Micropalaeontology, Palaeoenvironments and Sequence Stratigraphy of the Sulaiy Formation of Eastern Saudi Arabia

Saleh Sfoog M. AlEnezi

A thesis submitted to Plymouth University in Partial fulfilment for the degree of

PhD Geological Science

School of Geography, Earth and Environmental Sciences

Faculty of Sciences and Technology

May 2016

Saleh Sfoog AlEnezi, *Micropalaeontology, Palaeoenvironments and Sequence Stratigraphy of the Sulaiy Formation of Eastern Saudi Arabia*

The Sulaiy Formation, which is the oldest unit in the Lower Cretaceous succession, is conformably overlain by the Yamama Formation and it is a challenge to identify the precise age of the two formations using foraminifera and other microfossil assemblages. In the eastern side of Saudi Arabia, the Sulaiy Formation and the base of Yamama Formation are poorly studied. The main objectives of this study is to enhance the understanding of the Sulaiy Formation sequence stratigraphical correlation, regional lateral variations and palaeoenvironmental investigation.

Lithological and semi-quantitative micropalaeontological analysis of 1277 thin sections taken from core samples from nine cored wells providing a geographically representative distribution from the Saudi Arabian Gulf. These cores intersected the base of the Yamama Formation and the Sulaiy Formation in the total thickness of cored wells of 843.23 meters (2766.5 feet).

On the evidence provided by the foraminifera, the Sulaiy Formation is considered to represent the Berriasian to the lowermost Valanginian. The investigation of the micropalaeontology has provided considerable insights into the biocomponents of Sulaiy and the base of Yamama formations in order to identify their biofacies. These microfossils include rotalid foraminifera, miliolid foraminifera, agglutinated foraminifera, calcareous algae, calcispheres, stromatoporoids, sponge spicules, problematica (e.g. *Lithocodium aggregatum*), molluscs, corals, echinoderms and ostracods. Systematics of planktic and benthic foraminifera is accomplished using the foraminiferal classification by Loeblich and Tappan (1988) as the main source.

The assemblage contains foraminifera that recorded for the first time in the Sulaiy Formation. Other microfossils were identified and recorded to help in the identification of the sedimentary environments.

The investigation of the micropalaeontology and the lithofacies analysis have provided evidence the identification of the various lithofacies. About twenty four microfacies were identified on the basis of their bio−component and non-skeletal grains. The lithofacies and the bio−component results have provided the evidence of the sedimentary palaeoenvironmental model namely the Arabian Rimmed Carbonate Platform. This palaeoenvironmental depositional model is characterised by two different platform regimes. They are the Platform Interior and the Platform Exterior each of which have unique sedimentary lithofacies zones that produce different types of lithofacies. Each lithofacies is characterised by special depositional conditions and palaeobathymetry that interact with sea level changes and the accommodation space. The important palaeoenvironments are intertidal, restricted lagoon (subtidal), open marine, deeper open marine, inner shoal, shoal and platform margin.

Generating, and testing, a depositional model as a part of formulating a sequence stratigraphical interpretation of a region is a key to understanding its geological development and – ultimately – reservoir potential. The micropalaeontology and sedimentology of the Sulaiy Formation in the subsurface have indicated a succession of clearly defined shallowing−upwards depositional cycles. These typically commence with a deep marine biofacies with wackestones and packstones, capped with a mudstone-wackestone maximum flooding zone and an upper unit of packstone to grainstones containing shallow marine biofacies. The upper part of the Sulaiy Formation is highstand-dominated with common grainstones that host the

Lower Ratawi reservoir which is capped by karst that defines the sequence boundary. This karst is identified by its abundant moldic porosity that enhanced the the reservoir quality by increasing its porosities into greater values. Integration of the sedimentology and micropalaeontology has yielded a succession of shoaling−upwards depositional cycles, considered to be 4th order sequences, that are superimposed on a large scale 3rd order system tract shallowing−upwards, highstand-associated sequence of the Sulaiy Formation.

The Lower Ratawi Reservoir is located within the latest high-stand portion of a third-order Sulaiy Formation sequence. The reservoir consists of a succession of several sequences, each of which is sub-divided into a lower transgressive systems tract separated from the upper highstand systems tract by a maximum flooding surface (MFS/Z). The last of these depositional cycles terminates in beds of porous and permeable ooid, or ooidal-peloidal, grainstone. The reservoir is sealed by the finer-grained sediments of the Yamama Formation.

Table of contents

CHAPTER FOUR: SYSTEMATICS

CHAPTER FIVE: PALAEOENVIRONEMENTAL DEPOSITIONAL MODEL

CHAPTER SIX: SEQUENCE STRATIGRAPHY AND PALAEOENVIRONMENTAL MAPS

List of Figures

List of Tables

AUTHOR'S DECLARATION

At no time during the registration for the degree of Doctor of Philosophy has the author been registered for any other University award without prior agreement of the Graduate Committee.

Work submitted for this research degree at the Plymouth University has not formed part of any other degree either at Plymouth University or at any other establishment.

External Contacts:

Saleh Sfoog M. AlEnezi.

Office phone: 00966-13-873-2822.

Mobile 00966-563792116.

saleh.enezi.4@aramco.com

senezyoo@hotmail.com

Saudi Aramco P. O. Box 5810.

Dhahran 31311.

Saudi Arabia.

Word count of main body of thesis: **58, 022 .**

Signed_____

Date_____

CHAPTER ONE

INTRODUCTION, AIMS AND OBJECTIVES

CHAPTER ONE– INTRODUCTION, AIMS AND OBJECTIVES

1.1 INTRODUCTION

The Cretaceous hydrocarbon reservoirs of the Arabian Gulf region are economically very important. Considerable volumes of recoverable oil are produced from 90 oil fields, which include 17 from Cretaceous reservoirs (Figures 1.1 and 1.2). The Arabian Gulf presently holds 56 percent of the world's hydrocarbon reserves (Kendall *et al.,* 2010) and the Cretaceous oil fields in the Arabian Gulf countries are producing approximately 361 million barrels per year (Christian, 1997). This has stimulated exploration activity in the region, resulting in increased research and geological studies (Christian, 1997).

This research project aims to improve our understanding of Cretaceous stratigraphy, micropalaeontology, lithofacies and sequence stratigraphy.

The Cretaceous rocks in Saudi Arabia can be subdivided into three lithostratigraphical groups that are separated by two major unconformities (Figure 1.3). At the base is the Thamama Group (basal Lower Cretaceous), which is composed of very fine grained limestones to packstones, with grainstones at the top. The Wasia Group (top Lower Cretaceous) consists mainly of sandstones interbedded with shales and with some thin dolomite lenses at the top. The Aruma Group (Upper Cretaceous) forms the uppermost carbonate group and is composed of limestones with significantly less dolomite and shale. This study will focus on the lowest part of the Thamama Group; the Sulaiy Formation and the base of the Yamama Formation. The Sulaiy Formation, which include the Lower Ratawi reservoir,

has equivalent successions in the region of the Arabian Gulf areas (Figure 1.2) which have economic oil and gas production potential. In the offshore of Iran the equivalent reservoir is called the Fhliyan Formation. In southern Iraq it is also known as the Sulaiy Formation, and the Makhul Formation in the Mesopotamian Basin. In Kuwait the Sulaiy Formation equivalent is sub-divided into two formations; namely the Makhul Formation at the base and the overlying Managish Formation. The Managish reservoir is extremely significant as it produces almost one third of all Kuwaiti oil production. In Abu Dhabi and Oman the equivalent units are the Habshan and Rayda formations. The name Sulaiy Formation is also used in Bahrain and Qatar (Figure 1.2) (Christian, 1997).

1.2 RATIONALE

Bramkamp and Barger (1938) were the first people who identified the upper and lower boundaries of the outcrops of the Sulaiy and Yamama beds. Redmond (1962) has been revised the boundaries positions of the Sulaiy and Yamama beds based on their foraminiferal and lithological characters (Powers *et al.*, 1966). He was the first micropalaeontologist who identified and named benthic foraminifera taxon that were used to characterise the Sulaiy Formation from the Yamama Formation. However, Powers (1968) mentions that the sub-surface contacts between the Sulaiy and Yamama formations are conformable in the Uthmaniyah area of the Ghawar Field (Figure 1.1).

In the outcrop, the base of the Sulaiy Formation was selected above the late Jurassic unconformity on top of the Hith evaporate member and the Hith Transitional Member. In the sub-surface, the base of the Sulaiy Formation can be detected lithologically by the change from clean-grained limestone, dolomite or calcite-cemented ooidal grainstone of the upper-most Hith Transitional Member to the peloidal grainstones of the base of the Sulaiy (Powers *et al.*, 1966).

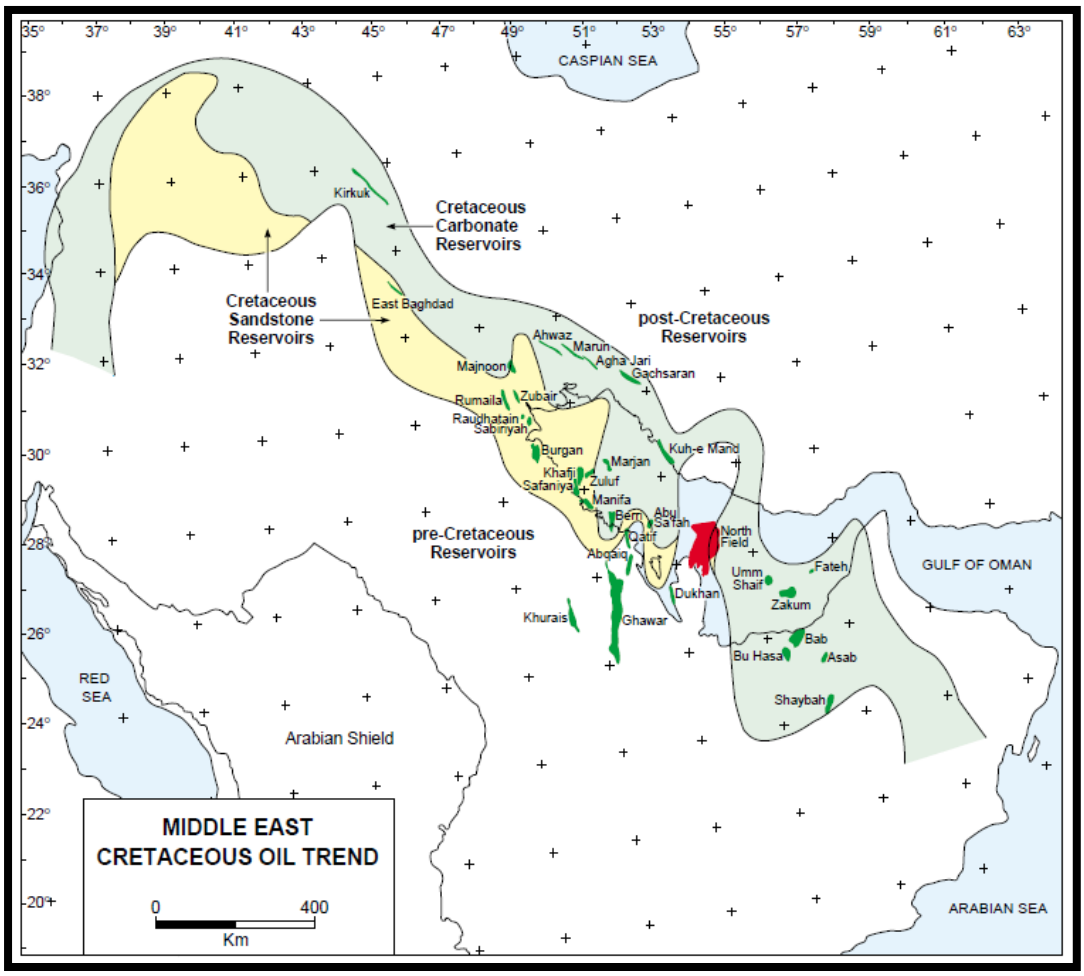

Figure 1.1. The Cretaceous oil fields in the Arabian Gulf Region include 17 of the super-giant oil fields of the 90 fields that are distributed in the Lower Cretaceous carbonate reservoirs (light green area) and the mid-Cretaceous sandstone reservoirs (yellow area). The main Saudi Arabian fields include those of Safaniya, Khafji, Manifa, Marjan, and Berri (after Christian, 1997).

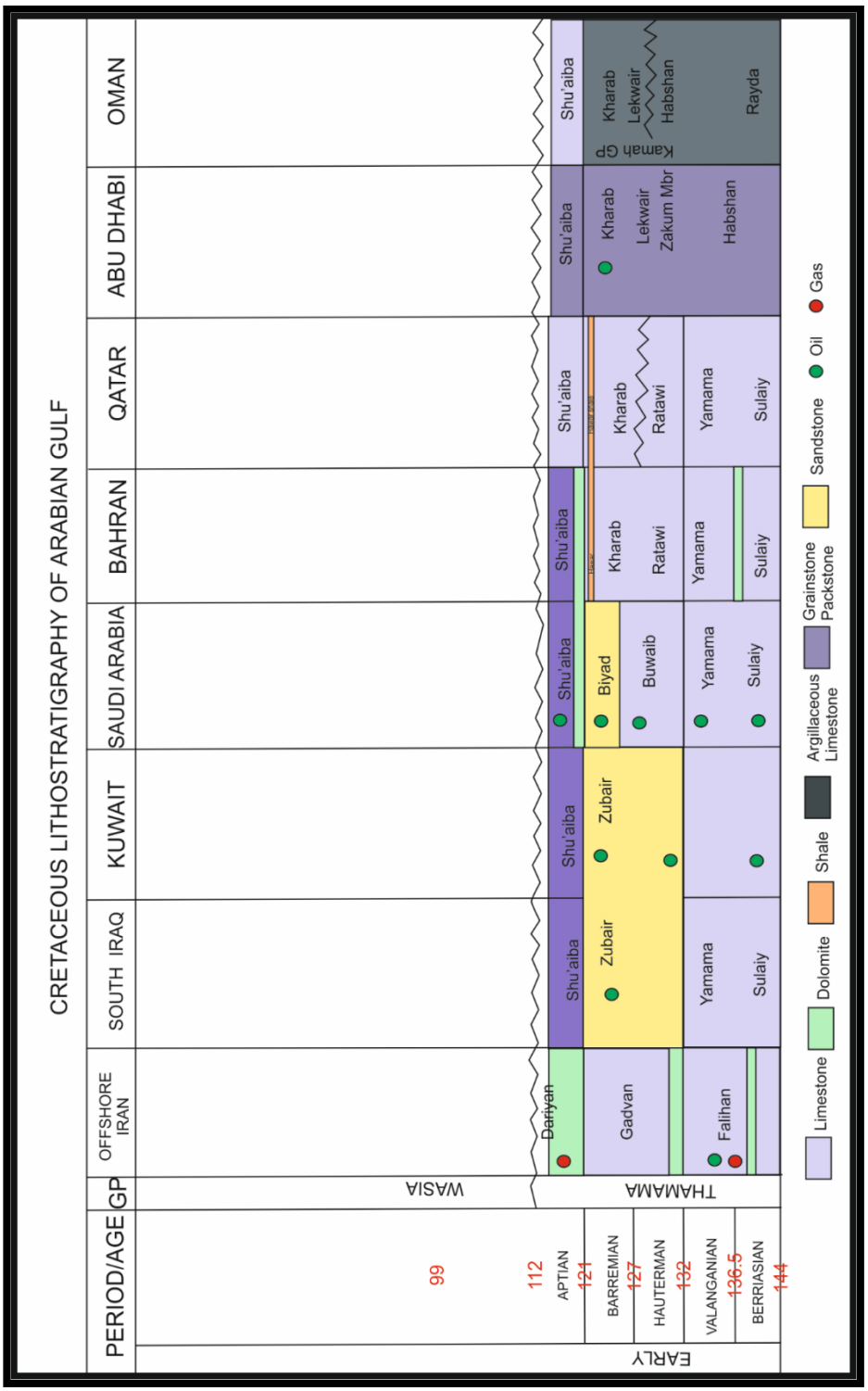

Figure 1.2. Comparison of nomenclature, stratigraphy and lithological columns of the Thamama group successions and reservoir systems of the Arabian Gulf countries (modified from Christian, 1997).

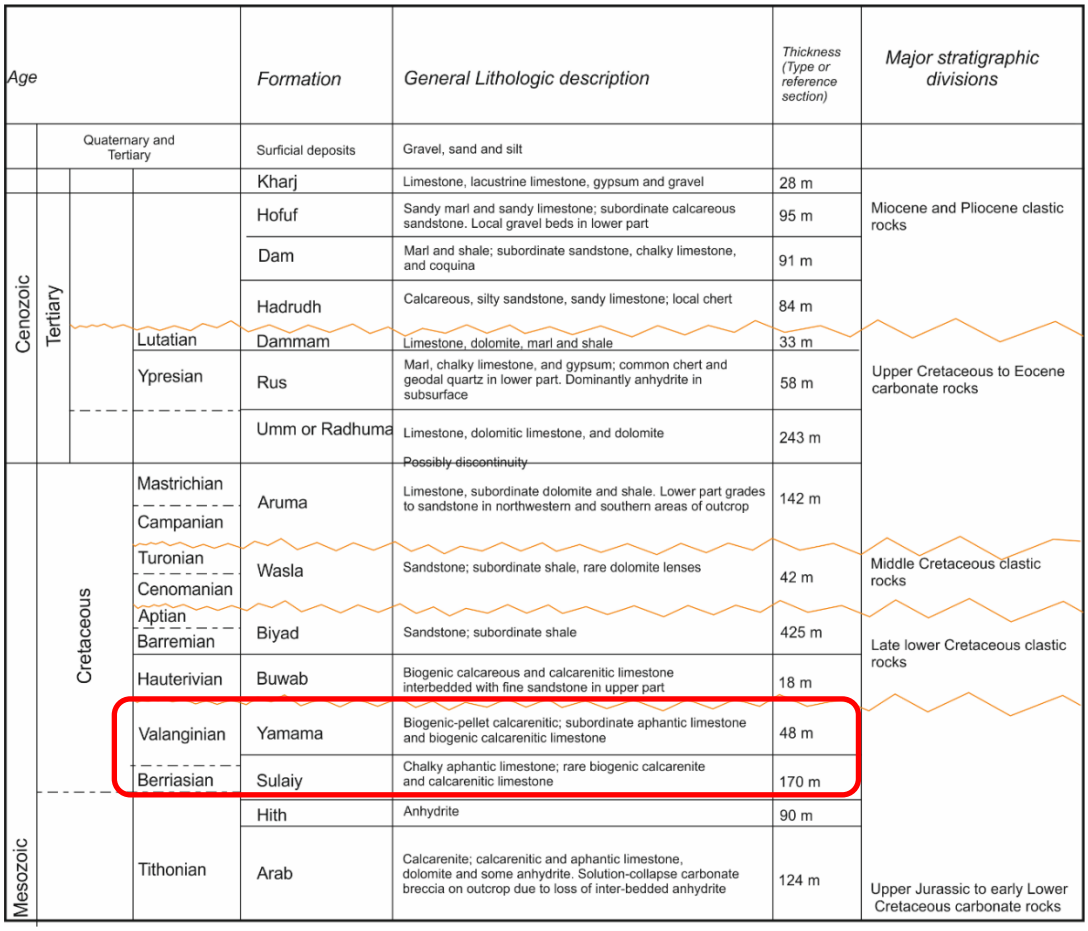

Figure 1.3. The Saudi Arabian geological column based on the geological field studies by the earliest Saudi Aramco geologists; after Powers *et al.* (1965), improved by AL Jallal and AlSharhan (2005). The red box encompasses the stratigraphical interval studied in this research.

Further details of regional studies on the Sulaiy Formation were discussed in Al Sharhan and Nairn (1986, 1988, 1990, and 1997). The first attempt to set up a depositional model of the Mesozoic succession outcrops (including the Sulaiy Formation) was suggested by Murris (1981), Al Sharhan and Nairn (1986, 1988, 1990, 1993, 1997), Shebl and Al Sharhan (1994, 2000) and Al Sharhan and Whittle (1997). Although they have suggested a carbonate Ramp platform model for the successions. The first sedimentary facies and the microfacies analysis using Dunham (1962) on the Sulaiy Formation outcrops were provided by Shebl and Al Sharhan (1994, 2000). These

microfacies analysis were missing the use of depth and palaeoenviromental diagnostic microfossils.

The global relative sea level changes and major/minor unconformities during Phanerozoic of the Middle East were discussed by Al Sharhan and Nairn (1997) using Vail *et al.* (1977) and Sloss (1963). The calibration of sea level changes throughout the succession were generated by Vail *et al.* (1977), Haq *et al.* (1988) and Haq and Al-Qahtani (2005). These have been followed by basic sequence stratigraphy (generalized) by Vailk *et al.* (1977) and Haq *et al.* in which they recognized all major 1st order cycles of the Middle East geological succession. The major tectonic events and the Arabian Plate sequence stratigraphy were discussed by Harris et al. (1984), Al Sharhan and Nairn (1997), Ziegler (2001) Sharland *et al.* (2001) and Pollastro (2003). They concluded that the Cretaceous successions of the Arabian Gulf area were separated by two major unconformities: the post-Shuaiba unconformity and the post-Wasia unconformity. These unconformities have been related to three major tectono-stratigraphic groups. The oldest group is the Thamama Group which includes the Sulaiy and the Yamama formations.

In the subsurface, the hydrocarbon preliminary evaluation results of the Kuwaiti Sulaiy Formation was discussed by Abdullah and Kinghron (1996). They have indicated that the Lower Sulaiy Formation (equivalent to the Makhul Formation) is the source rock of the Managish Formation which is equivalent to the Saudi Lower Ratawi reservoir. The first work on the sub-surface major sequence stratigraphy was presented by Hughes (2000a) and he concluded that the top of the Sulaiy Formation is resembles the end of a 3rd order cycle. The late highstand grainstones (Hughes, 2000a) of the Sulaiy Formation host the Lower Ratawi hydrocarbon reservoir, and the intra-

formational grainstones of the Yamama Formation host the Upper Ratawi reservoir. Saudi Aramco have recognised that the Lower Cretaceous reservoirs in the Sulaiy and Yamama formations of the Eastern part of Saudi Arabia are poorly understood with few publications on the regional distribution of palaeoenviromentally controlled biofacies and depositional models. The first use of microfossils to determine the palaeoenviromental variations and sequence stratigraphical responses was by Hughes (2013) when he employed microproblematica in the recognition of transgressive and regressive patterns. Although, this research will provide 12 groups of biocomponents to display a varied vertical distribution within the Sulaiy Formation, and can be used to support recognition of depositional cycles.

Both formations contain a variety of microscopic skeletal components for which the palaeoenviromental and sequence stratigraphic implications have yet to be fully understood. Current depositional models require the palaeoenviromental refinement that a regional micropalaeontological study will provide.

A more complete (higher resolution) stratigraphical framework is required to support further development studies of the Sulaiy and Yamama formation reservoirs. A specific problem exists in the determination of the boundary between the top of the Sulaiy Formation and the base of the Yamama Formation due to a lack of studies of regional palaeoenvironmentally–controlled biofacies. It is also important to understand the origin, nature and extent of the post-Sulaiy unconformity in order to understand the diagenesis that preserved the localised porous grainstones at the top of Sulaiy Formation. This study is aims to resolve these issues as will be explained in subsequent sections.

1.3 THE TYPE SECTION AND NOMENCLATURE OF THE LOWER THAMAMA GROUP

The Lower Thamama Group (Lower Cretaceous) type section in Central Saudi Arabia is located 150 km south of Riyadh, near to Al Kharj (Figure 1.4). The name is taken from Khasm a Thamama, which means the Thamama cliff, and this is the type locality. Steinke (1940) recognized that the outcrops were Cretaceous in age and established the newly named formation (Thamama Formation). They were previously (prior to 1940) considered to belong to the Tuwaiq and Riyadh formations of the Jurassic. The Thamama Formation was elevated to group status, the Thamama Group, because of the lithological sub–division into three formations (Buwaib, Yamama and Sulaiy formations) by Powers *et al*. (1966). Powers included the Biyadh Sandstone in the top of the Thamama Group (Figure 1.2), although this has now been included as a member of the overlying Wasia Formation. Stratigraphically, the Thamama Group overlies the Hith Anhydrite and the Hith Limestones (Late Tithonian). The Wasia Group overlies the Thamama Group, and the two units are separated by the regional pre-Wasia unconformity (late Aptian). In the Thamama Group outcrop and the sub-surface of Saudi Arabia, the regional, late Valanginian unconformity separates the Yamama Formation from the Buwaib Formation.

Sedimentation was interrupted in eastern Saudi Arabia by the late Valanginian to early Hauterivian hiatus, which produced the late Valanginian unconformity.

The Sulaiy Formation was originally defined by Burchfiel and Hoover (1935), in which it located within top beds between the unconformities of the post-Marrat (late Toarcian) and pre-Wasia (late Aptian). The beds were assigned to the Tuwaiq Formation. Steinke (1937) added some younger units to the Tuwaiq Formation and they are the Riyadh chalks and limestones, and the Biyadh and Wasia members. In 1938, Bramkamp and Barger (1938) re-studied the top of the Tuwaiq Formation and elevated the Riyadh chalks and limestones member to the Riyadh Formation which consists of the Hith Anhydrite and Riyadh Lower Member at the base, overlain by the Sulaiy Limestone Member, and the Yamama Detrital Member at the top. Steinke and Bramkamp (1952) separated the Sulaiy and Yamama detrital members from the Riyadh Formation and established the Thamama Formation, which was based on the presence of Lower Cretaceous fossils (Tithonian–Valanginian). A third member, unnamed, was added to the Thamama Formation. Later, Steinke and Bramkamp (1952) formally elevated the three beds to formations of the Thamama Group. They are, from base to top, the Sulaiy, Yamama, and Buwaib formations (Powers, 1968).

1.3.1 Sulaiy Formation

Origin of Name: The Sulaiy Formation is named after Wadi as Sulayy (Figure 1.4) at the base of the Hit Escarpment located in south Riyadh on the eastern side of Hit Town (lat. 24° 29’ 18’’ N.; long. 47° 00’ 06’’ E) where the Hith evaporites are exposed in a very deep sinkhole (Figure 1.5).

Age: The first age assigned to the Sulaiy Formation by Redmond (1962, 1964) was Late Jurassic–Early Cretaceous (Late Tithonian–Valanginian) based on both stratigraphical position and contained fossils. Vaslet *et al.* (1991) and Al-Husseini *et al.* (2006) have discussed the boundary between the base of the Sulaiy Formation and the Hith Anhydrite. They concluded that microfossils are not useful in determining the precise age for the base of the Sulaiy Formation. Al-Husseini *et al.* (2006) have provided the ages of the Hith and Sulaiy formations using Sr-isotopes, which indicate that the base of the Sulaiy Formation is mid–Late Tithonian in age.

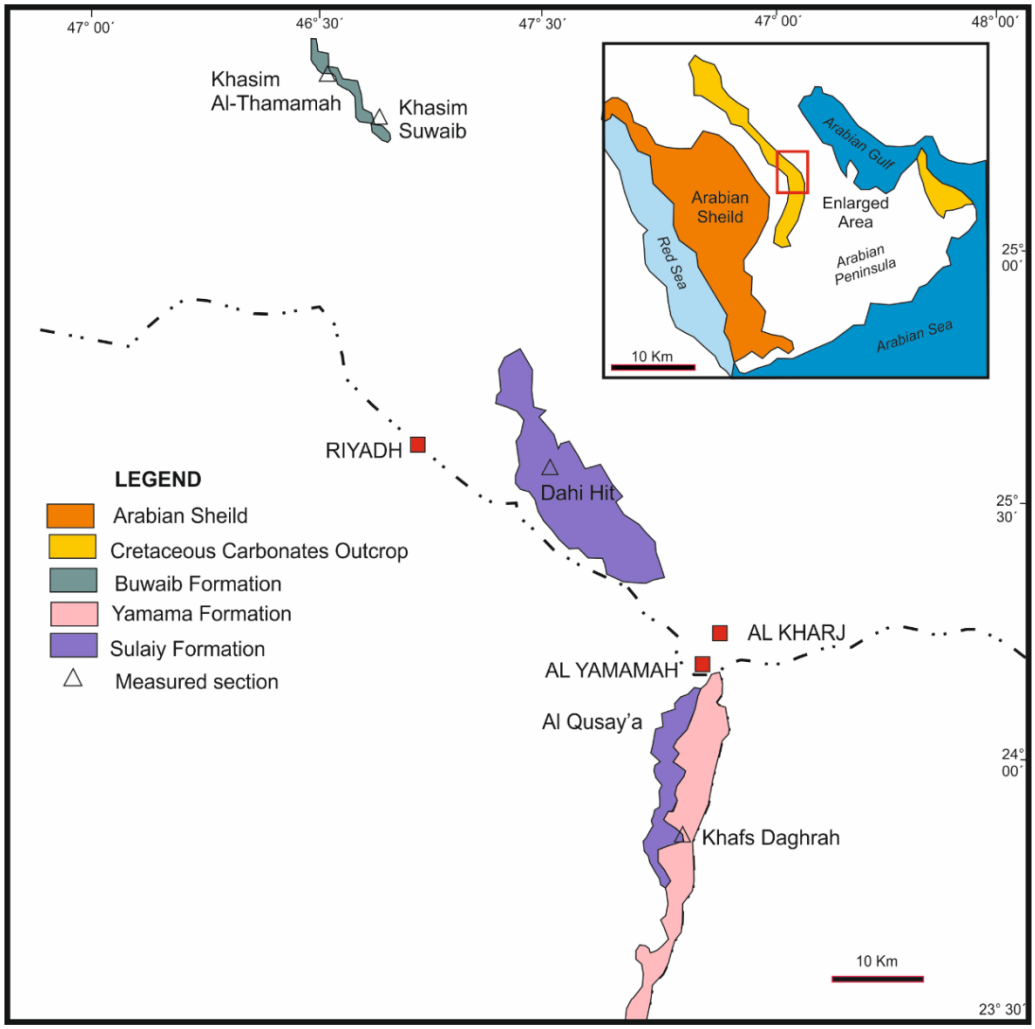

Figure 1.4. The type sections of the Lower Cretaceous rocks in Central Saudi Arabia. These are the type sections of the Lower Thamama Group of the Sulaiy, Yamama and Buwaib formations, with their exposure names and location coordinates (Shebl and AlSharhan, 2000).

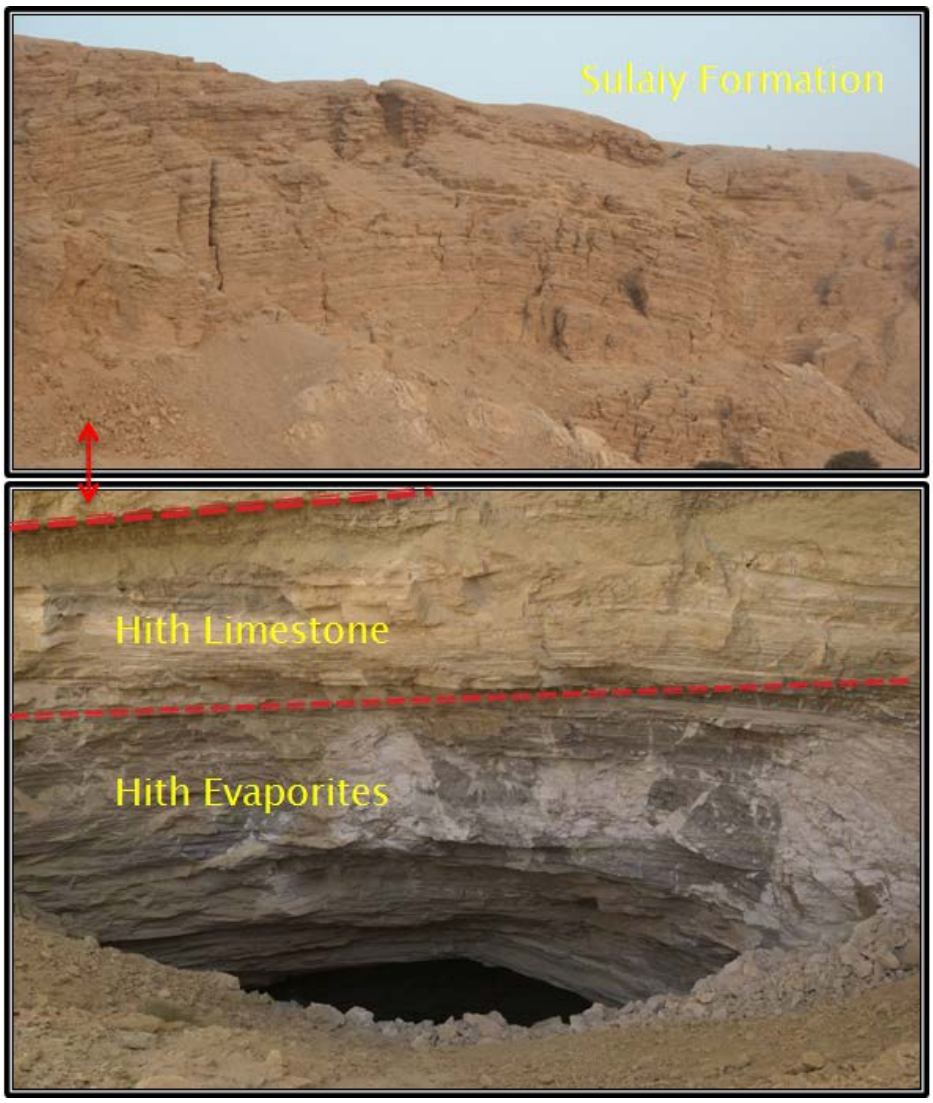

Figure 1.5. Dahl Hith. View of a sink-hole within the anhydrites of the Hith Formation, overlain by fractured and collapsed carbonates of the basal Sulaiy Formation. The Photograph were taken by Bob Lindsay in 2009. The double-headed arrow indicates the base of the Sulaiy Formation.

However, in this study, it is concluded that microfossils can be useful in accurately constraining the age of the Sulaiy Formation. There are several microfossils that can be used to determine the age of the Sulaiy Formation and that of the Lower Ratawi reservoir. The strontium isotope age dating of Al-Husseini *et al.* (2006) appears to agree with this biostratigraphy but the measured sample appears to come from within the top of the Hith Formation which is followed by the unconformity separating the top of Hith Formation

from the base of Sulaiy Formation. This will be discussed further in Chapter Four.

The age of the Sulaiy Formation is Berriasian to early Valanginian based on the planktic foraminiferid *Conoglobigerina* sp. cf. *C. gulekhensis* (Gorbatchick and Poroshina, 1979). The stratigraphical age of *Conoglobigerina* sp. cf. *C. gulekhensis* has been recorded by several authors in different places in the world including Berriasian to Valanginian by Grigelis and Gorbatchik (1980), Berriasian to Valanginian by Banner and Desai (1988) and Berriasian to Early Valanginian by Simmons *et al*. (1997). In this study it appears to follow the suggestion of Simmons *et al.* (1997).

The other foraminiferid that provides the same age range of Berriasian to early Valenginan is *Andersenolina delphynsis* (Arnaud-Vanneau, Boisseau and Darsac, 1988) which is recorded by several authors, including Arnaud-Vanneau *et al*. (1988), and Bucur *et al.* (1995) from the Carpathian Mountains, Chiocchini and Mancinelli (1979) and Chiocchini *et al.* (1994) from the Italian Alps, Velic (1997) from Croatia, Bucur and Săsăran (2005) from the carbonate platforms of Romania and Altiner (1991) from Turkey. The agglutinated benthic foraminiferid *Everticyclammina kelleri* (Henson, 1948), is also an indicator for the Sulaiy Formation, which ranges from Berriasian to Hauterivian (Banner and Whittaker, 1991). Similarly, the agglutinated foraminiferid *Pfenderina neocomiensis* (Pfender, 1938) ranges from Berriasian to Hauterivian (Olszewska, 2010).

The top of the Sulaiy Formation can be identified by the first appearance of *Neotrocholina valdensis* (Reichel, 1955). It is Late Berriasian to Valanginian in age, which has been determined by combining the age range results of

several authors (see Chapter 4: Systematics). The top of the Sulaiy Formation can also be identified by the first appearance of *Montsalevia salevensis* Charollais, Brönnimann and Zaninetti (1966), *Meandrospira favrei* Charollais, Bronnimann and Zaninetti (1966), *Ophthalmidium* sp., *Derventina filipescui* Neagu (1968), *Istriloculina eliptica* Iovcheva, *Gaudryina ectypa* Arnaud-Vanneau (1989) and *Nodobacularia* sp. This last species is an ideal index fossil for the base of the Lower Ratawi Reservoir.

Stratigraphy: The Sulaiy Formation, which is the oldest unit in the Lower Cretaceous succession, is conformably overlain by the Yamama Formation. As noted above, the type section is 170 m thick, and exposed in a cliff above Dahl Hith (Powers, 1968). The lower boundary is defined by the disconformity between the basal packstones and grainstones of the Sulaiy Formation and the underlying rudstones of the Hith Formation rocks (Powers, 1966, 1968) (Figure 1.5).

Lithology and Sedimentary Environment: The lithological character of the outcrop is mainly composed of alternations of very fine limestone and peloidal oolitic packstones and grainstones (Powers, 1968). The sedimentary environment representing by the outcrop is a succession of low energy, open shelf and lagoonal sediments of tan, chalky, thick-bedded, lime mudstones and wackestones interbedded with thin beds of skeletal and pellet packstones and grainstones. These stringers become more abundant in the lower part of the Sulaiy Formation. The basal bed contains moderate amounts of fine quartz sand (Powers, 1966, 1968).

Palaeontology: Based on Powers (1968), the formation contains a wide range of fossils and microfossils. The fossils are *Milleporidium* sp.

(demosponge), *Diceras* sp. (bivalve), but some fossils have been given incorrect names with recent ages such as *Aporrhais* sp. (gastropod), *Nerinea* sp. (gastropod), and *Ostrea* sp. (bivalve). The microfossils are mainly larger, agglutinated foraminifera and larger rotalids. Redmond (1964) recovered the following foraminifera from the upper-most part of the Sulaiy Formation: *Bramkampella arabica* (Redmond), *Everticyclammina* sp., *Iberina lusitanica* Egger (synonym of *Anchispirocyclina lusitanica* Jordan and Applin, 1952), *Nautiloculina* sp., *Pseudocyclammina sulaiyana* (Redmond), *Trocholina* sp. 1 (probably *Andersenolina elongata* Leupold), *Trocholina* sp. 2 (probably *Andersenolina albina* Leupold). The Jurassic age given to the formation is from the common distribution of *Nautiloculina* sp. which is located within the Lower Cretaceous (Powers, 1966). Maync (1959) has shown that *Iberina lusitanica* (*Anchispirocyclina lusitanica*) appears in the Lower Kimmeridgian and continues throughout the uppermost Jurassic and lowemost Cretaceous, until it disappears in the Lower Valanginian. Henson (1948), from the Qatar Dukhan well 2, has identified *Pseudocyclammina sulaiyana* Redmond as *Pseudocyclammina* aff. *lituus* (Yokoyama) in equivalent beds to the Sulaiy Formation. A very important palaeoenvironmental proxy of *Cladocoropsis* spp. was found common associated with sediments of the uppermost Jurassic beds and mentioned by Henson, 1948, and Powers, 1968.

1.3.2 Yamama Formation

Origin of Name: The type section of the Yamama Formation is 45.5 m thick, and is located 20 km North of Al Yamama which is now part of Ryiadh City in the Central Province of Saudi Arabia. Following the nomenclatural evolution of the Sulaiy Formation, the Yamama Formation was separated from the

Thamama Formation, which was then elevated to the Thamama Group (Powers *et al.*, 1966). The type section was described by Powers *et al.* (1966) and Powers (1968) from outcrops on the Al Quasaya upland. The definition of the Yamama type section was by Steinke (1940) who stated that it was the "*58 m of section between the dense Sulaiy limestone below and the pre-Buwaib unconformity above*" (Powers *et al.*, 1966).

Age: The Yamama Formation is confirmed as Valanginian in age and it is recognized by its restricted to open sub-tidal, lagoonal sedimentary environment. The age is given as Valanginian, based on the occurrence of *Everticyclammina eccentrica* Redmond (1964), *Everticyclammina elegans* Redmond (1964), *Pseudocyclammina cylindrica* Redmond (1964), *Pygurus rostratus* Agassiz 1839 (Echinodermata), and *Trematopygus* sp. cf. *T. grasi* d'Orbigny, 1857 (Echinodermata). Powers *et al.* (1966, p. D71) concluded that "none of these fossils are known outside Saudi Arabia, they have no value in defining the age of the formation".

Stratigraphy: In the reference section, the Yamama Formation has unconformable contact with the underlying Sulaiy Formation (Figure 1.5). There is a sharp lithological change from the light brown grainstones of the uppermost Sulaiy Formation to the mudstones and wackestones of the basal Yamama Formation (Powers *et al*., 1966). Overlying the Yamama Formation is the Buwaib Formation, separated by the pre-Buwaib unconformity. This is indicated by the change at the top of the Yamama Formation from golden-brown pellet grainstones to tan–coloured wackestones and mudstones (Powers *et al*., 1966).

Lithology and Sedimentary Environment: The carbonate sediments of the Yamama Formation are packstones to grainstones that indicate a shallow water environment. The sediments are mainly peloidal foraminiferal grainstones with some minor alternations of mudstones and wackstones. In the reference section, the main rock types are clean-washed grainstones and rudstones gradually replaced by mudstones, wackestones and packstones, with interbeds of the deep basin shales.

Palaeontology: Redmond (1964) provided a comprehensive list of fossils and the foraminifera recorded from the Yamama Formation. The foraminifera include *Cyclammina* spp., *Everticyclammina eccentrica* Redmond (1964), *Everticyclammina elegans* Redmond (1964), *Pseudocyclammina cylindrica* Redmond (1964), *Pseudocyclammina* sp., *Trocholina* spp., *Haplophragmium* sp., *Haplophragmoides* sp. and *Trochammina* sp. The macrofossils include *Astrocaenia*? sp. (scleractinian coral), *Milleporidium* sp. (demosponge) and echinoderms, including *Pygurus rostratus* Agassiz (1839), and *Trematopygus* sp. cf. *T. grasi* d'Orbigny (Powers, 1965). The gastropods are represented by *Aporrihais* sp., *Cerithium* sp., *Gyrodes* sp., *Natica* sp., *Pleurotomaria* sp. and *Trochos* sp. The bivalves include *Anisocardia* sp., *Corbis* sp., *Corbula* sp., *Chione* sp., *Cuculaea* sp., *Exogyra* spp., *Homoya* sp. Agassiz (1843), *Lima* sp., *Nuculana* sp., *Ostrea* sp., *Paphia* sp., *Pholadomya* sp. cf. *P. decussata*, *Tellina* sp., *Trigonia* sp. and *Venus* sp.

In this study the identified benthic foraminifera and calcareous algae are including *Haplophragmoides joukowskyi*, *Meandrospira faveri*, *Trocholina sagittaria*, *Andersenolina elongata, Andersenolina alpina, Derventina filipescue, Myancina* n. sp.1, *Paracoskinolina pfenderae* and *Gaudrina* sp. cf. *G. ectupa*. The calcareous algae include *Salpingoporella dinarica*, *S.*

istriana, S. anulata, S. hasi, S. pygmaea, Clypina sulcata, Permocalculus spp. and *Cylindroporella arabica.* Important diagnostic stratigraphical and palaeoenvironmental associations of benthic foraminifera that include *Protopeneroplis banatica*, *Pseudocyclammina littus, Textulariopsis jurassica, Verneuilinoides polonicus, Siphovalvulina variabilis* and *Lenticulina* spp.

Subsurface Distribution and Value: The formation extends regionally along the entire eastern, southern and the north–eastern flank of Arabia. In Saudi Arabia, it contains the oil producing Upper Ratawi reservoir within the offshore area of the Manifa Field. The thickness of the formation increases towards the east from 46 m in the outcrops, to 140 m in the Uthmaniyah wells of the giant Ghawar Field. The thickness change is attributed by the pre-Buwaib unconformity (Powers *et al*., 1966) across the shallower lithofacies and less truncated at the deep facies. Powers *et al.* (1966) indicated that the unconformity is absent in the Uthmaniyah wells, where the contact is conformable between the Yamama and Buwaib formations and also between the Sulaiy and Yamama formations.

1.4 AIMS

The aim of this investigation is to provide evidence for the lateral variations in the character of the uppermost Sulaiy and the lowermost Yamama formations in the eastern part of Saudi Arabia. There is a need to provide a stratigraphical and palaeoenvironmental framework that will improve the prediction of reservoirs in a group of oil fields both onshore, and offshore, eastern Saudi Arabia. This study is centred on the Lower Cretaceous Sulaiy Formation, which hosts the Lower Ratawi reservoir.

Such an investigation should also provide evidence for high-frequency depositional cycles and systems tract-associated biofacies variations that migrated across the extensive carbonate platform in response to short-term and long-term eustatic variations. Their preservation is probably due to a gradual subsidence of the platform and the interaction of these two variables will contribute significantly towards understanding the regional distribution of palaeoenvironmentally-controlled biofacies. Depositional models resulting from the investigation will have important implications for understanding the distribution of high-energy lithofacies that are of potential hydrocarbon reservoir significance.

Regional variations in the palaeoenvironments represented at the Sulaiy-Yamama boundary make consistent determination of this event problematical. This research will identify such lateral variations in the character of the uppermost Sulaiy and the lowermost Yamama formations.

Additional aspects of this investigation will include the significance of the post-Sulaiy unconformity and an appreciation of the intensity of the eustatic controls on this event. It is suggested that the localised preservation of grainstones in the uppermost Sulaiy Formation may represent late highstand shoal development, upon which post-Sulaiy Formation (late Berriasian) sub-aerial exposure would have a significant effect on diagenesis.

In the Sulaiy Formation, Redmond (1964) noted that most of the described microfossils were recovered from the uppermost part of the formation whereas, in the lower parts, recovery was poor due to changes in the sedimentary environments that are locally barren of microfossils. This research will investigate such variations in microfossil abundance and

diversity in the lower parts of the Sulaiy Formation by an analysis of the sub-surface data.

1.5 OBJECTIVES

The study involves, for the first time, a solely thin-section based semi-quantitative analysis of a number of wells in order to determine their micropalaeontology, microfacies distribution, depositional environments, sequence stratigraphy and the distribution of reservoir facies. Limitations on the original objectives have been imposed by poor core distribution and unavailability of complete runs of equally-spaced thin sections. In addition, the planned integration of the micropalaeontological data with wireline logs has not been possible. The planned study of the entire Sulaiy and Yamama formations, and the respective equivalents of the Lower and Upper Ratawi reservoirs, has, therefore, been curtailed. Despite this, the studied section has received little attention and provides an opportunity to document the micropalaeontological and lithofacies content of the Berriasian carbonates of eastern Saudi Arabia. Such information will, in addition to contributing to the palaeogeographic extent of certain benthonic foraminifera, provide insights into their preferred palaeoenvironments. Stacking of microfossil assemblages will enable definition of depositional cycles of different hierarchies, especially when combined with observations of a diagenetic nature. The nature of the contact between the Sulaiy Formation and the overlying Yamama Formation will be characterised both micropalaeontologically and petrographically. These aspects of the research will also have a practical application to improve understanding, exploration and exploitation of the associated Lower

and Upper Ratawi reservoirs that are hosted by these Berriasian and Valanginian carbonates. This investigation, therefore, has the following five principal objectives:

- To document semi-quantitatively, and illustrate, the distribution of the entire micropalaeontological content of most of the Sulaiy Formation (Berriasian, lowermost Cretaceous) and the basal Yamama Formation (Valanginian). This information will facilitate the consistent recognition of the Sulaiy Formation in future studies;
- To record petrographic and diagenetic features of all thin sections;
- To use the microfacies to interpret the variable hierarchies of depositional sequences and to determine the depositional environments represented by the microfossil assemblages within each cycle. This information will assist inter-well correlation and have significant implications for hydrocarbon exploitation by determining the potential paths of intra-reservoir flow;
- To produce event-constrained palaeoenvironmental maps for selected horizons, and provide insights for regional palaeoenvironmental variations, degree of open marine access and possible location of coral and stromatoporoid bioherms and biostromes; and
- To understand fully the nature of the globally significant Berriasian-Valanginian boundary, which is known to represent a global eustatic fall in sea level, using the microfacies and diagenetic features represented in the thin sections.

CHAPTER TWO

STUDY AREA AND GEOLOGICAL SETTINGS

CHAPTER TWO−STUDY AREA AND GEOLOGICAL SETTINGS

2.1 THE POTENTIAL OF THE STUDY AREA

The study area for this research is located on the north-east flank of the Arabian Peninsula (Figure 2.1), in an area known by the Saudi Aramco Company as the North-Eastern oil fields in eastern Saudi Arabia. This area includes both onshore and offshore oilfields. Globally the region is known as the Arabian (Persian Gulf in Iran) Gulf, which is the economic heart of the Middle East, and which is located to the east of the Mediterranean Sea. The study area is located within the upper western Arabian Gulf, where the major oilfields are currently producing from Cretaceous carbonate and sandstone reservoirs. It is an area that contains economically valuable hydrocarbon fields, both offshore and onshore. The productive Jurassic and Cretaceous reservoirs are in the deep sub-surface and there are no surface outcrops (Figure 2.2). The research area is located in the southern Mesopotamian Fore-deep (USGS code 2024) Basin of the Arabian Gulf Basins by the USGS (Pollastro, 2003). Notably, as seen in Figure 2.2, the southern Mesopotamian Fore-deep Basin includes Kuwait and the eastern Saudi Arabian offshore and onshore. However, the nearby Widyan Basin - Interior Platform (USGS basin code 2023) contains only Jurassic reservoirs. It is because these provinces contain almost all of the Cretaceous reservoirs, that the study wells were selected from within these provinces.

The location of the study area is bounded between the following longitudes and latitudes (Figure 2.3): in the north between latitudes N28°36'04" to

N26°44'56" and in the west between longitudes E047°44'59" to E050°45'13". The study wells are located in a polygonal-shaped area of about 60,558 square kilometers (Figure 2.3).

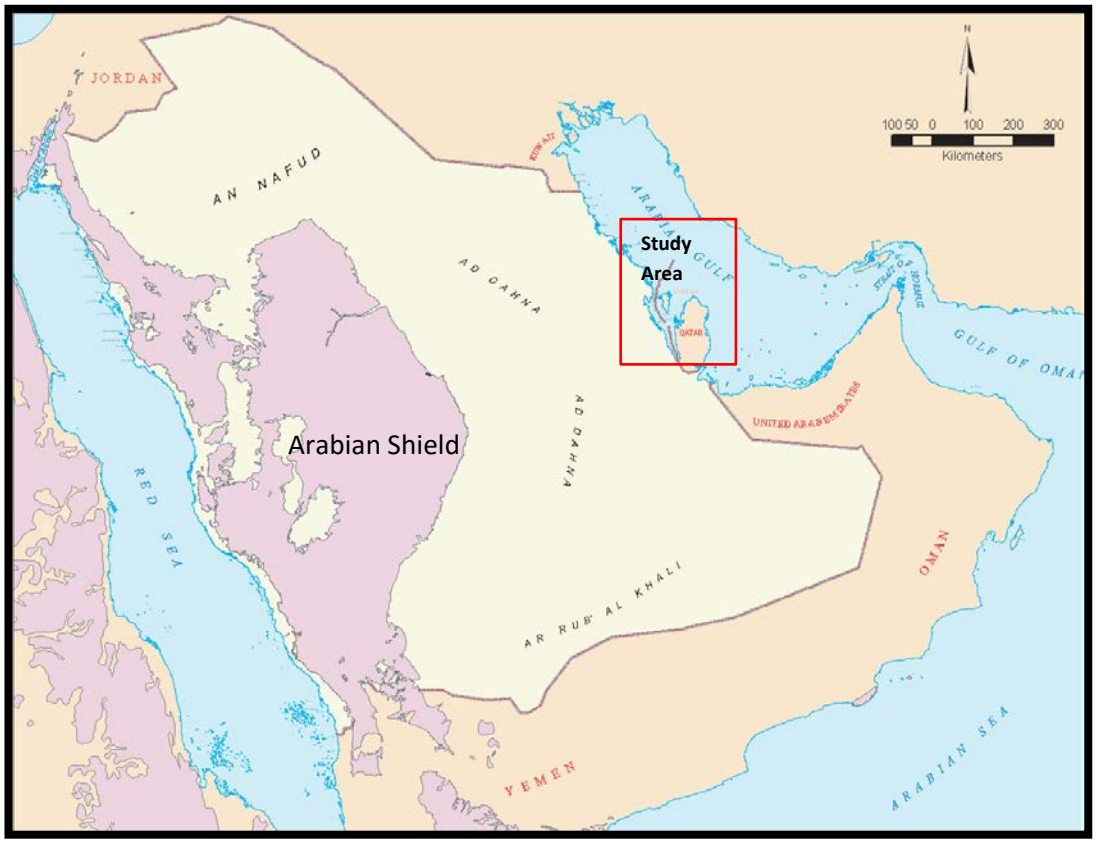

Figure 2.1. Map of Saudi Arabia showing the outline of the study area. Pink area is the Arabian Precambrian Shield and the pale yellow colour represents the sedimentary cover of the Arabian Peninsula (modified from Hughes, 2009).

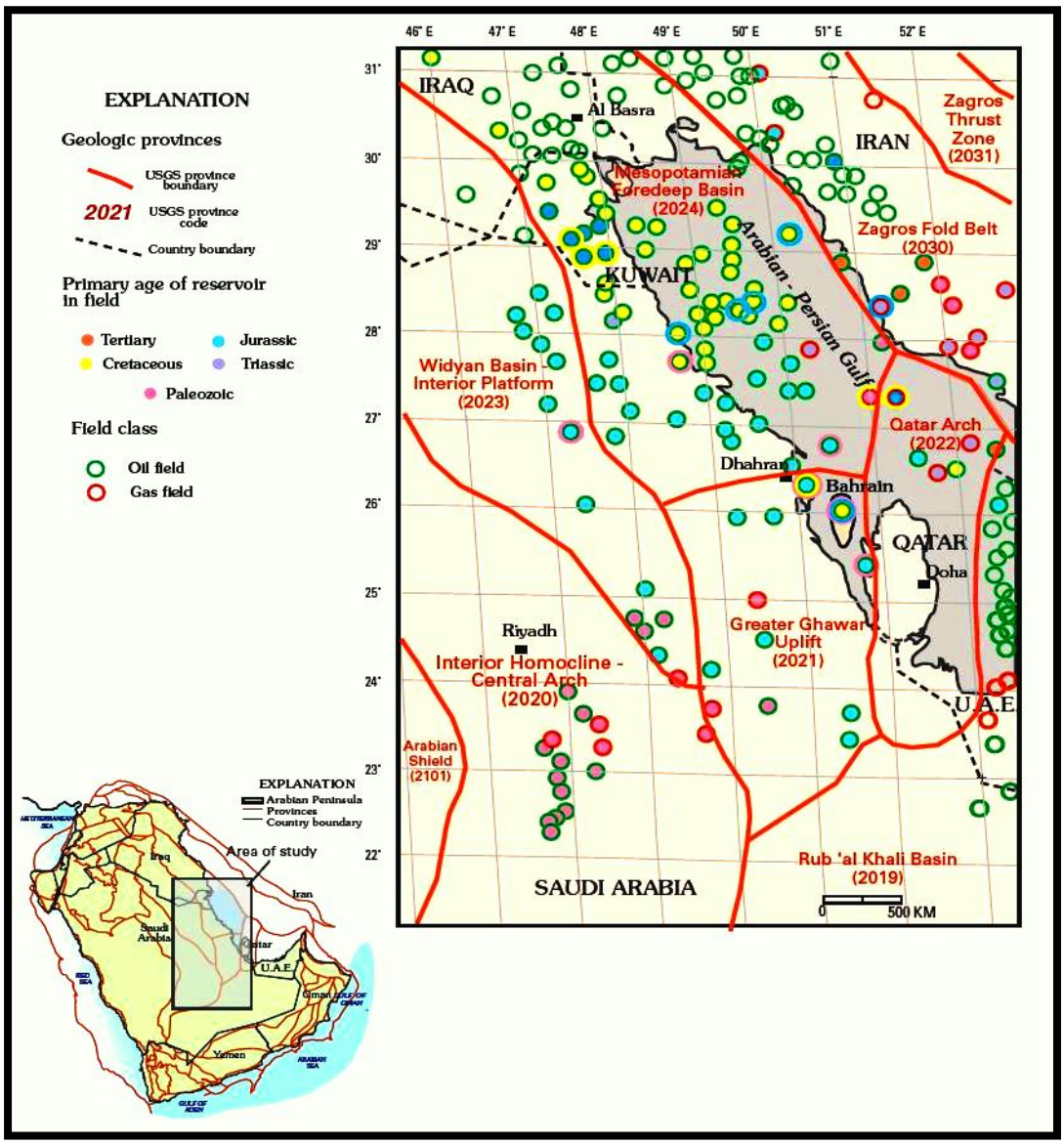

Figure 2.2. The distribution of the Jurassic and Cretaceous wells within the southern Arabian Gulf Provinces known as the Mesopotamian Fore-deep Basin. The Jurassic wells are in blue while the Cretaceous wells are shown in yellow. These wells are predominantly oil wells. The USGS gave a code for the Province as 2024 (Pollastro, 2003).

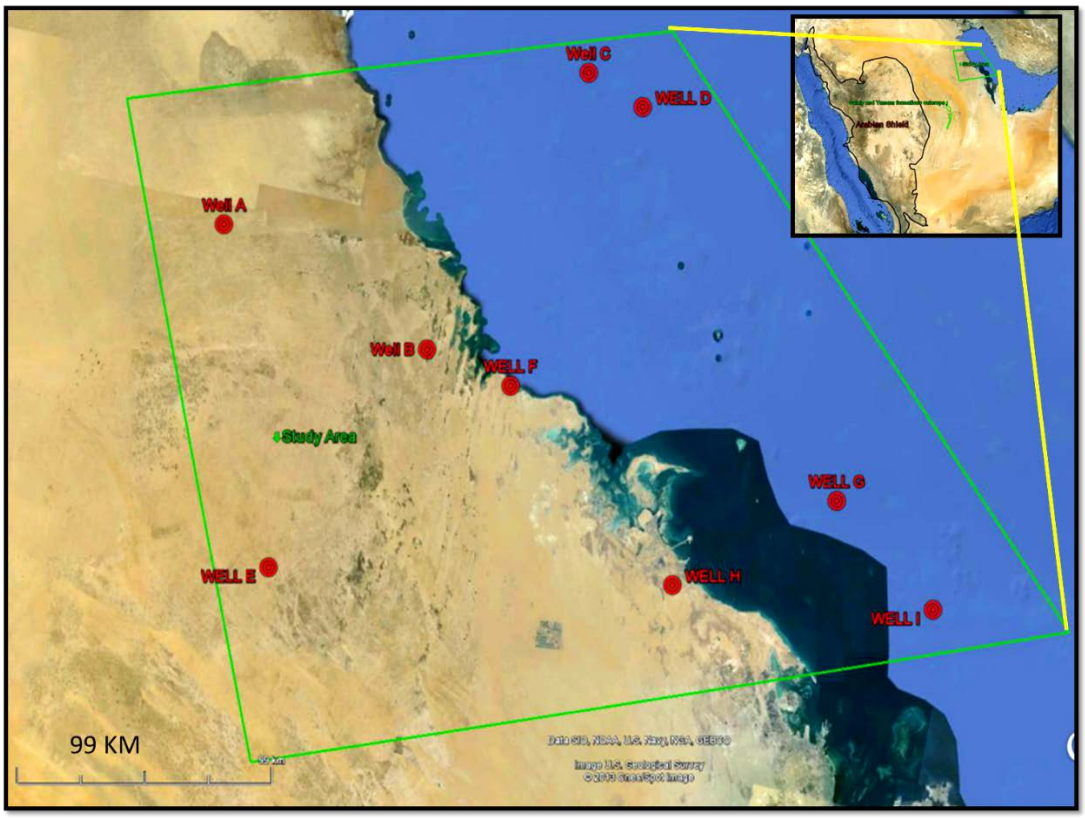

Figure 2.3. Satellite image of Saudi Arabia showing the study area outlined in green. The study area is shown in the inset map, also bordered in green. The locations of the studied wells are shown in red.

2.2 TECTONIC SETTING OF THE STUDY AREA

The Arabian Peninsula consists of the Arabian Precambrian Shield, exposed in the west, which is covered in the east by Palaeozoic, Mesozoic and Cenozoic sedimentary rocks (Figure 2.4) (Al-Hinai *et al.,* 1997). The Sulaiy and Yamama formations are sub-surface strata in the study area and their outcrop can only be found exposed around the margins of the Arabian Shield and located east from the Arabian Shield of the Arabian Plate. The outcrops of the Sulaiy and Yamama formations are located to the south-west side of Riyadh. They dip and plunge generally toward the east and the north-east of the Arabian Peninsula (Figures 2.5, 2.6).

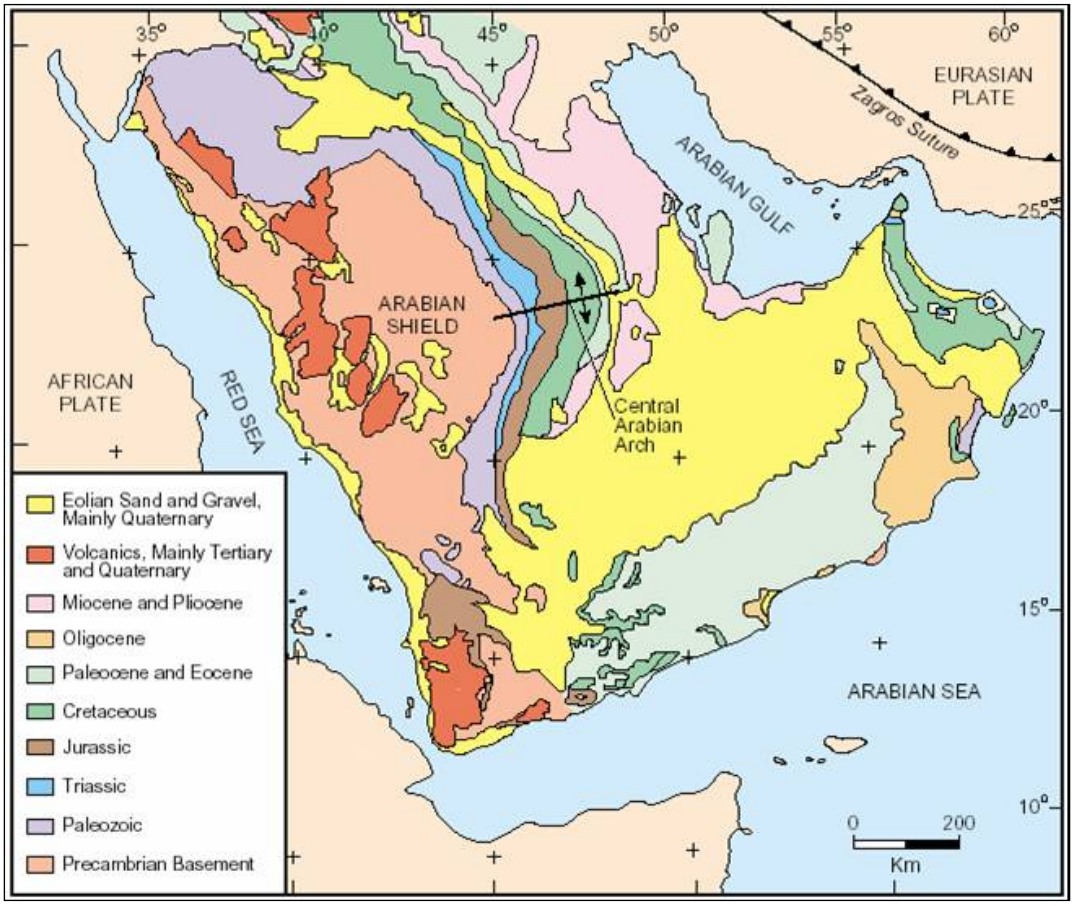

Figure 2.4. Generalized geological map of the Arabian Peninsula representing the outcrops geological groups including the Cretaceous (green) rocks near to the east of the Arabian Shield and in Oman (after Al-Hinai *et al*., 1997).

The structural pattern of the Arabian Peninsula includes four main tectonic zones (Henson, 1951; Beydoun 1966, 1988, 1991; Edgell, 1992). These compose the Arabian Shield, which includes cratonic Precambrian rocks, Stable Shelf, Unstable Shelf and the Zone of Marginal Troughs (Figure 2.6).

The Arabian Shield is made of cratonic Precambrian rocks which are exposed from the western side to the central area of the Arabian Peninsula and which extend beneath the Stable Shelf and the Unstable Shelf (Hariri, 2003). On the Unstable Shelf, the Precambrian rocks are affected by tensional block faulting that extends through the overlying sedimentary rocks of the Phanerozoic (Hariri, 2003). The Zone of the Marginal Troughs is

located in the north-eastern part of the Arabian Peninsula at its northern margin. It includes the Phanerozoic sedimentary rocks that are affected, and controlled, by compressional faults and fold structures. The Stable Shelf, or the interior Arabian Platform (Powers *et al.,* 1966), is the location of the sub-horizontally dipping Palaeozoic, Mesozoic and older Cenozoic strata, outcrops of which are located around the margins of the Arabian Shield. This includes the Sulaiy and Yamama formations (Figure 2.6) (Hariri, 2003). The stable shelf strata are thinner and not disturbed by the basement tectonics because they are palaeogeographically located directly next to the Arabian Shield in shallower elevations compared to the strata of the deeper Unstable Shelf strata (Figure 2.6) (Hariri, 2003).

The Unstable Shelf strata include all of the Arabian Phanerozoic succession that dip is gently eastwards and north-eastwards. They are interrupted by the underlying Precambrian reverse fault system (Hariri, 2003) and by the Precambrian salt diapiric folds of the Hormuz salt domes (Greig, 1958; Edgell, 1992; Konert *et al*., 2001). These faults and folds have created the hydrocarbon traps (Figure 2.7) in the study area. All of the major oil fields of the Arabian Gulf are within the Unstable Shelf (Figure 2.7), including those of study area.

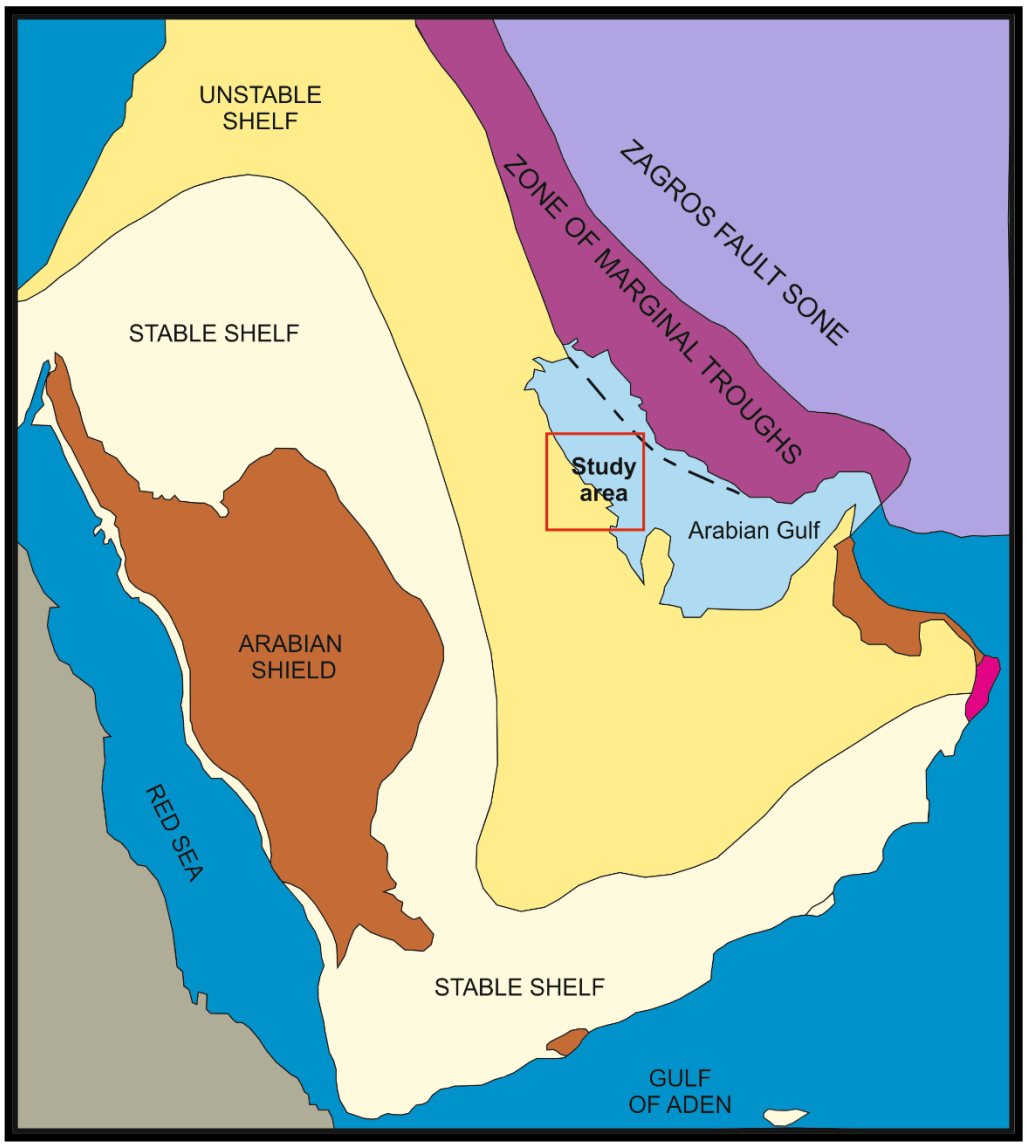

Figure 2.5 The major tectonic zones of the Arabian Peninsula. The study area is centred in the middle of the Unstable Shelf (Henson, 1951) which is a major tectono-stratigraphic province (Exterior Arabian Platform of Powers, 1966). It is formed Palaeozoic, Mesozoic and older Cenozoic strata that are gently dipping towards the east and the north-east (modified from Edgell, 1992).

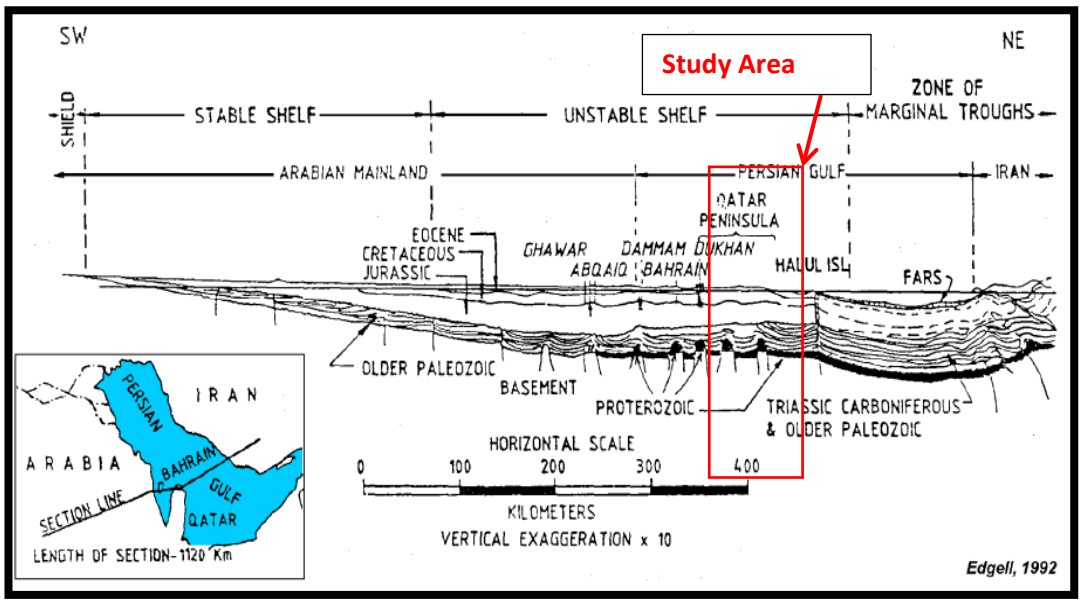

Figure 2.6. Geological cross-section along the eastern side of the Arabian Plate showing the distribution of the tectono-stratigraphic provinces (Exterior Arabian Platform of Powers *et al.*, 1966) and their relationship with the Arabian Precambrian Shield (Edgell, 1992). Note that the basement faults affected, and disturbed, all of the sedimentary cover during their deposition.

2.3 TECTONIC HISTORY OF THE STUDY AREA DURING THE LATEST JURASSIC AND THE EARLIEST CRETACEOUS (147.5-132 MA)

The palaeogeographical location of the study area during the Early Cretaceous was in the northern-east part of the Afro-Arabian Plate before the break-up and the rifting of the Red Sea the sedimentary basins were open platforms and intra-shelf basins of the Arabian Plate bordered by passive margins landward and with Tethys toward the North and the East of Arabia. Most of the Arabian Plate was a tectonically stable area, covered by a shallow, continental, shelf-sea located near the Equator (Figure 2.7). This shallow sea was a part of the Tethys Ocean, in which it was located at the north-east margin of the Gondwana continent (Beydoun, 1991). The

deposition and accumulation of Jurassic and Cretaceous rocks, including the Sulaiy and Yamama formations (Tithonian to Valanginian), was extensive with a palaeogeographical position close to the Equator and the wide shallow sea along the north-eastern and eastern parts of the Arabian Peninsula (Beydoun, 1991). During the Tithonian to Valanginian stages, major tectonic events took place in the Gondwana supercontinent that affected the Arabian Plate and influenced sea level changes (Haq and Al-Qahtani, 2005).

The break-up of the supercontinent Pangaea into Gondwana (south) and Laurasia (north) continued during the Jurassic and the earliest Cretaceous (Figure 2.7). The continental eastern flank of Arabia was covered by shallow seas during this period (Figure 2.7). In the Early Jurassic, the Indian Plate began to separate from the west of Gondwana and moved towards its present day location during the Cretaceous period (Figure 2.7). The separation of the Indian Plate from the Afro-Arabian side of Gondwana was completed during the Late Jurassic (Haq and Al-Qahtani, 2005). During the Early Cretaceous, Africa began moving northwards, and this resulted in the progressive closure of Tethys as the continents started to take up their present form and locations (BouDagher-Fadel, 2008).

Haq *et al.* (1988) found that the Tithonian-Valanginian interval was characterized by moderately high eustatic sea level, as the Cretaceous sedimentary basins of the eastern platform of the Arabian Plate were covered by the shallow-water carbonates of the Sulaiy, Yamama, Managish and Habshan formations. The rest of the Arabian Plate basins were the site of deposition of very fine limestones of the Sulaiy and Makhul formations.

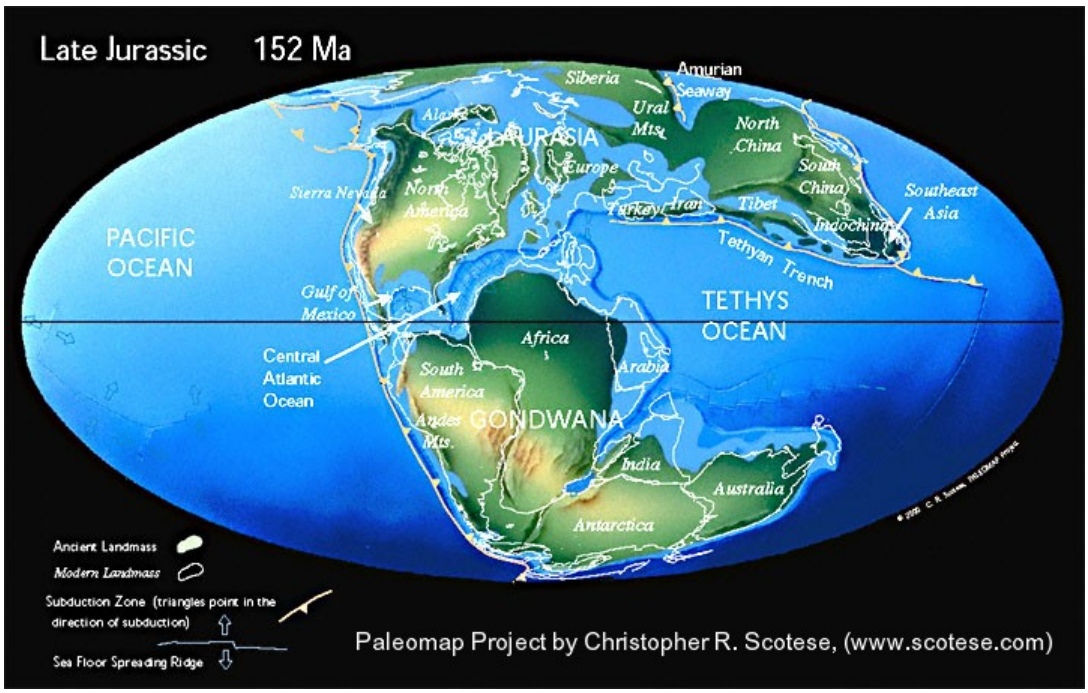

Figure 2.7. Palaeogeographical map showing a tectonic reconstruction of the Late Jurassic (152 million years ago) which is very similar to Tithonian-Valanginian tectonic reconstructions. This map shows the study area location in the northeast part of the Arab-African plate of the Gondwana supercontinent. The Equator is marked by the black line and the modern land boundaries as a white line.

This period of tectonic activity was accompanied by the deposition of considerable thicknesses of the Sulaiy, Yamama, Managish, Habshan and Rayda formations (Ziegler, 2001) on the eastern flank of Arabia and in Oman. The sedimentation was disturbed in the eastern part of the Arabian Peninsula by the hiatus from the latest Valanginian to the earliest Hauterivian, creating the late Valanginian unconformity. Al-Fares *et al.* (1998) explained that the hiatus was related to the remote plate tectonic stresses produced by the opening of the South Atlantic. An alternative view is that the late Valanginian hiatus is related to a short interval of global sea level fall related to a cooling episode within the normal Cretaceous greenhouse, which is supported by Nunn *et al.* (2010). In the southern and eastern areas of the Arabian Plate (Oman), deposition continued throughout

the early Cretaceous, without any indication of a late Valanginian hiatus (Figures 1.3, 2.8, 2.9, 2.10 and 2.11).

In the study area, The Cretaceous is sub-divided into three tectonic events separated by major unconformities. These events are the Lower tectonic event in which it produced the Thamama stratigraphical group; Middle produced the Wasia stratigraphical group and the Upper tectonic event in which it produced the Aruma stratigraphical group (Figure 2.8). The Sulaiy Formation is the base of the Thamama Group succession.

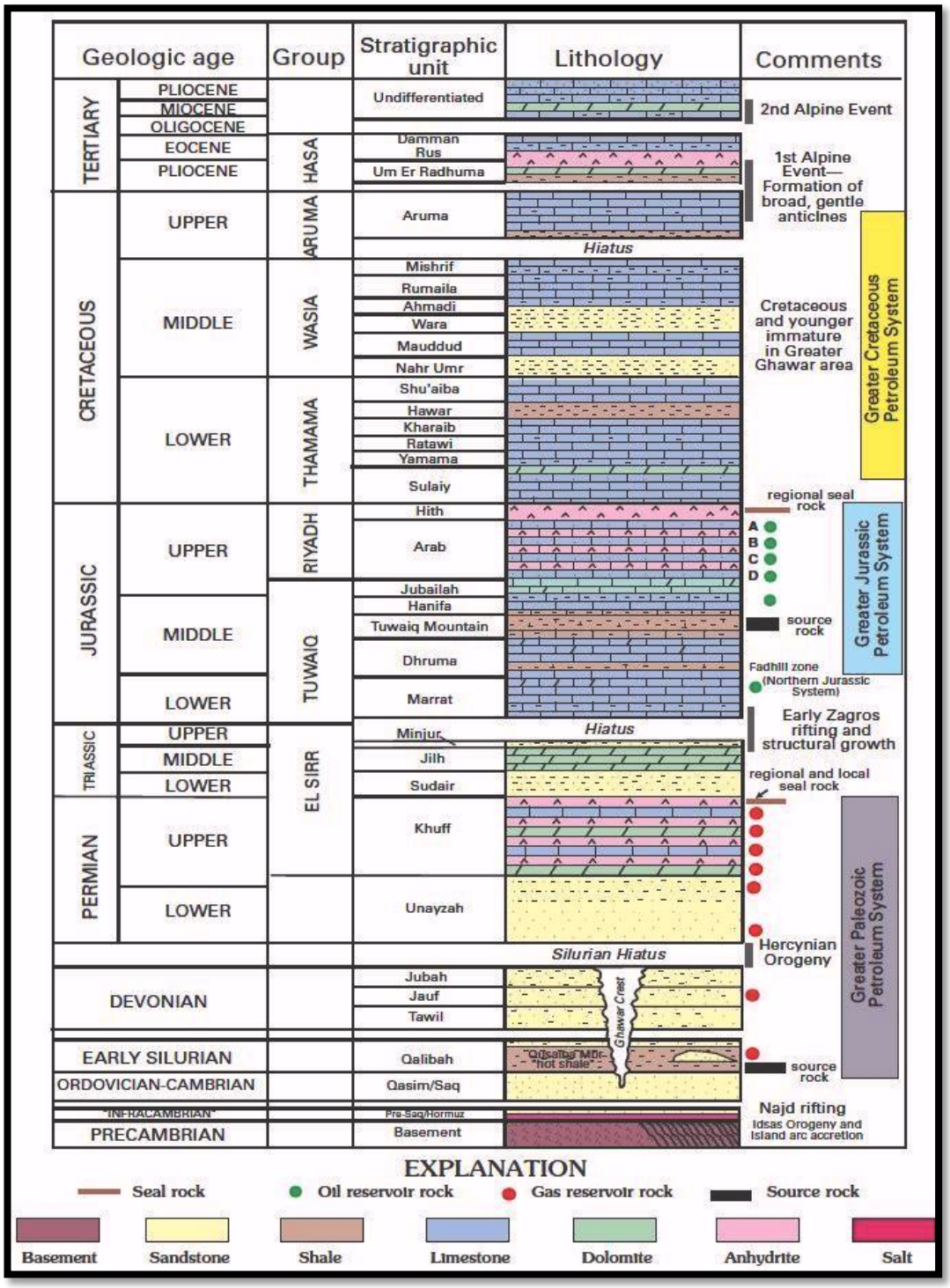

Figure 2.8. Generalized stratigraphical section of Palaeozoic, Jurassic and Cretaceous eastern Saudi Arabia showing the lithology and reservoir units (Pollastro, 2003).

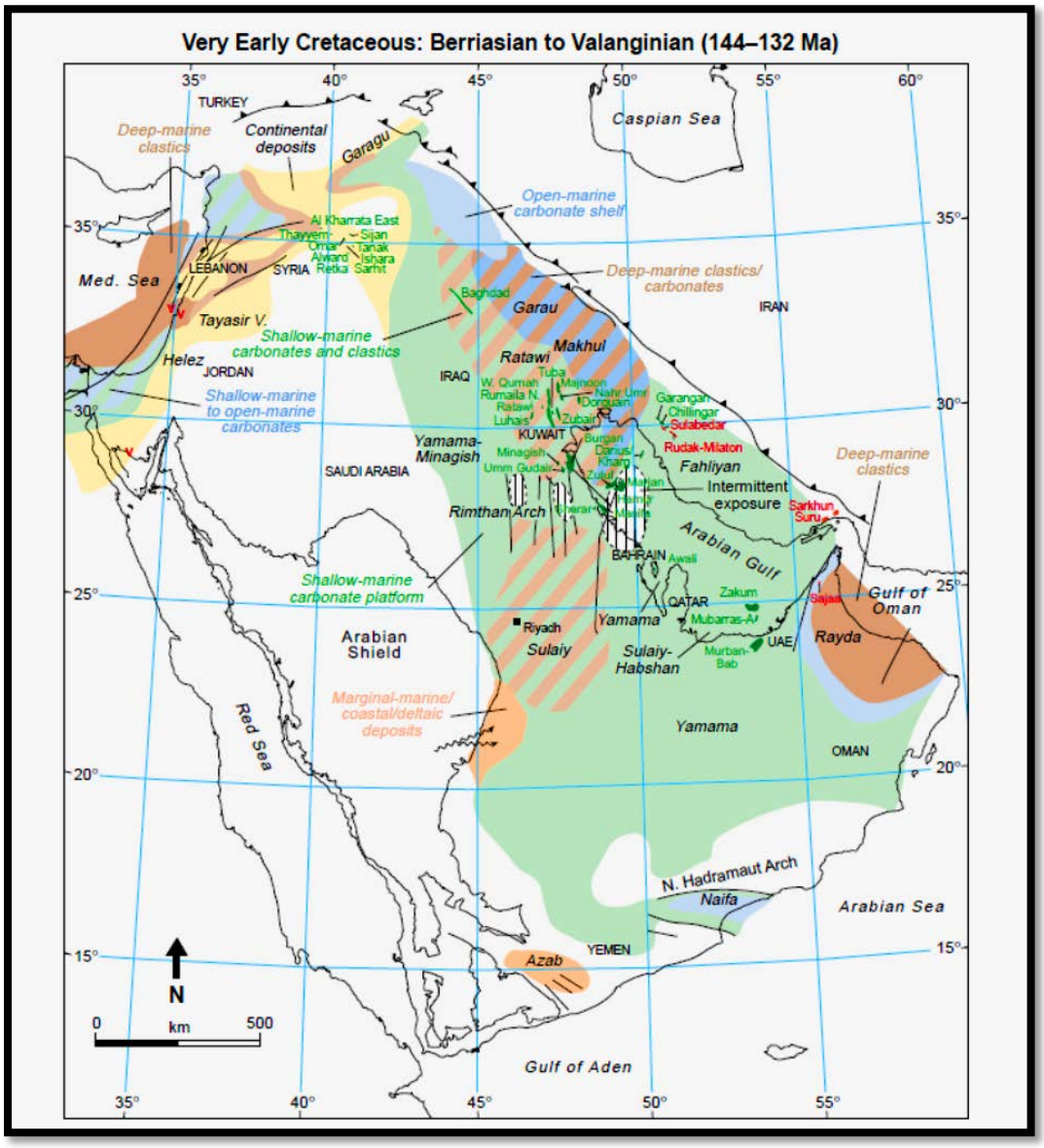

Figure 2.9. Generalized, subsurface palaeofacies map of the Sulaiy and the Yamama formations and their equivalent formations in the surrounding regions on the eastern side of the Arabian Peninsula (Ziegler, 2001).

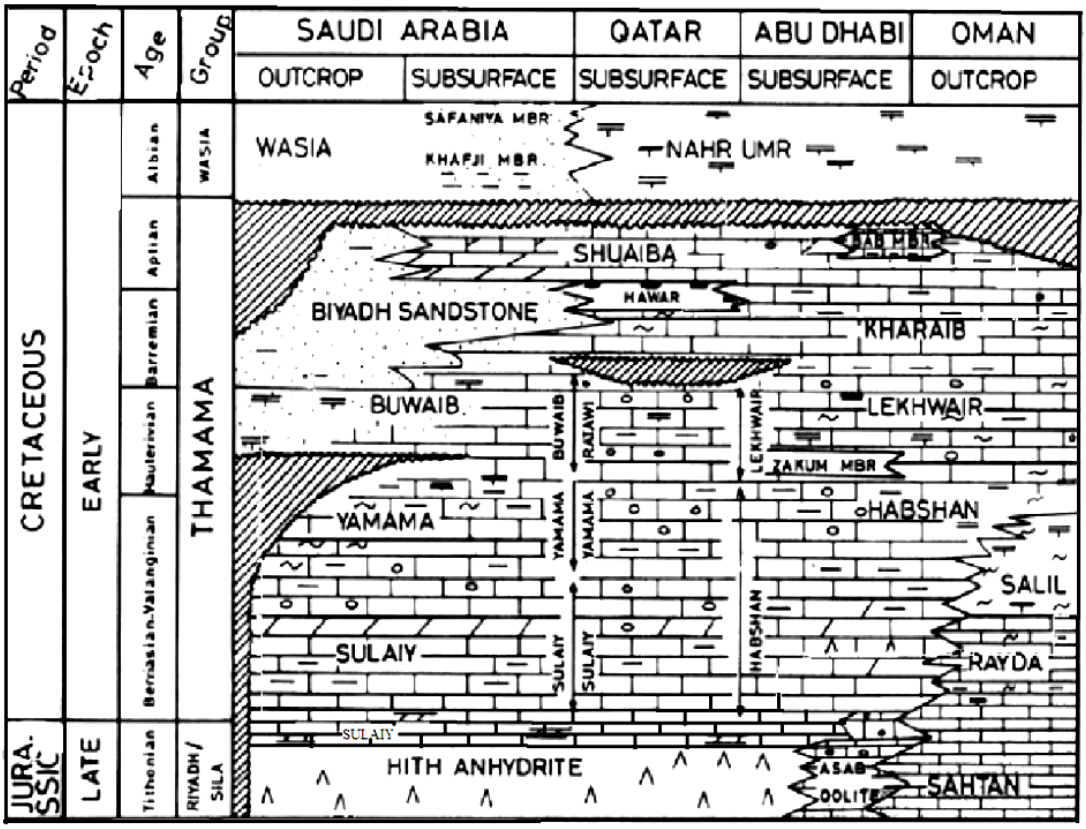

Figure 2.10. Regional stratigraphy of the Lower Cretaceous in the Arabian Gulf region. This is slightly modified from Shebl and AlSharhan (1994); their compilation was based on Powers *et al.* (1966), Sugden *et al*. (1975), AlSharhan and Nairn (1986) and Simmons and Hart (1987).

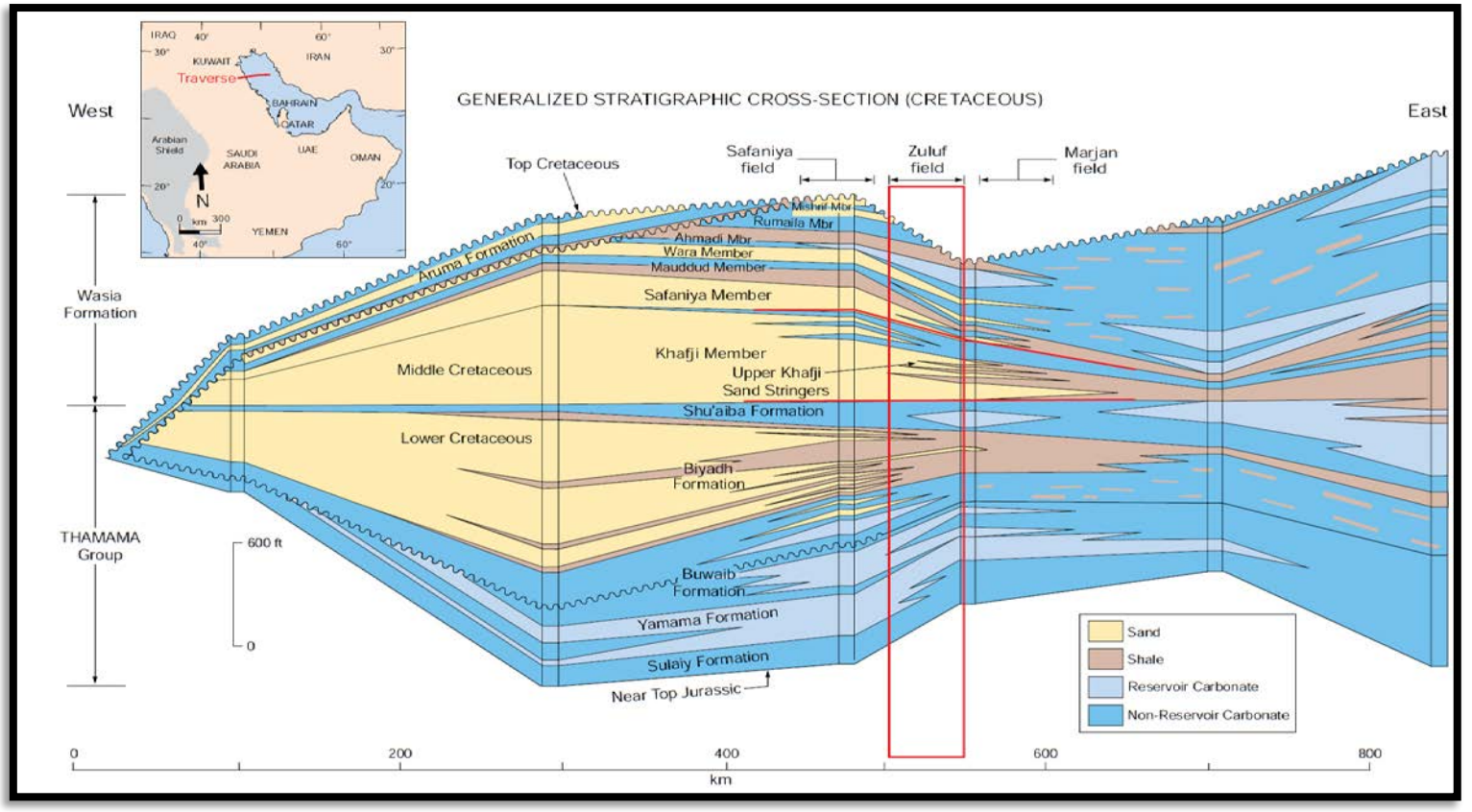

Figure 2.11. Generalized stratigraphical cross-section showing the reservoir bodies of the Cretaceous subsurface in 3D in the main oil fields of Safanyia, Zuluf and Marjan offshore fields in of eastern Saudi Arabia. This 3D cross-section is also representing the main unconformities and they are the late Jurassic, late Valanginian, late Aptian, middle Turonian and pre-Cenozoic unconformities (Modified by Macrides and Neves, 2008, after Grant and Al-Humam, 1999).

2.4 STRUCTURAL SETTING OF THE STUDY AREA

The study area is a part of the vast carbonate-rich stable shelf that extended over a wide area throughout the entire north-eastern Arabian Plate margin, bordered by the Zagros Mountains to the north-east and the Oman Mountains in the south-east. The topography of the Unstable Shelf tectonic zone was affected by regional tectonic events during the Miocene, associated with Red Sea spreading and the compressional effects of subduction along the Zagros Fold Belt (Al-Husseini, 2000) in the Zone of Marginal Troughs (Figure 2.6). Further, complex, structural features resulted from diapiric movements and uplift above lower Cambrian salt (Kassler, 1973).

The Cretaceous succession is a part of the Arabian Shelf sedimentary sequence which extends, and dips gently northwards and eastwards, across the Arabian Shield towards the Arabian Gulf Basin (Figure 2.12). The Stable Shelf sedimentary cover is usually located in the area of tectonic stability except further east in the Unstable Shelf tectonic zone, where it is interrupted by the Arabian basement reverse faults and the Precambrian salt diapirs of the north Gulf and south Gulf salt basins (Figure 2.6) (AlSharhan and Nairn, 1986). Structurally, the oil wells of the study area are located within the North Gulf Salt basin of Hormuz Salt (Figure 2.12) of the Unstable Shelf sedimentary tectonic zone (Edgell, 1992) (Figures 2.5 and 2.6). In this zone carbonate deposition was extensive during the Permian to Miocene interval, varying lithologically from deep water marls to shallow water grainstones and oolites, with occasional clastics and evaporites (Ziegler, 2001). A cross-section profile (Figure 2.13) by Konert *et al*., (2001) from the Arabian Shield

towards the middle of the Arabian Gulf Basin shows all of the sedimentary cover, including the Cretaceous successions as highly disturbed by reverse faults and by diapiric systems. However, the cross section profile is showing the North Field area was uplifted by the Qatar Arch tectonic event. Eventually, this type of block uplifting activity is not found in the study are which is evidenced by a cross section profile across the north side of the study wells showing a slight block uplifting that is just beyond the last study well in the Arabian Gulf (Well D) (Figure 2.11).

2.5 SEQUENCE STRATIGRAPHY

The Cretaceous succession of Saudi Arabia has been identified as Megasequence AP8 by Sharland *et al.* (2001) and consists, in Saudi Arabia, of the Sulaiy, Yamama, Buwaib, Biyadh, and Shu'aiba formations at the base and the Wasia and Aruma groups in the middle and upper part respectively (Figure 2.14). The interpretation of Sharland *et al.* (2001) places the Sulaiy/Yamama package within the K10, K20, K30 and K40 sequences of the transgressive-regressive cycles of the Arabian Plate (Figure 2.15). Sequence K40 is Early Valanginian to "middle" Hauterivian as indicated by nannofossils of KN48/49 zone age: The top of the Yamama limestones is marked by an unconformity within the lower part of the K40 sequence (within the Late Valanginian). Sequence K30 is latest Berriasian to earliest Valanginian with no palaeontological evidence from the Yamama Formation. K20 is Early to Late Berriasian defined by nannofossils of KN52/53 zone age.

K10 is mid-Tithonian to Early Berriasian defined by calpionellids of the *Calpionella alpine* biozone (Mike Bidgood, *pers. com.* 2011).

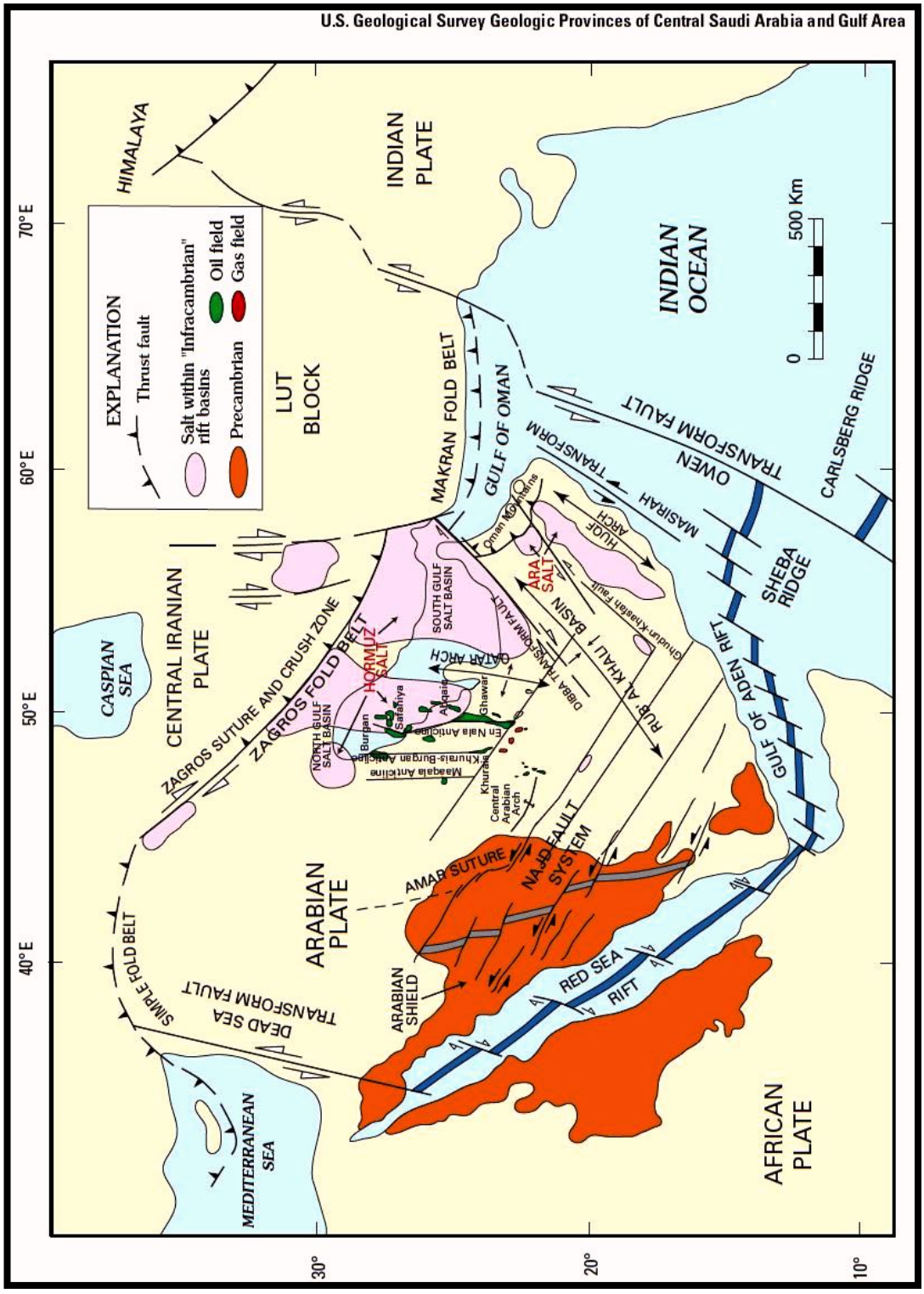

Figure 2.12. Arabian Plate tectonic and structural elements, Precambrian rift salt basins, and oil and gas fields of the Arabian Gulf region. The map is modified from Al-Husseini (2000) in Pollastro (2003).

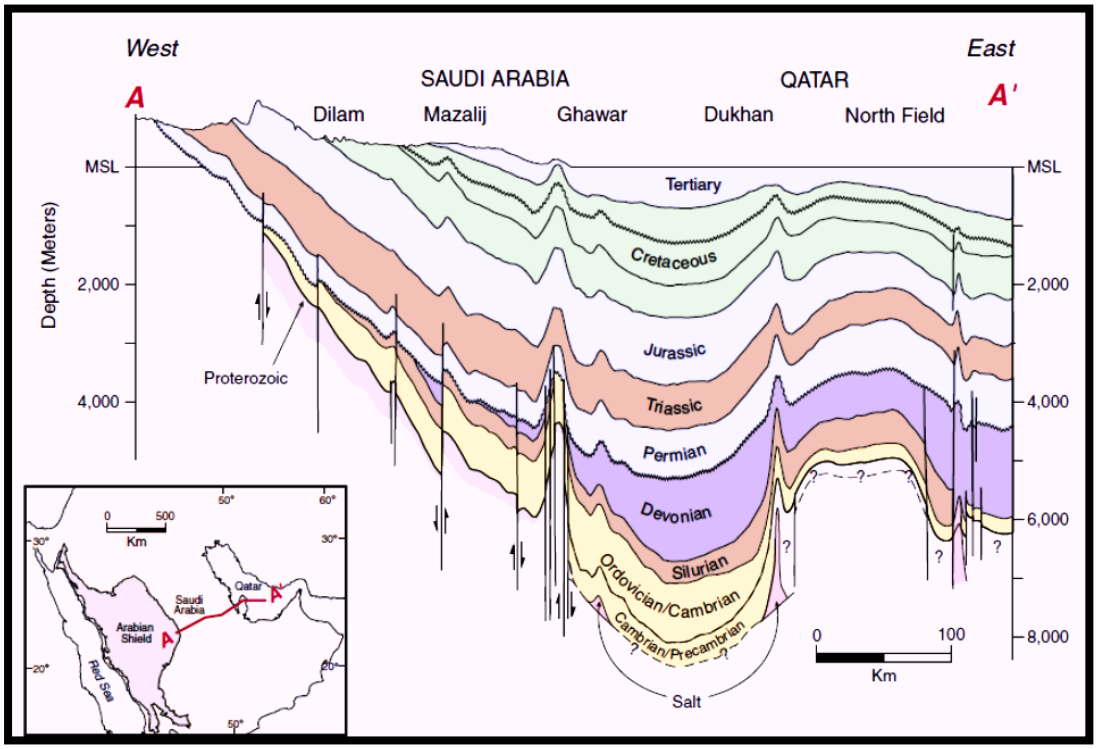

Figure 2.13. Geological cross-section across Saudi Arabia and Qatar from the Arabian Shield to the Arabian Gulf showing the Stable Shelf and the Unstable Shelf (Interior Platform sedimentary rocks) that have been interrupted by the Arabian basement reverse faults and the Precambrian salt domes. (Konert *et al*., 2001).

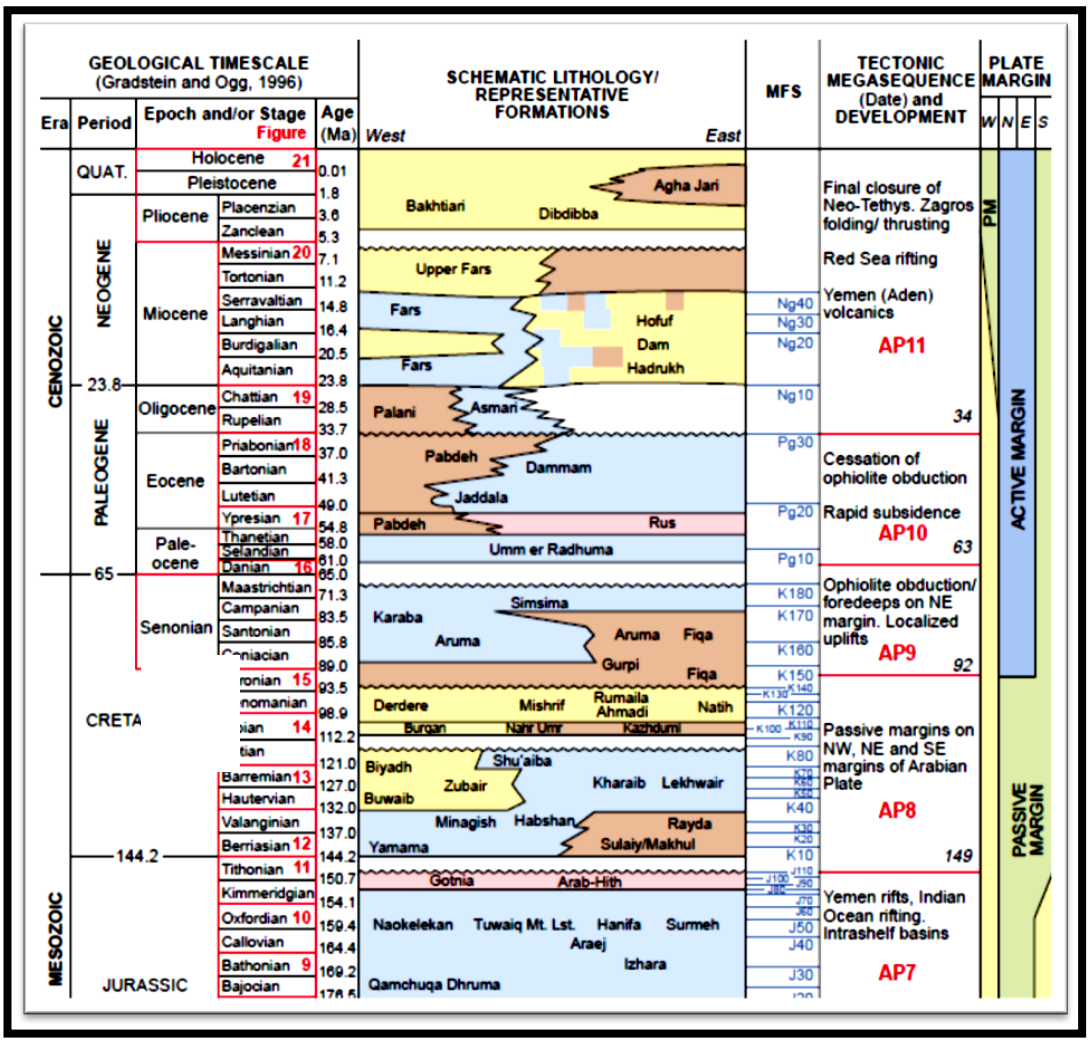

Figure 2.14. General stratigraphy of the Arabian Gulf subsurface representing the Cretaceous Megasequence AP8 of the Gulf region (modified by Ziegler, 2001, from Sharland *et al.*, 2001).

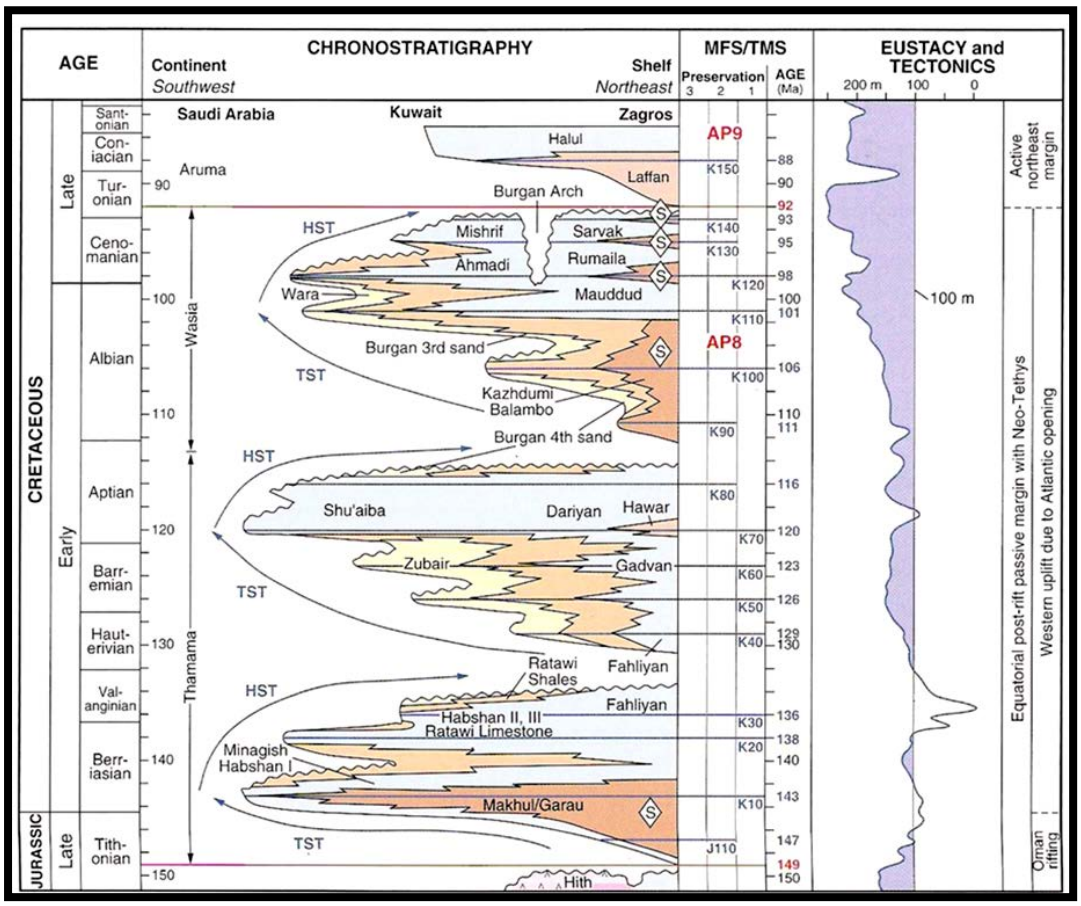

Figure 2.15. The sequence stratigraphy of the Cretaceous Megasequence AP8 of the Gulf region. Sharland *et al*. (2001) place the Sulaiy and Yamama package within the K10, K20, K30 and K40 sequences of the transgressive-regressive cycles of the Arabian Plate. This schematic column is based on data from Kuwait and Iran, with a lack of information and real data from the Saudi Arabian sub-surface. The chronostratigraphy of the Gulf region can be applied to the Sulaiy and Yamama formations of Saudi Arabia (Sharland *et al.*, 2001).

2.6 STRATIGRAPHY AND FORAMINIFERA BIOSTRATIGRAPHY

Redmond (1962) noted that the top of the Sulaiy Formation is recognized by a major faunal biofacies that is distributed regionally (Figure 2.16). *Pseudocyclammina sulaiyana* (Redmond 1964) is common throughout the Sulaiy Formation and can therefore, be used as the marker for the base of the Sulaiy Formation (Powers *et al.,* 1966). At outcrop, the contact is marked

by a sharp change in lithology from the tan-coloured mudstones and wackestones of the upper-most of Sulaiy Formation to the massive beds of non-cemented, clean grainstones of the Yamama Formation. Unfortunately, lithological changes in the sub-surface do not match those at outcrop. In the sub-surface, the top of the Sulaiy Formation, similar to the base of Yamama Formation at the outcrop, is formed of massive, clean, porous grainstones. This is followed by a compact limestone of the base of the Yamama Formation. The poorly defined lithological difference between the Sulaiy and Yamama formations in the sub-surface has highlighted the importance of using the foraminiferal evidence of the Sulaiy Formation (presence of *Pseudocyclammina sulaiyana)* to identify the top of the Sulaiy Formation (Powers *et al*., 1966).

In exposures, and in the sub-surface, the Yamama Formation is recognized by a change in lithology and the foraminiferal biofacies. *Pseudocyclammina sulaiyana* is an indicator of the Sulaiy Formation while *Everticyclammina elegans is* indicative of the base of the Yamama Formation (Figures 2.16 and 2.17). The Buwaib Formation lies above the Yamama Formation, separated by the Pre-Buwaib unconformity. In the sub-surface, the unconformity is difficult to detect except by using foraminiferal distributions, as suggested by Powers *et al.* (1966). He observed that the indicator of the top of Yamama is a horizon of *Everticyclammina eccentrica* and *Pseudocyclammina cylindrica* (Figure 2.16). The Buwaib Formation can be identified by the lithological change to shale, dolomite, calcarenite and aphanitic limestone and by the occurrence of C*yclammina greigi* and *Everticyclammina hensoni* (Powers *et al*., 1966).

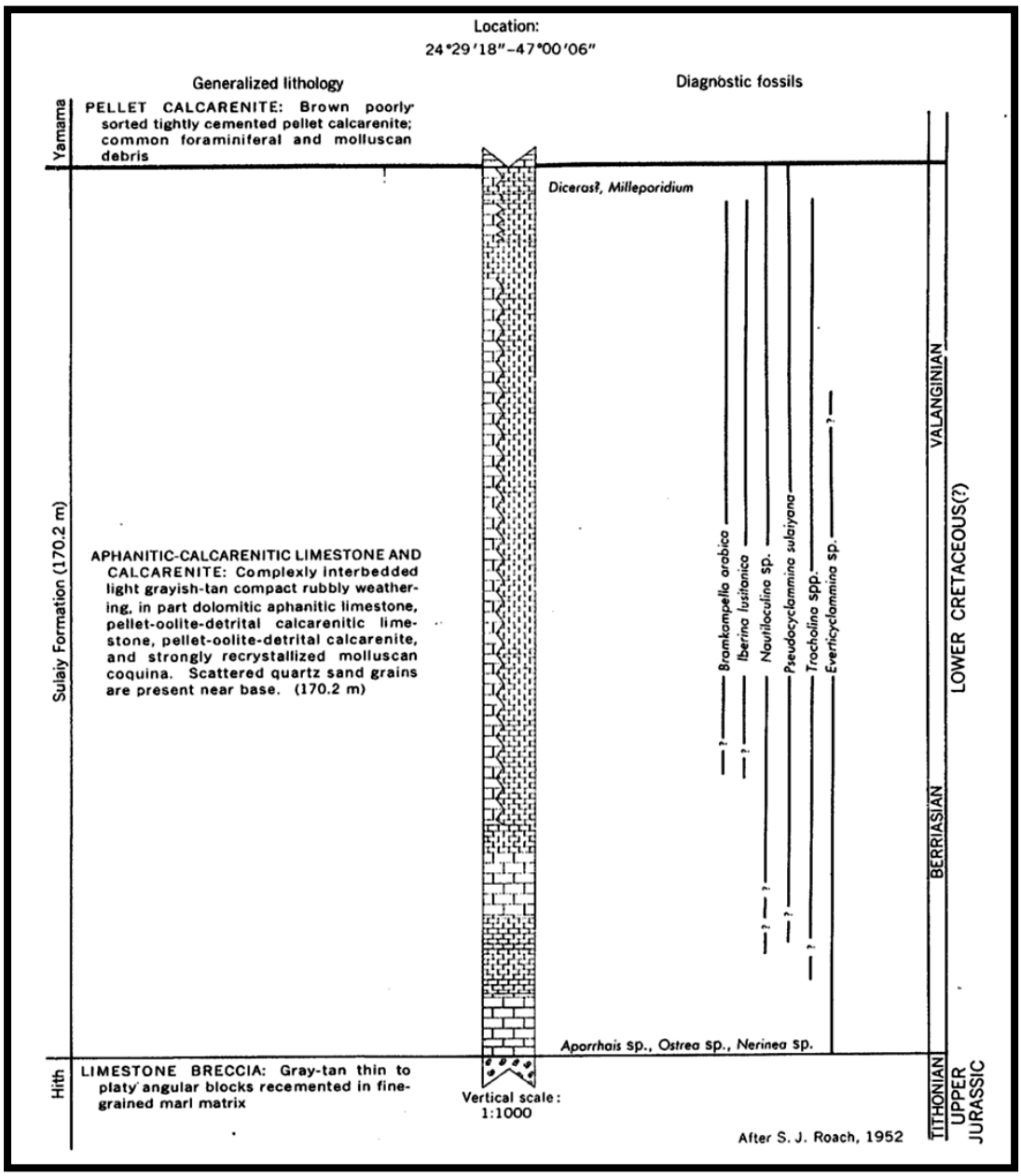

Figure 2.16. Type section of the Sulaiy Formation and the distribution of the principal foraminifera (Powers *et al.* 1966).

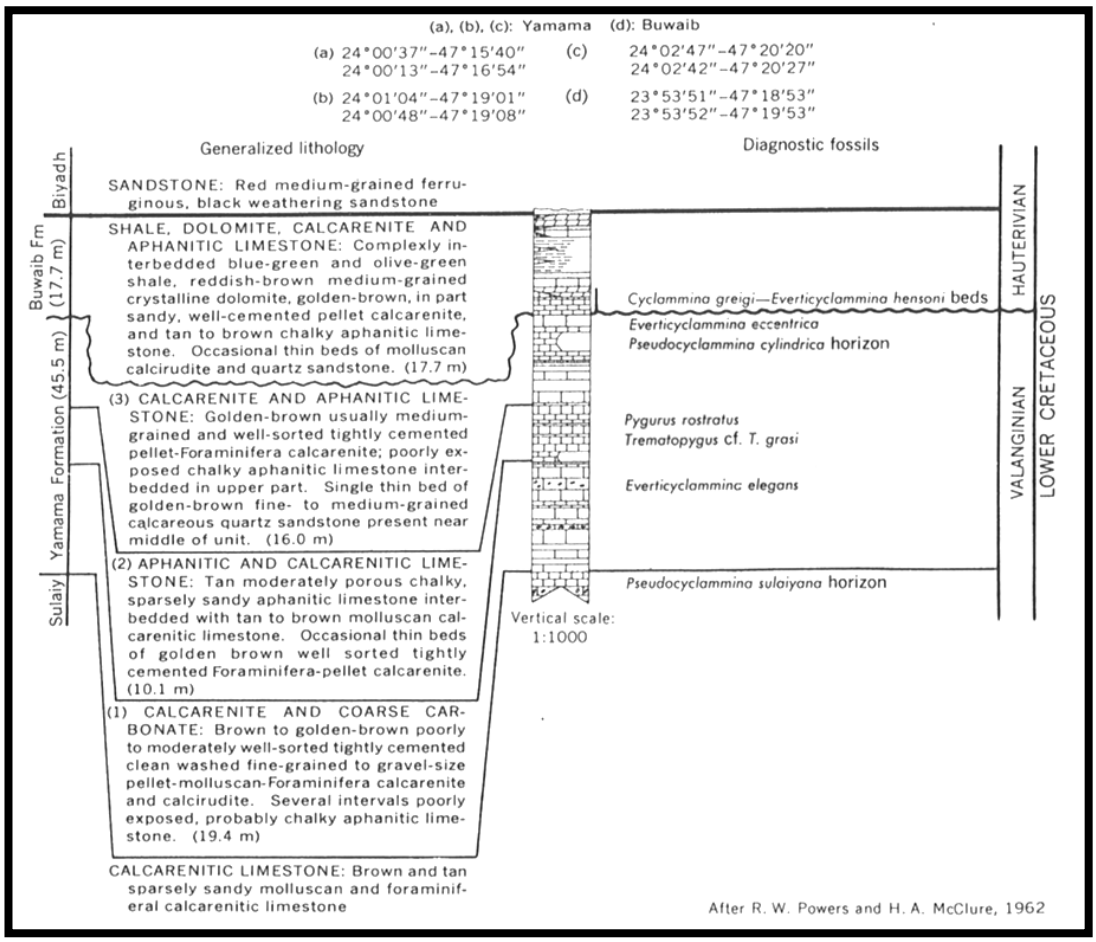

Figure 2.17. Type section summaries at Khasm al Buwaib of the Top Sulaiy, Yamama and Buwaib formations and the distribution of their principal foraminifera includes echinoids (Powers *et al*., 1966).

2.7 SUMMARY

This chapter has discussed the regional geology and the regional stratigraphy of the study area. The Lower and mid-Cretaceous hydrocarbon reservoirs are economically very important. This research aims to improve the interpretation of depositional environments, sequence stratigraphy and reservoir facies location and prediction. It should lead to the recognition of environmentally significant lithofacies and biofacies, of which their vertical variations will provide significant contributions towards on-going hydrocarbon

reservoir characterization studies. The results of the micropalaeontological analysis are presented in StrataBugs charts in the Enclosures. Lithological and semi-quantitative micropalaeontological analysis has provided a considerable insight into the bio-component composition, as well as providing evidence for the definition of various lithofacies and that also define the biofacies. To investigate the microfossil content, lithofacies, and palaeoenvironmental settings of the Sulaiy Formation (Thamama Group), thin sections prepared from trimmed plugs of cored carbonate rocks from on-shore and off-shore wells were examined and analysed using standard micropalaeontological techniques. The techniques and methodologies used in order to achieve the results are discussed in the next (Chapter 3).

CHAPTER THREE

MATERIALS AND METHODOLOGY

CHAPTER THREE-MATERIALS AND METHODOLOGY

3.1 SAMPLE LOCATIONS AND TYPES OF MATERIALS

Saudi Aramco Company in Dhahran (which is the sponsor company for this research) has given permission for a micropalaeontological study of thin sections prepared from trimmed plugs of cored carbonate rocks from a number of different locations among the hydrocarbon fields in the eastern province of Saudi Arabia. These samples are from on-shore and off-shore cored wells (Table 3.1). Figure 3.1 shows the locations of the cored wells for the thin-sectionsof the Sulaiy Formation (Table 3.1.). The cored wells have been given different letters (A, B, C, etc.) to protect their identity and the location of the actual fields. This is done as a part of the consignee agreement between the sponsor and the researcher in this study, in order to gain permission for this study.

Nine cored wells were selected by Saudi Aramco (GLTSD) for this investigation, providing a geographically representative distribution from the Saudi Arabian Gulf. They were acquired from the Saudi Aramco Core store in Dhahran, Saudi Arabia. These cores intersected the base of the Yamama Formation and the Sulaiy Formation. From the total thickness of cored wells of 843.23 meters (2766.5 feet) a total 1144 thin sections were prepared from plugs of semi-cicular geometry of 2.4 cm diameter. These thin sections were analysed micropalaeontologically and lithologically using a binocular microscope with a special head attachment for a digital camera (GXCAM-9

mega-pixel) to collect microphotographs of the principle microfossils and lithofacies.

3.2 METHODOLOGY SUMMARY

Semi-quantitative micropalaeontological analysis of thin-sections was undertaken using sub-surface, well cored samples. Most of the wells were closely spaced intervals to provide considerable insight into the biocomponents composition as well as providing evidence for defining the various biofacies. Other wells have some issues regarding the dolomitization and poor sampling recovery throughout the well.

The results of the micropalaeontological analysis will be presented in “StrataBugs” charts in the Enclosures. The research methodology involved the following steps in order to reach, and accomplish, the goals required for this onvestigation:

(a) The petrography of each thin-section, applying the Dunham (1962) rock texture classification, and some aspects of diagenesis related to porosity and permeability development were recorded in most of the wells.

(b) A semi-quantitative analysis of all the micro-biocomponents in the wells of closely spaced samples was undertaken. The semi-quantitative analysis logged each species into present (1 specimen), rare (2−5 specimens), common (6−20 specimens), abundant (20−50 specimens) and flood (> 50 specimens) categories.

(c) Completed the construction of biofacies and vertical species distribution (StrataBugs) charts, enclosures for each study well.

(d) Identified lithofacies by using the micropalaeontological contents in order to interpret the depositional environment of each lithofacies.

(e) Hierarchic depositional cycles were identified, recording deepening and shallowing-upwards cycles.

(f) The relationship of cycle boundaries and transgressive/regressive components were identified without appraisal of the gamma ray logs.

(g) The preparation of some examples of regional lithofacies maps and their systems tracts. This resulted in the identification of locations with good reservoir facies development.

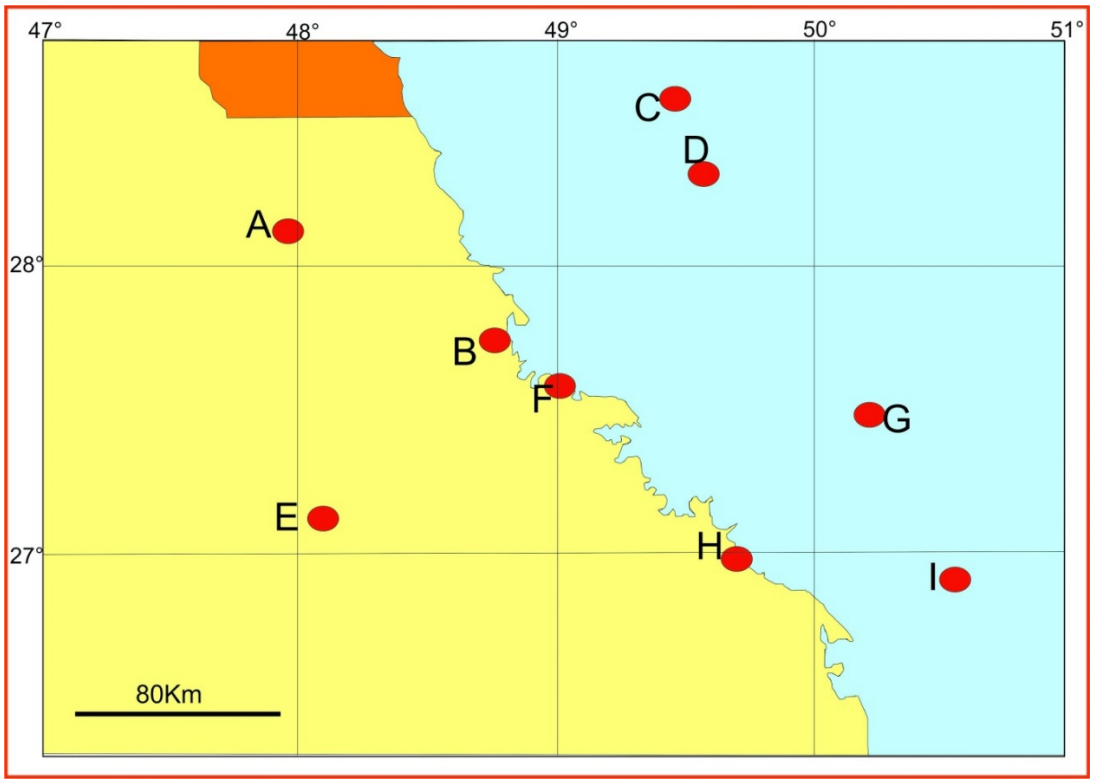

Figure 3.1. The location of wells in the northern Ghawar Area that include the cored wells that have been studied for the first time. The wells are cored only from the Sulaiy Formation.

WELL NAME	Formation	Core #	Top Core Depth (ft)	Bottom Core Depth (ft)	Footage (ft)	Top Plug No.	Base Plug No.	Slabbed	Plugged	Number of thin sections
D	Yamama		7957.2	8190.7	233.5	307	664	Y	Y	178
D	Sulaiy		8192.2	8644.2	687	665	8524	Y	Y	200
I	Sulaiy	3-5	5409	5543	134	96	279	Y	Y	89
E	?Sulaiy	6-9	10205.7	11222	1016.3	1	101		Y	100
H	Sulaiy	1	6380.5	6427.5	47	1	50	Y	Y	100
A	Sulaiy	1-2	4055.2	4147.2	92	1	90		Y	49
G	Sulaiy	5	6755.7	6811.3	55.6	46	102	Y	Y	93
F	Sulaiy	3-7	8142.5	8471.4	328.9	213	528	Y	Y	136
B	Sulaiy	4-5	8371	8431	60	62	171	Y	Y	100
C	Sulaiy	27-31	8226.3	8338.5	112.2	1317	1500		Y	99
									Total	1144

Table 3.1. Study wells of the Sulaiy Formation represented by capital letters showing top and base Sulaiy or Yamama Formation, total thickness footage, the top and base plug numbers and number of thin sections.

3.3 THIN SECTION DATA RECOVERY OF STUDY WELLS AND PROBLEMS

A number of problems have affected the deliverability of results and analyses. These were encountered during the analysis and include the following:

Unfortunately, not all of the selected study wells with core provided a geographically representative distribution because of poor recovery of samples (e.g., wells A, C and D) and there is one well that is not part of the study (Well E). Well D has a problem in that the thin-sections are not closely enough spaced and did not cover the whole well. These four wells are excluded from the sequence stratigraphical analysis. Most of the wells were cored from the top of the Sulaiy Formation creating difficulties correlation of the middle and base of the Sulaiy Formation sequences. Well A is fully dolomitised, making it defficult to identify its lithofacies and in assigning sequence cycles.

The need to sample and prepare more thin-sections with continuous physically log the cores from which the thin-sections were sampled in order to understand the boundary relationships This is an important future step after this research to identify the missing sequences boundaries.

Some of the thin-sections with low quality or damage will require preparation of replacements in order to log their petrography and microfossils properly and to avoid errors in the subsequent analysis.

3.4 THIN SECTION ANALYSIS

The lithology (e.g., limestone, dolomite, mixed limestone with shale and silt) and principal grain features (e.g., size, shape, sorting and porosity) were described from analysis of the thin sections and this was an integral part of the research. The carbonate classification follows the extended Dunham classification (Dunham 1962; Embry and Klovan, 1971) in addition to a new category that was previously added to the scheme by Saudi Aramco geologists. This category is located between packstone and grainstone and is described as a mud-lean packstone. It is possible, to identify the transition to another formation of some horizons were approximately established together with the environment of deposition using the microfossil content and lithological texture classification and in this case the identification of the base of the Yamama Formation from the top of the Sulaiy Formation at a gradual, conformable stratigraphical contact.

The microfossils in each thin-section from every core sample were listed and the abundance was counted on the basis of the Saudi Aramco micropalaeontological standard for semi-quantitative analysis. The standard semi-quantitative categories are the following: present (one specimen), rare (2 to 5 specimens), common (6 to 20 specimens), abundant (21 to 50 specimens) and flood (over 50 specimens). These categories include both small and large sizes of microfossils. Non-skeletal components were recorded as were the diagenetic changes to the carbonate rocks grains during deposition, exposure and burial. Visible porosity was estimated from the abundance of blue epoxy resin in thin-sections, as well as any

dolomitization present. The silt and sand content were estimated on the basis of the semi-quantitative Saudi Aramco standard.

3.5 DATA COLLECTION FROM THIN–SECTIONS

This section is written following personal communication with Dr Geraint Wyn Hughes, the founder of the industrial semi-quantitative recording methods used by Saudi Aramco.

It is worth considering an important aspect of thin-section micropalaeontology and microfacies relating to the validity of quantitative versus semi-quantitative recording of information. With disaggregated samples, a hopefully microfossil-bearing washed residue is sieved and distributed on a tray for picking and the recording of species abundance and diversity. Thin-sections, in contrast, display much more information that hinders the routine quantitative approach due to the presence of various porosity cement types, in addition to the random thin-section views of the microfossils and macrofossil fragments of various sizes. There are various ways in which quantitative microfacies analysis of thin-sections can be performed (Figure 3.2) (Flügel, 2010, figure 6.7; section 6.2.1.).

Following the recommendations of Flügel (2010), the methodology needs to be guided by the objectives. In industrial micropalaeontology and microfacies analysis, the objectives include age determination, palaeoenvironmental interpretation of the well section, recognition of depositional cycles of different hierarchies (sequences), palaeoenvironmental interpretation between wells and aspects of hydrocarbon significance.

Unlike processed and picked micropalaeontological residues, where microfossils are picked methodically and to a statistically valid total, thin sections contain a number of important elements that supplement the microfossils, such as inorganic grain types, macrofossil fragments, various cement types and porosities. As there is a need to maximize the data collected from the entire thin-section, a pragmatic method should be established that accurately captures the foraminiferal species diversity and abundance and adequately captures the diversity and abundance of microfossils and allochems that often are present in abundance. While quantitative recording of the primary microfossils, especially foraminifera, ostracods, and calcareous algae is achievable within a reasonable time-frame other microfossils, such as echinoid and bivalve fragments, sponge spicules, peloids and ooids, would be extremely time consuming and their absolute abundance would not be so significant. For these, semi-quantitative methods are deemed suitable, and this hybrid of quantitative with semi-quantitative approach seems to be favorably received by industry-based micropalaeontologists and carbonate sedimentologists.

Of the various methods discussed by Flügel (2010), none would provide us with the most accurate recording of data for the entire thin-section, as the presence of a single specimen of a rare species could be missed. The thin-section can be analysed in any one of four ways, as illustrated in Figure 3.2 (Flügel, 2010). Of these, point counting is considered not to be appropriate for micropalaeontology and microfacies recording because some foraminiferal species may only be present singly and their recording could easily be missed if only the point location was recorded.

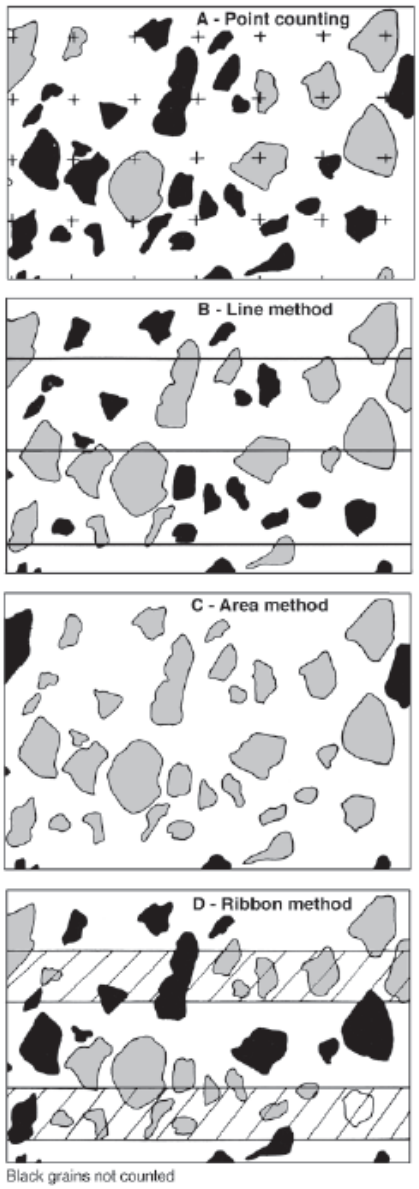

Figure 3.2. Comparison of A - point counting, B - line method, C - area method, and D – ribbon method used in evaluating frequency values. Solid black grains are those not counted. Note that ribbon counting measures only those grains which are totally, or almost totally, included within the ribbon (hatched area) (Flügel, 2010; figure 6.5).

Similarly, point counting of the often poorly-sorted nature of carbonates could lead to over estimation of macrofossil fragments, despite the cautious two-fold methodology described by Flügel (2010) for such circumstances. The line method suffers from a similar handicap, because of its restricted recording of specimens that are intersected by the sampling line. The ribbon method counts all grain types within ribbons separated by un-assessed

ribbons of a width equal to, or twice the diameter, of the largest grain or just spaced randomly. This method is not suitable for detailed micropalaeontology and microfacies because unacceptably large areas of the thin section would remain un-analyzed. The area method counts all grains lying within a defined thin-section area. Although this may apply reasonably accurately to very small microfossils, such as planktonic foraminifera, spicules and calcispheres, it cannot retain its accuracy when records are multiplied to estimate numbers occupying the entire thin-section area.

The method that is most accurate, after much investigation, is the “consecutive ribbon method” (Figure 3.3). This method involves analyzing the entire thin section by adjacent areas covered by the field of view, running repeatedly a right-to-left, then left-to-right pattern until the entire thin section has been analysed. The size of the field of view is, of course, based on the microscope objective selected and this will be based on the average grain size of the thin-section. Normally, a low power sweep of the entire thin-section is performed before deciding on the size of the field of view considered to be most appropriate in order to record the smallest microfossils. Quantitative recording of foraminifera is essential, followed by the semi-quantitative recording of associated microfossils. Porosity and cement types are recorded with visual estimates of their percentage. This method can be modified to capture, quantitatively, those elements that are of particular interest, such as dasyclad algae, ostracods, sponge spicules etc., if their presence is not typically abundant and their absolute abundance is deemed significant to the study.

Following meticulous analysis of thin sections for microfacies, the task of interpreting depositional cycles and palaeoenvironments from the wealth of data provides the next hurdle for inexperienced micropalaeontologists.

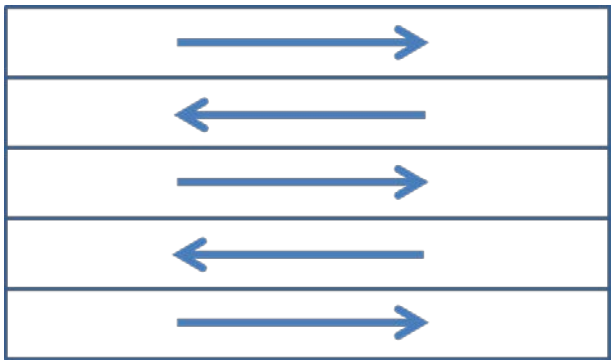

Figure 3.3. The consecutive ribbon method of thin-section analysis. This method can be adapted to quantitative, semi-quantitative or combined quantitative – semi-quantitative microfacies analysis.

3.6 MICROFOSSIL IDENTIFICATION

Most of the calcareous microfossils were identifiable by using their morphological differences and the skeletal microstructures observed in the thin-sections. Difficulties were mainly encountered in the identification of some of the agglutinated foraminifera, planktonic foraminifera and calcareous algae. The difficulty in identifying the taxonomy of some of the agglutinated species is the result of the random section cut through the foraminiferal test which, in extreme cases, meant that some agglutinated foraminifera are unidentified. The other difficulty is rareness and the random cut orientation of microfossil hard remains in which parts of the microfossils cannot be identified to upgrade the identification into species level. Diagenetic alteration (e.g., micritization, rim cements and dolomitization) has

created some confusion in the identification of some microfossils because of their effect on microstructure of some microfossils such as microproblematica, *Lithocodium aggregatum, Terebella lapilloides* and calcispheres. Another difficulty is the confusion of some authors who dealt with the same microfossil but have given them different names or placed them in an incorrect systematic position (e.g., *Trocholina* versus *Andersenolina* or *Redmondoides*, *Praechrysalidina* versus *Verneuilinoides*). In some cases, the age range of the same benthic foraminiferid species is not unified and they are different from author to author. In this study, some of the age ranges given by different authors are reported in Chapter Four: systematics chapter.

The remains of the calcareous microfossils were either composed of aragonite that had been replaced by calcite or micrite. In many cases they are unidentifiable. Most of these microfossils were recorded as microproblematica due to their limitation of identification.

The main microfossil groups encountered in all of the study wells thin sections are benthic foraminifera, planktonic foraminifera, calcareous algae, calpionellids, calcareous dinocysts (calcispheres), annelids worm tubes, sponges and related groups, corals, brachiopods remains, molluscs (gastropods, bivalves), echinoderm plates, ostracods, pelagic ostracods, favereinids and microproblematica which include *Lithocodium aggregatum* reef encrusters.

Some photomicrographs were taken of these microfossils and their morphology, mineralogy, association with other assemblages and systematics were documented. Literature from Eastern Europe and other

publications on Tethyan carbonate studies of Upper Jurassic and Lower Cretaceous microfossils have been studied.

3.7 CRITERIA USED FOR THE IDENTIFICATION OF THE SULAIY FORMATION LITHOFACIES DISTRIBUTION

The various lithofacies zones are characterised on the basis of their depositional energy (hydrodynamic control) which is reflected by the carbonate components. These are the grain types, matrix, cement, porosity type and the carbonate texture distribution. Grains include microfossils, peloids, oolites or ooids, oncoliths or oncoids and types of lithoclasts (extraclasts, intraclasts, grapestones or aggregates, micrite and breccia): see Flügel (2004, pp. 588−593). Depositional energy is controlled by sea level changes through time. However, the relationship between energy levels and the lithofacies grains involves the assessment of texture criteria such as roundness, matrix or primary micrite amount and grain sorting which are illustrated in Figure 3.4 Grain texture criteria provide an indicator for the level of the water energy. Energy levels can be categorised into five levels following Flügel (2004), as shown in Figure 3.4. These are very low energy, intermediate agitated, slightly agitated, moderately agitated and strongly agitated (Figure, 3.4)

Microfossils include foraminifera, gastropods, bivalve, ostracods, calcareous algae, fish remains, microproblematica (*Lithocodium/Bacinella* oncoids, *Crescentiella morronensis*), calcispheres and sponge spicules. Microfossils

are very good indexes for the type of sea water, either restricted or circulated from open marine and in which they are indirect indicators for sea level changes. An example of deeper marine, low energy microfossils are planktonic foraminifera, calcispheres, *Lithocodium* oncoids and sponge spicules. On the other hand, the high energy shallow environments are often represented by gastropods, bivalves, thick walled ostracods, and large, benthic foraminifera. Corals and reefal organisms represent higher energy levels in shallow water in a subtidal platform margin or inner shoal (Flügel, 2004, Krajewski, 2008, 2010). *Crescentiella morronensis* is a good indicator for the distal part of the platform margin, which may be characterised by quite intensive, water turbulence.

Ooids or oolites are spherical−shaped grains, usually less than 2mm diameter, with one or more regular, concentric carbonate lamellae that envelope a nucleus. They are an indicator of very agitated environments that are formed on ooid banks or shoals where depth is normally less than 5 m. Figure 3.5 shows the types of ooids that are produced in different sedimentary environments related to the intensity of the water energy.

Oncoliths or oncoids, greater in size which is over 2 mm, made of different origin of cortex from those of ooids. These are several types, including photic zone, low energy, cyanobacterial *Lithocodium* and *Bacinella* oncoids (Flügel, 2004, Krajewski, 2010). The smaller size oncoids are characterised by one (cortoids) or more of micritic laminations enveloping a nucleus. These usually reflect shallow water moderate to high energy marine environments.

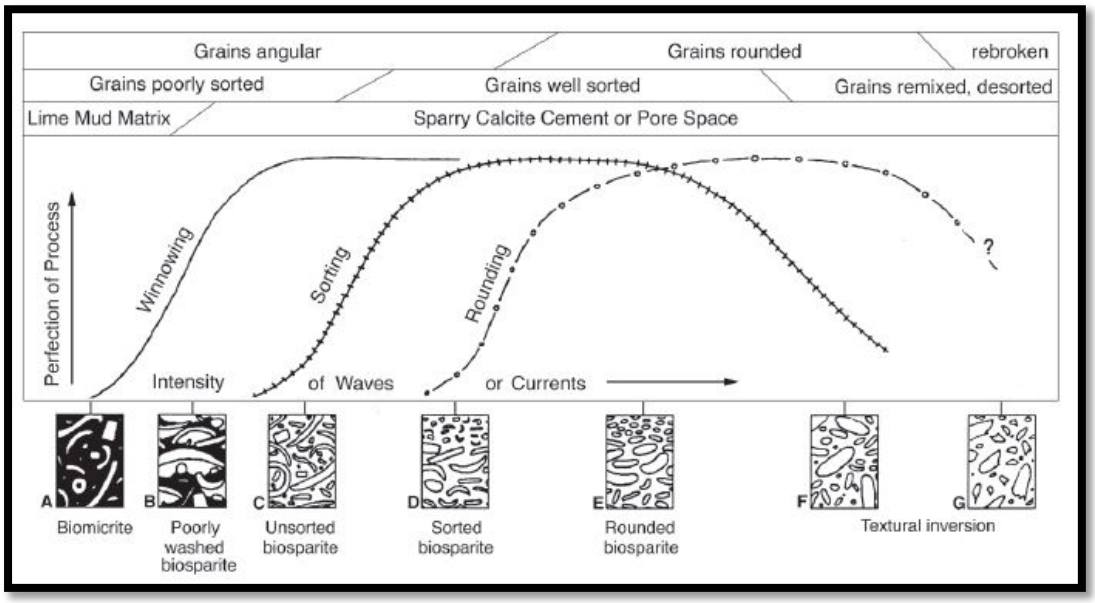

Figure 3.4. Classification of lithofacies grains and matrix that result from the strength of waves and currents (after Folk 1962 from Flügel, 2004).

However, they are sometimes transported and deposited in the subtidal lagoonal floatstones and wackestones. In extreme high energy environments, thin micrite films envelope skeletal grains at the shallower platform edge in highly turbulent conditions. These are represented as Microbial digester of skeletal bodies, formed in the lagoonal environment. These are turning the skeletal edges into microbial micrite and later turning the whole skeletal fragment into micrite mould. Grapestones, or aggregates, represent types of low energy environment that are made of two grains or more that have been enveloped by Irregular shaped micritic or micrite of microbial.

Lithoclasts are subdivided into two types: intraclasts and extraclasts. These are produced in high energy environments, but extraclasts can be transported into subtidal open marine environment. Micrite breccia is produced in low to moderate energy levels in intertidal to supratidal sedimentary environments.

	Microfabric of the cortex	Mineralogy, modern examples	Environment
Concentric (tangential) **ooids** 	Concentric laminae consisting of tangentially arranged crystals whose long axes are aligned to the surface of the laminae. High microporosity	Aragonite: Bahamas, Yucatan, Abu Dhabi, Persian Gulf	Very shallow, warm low-latitudinal seas; *common in high-energy settings*
		(Great Salt Lake/Utah)	Lacustrine-hypersaline
		Low-Mg calcite: Caliche ooids*	Terrestrial
Radial (radial-fibrous) **ooids** 	Laminae consisting of radially arranged crystals; long crystal axes perpendicular to the laminae surface	Aragonite: Persian Gulf, Great Barrier Reef, (Yucatan, Shark Bay, Mediterranean)	Shallow marine, *common in low-energy settings*
		Gulf of Aqaba	Sea-marginal hypersaline pool
		Great Salt Lake/Utah	Lacustrine-hypersaline
		Mg-calcite: (Baffin Bay/Texas)	Marine-hypersaline
		Calcite and Low-Mg calcite: e.g. Cave pearls*	Non-marine
Micritic (random) **ooids** 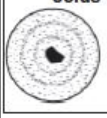	Laminae composed of randomly arranged microcrystalline crystals or Laminae obliterated or absent, due to a pervasive micritization of the cortex	Aragonite: Bahamas	Shallow-marine

Figure 3.5. Summary of ooid types and the identification of host environments in which they are created (after Flügel, 2004).

Matrix is the primary micrite of marine origin that decreases in amount as the sedimentary energy level increases. In other words, it can be a good proxy for low energy environments, using the ratio of micrite in the textural fabrics (Dunham, 1962). Generally the energy levels represented by the matrix−supported fabrics include mudstone and wackestone. On the other hand, the grain−supported fabrics are indices for higher to high energy levels such as mud−dominated packstone, grain−supported packstone and grainstone. These have been summarised by Flügel (2004) and are shown in Figure 3.6. The expanded classification suggested by Embry and Klovan (1971) has considered the grain size, source of grains, and whether allochthonous or autochthonous (Figure 3.7).

In conclusion, energy levels are controlled by water depth and wave amplitude. High energy levels characterise the intertidal zone, shallow open marine platform margin, inner shoal and shoal. The low energy sedimentary

environments are found within protected open marine, lagoonal and subtidal open marine settings (Flügel, 2004, Krajewski, 2010). Each sedimentary environment is characterised by the intensity of hydrodynamical energy, which can be obtained from the carbonate lithofacies components.

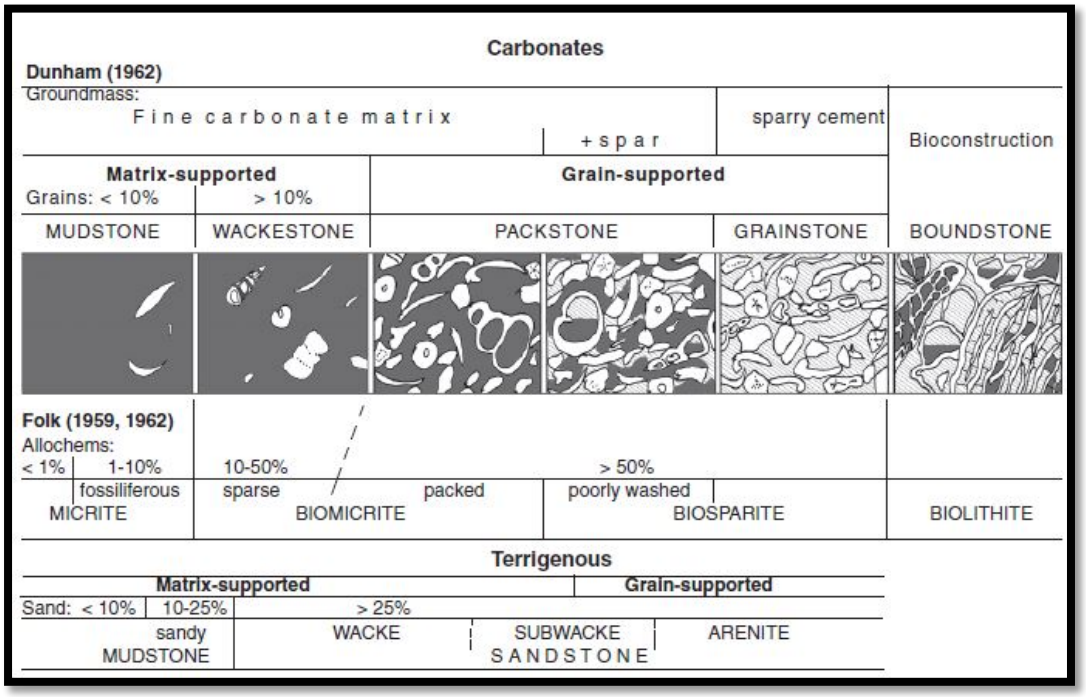

Figure 3.6. Carbonate microfacies textural classifications which were established on the basis of sedimentary energy levels. Classification and distribution is after Folk (1959, 1962) and Dunham (1962) (from Flügel, 2004).

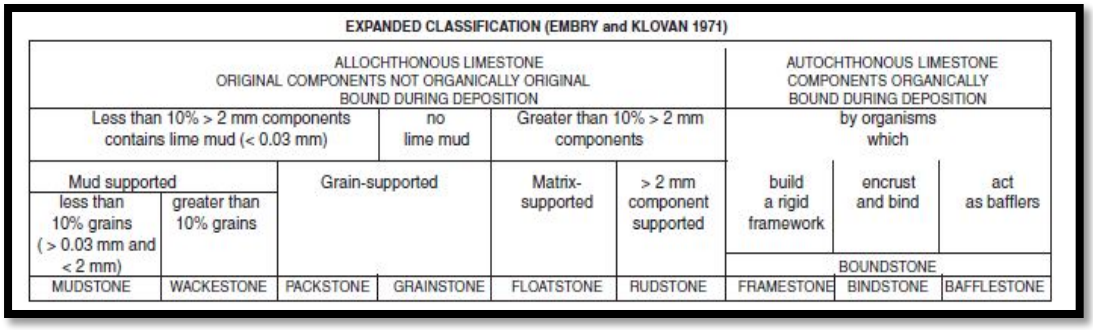

Figure 3.7. Expanded textural classification by Embry and Klovan (1971) based on Dunham (1962). It is based on the energy levels that produces certain lithofacies, taking into account the grain sizes, source of grains and whether allochthonous or autochthonous.

3.8 CRITERIA USED FOR THE IDENTIFICATION OF THE SEQUINCE STRATIGRAPHY DEPOSTIONAL CYCLES

The following stages have been used as a procedural guide to identify the location of each depositional cycle boundaries using the microfossils and microfacies analysis that are ploted in StrataBugs Charts.

1. Observe the distribution of foraminifera taxon and all associated microfossils in the studied section by hand coloring their presence. This exercise in itself will begin to provide suggestions of microfossil associations and packaging (Figure 3.8).

2. Hand colour the location of grainstone samples within the studied section. This first screening can reveal the tops of shoaling-upwards cycles. The mud to grain ratios used by Dunham (1962) serve to assist this determination and the Dunham textural scheme should be applied to each sample during analysis (Figure 3.8).

3. Hand colour the locations of mudstone samples within the studied section. This action can highlight zones that may equate to maximum flooding events, based on the premise that the site of deposition would be well below fair weather wave base and possibly represent an episode of reduced organic activity due to temporary flooding in excess of the organisms' depth preference (Figure 3.9).

4. Observe any periodicity in the vertical distribution of these grain types. Ideally, the highlighted lithologies will display a reasonably well-ordered distribution through the analyzed section (Figure 3.9).

5. If there are any “gaps” in the periodicity, search for episodes of mud-lean packstones or packstones. Such fabrics may represent shallowing-upwards successions in deeper settings where the end of the depositional cycle did not terminate shallow enough to experience the elevated energy levels associated with the results of fair weather wave-induced agitation.

6. Integrate the fabric-identified potential depositional cycles with peaks or locally continuous samples containing specific microfossils or macrofossil fragments.

7. This action will relate the microfossil assemblages to the rock fabrics and suggest environmental associations between the two (Figure 3.9).

8. The depositional cycles recognized by this exercise will probably represent 5^{th} order parasequences (Figure 3.9).

9. Note the distribution of different microfossil associations through the section, and commence more detailed interpretations relating the differences to lateral variations in the site of deposition experienced as the transgressive-regressive water depth variations cause the environmental belts to migrate landwards and seawards respectively (Figure 3.10).

10. Observe any packaging of the newly-recognized depositional cycles. These could represent candidate fourth order sequences (Figure 3.9).

11. List of the explanations of abbreviations: MFS (maximum flooding surface); MFZ (maximum flooding zone); MFS/Z (maximum flooding surface or zone); TST (transgressive system tract); HST (high stand system tract); SMF (Standard Microfacies Types, Flügel, 2004, pp. 680-711) (Figure 3.10).

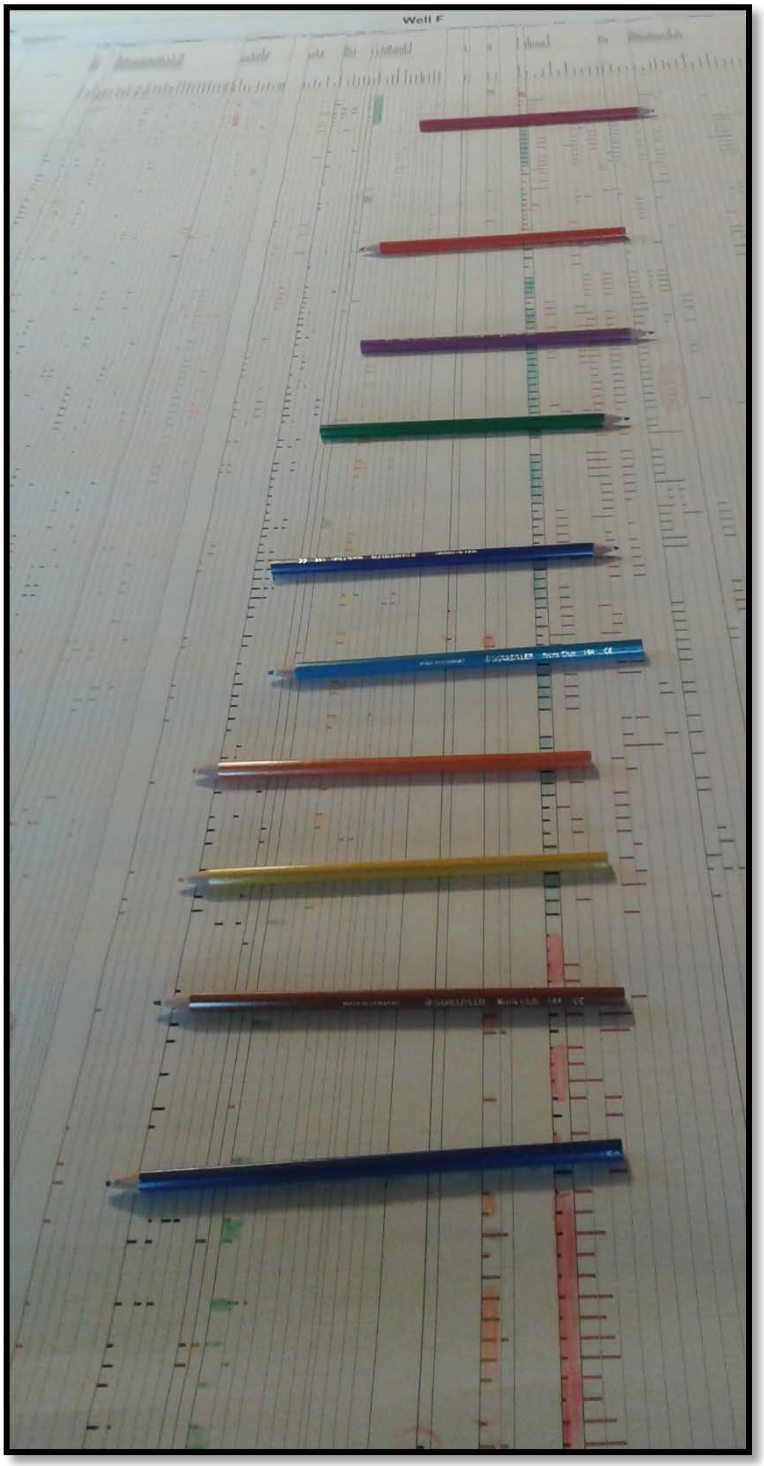

Figure 3.8. An illustration showing the observed distribution of foraminifera taxon with its associated microfossils and Dunham (1962) textures which are hand coloured. The colouring pencils are showing the different packages identified in this stage.

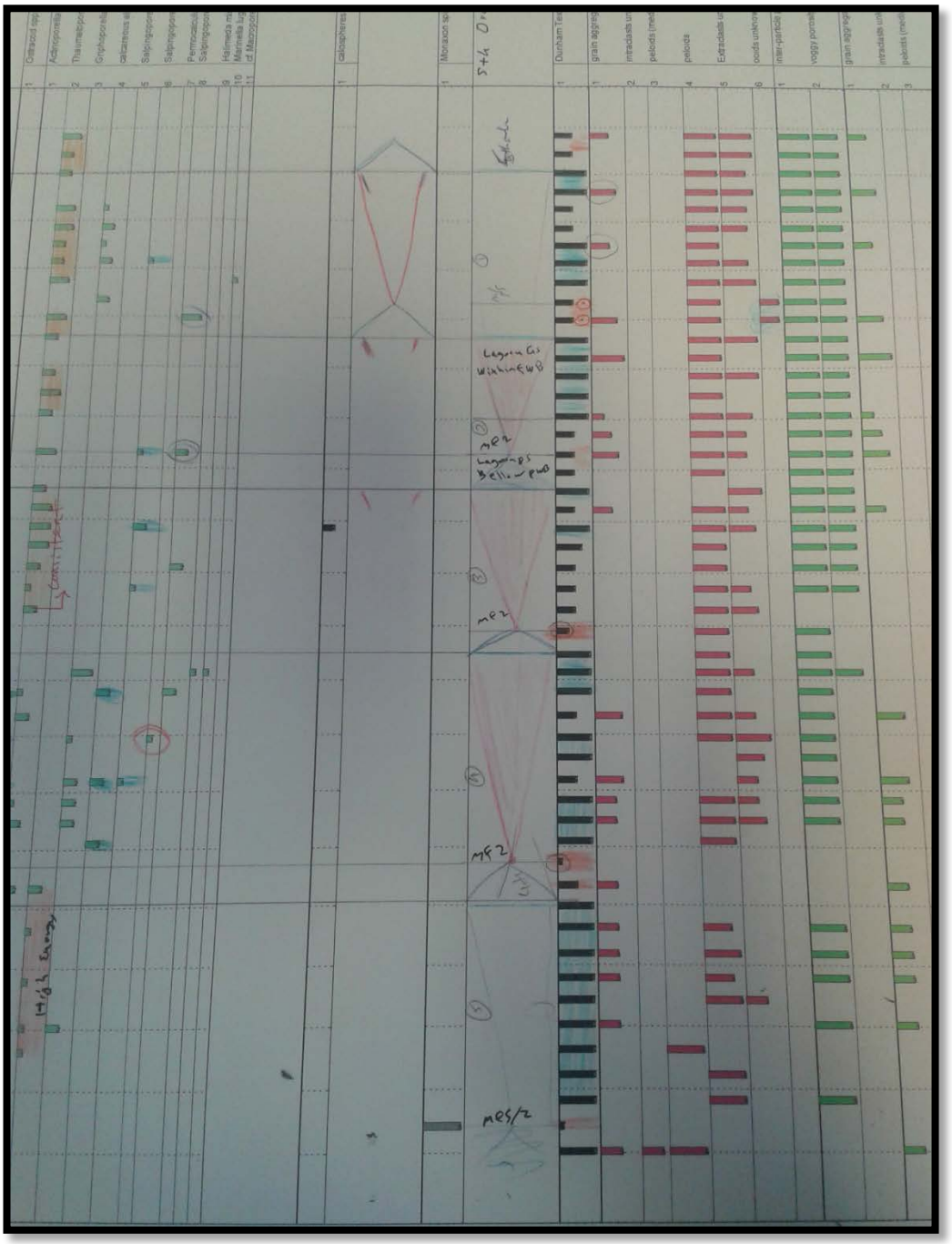

Figure 3.9. An illustration showing the highlighted zones of maximum flooding surfaces or zones with other constructed depositional cycles and parasequences. Each part of the identified cycles is associated with diagnostic microfossils association.

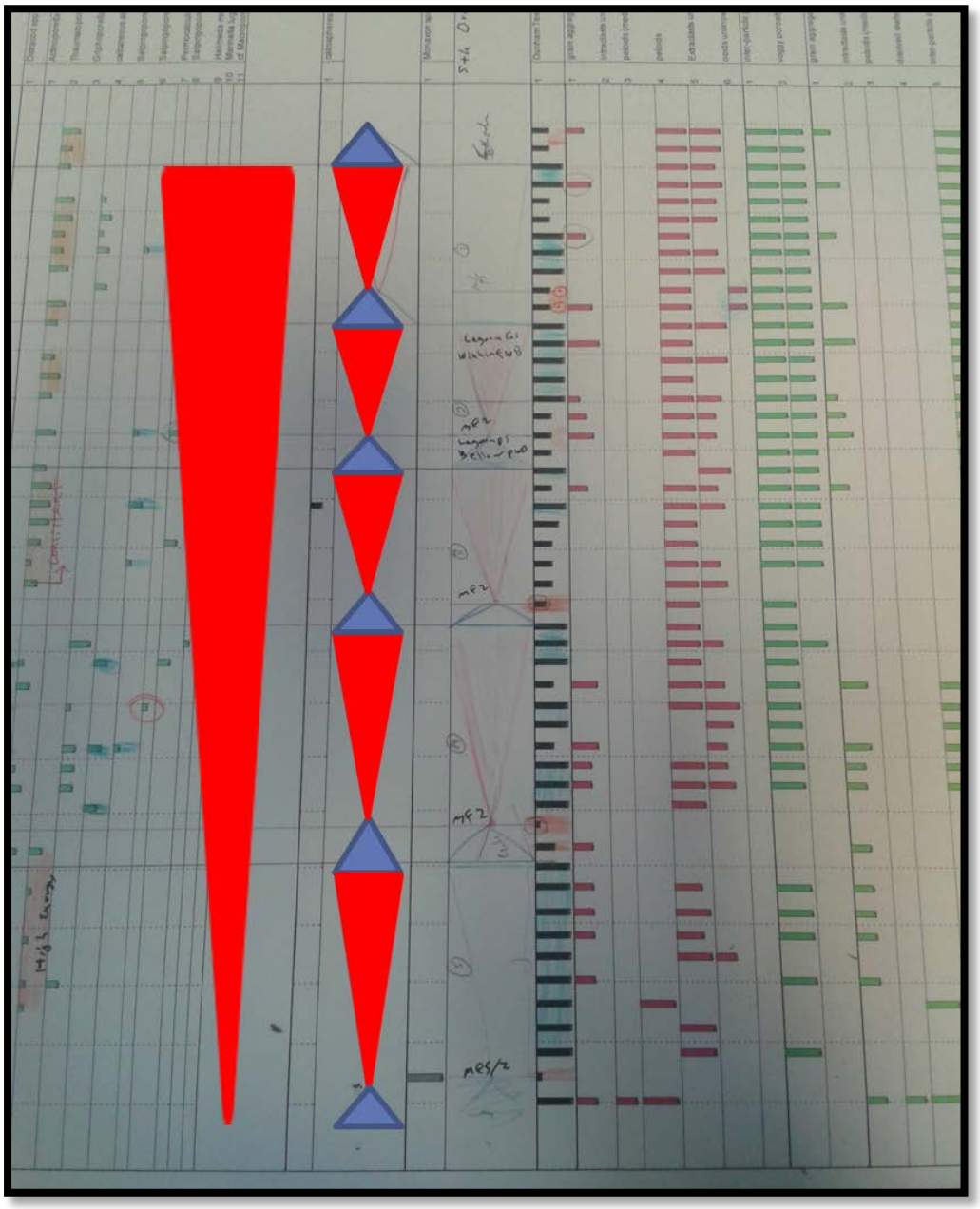

Figure 3.10. An illustration showing the observed recognized depositional cycles that are the transgressive-regressive components. These are including MFS (maximum flooding surface); MFZ (maximum flooding zone); MFS/Z (maximum flooding surface or zone); TST (transgressive system tract); HST (high stand system tract). Note the observed succession of shoaling upwards depositional cycle, which considered to be a 4th order sequence, that is superimposed on a large scale 3rd order system tract shallowing upward, in which it is a highstand-associated sequence of the Sulaiy Formation.

CHAPTER FOUR

SYSTEMATICS

CHAPTER FOUR

SYSTEMATICS

4.1 SYSTEMATICS OF FORAMINIFERA

Foraminifera are the most diverse and frequently abundant group found in the studied thin-sections. They represent the most important group used for biostratigraphy and biofacies identification. Additionally, most of the foraminifered tests were possible to describe and identify as a result of their great abundance and their good preservation quality in carbonate sediments. Using one scheme through the foraminiferal taxa classification history for foraminiferal taxonomy is difficult for agglutinated foraminifera of the Upper Jurassic and the Lower Cretaceous carbonate rocks. This difficulty is a consequence of the different basis that they have been classified by several authors. Accordingly, it is very important to understand the different basis of these classifications by reviewing the most important foraminiferal systematic schemes.

The foraminifera have undergone several assessments, with on-going upgrades of the basis of their classification. During 1927 and 1928, the name of Joseph A. Cushman was associated with foraminiferal taxonomy, in which he recognized and described about 600 genera (Haynes, 1981, 1990) from fifty families in the final edition of his book *Foraminifera* (Cushman, 1947). The basis of Cushman's classification was the wall structure, chamber arrangement and apertural form.

In the same way, Glassner (1945) used almost the same criteria for his foraminiferal classification in which he established higher categories, including seven superfamilies (Haynes, 1981, 1990). These classifications, however, were difficult to use as the stratigraphical evidence for linking these foraminiferal families into phylogenetic lines or evolutionary tracking was lacking (Haynes, 1981, 1990).

Thereafter, the new classifications began taking into account the biostratigraphy linkage and the biological interpretations in the fossil record. The fundamental of foraminiferal classification was based on the wall structure of subdividing foraminifera (Haynes, 1981, 1990). This change in procedure is represented by Wood (1947, 1949) and Loeblich and Tappan (1964). The most famous publication is the *Treatise of Invertebrate Paleontology* of Loeblich and Tappan (1964) which is a compilation of all the described genera at the time of publication. The *Treatise* was based mainly on wall structure in which 244 supra-generic categories were identified, from total of 1194 genera from 17 super-families and five sub-orders. It was used as the basic classification of the foraminifera for approximately a quarter of a century and some still use it by choice.

Haynes (1981) suggested advances in Foraminifera classification by recognizing nine orders with re-using the class category level. Hence, Loeblich and Tappan (1985) proposed some changes to their earlier classification and introduce further changes in 1987 when their revised "*Treatise*" was published by commercial printers (Loeblich and Tappan, 1987, 1988). The changes proposed in 1987 included the Order Foraminifera subdivided into 12 suborders,

63 superfamilies, 253 families and a total number of 591 supra-generic taxa (Loeblich and Tappan, 1984). Consequently, Loeblich and Tappan prepared the *Foraminiferal Genera and their Classification* which added more classification changes based on their supra-generic classification and description of most of species on the basis of their test characteristics and morphology (Loeblich and Tappan, 1987). These changes are 12 suborders, 74 superfamilies, 296 families, 302 subfamilies and a total number of 3620 genera.

Since this time, the agglutinated foraminifera have been the subject of proposed changes by Mikhalevich and Kaminski, partly related to the “Working Group on the Classification of Agglutinated Foraminifera”. They produced *the year 2000 Classification of the agglutinated foraminifera* in which Mikhalevich and Kaminski (2000) used the classification of Loeblich and Tappan (1992) in updating the agglutinated foraminifera classification. They re-classified the agglutinated foraminifera (as Subclass Textulariia) including four orders, 17 suborders, 27 superfamilies, 125 subfamilies that contain a total of 747 genera. This includes the new genera that had been renamed and re-classified by several authors including Desai and Banner (1987), Banner, Simmons and Whittaker (1991), and Theodor Neagu and Mircea Neagu (1995). Similarly, the stratigraphical ranges are subject to on-going revision by Kaminski (2004) and by a number of different authors from all around the world which will be mentioned within each of the species described in this study. Lately, Kaminski *et al.* (2008) have revised and updated 764 genera including the modification of 218 genera and re-description 136 genera of agglutinated foraminifera.

Finally, this study will use the foraminiferal classification of Loeblich and Tappan (1987) as the main source for systematics, with additional information being provided by Desai and Banner (1987), Septfontaine (1988), Banner *et al.* (1991), Wernli and Fookes (1992), Bucur (1993), Neagu (1994; 1995; 2000; 2004), Neagu and Palton (1994), Neagu and Neagu (1995), Bucur *et al.* (1996), Simmons *et al*. (1997) and Kaminski (2004).

The following publications were also used in getting the synonyms of Foraminifera and some calcareous algae from microfossils in thin sections. These references are Redmond (1964), Bucur (1988), Altiner (1991), Bucur *et al.* (1995; 1996; 2004; 2007; 2010; 2011), Schlagintweit and Ebli (1999), Pop and Bucur (2001), Hughes (2000; 2004; 2009), Ivanova and Kolodziej (2004; 2010), Bucur and Săsăran (2005; 2011), Husinec and Sokac (2006), Kobayashi and Vuks (2006), Krajewski and Olszewska (2007), Velic (2007), Hughes and Naji (2008), Hughes *et al.* (2008), Ivanova *et al.* (2008), Olszewska *et al.* (2008), Omana and González Arreola (2008), Vedrine (2008) and Görög and Wernli (2013).

The reference lists provided in this taxonomic section are not exhaustive but give information on the most important accounts of each species.

Order **FORAMINIFERIDA** Eichwald, 1830

Suborder **ALLOGROMIINA** Loeblich and Tappan, 1961

Superfamily **HORMOSINACEA** Haeckel, 1894

Family **TELAMMINIDAE** Loeblich and Tappan, 1985

Genus ***Troglotella*** Wernli and Fookes, 1992

Troglotella incrustans Wernli and Fookes, 1992

Plate 1, Figures A-B, Plate 2, Figures A-B, Plate 3, Figure A.

1992 *Troglotella incrustans* Wernli and Fookes, pp. 97, 98, 100, 102; fig. 1a- b pars, figs 3-10.

1996 *Troglotella incrustans* Wernli and Fookes; Bucur *et al*., pp. 71, 76; pl. 2, figs 3, 5; pl. 5, figs 6,9,10.

1997 *Troglotella incrustans* Wernli and Fookes; Kolodziej, pp. 252, 253; fig. 2 a-f pars, fig. 3.

1999 *Troglotella incrustans* Wernli and Fookes; Schlagintweit and Ebli, p. 391; pl. 3, fig. 4; p. 399, pl. 6, figs 7, 10-11.

2007 *Troglotella incrustans* Wernli and Fookes; Krajewski and Olszewska, p. 296; fig. 4b.

2008 *Troglotella incrustans* Wernli and Fookes; Vedrine, p. 6; fig. 5b.

2008 *Troglotella incrustans* Wernli and Fookes; Ivanova *et al*., p. 79; fig. 13e.

2012 *Troglotella incrustans* Wernli and Fookes; Schlagintweit: pp. 18- 23, 25; figs 1a-b, 3a-e, 4a-f, 5a-j, 6a-d, 7a-b, 8a-d, 9a-b, 11a-f, 12a-b and 15a-c.

***Diagnosis*:** A species of *Troglotella* with a calcareous test composed of uniserial and unilocular chambers that are sub-globular to oval in shape.

***Remarks*:** *Troglotella incrustans* is a rare, palaeoenvironmentally sensitive, boring foraminifera. It appears to have a life association with encrusting *Lithocodium aggregatum* (Elliot, 1956). It is a diagnostic foraminifera for oxygenated, normal marine conditions with high energy at the platform margin. Based on its life association with *Lithocodium aggregatum, T. incrustans* is always located within the calcified basal, chambers of *Lithocodium aggregatum* (Kolodiej, 1997, Schlagintweit, 2012). It has been shown by Vedrine (2008) that

the encrusting type of *Lithocodium aggregatum* is more abundant with *Mohlerina basiliensis* in the sedimentary zone of the platform margin.

***Stratigraphical Range*:** The stratigraphical age has been recorded by several authors as Kimmeridgian to Early Cenomanian. *T. incrustans* is recorded from the Tithonian to Berriasian of the Polish Carpathians (Kolodzeij, 1997) and the Kimmeridgian to Berriasian (Krajewski and Olszewska, 2007) of the Crimean Mountains, South Western Russia (formerly Southern Ukraine). Biostratigraphical work at several locations in France and in Eastern Europe suggest a range from the Kimmeridgian to Lower Cenomanian (Schlagintweit, 2012).

Suborder **GLOBIGERININA** Delage and Hérouard, 1896

Superfamily **FAVUSELLACEA** Longoria, 1974, emend. Banner and Desai, 1988

Family CONOGLOBIGERINIDAE Simmons *et al.,* 1997

Genus ***Conoglobigerina*** Morozova, 1961

Remarks*:* This genus is thought to represent as the oldest planktonic foraminifera (Simmons *et al*., 1997, Hart *et al*., 2012) from the Toarcian/ Aalenian to Early Valanginian (Banner and Desai, 1988, Simmons *et al*., 1997, Görög and Wernli, 2013). It was first identified by Morozova (1961), based on the umbilical position of the aperture and the surface ornamentation of the test (Grigelis and Gorbatchik, 1980). Since then, the systematic position of the genus has been uncertain with different authors having a range of views. These are summarized in Grigelis and Gorbatchik (1980, table 1, p. 7). *Caucasella* was

a re–named synonym given by Longoria (1974) which was rarely used by other authors; see, for example, Grigelis and Gorbatchik (1980) and Premoli Silva and Verga, (2004). Between 1981 and 1997, the systematic position of *Conoglobigerina* has been documented by Loeblich and Tappan (1987), Banner and Desai (1988), Simmons *et al*., (1997) and Görög and Wernli (2013). These views are summarized in Table 4.1. The definition of the genus was emended by Banner and Desai (1988) and Simmons *et al.* (1997) to confirm the genus in a modern manner. Hart *et al*. (2012) found that the separation of *Globuligerina* from *Conoglobigerina* is difficult and un-reliable based on the loop-shaped aperture used by Simmons *et al*. (1997). They evidenced this using several specimens of the Middle Bathonian *Conoglobigerina bathonica* (Pazdrowa) in which Hart *et al*. (2012, Plate 1 and Plate 2) illustrated different height/width ratios and highly variable loop-shaped apertures within the same assemblage. The origin of the genus from a benthic genus is probably responsible for its aragonitic wall composition (Simmons *et al*., 1997, Hart *et al*., 2012). It has been suggested that early *Conoglobigerina* evolved from *Oberhauserella* by way of *Praegubkinella* (Görög and Wernli, 2003; Hart *et al*., 2012) although Loeblich and Tappan (1987) regarded these two genera as synonyms.

Hart *et al*. (2012) discussed the phylogenetic lineages of *Conoglobigerina* and its separation from the genus *Globuligerina* by the height of spiral side. They found that this is a species with both high and low trochospiral chamber arrangements within the well-preserved assemblages from Ogrodzieniec (Poland). This is followed by the low trochospiral species *Conoglobigerina*

oxfordiana and *Conoglobigerina caucasica* and the high to medium-spired *Conoglobigerina gulekhensis* (Hart *et al*., 2012).

Favusella, a commonly used generic name in the uppermost Jurassic and Lower Cretaceous, probably evolved from *Conoglobigerina gulekhensis* by the development of a favose wall texture (honeycomb ornamentation). The wall surface texture of *C. gulekhensis* is irregularly reticulate (Hart *et al*., 2012).

Author and Year	Grigelis and Gorbatchik, 1980	Loeblich and Tappan, 1988	Banner and Desai, 1988	Simmons *et al.* 1997	Görög and Wernli, 2013
Order	Foraminiferida				Globigerinida
Suborder	Globigerinina				
Superfamily	Globigerinacea	Rotaliporacea	Favusellacea		Favuselloidea
Family	Favusellidae	Globuligerinidae		Conoglobigerinidae	
Genus	*Conoglobigerina*				

Table 4.1. Summary of the systematic position of *Conoglobigerina* given by different authors. This research follows Simmons *et al*., (1997) as this position is accepted by Hart *et al*. (2012) and Görög and Wernli (2013).

Conoglobigerina sp. cf. *C. gulekhensis* (Gorbatchik and Poroshina, 1979)

Plate 3, Figure B, Plate 4, Figures A-B, Plate 5, Figures A-B.

1979 *Globuligerina gulekhensis* Gorbatchick and Poroshina, pp. 24-26, figs 1a-d, text-fig. 1a-c.

1981 *Globuligerina gulekhensis* Gorbatchick and Poroshina, 1979; Grigelis and Gorbatchik: p. 13; pl. 2, fig. 2.

1988 *Conoglobigerina gulekhensis* (Gorbatchik and Poroshina); Banner and Desai, p. 153; pl. 2, fig. 5.

1997 *Conoglobigerina gulekhensis* (Gorbatchik and Poroshina); Simmons *et al.*, p. 43; pl. 2.6, figs 13-15.

***Diagnosis*:** A high-spired form of *Conoglobigerina* composed of three whorls, with 4−5 sub-globular chambers in the final whorl.

Description: The test is a high-spired trochospiral with a minimum of three whorls and five chambers in the last whorl. *Conoglobigerina* sp. cf. *C. gulekhensis* shows affiliation to *Conoglobigerina gulekhensis*, but no clear sections through the aperture have been seen to confirm the identification. The conical trochospiral whorl's height is higher than the last whorl, and the ratio of the height/length is from1.18 to 1.22. The growth rate of the chambers is medium. In the last whorl the umbilical side is totally evolute while the trochospiral side is involute. The wall has random external perforations with unclear ornamentation type as a result of dissolution of the original test which has been replaced by micrite and only some of the original structures retained.

***Remarks*:** This species appears very close to *Conoglobigerina conica* (Iovceva and Trifonova, 1961) but this taxon was apparently defined using internal, glauconitic molds (Masters, 1977; Simmons *et al.*, 1997, p. 24). This lack of available holotype or paratype makes *C. conica* an invalid species, leaving *C. gulekhensis* as the only viable point of reference. As the specimens recovered in this investigation lack an original test wall and, as only seen in thin-section, do

not give a clear view of the aperture, only the tentative determination is given as *Conoglobigerina* sp. cf. *C. gulekhensis.* The specimens were encountered from the offshore Well D.

***Stratigraphical Range*:** The stratigraphical range has been recorded by several authors in different places in the world including Berriasian to Valanginian by Grigelis and Gorbatchik (1981), Berriasian to Valanginian by Banner and Desai (1988) and Berriasian to Early Valanginian by Simmons *et al*. (1997). In this study the stratigraphical range given by Simmons *et al.* (1997) is followed.

Suborder **INVOLUTININA** Hohenegger and Piller, 1977

Superfamily INVOLUTINOIDEA Bűtschli, 1880

Family TROCHOLINIDAE Kristan-Tollmann, 1963 (formerly **INVOLUTINIDAE** Bűtschli, 1880), emended by Riguard *et al*., 2013, pp. 321-323.

Subfamily TROCHOLININAE Kristan-Tollmann, 1963, (formerly **AULOTORTINAE** Zaninetti, 1984), emended by Riguard *et al*., 2013, p. 329.

Genus *Coscinoconus* Leupold in Leupold and Bigler, 1936 (formerly ***Andersenolina*** Neagu, 1994), emended by Riguard *et al*., 2013, pp. 329-330.

Diagnosis: The test morphology is from lenticular to high cylindrical conical; the proloculus is followed by a trochospirally coiled tubular chamber. Each coiling stage is secreted with a singular lamella and the wall was originally composed of aragonite that has now been replaced by calcareous micrite. The pseudo-

pillar structures are thicker toward the umbilical part; the trochospiral part is evolute with different ranges of heights; the involute umbilical part is semi-flat to slightly concave (*C. chouberti*). The umbilical side is constructed of a secreted, perforate, lamellae added with each whorl.

***Preliminary Remarks*:** *Coscinoconus* was often known as *Andersenolina and Trocholina*. The genus *Trocholina* was elevated into a group and sub–divided into five genera by Neagu (1994, 1995). This group includes *Trocholina*, *Neotrocholina*, *Ichnusella*, *Andersenolina* and *Bancilina*. This approach by Neagu is, of course, outside the "Rules of Zoological Nomenclature" and 'Group' has no taxonomic status. However, as all fossil species are by default "morphospecies" and are not biological species in the true sense, then this approach may have practical value to those working on these taxa. However, Riguard *et al*. (2013) re-used the original name suggested by Leupold (1936) and they emended their descriptions and their classification position. They suggested re-using the Superfamily INVOLUTINOIDEA Bűtschli (1880) in the classification of *Coscinoconus.*

The sub-generic classification used in this study will be based on the number of whorls, aperture shape and height, test morphology and height/width ratio. This genus can be used to identify the Sulaiy Formation from the base of the Yamama Formation. Authors using the new classification and new generic names are Bucur and Săsăran (2005), Krajewski and Olszewska (2007), Olszewska (2010) and Riguard *et al*. (2013).

Coscinoconus alpina Leupold in Leupold and Bigler, 1936

Plate 6, Figures A-B, Plate 7, Figures A-B.

1936 *Coscinoconus alpinus* Leupold in Leupold and Bigler, 1936, p. 610; pl.18, figs 1-8.

1991 *Trocholina alpina* (Leupold); Altiner, p. 199, pl. 9, figs 1-4.

1994 *Andersenolina alpina* (Leupold); Neagu, pp. 443, 444, 452, 450; pl. 7, figs 8-9, pl. 8, figs 1-10, pl. 12, figs 1-5, text-fig. 4, fig. 3-4.

1995 *Trocholina alpina* (Leupold); Bucur *et al*., p. 361 ; pl. 2, figs 8, 10.

1996 *Trocholina alpina* (Leupold); Bucur *et al*., p. 72 ; pl. 3, figs 1, 2.

2004 *Andersenolina alpina* (Leupold); Bucur and Săsăran, p. 66 ; pl. IV, fig. 1.

2005 *Andersenolina alpina* (Leupold); Bucur and Săsăran, pp. 36, 38 ; pl. II, fig.1, pl. IV, fig. 13.

2007 *Andersenolina alpina* (Leupold); Krajewski and Olszewska, p. 300; fig. 6J.

2008 *Trocholina albina* (Leupold); Ivanova *et al*., p. 72; fig. 7q-r.

2010 *Andersenolina alpina* (Leupold); Olszewska, pl. VII, fig. 8.

***Diagnosis*:** *Coscinoconus alpina* has a conical, trochospiral test of medium height. The trochospiral side is an equilateral triangular shape. The umbilical side is high and it is constructed of a thick lamella added on each whorl.

***Remarks*:** *Coscinoconus alpina* is common in the Sulaiy Formation. It is associated with a proximal shallow platform interior palaeoenvironment. The disappearance *of C. alpina* is at the base of Yamama Formation in the Saudi Arabian offshore wells.

***Stratigraphical Range*:** The stratigraphical age of this species has been recorded by several authors in different places in the world and these are

summarized in Table 4.2. In this study the stratigraphical range is Tithonian to Early Valanginian, in agreement with the stratigraphical age ranges provided by Chiocchini and Mancinelli (1979), Altiner (1991), Chiocchini *et al.* (1994), Bucur and Săsăran (2005), Krajewski and Olszewska (2007) and Olszewska (2010). Age ranges and occurrences are recorded as Tithonian to Lower Valanginian in South East Poland by Olszewska (2010), Tithonian to Early Valanginian in the Crimea Mountains by Krajewski and Olszewska, (2007) Upper Bajocian to Hauterivian in Croatia by Velic (1997), Tithonian to Upper Berriasian in the Italian Alps by Chiocchini and Mancinelli (1979) and Chiocchini *et al.* (1994), Upper Kimmeridgian to Middle Valanginian in the Carpathian by Mountains by Bucur *et al.* (1995), Upper Oxfordian to Lower Valanginian by Bucur and Săsăran (2005) of the carbonate platforms of Romania, Upper Kimmeridgian to Lower Valanginian by Altiner (1991) of Turkey and Middle Kimmeridgian to Valanginian of Ukraine by Ivanova *et al.* (2008).

Coscinoconus delphinensis (Arnaud-Vanneau *et al.* 1988)

Plate 8, Figures A-B, Plate 9.

1988 *Trocholina delphinensis* Arnaud-Vanneau *et al.*; p. 358, pl. 1, fig. 1, pl. 3, figs 1-8.

1991 *Trocholina delphinensis* Arnaud-Vanneau *et al.*; Altiner, p. 199, pl. 9, figs 10-16.

1994 *Andersenolina delphinensis* (Arnaud-Vanneau *et al.*); Neagu, pp. 443, 450, 451, 455, pl. 7, figs 1-7, pl. 11, figs 22, 26, pl. 13, figs 10-12, 18, text-fig. 4, fig. 1.

1995 *Trocholina delphinensis* Arnaud-Vanneau *et al.*; Bucur *et al*., p. 361, pl. 2, figs 6, 12, 13.

2005b *Andersenolina delphinensis* (Arnaud-Vanneau *et al.*); Bucur and Săsăran, p. 38, pl. IV, fig. 14.

***Diagnosis*:** *Coscinoconus delphinensis* has a high, conical, trochospiral test of up to eight whorls; the umbilical side is highly convex with fairly thick perforate lamella added with each whorl.

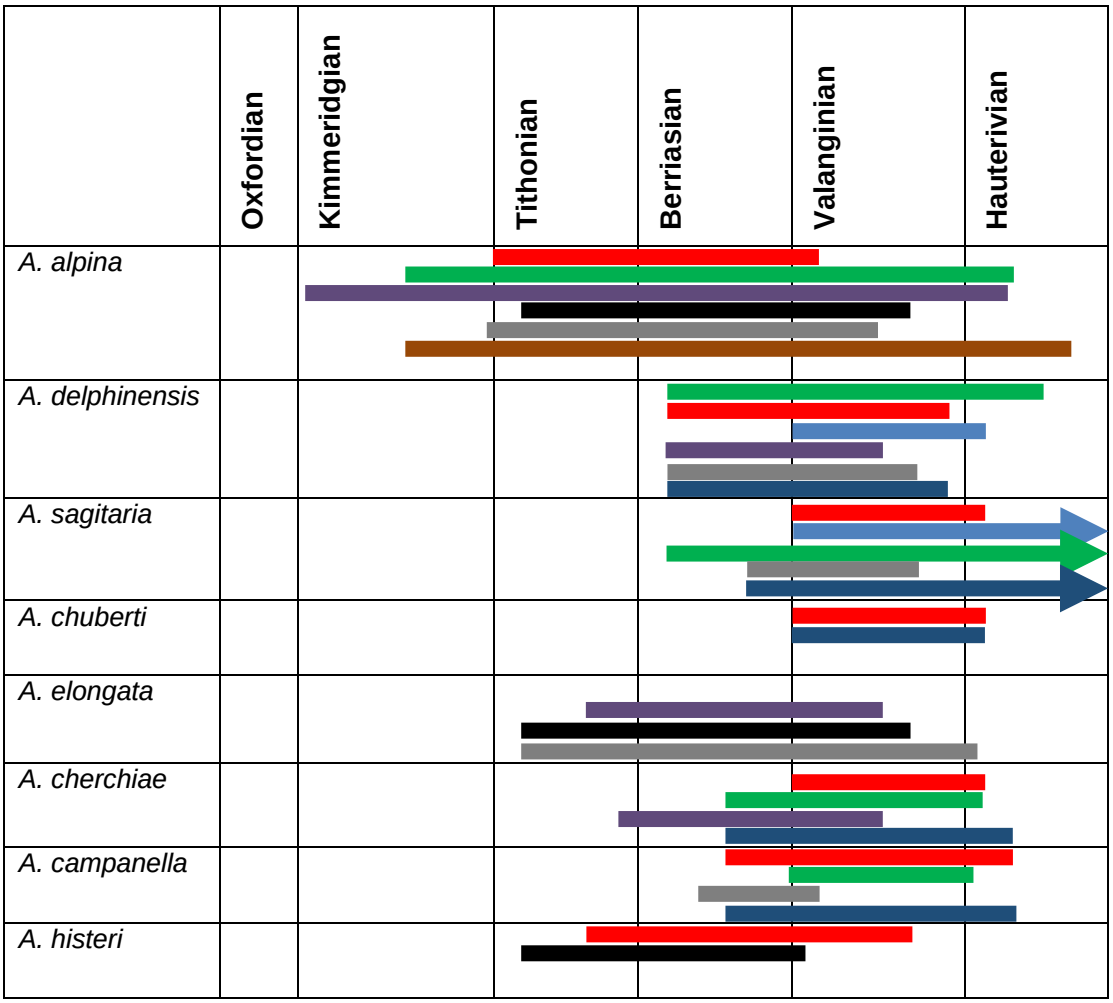

Table 4.2. The summary of the important *Coscinoconus* (*Andersenolina*,*Trocholina*) species stratigraphical ranges during the Lower Cretaceous from other authors. The colored bar are referring to the ranges given by the following authors (author names colour legend): **Chiocchini and Mancinelli, 1979, Chiocchini *et al.*, 1994, Krajewski and Olszewska, 2007, Olszewska, 2010, Bucur *et al.* 1995 Bucur and Săsăran, 2005, Altiner, 1991, Ivanova *et al.*, 2008, Arnaud-Vanneau *et al.*, 1988.**

***Remarks*:** *Coscinoconus delphinensis* shape is generally low sub-oval; trochospiral side shape is similar to cathedral extended leg sides; following the

trochospiral side shape is the pseudo- pillar structures in which they have two stages of enlargement, the first one is the apex pseudo- pillar enlargement rate is high while the pseudo- pillar enlargement rate of the rest of the trochospiral side is slow; the pseudo- pillar shape is curvilinear triangular with lower convex and upper plano- to semi-concave.

It is common in the Sulaiy Formation and the lower part of the Yamama Formation in the Saudi Arabian offshore wells along the western side of the Arabian Gulf. The first appearance of *C. delphinensis* is an indicator of the Berriasian stage. It is palaeoenvironmentally associated with the subtidal lagoon to shallow lagoon shallow platform interior and platform margin. ***Stratigraphical Range*:** It is recorded by several authors from the Berriasian to Middle Valanginian. The stratigraphical ranges provided by different authors are summarized in Table 4.2.

Coscinoconus elongata Leupold in Leupold and Bigler, 1936

Plate 10, Figures A-B.

1936 *Coscinodiscus elongatus*; Leupold in Leupold and Bigler, 1936, p. 617, pl. 8, figs 12-14.

1988 *Trocholina elongata* (Leupold); Bucur, p. 387, pl. II, fig. 22.

1991 *Trocholina elongata* (Leupold); Altiner, p. 199, pl. 9, figs 1-4.

1994 *Andersenolina elongata* (Leupold); Neagu, pp. 436, 440, 452, 449, pl. 4, figs 1-22, pl. 6, figs 12-14, pl. 12, figs 13-17, text-fig. 3, fig. 7.

2005b *Andersenolina elongata* (Leupold); Bucur and Săsăran, p. 38, pl. IV, figs 16-17.

2007 *Andersenolina elongata* (Leupold); Krajewski and Olszewska, p. 300, fig. 6K.

***Diagnosis*:** A species of *Coscinoconus* with a long cylindro-conical, trochospiral test of 10-13 whorls. The umbilical part is low to medium convex in shape. The pseudo–pillar structures are globular.

***Remarks*:** *Coscinoconus elongata* is common in the Sulaiy Formation and its disappearance at the top of the Sulaiy Formation is an indication of the transition into the base of the Yamama Formation. Palaeoenvironmentally, it is often associated with shallow lagoons. It is also associated with shoaling−upwards sequences at the top of each sequence of the depositional cycles in the Sulaiy Formation.

Stratigraphical Range: The age recorded for this species is Tithonian to Early Valanginian by Krajewski and Olszewska (2007) in the Crimea Mountains from Southern East of Russia (formerly Southern Ukraine).

Coscinoconus cherchiae Arnaud-Vanneau *et al.*1988

Plate 11, Figures A-B.

1988 *Trocholina cherchiae* Arnaud-Vanneu *et al.*; p. 357, pl. 2, figs 1-21, text-fig. 2.

1994 *Andersenolina cherchiae* Arnaud-Vanneau *et al.*; Neagu, pp. 439, 440, 452, 449, pl. 5, figs 1-14, pl. 6, figs 1-11, pl. 12, figs 18-23, text-fig. 3, fig. 8a-c, text-fig. 4, fig. 2a-c.

1995 *Trocholina cherchiae* (Arnaud-Vanneau *et al.*); Bucur *et al*., p. 361; pl. 2, figs 3, 11.

2005 *Andersenolina alpina* Arnaud-Vanneau *et al.*; Bucur and Săsăran, p. 38, pl. IV, fig. 15.

***Diagnosis*:** *Coscinoconus cherchiae* has a cylindro-conical, trochospiral coiling test of eight to nine whorls. The general shape is oval with an apical angle that is twice that of the apical angle in *C. elongata*.

***Remarks*:** Pseudo-pillar shape is globular to an irregular curvilinear triangle. The trochospire has two stages of enlargement with the apical part showing slower enlargement of the chambers and occupies 35% of the test; the remaining 65% of the test shows rapid enlargement of the chambers toward the umbilical part. The umbilical part is high and composed of a thick perforated plate. The appearance of *C. cherchiae* is an indicator of the base of the Yamama Formation in some of the studied wells.

***Stratigraphical Range*:** The age is recorded as Late Berriasian to Valanginian (Table 4.2) according to Chiocchini and Mancinelli (1979), Arnaud-Vanneau *et al*. (1988) and Chiocchini *et al.* (1994).

Coscinoconus sagittaria Arnaud-Vanneau *et al.,* 1988

Plate 12, Figures A-B, Plate 13, Figures A-B, Plate 14, Figure A.

1988 *Trocholina sagittaria* Arnaud-Vanneau *et al.*, p. 367, pl. 1. fig. 5, p. 377, pl. VI, figs1-10.

1991 *Trocholina sagittaria* Arnaud-Vanneau *et al.*; Altiner, p. 199, pl. 9, figs 17-19.

1995 *Trocholina sagittaria* Arnaud-Vanneau *et al.*; Bucur *et al*., p. 361, pl. 2, fig. 5.

2004 *Andersenolina sagittaria* (Arnaud-Vanneau *et al*.); Bucur and Săsăran, p. 66, pl. IV, fig. 2.

2008 *Trocholina sagittaria* Arnaud-Vanneau *et al.*; Hussaeini and Conrad, p. 227, pl. 5, fig. E.

***Diagnosis*:** *Coscinoconus sagittaria* is a short, cylindro-conical, trochospirally coiled species of *Coscinoconus*. The umbilical side is semi-flat to slightly convex and number of whorls varies from 7 to 12.

***Remarks*:** This species is widely distributed within the Sulaiy and Yamama formations. The level of occurrence is from present to rare in thin section. It is often associated with high-energy environments at the platform margin.

***Stratigraphical Range*:** *Coscinoconus sagittaria* appears to have a wide stratigraphical range from Berriasian to Aptian. Arnaud-Vanneau *et al*. (1988), Altiner (1991) and Bucur *et al.* (1995) indicate that the first appearance is in the Berriasian stage. *Coscinoconus sagittaria* is also reported from Aptian carbonates (Bucur and Săsăran, 2004). Chiocchini and Mancinelli (1979) and Chiocchini *et al.* (1994) indicated only a Valanginian age (Table 4.2). Finally, the stratigraphical range is from the mid-Berriasian to Aptian based on authors mentioned in Table 4.2.

Genus ***Neotrocholina*** Reichel, 1955

Diagnosis: Wall is made of visible radial-hyaline calcite; the proloculus is followed by trochospiral coiling of the tubular second chamber. The wall has no secondary lamellae on the trochospiral side.

Neotrocholina valdensis Reichel, 1955

Plate 14, Figure B.

1955 *Neotrocholina valdensis* Reichel, p. 404, pl. 16, fig. 5a-b (holotype), fig. 3 (thin section)

1963 *Neotrocholina valdensis* Reichel; Dessauvagie, pp. 72-74, text figs 2-6, pl. 1, figs a-d, pl. 2 figs a-g.

1988 *Neotrocholina valdensis* Reichel; Bucur, p. 387, pl. II, fig. 24.

1995 *Neotrocholina valdensis* Reichel; Neagu, pp. 11, 14, 17, 18, 21, 30, 37, text figure 4-E, pl. 2, figs 13-21, 28-44, 49-51; pl. 3, figs 1-9, 37-39, pl. 4, figs 36-47, 52-66, pl. 5, figs 57-60, pl. 10, figs 1-10, pl. 13, figs 1-4, 9, 17, 23.

1995 *Neotrocholina valdensis* Reichel; Bucur *et al*., p. 361, pl. II, fig.9.

2004 *Neotrocholina valdensis* Reichel; Bucur *et al*., p. 66, pl. IV, figs 5, 6.

2004 *Neotrocholina valdensis* Reichel; Ivanova and Kolodziej, p. 71, figs 1.I-J

2008 *Neotrocholina valdensis* Reichel; Ivanova *et al*., p 72, fig. L

***Diagnosis*:** *Neotrocholina valdensis* has a conical test of medium height. The proloculus is followed by trochospiral coiling of the tubular second chamber. The trochospiral side is medium to high convex while the umbilical side is flat. There are 5-6 whorls visible. The wall is calcareous, radiate without any secondary lamellae on the trochospiral side. The thickness of the wall in the trochospiral part remains the same in all whorls and the shape of the coiled, tubular chamber in each whorl is a globular to inflated semi-rectangular shape; the umbilical part is finely perforated.

***Remarks*:** *Neotrocholina valdensis* appears in the uppermost Sulaiy Formation or the lowermost Yamama Formation. Schlagintweit and Ebli (1999) reported the association of *Neotrocholina valdensis* with *Meandrospira favrei* in the Northern Alps in Lower Valanginian. Ivanova and Kolodziej (2004) recorded its association with *Montsalevia salevensis*, *Meandrospira favrei* and *Patellina turriclata* in the coral bearing limestones of the Stramberk Mountains, Polish Outer Carpathians.

***Stratigraphical Range*:** This species is Late Berriasian to Valanginian in age from combining the stratigraphical results of several authors. According to

Reichel (1955) it is recorded from the Valanginian in the Swiss Alps. Dessauvagie (1963) recorded that it is Late Tithonian? to Valanginian in age in NE Turkey. Altiner (1991) recorded it as Late Berriasian to Middle Valanginian in Turkey. Bucur *et al.* (1995) recorded it from the Late Berriasian to Valanginian in Eastern Serbia. Schlagintweit and Ebli (1999) recorded that it is Late Berriasian to Valanginian age in the Northern Calcareous Alps. Bucur and Săsăran (2005) recorded it from the Late Berriasian to Early Valanginian in Romania, while Bucur *et al.* (2004) suggested Berriasian to Valanginian. Ivanova (2008, 2010) restricted it to the Valanginian in SW Bulgaria and the Polish Outer Carpathians, while Neagu (1995) suggested only Valanginian in age. It is Late Berriasian to Valanginian in age according to Schlagintweit and Ebli (1999) in the Northern Alps but is recorded as Late Berriasian to Valanginian in the Polish Outer Carpathians by Ivanova and Kolodziej (2004).

Family **VENTROLAMINIDAE** Weynschenck, 1950

Genus ***Protopeneroplis*** Weynschenck, 1950

Diagnosis**:** *Protopeneroplis* has an involute, lenticular test with a maximum size of 0.8 mm in diameter; the coiling is ranging from a loose planispiral to trochospiral. The last whorl contains from twelve to sixteen chambers; the wall is thick, calcareous, hyaline (0.42 mm) with two micro-layers, an internal microgranular and external pure hyaline layers that thickened in every new added chambers of added whorls; in thin section the wall appears as dark and light bands reflecting the repeated two micro-layers for every chamber wall in each whorl.

***Remarks*:** Several authors have reviewed the species of *Protopeneroplis* and a new species was identified by Bucur (1993, 1997) and Bucur *et al.* (1996). The best known species of the genus are the Jurassic *Protopeneroplis striata* Weynschenck (1950), *Protopeneroplis ultragranulata* Gorbatchik (1971), *Protopeneroplis trochoangulata* (Septfontaine,1974; it is a synonym for *P. ultragranulata*), and *Protopeneroplis banatica* Bucur (1993). The last two species are from the Lower Cretaceous and their stratigraphical range and phylogenetic relationships are reported by Bucur (1997, p. 68, figure 3).

Protopeneroplis ultragranulata (Gorbatchik, 1971)

Plate 15, Figures A-F, Plate 16, Figures A-F, Plate 17, Figures A-C.

1971 *Hoeglundina ultragranulata* Gorbatchik, p. 135, pl. 26, fig. 2.

1988 *Protopeneroplis trochangulata* Septfontaine; Bucur, p. 387, pl. II, figs 15-19.

1991 *Protopeneroplis trochangulata* Septfontaine; Altiner, p 194, pl. 7, figs 1-5.

1993 *Protopeneroplis ultragranulata* (Gorbatchik); Bucur, p. 221, pl. 2, figs 1, 2, 5, 8, 11, 12.

1995 *Protopeneroplis ultragranulata* (Gorbatchik); Bucur *et al*., p 367, pl. V, figs 5-7.

1996 *Protopeneroplis ultragranulata* (Gorbatchik); Bucur *et al*., p 73, pl. 3, figs 14-17.

1997 *Protopeneroplis ultragranulata* (Gorbatchik); Bucur *et al*., pp. 72-74, pl. 6.I, figs 13-16, pl. 6.II, figs 1-14 pl. 6.III, figs 1-3.

2004 *Protopeneroplis ultragranulata* (Gorbatchik); Bucur *et al*., p. 66, pl. IV, figs 7-12.

2005 *Protopeneroplis ultragranulata* (Gorbatchik); Bucur and Săsăran, p 38, figs 10, 11.

2007 *Protopeneroplis ultragranulata* (Gorbatchik); Bruni *et al*., p 54, pl. III, figs 5-6.

2008 *Protopeneroplis ultragranulata* (Gorbatchik); Bucur *et al*., p 72, figs 7e-f.

2010 *Protopeneroplis ultragranulata* (Gorbatchik); Ivanova and Kolodziej, p 31, pl. 5, figs 1-6.

***Diagnosis*:** *Protopeneroplis ultragranulata* has a lenticular, trochospirally coiled test. The wall is thick, made of two layers, the external layer is microgranular and the internal layer is hyaline; the outer surface ornamentation is pustulate on the spiral part. The periphery is angular in shape and the size is generally large.

***Remarks*:** Bucur *et al.* (1997, p. 67) have discussed the synonyms of this species, which was named by Gorbatchik (1971) as *Hoeglundina* (?) *ultragranulata*. It was known by earlier authors as *Protopeneroplis trochangulata* Septfontaine (1974) but it was later shown by Bucur (1997) that it is a synonym of *P. ultragranulata*. *P*. *ultragranulata* occurrences extend to the Valanginian deposits of the Yamama Formation in Saudi Arabia.

***Stratigraphical Range*:** According to Bucur *et al.* (1996) and Bucur (1997) it ranges from Middle Tithonian to Lower Barremian.

Protopeneroplis banatica Bucur, 1993

Plate 17, Figures D-E.

1988 *Protopeneroplis* aff. *trochangulata* Septfontaine; Bucur, p. 387, pl. II, figs 20-21.

1993 *Protopeneroplis banatica* Bucur, pp. 219, 221, pl. 1, figs 1-37, pl. 2, figs 3, 4, 6, 7, 9, 10, 13.

1995 *Protopeneroplis banatica* Bucur; Bucur *et al*., p 367, pl. V, fig. 8.

1997 *Protopeneroplis banatica* Bucur; Bucur *et al*., p 74, pl. 6.III, figs 4-19.

2004 *Protopeneroplis* cf. *banatica* (Bucur); Bucur *et al*., p. 66, pl. IV, figs 13-15.

***Diagnosis*:** *Protopeneroplis banatica* is trochospirally coiled and involute. The wall is composed of two micro-layers. The internal wall layer is composed of radial hyaline calcite and this is followed by external microgranular layer. The

hyaline layer is well developed on the spiral side, but shows no development of pustules. The peripheral chamber is angular or slightly rounded. There are from one to five whorls and the final whorl contains from seven to eight chambers.

***Remarks*:** The appearance of *Protopeneroplis banatica* up-section is an indicator of the base of the Yamama Formation.

***Stratigraphical Range*:** The stratigraphical range of *Protopeneroplis banatica* is given as Valanginian to Lower Hauterivian by Bucur *et al*. (1995). More recently, Bucur *et al.* (2004) have indicated the presence of related forms from Berriasian to Valanginian.

Sub Order **LAGENINA** Delage and Hérouard, 1896

Superfamily **NODOSARIACEA** Ehrenberg, 1838

Family **LENTICULINIDAE** Chapman, Parr and Collins, 1934

Subfamily **LENTICULININAE** Chapman, Parr and Collins, 1934

Genus ***Lenticulina*** Lamarck, 1804

Lenticulina spp.

Plate 17, Figure F, Plate 18, Figures A-F

***Diagnosis*:** *Lenticulina* has a calcareous, perforate, radial, hyaline test. Coiling is planispiral, and the test is lenticular. Most specimens are symmetrical but some may show asymmetrical shapes. Chambers increase slowly in size with growth and the last one or two chambers may be partially uncoiled.

***Remarks*:** *Lenticulina* spp. occur throughout Jurassic–Cretaceous sediments and, in the Middle East, are known from deep ramp to basinal biofacies (Murillo-Muneton and Dorobek, 2003; Hughes *et al.*, 2008) in particular within the *Lenticulina*-spicules biofacies. The genus is associated with small foraminifera including *Nodosaria* spp.*, Astacolus* spp., *polymorphinids* and *Bolivina* spp. Agglutinated foraminifera are also associated with *Lenticulina,* including *Kurnubia palastiniensis, Nautiloculina oolithica, Pseudocyclammina lituus, Praedorothia* sp.*, Protomarssonella kummi, Gaudryina ectypa, Verneuilina minuta* and *Gaudryinella* sp*.* Other, deeper marine microfossils may also be associated with this genus including calcareous dinocysts and sponge spicules (Hughes *et al.*, 2008). *Lenticulina* is associated with finer–grained lithologies including mudstones and wackestones (Hughes *et al.*, 2008). It must be noted that *Lenticulina* is a highly variable genus with species being identified by overall shape, degree of uncoiling and surface ornamentation; mostly characters that may not be assessed using thin-sections.

***Stratigraphical Range*:** The stratigraphical range of *Lenticulina* is given as Triassic to Recent by Loeblich and Tappan (1987).

Family **POLYMORPHINIDAE** d'Orbigny, 1839

Subfamily **POLYMORPHININAE** d'Orbigny, 1839

Genus ***Pyrulinoides*** Marie, 1941

Pyrulinoides sp.

Plate 19, Figure A.

***Diagnosis*:** *Pyrulinoides* is characterized by a biserial, elongate, fusiform test that tapers at both ends. Later chambers show rapid enlargement and the last two chambers occupy three quarters of the test size. The wall is thin, radial, and calcareous with a smooth surface.

***Remarks*:** *Pyrulinoides* sp. is given as the informal name for the polymorphinids by Kuznetsova *et al*. (1996), Hughes (2000a), Kobayashi and Vuks (2006), Hughes (2008), Hughes *et al.* (2008a and 2008b) and Olszewska (2010). It is often associated with the foraminifera and other microfossils associated with *Lenticulina* sp. in the *Lenticulina*-spicules biofacies. The palaeoenvironment of *Pyrulinoides* sp. is moderate to deep, normal marine conditions located in the middle to outer ramp, or the intra-shelf basin, facies (Hughes, 2000a, 2008).

***Stratigraphical Range*:** According to Loeblich and Tappan (1987) this genus ranges from Upper Triassic (Rhaetian) to Lower Oligocene.

Family **NODOSARIIDAE** Ehrenberg, 1838

Subfamily **NODOSARIINAE** Ehrenberg, 1838

Genus ***Nodosaria*** Lamarck, 1812

Nodosaria spp.

Plate 19, Figure B, Plate 20, Figure A.

***Diagnosis*:** *Nodosaria* spp. has an elongate test with uniserial chambers that are globular, and rectilinear or oval in shape. The sutures are often depressed and constricted. The wall is radial, perforate, calcareous or hyaline and the external surface is often ornamented.

***Remarks*:** The test is usually small and often fragmentary. It is associated with foraminifera and other microfossils, including *Lenticulina* sp., in the *Lenticulina*-spicules biofacies. The palaeoenvironment of *Nodosaria* spp. is moderate to deep, normal marine conditions located in the middle to outer ramp or the intra-shelf basin (Hughes, 2000a and 2008).

***Stratigraphical Range*:** The genus ranges from Lower Jurassic to Holocene (Loeblich and Tappan, 1987).

SubOrder **MILIOLINA** Delage and Hérouard, 1896

Superfamily **CORNUSPIRACEA** Schultze, 1854

Family **OPHTHALMIDIIDAE Wiesner, 1920**

Genus ***Ophthalmidium*** Kübler and Zwingli, 1870

Ophthalmidium sp.

Plate 21, Figures A-F, Plate 22, Figure A.

1968 *Ophthalmidium minima* Tappan; Neagu, p. 572, pl. 4, fig. 20.

2006 *Ophthalmidium* sp. (Kübler and Zwingli); Kobayashi and Vuks: p 841, fig. 6.22.

2010 *Ophthalmidium* sp. (Kübler and Zwingli); Ivanova and Kolodziej: p 25, pl. 2, fig. 20.

***Diagnosis*:** *Ophthalmidium* sp. is a small, elongate miliolid with an oval shape. The proloculus is flat and inflated followed by tubular chambers that are planispirally coiled; each chamber is rapidly enlarging, overlapping the earlier chambers; the wall is porcelaneous with a variable thickness; the last chamber often has a long neck, tapering to the aperture.

***Remarks*:** This genus is recorded by Hughes (2008) and has been shown to prefer external platform zones such as slope and deep slope environments (Haas *et al.*, 2006). This species is often associated with *Nodobacularia* sp., *Nubecularia* sp., *Crescentiella morronensis* forma *morronensis* (Crescenti, 1969) and *Terebella* sp. cf.*T. lapilloides* Münster (1833).

***Stratigraphical Range*:** It ranges from Berriasian to Barremian (Neagu, 1968; Kobayashi and Vuks, 2006).

Family **CORNUSPIRIDAE** Schultze, 1854

Subfamily **MEANDROSPIRINAE** Saidova, 1981

Genus ***Meandrospira*** Loeblich and Tappan, 1946

Meandrospira favrei (Charollais *et al.*, 1966)

Plate 22, Figures B-F, Plate 23, Figures A-B.

1966 *Citaella? favrei*: Charollais *et al.*, pp. 37-47, pl. 2, figs 3, 4, pl. 3, figs 1-5, pl. 5, figs 1, 2; text-figs 4-6.

1995 *Meandrospira, favrei* (Charollais *et al.,* 1966): Bucur *et al*., p. 367, pl. V, figs 13-15.

2008 *Meandrospira favrei* (Charollais *et al.,* 1966); Ivanova *et al.*, p. 72, fig. 7n-o.

2010 *Meandrospira favrei* (Charollais *et al.,* 1966); Ivanova and Kolodziej, p. 25, pl. 2, figs 8-9.

***Diagnosis*:** A species of *Meandrospira* with a very small test; the proloculus is followed by a spirally enrolled tubular secondary chamber; later stages of enrolment possess bends and tend to follow meandering-planispiral coiling; wall

calcareous, porcelaneous, imperforate and of uniform, thin thickness; second chamber cross section is small and rounded.

Remarks: The appearance of *Meandrospira favrei* is an indication of the Yamama Formation. It is associated with mudstones and wackestones of deeper water biofacies.

Stratigraphical Range**:** Ivanova and Kolodziej (2010), Ivanova (2008), Bucur *et al*. (1995) and Altiner (1991) all recorded this species as Valanginian in age.

Family **NUBECULARIIDAE** Jones, 1875

Subfamily **NUBECULARIINAE** Jones, 1875

Genus ***Nubecularia*** Defrance, 1825

Nubecularia spp.

Plate 23, Figures C-F, Plate 24, Figures A-F.

1995 *Nubecularia* sp. Bucur *et al*., p. 362, pl. 3, fig. 12.

1996 unidentified miliolids; Bucur *et al*., p. 70; pl. 2, figs 7-17.

Diagnosis**:** Encrusting species of *Nubecularia* with a porcelaneous, calcareous wall; the proloculus is followed by a number of uncoiled whorls with few chambers.

Remarks**:** *Nubecularia* spp. is common in the deeper water facies of the Sulaiy Formation. It is associated with fine pellet grainstones of subtidal, marine facies. In thin section it is impossible to identify the species that are found in ‘normal’ residues. It appears irregularly and randomly coiled, especially the last few chambers which often become uncoiled.

***Stratigraphical Range*:** The genus has a range of Jurassic to Holocene (Loeblich and Tappan, 1987).

Sub Family **NODOBACULARIINAE** Cushman, 1927

Genus ***Nodobacularia*** Rhumbler, 1895

Nodobacularia n. sp.

Plate 25, Figures A-C.

***Observation*:** This is a new species of *Nodobacularia* found in from the Sulaiy Formation. This species has a characteristic morphology, wall structure and composition.

***Diagnosis*:** A species of *Nodobacularia* with a bilamellar test. The internal micro−layer is five to six times thicker than the external micro−layer. The internal micro−layer is composed of imperforate, porcelaneous calcite while the thin, external micro−layer is composed of very finely agglutinated materials of *Crescentiella morronensis* forma *morronensis* (Crescenti 1969). The early coiling is triloculine of the early three chambers followed by an uncoiled, uniserial, semi-rectilinear, elongate, tubular to ovate overlapping chambers which taper at the end. The chamber sizes are gradually increasing in the uniserial semi-rectilinear part, although the last chamber is often broken.

***Remarks*:** This species is easily confused with the associated problematica *Crescentiella morronensis* which can be distinguished from *Nodobacularia* sp. by its early zig-zag chamber arrangement and the thick agglutinated wall. The size in the best specimen is 0.2 mm width by length of 0.81 mm. *Nodobacularia* (Rhumbler, 1985) has not previously been reported from Tethyan carbonate

rocks. According to Loeblich and Tappan (1987), it is found in the Lower Cretaceous sedimentary rocks of England and Germany (e. g., Carter and Hart, 1977). The species is often associated with *Nubecularia* spp.

***Stratigraphical Range*:** This genus has never been reported from Tethyan carbonate successions. The specimen was found in the lower part of Lower Ratawi of Sulaiy Formation in which it is believed to be of late Tithonian to Berriasian age. It was only found in Well-H in this study.

Superfamily **MILIOLACEA** Ehrenberg, 1839

Family **HAUERINIDAE** Schwager, 1876

Subfamily **HAUERININAE** Schwager, 1876

Genus ***Derventina*** Neagu, 1968

Derventina filipescui Neagu, 1968

Plate 25, Figures D-F, Plate 26, Figure A.

1968 *Derventina filipescui* Neagu, pp. 566, 568 , pl. 5, figs 1-13, pl. 7, figs 4-6.

1995 *Derventina filipescui* Neagu; Bucur *et al*., p. 362, pl. 3, fig. 5.

***Diagnosis*:** A species of *Derventina* with a flat-sided, discoidal test. The early stage shows quinqueloculine coiling, which is later followed by a planispiral coil; the wall is calcareous imperforate and porcelaneous.

***Remarks*:** *Derventina filipescui* is associated with *Meandrospira favrei*. Its appearance is indicative of the base of the Yamama Formation. It is associated with mudstones and wackestones of a deeper water biofacies.

Stratigraphical Range: This species ranges from Valanginian to Lower Aptian according to Bucur *et al*. (1995).

Genus ***Istriloculina*** Neagu, 1984

Istriloculina emiliae Neagu, 1984

Plate 26, Figures B-C.

1984 *Istriloculina emiliae* Neagu, p. 88, pl. 2, figs 22-25.

1995 *Istriloculina* sp (Neagu); Bucur *et al*., p 362, pl. 3, figs 14-15.

2008 *Istriloculina emiliae* Neagu; Ivanova *et al.*, p. 72, fig.7 k.

2010 *Istriloculina emiliae* Neagu; Ivanova and Kolodziej, p. 14, pl. 2, figs 24-26.

2014 *Istriloculina emiliae* Neagu; Dragastan *et al.*, p. 251, pl. IV, fig. 4.

***Diagnosis*:** *Istriloculina emiliae* varies from globular to subglobular in shape; the coiling in the first stage is quinqueloculine followed by an adult stage of semi-triloculine to biloculine coiling; each whorl has three chambers without floors; wall is porcelaneous, calcareous;

***Remarks*:** Uncommon in the Sulaiy Formation, it is associated with other miliolid species.

***Stratigraphical Range*:** The age is Tithonian to Barremian according to Ivanova and Kolodziej (2010).

Istriloculina eliptica (Iovcheva, 1962)

Plate 26, Figures D-E.

1962 *Pyrgo eliptica* Iovcheva; p. 52, pl. 2, figs 7-11.

1986 *Istriloculina elliptica* (Iovcheva); Neagu, p. 344, pl. 5, figs 25-34, figs 6a-m.

2010 *Istriloculina eliptica* (Iovcheva); Ivanova and Kolodziej, p 14, pl. 2, figs 22-23.

***Diagnosis*:** *Istriloculina eliptica* test is elongate to ovate in shape; early coiling is quinqueloculine followed by an adult stage of semi triloculine to biloculine coiling; last whorl has two chambers; wall is thin porcelaneous calcareous.

***Remarks*:** This species is rare in the Sulaiy Formation where it is associated with other miliolid species.

***Stratigraphical Range*:** The range is reported as Middle Berriasian to Aptian by Ivanova and Kolodziej (2010).

Genus ***Quinqueloculina*** d'Orbigny, 1826

Quinqueloculina egmontensis Lloyd, 1962

Plate 26, Figure F, Plate 27, Figures A-F.

1962 *Quinqueloculina egmontensis*, Lloyd, p. 376, pl. 2, fig. 7a-c.

1985 *Rumanoloculina robusta* (Neagu); Neagu, p. 213, pl. 5, figs 21-24.

1991 *Quinqueloculina robusta* Neagu; Altiner, pl. 10, figs 1-4.

1995 *Rumanoloculina robusta* (Neagu); Bucur *et al*., p 362, pl. 3, figs 6-9.

1996 Unidentified miliolids Bucur *et al*., p 66, pl. 1, figs 13, 16.

1999 *Rumanoloculina robusta* (Neagu); Ivanova, pl. 2, figs 9, 10.

2006 *Quinqueloculina podlubiensis* Terestschuk; Kobayashi and Vuks, p 841, fig. 6.

2007 *Decussoloculina barbui* Neagu*;* Krajewski and Olszewska, p. 303, fig. 7, d.

2007 *Quinqueloculina semisphaeroidalis* Danitsch; Krajewski and Olszewska, p. 303, fig.7, h.

2007 *Rumanoloculina mitchurini* Dain; Krajewski and Olszewska, p. 304, fig. 7, e.

2007 *Rumanoloculina verbizhiensis* (Dulub); Krajewski and Olszewska, p. 305, fig. 7, i, j.

2008 *Quinqueloculina robusta* Neagu; Ivanova *et al*., p 72, fig. 7.c-d.

2010 *Quinqueloculina egmontensis* Lloyd; Ivanova and Kolodziej, p. 25, pl. 2, figs 29-36.

***Diagnosis*:** A species of *Quinqueloculina* with an oval to globular test and a rounded periphery with quinquloculine coiling. Chamber walls are thickened at every newly added chamber. The wall is secreted calcareous, porcelanous type. In thin-sections, the *Q. egmontensis* aperture is difficult to recognize.

***Remarks*:** *Quinqueloculina egmontensis* was renamed with several synonyms and subdivided into different *Quinqueloculina* species that share the same morphological characteristics. In thin section, all of these synonyms will be treated as *Q. egmontensis* due to difficulties in recognition of clear differences between them. These synonyms are summarized and discussed in Ivanova and Kolodziej (2010, p. 15) and include the following: *Quinqueloculina rubusta* Neagu (1968)*, Rumanoloculina robusta* Neagu (1968), *Quinqueloculina podlubiensis* Terestschuk (1964), and *Decussoloculina barbui* Neagu (1968). *Quinqueloculina egmontensis* is usually associated with other miliolids in lagoonal palaeoenvironments. It is common in the middle to upper part of the Sulaiy Formation.

***Stratigraphical Range*:** it is recorded from Uppermost Oxfordian to Albian by Ivanova and Kolodziej (2010).

Quinqueloculina spp.

Plate 28, Figures A-F.

***Remarks*:** These are all *Quinqueloculina* species that are not easy to speciate and all representing mainly a lagoonal palaeoenvironment.

Superfamily **DISCORBACEA** Ehrenberg, 1838

Family **DISCORBIDAE** Ehrenberg, 1838

Genus ***Mohlerina*** Bucur *et al.* 1996

Remarks: The genus *Mohlerina* was re-named and re-classified by Bucur *et al*. (1996) and included in the Family Discorbidae (Ehrenberg, 1838), Suborder Rotaliina (Delage and Hérouard, 1896), under the old name of *Conicuspirillina* (Cushman, 1927). Loeblich and Tappan (1987) based their views on the characteristics of its wall and inner microstructure. Dragastan (2011) suggested retaining *Mohlerina* (Bucur *et al*., 1996) in the Family Spirillinidae (Reuss and Fritschm, 1861) as a re-named genus in Loeblich and Tappan (1987). However, he also suggested that the genus might be placed in the Subfamily Polymorphininae of the Family Lagenidae (Dragastan, 2011).

Mohlerina basiliensis (Mohler, 1938)

Plate 29, Figures A-C.

1938 *Conicospirillina basiliensis* Mohler, p. 27, pl. 4, fig. 5.

1988 *Conicospirillina basiliensis;* Mohler; Bucur, pp. 380-382, pl. 2, figs 27-28.

1991 *Conicospirillina basiliensis* Mohler; Altiner, pp. 171, 173, pl. 3, figs 8, 9; pl. 7, figs 6-8.

1996 *Mohlerina basiliensis* (Mohler); Bucur *et al*., pp. 73, 75, pl. 3, figs 3-6; pl. 4, figs 2,3, 5-9.

1999 *Mohlerina basiliensis* (Mohler)*;* Schlagintweit and Ebli, p. 400, pl. 6, figs 1-2.

2005 *Mohlerina basiliensis* (Mohler); Bucur and Săsăran, p. 36, pl. II, fig. 12

2007 *Mohlerina basiliensis* (Mohler); Krajewski and Olszewska, p. 305, fig. 8a.

2008 *Mohlerina basiliensis* (Mohler); Vedrine, p. 5, pl. 1, figs 1-13. .

2008 *Mohlerina basiliensis (*Mohler); Ivanova *et al*., p. 71, fig. 6.n-q.

2010 *Mohlerina basiliensis (*Mohler); Olszewska, p. 43, pl. II, fig. 4.

2010 *Mohlerina basiliensis* (Mohler); Ivanova and Kolodziej, p. 31, pl. 5, figs 12-18.

Diagnosis: A species of *Mohlerina* that is multi-locular, in a low trochospiral coil. The spiral side is convex and the umbilical side concave (Bucur *et al.,* 1996). In thin section, the chambers vary in shape from oval to rounded shape to arched or semi-circular. The test wall is composite, with an external lamellar, fibrous to radial calcitic hyaline type of wall with an internal, thin, micrite micro-layer.

Remarks**:** *Mohlerina basiliensis* is associated with microfossils from deep ramp to basinal biofacies (Murillo-Muneton and Dorobek, 2003; Hughes and Naji, 2008) in particular the *Lenticulina*-Spicule biofacies. It is associated with small foraminifera including *Nodosaria* spp*., Astacolus* spp. and polymorphinids spp. Agglutinated foraminifera are also associated with this species, including *Kurnubia palastiniensis, Nautiloculina oolithica, Pseudocyclammina lituus, Praedorothia* sp., *Protomarssonella kummi, Gaudryina ectypa, Verneuilina minuta* and *Gaudryinella.* Other, deeper marine microfossils, can also be associated, including calcareous dinocysts and sponge spicules (Hughes *et al.*, 2008a). It is associated with finer lithologies including mudstones and wackstones (Hughes *et al.*, 2008a).

***Stratigraphical Range*:** It ranges from Oxfordian to Valanginian according to Ivanova and Kolodziej (2010) and Olszewska (2010).

Sub Order **TEXTULARIINA** Delage and Hérouard, 1896

Superfamily **HORMOSINACEA** Haeckel, 1894

Family **HORMOSINIDAE** Haeckel, 1894

Subfamily **REOPHACINAE** Cushman, 1910

Genus ***Reophax*** de Montfort, 1808

Reophax spp.

Plate 29, Figures D-E.

***Diagnosis*:** *Reophax* has an agglutinated, elongated test of uniserial chambers; chambers are inflated to globular; wall thickness varies depending on the agglutinated materials used in the test; the cemented materials contain a variety of grains and other materials.

***Stratigraphical Range*:** The overall stratigraphical range is Middle Ordovician to Holocene (Loeblich and Tappan, 1987), and so the genus (or species) has limited stratigraphical value.

Superfamily **LITUOLACEA** de Blainville, 1827

Family **HAPLOPHRAGMOIDIDAE** Maync, 1952

Genus ***Haplophragmoides*** Cushman, 1910

Haplophragmoides joukowskyi Charollais *et al.* 1966

Plate 29, Figure F, Plate 30, Figures A-F.

1966 *Haplophragmoides joukowskyi* Charollais *et al.,* pp. 32, 33, 54, pl. II, figs 1,5,7. text-figs 2, 3.

1995 *Haplophragmoides joukowskyi* Charollais *et al.*; Bucur *et al*., p. 367, pl. VI, figs 9, 11-12.

2005 *Haplophragmoides joukowskyi* Charollais *et al.*; Bucur and Săsăran: p. 38, pl. IV, figs 1-2.

2007 *Haplophragmoides joukowskyi* Charollais *et al.*; Bruni *et al*., p. 54, pl. III, figs 9, 3-4.

2008 *Haplophragmoides joukowskyi* Charollais *et al.*;Ivanova *et al.,* p. 72, fig. 7. I.

2010 *Haplophragmoides joukowskyi* Charollais *et al.*;Olszewska, p.20, pl. VI, fig. 9.

2014 *Haplophragmoides joukowskyi* Charollais *et al.*;Bucur *et al*., p. 205, pl. 3, figs A-G.

***Diagnosis*:** Test is spherical in horizontal section; it is planispirally coiled, involute; biumbilical less flattened sides; chambers are sub-globular and enlarging slowly with growth; wall is thinly agglutinated.

***Remarks*:** The appearance of *Haplophragmoides joukowskyi* supports the identification for for the base of the Yamama Formation. It is often associated with *Meandrospira favrei.*

***Stratigraphical Range*:** Its range is given as Berriasian to Valanginian by Olszewska (2010).

Family **NAUTILOCULINIDAE** Loeblich and Tappan, 1985

Genus ***Nautiloculina*** Mohler, 1938

Remarks: The systematic classification used here is based on Loeblich and Tappan (1987). Kaminski (2004) has relocated the genus *Nautiloculina* (Mohler, 1938) and the Family Nautiloculinidae (Loeblich and Tappan, 1985) as a sub-

division of the Superfamily Nezzazatacea (Hamaoui and Saint-Marc, 1970) within the Suborder Nezzazatina.

Nautiloculina bronnimanni Arnaud-Vanneau and Peybernes, 1978

Plate 31, Figures A-D.

1978 *Nautiloculina bronnimanni* Arnaud-Vanneau and Peybernes; p. 70, pl. 1, figs 6-8; pl. 2, figs 4-11.

1983 *Nautiloculina bronnimanni* Arnaud-Vanneau and Peybernes; Darsac, p. 208, pl. 6, figs 26-27.

1989 *Nautiloculina bronnimanni* Arnaud-Vanneau and Peybernes; Arnaud-Vanneau and Masse, p. 264, pl. 1, fig. 9.

2003 *Nautiloculina bronnimanni* Arnaud-Vanneau and Peybernes; Dragastan and Richter, p. 93, pl. 1, fig. 2; pl. 9, figs 10, 11, 16.

2004 *Nautiloculina broennimanni* Arnaud-Vanneau and Peybernes; Bucur *et al*., pl. 3, fig. 22.

2004 *Nautiloculina bronnimanni* Arnaud-Vanneau and Peybernes; Ivanova and Kolodziej, fig. 1 D.

2005 *Nautiloculina cretacea* Peybernes; Olszewska, p.35, pl. 4, fig. 3.

2007 *Nautiloculina bronnimanni* Arnaud-Vanneau and Peybernes; Krajewski and Olszewska, p. 297, fig. 4 H.

2008 *Nautiloculina* cf. *bronnimanni* Arnaud-Vanneau and Peybernes; Husseini & Conrad, p. 229, pl. 6, fig. K.

2010 *Nautiloculina bronnimanni* Arnaud-Vanneau and Peybernes; Ivanova and Kolodziej, p. 25, pl. 2, figs 2-4.

2010 *Nautiloculina cretacea* Peybernes (1976); Olszewska, p. 49, pl. V, fig. 10.

Diagnosis: *N. bronnimanni* is multi-chambered, planispiral and involute with five complete whorls. Wall is canalicular agglutinated.

***Remarks*:** The axial plane of the test is oval while the transverse plane is ellipse. Sutures are depressed and canalicular. Chambers are quadrangular in

shape and the periphery last chamber is symmetrical, acute. The septum is approximately about 40º perpendicular to the whorl surface. *Nautiloculina bronnimanni* Arnaud-Vanneau & Peybernes (1978) has another synonym which is *Nautiloculina cretacea* Peybernes (1976).

***Stratigraphical Range*:** Using data from several authors' the range of *Nautiloculina bronnimanni* is Berriasian to Hauterivian. Other ranges recorded are:

- From Berriasian to Upper Albian by Arnaud-Vanneau and Peybernes (1978) from the Pyrénées between France and Spain.
- Berriasian by Altiner (1991) from Turkey.
- Berriasian to Aptian by Bucur *et al.* (1995) from Eastern Serbia.
- Ivanova and Kolodziej (2004) followed the age range by Arnaud-Vanneau and Pyrénées Mountains (1978).
- From Berriasian to Hauterivian by Krajewski and Olszewska (2007) from Southern Ukraine.
- Berriasian to Lower Valanginian by Ivanova *et al.* (2008) from SW Bulgaria.
- Berriasian to Hauterivian by Olszewska (2010) from Southeast Poland.

Nautiloculina oolithica Möhler, 1938

Plate 31, Figures E-F, Plate 32, Figures A-B.

1938 *Nautiloculina oolithica* Möhler; pp. 18, 19, pl. 4, figs 1-3; text-fig. 6. (Ellis and Messina 1941-2011).

1988 *Nautiloculina oolithica* Möhler; Loeblich and Tappan, p. 71, pl. 54, figs 10-12.

2004 *Nautiloculina oolithica* Möhler; Hughes, p. 88, pl. 6. figs 5-6.

2006 *Nautiloculina oolithica* Möhler; Kobayashi and Vuks, p. 838, figs 4.1-4.

2007 *Nautiloculina oolithica* Möhler; Krajewski and Olszewska, p. 296, fig. 4H.

2008 *Nautiloculina oolithica* Möhler; Omana and Gonzalez Arreola, p. 810, fig. 9d.

2008 *Nautiloculina oolithica* Möhler; Hughes *et al.,* p. 27, pl. 1, figs 6-8.

2010 *Nautiloculina oolithica* Möhler; Olszewska, p. 45, pl. III, fig. 2.

***Diagnosis*:** An involute, planispiral species of *Nautiloculina*. The final whorl contains 14 chambers, the penultimate whorl 12 chambers and the proceeding whorl about 10 chambers. The outer shape of an axial plane section is circular and the transverse section is elliptical. Sutures in the early whorls are radial but in the last whorl they are oblique to the wall surface. The early chambers are globular in shape and the later chambers are gradually decreasing in size, with smaller chambers in each whorl. The wall is single-layered, calcareous and microgranular, almost appearing similar to an agglutinated form. Chambers are symmetrical and semi-circular in shape.

***Remarks*:** *Nautiloculina oolithica* is usually encountered from facies within the intra-shelf basin from shallow lagoonal to back bank and often in association *Kurnubia palastiniensis,* echinoid fragments*,* calcareous algae and *Quinqueloculina* spp. (Hughes *et al.*, 2004c).

Stratigraphical Range: The best reported age range is from Bajocian to Maastrichtian by Kobayashi and Vuks (2006) from the Kanto Mountains of Japan. Other recorded ranges from other authors include the following:

- Late Oxfordian to Berriasian by Krajewski and Olszewska (2007) in Southern Ukraine.
- Berriasian to Valanginian by Husseini and Conrad (2008) in SW Iran.
- Middle Jurassic to Lower Cretaceous by Olszewska (2010) from South-east Poland.

Family **MAYNCINIDAE** Loeblich and Tappan, 1985

Genus ***Freixialina*** Ramalho, 1969

Freixialina planispiralis Ramalho, 1969

Plate 32, Figures C-D.

1969 *Freixialina planispiralis* Ramalho; p. 37, pl. 2, fig.1.

2006 *Freixialina planispiralis* Ramalho; Kobayashi and Vuks, p. 838, figs 4.5-10.

2008 *Freixialina planispiralis* Ramalho; Boudagher-Fadhel, p. 165, pl. 4.3, fig. 3.

2008 *Freixialina planispiralis* Ramalho; Omana and Gonzalez Arreola, p. 810, fig. 9g.

2010 *Freixialina planispiralis* Ramalho; Ivanova and Kołodziej, p. 8, pl. 2, fig. 1.

***Diagnosis*:** The test of *Freixialina planispiralis* is evolute, planispirally coiled; overall shape is discoidal; total number of chambers can reach 16 in the last whorl with a rapid enlargement in size; the septa of each chamber represents curved and oblique sutures; wall is agglutinated non-canalicular.

***Remarks*:** *Freixialina planispiralis* is reported for the first time in Saudi Arabia. Loeblich and Tappan (1987) noted that the difference from *Daxia* is that genus has a non-planispiral, evolute test. Loeblich and Tappan (1987) also noted that *Freixialina planispiralis* is older and may be an ancestor of *Daxia*.

***Stratigraphical Range*:** The range given by Ivanova and Kołodziej (2010, p. 8) is Kimmeridgian to Barremian based on the recorded ranges from a number of different authors.

Family **LITUOLIDAE** de Blainville, 1827

Subfamily **AMMOMARGINULININAE** Podobina, 1978

Genus ***Ammobaculites*** Cushman, 1910

Ammobaculites sp. aff. *celatus* Arnaud-Vanneau, 1980

Plate 32, Figures E-F.

1980 *Ammobaculites celatus* Arnaud-Vanneau, pp. 320-325, pl. 63, figs 8-9, text-figs 107-109.

1995 *Ammobaculites celatus* Arnaud-Vanneau; Ivanova *et al*.; p. 215, pl. 1, fig. 6.

1999 *Ammobaculites* sp. aff. *celatus* Arnaud-Vanneau; Schlagintweit and Ebli, p. 397, pl. 5, figs 5-6.

2008 *Ammobaculites celatus* Arnaud-Vanneau; Ivanova *et al.:* p 72, fig. 7.v.

2013 *Ammobaculites* sp.; Bucur *et al*., p. 28, fig. 4 I.

***Diagnosis*:** *Ammobaculites* sp. aff. *celatus* is small and characterized by an elongate test; the early growth stage is rounded, coiled while later stages are uniserial, uncoiled; chambers rectilinear with slightly twisted sutures; the wall is made of medium to large−sized coa3rse agglutinated material.

***Remarks*:** *Ammobaculites celatus* is well known from the Aptian stage and it may extend back to the Valanginian where this species is encountered. This is the first record in Saudi Arabia. In this study, the first appearance indicates the

base of the Yamama Formation. This may not be a correct interpretation as some authors have recorded it from the Upper Tithonian.

***Stratigraphical Range*:** The recorded range is from the Upper Tithonian to Aptian. This age range is based on information from the following authors:

- Aptian by Arnaud-Vanneau and Premoli Silva (1995) from Japan.
- Aptian recorded by Schlagintweit and Ebli (1999) from the Northern Alps.
- Upper Tithonian to Aptian by Ivanova *et al.* (2008) from SW Bulgaria.

Ammobaculites subcretaceus Cushman and Alexander, 1930

Plate 33, Figures A-D.

1930 *Ammobaculites subcretaceus* Cushman and Alexander, p. 6, pl. 2, figs 9-10.

1950 *Ammobaculites subcretaceus* Cushman and Alexander, Loeblech and Tappan, p. 7, pl. 1.1, figs 21a, 22.

2008a *Ammobaculites* sp., Hughes, p. 76, fig.10.2.

2010 *Ammobaculites subcretaceus* Cushman and Alexander, Ivanova and Kołodziej, p. 23, pl. I, figs 14-15.

2013 *Ammobaculites* sp.; Bucur *et al*., p. 28, figs 4 K, N, W.

***Diagnosis*:** *Ammobaculites subcretaceus* is characterised by a free, elongate, medium sized test; first stage whorl is made of up to five chambers; later stage is uniserial and uncoiled; chambers are rectilinear; wall is finely agglutinated with medium thickness

***Remarks*:** *Ammobaculites subcretaceus* is encountered in the deeper, lagoonal shelf facies (Hughes, 2008a).

***Stratigraphical Range*:** This species ranges from Oxfordian to Cenomanian according to Ivanova and Kołodziej (2010).

Superfamily **BIOKOVINACEA** Gusic, 1977

Family **CHARENTIIDAE** Loeblich and Tappan, 1985

Genus ***Charentia*** Neumann, 1965

Charentia cuvillieri Neumann, 1965

Plate 33, Figure E.

1965 *Charentia cuvillieri* Neumann, p. 63, pl. 2, figs 6-12.

1985 *Charentia cuvillieri* Neumann; Loeblich and Tappan, p. 96, pl. 3, figs 1-13.

1987 *Charentia cuvillieri* Neumann; Loeblich and Tappan, p. 89, pl. 78, figs 1-10., pl. 79, figs 1-3.

1995 *Charentia cuvillieri* Neumann; Bucur *et al.*, p. 359. pl. 1, figs 10-11.

1999 *Charentia cuvillieri* Neumann; Schlagintweit and Ebli, p. 397, pl. 5, figs 1-3.

2008 *Charentia cuvillieri* Neumann; Ivanova *et al*., p. 72; fig. 7.g-h.

2008 *Charentia cuvillieri* Neumann; Boudagher-Fadhel, p. 226, pl. 5.5, fig. 12.

2010 *Charentia cuvillieri* Neumann; Ivanova and Kołodziej, p. 27, pl. III, figs 5-10.

***Diagnosis*:** *Charentia cuvillieri* has a lenticular, planispirally coiled test; the early stage is planispirally coiled; the last whorl is semi-uncoiled with at least two chambers; wall is fine grained, agglutinated.

***Remarks*:** This species is reported for the first time in Saudi Arabia. It is encountered in the shallow to deeper lagoonal facies and in the lagoon bank.

***Stratigraphical Range*:** Ivanova and Kołodziej (2010, p. 9) give a range of Upper Tithonian to Cenomanian. Other age ranges are recorded as Berriasian-Valanginian (Ivanovna *et al*., 2008), and Tithonian to Cenomanian (Kuznetsova *et al.*, 1996; *Bucur et al*., 1995).

Charentia evoluta (Gorbatchik, 1968)

Plate 33, Figure F, Plate 34, Figure A.

1968 *Tonasia evoluta* Gorbatchik, pp. 8-9, pl. 2, figs 1-5.

2006 *Charentia evoluta* (Gorbatchik); Kobayashi and Vuks, p. 838, figs 4.27-32.

2008 *Charentia evoluta* (Gorbatchik), Olszewska *et al.*, p. 44, fig. 7.S.

2007 *Charentia evoluta* (Gorbatchik); Krajewski and Olszewska, p. 298, figs 5. G,H.

2011 *Charentia evoluta* (Gorbatchik); Olszewska *et al.*, pl. VI, figs 1-2.

2011 *Charentia evoluta* (Gorbatchik); Bucur *et al.,* p. 86, pl. IV, fig.11.

***Diagnosis*:** The test of *Charentia evoluta* is large asymmetrical discoidal to lenticular; early stage is planispiral which then becomes uniserial coiling to uncoiled; chambers are rectilinear, arranged with very weak septal to non-septal depressions between chambers; in the final uncoiled stage, chambers are extremely enlarged and septa are well developed between chambers; there are four chambers in the last whorl.

***Remarks*:** This species is reported for the first time in Saudi Arabia. It is encountered in the shallow to deeper lagoonal facies and in the lagoon bank.

***Stratigraphical Range*:** This species is recorded as ranging from Upper Kimmeridgian to Valanginian (Olszewska *et al.*, 2011). Kuznetsova *et al.,*

(1996), gives a range of “Neocomian” in Syria but this stratigraphic term is too vague and the Sub-Commission on Cretaceous Stratigraphy has rejected its use.

Family **MONTSALEVIIDAE** Zaninetti *et al.*, 1987

Genus ***Montsalevia*** Zaninetti *et al.*, 1987

Remarks: This new genus and new family was identified by Zaninetti *et al.* (1987). It is placed within the Superfamily Biokovinacea of the Loeblich and Tappan systematic scheme (1987). The old synonym of *Montsalevia* is *Pseudotextulariella* by Charollais *et al.* (1966). It is classified under the Family Cuneolinidae in the Superfamily Ataxophragmiacea (Loeblich and Tappan, 1987). Zaninetti *et al.* (from Kaminski, 2000) believe that it is a sub-classification from the Subfamily Sabaudiinae from the Family Cuneolinidae, and from the Superfamily Ataxophragmiacea (Loeblich and Tappan, 1987).

Montsalevia salevensis Charollais *et al.*, 1966

Plate 34, Figures B-C.

1966 *Montsalevia salevensis* Charollais *et al.*, pp. 28-34, pl. I, figs 1-5, pl. II, figs 2, 6, text-fig 1.

1995 *Montsalevia salevensis* Charollais *et al.*; Bucur *et al*., p. 364, pl. IV, figs 11-15.

2005 *Montsalevia salevensis* Charollais *et al.*; Bucur and Săsăran, p. 38, pl. IV, figs 3-8.

2006 *Montsalevia salevensis* Charollais *et al.*; Schlagintweit and Gawlick, p. 58, figs 7-8.

2007 *Montsalevia salevensis* Charollais *et al.*; Bruni *et al*., pl. III, figs 1-2.

2007 *Montsalevia salevensis* Charollais *et al.*; Krajewski and Olszewska, p. 298, fig. 5k.

2010 *Montsalevia salevensis* Charollais *et al.*; Ivanova and Kołodziej, p. 25, pl. 2, fig. 10.

2010 *Montsalevia salevensis* Charollais *et al.*; Olszewska, pl. V, fig. 1.

2014 *Montsalevia salevensis* Charollais *et al.*; Bucur *et al*., p. 204, pl. 2, figs A-I.

***Diagnosis*:** *Montsalevia salevensis* is recognized by its chamber arrangement with low height while width is greater than height; shape generally is a low, conical test that is initiated by trochospiral coiling followed by a biserial arrangement of chambers; the periphery is sub-rounded to rounded; wall formed of non-canaliculate, microgranular, calcite.

***Remarks*:** The first occurrence of *Montsalevia salevensis* is at the base of the Yamama Formation. It is recorded in the deeper lagoonal facies. It is often associated with *Haplophragmoides joukowskyi*.

***Stratigraphical Range*:** The stratigraphical range is recorded as Late Berriasian to Hauterivian (Krajewski and Olszewska, 2007; Ivanova and Kołodziej, 2010).

Superfamily **LOFTUSIACEA** Brady, 1884

Family **SPIROCYCLINIDAE** Munier-Chalmas, 1887

Genus ***Anchispirocyclina*** Jordan and Applin, 1952

Anchispirocyclina lusitanica (Egger, 1902)

Plate 34, Figures D-F, Plate 35, Figures A-E.

1902 *Dicyclina lusitanica* Egger, p. 585, pl. 7, figs 4, 11,12, 14, pl. 8, figs 1-4.

1967 *Anchispirocyclina lusitanica* (Egger); Hottinger, p. 74, pl.13, figs 6-8, text−fig. 37 A-B.

1985 *Anchispirocyclina lusitanica* (Egger); Dupeuble *et al*., p. 105, pl.3, figs 1-2.

1996 *Anchispirocyclina lusitanica* (Egger); Kuznetsova *et al.*, pp. 228, 252, pl. IX, figs 1 A-C; pl. XXI, fig. 3

1999 *Anchispirocyclina lusitanica* (Egger); Schlagintweit and Ebli, p. 397, pl. 5, fig. 9.

2007 *Anchispirocyclina lusitanica* (Egger); Krajewski and Olszewska, p. 300, figs 6 D,E.

2008 *Anchispirocyclina lusitanica* (Egger); Boudagher-Fadhel, p. 184, pl. 4.12, figs 6-7.

2009 *Anchispirocyclina lusitanica* (Egger); Hughes, pp. 140, 149, pl. 5, fig. 5.12, text-fig. 3.

2010 *Anchispirocyclina lusitanica* (Egger); Krajewski and Olszewska, pp. 29, 64, table 4.1, fig. D, table 4.14, fig. A

2011 *Anchispirocyclina lusitanica* (Egger); Dragastan, pp. 108−110, pl. 1, figs 1-7, pl. 2, figs 1-6.

2013 *Anchispirocyclina lusitanica* (Egger); Bucur *et al.*, p. 27, fig. 3 c-i.

Diagnosis: *Anchispirocyclina lusitanica* is plano-planispirally coiled with an asymmetrical, flat discoidal test; early stage is a perfect planispiral and later stage is peneropline-like coiling; chambers in the early stage are arcuate followed by cyclic chambers with a width greater than their height; the wall is non-canaliculate agglutinated, composed of calcareous grains.

***Remarks*:** This species was first described as *Dicyclina lusitanica* by Egger (1902) and then redefined and placed in the genus *Anchispirocyclina* by Hottinger (1967). It is commonly encountered in Tithonian–Berriasian sedimentary rocks of Northern Iran and Eastern Europe (Bucur *et al.*, 2013).

Anchispirocyclina lusitanica is usually associated with *Andersenolina alpina*, *Andersenolina elongata*, *Bramkampella arabica*, *Pseudocyclammina lituus*, *Mohlerina basiliensis*, *Protopeneroplis ultragranulata* and *Protopeneroplis banatica*. It is recorded in a range of sedimentary environments of shallow water

facies that are either lagoonal or intertidal (Bucur and Săsăran, 2005; Hughes, 2009).

In the past, *Anchispirocyclina lusitanica* was considered to be an index fossil for the Tithonian stage of the subsurface of the Grand Banks of Newfoundland, Canada (Gradstein, 1978). However, this was rejected by Granier and Bucur (2011) as they reported it in the younger Berriasian rocks of the Bias do Norte section in Portugal.

Anchispirocyclina lusitanica is often confused with *Anchispirocyclina neumannae* in Velic (2007) from the Late Tithonian carbonate rocks of Southern Croatia. It can also be confused with cf. *Timidonella sarda* of the Saudi, Lower Tuwaiq Mountain Formation, which is Late Callovian in age (Hughes, 2009). These other records have caused problems in the identification of a stratigraphical range for *Anchispirocyclina lusitanica*.

***Stratigraphical Range*:** This species ranges from Tithonian to Valanginian where it is encountered in the Yamama Formation. Several other authors have recorded different stratigraphcal ranges and they are:

- *Anchispirocyclina lusitanica* ranges from Tithonian to Early Berriasian according to Schlagintweit and Ebli (1999) and Krajewski and Olszewska (2007).
- From Tithonian to Valanginian which is evidenced from the associated *Protopeneroplis banatica* in Romania (Bucur and Săsăran, 2005).
- From Kimmeridgian to Valanginian by Boudagher-Fadhel (2008).

Family **CYCLAMMINIDAE** Marie, 1941

Subfamily **BUCCICRENATINAE** Loeblich and Tappan, 1985

Genus ***Everticyclammina*** Redmond, 1964

***Remarks*:** The *Everticyclammina* genus wall was described by Redmond (1964) and Banner and Whittaker (1991) to be of an alveoli agglutinated type but from thin sections they displayed this is not accepted. The wall type is seen to be a canaliculate agglutinated type. On the other hand, *Buccicrenata* is actually made alveoli, thick agglutinated wall type. Despite that, *Buccicrenata* shares all other characteristics with *Everticyclammina*. This important difference was recognized in Loeblich and Tappan (1987) and extensively explained with some new species defined and named by Dragastan (2011). The alveolar agglutinated wall type of *Everticyclammina praekelleri* (Banner and Highton, 1990, p. 8-10, pl. 1, fig. 1; pl. 3, fig. 5; pl. 4, figs 1-11) must be amended and renamed as *Buccicrenata praekelleri* (Banner and Highton).

Everticyclammina kelleri (Henson, 1948)

Plate 35, Figure F, Plate 36, Figures A-F.

1948 *Pseudocyclammina kelleri* Henson, pp. 16, 17, pl. 9, figs 4, 5, 7.

1964 *Everticyclammina elegans* Redmond, p. 411, pl. 1, figs 19-21.

1991 *Everticyclammina eccentric* Redmond; Banner and Whittaker, p. 55, pl.4, figs 4-8.

1991 *Everticyclammina elegans* Redmond, Banner and Whittaker, pp. 55, 57, pl.4, figs 9-11; pl. 5, figs 1-4.

2007 *Everticyclammina kelleri* (Henson); Krajewski and Olszewska, p. 298, fig 5.E.

2008 *Everticyclammina kelleri* (Henson); Boudagher-Fadhel, p. 186, pl. 4.13, fig. 4.

***Diagnosis*:** *Everticyclammina kelleri* is planispirally coiled, involute; the general shape is lenticular; chambers are wide and inflated almost a wedge shape; late added chamber is positioned semi-perpendicular to the previous chamber while earlier ones are sub-parallel; wall is canaliculated, thin and agglutinated; sutures are arranged radially, slightly curved; septal, pillars are short to undeveloped, arranged perpendicular to the coiling line.

***Remarks*:** The *Everticyclammina* wall was described by Redmond (1964) and Banner and Whittaker (1991) to be alveoli agglutinated type but from thin sections they illustrated this is not accepted. The wall type is seen to be of a perforated, agglutinated type.

***Stratigraphical Range*:** This species ranges from Berriasian to Hauterivian (Banner and Whittaker, 1991). More recently, Krajewski (2010) has shown the range to be Berriasian to Valanginian in the Crimea Mountains of Russia (formerly southern Ukraine).

Everticyclammina virguliana Koechlin, 1942

Plate 37, Figures A-D.

1995 *Everticyclammina virguliana* Koechlin; Bucur *et al.*, p. 359, pl. 1, figs 7- 8.

1996 *Everticyclammina virguliana* Koechlin; Bucur *et al*., p. 67; pl. 1, figs 7.

2006 *Everticyclammina virguliana* Koechlin; Kobayashi and Vuks, pp. 838, 840, figs 4.46-50; fig. 5.1.

2008 *Everticyclammina virguliana* Koechlin; Boudagher-Fadhel, p. 184, pl. 4.12, fig. 5.

2008b *Everticyclammina* sp. Koechlin; Hughes *et al*., p. 29, pl. 2, fig. 15.

2008 *Everticyclammina virguliana* Koechlin; Omana and Gonzalez Arreola, pp. 806, 809, figs 5.d., 8.d.

***Diagnosis*:** *Everticyclammina virguliana* is planispirally coiled, extremely involute, with a complete circular shape in transverse section;

Remarks: Overall, shape is lenticular; chambers are wide and inflated, similar to a wedge shape; later added chambers are positioned semi-perpendicular to the previous chamber, while earlier ones are sub-parallel; wall thinly agglutinated with alveoli; sutures are arranged slightly radial with curvature; septal pillars are short to undeveloped, arranged perpendicular to the coiling direction.

***Stratigraphical Range*:** This species ranges from Kimmeridgian to Lower Berriasian by Omana and Gonzalez Arreola (2008).

Subfamily **CHOFFATELLINAE** Maync, 1958

Genus ***Bramkampella*** Redmond, 1964

Bramkampella arabica Redmond 1964

Plate 37, Figures E-F, Plate 38, Figures A-C.

1959 ? *Haurania* sp. Dunnington *et al.,* p.306.

1964 *Bramkampella arabica* Redmond, pp. 409-412, 414, text-fig. 2 pl. 1 figs 26-29.

1987 *Bramkampella arabica* Redmond; Loeblich and Tappan, pp. 101-102, pl. 100, figs 14-18.

1991 *Bramkampella arabica* Redmond, Banner and Whittaker, p.45, pl. 2, figs 1-7.

2005 *Bramkampella arabica* Redmond; Bucur and Săsăran: p 30, pl. II, figs 6-7.

2011 *Bramkampella arabica* Redmond; Bucur and Săsăran, p 89, pl 19, figs 6-7.

***Diagnosis*:** *Bramkampella arabica* is initiated by a planispirally, involute coiling early stage that is followed by later stage, evolute and uncoiled test; wall is thick alveolar and is composed of microgranular, agglutinated material; partitions within the wall are arranged radially and can extend up to the axis; chambers are increasing in size rapidly.

Description: This species shape in thin−sections is rectilinear and circular and the test shape is conical to sub-conical. *Trochamijiella* and *Amijiela* are different from *Bramkampella* by their different early coiling stages which is initially trochospiral, while this species is planispiral and involute (Athersuch *et al*., 1992).

***Remarks*:** This species was identified and described by Redmond (1964) and found with *Everticyclammina* sp., *Anchiospirocyclina lusitanica* (Egger), *Nautiloculina* sp., *Pseudocyclammina sulaiyana* Redmond and *Trocholina* spp. It is located within the uppermost section of the Sulaiy Formation at the outcrop location of Dahl Hith (Powers *et al.*, 1966). The topotype specimen was presented by Aramco to the British National History Museum in which it was given registration numbers P47544 and P47545 (Banner and Whittaker, 1991). Other known localities in the world are the Crimea Mountains (Southern Russia), in the Berriasian successions, by Gorbatchik and Mohamad (1997). It

is reported by Noujaim Clark and Boudaher-Fadel (2001) from the Upper Berriasian-Lower Valanginian limestones of Lebanon and identified as an index fossil for the Lower Cretaceous of Lebanon. In Romania it is recovered within Upper Jurassic-Lower Cretaceous deposits from the Trascău Mountains (Bucur and Săsăran, 2005). It is associated with an assemblage that include *Andersenolina alpina, A.elongata, Anchispirocyclina lusitanica, Pseudocyclammina lituus, Neokilianina* sp*., Mohlerina basiliensis, Protopeneroplis* cf*. banatica* and *Protopeneroplis ultragranulata* (Bucur and Săsăran, 2005).

***Stratigraphical Range*:** It ranges from Upper Berriasian to Lower Valanginian and it was not reported in the Upper Jurassic by Banner and Whittaker (1991), while Bucur and Săsăran (2005) recorded it in three different depositional units that range from Kimmeridgian to Upper Tithonian and questionable Berriasian successions. Other age ranges from other authors are:

- Identified as Berriasian age by Gorbatchik and Mohamad (1997) in the Crimea Mountains (Southern Russia).
- Recorded as Upper Berriasian-Lower Valanginian by Noujaim Clark and Boudaher-Fadel (2001).

Genus ***Pseudocyclammina*** Yabe and Hanzawa, 1926

Remarks: *Pseudocyclammina* earliest coiling types vary from planispiral to rare streptospiral followed by involute, sub-spherical to flattened intermediate coiling stage and lately followed by uncoiled stage. Wall is made of coarse agglutinated materials which are perforated by large perforations. Endoskeleton wall layer

contains thick septa while the exoskeleton contains few, irregular, pillars. Stratigraphical range of this genus varies from Lower Jurassic (Domerian) to Upper Cretaceous (Coniacian) (Loeblich and Tappan, 1987).

Pseudocyclammina cylindrica Redmond, 1964

Plate 38, Figures D-F, Plate 39, Figure A.

1959 *Pseudocyclammina vasconica* Maync, p. 180, pl. 1, figs 1-9, pl. 2, figs 1-14.

1964 *Pseudocyclammina cylindrica* Redmond, pp. 411, 413, pl. 1, fig. 1, pl. 2, figs 1-2, 9.

1991 *Pseudocyclammina vasconica* Maync *cylindrica* Redmond; Banner and Whittaker, pp. 56-59, pl. 5, figs 5a-7, pl. 6, figs 1-4.

1991 *Pseudocyclammina*? sp., Altiner, pp. 204-205, pl. 12, figs 3-6.

2006 *Pseudocyclammina lituus* (Yokoyama); Kobayashi and Vuks, p. 840, fig. 5.7.

2007 *Pseudocyclammina* sp., Bruni *et al*., p. 54, pl. III, fig. 23.

2008 *Pseudocyclammina lituus* (Yokoyama); Omana and Gonzalez Arreola, p. 812, fig. 4.c-d.

2010 *Pseudocyclammina cylindrica* Redmond; Olszewska, p. 23, pl. V, fig. 6.

***Diagnosis*:** Early coiling of *Pseudocyclammina cylindrica* is thick, planispiral with wide rounded margins followed by a sub-spherical and flattened intermediate stage and which is later uncoiled forming the main cylindrical stage. Wall is composed of coarsely, agglutinated material with large perforations and coarse sub-epidermal network. Exoskeleton includes some irregular pillars and the endoskeleton wall layer includes thick septa.

***Remarks*:** The final coiling of the uniserial cylindrical uncoiled stage containing about seven to eight chambers. Chambers are inflated to slightly inflated in the planispiral stage, followed by flattened chambers in the cylindrical stage. The

sub-epidermal surface relief is thin and made of fine, mesh−like structures. Aperture is not recognizable in thin sections. This species was identified and described by Redmond (1964). It was recovered from the Yamama Formation. The holotype and paratypes were given by Arabian American Oil Company (former name of the Saudi Aramco company) to the American Museum of Natural History (slides FT-1220, FT-1221 and FT-1222).

***Stratigraphical Range*:** In Saudi Arabian deposits, *Pseudocyclammina cylindrica* ranges only from Upper Berriasian to Valanginian. This species was recovered, with common occurrence, by Arabian American Oil Company (former name of the Saudi Aramco company) from drilled wells in the lower and middle Yamama Formation (Redmond, 1964). However, other occurrences recorded by other authors indicate a range from Berriasian to Valanginian and they are:

- It is reported from Berriasian to Valanginian in South Iraq in the Ratawi Formation by Henson (1948). It was also recovered by the same author from Qatar and the United Arab Emirates.
- It was recorded from Berriasian to Valanginian in the Polish Babczyn Formation by Olszewska (2010).

Pseudocyclammina lituus Yokoyama, 1890

Plate 39, Figures B-F, Plate 40, Figures A-D.

1890 *Cyclammina lituus* Yokoyama, p. 26, pl. 5, fig. 7.

1964 *Pseudocyclammina sulaiyana* Redmond, pp. 411, 413, pl. 1, figs 9-11, pl. 2, fig. 9.

1988 *Pseudocyclammina lituus* (Yokoyama); Sartorio and Venturini, p. 92, fig, 1.

1988 *Pseudocyclammina lituus* (Yokoyama); Bucur, p. 385, pl. 1, figs 5, 11.

1991 *Pseudocyclammina lituus* (Yokoyama); Banner and Whittaker, pp. 56-59, pl. 5, figs 8-11, pl. 6, fig. 5.

1991 *Pseudocyclammina* sp., Altiner, pp 204-205, pl. 12, figs 7-8.

1995 *Pseudocyclammina lituus* (Yokoyama); Bucur *et al.,* p. 359, pl. 1, figs 3-4.

2004 *Pseudocyclammina lituus* (Yokoyama); Bucur *et al.,* p. 65, pl. 3, fig. 1.

2004b *Pseudocyclammina lituus* (Yokoyama); Hughes, p. 216, pl. 1, figs e-l.

2004 *Pseudocyclammina lituus* (Yokoyama); Ivanova and Kolodziej, p. 71, fig.1.B.

2006 *Pseudocyclammina lituus* (Yokoyama); Kobayashi and Vuks, p. 840, figs 5.7-14.

2007 *Pseudocyclammina lituus* (Yokoyama); Krajewski and Olszewska, p 301, fig. 6F.

2008 *Pseudocyclammina lituus* (Yokoyama); Ivanova *et al*., p 72, fig. 7a.

2008 *Pseudocyclammina lituus* (Yokoyama); Omana and Gonzalez Arreola, pp. 805-806, figs 4.a-b, 5.a-c.

2008 *Pseudocyclammina lituus* (Yokoyama); Hosseini and Conrad, p 227, pl. 5, fig. O.

2008b *Pseudocyclammina lituus* (Yokoyama); Hughes and Naji, p. 70, pl. 3, fig. 9.

2009 *Pseudocyclammina lituus* (Yokoyama); Hughes, p. 139.

2010 *Pseudocyclammina lituus* (Yokoyama); Ivanova and Kolodziej, p. 29, pl. IV, figs 1-10.

2010 *Pseudocyclammina lituus* (Yokoyama); Olszewska, pl. v, fig. 2.

2011 *Pseudocyclammina lituus* (Yokoyama); Bucur and Săsăran, p. 89, pl. 19, figs 1-3.

2013 *Pseudocyclammina lituus* (Yokoyama); Bucur *et al*., p. 27, fig. 3.a-.b.

***Diagnosis*:** Early coiling of *Pseudocyclammina lituus* is planispiral, followed by a sub-spherical and flattened intermediate stage with the later coiling stage is uncoiled. Sutures are oblique in all coiling stages. Wall is coarsely agglutinated with large perforations and a coarse sub-epidermal network. Exoskeleton

includes some irregular pillars and the endoskeleton wall layer includes thick septa.

***Remarks*:** It was first identified and described from Japan by Yokoyama (1890) and was also described in Saudi Arabia by Redmond (1964). He identified it as a synonym of *P. lituus* and named it *Pseudocyclammina sulaiyana.*

***Stratigraphical Range*:** *Pseudocyclammina lituus* ranges from Oxfordian to Hauterivian (Banner and Whittaker, 1991; Hughes, 2004; Ivanova and Kolodziej, 2010).

Superfamily **SPIROPLECTAMMINACEA** Cushman, 1927

Family **TEXTULARIOPSIDAE** Loeblich and Tappan, 1982

Genus ***Plectinella*** Marie, 1956

Plectinella virgulinoides Marie, 1956

Plate 40, Figures E-F, Plate 41, Figures A-E.

1956 *Plectinella* Marie, B240.

1958 *Arenovirgulina* Said and Barakat, p. 243.

1964 *Pseudobolivina* Wiesner, Loeblich and Tappan, p. C255, pl. 167, fig. 4.

1982 *Plectinella virgulinoides* Marie, Loeblich and Tappan, p. 66.

1987 *Plectinella virgulinoides* Marie, Loeblich and Tappan, p. 115, pl. 22, figs 18-23.

***Diagnosis*:** *Plectinella virgulinoides* has an irregular, biserial chamber arrangement with inflated, high chambers that are occasionally twisted; wall is non-perforate, agglutinated; aperture is areal with a tendency to be terminal.

***Remarks*:** This is the first record in Saudi Arabia. Loeblich and Tappan (1982) mentioned that *Plectinella* has two synonyms; *Arenovirgulina* (Said and Barakat, 1958) and *Pseudobolivina* (Loeblich and Tappan, 1964).

***Stratigraphical Range*:** The species is recorded from the Callovian to Maastrichtian (Loeblich and Tappan, 1982, 1987).

Genus **Textulariopsis** Banner and Pereira, 1981

Textulariopsis jurassica (Gümbel, 1862)

Plate 52, Figures C-F, Plate 53, Figures A-C.

1862 *Textilaria jurassica* Gümbel, p. 228, pl. 4, fig. 17

1996 *Textularia* sp. Bucur *et* al, p. 67; pl. 1, fig. 8.

2001 *Textulariopsis* sp. Boudagher-Fadel *et al*., p. 609, pl. 2, figs 5-7.

2008 *Textulariopsis jurassica* (Gümbel); Olszewska *et al.,* p. 48, fig. 10-J.

2010 *Textulariopsis jurassica* (Gümbel); Olszewska, p. 44, pl. 3, fig.1.

2010 *Gaudryinopsis* sp. Ivanova and Kołodziej, p. 23, pl. 1, figs 9-10.

***Diagnosis*:** *Textulariopsis jurassica* shows biserial coiling with slow enlargement of newly added chambers; later chambers are ovoid in shape. The wall is thick, solid agglutinated.

***Remarks*:** This is the first record in Saudi Arabia. The relatively unknown synonym of this genus is *Gaudryinopsis* (Podobina, 1975) which was identified and described in Loeblich and Tappan (1987).

***Stratigraphical Range*:** The first appearance may be Bajocian, with the last in the Valanginian (Olszewska, 2010).

Superfamily **VERNEUILINACEA** Cushman, 1911

Family **PROLIXOPLECTIDAE** Loeblich and Tappan, 1985

Genus ***Eomarssonella*** Levina, 1972

Eomarssonella sp.

Plate 41, Figure F, Plate 42, Figures A-D.

***Diagnosis*:** This form of *Eomarssonella* is cone-shaped, with a trochospiral early stage followed by a triserial chamber arrangement; chambers are inflated with greater height enlargement with growth; sutures are depressed; wall is non-canaliculate, agglutinated.

***Remarks*:** This form is recorded for the first time in Saudi Arabia. *Eomarssonella* sp. can be distinguished from *Praedorothia* sp. by its conical shape. The adult stage of *Praedorothia* has a biserial chamber arrangement with almost parallel sides. However, they have a solid, non-perforate agglutinated wall. *Eomarssonella* sp. is often associated with other agglutinated foraminifera such as *Nautiloculina oolithica, Pseudocyclammina lituus, Praedorothia* sp., *Protomarssonella kummi, Gaudryina ectypa, Verneuilina minuta* and *Gaudryinella* sp.

***Stratigraphical Range*:** The genus has a recorded range from Oxfordian to Berriasian (Loeblich and Tappan, 1987) but this form has no record with which to determine the stratigraphic range.

Family **TRITAXIIDAE** Plotnikova, 1979

Genus ***Bitaxia*** (Plotnikova, 1978)

Bitaxia spp.

Plate 42, Figure E.

***Diagnosis*:** *Bitaxia* has a long test with an early triserial stage and triangular shape followed by an adult, biserial, chamber arrangement; chambers have carinate corners; the wall is solid agglutinated; internal, sub-cylindrical siphon extending internally with a Y-shaped base.

Remarks: This genus is recorded for the first time in Saudi Arabia. This genus is associated with microfossils from the deep ramp to basin biofacies (Murillo-Muneton and Dorobek, 2003; Hughes *et al.*, 2008) in particular the *Lenticulina*-Spicule biofacies. It is associated with small foraminifera including *Nodosaria* spp.*, Astacolus* spp., polymorphinids and *Bolivina.* Agglutinated foraminifera that are associated with this genus are *Kurnubia palastiniensis, Nautiloculina oolithica, Pseudocyclammina lituus, Praedorothia* sp., *Protomarssonella kummi, Gaudryina ectypa, Verneuilina minuta* and *Gaudryinella.* Other deeper marine microfossils, including calcareous dinocysts and sponge spicules (Hughes *et al.*, 2008), are often associated with this genus which is characteristic of mudstones and wackestones (Hughes *et al.*, 2008).

***Stratigraphical Range*:** The range is given as Upper Tithonian to Berriasian in the Crimea, Russia (formerly Ukraine) by Olszewska (2010).

Family **VERNEUILINIDAE** Cushman, 1911

Subfamily **VERNEUILINOIDINAE** Suleymanov, 1973

Genus ***Uvigerinammina*** Majzon, 1943

Uvigerinammina uvigeriniformis (Seibold and Seibold, 1960)

Plate 42, Figure F, Plate 43, FigureS A-B

1960 *Gaudyina uvigeriniformis* Seibold and Seibold, pp. 334-335, text-fig. 8, pl. 7, fig. 4.

1995 *Uvigerinammina uvigeriniformis* (Seibold and Seibold); Neagu and Neagu, p. 218, pl. 2, figs 28-43, pl. 6, figs 11-14.

2007 *Uvigerinammina uvigeriniformis* (Seibold and Seibold); Krajewski and Olszewska, p. 297, fig. 4G.

2005 *Uvigerinammina uvigeriniformis* (Seibold and Seibold); Olszewska, p. 34, pl. 5, fig. 1.

2010 *Uvigerinammina uvigeriniformis* (Seibold and Seibold); Ivanova and Olszewska: p 23, pl. I, fig. 13.

2010 *Uvigerinammina uvigeriniformis* (Seibold and Seibold); Olszewska, p. 21, pl. V, fig. 4.

Diagnosis: *Uvigerinammina uvigeriniformis* is characterised by an irregular, triserial chamber arrangement; chambers are arranged as three per whorl and they are inflated, rapidly increasing in size; wall is non-canaliculate agglutinated fine grained; sutures are depressed.

Remarks: Kowal *et al.* (2011), in the Polish Uppermost Jurassic–Lower Cretaceous, found it associated with *Andersenolina alpina, Haghimashella arculata, Mohlerina basiliensis, Protomarssonella kummi, Protopeneroplis ultragranulata, Scythiloculina confusa, Siphovalvulina variabilis, Neotrocholina conica, Neotrocholina molesta,* and *Crassicolaria brevis.*

***Stratigraphical Range*:** The stratigraphic range of *Uvigerinammina uvigeriniformis* is Oxfordian to Lower Valangian (Olszewska, 2010). Other recorded age ranges are:

- In Romania it was first recorded by Neagu and Neagu (1995) from the Lower Kimmeridgian.
- Krajewski and Olszewska (2007) recorded its straticraphic range between Middle Oxfordian and Early Valanginian. In the Crimea Mountains (South Russia).

Genus ***Verneuilinoides*** Loeblich and Tappan, 1949

Verneuilinoides neocomiensis Mjatliuk, 1939

Plate 43, Figures C-F, Plate 44, Figure A.

1939 *Verneuilinoides neocomiensis* Mjatliuk, p. 50, pl. 1, figs 12-13.

2006 *Valvulina* spp; Kobayashi and Vuks, p. 841, fig. 6.(9, 10, 11, 14).

2010 *Verneuilinoides neocomiensis* Mjatliuk; Ivanova and Kołodziej, p. 7, pl. I, figs 1-5.

Diagnosis**:** *Verneuilinoides neocomiensis* is characterised by a triserial, elongate test with rounded sides in cross-section; chambers are inflated to globular in shape; sutures are depressed; the wall is non-canaliculate, agglutinated.

Remarks**:** This species is recorded for the first time in Saudi Arabia. It can be confused with the *Redmondoides lugeoni,* but can be differentiated by its non-perforate wall. *Redmondoides lugeoni* has a canaliculated, agglutinated, wall structure.

Stratigraphical Range**:** The range is given as uppermost Tithonian to Aptian (Ivanova and Kołodziej, 2010).

Verneuilinoides polonicus (Cushman and Glazewski, 1949)

Plate 44, Figures B-F, Plate 45, Figures A-C.

1949 *Verneuilina polonica* Cushman and Glazewski, p. 7, pl. 1, figs 14-15.

2006 *Valvulina* spp; Kobayashi and Vuks, p. 841, fig. 6.12.

2007 *Verneuilinoides polonicus* (Cushman and Glazewski); Krajewski and Olszewska, p. 306, fig. 8 B.

2008 *Verneuilinoides polonicus* (Cushman and Glazewski); Ivanovna *et al*., p. 72; fig. 7.b.

***Diagnosis*:** *Verneuilinoides polonicus* is a large agglutinated foraminifera, characterised by its triserial chamber arrangement; chambers are inflated but enlargement rate for later chambers is slower than other species; chambers are wider than high; wall is thick, non-canaliculate, agglutinated.

***Remarks*:** This is the first time this species has been recorded in Saudi Arabia. It can be confused with the *Redmondoides lugeoni* but it is can be differentiated by its solid, imperforate wall as *Redmondoides lugeoni* has a perforated, agglutinated wall.

***Stratigraphical Range*:** The range is given as Tithonian to Early Valanginian by Krajewski and Olszewska (2007).

Genus ***Siphovalvulina*** Septfontaine, 1988

Siphovalvulina variabilis Septfontaine 1988.

Plate 45, Figures D-F.

1988 *Siphovalvulina variabilis* Septfontaine, p. 245, text-fig. 5.

2006 *Siphovalvulina* sp. Septfontaine; Kobayashi and Vuks, p. 841, figs 6.1-5.

2007 *Siphovalvulina variabilis* Septfontaine, Krajewski and Olszewska. P. 301, fig. 6A.

2008 *Siphovalvulina variabilis* Septfontaine; Ivanovna *et al*., p. 71; fig. 6.r.

2010 *Siphovalvulina variabilis* Septfontaine; Ivanova and Kołodziej, p. 23, pl. I, fig. 19.

Diagnosis**:** *Siphovalvulina variabilis* is characterized by trochospiral coiling in which each whorl contains three sub-globular chambers. However, these chambers are increasing in size per newly added whorl. The internal canal suture is very depressed and it is parallel to the axes of growth.

Remarks: This species is common within shallow carbonate platforms (Olszewska, 2010).

Stratigraphical Range**:** In this research it ranges from Middle Jurassic to Upper Barremian. The first age range was reported by Septfontaine (1988) as Hettangian to Upper Barremian to? Upper Cretaceous. In contrast, it was given as Middle Jurassic to Tithonian by Krajewski and Olszewska (2007).

Subfamily **VERNEUILININAE** Cushman 1911

Genus ***Gaudryina*** d'Orbigny 1839

Gaudryina ectypa Arnaud-Vanneau 1988

Plate 46, Figure A.

1980 *Gaudryina ectypa* Arnaud-Vanneau, pp. 407-412, pl. 45, figs 2-4, pl. 70, figs 1-6, figs 152-153.

1988 *Gaudryina* cf. *ectypa* Arnaud-Vanneau; Bucur pl. 1 figs 22-23.

2004 *Gaudryina* sp. Bucur *et al.,* p.65, pl. 3 fig. 2.

***Diagnosis*:** *Gaudryina ectypa* has a long, free test with an early triserial stage and triangular shape, followed by a later biserial, chamber arrangement; the wall is non-perforate, agglutinated.

***Remarks*:** This the first time that this species is recorded in Saudi Arabia.

***Stratigraphical Range*:** The stratigraphical range of *Gaudryina ectypa* is given as Berriasian to Barremian by Bucur *et al*. (2014).

Genus ***Gaudryinella*** Plummer, 1931

Gaudryinella sp.

Plate 46, Figures B-F.

Diagnosis: *Gaudryinella* sp. is characterised by a long test that begins with a triserial chamber arrangement followed by an irregular, biserial form with a tendency to be uniserial in the last few chambers; chambers are globular, inflated, increasing rapidly with grouth; wall is finely agglutinated, non-canaliculate, sutres are depressed and it has a rough external surface.

Remarks: This is recorded in Saudi Arabia for the first time. It is very similar to the younger *Bigenerina* sp., a name that is used by mistake in some publications. In some cases it is confused with the older, *Bicazammina jurrassica* (Neagu and Neagu, 1995), which is restricted to the Lower Kimmeridgian and may possibly be an ancestral form of the genus *Gaudryinella*. It differs from this specis by the initial biserial stage, which then follows a loosely uniserial arrangement. The chamber size and shape are very similar. It is associated with microfossils from deeper lagoonal to shallow shoal (Murillo-Muneton and Dorobek, 2003; Hughes *et al*., 2008).

Stratigraphical Range: It is found within the Sulaiy Formation, which extends its age to Berriasian, although it is recorded up to the Cenomanian by Loeblich and Tappan (1987).

Genus ***Verneuilina*** d'Orbigny, 1839

Verneuilina minuta Wiesner, 1931

Plate 47, Figures A-B.

1931 *Verneuilina minuta* Wiesner, p. 99, fig. 4.10 (1, 2, 3, 5).

1996 *Verneuilina minuta* Wiesner; Bucur *et al*.: p 76; pl. 5, figs 4.

1996 *Verneuilinoides subminuta* (Gorbatchik); Kuznetsova *et al.*, p. 234, pl. XIII, fig. 6a, 6.

Diagnosis**:** *Verneuilina minuta* is characterized by its elongate test with triserial chamber arrangement; wall is agglutinated, non-canaliculate, composed of fine-grained agglutinated materials; margins are triangular, subcarinate.

Remarks**:** This species is recorded in Saudi Arabia for the first time.

Stratigraphic Range: The range is given as Upper Tithonian to Lower Aptian by Kuznetsova *et al.*(1996).

Super Family **ATAXOPHRAGMIACEA** Schwager, 1877

Family **DOROTHIIDAE** Balakhmatova, 1972

Subfamily **DOROTHIINAE** Balakhmatova, 1972

Genus ***Protomarssonella*** Desai and Banner, 1987

Protomarssonella kummi (Zedler, 1961)

Plate 47, Figures C-E.

1961 *Marssonella kummi* Zedler, pp. 31-32, pl. 7, fig. 1.

1984 *Dorothia kummi* (Zedler); Moullade, pl. 7, figs 19-20, figs 23-24, figs. 21-22.

1987 *Marssonella kummi* Zedler, Desai and Banner, p. 24, pl. 5, figs 2a-e.

2010 *Protomarssonella kummi (*Zedler); Ivanova and Kołodziej, p. 7, pl. 1, figs 11-12.

2010 *Protomarssonella kummi (*Zedler); Olszewska, p. 21, pl. V, fig. 5.

***Diagnosis*:** *Protomarssonella kummi* is characterised by an elongate narrow conical test with an early trochospiral chamber arrangment followed by a biserial chamber arrangment. Wall is non-perforate and solid, agglutinated.

***Remarks*:** This species is recorded in Saudi Arabia for the first time. A diagnostic feature is the slightly non-parallel sides in which it can differ from the *Praedorothia*. It was emended from *Marssonella* to *Protomarssonella* by Desai and Banner (1987). However, they have the same coiling mode, septa and aperture but wall is not perforated by canaliculation or alveoli.

Stratigraphic Range: The range is given as Upper Tithonian to Hauterivian by Olszewska (2010) and Upper Tithonain to Albian by Ivanova and Klodziej (2010).

Genus ***P****raedorothia* Desai and Banner, 1987

Praedorothia sp. cf. *P. praehauteriviana* (Dieni and Massari, 1966)

Plate 47, Figure F, Plate 48, Figure A.

1966 *Dorothia praehauteriviana* Dieni and Massari, p. 108, pl. 2, figs 23a-24b; pl. 10, figs 9-13.

1987 *Praedorothia praehauteriviana* (Dieni and Massari, 1966), Desai and Banner, p. 18, pl. 4, figs 2a-d.

1992 *Praedorothia praehauteriviana* (Dieni and Massari, 1966), Kaminski *et al.*, p. 255, pl. 6, figs 7-8.

***Diagnosis*:** *Praedorothia* sp. cf. *P. praehauteriviana* has a parallel−sided, semi−cylindrical to conical and elongate test; the early coiling is trochospiral followed by a later biserial arrangment; Wall is non-perforate and solid agglutinated.

***Remarks*:** This species is recorded in Saudi Arabia for the first time. A diagnostic feature is the slightly parallel sides in which it can differ from the *Protomarssonella*. It was emended from *Dorothia* to *Praedorothia* by Desai and Banner (1987). However, they have the same coiling mode, septa and aperture but wall is not perforated by canaliculation or alveoli.

Stratigraphic Range: The range is given by Desai and Banner (1987) as Tithonian to Valanginian.

Family **PFENDERINIDAE** Smout and Sugden, 1962

Subfamily **KURNUBIINAE** Redmond, 1964

Genus ***Kurnubia*** Henson, 1948

Kurnubia palastiniensis Henson, 1948

Plate 48, Figures B-F, Plate 49, Figures A-E.

1948 *Kurnubia palastiniensis* Henson, p. 609, pl. 16, figs 8,11, pl. 18, figs 10-11.

1987 *Kurnubia palastiniensis* Henson; Loeblich and Tappan, p. 154, pl. 165, figs 1-6.

2001 *Kurnubia palastiniensis* Henson; Pop and Bucur, p. 86, pl.III, fig. 9.

2008 *Kurnubia palastiniensis* Henson; Ivanova *et al.*, p. 71, fig. 6.a.

2011 *Kurnubia palastiniensis* Henson;Turi *et al*., p. 21, pl.II, fig. 11.

Diagnosis: *Kurnubia palastiniensis* is characterised by an elongate, sub-conical test with early trochospirall coiling followed by an uncoiled uniserial chamber; Chambers along the axis of coilng are inclined; wall is perforated, agglutinated and the exoskeleton part of the wall is formed of a alveolar network.

Remarks**:** This species is diagnostic of the base of the Sulaiy Formation in the sub-surface. It typifies to the uppermost part of the Jurassic. It is associated with *Everticyclammina virguliana*, *Nautiloculina oolitica*, *Pseudocyclammina littus*, and *Verneuilinoides polonicus*.

Stratigraphic Range: It ranges from the Callovian and Oxfordian (Hughes, 2004) to Early Tithonian (Turi *et al*., 2011). It is also recorded from Căprioara (Mureş Trough), Romania, as Upper Jurassic by Serban *et al*. (2011). This species is a diagnostic marker for the base of the Sulaiy Formation.

Subfamily **PFENDERININAE** Smout and Sugden, 1962

Genus ***Pfenderina*** Henson, 1948

Pfenderina neocomiensis (Pfender, 1938)

Plate 49, Figure F, Plate 50, Figures A-F, Plate 51, Figures A-D.

1938 *Eoruperia neocomiensis* Pfender, p. 236, figs 1-7.

1975 *Pfenderina neocomiensis* (Pfender); Mansour, p. 128, pl. 3, fig. 2.

1995 *Pfenderina* cf. *neocomiensis* (Pfender); Bucur *et al*., p. 367, pl. VI, figs 4-6.

2008 *Pfenderina neocomiensis* (Pfender); Saad, pl. I, fig. 14.

2010 *Pfenderina neocomiensis* (Pfender); Olszewska, p. 49, pl. V, fig. 7.

***Diagnosis*:** *Pfenderina neocomiensis* has a high, trochospirally coiled test; each whorl contains from five to seven chambers; the septa, position is perpendicular to the test axis; wall is imperforate, finely agglutinated to microgranular.

***Remarks*:** This species is common in the top of the Sulaiy Formation as well as the base of the Yamama Formation. *Pfendrina neocomiensis* is associated with other agglutinated foraminifera that prefer a deep lagoonal environment (Hughes, 2009).

***Stratigraphical Range*:** Recent studies show that it has a range from Berriasian to Hauterivian (Olszewska, 2010). Bucur *et al*. (1995), recorded a range of Upper Berriasian to Valanginian.

Superfamilie **TEXTULARIACEA** Ehrenberg, 1838

Family **TEXTULARIIDAE** Ehrenberg, 1838

Subfamily **TEXTLARIINAE** Ehrenberg, 1838

Genus ***Haghimashella*** Neagu and Neagu, 1995

Haghimashella arcuata (Haeusler, 1890)

Plate 51, Figures E-F, Plate 52, Figures A-B.

1890 *Bigenerina arcuata* Haeusler, p. 73, pl. 12, figs 14-22.

1995 *Haghimashella arcuata* (Haeusler); Neagu and Neagu, p. 221, pl. 2 figs 1-11.

2007 *Haghimashella arcuata* (Haeusler); Krajewski and Olszewska, p. 296, fig. 4-d.

2008 *Haghimashella arcuata* (Haeusler); Olszewska *et al.*, p. 48, fig. 10-H.

2010 *Haghimashella arcuata* (Haeusler); Ivanova and Kołodziej, p. 7, pl. 1, fig. 17.

2010 *Haghimashella arcuata* (Haeusler); Olszewska, p.43, pl. II, fig. 11.

***Diagnosis*:** *Haghimashella arcuata* has a non-canaliculate agglutinated wall; test elongate, smooth; test formed of two stages, a small biserial, juvenile stage followed by a larger, uniserial, adult stage; chambers are inflated, globular in shape.

***Remarks*:** This species is recorded in Saudi Arabia for the first time. This species was described by Haeusler (1890) as *Bigenerina arcuata* but then it was redefined by Neagu and Neagu (1995) as *Haghimashella arcuata*. It is an indicator for the lower part of the Sulaiy Formation. It can be confused with *Bicazammina jurassica* (Haeusler, 1890) and it differs from this species by having a larger early biserial stage followed by a finally uniserial chamber arrangement.

***Stratigraphical Range*:** The range given by Olszewska (2010) is Callovian to Valanginian.

4.2 SYSTEMATICS OF MICROPROBLEMATICA

Microproblematica are those microfossils with a non-determined biological classification and often with uncertain affinities. In many cases they have a valuable stratigraphical and palaeoenvironmental distribution (Hughes, 2013). This group includes the following microfossils:

- *Aeolisaccus dunningtoni* Elliot*, 1958*
- *Hensonella* sp

- *Lithocodium aggregatum* Elliott, 1956
- *Pseudolithocodium carpathicum* Misik (1979)
- *Crescentiella morronensis* (Crescenti 1969)

Genus ***Aeolisaccus dunningtoni*** Elliott, 1958

Aeolisaccus dunningtoni Elliott, 1958

Plate 67, Figures A-F

1958 *Aeolisaccus dunningtoni* Elliott; pp. 422-424, pl. 3, figs 5-6, 8-9.

2008 *Aeolisaccus inconstans* Radoicic; Husseini and Conrad, p. 229, pl. 6, fig. j.

2013 *Aeolisaccus dunningtoni* Elliott; Hughes, pp. 60, 62-63, fig. 3, figs 4.1-15.

***Diagnosis*:** The test is composed of homogeneous microgranular calcite. It is a free, single, elongate tubular chamber, with no internal septal. The wall is variable in thickness. The test is slightly tapering and appears to have an open aperture.

***Remarks*:** The affinities of *Aeolisaccus dunningtoni* are not clear and there are two possibilities. It may be the fossilized tubes of cyanobacteria or a type of foraminifera (Loeblich and Tappan, 1988, Hughes, 2013). It is classified as microproblematica, following the latest study by Hughes (2013). In the Saudi Arabian sub-surface it is associated with supra–tidal flats and intertidal palaeoenvironments and recorded in carbonate mudstones, wackestones and packstones (Hughes, 2013).

***Stratigraphical Range*:** The range given by Hughes (2013) is Early Permian to Late Jurassic of the Arabian Plate, Berriasian- Aptian (Ivanovna *et al.*, 2008),

Upper Berriasian to Lower Aptian (Bucur *et al*., 1995) and Uppermost Tithonian to Valanginian in North-Western Anatolia, Turkey (Altiner, 1991).

Genus ***Hensonella*** Elliott, 1959

***Remarks*:** This genus has been extensively discussed by Simmons *et al*. (1991, p. 957) and Scholle and Ulmer-Scholle (2003, pp 208, 213). Several previous authors have assigned *Hensonella* tubes to scaphopods, red algae, or dasycladacean algae. *Hensonella* is widely observed throughout the Middle East in Hauterivian to Albian sediments deposited within open marine, shelf margin palaeoenvironmental settings (Scholle and Ulmer-Scholle 2003, p. 213). The current author has recently observed a new species within the Berriasian Sulaiy Formation of eastern Saudi Arabia. This new species is much greater in size than those of the Hauterivian-Albian forms.

Hensonella n. sp.

Plate 68, Figures A-C

***Diagnosis*:** This *Hensonella* species is characterized by a large, long tube which tapers at one end and is parallel-sided and straight at the other end; the calcareous wall is composed of an internal, dark colored, microgranular layer and external radiating prisms that are perpendicular to the wall. The outer layer prisms are enlarged in size within the isopachous cement layer. *Hensonella* tubes are incomplete as a result of syn-depositional, crushing and alteration to micrite by the syn-deposition microbialite bio-alteration. The maximum length is 8.2 mm and width is from 0.4 to 0.7 mm.

***Remarks*:** This species is deposited with peloidal, skeletal packstones and wackestones. It is associated with open marine biota such as *Saccocoma* sp., crinoid plates, calcispheres (*Stomiosphaera wanneri*, *Colomisphaera conferta*), *Lithocodium aggregatum*, *Thaumatoporella parvovesiculifera* and large agglutinated foraminifera (*Everticyclammina kelleri*).

Stratigraphical Range: This species is assigned to the Berriasian age by the association with diagnostic calcispheres such as *Stomiosphaera wanneri* and *Colomisphaera conferta*.

Genus ***Lithocodium*** Elliott 1956

Lithocodium aggregatum Elliott, 1956

Plate 68, Figures D-F, Plate 69, Figures A-F, Plate 70, Figures A-F, Plate 71, Figures A-F

1956 *Lithocodium aggregatum* Elliott; p. 331, pl. 1, fig. 2, pl. 1, figs 4-5.

1971 *Lithocodium aggregatum* Elliott; Basson and Edgel, pp. 416-417, pl. 1, fig. 1.

1990 *Lithocodium aggregatum* Elliott; Banner *et al*., pp. 28-30, pl. 1, figs 1-4, pl. 2, figs 1-4, pl. 3, fig. 1, pl. 4, fig. 1.

2004 *Lithocodium aggregatum* Elliott; Bucur *et al*., pl. II, fig. 24.

2005 *Lithocodium aggregatum* Elliott; Radoičić, p. 33, pl. 5, figs 1-8, pl. 6, figs 1-4, 8, pl. 7, figs 1-2, pl. 8, figs 3-6, 9.

2010 *Lithocodium aggregatum* Elliott; Schlagintweit *et al*., pp.519-522, figs. 3a-c, b–e pars, f, h pars, figs 4a–h, figs 5a–e g, i, figs 6a–g, figs 7a–i. figs 8a–d, fig.13a pars, figs 14a–f pars, figs 16a–j.

***Diagnosis*:** The taxon is made of alveolar layer that is surrounding one or more empty chambers. This chamber is bearing multiples radiating canals and is characterised by irregular shapes and sizes from 0.5 mm to 2 mm (Schlagintweit *et al*., 2010).

***Remarks*:** For further definitions, see Elliot (1956), Radoičić (2005) and Schlagintweit *et al*. (2010). The origin and the systematics position is controversial and this is discussed in detail by Schlagintweit *et al.* (2010, p. 511, table 1). Usually they are in forms such as oncoids, encrusters and lumps. However, they are more usually found encrusting the hard skeletons of corals and multi-layered bivalves. They act as microbialitic micritizers and corroders of skeletal grains (Radoičić, 2005). This taxa is usually associated with the inner platform (restricted or circulated) and platform margin facies where sea water is moderate to highly agitated (Schlagintweit and Ebli, 1999). This taxa is diagnosticof the *Lithocodium aggregatum* microfacies that was deposited under shallow and normal marine condions. However two palaeoenvironments can be recognized based on *Lithocodium* shape and size. The low energy *Lithocodium aggregatum* are large oncoids in categories 3 and 4 of Vědrine (1977) in which they are characterized by encrusting microbial meshwork shapes. On the other hand, the high energy *Lithocodium aggregatum* is made of semi-spheroids or lumps of smaller oncoids characterized by a thick micric cortex which has been described by Vědrine (1977) and Michetiuc *et al.* (2012) as category of oncoids.

Stratigraphical Range: This taxa is commonly distributed between the Kimmeridgian to Albian in the limestones of the Middle East (Banner *et al.,* 1991).

Genus ***Pseudolithocodium*** Míšík 1979

Pseudolithocodium carpathicum Míšík 1979

Plate 72, Figure A

1979 *Pseudolithocodium carpathicum* Míšík, p. 709, pl.2, figs 2-8.

1999 *Pseudolithocodium carpathicum* Míšík; Schlagintweit and Ebli, p. 410, pl. 10, figs 3-5.

***Diagnosis*:** The body is composed of a mesh−work of narrow tubes separated by micrite layers that are very densely packed.

***Remarks*:** This taxa was described by Schlagintweit and Ebli (1999) and it occurs in the platform margin limestones of the Krashtein Mountains. It is found associated with *Thaumatoporella parvovesiculifera* (Raineri). The origin and the systematic position of the taxon is controversial and has been discussed by Schlagintweit and Ebli (1999, p. 410). It was found within the restricted platform interior of the lagoonal environment setting (Haas *et al.*, 2006, p. 156).

Stratigraphical Range: The age is controversial and is given by Schlagintweit and Ebli (1999) as Tithonian.

Genus ***Crescentiella*** Senowbari-Daryan *et al.* 2007

Crescentiella morronensis forma *morronensis* (Crescenti 1969), emend.

Senowbari-Daryan *et al*., 2007

Plate 72, Figures B-F, Plate 73, Figures A-E

1969 *Crescentiella morronensis* Crescenti, pp. 35-37, figs 10, 20-22.

1999 *Crescentiella morronensis* (Crescenti); Schlagintweit and Ebli, p. 412, pl. 2, fig. 5; pl. 4, fig. 7, pl. 12,

figs 4-5.

2000 *Crescentiella morronensis* Crescenti; Bucur and Onac, p. 15, pl. 2, fig. 9.

2007 *Crescentiella morronensis* forma *morronensis* (Crescenti, 1969); Senowbari-Daryan *et al*., pp. 187-196, text-figs. 1–3, 8; pl. 1, fig. a–i; pl. 2, fig. a–h; pl. 3, fig. a–g; pl. 4, fig. b–h; Pl. 5, fig. b, d–h; pl. 6, fig. a–h.

***Diagnosis*:** This taxon is characterized by colonies of tubes that are formed of dark, concentric banded micrites. These micrite layers surround internal cavities of uniserial miliolids such as *Nodobacularia* or *Nubecularia.*

***Remarks*:** This genus appears to have been been living in co−operation with *Nodobacularia* or *Nubecularia* species. This genus was amended from *Crescentiella morronensis* by Senowbari-Daryan *et al*. (2007). It is a critical depth marker based on its wall thicknesses (Leinfelder, 1996, figure 5, p. 231). However, it is associated with slope and deep slope successions that are deposited by occasional gravity storm flows such as in the microfacies HMF3.

Stratigraphical Range The species *Crescentiella morronensis* forma *morronensis* (Crescenti 1969) is recorded from the Upper Jurassic to Lower Cretaceous by Senowbari-Daryan *et al*. (2007).

4.3 SYSTEMATICS OF THE SPONGE GROUP

This group include all of the skeletal remains of the Phylum Porifera that prefer normal oxygenated water. However, some parts are usually allocthonous such

as sponge spicules of the Class Demospongiae. Sessile reef builders are represented by *Cladocoropsis mirabilis* and the stromatoporoid remains which contribute to the reef buildups within the back-shoal area and parts of the platform margin (Flügel, 2004).

Sponge Spicules

Remarks : Rocks with spicules in extremly high numbers are called spiculites and this facies is equivalent to the slope facies SMF1 of the Rimmed Carbonate Platform and the Outer Ramp basin facies SMF1 of the ramp model which been discribed by Flügel (2004, pp. 721-722). The spiculites and the peloidal calcisiltite spicule-rich facies are attributed to deeper environments within the deep intra-shelf basin or the slope area. This includes large monaxons, smaller monaxons and triaxons. They are often associated with the *Lenticulina* biofacies in the deeper marine, slope areas. Other associated microfossils include *Nodosaria* spp., polymorphinids and agglutinated foraminifera such as *Gaudryinella* sp. and *Kurnubia palastiniensis*.

Phylum **PORIFERA** Grant, 1836

Class **DEMOSPONGIAE** Sollas, 1885

Large spicules

Plate 54, Figures A-B.

***Diagnosis*:** A large, single, axis spicule is defined as being over 130 µm.

Monaxon sponge spicules

Plate 53, Figures D-F, Plate 54, Figures C-D.

***Diagnosis*:** A smaller, single, axis spicule is defined as being less than 100 µm.

Triaxon sponge spicules

Plate 53, Figure E, Plate 54, Figures E-F.

***Diagnosis*:** This is a large spicule, basically consisting of three axes and about six rays.

Class **STROMATOPOROIDEA** Nicholson and Murie, 1878

Stromatoporoid sp.

Plate 55, Figure A, F.

***Diagnosis*:** Stromatoporoid species are usually of an encrusting or domal type that act as a reef builder organism. The organism accretes its structure from calcium carbonate as laminae and pillars. The structures are parallel and reticulate and appear in thin-section as double layers. The size ranges from several centimeters to meters.

Genus ***Cladocoropsis*** Felix, 1907

Cladocoropsis mirabilis Felix (1927)

Plate 55, Figures B-E,

Diagnosis: This taxon is a branching type of stromatoporoid that normally occurs in a columnar form. Tabular laminae are seen to coat the external wall of the *Cladocoropsis mirabilis*.

Remarks: *C. mirabilis* is often associated with *Thaumatoporella parvovesiculifera* (Raineri) and is diagnostic of shallow marine and reefal

conditions (Basson and Edgell, 1971; Bucur *et al*., 2004; Hughes *et al*. 2009). It is recorded from Saudi Arabian Oxfordian carbonates and indicates moderate to low energy conditions within the distal part of the lagoonal palaeoenvironment (Hughes *et al.,* 2009).

Stratigraphical Range: *Cladocoropsis mirabilis* is recorded from the Bathonian (Middle Jurassic) to the lowermost Cretaceous (Berriasian) by Senowbari-Kano *et al*. (2007).

4.4 SYSTEMATICS OF THE CALCISPHERES

Calcispheres are believed to be the small (up to 0.5mm diameter) spherical cysts of dinoflagellate organisms that are common in the pelagic seas of the Palaeozoic and Mesozoic eras. They are hollow spheroids, often filled by sparry calcite, with micrite walls (Allaby and Allaby, 1990). This group have several common names such as calcispheres (Masters and Scott, 1978; Hart, 1991; Bucur *et al.*, 2014), calcareous dinoflagellates (Reháková, 2000) and calcareous dinocycts (Krajewski and Olszewska, 2007; Olszewska, 2010). Masters and Scott (1978) referred this group to "*Incertae Sedis*" which means unknown microfossils. This group includes the following old taxa:

Bonetocardiella Dufour, 1968.

Stomiosphaera Wanner, 1940.

Pithonella Lorenz, 1902.

Cadosinopsis Schiebner, 1967

An attempt by Masters and Scott (1978) to organise these assorted forms of calcispheres was problematic as many were shown to be recrystallized.

Keupp (1978, 1979) has described the probable link to dinoflagellte cysts. From 1979-1992 Keupp and co-workers gradually developed the link between calcispheres and dinocysts. This has been carried on by Willems and Wendler (2002), but only a very few taxa show the paratabulation that proves that they are dinocycts. Extensive dinoflagellate studies are reported by Reháková (2000, p. 229). In thin-section, it is almost impossible to see the platelets or the aperture (archeopyle of the dinocyst).

Reháková (2000) was effectively taking the Masters and Scott (1978) approach and - using thin-sections – was only able to use the wall structure. The author is also taking this approach to speciate clacispheres in thin-sections as it is the only available method, since the disaggregation from carbonate samples is almost impossible.

Order **PERIDINIALES** Haeckel, 1894

Family **CALCIODINELLACEAE** Deflandre, 1947 emend. Bujak and Davies, 1983

Dinocyct spp.

Plate 56, Figures B, D, F.

***Diagnosis*:** Calcareous dinoflagellate spheres made of hollow spheroids, filled by sparry calcite, with walls made of micrite and calcareous, radiating layers.

***Remarks*:** The palaoenvironmental distribution of calcispheres is usually associated with the protected back reef sediments of the carbonate platform (Ka´zmierczak and Kremer, 2005). However, Masters and Scott (1978) reported rare calcispheres from the back reefal lagoonal accumulations from Arizona's Lower Cretaceous. The occurrences of these species are also rare is this research and they probably record higher sea levels.

Genus ***Comittosphaera*** Řehánek, 1985

Comittosphaera sublapidosa (Volger, 1941)

Plate 56, Figure C.

1941 *Cadosina sublapidosa* Volger, p. 280, pl. 2, fig. 5.

2005 *Comittosphaera sublapidosa* (Vogler); Olszewska, p. 31, pl. 3, fig. 7.

2007 *Comittosphaera sublapidosa* (Vogler); Krajewski and Olszewska, p. 305, fig. 8F.

Diagnosis: Calcareous dinoflagellate spheres, composed of two, uneven, inner and outer wall layers; the inner micritic layer is extremely variable in thickness while the outer layer is formed of radiating, uneven calcitic crystals

***Stratigraphical Range*:** The species was recorded as ranging from Tithonian to Hauterivian by Krajewski and Olszewska (2007) in the Southern Crimea Mountains (South-West Russia).

Genus ***Colomisphaera*** Nowak,1968

Colomisphaera cieszynica Nowak,1968

Plate 56, Figure E.

1968 *Colomisphaera cieszynica* Nowak, pp. 309-310, pl. 30, figs 1-5.

2005 *Colomisphaera cieszynica* Nowak; Olszewska, p. 30, pl. 2, fig. 9.

2010 *Colomisphaera cieszynica* Nowak; Olszewska, pp. 28-29, pl. VIII, fig. 4.

Diagnosis: Calcareous dinoflagellate spheres, composed of a single wall layer; formed of longitudinal, radiating calcareous crystals. Both margins are irregular and uneven.

***Stratigraphical Range*:** The species was recorded by Olszewska (2010) from the Kimmeridgian to Lower Valanginian of S.E. Poland.

Colomisphaera conferta Řehánek, 1985

Plate 58, Figure B.

1985 *Colomisphaera conferta* Řehánek, pp. 171-173, pl. 1, figs 1-8.

2005 *Colomisphaera conferta* Řehánek; Olszewska, p. 30, pl. 2, fig. 13.

2010 *Colomisphaera conferta* Řehánek; Olszewska, p. 29, pl. VIII, fig. 5.

Diagnosis: Calcareous dinoflagellate, sub-oval in shape, composed of one wall layer; this layer is made of short, radiating calcareous crystals. Both margins are uneven and the inner margin has a lining of thin micrite.

***Stratigraphical Range*:** The species was recorded by Olszewska (2010) from the Upper Berriasian to Valanginian of S.E. Poland.

Genus ***Crustocadosina*** Řehánek, 1985

Crustocadosina semiradiata (Wanner, 1940)

Plate 58, Figures C-D.

1940 *Cadosina semiradiata* Wanner, p. 81, pl. 1, figs 36-37.

2005 *Crustocadosina semiradiata* (Wanner, 1940); Olszewska, p. 33, pl. 2, fig. 1.

2007 *Crustocadosina semiradiata* (Wanner, 1940); Krajewski and Olszewska, p.307, fig. 8H.

2010 *Crustocadosina semiradiata* (Wanner, 1940); Olszewska, p.30, pl. II, fig. 12.

Diagnosis: Calcareous dinoflagellate, oval to sub-oval, in shape, composed of two, even, inner and outer wall layers; the outer layer is formed of short, radiating calcareous crystals. The inner layer is formed of thicker micritic calcite than the outer layer.

***Stratigraphical Range*:** The species was recorded by Olszewska (2010) from the Upper Oxfordian to Early Aptian of S.E. Poland.

Genus ***Stomiosphaera*** Wanner, 1940

Stomiosphaera wanneri Borza, 1969

Plate 57, Figure B; Plate 58, Figures A-B.

1969 *Stomiosphaera wanneri* Borza, pp. 62-63, pl. 61, figs 4-13.

2005 *Stomiosphaera wanneri* Borza; Olszewska, p. 29, pl. 2, fig. 11.

2010 *Stomiosphaera wanneri* Borza; Olszewska, p.28, pl. VIII, fig. 11.

Diagnosis: Calcareous dinoflagellate, spheroidal, composed of one smooth radiating wall layer with an uneven external margin; in cross polarized light, the wall displays an extinction cross.

***Stratigraphical Range*:** The species was recorded by Olszewska (2010) from the Upper Berriasian to Hauterivian of S.E. Poland.

4.5 SYSTEMATICS OF THE CALCAREOUS ALGAE

Systematic data were obtained from Elliott (1957, 1958, 1968), Basson and Edgell (1971), Roux and Deloffre (1990), Kuss and Conrad (1991), Okla (1991), Kuss (1994), Yilmaz (1999), Bucur *et al.* (2005, 2014), Schlagintweit *et al*. (2009), Olszewska (2010) and Bucur (2011).

The Saudi Arabian Sulaiy and Yamama formations contained significant number of dasyclads, green algae and red algae. The occourences of these taxa were recorded from rare to common in the Sulaiy Formation but recorded very as common in the Yamama Formation.

Phylum **THALLOPHYTA** Unger, 1838

Class **CHLOROPHYCEAE** Kuetzing, 1833

Order **DASYCLADALES** Pascher, 1931

Family **ACETABULARIACEAE** Häuck, 1885

Genus ***Actinoporella*** (Gumble in Alth, 1881), emend. Conrad *et al.*, 1974

Actinoporella podolica (Alth, 1878), emend. Conrad *et al.* 1974

Plate 59, Figures A-E

1878 *Gyroporella podolica* Alth, pl. VI, figs 1-8 (not fig 5).

1968 *Actinoporella podolica* (Alth); Elliott, p. 19, pl. 3, figs 2, 4, 7.

1971 *Actinoporella podolica* (Alth); Basson and Edgell, p. 417, pl. I, figs 1-2.

1974 *Actinoporella podolica* (Alth); emended by Conrad *et al.,* pp. 6-13, figs 1 (1-8), 2 (1-7), 4-12.

1976 *Actinoporella podolica* (Alth); Conrad and Peyberněs, p. 180, fig. 5-b.

1999 *Actinoporella podolica* (Alth); Yilmaz, p. 85, pl. 1, fig. 1.

1999 *Actinoporella podolica* (Alth); Bucur, p. 57, pl. III, figs 14, 15, 20.

2011 *Actinoporella podolica* (Alth); Bucur *et al.*, pp. 621-623, pl. 1, figs 1-5, pl. 3, figs 1-3, pl. 4, figs 1-6, pl. 6, figs 6-7, 11, pl. 7, figs 1-6.

2014 *Actinoporella podolica* (Alth); Bucur *et al.*, pp. 664-665, figs 3 a-e.

Diagnosis: Disaggregated thallous verticils, with axial cavity, characterised disc shapes, which are made of elongate, interconnected laterals.

Remarks: This species is best described by Conrad et al (1974, pp. 7-9) and Bucur et al. (2011, pp. 621-623). It was recorded as common to abundant in the Saudi Arabian Sulaiy and Yamama formations. It is a diagnostic calcareous algae for the lagoonal sedimentary zone.

***Stratigraphical Range*:** The range is given as mid-Tithonian to mid-Aptian by Bucur *et al.* (2011). Although Bucur *et al.* (2014) recorded this species between the uppermost Tithonian to Berriasian of the Southern Crimea (South-East Russia). This study extends the range to the Valalnginian.

Family **POLYPHYSACEAE** (Kützing, 1841)

Genus ***Clypeina*** (Michelin, 1845), emend. Rezack, 1959

Clypina isabellae Masse *et al.* (1999), emend. Schlagintweit *et al.* (2009)

Plate 64, Figures C-E

1999 *Clypina isabellae Masse et al.*, p. 237, pl. 2, figs 1-8.

2004 *Clypina sulcata* (Alth); Bucur *et al.* p. 60, pl. II, fig. 10.

2009 *Clypina isabellae Masse et al.*; Schlagintweit *et al.*, pp. 49-50, pl. 2, figs 1-24, pl. 3, figs 1-20..

Diagnosis: This species is made of an elongated, cylindrical thallus that is surrounded by irregularly arranged branches. These branches are double thick, walled and sub-parallel to the thallus axes. An extended description can be obtained from Schlagintweit *et al*. (2009, p. 49).

***Remarks*:** The palaoenvironmental distribution of the *Clypina isabellae* is usually within the protected lagoonal sediments of the carbonate platform. The species is often associated with *Salpingoporella* spp. and miliolids.

***Stratigraphical Range*:** The range is given as Kimmeridgian to Berriasian by Bucur *et al*. (2005) and Schlagintweit *et al*. (2009).

Iranella inopinata Gollestaneh,1965

Plate 64, Figure F

1965 *Iranella inopinata* Gollestaneh, p. 250, pls. 68-69.

2008 *Salpingoporella? inopinata* Gollestaneh; Abolfazl Hosseini and Conrad, pp. 216-217, pl. 1, figs J-M, T, pl. 2, figs n-p, pl. 3, fig. F, pl. 4, figs D, L-P.

Diagnosis: This species is made of a thallus and an axial hollow with a cylindrical shape; lateral branches are usually wider at the outer margins and in sections they are elliptical and elongated followed by rounded shapes in random sections. The wall is made of colourless, calcareous sparry cement replacing the original aragonite crystals.

***Stratigraphical Range*:** The range is given as Berriasian to Valanginian by Abolfazl Hosseini and Conrad (2008).

Family **TRIPLOPORELLACEAE** Berger and Kaever, 1992, (prev. **DASYCLADACEAE** Kuetzing, 1843, emend. Stizenberger, 1860)

Tribe **DIPLOPOREAE** Pia, 1920

Genus ***Salppingoporella*** Pia in Trauth, 1918, emend. Carras *et al.*, 2006

Salpingoporella annulata Carozzi, 1953

Plate 60, Figures A-F, Plate 61. Figures A-F

1953 *Salpingoporella annulata* Carozzi, p. 382, text-figs 1-55,

1968 *Salpingoporella annulata* Carozzi; Elliott, pp. 72-73, pl. 20, figs 3, 4, 6, 7.

1971 *Salpingoporella annulata* Carozzi; Basson and Edgell, p. 420, pl. 4, fig. 3.

1991 *Salpingoporella annulata* Carozzi; Okla, p. 188, pl. 2, figs 4-7.

1995 *Salpingoporella annulata* Carozzi; Bucur *et al.*, p. 357, pl. VIII, fig. 1.

1999 *Salpingoporella annulata* Carozzi; Yilmaz, pp. 87-88, pl. 2, fig. 27.

2001 *Salpingoporella annulata* Carozzi; Tasli, p. 12, pl. III, fig. 11.

2006 *Salpingoporella annulata* Carozzi; Carras *et al*., pp. 464-468, pl. 1, figs 1-5.

2014 *Salpingoporella annulata* Carozzi; Bucur *et al.*, p. 67, fig. 6 g-k.

Diagnosis: This species is characterised by a small, cylindrical thallus made of eight to twenty radiated branches. These are wider in the outer margin and wall is composed of colorless, sparry calcite.

Remarks: *Salpingoporella annulata* Carozzi is a very comon dasyclad in the Sulaiy and the Yammam formations. However, they are the most common

calcareous algae in the lagoonal depositonal zone in the Middle Jurassic to the Lower Cretaceous carbonate successtions.

***Stratigraphical Range*:** This species, range is given as middle Bathonian to Early Barremian by Carras *et al.* (2006).

Salpingoporella circassa Farinacci and Radoičić, 1991

Plate 62, Figures A-B

1991 *Salpingoporella circassa* Farinacci and Radoičić, p. 140, pl. 4, figs 1-18, pl. 5, figs 1-2.

1995 *Salpingoporella circassa* Farinacci and Radoičić; Bucur *et al.*, p. 357, pl. VIII, figs 5-8.

1999 *Salpingoporella* aff. *circassa* Farinacci and Radoičić; Yilmaz, p. 88, pl. 2, figs 33-34.

2006 *Salpingoporella circassa* Farinacci and Radoičić; Carras *et al*., pp. 469-470, pl. II, figs 6-10.

Diagnosis: This species is characterised by a small verticils in which it has five to six lateral branches for every verticil.

Remarks: This species is recorded in the lagoonal facies in association with other species of *Salpingporella*.

***Stratigraphical Range*:** The range is given as Berriasian to Hauterivian by Carras *et al.* (2006).

Salpingoporella katzeri Conrad and Radoičić, 1978,

emend Carras *et al*., 2006.

Plate 62, Figure C

1978 *Salpingoporella katzeri* Conrad and Radoičić, pp. 69-71, pl. 1, figs 1-6, pl. 2, figs 1-11.

1999 *Salpingoporella katzeri* Conrad and Radoičić; Yilmaz, p. 89, pl. 3, figs 40-41.

2006 *Salpingoporella katzeri* Conrad and Radoičić; Carras *et al.,* p. 478, pl. II, figs 11-14.

Diagnosis: The thallus is disarticulated, small verticils. Each verticil contains five to seven branches; the sections of the branches are started as rhomb and hexagonal shapes. Branches are widening towards the outer margins.

Remarks: This species is recorded as present to rare in the lagoonal and platform margin facies.

***Stratigraphical Range*:** The species range is given as Berriasian to Valanginian by Carras *et al.* (2006).

Salpingoporella gr. *pygmaea* (Gümbel, 1891), emend. Carras *et al.,* 2006.

Plate 62, Figures D-F, Plate 63, Figures A-B, Plate 64, and Figures A-B

1891 *Gyroporella pygmaea* Gümbel, p. 306, figs 6-7.

1999 *Salpingoporella* gr. *pygmaea* (Gümbel); Yilmaz, p. 90, pl. 3, figs 48-49.

1999 *Salpingoporella* gr. *pygmaea* (Gümbel); Schlagintweit and Ebli, p. 394, pl. 8, figs 5, 8, 10-11.

2004 *Salpingoporella* gr. *pygmaea* (Gümbel); Bucur *et al.,* p. 60, pl. II, figs 8-9.

2005 *Salpingoporella* gr. *pygmaea* (Gümbel); Bucur *et al.,* pp. 116-118, pl. 1, figs 1-19.

2006 *Salpingoporella* gr. *pygmaea* (Gümbel); Carras *et al.,* pp. 484-488, pl. IX, figs 1-12.

2010 *Salpingoporella* gr. *pygmaea* (Gümbel); Olszewska, p.31, pl. VIII, fig. 3.

2014 *Salpingoporella* gr. *pygmaea* (Gümbel); Bucur *et al.*, p. 67, fig. 7 a-k.

Diagnosis: *Salpingoporella pygmaea* is characterised by a medium to large thallus; branches are arranged quincunxes and there are fifteen to thirty-five per verticil; the sections of the branches are first narrow and then slightley wider at the outer margins; section shapes are semi-rounded to polygonal and occationally at vertical sections the shapes are semi-elliptical.

Remarks: This species is recorded as rare to common in the open marine part of the inner shoal and platform margin facies. It is associated with *Thaumatoporella parvovesiculifera* (Raineri).

Stratigraphical Range**:** The range is given as Bathonian to Aptian by Carras *et al.* (2006).

Salpingoporella dinarica Radoičić, 1959

Plate 64, Figures B-C, Plate 65, Figure A

1959 *Salpingoporella dinarica* Radoičić*,* pl. 3, fig. 1, pl. 4, figs 1-4, pl. 5, figs 1-4.

1968 *Salpingoporella dinarica* Radoičić; Elliott, pp. 75-77, pl. 21, fig. 4, pl. 22..

1991 *Salpingoporella dinarica* Radoičić*;* Kuss and Conrad, pp. 874-876, fig.4.15.

1999 *Salpingoporella dinarica* Radoičić; Yilmaz, p. 88, pl. 2, fig. 35.

2006 *Salpingoporella dinarica* Radoičić; Carras *et al.,* pp. 470-472, pl. II, figs 11-14.

Diagnosis: *Salpingoporella dinarica* is a thalli similar to rod that has a funnel shaped branches arranged perpendicularly to the axial hollow; the branches are from four to ten and are made of openings similar to the honeycomp patterns; the colour is yellow to whitish yellow under transmitted light.

Remarks: This species was recorded as rare to common in the Sulaiy and the Yamama formations. It is a diagnostic calcareous algae for the lagoonal and platform marginal reef sedimentary zone.

***Stratigraphical Range*:** The range is given as Berriasian to Albian by Carras *et al.* (2006).

Genus ***Holosporella*** Pia, 1930

Holosporella arabica Granier and Brunn, 1991

Plate 59, Figure F

Diagnosis: This species is characterised by a hollow cylindrical thallus with a thick, single layered wall; the wall is axially perforated.

Remarks: This calcareous algae is recorded in Saudi Arabia for the first time.

***Stratigraphical Range*:** The range given as Berriasian to Aptian by Granier and Brun (1991) from off-shore of Abu Dhabi.

Family **SELETONELLACEAE** (Korde, 1950), emend. Bassoullet *et al.,* 1975

Tripe **DASYPORELLEAE (**Pia, 1920), emend. Bassoullet *et al.,* 1979

Genus ***Macroporella*** **(**Pia, 1912), emend. Bassoullet *et al.,* 1978

Macroporella praturloni Dragastan, 1971.

Plate 58, Figures E-F

1971 *Macroporella praturloni* Dragastan, p. 209, pl. 3, figs 2-3.

1995 *Macroporella praturloni* Dragastan; Bucur *et al.*, p. 357, pl. IX, fig. 5.

Diagnosis: This species is characterised by a cylindrical thallus and it is made of a very thick central stem; the branches are thick, tabulated with a primitive alternating arrangement.

Remarks: This species of calcareous algae is recorded in Saudi Arabia for the first time.

***Stratigraphical Range*:** This species age is given as Berriasian by Granier and Brun (1991) and Berriasian to Valanginian by Bucur (1995).

Genus ***Arabicodium*** Elliott, 1957

Arabicodium aegagrapiloides Elliott, 1957

Plate 66, Figure E

1957 *Arabicodium aegagrapiloides* Elliott, pp. 228-230, pl. 1, figs 17-10.

Diagnosis: *Arabicodium aegagrapiloides* is characterised by segements of a cylindrical thalli that appear rounded in thin-section; internal structures are formed of fine irregular, twisted threads that extend to the external margins.

Remarks: This species is an udoteacean green algae with rare abundances in the Sulaiy Formation. This may appear similar to *Cayeuxia* and *Halimeda* but differs in the presence of a central, internal structure which is not typical of *Cayeuxia* or *Halimeda.*

***Stratigraphical Range*:** The range is given as Lower Cretacous by Elliott (1957).

Class **RHODOPHYCEAE** Rabenhorst, 1863

Order **CRYPTONEMIALES** Schmitz (in Engler), 1892

Family **GYMNOCODIACEAE** Elliott, 1955

Genus ***Permocalculus*** Elliott, 1955

Permocalculus ampullaceus Elliott, 1959

Plate 65, Figures A, D-F

1959 *Permocalculus ampullaceus* Elliott, p. 218, pl. 2, figs 3-4.

1971 *Permocalculus ampullaceus* Elliott; Basson and Edgell, p. 426, pl. 6, fig. 4.

Discription: These are often reworked parts of cylindrical thallus shapes. These are characterized by segmentations in the cortical crenulations.

Remarks: These forms are recorded as common to abundant in the Saudi Arabian Yamama Formation. It is a diagnostic, coralline red calcareous algae for the lagoonal and platform margin sedimentary zones.

***Stratigraphical Range*:** The range is given as Tithonian to Hauterivian by Basson and Edgell (1971).

Genus ***Thaumatoporella*** Pia, 1927

Thaumatoporella parvovesiculifera (Raineri, 1922), emend. Pia 1927.

Plate 66, Figures B-D

1957 *Polygonella incrustata* Elliott, p. 230, pl. 1, figs 11-12.

1971 *Polygonella incrustata* Elliott; Basson and Edgell, p. 428, pl. 7, figs 5-6.

2001 *Thaumatoporella parvovesiculifera* (Raineri); Tasli, p. 12, pl. III, fig. 12.

2014 *Thaumatoporella parvovesiculifera* (Raineri); Bucur *et al.*, p. 74, fig. 14 o-p.

Diagnosis: This species is a type of incruster made of a layer contains large, cellolar openings; these openings are of pentagonal shapes.

Remarks: This species was recorded as rare to common in the Sulaiy and the Yamama formations. It is a diagnostic calcareous algae for the lagoonal sedimentary zone.

***Stratigraphical Range*:** The range is given as Late Triassic to Cretaceous by Bucur *et al*. (2005).

Order **RHODOPHYTA** Wettstein, 1901

Family **CORALLINACEAE** Lamouroux, 1816

Genus ***Marinella*** Pfender, 1939

Marinella lugeoni Pfender, 1939

Plate 66, Figure F

1939 *Marinella lugeoni* Pfender, pp. 215-216, pl. I, fig. 1, Pl. II, figs. 1-2.

1994 *Marinella lugeoni* Pfender; Kuss, pp. 298-299, pl. 1, figs 1-4.

2010 *Marinella lugeoni* Pfender; Olszewska, p.31, pl. III, fig. 8.

Diagnosis: *Marinella lugeoni* is characterised by a thallus of fan-like shape to semi-circular that is radially branched from the base.

Remarks: This species is recorded with rare occurrences in the Sulaiy and the Yamama formations. It is a diagnostic calcareous algae of the distal parts of the inner platform's, protected open marine part and the platform margin areas.

***Stratigraphical Range*:** The range is given as Late Jurassic to Cretaceous by Bucur *et al*. (2005).

4.6 SYSTEMATICS OF CALPIONELLIDS

Order **TINTINIDA** Corliss, 1956

Family **CALPIONELLIDAE,** Bonet, 1956

Definition: The Family Calpionellidae Bonet (1956) is a subdivision of the Order Tintinida Corliss (1956) that are characterized by a calcareous, hyaline, lorica (Nowak, 1980).

Diagnosis: Calpionellids are small sized, 45 to 150 µm; single-chambered, calcareous hyaline lorica, that is like a cup or vase, usually with collar (neck); wall is well preserved which is made of low magnesium radiating calcite; an additional external, dark micritic wall layer may be present in some genera (Scholle and Ulmer-Scholle, 2003, p. 52).

Remarks: Calpionellids are important micro-plankton during their time range and are present in many Tethyan, pelagic carbonate sediments (Reháková and Michalík, 1997, Reháková, 2000). They are restricted to open marine, pelagic limestones and they are restricted to the warm waters of the Tethyan Realm at latitudes between 30° to 35° (Scholle and Ulmer-Scholle, 2003, p. 52). Calpionellids provide an essential age−dating adjacent to the Jurassic−Cretaceous boundary. Their rapid evolution and characteristic

appearance has provided a series of valuable biozones (Lakova *et al.,* 1999, p. 152).

Stratigraphic Range: This family is stratigraphically restricted to the time range from Late Tithonian to Valanginian. The range charts of the calpionellid genera and species used in this research are provided by Remane (1989, figure 7, p. 560), Remane (1998, figure 8, p. 166, table 1, p. 168), Lakova *et al.* (1999, figure 9, p. 160), Akyazi *et al*., (2001, table 1, p. 124; table 3, p. 127, table 15, p. 140) and Andreini *et al.* (2007, fig. 4, p. 184).

Genus ***Calpionella*** Lorenz, 1902

Calpionella alpina Lorenz, 1902

Plate 73, Figures B-C.

1902 *Calpionella alpina* Lorenz, p. 60, pl.9, fig. 1.

1999 *Calpionella grandalpina* Nagy; Lakova *et al.*, p. 162, pl. 1, fig. 7.

2001 *Calpionella alpina* Lorenz; Akyazi *et al.*, pp. 133-134, pl. 1, fig. 12, pl. 2, figs 1-4.

2004 *Calpionella alpina* Lorenz; Bucur *et al*., p. 61, pl. IV, figs 19, 20.

2005 *Calpionella alpina* Lorenz; Olszewska, p. 28, pl. 1, fig. 5.

2008 *Calpionella alpina* Lorenz; Olszewska *et al*., p. 42, fig. 7 B..

2010 *Calpionella alpina* Lorenz; Olszewska, p. 30, pl. VIII, fig. 3.

2012 *Calpionella alpina* Lorenz; Benzaggagh *et al.*, p.19, figs 6 K-L, R-T, figs 17 A, C

2013 *Calpionella alpina* Lorenz; Krische *et al.*, p.38, fig. 12 (C-D)

2014 *Calpionella alpina* Lorenz; Platonov *et al.*, p.70, fig. 6 (30-37)

2015 *Calpionella alpina* Lorenz; Zell *et al.*, p. 46-47, figs. 10 D, N, F and L, fig. 11 B.

Diagnosis: *Calpionella alpina* is a polymorphic lorica characterized by a small lorica, more or less spherical, slightly higher than wide. The collar is short, cylindrical or absent and rarely well developed.

Remarks: This collar form of *Calpionella alpina* is comparable with the collar form number 15 of Remane (1998, fig. 8, p. 166) and the intermediate form of lower and upper B zone of Remane (1989, fig. 6, p. 559).

***Stratigraphical Range*:** The range is given as uppermost Tithonian to lowermost Berriasian by Remane (1989, 1998). This form is known extend up to the upper Berriasian in association with the *Calpionellopsis simplex* (Andreini *et al.*, 2007)

Genus ***Crassicollaria,*** Remane, 1962

Crassicollaria brevis Remane, 1962

Plate 73, Figure A.

1962 *Crassicollaria brevis* Remane, pl. 1, fig. 9.

1999 *Crassicollaria brevis* Remane; Lakova *et al.*, p. 162, pl. 1, fig. 6.

2001 *Crassicollaria brevis* Remane; Akyazi *et al.*, p. 133, pl. 1, fig. 9.

2004 *Crassicollaria brevis* Remane; Bucur *et al*., p. 61, pl. IV, fig. 22.

2014 *Crassicollaria brevis* Remane; Platonov *et al*., p. 70, fig. 6 (16)

Diagnosis: This species is characterised by intermediate height of lorica and invisible collar in a random section (Remane, 1989, 1998).

Remarks: This species is very rare and if often associated with *Calpionella alpina* Lorenz.

***Stratigraphical Range*:** The range is given as uppermost Tithonian by Andreini *et al.* (2007).

Genus ***Calpionellopsis*** Colom, 1948

Calpionellopsis simplex (Colom, 1939)

Plate 73, Figures F

1939 *Calpionella simplex* Colom, 1939, pl. 2, fig.11, pl. 3, figs 6-9.

1999 *Calpionellopsis simplex* (Colom, 1939); Lakova *et al.*, p. 162, pl. 1, fig. 12.

2001 *Calpionellopsis simplex* (Colom, 1939); Akyazi *et al.*, pp.136-137, pl. 3 fig. 3.

2012 *Calpionellopsis simplex* (Colom, 1939); Benzaggagh *et al.*, pp.31-32, fig. 9 G-M, fig. 17 I, K

2015 *Calpionellopsis simplex* (Colom, 1939); Zell *et al.*, pp.46-47, fig. 10 A and F and L, fig. 11 E.

Diagnosis: *Calpionellopsis simplex* has an elongated, narrow, taller then wide lorica. The lorica walls are parallel to slightly convex.

***Remarks*:** The opening is wide, with a small collar that is located inside the lorica. (Benzaggagh *et al*., 2012). This species is an indicator of the middle to upper part of the Sulaiy Formation. *Calpionellopsis simplex* is a diagnostic indicator of the slope and deep slope areas.

***Stratigraphical Range*:** The range is given as Upper Berriasian by Remane (1989, 1998), Lakova *et al.* (1999) and Andreini *et al*. (2007).

4.7 SYSTEMATICS OF ANNELIDS (WORM TUBE) GROUP

Phylum **ANNELIDA**

Class **POLYCHAETA** Grube, 1850

Order **SEDENTARIA** Lamarck, 1818

Family **SERPULIDAE** Rafinesque, 1815

Serpulid sp.

Plate 74, Figure D-E

***Diagnosis*:** Serpulid sp. is a series of calcareous, secreted tubes with semi-circular to elliptical shapes; external and internal marg*ins are smooth and tend to occur as clusters of encrusting calcareous worm tubes.

***Remarks*:** This worm tube is encrusts on hard surfaces and on skeletal remains such as bivalves and other reef organisms. It is an indicator of marine and often hypersaline conditions. However, they are very common in very shallow subtidal zones and intertidal environments.

Stratigraphical Range: This group is distributed between Precambrian and Recent and has little stratigraphical value.

Family **TEREBELLIDAE** Grube, 1851

Genus ***Terebella*** Linnè, 1758

Terebella sp. cf.*T. lapilloides* Münster, 1833

Plate 74, Figure F

1833 *Terebella lapilloides* Münster, pl.71, figs 16.

2010 *Terebella lapilloides* Münster; Olszewska, p. 31, pl. I, fig. 10.

***Diagnosis*:** This sepcies of *Terebella* has an agglutinated sinuous tube that has an elliptical interior margin and a semi-smooth external margin. Measured length is about 0.45 mm and width is 0.15 mm.

***Remarks*:** This species is typical of dysoxic marine conditions within the deeper and distal palaeoenvironments of the Platform Margin and the upper Slope zones (Olszewska, 2010). It is associated with *Crescentiella morronensis* (Crescenti 1969), sponge spicules and species of *Nodobacularia* and *Nubecularia*.

Stratigraphical Range: This species is known from the Upper Triassic to Jurassic (Olszewska, 2010), but this new form appears restricted to the Berriasian.

4.8 SYSTEMATICS OF CORALS GROUP

Phylum **CNIDARIA**

Class **ANTHOZOA**

Sub-class **ZONATHARIA**

Order **SCLERACTINIA**

Scleractinian coral

Plate 75, Figure A.

***Diagnosis*:** The coral body is not preserved, and the original aragonitic structure has been replaced by micrite.

***Remarks*:** Corals are very rare and may represent solitary occurrences in patch reefs of the lagoonal and Platform Margin palaeoenvironments (Scholle and Ulmer-Scholle, 2003, p.113)

Stratigraphical Range: Scleractinian corals are recorded from Middle Triassic to Recent, and they have little stratigraphical value in a fragmentary state (Scholle and Ulmer-Scholle, 2003, p.113).

4.9 SYSTEMATICS OF MOLLUSC GROUP

Phylum **MOLLUSCA**

Sub-Phylum **CYRTOSOMA**

Class **GASTROPODA**

Gastropoda sp.1. (? semi-pelagic)

Plate 75, Figure B

***Diagnosis*:** A gastropod species that is made of an un−chambered trochospiral shell; the shell is thin and has been dissolved and replaced by calcite cement. Width is 0.95 mm and length is 0.8 mm.

Remarks: This type of gastropod is possibly a semi-pelagic type and prefers only the normal marine conditions since it is associated with the sponge spicules.

Gastropoda spp.

Plate 75, Figure D-F

***Diagnosis*:** Equatorial and transverse sections of gastropod species that are made of an un−chambered trochospiral shell; these shells are thick and have been dissolved and replaced by calcite cement or pelleted grains.

Remarks: The shell thickness is suggestive of a higher energy environment and many of these may have been transported from their actual habitats.

Order **CERITHIIDAE**

Cerithiidae

Plate 75, Figure C

***Diagnosis*:** Species of the Cerithiidae formed of un−chambered cone-like turreted shell; the shell has been dissolved and replaced by calcite cement.

Remarks: This group of gastropods is common in the nearshore environments such as intertidal, subtidal and lagoonal.

Class **BIVALVIA**

Bivalve fragments.

Plate 76, Figures A-C

***Diagnosis*:** Bivalve shells with bilateral symmetry formed of replaced calcite (originally aragonite); mostly broken and compressed.

Remarks: These species are common in nearshore environments such as intertidal, lagoonal subtidal, inner shoal, open marine protected lagoon, and the platform margin.

Costate bivalve spp.

Plate 76, Figures D and F

***Diagnosis*:** These are costate types of bivalves that have thick shells.

Remarks: These species are good indicators of high energy conditions since they have robust, thick shells.

Inoceramus sp. (fragments)

Plate 76, Figure E

***Diagnosis*:** Fragmented type of very thick bivalves that are characterized by a prismatic layer that are often found in individual prisms.

Remarks: Inoceramids are a feature of the platform margin and the platform slope.

Stratigraphic Range: *Inoceramus* spp. occur throughout the Cretaceous (Scholle and Ulmer-Scholle, 2003).), and they have little stratigraphical value in a fragmentary state.

(Oyster)

Plate 77, Figures A-C

***Diagnosis*:** It is a very thick type of bivalve characterized by a multi-layered internal structure. The first layer is original calcite followed by two layers of replaced calcite cement (originally aragonite).

Remarks: These species are an indicator of platform margin areas.

4.10 SYSTEMATICS OF ECHINODERMATA

This group includes echinoid plates, echinoid spines, crinoid plates and *Saccocoma* sp. However, they are excellent calcareous microfossils that help in the identification of palaeoenvironments and the hydrodynamic energy. Often found fragmentary, they can still be attributed to the organism. Their occurrences frequently help to recognize sequences and the sea level history of a succession of carbonate rocks.

Phylum **ECHINODERMATA**

Sub-Phylum **ECHINOZOA**

Class **ECHINOIDEA**

Order **ECHINOIDA** Claus, 1876

Echinoid plates and echinoid spines

Echinoid plates: Plate 77, Figures E-F, Plate 78, Figures A-C ; echinoid spines: Plate 79, Figures A-D

***Diagnosis*:** These are fragments of plates and spines, in which each individual is made of a single calcite crystal. These crystals are characterized with unit extinction and a meshwork perforation that are often filled with syn-sedimentatry materials such as micrite. Usually syntaxial cement overgrowth is associated with echinoid and crinoid plates (Scholle and Ulmer-Scholle, 2003, p. 178).

***Remarks*:** The echinoid plates and spines are derived from sea urchins which can live only in normal marine conditions from shoreface to deep slope and abyssal basins (Scholle and Ulmer-Scholle, 2003, p. 178). However, they are very common in the normal marine subtidal zones and the platform margin zone. The common occurrence of echinoid spines is a direct indication of the distal parts of the platform margin zone (Scholle and Ulmer-Scholle, 2003, p. 183; Flügel, 2004, pp. 556-558). Regular (surface dwelling) and irregular (burrowing) forms can often be identified by their distinctive spines.

Stratigraphic Range: The overall stratigraphical range is given as Late Ordovician to Recent by Scholle and Ulmer-Scholle (2003), and they have little stratigraphical value in a fragmentary state.

Sub-Phylum **PELMATOZOA**

Class **CRINOIDEA** Miller, 1821

Crinoid plates

Plate 78, Figures E-F

***Diagnosis*:** Crinoid plate formed of a large, single calcite plate made of high-Mg calcite (3-8 mole % Mg). It is perforated by multiple small pores.

***Remarks*:** The crinoid plates are detached columnal ossicles and arm plates from crinoid stems and arms. These only prefer marine conditions and have very little tolerance of salinity changes (Scholle and Ulmer-Scholle, 2003, p. 184; Flügel, 2004, pp. 550-554). The plates are associated with calcite syntaxial overgrowth cementation and has unit extinction (Scholle and Ulmer-Scholle, 2003, p. 184).

Stratigraphic Range: The stratigraphical range is given as early Ordovician to Recent by Scholle and Ulmer-Scholle (2003), and they have little stratigraphical value in fragmentary state.

Order **ROVEACRINIDA** Sieverts-Doreck, 1933

Family **ROVEACRINIDAE** Peck, 1943

Genus ***Saccocoma*** Agassiz, 1835

Saccocoma sp.

Plate 79, Figures E-F

Diagnosis: *Saccocoma* are formed of twin radiating calcareous plates with different extinction directions. They have variable shapes similar to harpoon heads.

***Remarks*:** The plates are separated parts of the pelagic *Saccocoma* skeleton in which they represent radiating calcareous plates with higher extinction in comparison with echinoid plates and spines. This genus is restricted to the pelagic carbonates of the platform margin and slope.

***Stratigraphical Range*:** The range is given as Middle Oxfordian to Lower Kimmeridgian by Olszewska (2010). Although this form can extend up to the Upper Tithonian and Berriasian of the Sulaiy Formation, this is likely to be a partial range.

Sub-Phylum **ASTEROZOA**

Class **ASTEROIDEA** (star fish)

Asteroid sp.

Plate 77, Figure D

***Diagnosis*:** Asteroids are made of plates with an irregular shape that have a high mesh−work perforation and highly porous appearance. Similarly with echinoids and crinoids, it has the unit extinction property under the cross polarized light (Scholle and Ulmer-Scholle, 2003, p. 190).

***Remarks*:** The asteroids occur in a wide range of palaeoenvironments from intertidal to deep basins. They are slightly more tolerant of changes in salinity than echinoids and crinoids (Scholle and Ulmer-Scholle, 2003, p. 183).

Stratigraphic Range: Asteroids have a stratigraphical range from early Ordovician to Recent by Scholle and Ulmer-Scholle (2003), and they have little stratrigraphical value in a fragmentary state.

4.11 SYSTEMATICS OF OSTRACODA

Phylum **ARTHOROPODA**

Super-Class **CRUSTACEA**

Class **OSTRACODA**

Ostracoda spp.

Plate 80, Figures A-E.

***Diagnosis*:** The bivalved carapace of ostracoda is made of well preserved, radiating calcite with a variable thickness and shape. The carapace is usually small and biconvex with smoth internal and external margins. Different valves sizes and thicknesses are observed as the animal moults during life (Scholle and Ulmer-Scholle, 2003, p.198).

Remarks: It is almost impossible to identify to the generic or species level using thin−sections. However, they are common in the following palaeoenvironments: lacustrine, brackish supratidal, intertidal and lagoonal zones.

Stratigraphic Range: The Ostracoda have a stratigraphical range from early Cambrian to Recent (Scholle and Ulmer-Scholle, 2003), and separated forms must be identified to the species level to have any stratigraphical value.

4.12 SYSTEMATICS OF MICROTRACEFOSSIL

Class **MALACOSTRACA** Latreille, 1803

Order **DECAPODA** Latreille, 1803

Tribe **THALASSINIDEA**

Family **FAVREINIDAE** Vialov, 1978

Genus ***Favreina*** Brönnimann, 1955

Favreina sp. *cf. F. dinarica* Brönnimann, 1976

Plate 80, Figure F., Plate 81, Figure A

1975 *Favreina* aff.*salevensis* (Parejas, 1948); Lehmann, pp. 827-828, pl. 1, figs 1-13, pl. 2, figs 1-17,

text- figs 1-2.

1976 *Favreina dinarica* Brönnimann, p. 40, pl. 7, figs 1-14.text-fig. 4D.

2010 *Favreina* cf. *salevensis*; Ketzmann and Palma, p. 59, fig. 3A.

2010 *Favreina* cf*. dinarica* Brönnimann; Olszewska, p.32, pl. VIII, fig. 14.

Diagnosis: Calcareous crustacean coprolite with a deformed semi-circular outline of about 0.5 mm diameter; it is formed of 2 bilateral, semi-symmetric and contains about fourty internal canals.

***Remarks*:** This species is similar to *Favreina dinarica* Brönnimann (1976, text-figure 4 D, 49-48 pp.).This calcareous crustacean faecal pellet is restricted to the shallower and subtidal palaeoenvironmetns of the inner platform area (Brönnimann, 1976). This fossil is very rare and it has usually been transported from shallower facies to the nearby deeper sediments.

***Stratigraphical Range*:** The stratgraphical range of *Favreina dinarica* Brönnimann is given as Berriasian to Hauterivian (Neocomian) by Olszewska (2010).

4.13 SUMMARY

The main microfossil groups encountered are foraminifera, microproblematica, sponge group, calcispheres, calcareous algae, calpionellids, molluscan bioclasts, ostracoda and other microfossils. Photomicrographs have been taken of these microfossils and their morphology, mineralogy, association with other assemblages and systematics documented. Literature on Tethyan carbonate studies of Upper Jurassic and Lower Cretaceous microfossils have been studied.

On the evidence provided by the foraminifera, the Sulaiy Formation is considered to be transitional from the uppermost Jurassic (Tithonian) to the lowermost Cretaceous (Berriasian to the lowermost Valanginian). The use of index fossils range zones of calpionellids, benthic foraminifera and dasyclad algae has confirmed the chronostratigraphic age of the upper Sulaiy Formation as Berriasian to lowermost Valanginian, and the Yamama Formation as Valanginian.

Microlithological and semi-quantitative micropalaeontological analysis of the studied wells samples has provided considerable insight into the biocomponent composition as well as providing evidence for defining various microfacies

sedimentary zones and will define microfacies in the following chapter of this research (Chapter five).

CHAPTER FIVE

PALAEOENVIRONMENTAL DEPOSITIONAL MODEL

CHAPTER FIVE

PALAEOENVIRONMENTAL DEPOSITIONAL MODEL

5.1 INTRODUCTION

In order to generate a stratigraphical framework and sequence stratigraphical interpretations for each well it is important to have a depositional model which includes facies characteristics and their distribution in space and time. This model should include both lithofacies and microfacies characteristics, both of which contribute to the identification of Facies Zones. An understanding of these zones, within a chrono-stratigraphic framework, will allow the identification of potential reservoirs in the Lower Ratawi group of oilfields both on-shore and off-shore eastern Saudi Arabia.

Key to developing such a depositional model is an understanding of the microfossil assemblage (including molluscs, calcareous algae, agglutinated foraminifera, rotalid foraminifera, miliolids, planktonic foraminifera, calpionellids, problematica, etc.) and their relationship with palaeobathymetry. Allochthonous microfossils must also be identified and interpreted correctly, especially where they are an important component of the assemblage (e.g., calciturbidites; see Flügel, 2004).

Carbonate basins and platforms record subtle changes in water depth, as the variation in depositional parameters controls the generation of carbonate and, ultimately, lithofacies. Understanding the palaeogeography of an area requires knowledge of the areal distribution of facies on both the local and regional scale, and leads to the production of palaeogeographical maps.

5.2 SULAIY FORMATION PALAEOENVIRONMENTAL MODEL.

5.2.1 Introduction.

Generating, and testing, a depositional model as a part of formulating a sequence stratigraphical interpretation of a region is a key to understanding its geological development and – ultimately – reservoir potential. In general, the carbonate Platform models have been developed by Simmons and Williams (1992), Emery and Myers (1996), Spence and Tucker (1999, 2000, and 2007), Spence *et al.* (2004) and Ahr (2008). Investigations of Lower Cretaceous shallow marine carbonates have been conducted by Hughes (2000), El-Azabi and El-Arabi (1996, 2007), Strohmenger *et al.* (2006) and Hosseini and Conrad (2008).

5.2.2 Depositional Model for the Arabian Shallow Platform.

Selecting an appropriate depositional model must take into consideration four essential factors:

1. The palaeogeographical setting of the area in the Berriasian;
2. The tectonic setting of the area in terms of any structures, rifts, etc., that will control or influence sedimentation patterns;
3. Sea level changes (eustasy), and how these palaeobathymetrical changes will affect the carbonate factories of the Arabian Platform and, ultimately, control the development of facies; and
4. The microfacies analysis with eventual biofacies analysis has provided distinguishable facies zones that observed carbonate

platform evolution from ramp facies to carbonate platform with localised ooid shoals as distal build-up. Although, lateral facies changes have been used to generate and demonstrate palaeogeographical maps of the studied wells.

The depositional model for the Sulaiy Formation will, therefore, include an assessment of the whole of the shallow platform of this passive margin and how it relates to the whole of the Peri-Tethys area (Figure 5.1). The shallow platform models of passive margins has been discussed in general by Kauffman and Hart (1996), Scotese (1997), Dercourt *et al.* (2000) and Skelton (2003).

The Arabian Platform, during the Berriasian, was on the edge of the super-continent of Pangaea both before, and during, its breakup in the early to mid-Cretaceous. The field area was located in the north-eastern part of the African Plate. All of Arabia, excluding the Nubian-Arabian shield and land, was a shallow continental passive margin covered by a shallow sea (Figure 5.1). The tectonic activity during the Tithonian stage (uppermost Jurassic) was very weak across the Arabian Plate and this led to the development of the extended passive margin of Arabia (Dercourt *et al.,* 2000). However, this passive margin was originally created by slow, normal palaeo-rifting, in which it has minimal effect on the sea level fluctuations. Eventually, that was a response to the, slow continuous marginal rifting in some parts of the Arabian Platform created by S-SW to N-NE normal faults (Figure 2.6) during the Berriasian stage (Dercourt *et al.,* 2000). This ancient rifting possibly increased the sedimentation rate and accommodation space locally in some parts of the Arabian Platform. The passive margin contributed to the global

measurement of ocean crust production (Figure 5.2) during the Berriasian stage which is within minimal rates at 20 × 10^6 km^3/m.y. (Larson, 1991; Kauffman and Hart, 1996). Though still within the Cretaceous 'greenhouse' (Skelton, 2003, pp. 174-179), the earliest Cretaceous does record slightly lower temperatures, with a cooler phase extending throughout the Berriasian and Valanginian (Hart *et al.*, 2009; Nunn *et al.*, 2010). It was only during the Barremian stage (Fig. 5.2) that palaeotemperatures began to rise, possibly linked to the increasing rate of ocean crust production (Larson, 1991; Kauffman and Hart, 1996; Dercourt *et al.*, 2000). The early Cretaceous was, therefore, characterised by the presence of wide, shallow-water, carbonate platforms (Figures 2.6, 2.7, 5.2 and 5.3). All of the regional evidence, and the present detailed investigation of the lithofacies, indicates the presence of an extensive shallow-water, carbonate platform. In this study it is called the 'Standard Arabian Rimmed Shallow Carbonate Platform (Figure 5.3).

Based on the evidences discussed previously and from the analysed lithofacies of Sulaiy Formation, the correct palaeoenvironmental depositional model is that of a shallow carbonate platform. It is named in this study as the Arabian Rimmed Shallow Platform; abbreviated as ARSP in this investigation (Figure 5.3).

5.2.3 Arabian Rimmed Shallow Platform (ARSP) Model.

There are a number of classifications for shallow-water carbonate platforms that have been generated. These include those by Wilson (1970, 1974), Ahr (1973, 2008), Read (1982, 1985) Walker (1992) Tucker and Wright (1990), Schlager (2002) and Flügel (2004). Ahr (2008, p. 77) defined any sedimentary platform as "all depositional surfaces, regardless of their

physiography, or bathymetry". The first rimmed carbonate platform model was generated by Wilson (1975) where he described a number of Standard Facies Zones (FZ) and their Standard Microfacies Types (SMF). The differentiation and comparison between different carbonate platforms was discussed by Flügel (2004) and Ahr (2008). These models helped to identify the ideal sedimentary platform geomorphology and model used in this research. The palaeogeographical setting and the results of a lithofacies analysis provide evidence of the type of depositional model appropriate for the lower Cretaceous.

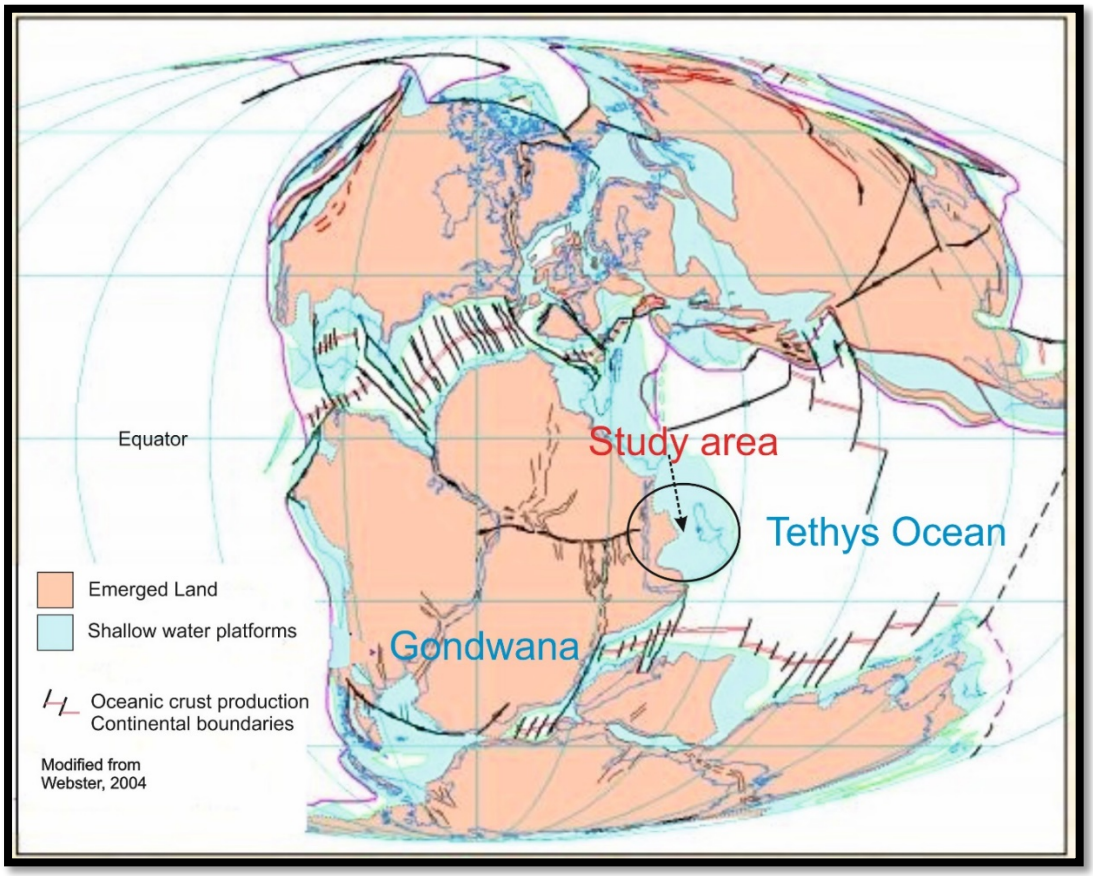

Figure 5.1. The position of the study area and the Equator during the Berriasian are shown in this palaeotectonic map. Note the extensive, passive margin (the Arabian shallow marine platform) of the Arabian Plate on the eastern edge of the African Continent (modified from Webster, 2004).

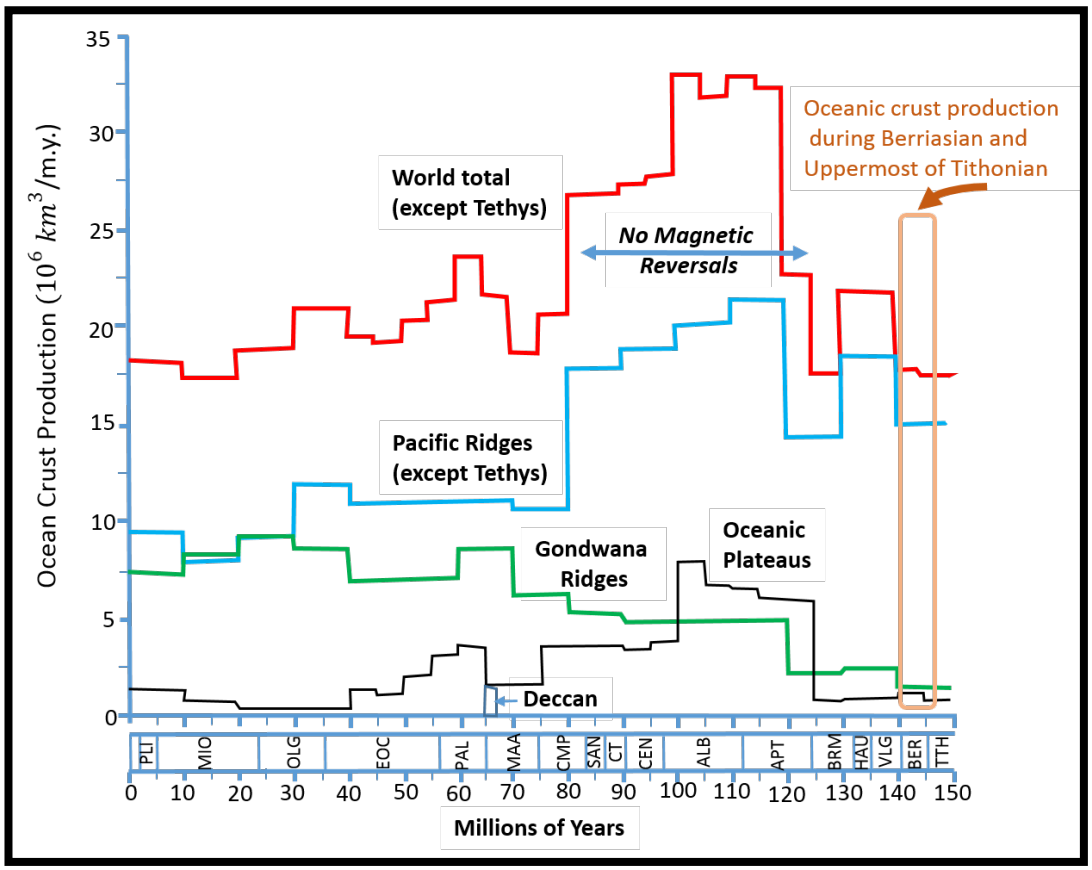

Figure 5.2. Chart showing the Berriasian stage (Orange box), which is a time of normal oceanic crust production (modified from Larson, 1991; Kauffman and Hart, 1996). The period of enhanced rifting began in the Barremian and continued into the Campanian.

This is known as the Rimmed Platform. This platform is an independent category that differs slightly from a Rimmed Shelf and which is quite different from the Monoclinal Ramp, Open Shelf, Distally Steepened Ramp or Eperic Platform. This depositional model is characterised by a wide, flattened, shallow platform with only gentle slopes. This slope is definitely different from the quite steep angle that is typical of a ramp. The Arabian Rimmed Shallow Platform was developed on the very wide, submerged, Arabian Plate (Figure 5.3). This platform is similar to the depositional models produced by the following authors in nearby regions: Schulze *et al.* (2005), Strohmenger *et al.* (2006) and Hosseini and Conrad (2008). The hydrodynamics of the sea

water that developed the Arabian Rimmed Platform is perfectly explained by Ahr (2008). The descriptions of the lithofacies zones from Flügel (2004) are also appropriate for use in this study.

From Recent rimmed shelf studies, the hydrodynamical settings of rimmed platforms can be obtained from the Florida Keys or the Great Bahama Banks (Ahr, 2008). Any waves that interact directly on the platform margin and the platform shoal, cause erosional effects on the platform margin and disturb the environments on the platform shoal. Strong storms will rip up lithoclasts from the substrate and, mixed with different skeletal grains, will be transported throughout the slope and the deep slope where they will accumulate. Wave energy will be largely absorbed before the platform shoal and only weak waves will reach beyond this to the protected open marine subtidal zone. These will have only a minimum effect within the lagoonal zone (Figure 5.3). As a consequence of this energy distribution, the amount and distribution of marine micrite will increase in the sediments of the protected open marine zone and lagoon. Thus, lithofacies types reflect the amount of micrite in the carbonate sediments, with the lowest energy regime supporting the highest micrite production. During any storm events this situation will shift below storm wave base to the deep slope and even the basin. The amount of wave and current energy, along with the palaeobathymetry depths, has controlled the lithofacies depositional zones of the Rimmed Arabian Platform depositional model. Thus, the depth of the fair weather wave base (FWWB) is between 10 m to 30 m and the storm wave base (SWB) is between 25 m to 100 m based on the evidence presented by Flügel (2004), Strohmenger *et al.* (2006), Ahr (2008) and Katz *et al*. (2013).

Overall, this palaeoenvironmental depositional model is characterised by two different platform regimes. These are the Platform Interior and the Platform Exterior in which they have unique sedimentary environments that produce different types of microfacies. Each microfacies is characterised by quite special depositional conditions and palaeobathymetry that are interact differently with sea level changes and the accommodation space.

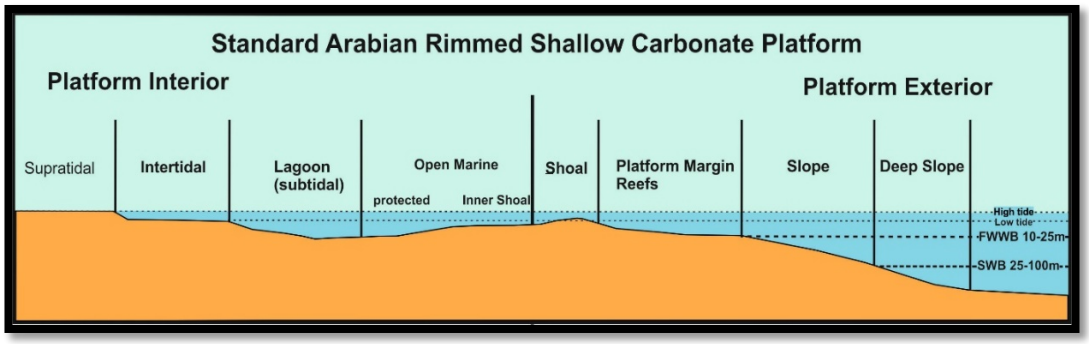

Figure 5.3. A palaeoenvironmental depositional model for the Sulaiy Formation which is named, in this study, the Standard Arabian Rimmed Shallow Carbonate Platform. It is subdivided into two parts: the Platform Interior and the Platform Exterior.

5.3 DEPOSITIONAL ZONES.

Flügel (2004, p. 657) defined Facies Zones (FZ) as" belts differentiated according to the changes of sedimentological and biological criteria across shelf- slope- basin transects". Microfacies are similar but these are obtained by petrographical analysis using a polarising microscope. In this study the term used for both microfacies and facies is lithofacies (Ahr, 2008). However, these microfacies were accumulated in microfacies zone(s) in which they were produced by sedimentary processes within a specific palaeobathymetry

and under specific hydrodynamic conditions. Microfacies Depositional Zones (MDZ) are identified by using information provided by Wilson (1975), Lucia (1995), D' Argenio *et al.* (1999), Flügel (2004), Schulze *et al.* (2005), Strohmenger *et al.* (2006) and Ahr (2008). The zones (MDZ) in this study are slightly different from those of the above-mentioned authors and are probably restricted to the Arabian Platform (Figure 5.3). The Arabian Rimmed Platform is described in two parts: the Platform Interior and the Platform Exterior.

The Platform Exterior is composed of four different Microfacies Depositional Zones. These have been given codes in this study and these are the Deep Slope (MDZ-1), Slope (MDZ-2), Platform Margin (MDZ-3) and Platform Shoal (MDZ-4). The Platform Interior zones are Open Marine (MDZ-5), which is formed of a protected subtidal Open Marine Subzone and the shallower Inner Shoal Subzone. The Platform Interior is, additionally, formed of the Subtidal Lagoonal Zone (MDZ-6), Intertidal Zone (MDZ-7) and the Supratidal Zone (MDZ-8). The Supratidal Zone has not been encountered and probably located in a very narrow facies belt adjacent to the land. Distal lithofacies zones are located above fair weather wave base (FWWB) where carbonate materials are re-sedimented. These distal microfacies sedimentary zones are Platform Margin (MDZ-3) and Platform Shoal (MDZ-4). The deepest palaeoenvironment is the Deep Slope (MDZ-2) in which microfacies have been accumulated below the storm wave base (SWB). The Platform Shallow Margin (MDZ-3) is a very narrow belt in which microfacies have been accumulated above the fear weather wave base (FWWB).

These microfacies zones are best described by Wilson (1975) and Flügel (2004, pp. 662, 666). The Microfacies Depositional Zones (MDZ) of the

Sulaiy Formation and the Base of the Yamama Formation are explained as follows:

Platform Exterior's Deep Slope, below SWB (MDZ-1)

Synonymies: Outer Neritic (Koutsoukos and Hart 1990; Katz *et al.,* 2013); Middle and Lower Slope (Koutsoukos and Hart 1990); Platform Margin Slope (Alsharhan and Nairn, 1993); Steep Erosional Slope with Depositional Terraces (Haas, 1999, p. 63); Toe-Of-Slope (Flügel, 2004, pp. 662, 721; Haas *et al.,* 2006, p. 63); Deep Shelf Margin (Flügel, 2004, p. 662); Outer Ramp (Flügel, 2004, pp. 386, 666; Krajewski, 2006); Open Platform's Lower Ramp (Strohmenger, 2006); Lower Platform Slope (Krajewski, 2010).

Description: This zone is located below the storm wave base (SWB).

Sediments: The sedimentation rate of the Deep Slope Zone is low due to the mesotrophic conditions of medium levels of nutrients content in the sea water. This zone is characterized by mainly low to moderate energy. The sediment input is often dominated by allochthonous material (fine to medium-grained), carbonate sediments and a minority of autochthonous, pelagic, mudstone. However, occasional, storm derived and reworked sediments have been accumulated as interbeds, during times of lowered sea levels and during storm events. Abundant mixed lithoclasts and finely broken skeletal debris have been accumulated as calcisiltite (Flügel, 2004, p. 666).

Associated microfossils: The associated biota are usually small agglutinated foraminifera and planktonic foraminifera, crinoid plates, *Saccocoma* sp, echinoderm plates, echinoderm spines, sponge spicules, calpionellids and some problematica. Very important, common, microfossils

are *Conoglobigerina* sp. cf. *C. gulekhensis* (Gorbatchik and Poroshina, 1979), *Ophthalmidium* spp., Serpulid sp, *Terebella lapilloides* and *Crescentiella morronensis* forma *morronensis* (Crescenti, 1969).

Platform Exterior's Upper Slope, below FWWB and above SWB, (MDZ-2)

Synonymies: Middle Neritic (Koutsoukos and Hart 1990; Katz *et al.,* 2013, Hughes, 2013); Upper Slope (Koutsoukos and Hart 1990); Platform Margin Slope or Fore-Reef (Alsharhan and Nairn, 1993); Distal and Proximal Slope Terrace (Haas, 1999, p. 59); Upper Slope (Chlagintweit *et al.*, 2000), Slope (Flügel, 2004, p. 662; Haas *et al.,* 2006); Mid-Ramp (Flügel, 2004, pp. 386, 666; Krajewski, 2016); Mid-Shelf (Flügel, 2004, p. 667), Open Platform's Middle Ramp (Strohmenger *et al*., 2006); Slope (Krajewski, 2010).

Description: This zone is located below Fair Weather Wave Base (FWWB) and above Storm Waves Base (SWB). The sea floor of this part is inclined toward the Deep Slope and the Deep Shelf (Flügel, 2004, p. 662).

Sediments: This environment is dominated by high energy materials reworked from the shallower Platform Margin. During lower energy periods these materials are mixed with pelagic micrites and other skeletal remains. The produced lithofacies from the Upper Slope sedimentary environment are mudstone, reworked materials packestone, rudstone, grainstone, and floatstone. (Flügel, 2004, p. 662).

Associated microfossils: The associated biota are usually *Mohlerina basiliensis* (Mohler, 1938), *Lenticulina* sp. and *Nodosaria* sp., small agglutinated foraminifera, crinoid plates, echinoderm plates and spines and sponge spicules. Important common microfossils are *Ophthalmidium* sp.,

Serpulid sp, *Terebella* sp. cf.*T. lapilloides* Münster (1833) and *Crescentiella morronensis* forma *morronensis* (Crescenti, 1969).

Platform Exterior's Margin, above FWWB, (MDZ-3)

Synonymies: Inner Neritic (Koutsoukos and Hart 1990; Katz *et al*., 2013); Inner Shelf or Inner Neritic (Koutsoukos and Hart 1990; Hughes, 2013); Reef Margin (Alsharhan and Nairn, 1993; Haas *et al*., 2006); Platform Margin (Chlagintweit *et al*., 2000; Flügel, 2004, p. 721; Krajewski, 2010); External Platform (Colombie and Strasser, 2005); Outer Platform (Michetiuc and Bucur, 2012); Open Platform's Upper Ramp (Strohmenger *et al*., 2006); Inner Ramp (Krajewski, 2016).

Description: This zone is normal marine on the Platform Exterior and located above the Fair Weather Wave Base (FWWB). This part is usually very shallow next to the shoal bank and it is characterized by high to moderate wave energy.

Sediments: The sediments of this zone are characterised by large reworked skeletal and lithoclasts materials from nearby shallower zones or from the Platform Margin itself. There are common stromatoporoids and large *Lithocodium* nodules' microfacies that may be forming the rim of the platform.

Associated microfossils: The zone is characterised by colonial encrusters such as encrusting *Lithocodium* and *Thaumatoporella*. Encrustinfg foramnifera such as *Nubecularia* spp. and *Nodobacularia* sp. are common. Calcareous algae are common and represented by *Thaumatoporella parvovesiculifera* (Raineri, 1922), *Marinella lugeoni* Pfender (1939), *Salpingoporella* gr. *pygmaea* (Gümbel, 1891) and *Actinoporella podolica*

(Alth, 1878). Crinoid plates are common with echinoderm plates and spines. However, Serpulid sp., multi-layered bivalves and *Inoceramus* sp. (fragment) are also common. *Crescentiella morronensis* forma *morronensis* (Crescenti 1969) also characterizes the higher energy part of this zone. The trocholinids (*Coscinoconus* spp.) are common, together with biserial agglutinated foraminifera.

Platform Exterior's Shoal (MDZ-4)

Synonymies: Paralic Shoal (Koutsoukos and Hart 1990); Shoal or Sand Shoal (Alsharhan and Nairn, 1993; Haas *et al*., 2006; Krajewski, 2010); Outer Shoal (D'Argenio *et al*., 1999); Platform Exterior's Sand Shoal (Flügel, 2004, p. 721); Internal Platform's External Shoal (Colombie and Strasser, 2005); Open Platform's Shoal (Strohmenger *et al*., 2006); Outer Platform's Shoals (Michetiuc and Bucur, 2012).

Description: This Zone forms the edge of the Platform Interior and is located above the shallower, normal wave base. The shoal zone is characterised by high energy agitating waves (Flügel, 2004, p.663).

Sediments: This zone is dominated by ooid grainstones, peloidal grainstone and packstone that is usually clean from micritic materials.

Associated microfossils: The ooid shoal contains a less diverse biota with rare with foraminifera and calcareous algae. However, the more protected tidal channels may contain bivalves and gastropods with encrusting *Thaumatoporella* and *Lithocodium* nodules. It is also quite common to find echinoderm and crinoid plates.

Platform Interior's Inner Shoal (back shoal) Zone (MDZ-5A)

Synonymies: Back Shoal (Alsharhan and Nairn, 1993); Inner Shoal (D'Argenio *et al*., 1999; Krajewski, 2010); Back-Reef (Chlagintweit *et al*., 2000); Internal Platform's Internal Shoal (Colombie and Strasser, 2005); Restricted Platform's Inner Shoal (Strohmenger *et al*., 2006); Middle Platform's Subtidal Sand Bars (Michetiuc and Bucur, 2012); moderate- to high-energy Inner Ramp (Krajewski, 2016).

Description: This zone is intertidal to shallow subtidal and is located at the back of the platform shoal which is characterised by less wave energy intensity and may be protected. However, it remains an open marine part of the Lagoon. It is still affected by the normal marine conditions (Flügel, 2004, p. 663).

Sediments: The Platform Interior's Inner Shoal contains variable types of microfacies and sediments beginning with wackestones on the lagoon side to packstones and grainstone at the ooid shoal bank side. Winnowed and clean peloidal to pellet grainstone is common at the lagoon side, created by high energy waves.

Associated microfossils: This zone is characterized by a shallow-marine biota such as benthic foraminifera and calcareous algae. Molluscs, such as bivalves and gastropods, are common together with *Cladocoropsis mirabilis* Felix (1927).

Platform Interior's Protected, Open Marine, Lagoonal Zone (MDZ-5B)

Synonymies: Protected Lagoon (D'Argenio *et al.*, 1999); Platform Interior's Protected, Open Marine (Flügel, 2004, pp. 662, 721); Internal Platform's Sheltered Lagoon (Colombie and Strasser, 2005); Restricted Platform's

Subtidal (Strohmenger *et al*., 2006); Platform Interior Normal Marine (Haas *et al*., 2006); Subtidal, Open Marine (Krajewski, 2010).

Description: This zone is represented by the flat subtidal part to deep subtidal of the marine protected lagoon next to the inner-shoal and bordered by the restricted Lagoonal Zone. This zone is affected by marine conditions with low to moderate energy intensity. Water depth is a maximum of a few tens of meters and it is the deepest part of the Platform Interior (Flügel, 2004, p. 663).

Sediments: It is characterised mudstone to wackestone at the lagoon side. Winnowed fine sediments from the shallower inner-shoal are accumulated in this zone.

Associated microfossils: This zone contains a very high biotic diversity and contains most of the benthos of the lagoonal zone. Benthic foramnifera are commonly recorded, including large lituolids such as *Kurnubia palastiniensis* Henson (1948), *Coscinoconus* spp. and *Nautiloculina oolithica* Möhler (1938). Clacareous algae are common, including *Thaumatoporella parvovesiculifera* (Raineri, 1922), *Marinella lugeoni* Pfender (1939), *Salpingoporella* spp.and *Actinoporella podolica* (Alth, 1878). This zone is also characterised by the presence of calcispheres (Dinocyct spp.).

Platform Interior's restricted Lagoonal Zone (MDZ-6)

Synonymies: Paralic Lagoon (Koutsoukos and Hart 1990); Platform Lagoon (Alsharhan and Nairn, 1993); Restricted Lagoon (D'Argenio *et al*., 1999; Krajewski, 2010); Platform Interior's Restricted (Flügel, 2004, pp. 662, 721; Haas *et al*., 2006); Internal Platform's Semi Restricted and Restricted

Lagoon (Colombie and Strasser, 2005); Restricted Platform's Subtidal (Strohmenger *et al*., 2006); Outer Platform (Michetiuc and Bucur, 2012).

Description: This zone is a restricted part of the Internal Platform, which is separated from the open marine, protected, part of the lagoon by the internal-shoal. This zone is, however, characterised by elevated salinities and relatively low energy conditions (Flügel, 2004, p. 663).

Sediments: This zone is dominated by mudstone and wackestone with minor peloidal packstones.

Associated microfossils: The biota includes common miliolids, ostracods and calcareous algae. Gastropods and bivalves are rare to common with some records of cyanobacteria.

Platform Interior's Intertidal Zone (MDZ-7)

Synonymies: Paralic Tidal Flat (Koutsoukos and Hart 1990); Tidal Flat (D'Argenio *et al*., 1999); Restricted Platform's Intertidal (Strohmenger *et al*., 2006); Platform Interior's Evaporitic or Brackish (Flügel, 2004, pp. 662-663, 721); Mid-Ramp (Flügel, 2004, p. 666; Krajewski, 2016); Internal Platform's Tidal Flat and Intertidal (Colombie and Strasser, 2005); Intertidal (Krajewski, 2010); Inner Platform (Michetiuc and Bucur, 2012); Proximal and Distal Intertidal Hypersaline (Hughes, 2013).

Description: This zone is located in the intertidal zone and bordered by the supratidal sabkha zone (Flügel, 2004, p. 663).

Sediments: This zone is dominated by shallow intertidal mudstone, which may be associated with mudcracks and evaporite minerals such as anhydrite and gypsum.

Associated microfossils: This environment is barren of foraminifera but may contain ostracods and thin bivalves with rare gastropods (including species of the Cerithiidae). Cyanobacterial mats and stromatolites are commonly recorded.

5.4. MICROFACIES DISTRIBUTION OF SULAIY FORMATION DEPOSITIONAL MODEL

The microfacies were assigned and identified using information from Ahr (1973, 2008), Wilson (1975), Read (1982, 1985), Tucker and Wright (1990), Walker (1992), Schlager (2002), Flügel (2004) and Krajewski (2008, 2010). The best lithofacies analysis, based on microfossil content and non-skeletal grain changes, is provided by Krajewski (2008, 2010). The work of Krajewski (2010) on microfacies palaeoenvironmental analysis has been used as the main reference in the determination of microfacies depositional zones related to sea level changes. The reason for using Krajewskis' (2010) microfacies analysis is that it provides evidence from field lithofacies and lithofacies distribution analysis within the shallow water carbonate platform of the Tethys carbonate region during Berriasian times. Krajewski (2010) analysed the microfacies and sedimentary zones using the classical rimmed platform from the Crimea (Southern Russia). These carbonate formations appear to be the closest analogue to the Arabian Rimmed Carbonate Platform. The exposures of the Sulaiy Formation are not well studied as a result of structural disturbance.

Each of the microfacies is explained and illustrated. Data presented include their microfacies name, Dunham textural classification, reservoir quality, sedimentary features, microfossils and any depositional settings that are suggested twenty-four microfacies are identified, discussed and located within a Microfacies Depositional Zone (MDZ). Figure 5.4 is the summary and the distribution of most important microfacies in the Sulaiy Formation.

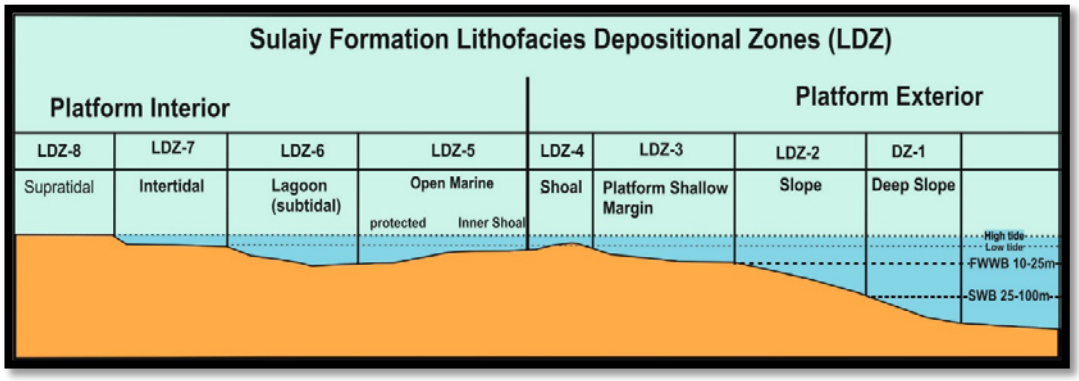

Figure 5.4. The distribution of microfacies along the Arabian Rimmed Platform of the Sulaiy Formation.

5.4.1 Microfacies Characterization of Each Well

Microfacies Depositional Textures are based on Dunham (1962) and Embry and Klovan (1971). Porosity types are based on Choquette and Pray (1970). The most important microfacies were obtained from representative wells such as wells H and D.

Well-H

This onshore well is located in the centre of the southern part of the study area. It is, however, an important cored well as it has been sampled every foot. The samples were taken from the 48 feet core that provided 50 thin sections for analysis. The core top depth is 8380.5’ and the core base is at 8427.5’. The analysis has revealed the following microfacies types:

Well-H Microfacies 1 (HMF 1): Porous, Intraclastic, Foraminferal and Peloidal Packstone (Plate 82, Figures A-B).

Description: This microfacies is characterised by lithoclasts, peloids, intraclasts, benthic foraminifera and aggregates.

Depth: This microfacies is recorded from a depth of 6427.5 ft in Well-H.

SMF Type: The microfacies is close, or equivalent, to SMF 21, fenestral packstone or bindstone. This is from the restricted facies zone (FZ8) of Flügel (2004, p. 721). The biodiversity of HMF 1 is, however, greater and it contains protected open marine microfossils.

Palaeoenvironment: This microfacies is mainly attributable to the distal, intertidal part of the lagoonal part (MDZ-7) and the microfossil content is suggestive of the intertidal part of the back-shoal of the protected open marine facies zone (MDZ-5). However, this is a shallow-water, intertidal, palaeoenvironment in Well-H during this part of the sequence (TST).

Primary porosity: This microfacies is highly porous (~20%) and has potential reservoir quality with fenestral (FE), interparticle (BP) and intraparticle (IP) porosities.

Microfossil content: This microfacies contains common *Verneuilinoides polonicus* and *Nautiloculina bronnimanni*. Other, rarer microfossils include *Ammobaculites subcretaceus*, *Protopeneroplis ultragranulata*, *Quinqueloculina* spp., *Coscinoconus alpina*, *C. delphinensis*, *Ophthalmidium* sp., *Salpingoporella pygmaea*, *Thaumatoporella parvovesiculifera* and fragments of costate bivalves.

Well-H Microfacies 2 (HMF2): Finely Laminated Mudstone (Plate 83, Figures A-B).

Description: This is a microfacies characterised by the presence of laminated mudstones. Most of the included fragments have been leached out leaving a rare moldic porosity.

Depth: This microfacies was recorded between a depth of 6426.5 ft and 6415.7ft in Well-H.

SMF Type: This is equivalent to SMF 22, the laminated mudstone. This is probably representative of FZ7, FZ8 and FZ9 of Flügel (2004, p. 721).

Palaeoenvironment: The laminated mudstone microfacies was deposited along the intertidal and subtidal parts of the lagoon where energy levels were very low, interrupted by occasional, storm-induced, periods of gravity flows and storm-material suspensions.

Primary porosity: The HMF 2 microfacies porosity is from 0 % to <0.5 % of a moldic (MO) porosity type. Almost all of the porosity is formed by the empty spaces left by dissolved grains.

Microfossil content: This microfacies is characterised by being barren of microfossils to one of very low biodiversity. It only contains occasional, thin-walled ostracods.

Well-H Microfacies 3 (HMF 3): Peloidal, Foraminiferal and Intraclastic Packstone (Plate 84, Figures A-B; Plate 85, Figures A-B; Plate 86, Figures A-B). Description: This microfacies is characterized by fine grained packstone and grainstone made of allochthonous peloids, ooids, coated

grains, lithoclastics and benthic foraminifera. This microfacies is, sometimes, typified by a form of peloidal lamination with low porosity values (~5%).

Depth: HMF3 microfacies was recorded from depths (6425.5 ft to 6424.5 ft; 6414.8; 6410.2 ft to 6409.2 ft; 6413 ft) in Well-H.

SMF Type: This microfacies is equivalent to SMF 16, a non-laminated peloidal packstone and it is attributed to restricted platform interior zone (FZ8) of Flügel (2004, p. 721).

Palaeoenvironment: The HMF3 microfacies is mainly characterized by moderately agitated to intermediate energy levels. This formed in a subtidal, peloidal bank (inner shoal of MDZ-5) with no restriction from open water agitation and was formed above fair weather wave base (FWWB). This bank, however, created a restriction to the lagoonal part of the platform interior.

Primary porosity: The HMF3 microfacies has a potential reservoir quality with highly porous (5–20%) interparticle (BP) and intraparticle (IP) porosities. This moldic porosity resulted from diagenesis during long-term subaerial exposures.

Microfossil content: This microfacies contains diagnostic microfossils indicating a lagoonal to protected open marine environment. The assemblage includes *Salpingoporella pygmaea*, bivalve fragments, gastropod (at 6414.8'), *Pseudocyclammina lituus*, *Protopeneroplis ultragranulata*, *Quinqueloculina* spp., miliolids, *Istriloculina* spp., *Pfenderina neocomiensis*, *Coscinoconus alpina, C. delphinensis*, *Gaudryinopsis* sp., *Verneuilinoides polonicus, Protomarssonella kummi, Haghimashella arcuata,* common echinoderm plates and spines, and *Lithocodium* intraclasts.

Well-H Microfacies 4 (HMF 4): Lithocodium, Intraclastic and Peloidal Wackestone-Packstone-Grainstone-Rudstone (HMF 4a: Plate 87, Figures A-B; Plate 88, Figures A-B; Plate 89, Figures A-B; Plate 90, Figures A-B; HMF 4b: Plate 91, Figures A-B).

Depth: This microfacies is recorded at depths (6423.5 ft to 6416.7 ft; 6412.1 ft to 6411.1 ft; 6407.2 ft to 6406.4 ft; 6400.4 ft) from Well-H.

SMF Type: The microfacies is close, or equivalent, to SMF13, the oncoid rudstone or grainstone. It represents the shallow open marine microfacies zones FZ7, FZ6 and FZ5 of Flügel (2004, p. 721).

Description and Palaeoenvironment: This microfacies is diagnostic of shallow-water normal marine conditions. It is located in the open marine part of the platform interior and extends to the shallower banks of the platform margin. The shape and size of *Lithocodium* microfacies can characterise two sub-palaeoenvironments:

- HMF4a: The low energy *Lithocodium aggregatum* are large oncoids falling into the categories 3 and 4 of Vědrine *et al*. (2007) and Michetiuc *et al.* (2012), in which they are characterized by encrusting microbial meshwork shapes.
- HMF4b: The high energy *Lithocodium aggregatum* is formed of semi-spheroids or lumps of smaller oncoids that are characterized by a thick micric cortex which was described by Vědrine *et al*. (2007) and Michetiuc *et al.* (2012) as category one of *Lithocodium aggregatum* smaller oncoids.

Michetiuc *et al.* (2012) have recorded microbial traces produced by *Lithocodium aggregatum* organisms such as encrustation, boring, fracturing,

burrowing and the final stage is micritization. However, all of these microbial remains were recorded from the *Lithocodium* microfacies. Michetiuc *et al.* (2012) also found that HMF4 microfacies is indicative of low accumulation and sedimentation rates.

Primary porosity: This microfacies has potential reservoir quality with intermediate to highly porous moldic (Mo), interparticle (IP) and intraparticle (BP) porosities, with a range of porosity from 5% to 20%.

Microfossil content: HMF4 is characterised by relatively low biodiversity and only contains shallow-water, open marine microfossils. *Lithocodium aggregatum* Elliott is the main biotic component of the HMF4 microfacies together with other normal, marine microfossils such as benthic foraminifera, corals, echinoid plates and oysters.

Well-H Microfacies 5 (HMF 5): *Terebella*, *Crescentiella, Ophthalmidium* and Allochthonous Bio-lithoclastic Packstone/Grainstone (Plate 92, Figures A-B; Plate 93, Figure A).

Description: This microfacies is characterized by fine grained packstone and grainstone formed of allochthonous peloids, ooids, coated grains, lithoclastics and allochthonous benthic foraminifera. These are an admixture of reworked sediments transported by gravity flows from both the platform interior and platform margin.

Depth: Microfacies HMF5 was recorded from a depth of 6417.6 ft in Well-H.

SMF Type: This is the equivalent to SMF 5, the allochthonous bioclastic grainstone. It represents the slope and the toe-of-slope zones (respectively FZ4 and FZ3) of Flügel (2004, p. 721).

Palaeoenvironment: Microfacies HMF 5 is commonly found on the deep slope, lying below storm wave base (SWB) during quite continuous episodes of gravity storms.

Primary porosity: The HMF5 microfacies has potential reservoir quality with highly porous (~20%) with both interparticle (BP) and intraparticle (IP) porosities.

Microfossil content: This microfacies was deposited above the storm wave base (SWB) and contains diagnostic microfossils indicating a slope and deep slope biota such as *Ophthalmidium* sp., *Terebella* sp. cf*. T. lapilloides* and *Crescentiella morronensis* forma *morronensis*. Other benthic microfossils are allochthonous transported by gravity flows from shallower zones such as *Protopeneroplis ultragranulata*, *Quinqueloculina* spp., *Pfenderina neocomiensis*, *Coscinoconus alpina*, *C. delphinensis*, *Gaudryinopsis* sp., *Verneuilinoides polonicus, Protomarssonella kummi, Haghimashella arcuata,* common echinoderm plates and spines, and *Lithocodium* extraclasts.

Well-H Microfacies 6 (HMF 6): Laminated Peloidal Packstone/Grainstone/Bindstone (Plate 93, Figure B; Plate 94, Figures A-B).

Description: This microfacies is characterized by alternations of micrite and fine peloidal laminations. It is composed of fine grained packstone and grainstone.

Depth: Microfacies HMF6 was recorded from depths 6406.2 ft and 6405.3 ft in Well-H.

SMF Type: This microfacies is equivalent to SMF16, the laminated from open marine platform interior zone (FZ7) of Flügel (2004, p. 721).

Palaeoenvironment: Microfacies HMF6 commonly forms subtidal banks in the protected Open Marine Zone (MDZ-5). It represents the upper part of the highstand system tract (HST).

Porosity type: HMF5 has a potential reservoir quality with an interparticle (BP) porosity of ~5%.

Microfossil content: This microfacies has a relatively low biodiversity but contains benthic foraminifera such as *Protopeneroplis ultragranulata*, *Quinqueloculina* spp., *Coscinoconus alpina*, *C. delphinensis* and *Verneuilinoides polonicus.*

Well-D

This offshore well is located in the eastern corner of the northern part of the study area. However, this cored well has revealed no value in the sequence stratigraphy analysis because of the missing and non-cored intervals required for the identification of the maximum flooding zones. On the other hand, it has provided a variety of microfacies that are used for setting the sequences and para-sequences in this research. The recovered samples were taken from the 452 feet core that provided 214 thin sections for analysis. The core top depth is 8192.2' and the core base is at 8644.2'. The analysis has revealed the following microfacies types:

Well-D Microfacies 1 (DMF 1): Spiculite, Calcisiltite Wackestone (Plate 95, Figures A-B).

Description: Texture is mainly made of wackestone. The matrix is mainly of spicule-rich, fine, commuted skeletal grains (calcisiltite) wackestone with transported benthic foraminifera, small gastropods and small bivalves. The wackestone micrite is associated with dark pellets, which are diagnosis of low energy condition.

Depth: This microfacies is located in cored Well D at a depth of 8644.2 ft.

SMF type: The DMF1 microfacies is equivalent to the spiculite wakestone/packstone and the microbioclastic peloidal calcisiltite of Flügel (2004) Standard Microfacies (SMF 1 and SMF 2 respectively).

Palaeoenvironment: This microfacies is only located in the Exterior Platform, in which it is located in the Deep Slope (MDZ-1). It is located in the deepest part of the slope which may indicate the highest sea level of a maximum flooding zone (MFZ).

Porosity type: This microfacies has very poor reservoir quality as it contains no porosity. The microfacies is probably a source rock for hydrocarbons.

Microfossil content: This microfacies is characterised by deeper slope microfossils that includes common echinoderms, triaxon spicules, monaxon spicules, planktonic foraminifera and calpionellids. Triaxon spicules, monaxon spicules, planktonic foraminifera (*Conoglobigerina* sp. cf. *C. gulekhensis*) and calpionellids are indicators of the deepest part of slope sedimentary environment.

Well-D Microfacies 2 (DMF 2): Extraclastic, *Nodosaria*, *Lenticulina* and *Saccocoma* Packstone (Plate 96, Figures A-B).

Description: Texture is mainly that of packstone. It is mainly composed of angular, well-sorted lithoclasts and echinoderm fragments. The main matrix is transported lithoclasts in the form of microbreccia. Oil stains are common and implicating fair porosity.

Depth: This microfacies is located in cored Well D at a depth of 8642.7 ft.

SMF type: This is equivalent to the microbreccia, bio-lithoclastic packstone of Flügel (2004) Standard Microfacies (SMF 4).

Palaeoenvironment: The microfacies is characteristic of a slope area. The DMF2 microfacies is located between the fair weather wave base FWWB and the storm wave base SWB within the Platform Exterior. It is located in the Slope Depositional Zone (MDZ-2). Comparing it with DMF1, this microfacies is located in a shallower environment and it represents the high stand system tract HST of the sequence cycle for each bed. However, the high influx of echinoderm debris is an indicator of deeper, open marine sedimentary episodes of gravity flow followed by a low rate of sedimentation and low energy episodes of micritic strata, which settled down vertically in a calm environment.

Porosity type: This microfacies has fair reservoir quality as it contains reasonable levels of porosity that is evident from the oil staining.

Microfossil content: The DMF2 microfacies contain autochthonous pelagic *Saccocoma* spp. and rotalid foraminifera such as *Nodosaria* spp. and

Lenticulina spp. Allocthounous microfossils include common echinoderm fragments, rare gastropods, benthic foraminifera and thin-shelled ostracods.

Well-D Microfacies 3 (DMF 3): Slope-Laminated Peloidal Bindstone/ Wackestone/ Packstone (Plate 97, Figures A-B; Plate 98, Figures A-B).

Description: Textures are mainly made of packstone and bindstone. This microfacies is characterised by slope (above SWB) microfossils that include common echinoderm fragments triaxon spicules, monaxon spicules, planktonic foraminifera and benthic agglutinated foraminifera.

Depth: Location and depth range: this biofacies is located in cored Well D at depths between 8636.7 and 8627.7ft.

SMF type: This is equivalent to the laminated peloidal bindstone of Flügel (2004), Standard Microfacies (SMF 16-Laminated).

Palaeoenvironment: This microfacies is only located in the Exterior Platform in the Upper Slope (MDZ-2). The Upper Slope conditions are attributed to the presence of bioclasts such as common planktonic foraminifera and abundant sponge spicules.

The alternations of packstone to wackestone laminae are explained by the following:

- Some thin laminae contain planktonic foraminifera and sponge spicules that have been accumulated in low energy, deep slope micrites after episodes of gravity flows.
- Well sorted fine peloids, benthic foraminifera, small gastropods, and small bivalves have been transported from the Platform Margin and

the Platform Interior by the gravity flows. These have been deposited on the Upper Slope (MDZ-2) above the SWB.

Porosity type: This microfacies is densely packed and has poor reservoir quality as it contains no visible porosity. Chemical compaction and stylolite are very common.

Microfossil content: This microfacies is characterised by the presence of common planktonic foraminifera (*Conoglobigerina* sp. cf. *C. gulekhensis*), *Saccocom*a sp., triaxon spicules, monaxon spicules and small varieties of agglutinated foraminifera.

Well-D Microfacies 4 (DMF 4): *Lenticulina*, Oyster, Peloidal Packstone (Plate 99, Figure A).

Description: This microfacies texture is mainly that of packstone. The texture is abundant with very well sorted fine peloids and it is the main matrix. Many of the bioclasts are transported from shallower zones such as coated oyster bivalves and gastropods. Autochthonous *Lenticulina* spp., is also present.

Depth: This biofacies is located in cored Well D at a depth of 8630.7ft.

SMF type: It is the equivalent of the distal part of the allocthonous bioclastic grainstone/rudstone/packestone/floatstone, breccia of Flügel (2004) Standard Microfacies (SMF 5). The coated oyster bivalves are sourced from the Platform Margin's coated bioclastic grainstone microfacies (SMF 11).

Palaeoenvironment: This microfacies is located in the Exterior Platform in which it is located below fair weather wave base FWWB in the Upper Slope Depositional Zone (MDZ-2).

Porosity type: The microfacies has poor porosity with (<3%). It is commonly represented by a moldic (Mo) porosity.

Microfossil content: This microfacies is characterised by *Lenticulina* spp. and transported Platform Margin microfossils such as gastropods, oyster type of bivalves, echinoderms and agglutinated foraminifera.

Well-D Microfacies 5 (DMF 5): *Lenticulina,* Saddle Dolomite Wackestone (Plate 99, Figure B).

Description: This microfacies texture has mainly that of wackestone. The crystalline saddle dolomite is secondary that has possibly been developed by hydrothermal fluids. The main matrix in this lithofacies is very dolomitic, dense micrite. Solution seams and microstylolites are very common.

Depth: This biofacies is located in cored Well D at a depth of 8620.2 ft.

SMF type: It is the equivalent of the whole fossil wackestone and floatstone of Flügel (2004) Standard Microfacies (SMF 8).

Palaeoenvironment: This microfacies is only located in the Exterior Platform in which it is located in the slope, below fair weather wave base FWWB (MDZ-2).

Porosity type: The microfacies has very poor reservoir quality as it only contains a rare Intraparticle (WB) porosity. The secondary dolomite growth, microstylolite structures and solution seams has damaged most of the primary porosity.

Microfossil content: This microfacies is characterised by slope microfossils that include *Lenticulina* spp., *Nodosaria* spp., *Everticyclammina virguliana* and *Pseudocyclammina lituus.*

Well-D Microfacies 6 (DMF 6): *Protopeneroplis,* Peloidal Wackestone (Plate 100, Figures A-B).

Description: This microfacies texture is mainly that of peloidal wackestone. The well sorted fine peloids were created within the back-shoal side of the protected open marine floor and they are probably localised as a result of the very low energy conditions.

Depth: This biofacies is located in cored Well D at a depth of 8611.2ft.

SMF type: This is equivalent to the Platform Interior, Open Marine, whole fossil wackestone and floatstone of Flügel (2004) Standard Microfacies (SMF 8).

Palaeoenvironment: This microfacies is only located in the Interior Platform in which it is located in the Open Marine zone (MDZ-5). The open marine conditions of the Platform Interior are evidenced from the presence of benthic foraminifera, small gastropods, and small bivalves in the bioclast wackestone.

Porosity type: The microfacies has low reservoir quality as it contains no porosity.

Microfossil content: This microfacies is characterised by sheltered open marine microfossils that is include common gastropods, bivalves, echinoderm fragments, *Protopeneroplis ultragranulata*, *P. lituus* and thin-shelled ostracods.

Well-D Microfacies 7 (DMF 7): Foraminifera, Peloidal Mud-lean Packstone (Plate 101, Figures A-B).

Description: Texture is almost completely that of a mud-lean packstone. It is mainly formed of very fine and very well-sorted peloids. Bioclastic contents have been coated by micrite envelopes as a result of microbial activity.

Depth: This biofacies is located in cored Well D at a depth of 8584.2 ft.

SMF type: This is transitional between (SMF 18) grainstone/packstone with abundant foraminifera and (SMF 11) coated bioclastic grainstone of Flügel (2004) Standard Microfacies.

Palaeoenvironment: This microfacies has been deposited under moderate to high energy conditions. It is located in the Platform Interior of the inner shoal bank that separates the Lagoon Zone (MDZ-6) from the protected Open Marine zone (MDZ-5). Porosity type: The reservoir quality is poor as a result of the calcite cemented fabric.

Microfossil content: This microfacies is characterised by inner-shoal foraminifera with high diversity. It contains abundant, and variable, miliolids and other benthic, agglutinated foraminifera.

Well-D Microfacies 8 (DMF 8): *Nodosaria*, Peloidal Microstylolitic/Dolomitic Grainstone /Bindstone (Plate 102, Figures A-B).

Description: This microfacies is characterized by alternations of dolomitic, microstylolitic laminae with very well-sorted, fine peloidal laminations. Texture is mainly that of a peloidal grainstone, where peloids and dolomite

crystals are the main constituents. This microfacies has common signs of chemical dissolution and compaction.

Depth: Microfacies DMF 8 was recorded from a depth of 6563.2 ft in Well-D.

SMF Type: This microfacies is equivalent to the Platform Margin/slope SMF16, the laminated peloidal bindstone of Flügel (2004, p. 721).

Palaeoenvironment: This lithofacies is located in the edge of the Exterior Zone in which it is located above the fair weather wave base FWWB of the Platform Margin Zone (MDZ-3). The Platform Margin/Upper Slope conditions are attributed to the presence of bioclasts such as *Nodosaria* spp.

Porosity type: The microfacies has poor to fair porosities (~ 3%). The porosities have been destroyed by the chemical compaction and the stylolites. These laminae are densely packed and this results in poor reservoir quality; there is no visible porosity.

Microfossil content: The most important recorded microfossil is *Nodosaria* spp. with the following:

- Abundant, large, agglutinated foraminifera (*Everticyclammina greigi* and *Pseudocyclammina lituus*);
- Very common echinoderm fragments and debris with syntaxial cement; and
- Rare oyster bivalve fragments and ostracods.

Well-D Microfacies 9 (DMF 9): Peloidal, Reworked-Skeletal Wakestone (Plate 103, Figure A).

Description: This microfacies texture is mainly that of wakestone. Transported and reworked peloids and skeletal fragments are the main constituents. Planktic foraminifera are relatively common.

Depth: This biofacies is located in cored Well D at a depth of 8558.7 ft.

SMF type: This is equivalent to the toe-of-slope (FZ3) bioclastic packstone and wackestone with worn skeletal grains of Flügel (2004) Standard Microfacies (SMF 10).

Palaeoenvironment: This microfacies is only located in the Exterior Platform in the deep slope depositional zone (MDZ-1). It is located below the storm wave base SWB.

Porosity type: The microfacies is characterised by (IP) inter-particle porosity ranging from 3 % - 15%.

Microfossil content: This microfacies is characterised by the slope microfossils such as planktic foraminifera (*Conoglobigerina* sp. cf. *C. gulekhensis*), in association with the following transported microfossils:

- Rare agglutinated foraminifera (*Everticyclammina greigi* and *Pseudocyclammina lituus*);
- Very common fragments and debris of molluscs, including gastropods, and calcareous algae (*Salpingoporella annulata*); and
- Rare echinoderm fragments, bivalves and ostracods.

Well-D Microfacies 10 (DMF 10): *Conoglobigerina* sp., Extraclastic, Peloidal Wakestone (Plate 103, Figure B).

Description: This microfacies is that of wackestone and it is abundant with well sorted fine peloids.

Depth: This microfacies is located in cored Well D at a depth of 8542.2 ft.

SMF type: This is equivalent to the microbreccia, bio-lithoclastic packstone of Flügel (2004) Standard Microfacies (SMF 4).

Porosity type: The lithofacies is characterised by very poor moldic (Mo) porosity.

Microfossils contents: This microfacies is characterised by slope microfossil such as *Lenticulina* spp., planktonic foraminifera (*Conoglobigerina* sp. cf. *C. gulekhensis*) and benthic agglutinated foraminifera. It is associated with reworked and transported calcareous algae, gastropods, bivalves and echinoderm fragments.

Palaeoenvironmental: This microfacies is located below the fair weather wave base FWWB within the Platform Exterior in the Slope Depositional Zone (MDZ-2).

Well-D Microfacies 11 (DMF 11): *Lenticulina,* Peloidal Wackestone to Packstone (Plate 104, Figures A-B).

Description: This microfacies texture is mainly that of wackestone. The main matrix in this lithofacies is micrite that is abundantly recorded with moldic porosity. It is characterised by the presence of very well-sorted peloids that were created within the lagoon floor.

Depth: This Microfacies is located in cored Well D at a depth of 8540.7 ft.

SMF type: This is equivalent to the allochthonous bioclastic grainstone/rudstone/packstone/floatstone, breccia of Flügel (2004) Standard Microfacies (SMF 5).

Palaeoenvironment: This microfacies is only located in the Exterior Platform in which it is located on the slope, below fair weather wave base FWWB and above the storm wave base SWB (MDZ-1).

Porosity type: The microfacies has excellent reservoir quality in which it contains a moldic porosity type (Mo) ranging from 10% to 15 %. This is most likely to be an indication of a dramatic sea level fall in which a sequence boundary is identifiable.

Microfossil content: This microfacies is characterised by slope microfossils that include:

- Common *Lenticulina* spp ;
- Very common fragments and debris of molluscs and echinoderms;
- Rare polymorphinids; and
- Commonly transported *Nautiloculina* spp. from the lagoonal environment.

Well-D Microfacies 12 (DMF 12): Superficial Ooid Grainstone (Plate 105, Figure A).

Description: This microfacies texture is mainly that of grainstone. The main matrix is micritized concentric ooids with an abundant syntaxial cement growth surrounding echinoderm plates. Well-sorted concentric ooids have

been created within the shallow shoal and attributed to the very high energy conditions and the agitation of waves and currents within the platform sand bank.

Depth: This microfacies is located in cored Well D at a depth of 8406.2 ft.

SMF type: This is equivalent to the ooid grainstone with concentric ooids of Flügel (2004) Standard Microfacies (SMF 15-C).

Palaeoenvironment: This microfacies is located in both the proximal side of the Interior Platform (protected back-shoal of the Open Marine, MDZ-5) and in the distal side of the Platform Exterior (ooid sand shoal, MDZ-4). This is usually within the high energy conditions above the fair weather wave base FWWB.

Porosity type: This microfacies has very good reservoir quality in which it contains interparticle (IP) porosity ranging from 15% to 25 %. Meniscus cements, suggesting emergence, are formed in this environment by a relatively sharp fall in sea level.

Microfossil content: This microfacies is characterised by ooid sand shoal and back- bank shoal microfossils that include *Protopeneroplis* spp. and echinoderm fragments.

Well-D Microfacies 13 (DMF 13): Leached Superficial Ooid Grainstone (Plate 105, Figure B).

Description: This microfacies texture is mainly that of grainstone. The main matrix is leached concentric ooids that is characterised by an abundant syntaxial cement growth surrounding echinoderm plates.

Depth: This microfacies is located in cored Well D at a depth of 8410.7 ft.

SMF type: This is equivalent to the ooid grainstone with concentric ooids of Flügel (2004) Standard Microfacies (SMF 15-C).

Palaeoenvironment: This microfacies is located in the shallowest part of the distal side of the Platform Exterior (ooid sand shoal, MDZ-4). This is usually within the high energy conditions above the fair weather wave base FWWB.

Porosity type: This microfacies has very good reservoir quality in which it contains moldic (MO) and interparticle (IP) porosity above 25 %.

Microfossil content: This microfacies is barren of microfossils.

Well-D Microfacies 14 (DMF 14): Peloidal, Coated Bioclastics Packstone and Grainstone (**Plate 106, Figures A-B; Plate 107, Figure A).**

Description: This microfacies texture is mainly that of packstone and grainstone. Micritised peloids, ooids and coated skeletal fragments are the main constituents in association with common rounded lithoclasts and microbial micritization.

Depth: This microfacies is located in cored Well D at a depth of 8392.7 ft.

SMF type: This is equivalent to the coated bioclastic grainstone of Flügel (2004) Standard Microfacies (SMF 11).

Palaeoenvironment: This microfacies is created in the Platform Exterior in the platform margin depositional zone (MDZ-3).

Porosity type: This microfacies has very good reservoir quality in which it contains moldic (MO) and interparticle (IP) porosity ranging from 10 to 25 %.

Microfossil content: This microfacies is characterised by Platform Margin microfossils that include oyster bivalves and *Protopeneroplis* spp.

Well-D Microfacies 15 (DMF 15): *Lithocodium* Boundstone (Plate 107, Figure B).

Description: This microfacies texture is mainly that of boundstone to packstone. It is mainly composed of *Lithocodium aggregatum* large oncoids indicating categories 3 and 4 of Vědrine *et al*. (2007) and Michetiuc *et al.* (2012), in which they are characterized by encrusting microbial meshwork shapes.

Depth: This microfacies is located in cored Well D at a depth of 8385.2 ft.

SMF type: This is equivalent to the oncoids rudstone/grainstone of Flügel (2004) Standard Microfacies (SMF 13).

Palaeoenvironment: This microfacies is diagnostic of shallow-water/normal marine conditions. It is located in a very low energy setting of significant depth in the open marine part of the Platform Interior (MDZ-5). It is suggestive of a zone of maximum flooding of the platform.

Porosity type: This microfacies has very good reservoir quality in which it contains moldic (MO) and intraparticle (IP) porosity above 15 %.

Microfossil content: This microfacies is characterised by open marine microfossils that include:

- *Lithocodium aggregatum* oncoids and encrusters as reef ground stabilizers; and
- Between-grain encrusters are common (e.g., *Bacinella irregularis*).

Well-D Microfacies 16 (DMF 16): Non-Laminated Peloidal, Miliolids Grainstone (Plate 108, Figure A).

Description: This microfacies texture is mainly that of grainstone. The main matrix is clean fine, very well-sorted peloids that is abundant by syntaxial cement growth surrounding echinoderm plates. The very well sorted peloids have been created within the lagoonal floor.

Depth: This microfacies is located in cored Well D at a depth 8320.7 ft.

SMF type: This is equivalent to peloidal grainstone/packstone of Flügel (2004) Standard Microfacies (SMF 16-Non-Laminated).

Palaeoenvironment: This microfacies is located in the Interior Platform in the Lagoon Microfacies Depositional Zone (MDZ-6). The lagoonal conditions are indicated by the common to rare presence of miliolds, micritised peloids, small gastropod, and small bivalves.

Porosity type: This microfacies has very good reservoir quality in which it contains interparticle (IP) porosity of up to 20 %.

Microfossil content: This microfacies is characterised by lagoonal microfossils that include abundant *Quinqueloculina* spp, rare *Textulariopsis jurassica* and echinoderm fragments with syntaxial cement overgrowth.

Well-D Microfacies 17 (DMF 17): Peloidal Intraclastic Skeletal Grainstone (Plate 108, Figure B; Plate 109, Figure A).

Description: This microfacies texture is mainly that of grainstone. The main matrix is of non-laminated, fairly sorted, intraclastic, peloidal, *Quinquloculina* grainstone. This microfacies is associated with reworked lithoclasts and

coated skeletal fragments. These are very well-sorted peloids and minor to poorly sorted, sub-rounded lithoclasts.

Depth: This microfacies is located in cored Well D at a depth of 8249.7 ft.

SMF type: This is equivalent to the coated bioclastic grainstone of Flügel (2004) Standard Microfacies (SMF 18).

Palaeoenvironment: The microfacies (DMF 17) is a product of destructive, very high energy conditions. This microfacies is located in the shallowest part of the Platform Interior (inner shoals, MDZ-5 and MDZ-6). This is usually within the high energy conditions above the fair weather wave base FWWB.

Porosity type: This microfacies has very good reservoir quality in which it contains moldic (MO) and interparticle (IP) porosity above 35%.

Microfossil content: This microfacies is characterised by lagoonal and inner-shoal microfossils such as abundant miliolids, including *Quinquloculina* spp.

Well-D Microfacies 18 (DMF 18): Poorly sorted, Intraclastic Grainstone to Rudstone (Plate 109, Figure B; Plate 110, Figures A-B).

Description: This microfacies texture is mainly that of sparry calcite cemented rudstone and grainstone. The main matrix is leached out, poorly sorted, intraclastic peloids and coated reef skeletal fragments by micritic envelopes.

Depth: This microfacies is located in cored Well D at a depth of 8249.7 ft.

SMF type: This is equivalent to the densely packed reef rudstone of Flügel (2004) Standard Microfacies (SMF 6).

Palaeoenvironment and major diagenesis: It is located in the shallowest banks (not ooid bank) of the Platform Exterior (Platform Margin, MDZ-3). The poorly-sorted, sub-angular to sub-rounded grains were created within the platform margin in the very high energy conditions above FWWB. The micritic envelopes were created during sedimentation after which this microfacies was subjected to sub-aerial exposure diagenesis in which grain dissolution occurred. The aragonitic fragments have been leached out. The sparry calcite cement was created by the burial phreatic diagenesis. This is representative of a major sequence boundary of a third order cycle at the top of the Sulaiy Formation.

Porosity type: This microfacies has poor reservoir quality in which it contains a moldic (MO) porosity ~ 3 %.

Microfossil content: This microfacies is characterised by platform margin microfossils such as *Mohlerina basiliensis*, *Macroporella praturloni,* the encrusting type of *Lithocodium aggregatum* and the presence of oyster bivalves.

5.5 SUMMARY.

This research has improved the interpretation of depositional environments of the studied wells. This research has led to the identification of environmentally significant microfacies, of which their vertical distribution will provide a significant contribution towards on-going hydrocarbon reservoir characterization studies.

This part of the research has yielded the identification of twenty-four microfacies and the interpretation of their depositional palaoenvironment. These are summarized in Figure 5.5 and Table 5.1. The scaled photomicrographs of each microfacies are shown and explained in the Plates 82-110.

The results of the micropalaeontological and microfacies analysis have been presented in StrataBugs enclosures for Wells (A, B, D, F, G, H and I). These StrataBugs enclosures contain the construction of microfacies and vertical species distribution for each studied well. The sequence boundaries, maximum flooding surfaces and accommodation cycles were been assigned based on the StrataBugs microfossils and their host microfacies distribution.

The identification of deepening and shallowing-upwards biofacies and hierarchic depositional cycles were assigned. Sequence boundaries, maximum flooding surfaces and accommodation cycles are assigned in the following chapter (Chapter six). The microfacies were vertically constructed for linkage and correlation between the wells horizontally and this is represented in enclosure of correlation panel between Wells A-B-F-H-G-I. The horizontal relationship of cycle boundaries and transgressive regressive components has yielded the preparation of regional microfacies maps and their systems tracts in chapter six. This will result in the identification of locations with good reservoir microfacies development.

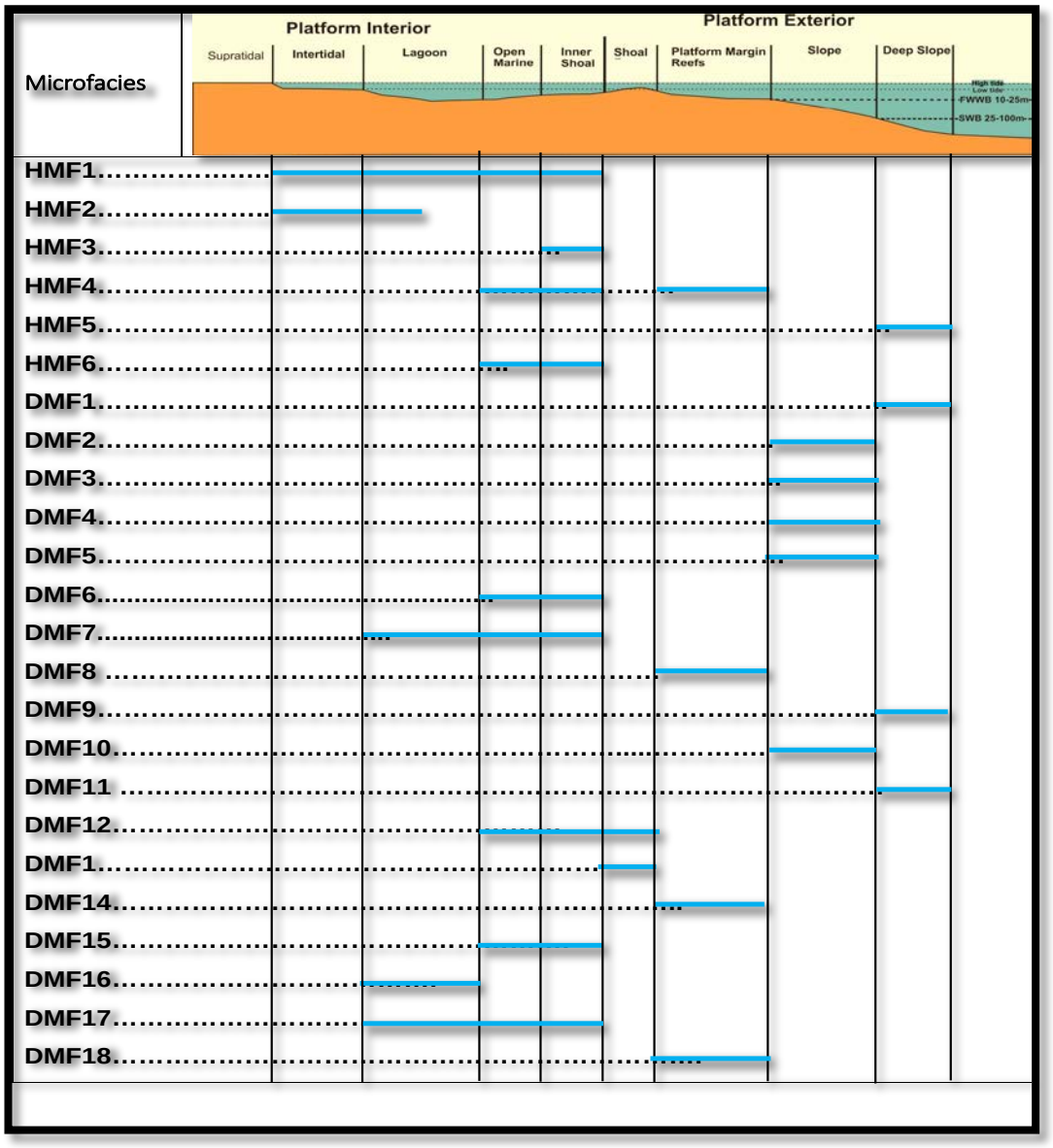

Figure 5.5. The summary table of the HMF and DMF types distribution in the Depositional Microfacies Zones (DMZ) of the Arabian Rimmed Shallow Platform (ARSP). These are the most abundant and common microfacies characterized by their contents of bio-components, litho-components and diagenetic characteristics.

Microfacies Code	Microfacies Type
HMF 1	Porous, Intraclastic, Foraminferal and Peloidal Packstone
HMF 2	Finely Laminated Mudstone
HMF 3	Peloidal, Foraminiferal and Intraclastic Packstone
HMF 4	Lithocodium, Intraclastic and Peloidal Wackestone-Packstone-Grainstone-Rudstone
HMF 5	*Terebella*, *Crescentiella, Ophthalmidium* and Allochthonous Bio-lithoclastic Packstone/Grainstone
HMF 6	Laminated Peloidal Packstone/Grainstone/Bindstone
DMF 1	Spiculite, Calcisiltite Wackestone
DMF 2	Extraclastic, *Nodosaria, Lenticulina* and *Saccocoma* Packstone
DMF 3	Slope-Laminated Peloidal Bindstone/ Wackestone/ Packstone
DMF 4	*Lenticulina,* Oyster, Peloidal Packstone
DMF 5	*Lenticulina,* Saddle Dolomite Wackestone
DMF 6	*Protopeneroplis,* Peloidal Wackestone
DMF 7	Foraminifera, Peloidal Mud-lean Packstone
DMF 8	*Nodosaria,* Peloidal Microstylolitic/Dolomitic Grainstone /Bindstone
DMF 9	Peloidal, Reworked-Skeletal Wakestone
DMF 10	*Conoglobigerina* sp., Extraclastic, Peloidal Wakestone
DMF 11	*Lenticulina,* Peloidal Wackestone to Packstone
DMF 12	Superficial Ooid Grainstone
DMF 13	Leached Superficial Ooid Grainstone
DMF 14	Peloidal, Coated Bioclastics Packstone and Grainstone
DMF 15	*Lithocodium* Boundstone
DMF 16	Non-Laminated Peloidal, Miliolids Grainstone
DMF 17	Peloidal Intraclastic Skeletal Grainstone
DMF 18	Poorly sorted, Intraclastic Grainstone to Rudstone

Table 5.1. The summary table of the twenty-four Microfacies identified in the studied wells H and D. these are used to describe transgressive (TST), highstand system tracts (HST) and maximum flooding zones or surfaces (MFZ/MFS).

CHAPTER SIX

SEQUENCE STRATIGRAPHY AND PALAEOENVIRONMENTAL MAPS

CHAPTER SIX

SEQUENCE STRATIGRAPHY AND PALAEOENVIRONMENTAL MAPS

6.1 SEQUENCE DETERMINATION

Sequence stratigraphy is largely founded on the ‘Exxon Model’ of seismic stratigraphy that was launched by publication of the AAPG Memoir (Payton, 1977). This volume included a number of papers, many of which acted as a foundation of sequence stratigraphy, including its complex terminology (Mitchum, 1977) and relationship to sea level changes (Vail *et al*., 1977). Galloway (1989) presented an alternative view for the recognition of sequence boundaries, using the MFS as the key marker, and for a number of years there was a debate as to the better method. This suggestion followed publication of the SEPM Memoir (Wilgus *et al*., 1988) on the role of sea level change throughout the Mesozoic and Cenozoic and its relationship to large-scale sequences. In the 1990s, sequence stratigraphy was becoming ‘mainstream’ and a number of texts appeared, many of which have become standard references for those in training (Walker and James, 1992; Emery and Myers, 1996; Miall, 1997). In more recent years a number of articles have documented the history of the development of sequence stratigraphy (Baum and Vail, 1998; Hinnov, 2000) and there is now a complete website [www.sepmstrata.org] that summarizes the development of sequence stratigraphy, the

literature base and the application of the methodology to carbonate environments such as the Arabian Peninsula (e.g., Kendall *et al.,* 1991).

The following section is written following personal communication with Dr Geraint Wyn Hughes concerning the industrial sequence determination method used by Saudi Aramco.

The main task is to subdivide the analyzed succession into depositional sequences of varying hierarchies, most which would be of fourth and fifth order sequences in typical formations and their associated reservoir facies. The resulting sequence-based interpretation provides a framework within which the micropalaeontological assemblages can be considered in relation to the petro−fabrics and result in the differentiation of local microfacies. Once these are identified, depositional environments can be determined, and their variation up and down the studied section can be related in a consistent and objective manner. Such an approach identifies the depositional settings that caused the development of reservoir, source and seal lithofacies. In addition to providing events for regional correlation that would be of a much higher resolution than by conventional biostratigraphy, they permit the construction of maps displaying regional depositional environments between the studied wells.

Carbonate sedimentation responds to transgressive-regressive cycles in shallow and deep marine settings in different ways, as described by Emery and Myers (1996) and Ahr (2008, chapter 5). The methodology of this part is provided in Section 3.8 of Chapter Three. This is a list of the abbreviations used in the text: MFS (maximum flooding surface); MFZ (maximum flooding zone); MFS/Z (maximum flooding surface or

zone); TST (transgressive system tract); HST (high stand system tract); SMF (Standard Microfacies Types, Flügel, 2004, pp. 680–711).

6.2 DEPOSITIONAL SEQUENCE STRATIGRAPHY OF STUDIED WELLS

Mitchum (1977) explained that a depositional sequence is a conformable succession of genetically, similar component strata that is bounded by unconformities and equivalent disconformities. Thus, the Sulaiy Formation is 3rd order sequence that is bounded by Hith Formation at the base and the Yamama Formation at the top. The sequence boundary at the base of the Sulaiy Formation has not been recorded in the studied wells whereas the top boundary between the Sulaiy and the Yamama formations has been identified as a disconformity. However, this top boundary was evidenced from the paleo-karstic features of cement types such as moldic and cavern porosities of the wells that are located paleogeographically within the Platform Interior. These diagenetic features are diagnostic of sub-aerial exposures, allowing the karstic and vadose diagenesis to characterize this boundary. This boundary was indicated in the eustatic cycle charts of Haq and AlQahtani (2005) and Sharland *et al.* (2001).This boundary was identified by Hughes *et al.* (2001) as a major 3rd order sequence boundary separating the top of the Sulaiy Formation from the base of the Yamama Formation. The cored part of the Sulaiy Formation is considered to be a highstand of a 3rd order sequence which it is located at the base of the Thamama Group (2nd order mega-sequence). In this research, it is possible to identify up to 12 (5th order) parasequences from the wells F and I, and 5 parasequences from the wells B, H, G. These parasequences were identified using an

integration between microfacies and micropaleontological analysis which identified successive layers of high-resolution, highstand, shoaling upwards depositional sequences. The thickness of parasequences has been discussed in Smith and Read (1999, p. 116) and it is between 1-12 meters thick and that is equivalent to the presently identified parasequence thicknesses. The parasequences is defined by Mitchum and Wagner (1991) as a relatively conformable bed(s) of similar genetic component strata that is bounded by marine maximum flooding surfaces.

6.3 5TH ORDER PARASEQUENCE MAIN ELEMENTS

Microfacies and micropalaeontological analysis are used to identify sequence boundaries (SB), transgressive system tracts (TST), maximum flooding zones or surfaces (MFS), highstand system tracts (HST) and the upper part of the highstand system tract (upper HST). From the analysis of the wells (B, D, E, F, G and H), it is shown that all of the studied wells are representing progressive parasequences that are identified from the transgression- associations of microfacies and microfossils. These dataare used in thedeterminationof the transgressive and highstand components of each depositional cycle for each well (Tables 1 to 6). Microfacies and biofacies characteristics of each well are shown in "StrataBugs"Enclosures(of the wells B, D, E, F, G and H).Each 5th order sequence is bounded by sequence boundaries (SB) (Figure 6.1). At the lower sequence boundary, the transgressive system tract part of each sequence (TST) is characterized by deepening upward microfacies(Figure 6.1). The

maximum flooding zone or surface (MFZ/S) is often identified using microfacies criteria and microfossils to determine the of water depth(Figure 6.1). In this research, it is very critical to trace the changes of deepening-upward and the shallowing-upward microfacies to identify the MFS. Often, the MFS is the deepest microfacies part of each sequence and it is followed by a highstand system track (HST) layer (Figure 6.1). This shallowing upward part of the sequence is terminated by the next sequence boundary (SB).

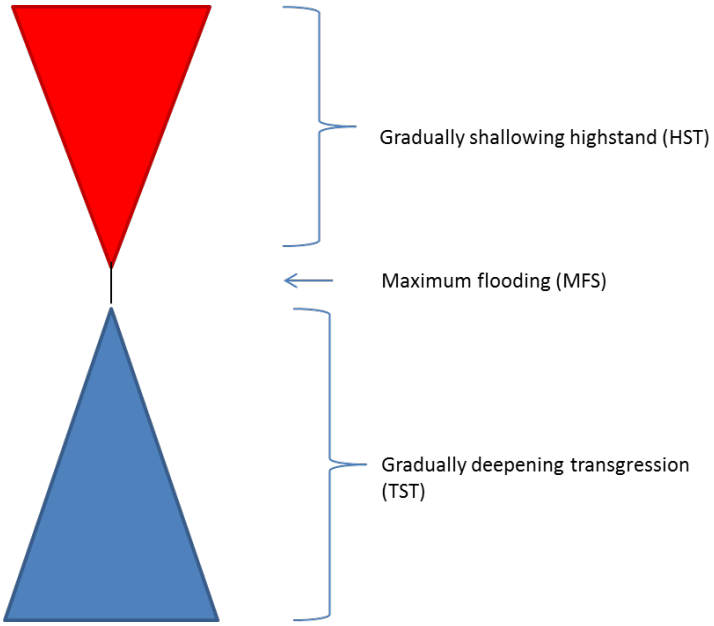

Figure 6.1 Diagram representing the main components of a 5thorder parasequence and their HST, MFS and TST elements.

Each recorded sequence has its characteristic pattern of the thickness changes between the shallowing-upward and the deepening-upward layers. This thickness is controlled by the depth of the microfacies palaoenvironment. However, the parasequence that deposited in greater depth palaoenvironmentis characterized by a higher accommodation space in which it produces the deep setting (Figure 6.2). On the

other hand, the shallow setting pattern is a characteristic of minimum accommodation space that is responsible for producing these parasequences, often this accommodation space is found within the Lagoonal environment or the intertidal sedimentary environment.

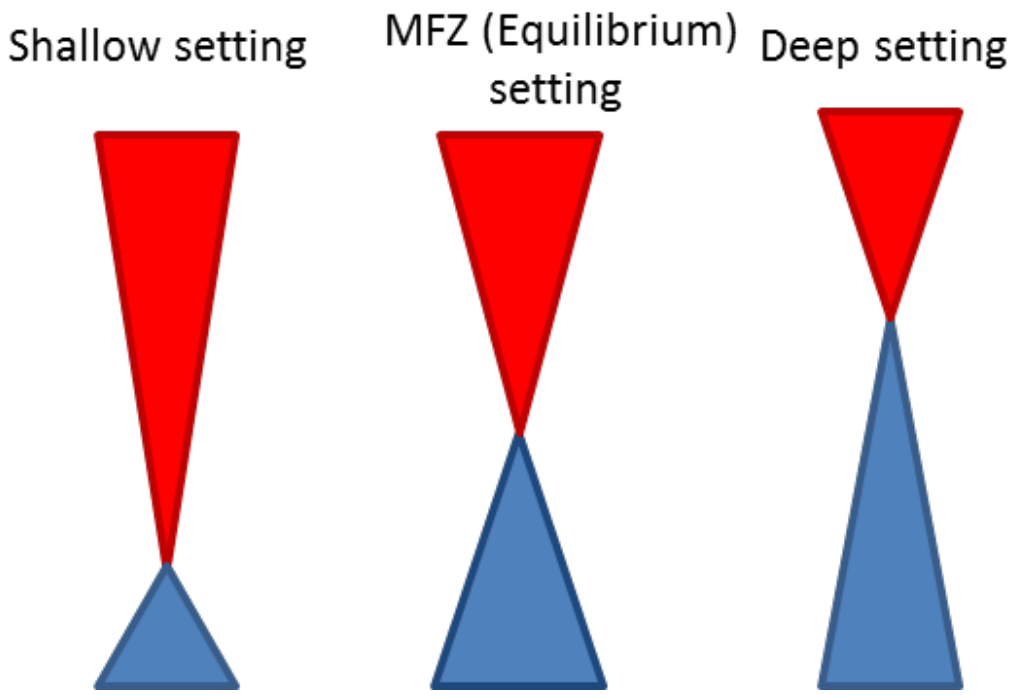

Figure 6.2 Diagram representing the difference between deep setting parasequence, maximum flooding zone setting and the shallow parasequence in terms of symmetry and thickness of the deepening and shallowing elements. An example of this type of parasequences patterns are represented in Figure 6.3.

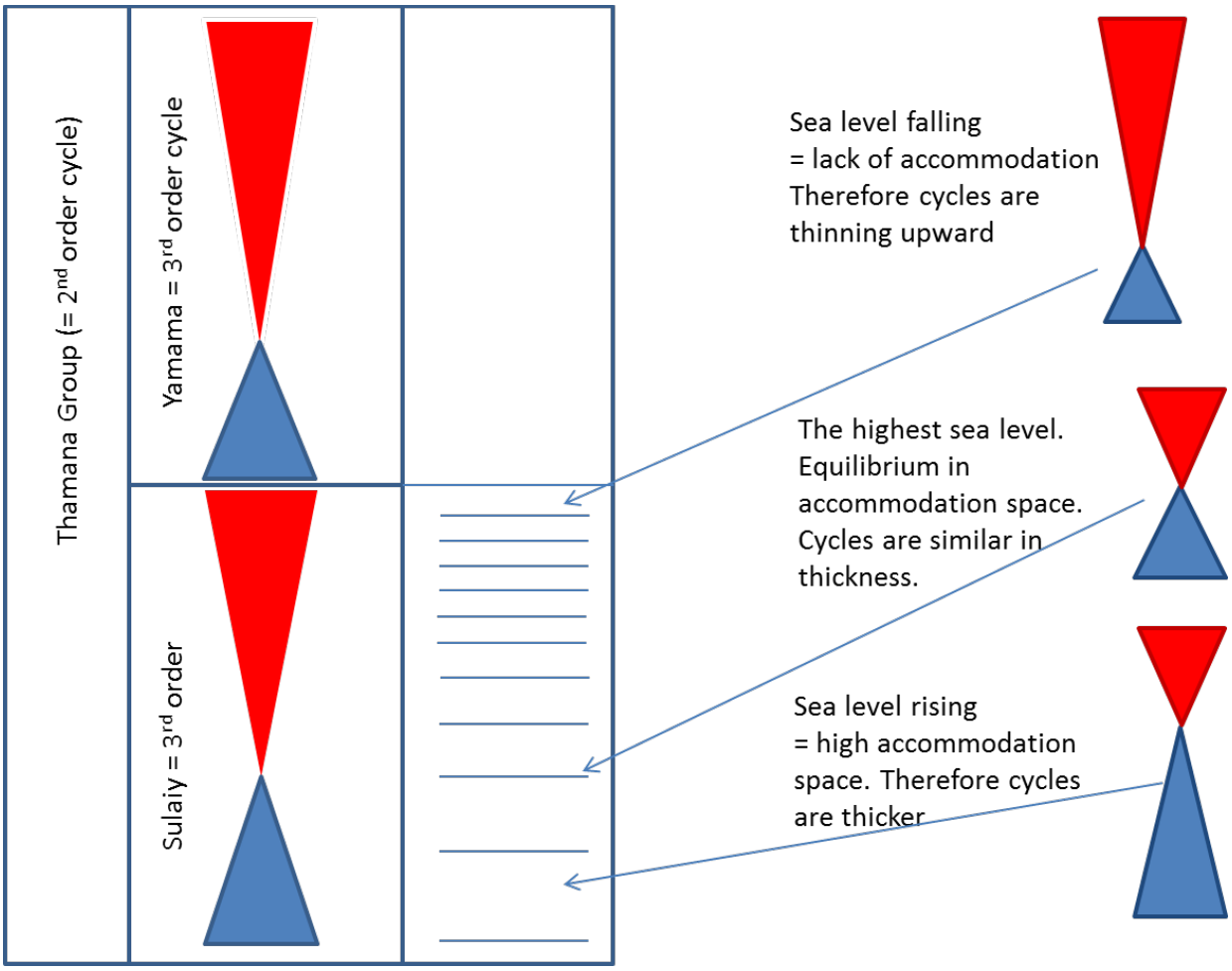

Figure 6.3 This diagram representsexamplesof a 5th order parasequence pattern from the highstand and the maximum flooding surface of the 3rd order sequence. Usually bed and layer thicknesses are getting smaller inthe shallowing upward part, while during the transgressive system tract, they are getting thicker.

6.4 5TH ORDER AND 4TH ORDER SEQUENCES OF EACH WELL

A total of twelve 5th order sequences have been identified across the study area, together with their deepening and shallowing sections (Enclosure of the correlation of wells A, B, F, H, G and I) in the Sulaiy Formation. The numbering is from top to bottom since they are only cored from top and never reached the bottom. The 4th order sequences are only identified at well F in which they can be correlated with the adjacent wells from the correlation chart of wells B, F, H, G and I. Each 4th order sequence contains at least two 5th order sequences (Table 6.1). They are compared with Haq's (2014, fig.1. p. 49) global short term sea level curve. These 4th order sequencesare summarised from Well-F in the following table:

Table 6.1 4th order sequences summary from Well-F and the equivalent codes from Haq (2014, fig.1. p. 49) with 5th sequences, depth, 4th order MFS and age.

4th Order sequence(Haq, 2014 SB code)	5thOrder sequences	Sequence Boundary depth in feet	4th Order MFS	Age million years
KVa2	1, 2	8202.5	8233.5	138
KVa1	3,4	8239.5	8245.5	139
KBe4	5, 6	8267.5	8337.5	140.2
KBe3	7, 8	8349.5	8365.5	141.4
KBe2	9, 10	8390.5	8402.5	142.7
KBe1	11, 12, 13	8423.5	8449.5	143.9

However, each well is characterized by sequences are grouped into sequence sets (Figure 6.3) of 5th order sequences. These are based on the stacking pattern of Figure 6.3 and the palaeographical location of the well (Figure 6.4). The palaeographical location of each well is based on the microfacies interpretation of overall depositional system of the studied area.

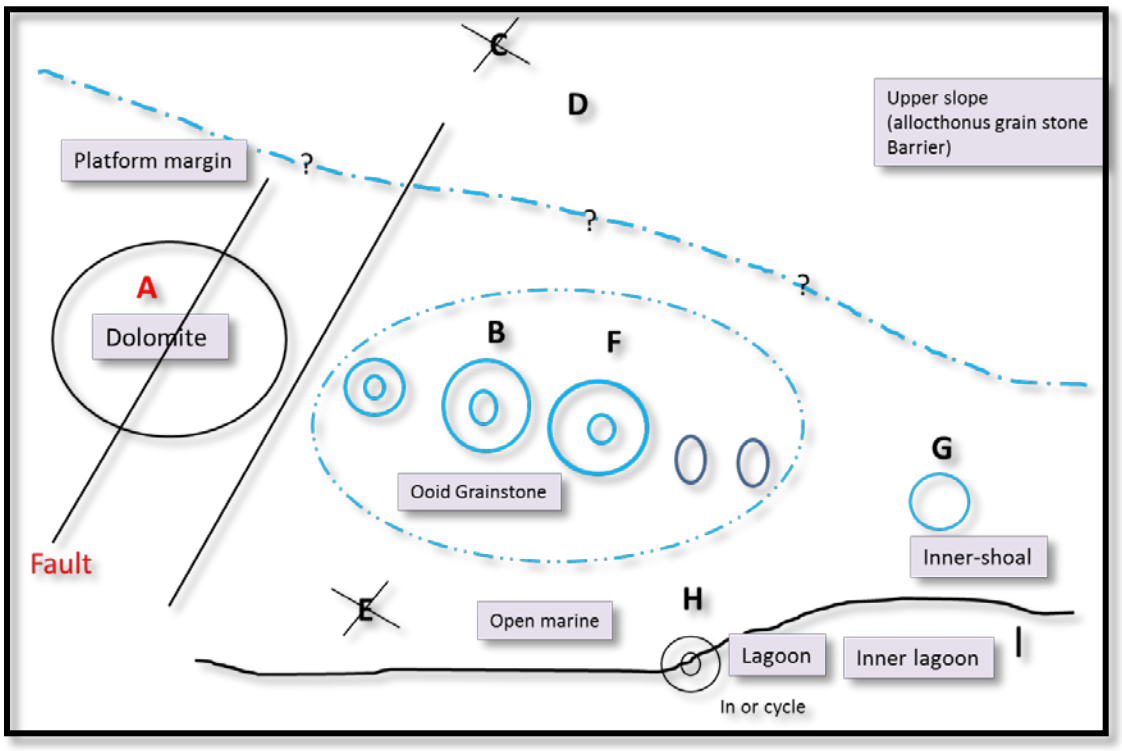

Figure 6.4 Generalized paleoenvironmental map showing the spatial distribution of microfacies and the microfacies sedimentary zones with wells location. Note that well A is totally dolomitised and it is excluded in this research with wells C and E.

The Sulaiy Formation micropalaeontological analysis has revealed that the depth diagnostic microfossils display a variable vertical distribution in which they are can be used to support recognition of depositional cycles.It is evident that certain species that are present in the transgressive system tract (TST) part of the studied section are absent in the highstand section (HST) of each 5th order sequence, or only present within

the maximum flooding sections of younger depositional cycles.This pattern reveals several depositional cycles, each of which is characterized by gradual replacement of deeper (deep setting) water species by shallower microfossils (shallow setting) (Figure 6.5).

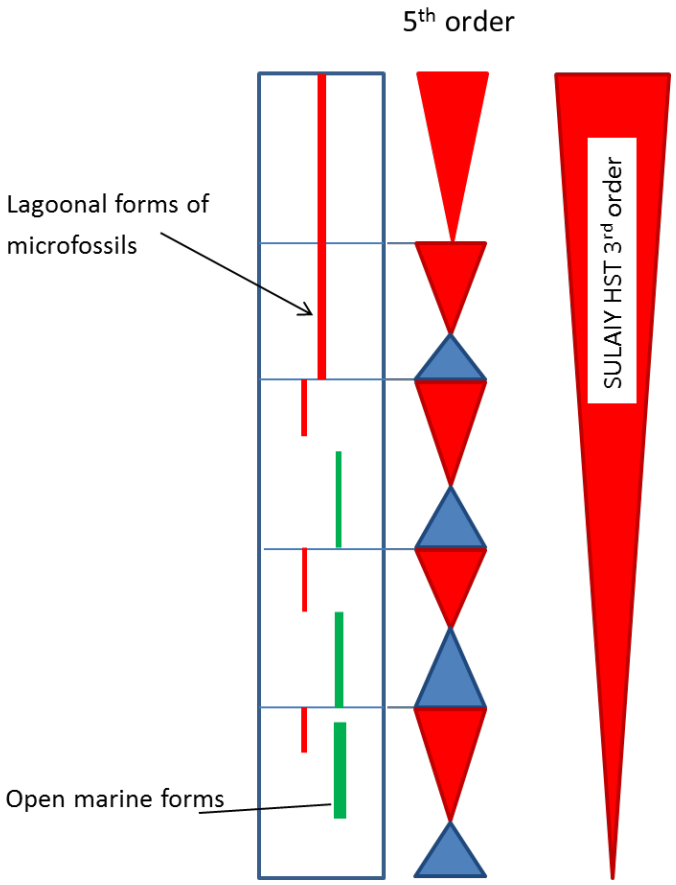

Figure 6.5 Example of distribution of shallow lagoonal and deep marine benthonic foraminifera in relation to high-frequency, parasequence-scale depositional cycles.

These microfossils responses has dissected each cycle of an parasequence of 5th order into transgressive system tract (TST), maximum flooding zone or surface (MFZ/S), transgressive highstand (HST) and the upper part of the highstand (Upper HST) (Figure 6.6).

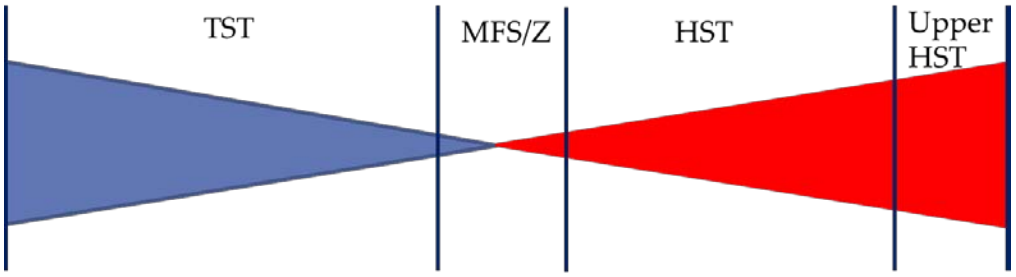

Figure 6.6 Diagram showing the dissected four sections that microfossils appearance and disappearance responses to each of 5th order cycle. They are dissected into transgressive system tract (TST), maximum flooding zone or surface (MFZ/S), transgressive highstand (HST) and the upper part of the highstand (Upper HST).

Each studied well sequences and their micropalaeontological responses in the four dissected parts of each depositional sequences are recorded, summarized and listed in each well sequence stratigraphy analysis.

Well-F

This well is characterized of twelve 5th order sequences (Table 6.2A) that are used as a base well for correlating the sequences layers in which six of 4th order sequences are identified (table 6.1). The 5th order sequences are numbered from top to bottom in the Sulaiy wells correlation enclosure of wells B, F, H, G and I. The generalised parasequences patterns of Well-F 5th order sequences are characterised as follows:

- Shallow setting patterns of the parasequences numbers 1, 2, 3, 4, 5, 6, 7, 8, 9 and 10. These comprise most of this cored well.
- Maximum flooding setting or equilibrium setting of the parasequences numbers 11 and 13.
- Parasequence 13 is the only one that is representing the deep setting pattern of Well-F.

This well is generally located within the ooid shoal bank in which it evidenced from the common shallow setting patterns and from the microfossils analysis (Figure 6.4 and Table 6.2B). However, the adjacent area may represent the best candidates for future drilling localities since it represents the best reservoir qualities.

Table 6.2A. Illustrates the interpreted sequence stratigraphic and palaeoenvironmental interpretations for Well-F.

Top depth (ft.)	**Base depth (ft.)**	**4TH Order SB**	**3rd order**	**5th order**	**Depositional environment**	**Microfacies**
	8202.5	**KVa2**			Base of Yamama Formation	
8202.5	8224.5		Highstand	HST	Ooid Shoal	Superficial ooid grainstone
8224.5				MFZ/S	Deeper open marine	Bioclastic, *Lithocodium* packstone
8224.5	8226.5			TST	Open marine	*Lithocodium* packstone
8226.5	8233.5			HST	Ooid shoal	Superficial ooid grainstone
8233.5		**MFS**		MFZ/S	Deeper open marine	*Lithocodium* spicules wackestone
8233.5	**8239.5**	**KVa1**		TST	Open marin	*Lithocodium* packstone
8239.5	8245.5			HST	Inner-shoal	Peloidal, bioclastic packstone
8245.5		**MFS**		MFZ/S	Deeper open marine	Spicules, bioclastic packstone
8245.5	8257.5			TST	Lagoon	Peloidal wackestone and mudstone
8257.5	8263.5			HST	Shoal to inner-shoal	Superficial ooid, peloidal grainstone
8263.5				MFZ/S	Inner-shoal	Pelletal packstone
8263.5	**8267.5**	**KBe4**		TST	NA	NA
8267.5	8285.5			HST	Ooid shoal	Superficial ooid grainstone
8285.5				MFZ/S	Deeper open marine	Bioclastic, calcipheres grainstone
8285.5	8291.5			TST	Lagoon	Pelletal packstone
8291.5	8311.3			HST	Ooid shoal	*Lithocodium,* superficial ooid graisntone
8311.3				MFZ/S	Deeper open marine	Bioclastic, *Lithocodium* grainstone

8311.3	8316.5			TST	Lagoon	*Quinqueloculina*,pelletal packstone
8316.5	8337.5			HST	Ooid shoal	Superficial ooid grainstone
8337.5		**MFS**		MFZ/S	Deeper open marine	*Lithocodium*, bioclastic grainstone/packstone
8343.5	**8349.5**	**KBe3**		TST	Open marine	*Lithocodium* packstone
8349.5	8365.5			HST	Ooids shoal	Superficial ooid, *Lithocodium* graisntone
8365.5		**MFS**		MFZ/S	Deeper open marine	*Lithocodium*, bioclastic grainstone/packstone
8365.5	8371.5			TST	Open marine	*Lithocodium* packstone
8371.5	8386.5			HST	Inner-shoal	Peloidal, grapestone grainstone
8386.5				MFZ/S	Deeper open marine	*Lithocodium* packstone
8386.5	**8390.5**	**KBe2**		TST	Open marine	*Lithocodium* grainstone
8390.5	8402.5		flooding	HST	Inner-shoal	Peloidal grainstone
8402.5		**MFS**		MFZ/S	Deeper open marine	*Lithocodium* packstone
8402.5	8406.5		Maximum zone setting	TST	Open marine	*Lithocodium* grainstone
8406.5	8415.5			HST	Shallow open marine	*Lithocodium* grainstone
8415.5				MFZ/	Deep open	*Lithocodium* mudstone
8415.5	**8423.5**	**KBe1**	Transgrssive	TST	Lagoon	Mudstone
8423.5	8435.5			HST	Open marine	*Lithocodium*, spicules packstone
8435.5				MFZ/S	Deeper open marine	*Lithocodium*, spicules, wackestone/packstone
8435.5	8443.5			TST	Lagoon to open marine	Bioclastic wackestone/mudstone
8443.5	8449.5			HST	Open marine	*Lithocodium,* spicules wackestone
8449.5		**MFS**		MFZ/S	Deeper open marine	Spicules wackestone
8449.5	8469.5			TST	Open marine	Spicules, *Lithocodium* mudstone

Table 6.2B. Display the interpreted microfossils vertical responses for each 5th order sequence for Well-F.

TST	MFS/Z	HST	UPPER HST	WELL-F microfossils distribution
Rare		Common		*Quinqueloculina egmontensis*
				Quinqueloculina pudubiensis
				Quinqueloculina robusta
				Quinqueloculina multicostata
				Quinqueloculina spp.
				Nubecularia spp.
				Nautiloculina oolithica
				Coscinoconus alpina
				Pfenderina neocomiensis
				Verneuilinoides neocomiensis
				Verneuilinoides polonicus
				Praedorothia praehauteriviana
				Mohlerina basiliensis
				Lenticulina spp.
				Gaudryinella sp.
				Salpingoporella annulata
				Salpingoporella spp.
				Thaumatoporella parvovesiculifera
				Permocalculus ampullaceus
				Lithocodium aggregatum
				echinoid fragments
				superficial ooid grains
PS / WS	MS	WS / PS	GS	Dunham (1962) texture
vadose, micro-stalactite dripstone cement				

Ooid shoal, diversity decreased compared to Well-H. The 5th order cycles of Well-F are thicker than those of Well-H. Blue is common and yellow is rare.

Well H

This well is characterized by seven 5th order sequences (Table 6.3A) that are used as a base well for correlating the sequences layers in which six of 4th order sequences are identified (Table 6.1). The 5th order sequences are numbered from top to bottom in the Sulaiy wells correlation enclosure of wells B, F, H, G and I. The generalised parasequence patterns of Well-H 5th order sequences are characterised as follows:

- Shallow setting patterns of the parasequences numbers 1, 2, 3, 4, 5, 6 and 7. These comprise most of this cored well.

This well is generally located within the open marine zoneor deep lagoon settings in which it evidenced from the common shallow setting patterns and from the microfossils analysis (Figure 6.4 and Table 6.3B).

Table 6.3A. Illustrates the interpreted sequence stratigraphic and palaoenvironmental interpretations for Well-H.

Top depth (ft.)	Base depth (ft.)	3rd order	5th order	Depositional environment	Microfacies
6380.5	6382.5	Highstand	TST	Lagoon	Peloidal packstone
6382.5	6389.2		HST	Inner-shoal	*Thaumatoporella,* bioclastic grainstone /packstone
6389.2			MFS	Inner-shoal, deeper	Bioclastic, ooidal packstone
6389.2	6391.1		TST	Lagoon	Bioclastic packstone
6391.1	6396.8		HST	Open marine inner shoal	Bioclastic, lithoclastic, echinoderm grainstone
6396.8			MFS	Open marine, deeper	*Lithocodium* packstone
6396.8	6398.6		TST	Open marine	Peloidal packstone

6398.6	6404.3		HST	Shallow open marine	*Thaumatoporella*,bioclastic, grainstone /*Lithocodium* packstone
6404.3			MFS	Open marine, deeper	*Lithocodium*, bioclastic packstone
6405.3	6406.4		TST	Lagoon	Rare bioclastic wackestone
6406.4	6414.8		HST	Shallow open marine	*Lithocodium*, crotoidal, micritized, bioclastic grainstone/packstone
6414.8			MFS	Deep lagoon	Bioclastic grainstone
6415.7	6417.6		TST	Lagoon	Bioclastic mudstone/packstone
6417.6	6423.5		HST	Shallow open marine	*Thaumatoporella,* bioclastic grainstone /*Lithocodium* packstone
6423.5			MFS	Open marine, deeper	*Lithocodium* grainstone
6423.5	6427.5		TST	Lagoon	Bioclastic, mudstone wackestone

Table 6.3B. Display the interpreted microfossils vertical responses for each 5th order sequence for Well-H.

TST	MFS/Z	HST	UPPER	WELL-H microfossils distribution
		Rare		*Quinqueloculina robusta*
				Quinqueloculina spp.
				Nubecularia spp.
				Protopeneroplis ultragranulata
common				*Pseudocyclammina lituus*
				Nautiloculina oolithica
				Nautiloculina bronnimanni
				Coscinoconus alpina
				Coscinoconus elongata
				Coscinoconus delphinensis
				Pfenderina neocomiensis
				Verneuilinoides neocomiensis
				Textulariopsis jurassica
				Siphovalvulina variabilis
				Charentia cuvillieri
				Everticyclammina virguliana

						Ammobaculites subcretaceus
						Reophax sp.
						Calcareous algae (reworked)
						Salpingoporella annulata
						Salpingoporella spp.
						Thaumatoporella parvovesiculifera
						Actinoporella podolica
						Permocalculus ampullaceus
						Lithocodium aggregatum
						echinoid fragments
						Rare, transported ooid grains in wackestone-packestone
PS	WS	MS	WS	PS	GS	Dunham (1962) texture classification
						isopachous cement
						meniscus cement
						vadose, micro-stalactite dripstone cement

Well G

This well is characterized by five 5th order sequences (Table 6.4A) that are used as a base well for correlating the sequences layers in which six of 4th order sequences are identified (Table 6.1). The 5th order sequences are numbered from top to bottom in the Sulaiy wells correlation enclosure of wells G, F, H, G and I. The generalised parasequence pattern of Well-G 5th order sequences are characterised as follows:

- Shallow setting pattern of the parasequences numbers 1, 2, 3, 4 and 5. These comprise most of this cored well.

This well is generally located within the Deep lagoon setting, adjacent to ooid shoal settings in which it is confirmed from the common shallow setting patterns and from the microfossil analysis (Figure 6.4 and Table 6.4B).

Table 6.4A. Illustrates the sequence stratigraphic and palaeoenvironmental interpretations for Well-G.

Top depth (ft.)	Base depth (ft.)	3rd order sequence	5th order parasequence	Depositional environment	Microfacies
6755.7				Base of Yamama Formation	
6756.5	6759.3	Highstand	HST	Ooidshoal	Superficial ooid, *Lithocodium,* agglutinated foraminifera and miliolids grainstone
6759.3			MFS	Deeper lagoon with ooids backstep	Bioclastic, *Lithocodium* grainstone
6759.3	6762.6		TST	Deeper open marine	Grapestone, bioclastic grainstone
6762.6	6771.6		HST	Ooids shoal and open marine	Superficial ooid, echinoderm, grainstone and *Lithocodium* grainstone

6771.6			MFS	Deeper open marine	*Lithocodium* boundstone
6771.6	6777.7		TST	Deeper lagoon	Bioclastic, pelletal, packstone/ grainstone
6777.7	6786.5		HST	Shoal, inner-shoal, open marine	Superficial ooid grainstone, bioclastic, pelletal grapestone, grainstone
6786.5			MFS	Deeper open marine	Bioclastic grainstone
6786.5	6790.6		TST	Lagoon	Bioclastic packstone
6790.6	6798.4		HST	Inner-shoal and open marine	Pelletal, calcispheres, bioclastic grainstone/packsone
6798.4			MFS	Deeper open marine	*Lithocodium* boundstone
6800.5	6798.4		TST	Open marine	Bioclastic packstone
6800.5	6804.6		HST	Inner-shoal	Pelletal grapestone/grainstone
6804.6			MFS	Deeper inner-shoal	Pelletal packstone
6804.6	6809.5		TST	Shallow Lagoon	Peletal,*Mohlerina, Lithocodium* packstone
6811.3			HST	Open marine	*Lithocodium* packstone

Table 6.4B. Display of the interpreted microfossils vertical responses for each 5th order sequence for Well-G.

TST	MFS/Z	HST	UPPER	WELL-G
		common		*Quinqueloculina robusta*
Rare		common		*Quinqueloculina* spp.
				Protopeneroplis ultragranulata
				Nautiloculina oolithica
				Coscinoconus alpina
				Coscinoconus elongata
				Coscinoconus delphinensis
				Ammobaculites subcretaceus
				Pfenderina neocomiensis
				Verneuilinoides polonicus
				Mohlerina basiliensis

						Lenticulina spp.
						Textulariopsis jurassica
						Salpingoporella annulata
						Salpingoporella pygmaea
						Salpingoporella spp.
						Actinoporella podolica
						Lithocodium aggregatum
						calcispheres
						costate bivalves
						Saccocoma sp.
						echinoid fragments
						superficial ooid grains
PS	WS	MS	WS	PS	GS	Dunham (1962) texture
						extraclastic grains
						vuggy and moldic ø

Well D

This well was difficult to characterize by its 5th order sequences (Table 6.5A. The 5th order sequences). This is because of missing cores between some of the candidate sequence boundaries. However Table 6.5A lists the proposed sequence boundaries with their depths.

This well is generally located within the debris flow sequences of the External Platform micro-biofacies. These represent the Platform Margin, Slope to Deep Slope sedimentary zones settings in which is supported by the common shallow setting patterns and from the microfossil analysis (Figure 6.4 and Table 6.5B).

Table 6.5A. Illustrates the interpreted sequence stratigraphic and palaeoenvironmental interpretations for Well-D.

Top depth (ft.)	Base depth (ft.)	3rd order	5th order	**Depositional environment**	Microfacies
8192.2	8211.7			Base of Yamama Formation	
8211.7		Highstand	HST	Open marine, inner-shoal bank	Peloidal grainstone, leached (MO) moldic porosity
8249.7			HST	Sand bank to platform margin	Poorly sorted, intraclastic grainstone to rudstone
8252.2			HST	Shoal bank	Superficial ooid grainstone
8320.7			TST	Lagoon	Non-laminated peloidal, miliolids grainstone
8329.2			HST	Shoal bank	Superficial ooid grainstone
8359.2			HST	Shoal bank	Superficial ooid grainstone
8377.7			HST	Shoal bank	Superficial ooid grainstone
8385.2			TST	Open marine to platform margin	*Lithocodium* boundstone
8386.7			HST	Platform margin	Peloidal, coated bioclastics packstone and grainstone
8480.2	8496.7		HST	inner-shoal	Peloidal,superficial ooid packstone
8496.7			MFZ/S	Deeper platform margin	Bioclastic, peloidal packstone
8496.7	8504.7		TST	Shallow platform margin	Peloids, bioclastic packstone
8504.7	8542.2		HST	Platform margin	Fine oncolitic, superficial ooid packstone
8542.2			MFZ/S	Slope	*Lenticulina,* peloidal wackestone to packstone
8542.2	8551.2		TST	Slope	*Conoglobigerina* sp., extraclastic, peloidal wackestone
8551.2			HST	Shoal	Superficial ooid, lithoclastic grainstone
8558.7				Deep slope	Peloidal, reworked-skeletal wackestone
8570.7			HST	Lagoon Inner-shaol	Peloidal grainstone
8579.7			HST	Open marine to inner-shoal	Peloidal, bioclastic grainstone
6563.2				Platform margin	*Nodosaria*, peloidal microstylolitic/dolomitic grainstone /bindstone

8584.2			MFZ/S	Inner-shoal	Foraminifera, peloidal mud-lean packstone
8611.2			?HST	Open Marine	*Protopeneroplis,* peloidal wackestone
8620.2			MFZ/S	Deep slope	*Lenticulina,* saddle dolomite wackestone
8630			TST	Upper slope	*Lenticulina*, oyster, peloidal packstone
8636.7			HST		Slope-laminated peloidal bindstone/ wackestone/ packstone
8642.7			HST	Platform margin	Extraclastic, *Nodosaria*, *Lenticulina* and *Saccocoma* packstone
8644.2			?MFZ/S	Deep slope	Spiculite, Calcisiltite Wackestone

Table 6.6B. Display of the microfossil interpretation and vertical responses for each 5th order sequence for Well-D.

TST	MFS/ Z	HST	UPPER HST	WELL-D microfossils distribution
common	MISSING CORE DATA			Planktic foraminifera
				Everticyclammina virguliana
				Pseudocyclammina lituus
				Nautiloculina oolithica
				Verneuilinoides polonicus
				Meandrospira faveri
				Miliolids
				Coscinoconus elongata
		Rare		*Lenticulina* spp.
				Nodosaria spp.
				Calpionellid
				Monaxon sponge spicules
				Triaxon sponge spicules
				Salpingoporella pygmaea
				reworked *Salpingoporella* spp.
				Permocalculus ampullaceus
				bivalve debris
				bivalves

					echinoid fragments
					Stromatoporoid
					coated grains and superficial ooid (transported)
PS	WS	MS	WS	PS-GS	Dunham (1962) texture

Well B

This well is characterized by five 5th order sequences (Table 6.7A) that are used as a base well for correlating the sequences layers in which six of 4th order sequences are identified (Table 6.1). The 5th order sequences are numbered from top to bottom in the Sulaiy wells correlation enclosure of wells G, F, H, G and I. The generalised parasequence patterns of Well-B 5th order sequences are characterised as follows:

- Shallow setting patterns of the parasequences numbers 1, 2, 3, 4 and 5. These comprise most of this cored well.

This well is generally located within the ooid shoal settings in which it is supported by evidence from the common shallow setting patterns and from the microfossil analysis (Figure 6.4 and Table 6.7B). Diversity is reduced in comparison to Well-H. The 5th order cycles of Well-F are thicker than those of Well-H.

Table 6.7A. This illustrates the sequence stratigraphic and palaeoenvironmental interpretations for Well-B

Top depth (ft.)	Base depth (ft.)	3rd order	5th order	Depositional environment	Microfacies
8349.4	8386.22			Base of Yamama Formation	
8387.7	8395.4	Highstand	HST	Ooidshoal to platform margin	Lithoclastic,superficial ooid, *Crescentiella*grainstone
8395.4			MFS	Deep open marine	*Lithocodium*, lithoclastic Grainstone
8395.4	8400.7		TST	Open marine, inner shoal	*Lithocodium*, bioclastic grainstone
8400.7	8408.3		HST	shoal to platform margin	Superficial ooid, lithoclastic, *Lithocodium*grainstone
8408.3			MFS	Deeper open marine	Peloidal, superficial ooid, bioclastic packstone
8408.3	8410.5		TST	Open marine	Lithoclastic,*Lithocodium*oncoidsgrainstone
8410.5	8417.3		HST	Shoal to platform margin	Lithoclastic,superficial ooid, *Crescentiella* grainstone
8417.3			MFS	Deeperopen marine	*Lithocodium* oncoids wackestone
8417.3	8422.6		TST	Open marine	*Lithocodium* oncoids packstone
8422.6	8430.3		HST	platform margin	Peloidal, *Lithocodium*,*Crescentiella*, bioclastic packstone
8430.3			MFS	Deeper open marine	Clacisphers,*Lithocodium* wackestone
8430.3	8440.20		TST	Deeper open marine	Bioclastic, *Lithocodium* packstone
8440.20	8446.7		HST	Ooid shoal	Superficial ooid, bioclastic,*Lithocodium* grainstone

Table 6.7B. This displays the microfossil interpretation for the vertical responses in each 5th order sequence for Well-B.

TST		MFS/Z	HST		UPPER HST	WELL-B microfossils distribution
Rare			Common			*Quinqueloculina pudubiensis*
						Quinqueloculina robusta
						Quinqueloculina multicostata
						Quinqueloculina spp.
						Nubecularia spp.
						Miliolids spp.
						Protopeneroplis ultragranulata
						Pseudocyclammina lituus
						Nautiloculina oolithica
						Coscinoconus alpina
						Coscinoconus elongata
						Pfenderina neocomiensis
						Verneuilinoides neocomiensis
						Verneuilinoides polonicus
						Mohlerina basiliensis
						cf. *Mohlerina basiliensis*
						Lenticulina spp.
						Gaudryinella sp.
						Praedorothia sp. cf. *P. praehauteriviana*
						Permocalculus ampullaceus
						Salpingoporella annulata
						Salpingoporella spp.
						Thaumatoporella parvovesiculifera
						Lithocodium aggregatum
						Crescentiella morronensis
						echinoid fragments
						superficial ooid grains
PS	WS	MS	WS	PS	GS	Dunham (1962) texture
						vuggy and moldic ø
						vadose, micro-stalactite dripstone cement

Well I

This well is characterized by twelve 5th order sequences (Table 6.8A) that are used as a base well for correlating the sequences layers in which six of 4th order sequences are identified (Table 6.1). The 5th order sequences are numbered from top to bottom in the Sulaiy wells correlation enclosure of wells B, F, H, G and I. The generalised parasequences patterns of Well-I 5th order sequences are characterised as follows:

- Shallow setting patterns of the parasequences numbers 1, 2, 3, 4, 5, 6, 7 and 8. These comprise most of this cored well.
- Maximum flooding setting or equilibrium setting of the parasequences numbers 11 and 12.

This well is generally located within the Lagoon and inner-shoal settings in which it is supported by the common shallow setting patterns and from the microfossil analysis (Figure 6.4 and Table 6.8B).

Table 6.8A. This illustrates the sequence stratigraphic and palaoenvironmental interpretations for Well-I.

Top depth (ft.)	**Base depth (ft.)**	**3rd order**	**5th order**	**Depositional environment**	Microfacies
5321.2	5379.7			Base of the Yamama Formation	
5379.7	5384.2	Highstand	HST	Inner shoal	Spicules, peloidal, extraclastic packstone/grainstone
5384.2			MFS	Deeper open marine	Spicules, fine peloidalpackstone
5384.2	5390.2		TST	Open marine	Bioclastic, spicules peloidalpackstone
5390.2	5396.2		HST	Inner-shoal	Intraclastic grainstone

5396.2			MFS	Deeper lagoon	Bioclastic calcisphere packstone
5396.2	5397.7		TST	Lagoon	Bioclastic intraclastic packstone
5397.7	5409.9		?HST	NA	NA
5409.9			MFS	Lagoon	Bioclastic, spicules wackestone
5409.9	5417.2		TST	Lagoon to open marine	Bioclastic, spicules packstone/wackestone
5417.2	5419.7		HST	Inner-shoal	Oolites intraclasticgrainstone
5419.7			MFS	Deeper open marine	Bioclastic, spicules wackestone
5419.7	5431.2		TST	Open marine	Bioclastics spicules packstone
5431.2	5435.2		HST	Inner-shoal	Extraclast peloids grainstone
5435.2			MFS	Open marine	Bioclastic, peloidal, spicules packstone
5435.2	5439.7		TST	Lagoon	Bioclastic, peloidalgrainstone
5439.7	5448.7		HST	Upper slope	Superficial ooid, spicules packstone/grainstone
5448.7			MFS	Deeper slope	Bioclastic, peloidal, spicules packstone
5448.7	5453.2		TST	Platform margin	Bioclastic, peloidalpackstone
5465.7	5471.7		HST	Inner-shoal	Bioclastic, peloidalpackstone
5471.7			MFS	Upper slope	Sperficial ooid, peloidal spicules Packstone
5471.7	5476.2		TST	Platform margin	Peloidal *Lithocodium* packstone/wackestone
5476.2	5482.2		HST	Opem marine	Lithocodium extraclast Grainstone
5515.2	5518.2		HST	Open marine	Extraclst lithocodium bioclast Grainstone
5518.2			MFS	Deeper lagoon	Extraclast peloids bioskeletal Grainstone
5518.2	5522.7		TST	Lagoon	Bioclastic echinoderms peloids Grainstone
5522.7	5528.7		HST	Shoal	Sperficial ooidgrainstone
5528.7			MFS	Deeper lagoon	Sperficial ooid packstone

5528.7	5533.2		TST	Open marine	*Lithocodium,* peloidal, extraclasticgrainstone
5533.2	5543.2		HST	Lagoon	Peloidalgrainstone

6.5 SELECTED PALAEOENVIRONMENTAL MAPS FROM SELECTED PARASEQUENCES SYSTEM TRACTS

The microfacies and the bio−component results have provided the evidence of the Arabian Rimmed shallow Platform (ARSP) sedimentary palaeoenvironmental model. The identified palaoenvironments are intertidal, restricted lagoon (subtidal), inner shoal, open marine, deeper open marine, ooid shoal, platform margin, slope and deeper slopeThe microfacies characteristics have assisted the recognition of a layered framework into which the regional variations of both facies types can be distributed. Transgressive, maximum flooding and highstand elements of each layer have been distinguished and enable 3 maps to be generated (Figures 6.9 to 6.11). These are from the highstand part of sequence-1 from the topmost of the Sulaiy Formation (Figure 6.9), the transgressive system tract part from sequence-3 (Figure 6.10) and the highstand par or the end of sequence-5 (Figure 6.11). These three maps show the well locations, the location of a postulated fault (see Fig. 6.4) and the facies boundaries. Well-A is excluded from this study for the reason of being totally dolomitized by probably hydrothermal fluids through North-East and South-West oriented faults. The facies boundaries some are represented by solid line and some are dotted lines. The solid lines are true boundaries based on microfacies data and the dotted lines are projected (or expected) boundaries but not from microfacies analysis. The boundaries colors are representing the sedimentary zone such as platform margin boundary is blue, ooid

shoal is orange, purple is representing the Inner-shoal, pale green is open marine, green is lagoon and the yellow color is representing the boundary of the intertidal sedimentary zone.

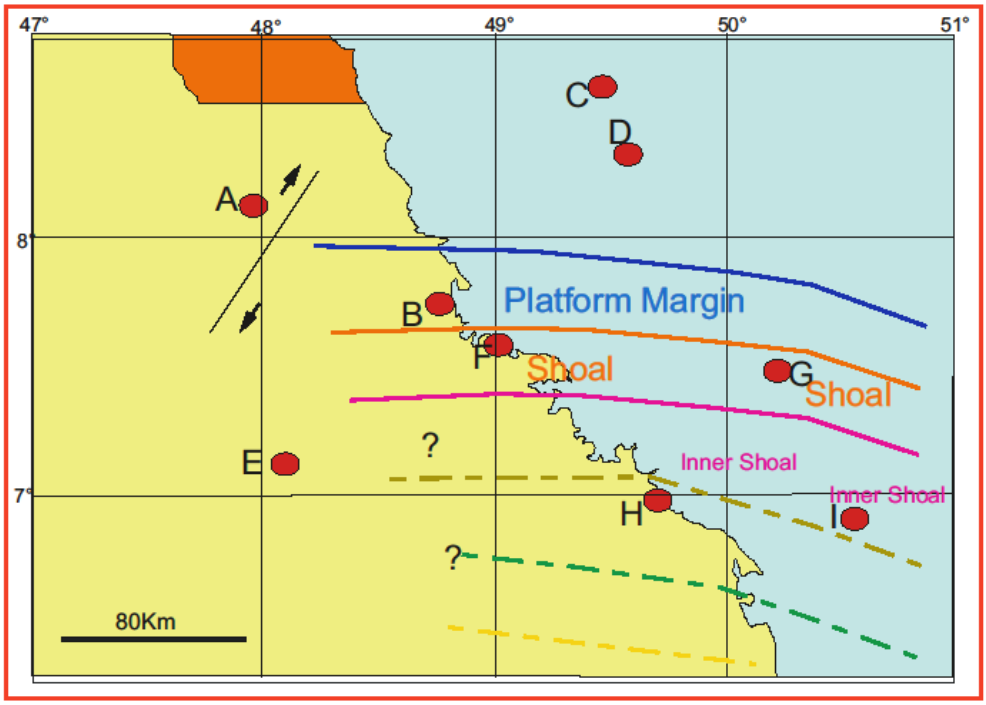

Figure 6.9. Paleogeographical map for the highstand part of sequence-1 from the topmost Sulaiy Formation.

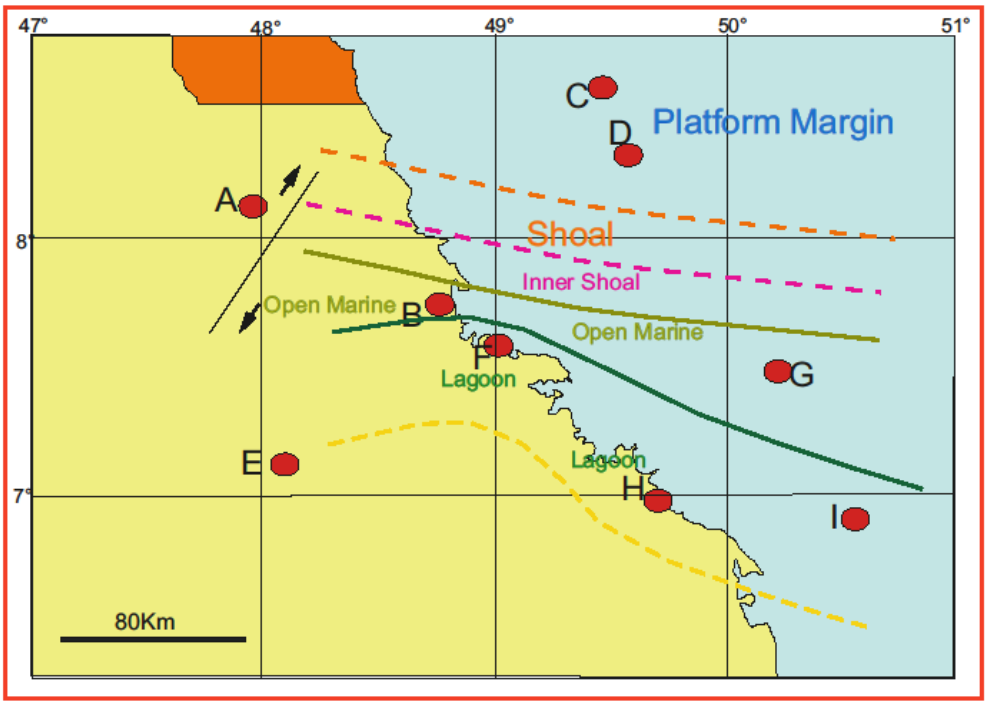

Figure 6.10 Paleogeographical map for the transgressive system tract part from sequence-3 of the Sulaiy Formation.

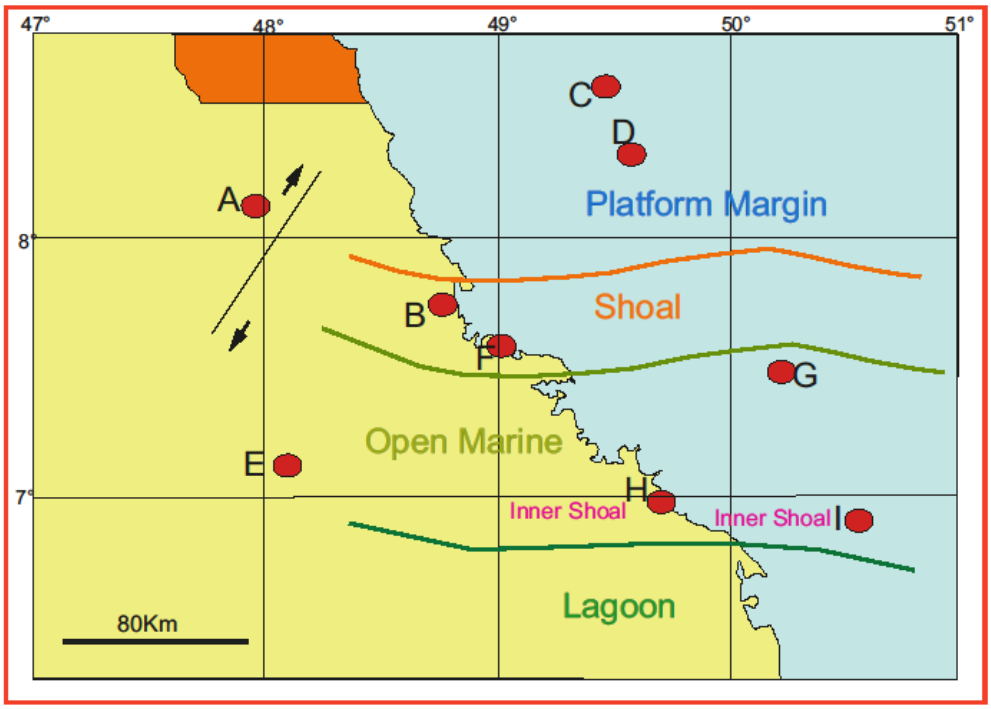

Figure 6.11 Paleogeographical map for the the highstand part or the end of sequence-5 of the Sulaiy Formation.

6.6 SUMMARY

The bio-components display a varied vertical distribution within the Sulaiy Formation, and can be used to support the recognition of depositional cycles. It is evident that certain species that are present in the lower part of the studied section are absent in the upper part, or only present within the maximum flooding sections of the younger depositional cycles. This pattern reveals several depositional cycles, each of which is characterized by gradual replacement of deeper water species by shallower forms. The entire studied section is probably related to an overall shallowing of the Upper Sulaiy Formation.

Integrated sedimentology and micropalaeontology has identified 10 sequences of shoaling upwards depositional cycles, considered to be 5^{th} order sequences that are superimposed on a large scale 3^{rd} order system tract shallowing upwards, highstand-associated sequence of the Sulaiy Formation. It has also identified 2 sequences of maximum flooding depositional cycles that are superimposed on a large scale 3^{rd} order system tract of maximum flooding zone (MFZ). Only one identified sequence of deepening upward setting depositional cycles, considered to be 5^{th} order sequences that are superimposed on a large scale, 3^{rd} order system tract, deepening upward pattern.

The Lower Ratawi Reservoir is located within the latest highstand portion of a 3^{rd} order Sulaiy Formation sequence. The reservoir consists of a succession of several sequences, each being sub-divided into a lower, transgressive systems tract separated from an upper highstand systems tract by a maximum flooding surface (MFS/Z). The

last of these depositional cycles terminates in beds of porous and permeable ooid, or ooid-pelloid, grainstone. The reservoir is sealed by the finer-grained sediments of the overlying Yamama Formation.

CHAPTER SEVEN

SUMMARY AND CONCLUSIONS

CHAPTER SEVEN

SUMMARY AND CONCLUSIONS

The Sulaiy Formation, which is the oldest unit in the Lower Cretaceous succession, is conformably overlain by the Yamama Formation and it has been a challenge to identify the precise age of the two formations using benthic foraminifera and associated microfossil assemblages. On the eastern side of Saudi Arabia, the Sulaiy Formation and the base of the Yamama Formation were poorly studied and this has been the focus of the present research.

The research has involved the lithological analysis of 1277 thin-sections, taken from core samples from nine wells which provide a geographically representative distribution within the Saudi Arabian Gulf. These cores intersected the base of the Yamama Formation and the Sulaiy Formation in the total thickness of cored wells of 843.23 meters (2766.5 feet) from a total number of 46 cores.

This research has involved the following:

- Selection of a series of cored wells which provided a geographically representative distribution of the Sulaiy Formation;
- The semi-quantitative micropalaeontological analysis of thin-sections from closely spaced samples;
- Construction of species distribution charts (using the software package “Strata-bugs”) for each studied well;
- Petrographical analysis of each thin-section, applying the Dunham classification (1962), and also recording aspects of their diagenesis;

- Determination of microbiofacies and the interpretation of their depositional environment;
- Identification of deepening and shallowing-upwards biofacies and their contribution to hierarchical depositional cycles in order to identify cycle boundaries and transgressive/regressive components; and
- Identification of some regional lithofacies and biofacies patterns and their position within systems tracts: data useful for the future identification of locations with good reservoir facies development.

This research has accomplished the following objectives:

- Investigated the microfossil diversity and abundance within the Sulaiy Formation up to, and including, the base of the Yamama Formation;
- Determined the age of the formations and the palaeoenvironments represented by the carbonate sediments;
- Enhanced the current understanding of the sequence stratigraphy of the Sulaiy Formation; and
- Determined the regional and lateral variations in palaeoenvironment.

The research has specifically investigated the micropalaeontology of the core samples from the selected wells and this has involved the following:

- The microfossils encountered included taxa from rotalid foraminifera, miliolid foraminifera, agglutinated foraminifera, calcareous algae, calcispheres, stromatoporoids, sponge spicules, problematica (e.g., *Lithocodium aggregatum*), molluscs, corals, echinoderms and ostracods;

- In general, the micropaleontological biodiversity of the Sulaiy Formation is less than that of the Yamama Formation which appears to be a result of the general low-stand situation;
- Systematic analysis of the planktic and benthic foraminifera was accomplished using the foraminiferal classification by Loeblich and Tappan (1987) as the main key reference, together with other key references from the literature on the Middle Eastern and Tethyan regions;
- The assemblages contain a number of foraminifera that are recorded for the first time in the Sulaiy Formation. Other microfossils were identified and recorded to help in the identification of the sedimentary environments;
- The use of index fossils or acme range zones of calpionellids, planktic and benthic foraminifera and calcareous algae has confirmed the chronostratigraphic age of the Sulaiy Formation as being the transitional interval from the uppermost Tithonian to the lowermost Cretaceous (Berriasian to the lowermost Valanginian);
- The base of the Sulaiy Formation is confirmed as uppermost Tithonian from the acme range zone of *Kurnubia palastiniensis* Henson (1948, Callovian to Tithonian), *Protopeneroplis ultragranulata* (Gorbatchik, 1971, Middle Tithonian to Lower Barremian), *Protomarssonella kummi* (Zedler, 1961, Upper Tithonian to Hauterivian), *Everticyclammina virguliana* Koechlin (1942, Kimmeridgian to Lower Berriasian), *Charentia cuvillieri* Neumann (1965, Upper Tithonian to Cenomanian), *Ammobaculites* sp. aff. *A.celatus* Arnaud-Vanneau (1980, Upper Tithonian to Aptian), *Verneuilina minuta* Wiesner (1931, Upper Tithonian to Lower Aptian), *Verneuilinoides neocomiensis* Mjatliuk (1939, uppermost

Tithonian to Aptian), *Anchispirocyclina lusitanica* (Egger, 1902, Tithonian to Valanginian), *Istriloculina emiliae* Neagu (1984, Tithonian to Barremian), *Coscinoconus elongata* (Leupold, 1935, Tithonian to Early Valanginian) and *Coscinoconus alpina* Leupold (1935, Tithonian to Early Valanginian). Non−foraminiferal microfossils include *Pseudolithocodium carpathicum* Míšík, (1979, Tithonian), *Comittosphaera sublapidosa* (Volger, 1941, Tithonian to Hauterivian), *Colomisphaera cieszynica* Nowak (1968, Kimmeridgian to Lower Valanginian),*Actinoporella podolica* (Alth, 1878, uppermost Tithonian to Berriasian), *Clypina isabellae* Masse *et al.* (1999, Kimmeridgian to Berriasian), *Salpingoporella katzeri* Conrad and Radoicic (1978, Berriasian to Valanginian), *Salpingoporella* ex. gr. *pygmaea* (Gümbel, 1891, Bathonian to Aptian), *Permocalculus ampullaceus* Elliott (1959, Tithonian to Hauterivian), *Calpionella alpina* Lorenz (1902,uppermost Tithonian to lowermost Berriasian), *Crassicollaria brevis* Remane (1962, uppermost Tithonian) and *Saccocoma* sp. (Upper Tithonian and Berriasian);

- The age of the Sulaiy Formation is confirmed as Berriasian to earliest Valanginian by the acme range zone of *Conoglobigerina* sp. cf. *C. gulekhensis* (Gorbatchik and Poroshina, 1979, Berriasian to Early Valanginian), *Pfenderina neocomiensis* (Pfender, 1938, Berriasian to Hauterivian), *Everticyclammina kelleri* (Henson, 1948, Berriasian to Valanginian), *Protopeneroplis ultragranulata* (Gorbatchik, 1971, Middle Tithonian to Lower Barremian), *Charentia cuvillieri* Neumann (1965, Upper Tithonian to Cenomanian), *Haghimashella arcuata* (Haeusler, 1890, Callovian to Valanginian), *Verneuilina minuta* Wiesner (1931,

Upper Tithonian to Lower Aptian), *Gaudryinella* spp.Plummer (1931, Berriasian to Cenomanian), *Nautiloculina bronnimanni* Arnaud-Vanneau and Peybernes (1978, Berriasian to Hauterivian), *Verneuilinoides polonicus (*Cushman and Glazewski, 1949, Tithonian to Early Valanginian), *Verneuilinoides neocomiensis* Mjatliuk (1939, uppermost Tithonian to Aptian), *Anchispirocyclina lusitanica* (Egger, 1902, Tithonian to Valanginian), *Charentia evoluta* (Gorbatchik, 1968, Upper Kimmeridgian to Valanginian), *Mohlerina basiliensis* (Mohler, 1938,Oxfordian to Valanginian), *Istriloculina eliptica* (Iovcheva, 1962, Middle Berriasian to Aptian), *Istriloculina emiliae* Neagu (1984, Tithonian to Barremian), *Nodobacularia* n. sp. (Tithonian to Berriasian), *Coscinoconus elongata* (Leupold, 1935, Tithonian to Early Valanginian) and *Coscinoconus alpina* Leupold (1935, Tithonian to Early Valanginian). Non−foraminiferal microfossils include *Hensonella* n. sp. (Berriasian), *Comittosphaera sublapidosa* (Volger, 1941, Tithonian to Hauterivian), *Colomisphaera cieszynica* Nowak (1968, Kimmeridgian to Lower Valanginian), *Actinoporella podolica* (Alth, 1878, uppermost Tithonian to Berriasian), *Clypina isabellae* Masse *et al.* (1999, Kimmeridgian to Berriasian), *Iranella inopinata* Gollestaneh (1965, Berriasian to Valanginian), *Salpingoporella annulata* Carozzi (1953, Bthonian to Early Brremian), *Salpingoporella katzeri* Conrad and Radoicic (1978, Berriasian to Valanginian), *Salpingoporella* ex. gr. *pygmaea* (Gümbel, 1891, Bathonian to Aptian),*Salpingoporella dinarica* Radoicic (1959, Berriasian to Albian), *Holosporella arabica* Granier and Brunn (1991,Berriasian to Aptian), *Macroporella praturloni* Dragastan (1971,Berriasian), *Arabicodium aegagrapiloides* Elliott, (1957, Lower Cretacous), *Permocalculus*

ampullaceus Elliott (1959, Tithonian to Hauterivian), *Saccocoma* sp. (Upper Tithonian and Berriasian) and *Favreina* sp. cf. *F.dinarica* Brönnimann (1976, Berriasian to Hauterivian);

- The uppermost boundary of the Sulaiy Formation (Upper Berriasian to lowermost Valanginian) is confirmed from the occurrences of *Bramkampella arabica* Redmond (1964,Upper Berriasian to Lower Valanginian), *Montsalevia salevensis* Charollais *et al.* (1966, Late Berriasian to Hauterivian), *Neotrocholina valdensis* Reichel, (1955, Late Berriasian to Valanginian), *Coscinoconus elongata* (Leupold, 1935, Tithonian to Early Valanginian), *Coscinoconus alpina* Leupold (1935, Tithonian to Early Valanginian), *Haplophragmoides joukowskyi* Charollais *et al.* (1966,Berriasian to Valanginian), *Istriloculina eliptica* (Iovcheva, 1962, Middle Berriasian to Aptian), *Derventina filipescui* Neagu (1968,Valanginian to Lower Aptian), *Ophthalmidium* spp. Kübler and Zwingli (1870,Berriasian to Barremian), *Meandrospira faverei* (Charollais *et al.,* 1966, Valanginian) an*d Protopeneroplis banatica* Bucur, (1993, Berriasian to Valanginian).
  Non−foraminiferal microfossils include *Hensonella* n. sp. (Berriasian), *Colomisphaera conferta* Řehánek (1985, Upper Berriasian to Valanginian), *Stomiosphaera wanneri* Borza(1969, Upper Berriasian to Hauterivian), *Iranella inopinata* Gollestaneh (1965, Berriasian to Valanginian)*,Salpingoporella* ex. gr. *pygmaea* (Gümbel, 1891,Bathonian to Aptian)*, Macroporella praturloni* Dragastan (1971, Berriasian)*, Arabicodium aegagrapiloides* Elliott, (1957, Lower Cretacous) and *Calpionellopsis simplex* (Colom, 1939, Upper Berriasian).

- *Lithocodium aggregatum* was found to be abundant in the Sulaiy Formation while *Cladocorobsis mirabilis* is reasonably rare to present. The presence and rare occurences of *Salpingoporella pygmaea* and *Meandrospira faveri* are characteristic of the Sulaiy Formation;
- The Yamama Formation is recognized by its restricted to open sub-tidal, lagoonal sedimentary environment. The evidence for this is the highly abundant and diverse assemblage of calcareous algae (most notably dasyclads); and
- The Valanginian age assigned for the Yamama Formation is confirmed from the occurrences of *Protopeneroplis banatica* Bucur, (1993, Berriasian to Valanginian), *Meandrospira favrei* (Charollais *et al*., 1966, Valanginian), *Haplophragmoides joukowskyi* Charollais *et al.* (1966, Berriasian to Valanginian), *Coscinoconus sagittaria* Arnaud-Vanneau *et al*., (1988, Late Berriasian to Valanginian), *Coscinoconus cherchiae* Arnaud-Vanneau *et al*. (1988, Late Berriasian to Valanginian), *Coscinoconus delphinensis* (Arnaud-Vanneau *et al.* 1988, Berriasian to Middle Valanginian), *Derventina filipescui* Neagu (1968, Valanginian to Lower Aptian*)*, *Istriloculina eliptica* (Iovcheva, 1962, Middle Berriasian to Aptian), *Ophthalmidium* spp. Kübler and Zwingli (1870, Berriasian to Barremian) *Pseudocyclammina cylindrica* Redmond (1964,Upper Berriasian to Valanginian), *Montsalevia salevensis* Charollais *et al.* (1966, Late Berriasian to Hauterivian), *Mohlerina basiliensis* (Mohler, 1938, Oxfordian to Valanginian), *Protopeneroplis ultragranulata* (Gorbatchik, 1971, Middle Tithonian to Lower Barremian) and *Textulariopsis jurassica* (Gümbel, 1862,Bajocian to Valanginian). Non−foraminiferal microfossils include calcareous algae such as *Iranella*

inopinata Gollestaneh (1965, Berriasian to Valanginian), *Arabicodium aegagrapiloides* Elliott, (1957, Lower Cretacous), *Salpingoporella annulata* Carozzi (1953, Bathonian to Early Brremian), *Salpingoporella* ex gr. *pygmaea* (Gümbel, 1891, Bathonian to Aptian), *Salpingoporella dinarica* Radoicic (1959, Berriasian to Albian), *Holosporella arabica* Granier and Brunn (1991, Berriasian to Aptian), *Salpingoporella katzeri* Conrad and Radoicic (1978, Berriasian to Valanginian) and *Permocalculus ampullaceus* Elliott (1959, Tithonian to Hauterivian), as well as fragments of *Inoceramus* sp. (Cretaceous).

The investigation of the micropalaeontology has provided considerable insights into the bio-components of the Sulaiy and the base of the Yamama formations which have all been used to identify their biofacies. The main results of this investigation include:

- The investigation of the various lithofacies. About twenty-four lithofacies units were identified on the basis of their bio−component and non-skeletal grains;
- The lithofacies and the bio−component results have provided the evidence of a sedimentary palaeoenvironmental model, namely the Arabian Rimmed shallow Platform (ARSP). This palaeoenvironmental depositional model is characterised by two different platform regimes. These are the Platform Interior and the Platform Exterior, each of which have unique sedimentary lithofacies zones that produce different types of lithofacies. Each lithofacies is characterised by special depositional conditions and a palaeobathymetric history that interacts with sea level changes and the available accommodation space;

- The important palaeoenvironments are intertidal, restricted lagoon (subtidal), inner shoal, open marine, deeper open marine, ooid shoal, platform margin, slope and deeper slope;
- Generating, and testing, a depositional model as a part of formulating a sequence stratigraphical interpretation of a region is a key to understanding its geological development and, ultimately, its reservoir potential;
- The micropalaeontology and sedimentology of the Sulaiy Formation in the subsurface have indicated a succession of clearly defined shallowing−upwards depositional cycles. These typically commence with a deep(er) marine biofacies with wackestones and packstones, capped with a mudstone-wackestone maximum flooding zone and an upper unit of packstone to grainstones representing a shallow marine biofacies;
- The upper part of the Sulaiy Formation is highstand-dominated with common grainstones that host the Lower Ratawi reservoir which is capped by karst that defines the sequence boundary. This karst is identified by its abundant moldic and cavern porosity that enhanced the reservoir quality by increasing porosities into greater values.This defines the post-Sulaiy unconformity and includes an appreciation of the intensity of the eustatic controls on events of late highstand system tracts.It is suggested that the localised preservation of grainstones in the uppermost Sulaiy Formation is represent late highstand shoal development, upon which post-Sulaiy Formation, late Berriasian sub-aerial exposure is a significant reservoir affecting diagenesis;

- Integration of the sedimentological and micropalaeontological information has identified a succession of shoaling−upwards depositional cycles, which are considered to be 5th and 4thorder para-sequences, that are superimposed on a large scale 3rd order system tract shallowing−upwards, highstand-associated, maximum flooding zones and deepening upward sequences of the Sulaiy Formation; and
- The Lower Ratawi Reservoir is located within the latest high-stand portion of a 3rd order Sulaiy Formation sequence. The reservoir consists of a succession of several sequences, each of which is sub-divided into a lower transgressive systems tract separated from the upper highstand systems tract by a maximum flooding surface (MFS/Z). The last of these depositional cycles terminates in beds of porous and permeable ooid, or ooidal-peloidal, grainstone. The reservoir is sealed by the finer-grained sediments of the Yamama Formation.

The results of this research, coupled with the available petrophysical data will improve the understanding, and prediction, of the distribution of hydrocarbon reservoir facies in this area and else here in the Arabian Gulf. It is also hoped that the data from this research will aid correlation of the Jurassic/Cretaceous boundary across the region following the determination of the J/K GSSP (Global Stratigraphic Section and Point).

This research has used general stratigraphical ranges of microfossils that are geographically distributed in the northern part of the Tethyan Region. It is required a precise study of localized stratigraphical ranges of the upper Jurassic and Lower Cretaceous formations biocomponents.

This research improved the interpretation of depositional environments, sequence stratigraphy and reservoir facies location prediction. This study will lead to the recognition of environmentally significant lithofacies and biofacies, of which their vertical collaboration will provide significant contributions towards on-going hydrocarbon reservoir characterization studies.The sequence stratigraphy model will be incorporated with the porosity and permeability data in Saudi Aramco Company in order to understand the porosity and permeability development relationship with the sequence stratigraphic position after the completion of this study. The constructed of microfacies succession of each well will provide a roadmap for the future Biosteering operations in drilling lateral wells in order to increase the production window of the reservoirs horizon.

In conclusion the preparation of regional lithofacies, microfacies maps and their systems tracts will result in the identification of locations with good reservoir facies development. It is extremly important to undertake the same type of reserch on the rest of the Saudi Arabian subsurface formations such as the Yamama Formation, Buwaib Formation, Shu’aiba Formation, Wasia Formation and members and Aruma Formation.

References

Abdullah, F. H. A., and Kinghorn, R. R. F.1996. A preliminary evaluation of Lower and Middle Cretaceous source rocks in Kuwait. *Journal of Petroleum Geology*, **19** (4), 461-480.

Abolfazl Hosseini, S. and Conrad, M.A. 2008. Calcareous algae, foraminifera and sequence stratigraphy of the Fahliyan Formation at Kuh-e-Surmeh (Zagros Basin, SW of Iran). *Geologia Croatica*, **61**(2-3), 215–237.

Ahr, W.M. 1973. The carbonate ramp, an alternative to the shelf model. *Transactions of the Gulf Coast Association of Geological Societies*, **23**, 221–225.

Ahr, W.M. 2008. *Geology of carbonate reservoirs: the identification, description and characterization of hydrocarbon reservoirs in carbonate rocks*. John Wiley and Sons Inc., Hoboken, NJ, USA, doi:10.1002/9780470370650.ch8.

Akyazi, M., Karabasoglu, A., Utar, A., Kesgìn, Ö, Erdem, N.Ö. and Ursavas, T.Ç. 2001. The calpionellid biostratigraphy of Jurassic-Cretaceous aged limestone in the Merzifon (Amasya) region. *Bulletin of Faculty of Engineering of Cumhuriyet University, Serie A - Earth Sciences*, **1**(2), 123–148.

Allaby, A. and Allaby, M. 1990. *The Concise Oxford Dictionary of Earth Sciences.* Oxford University Press, Oxford, 410pp.

Al-Fares A., Bouman, M. and Jeans, P. 1998. A new look at the Middle to Lower Cretaceous Stratigraphy, Offshore Kuwait. *GeoArabia*, **3(**4), 543–560.

Al-Hinai, K.G., Dabbagh, A.E., Gardner, W.C., Khan, M. and Saner, S. 1997. Shuttle imaging radar views of some geological features in the Arabian Peninsula. *GeoArabia*, **2**, 165–178.

Al-Husseini, M.I. 2000. Origin of the Arabian plate structures: Amar collision and Najd rift. *GeoArabia*, **5**(4), 527–542.

Al-Husseini, M. and Matthews, R.K. 2006. Stratigraphic Note: Orbital calibration of the Arabian Jurassic second-order sequence stratigraphy. *GeoArabia*, **11**(3), 161–170.

Al-Jallal, I.A. and Al-Sharhan, A.S. 2005. Arabia and the Gulf. *In*: Selley, R., Cocks, R. and Plimer, I. (eds), *Encyclopaedia of Geology*, Elsevier, Special Publication, 141–152.

Al-saad, H. 2008. Stratigraphic distribution of the Middle Jurassic foraminifera in the Middle East. *Revue de Paléobiologie, Genève* **27** (1), 1-13.

Alsharhan, A.S. and Nairn, A.E. 1986. A review of the Cretaceous formations In the Arabian Peninsula and Gulf: part I. Lower Cretaceous (Thamama Group) stratigraphy and paleogeography*. Journal of Petroleum Geology*, **9**(4), 365–391.

Alsharhan, A. S., and Nairn, A. E. M. 1988. A Review of the Ctretaceous Formations in the Arabian Peninsula and Gulf: Part ii. Mid-Cretaceous (Wasia Group) Stratigraphy and Paleogeography. *Journal of Petroleum Geology*, **11** (1), 89-112.

Alsharhan, A.S. and Nairn, A.E.M. 1993. Carbonate platform models of Arabian Cretaceous reservoirs. In: Simo, J.A.T., Scott, R.W. and Masse, J.-P. (eds), *Cretaceous carbonate platforms*, American Association of petroleum Geologists, Memoir **56**, 173–184.

Alsharhan, A.S. and Nairn, A.E. 1997. *Sedimentary basins and petroleum geology of the Middle East.* Elsevier, Amsterdam, New York, Oxford, 843pp.

Alsharhan, A.S. and Whittle, G.L. 1995. Carbonate-evaporite sequences of the Late Jurassic, southern and southwestern Arabian Gulf. *American Association of Petroleum Geologists, Bulletin*, **79**(11), 1608–1630.

Altiner, D. 1991, Microfossil biostratigraphy (mainly foraminifers) on the Jurassic-Lower Cretaceous carbonate successions in north-western Anatolia (Turkey). *Geologica Romana*, **27**, 167–213.

Andreini, G., Caracuel, J.E. and Parisi, G. 2007. Calpionellid biostratigraphy of the upper Tithonian–upper Valanginian interval in Western Sicily (Italy). *Swiss Journal of Geosciences*, **100**(2), 179–198.

Arnaud-Vanneau, A. 1980. Micropaléontologie et sédimentologie d'une platforms carbonatée de la marge passive de la Téhys : l'Urgonien du Vercors septentrional et de la Chartreuse (Alpes Occidentales). *Géologie Alpine, Mémoire*, **11**, 874pp.

Arnaud-Vanneau, A., Boisseau, T. and Darsac, C. 1988. Le genre *Trocholina* Paalzow 1922 et ses principales espèces au Crétacé. *Revue de Paléobiologie, Genéve*, **2**(6), 353–377.

Arnaud-Vanneau, A. and Peybernès, B. 1978. Les représentants éocrétacé du Genre *Nautiloculina* Mohler, 1938 (Foraminifera, Fam. Lituolidae ?) dans les châines subalpines septentrionales (Vercors) et les Pyrénées Franco-Espagnoles. Révision de *Nautiloculina cretacea* Peybernès, 1976 et description de *Nautiloculina bronnimanni* sp. *Geobios*, **11**(1), 67–81.

Arnaud-Vanneau, A. and Premoli Silva, I. 1995. Biostratigraphy and systematic description of benthic foraminifers from mid-Cretaceous shallow-water carbonate platform sediments at Sites 878 and 879 (Mit and Takuyo-Daisan Guyots). *In*: Haggerty. J.A., Premoli Silva, I., Rack, F. and McNutt, M K. (eds), *Proceedings of the Ocean Drilling Program, Scientific Results, College Station, TX*, **144**, 199–219.

D'Argenio, B., Ferreri, V., Raspini, A., Amodio, S. and Buonocunto, F.P. 1999. Cyclostratigraphy of a carbonate platform as a tool for high-precision correlation. *Tectonophysics*, **315**(1), 357–384.

Athersuch, J., Banner, F.T. and Simmons, M.D. 1992. On *Trochamijiella gollesstanehi*, gen. nov. et sp. nov. (Foraminiferida, Loftusiacea), an index for the Middle Eastern marine Late Bathonian. *Journal of Micropalaeontology*, **11**(1), 7–12.

Bachmann, M. and Hirsch, F. 2006. Lower Cretaceous carbonate platform of the eastern Levant (Galilee and the Golan Heights): stratigraphy and second-order sea-level change. *Cretaceous Research*, **27**(4), 487–512.

Banner, F.T. and Desai, D. 1988. A review and revision of the Jurassic-Early Cretaceous Globigerinina, with especial reference to the Aptian assemblages of Speeton (North Yorkshire, England). *Journal of Micropalaeontology*, **7**(2), 143–185.

Banner, FT., Gillmore, G.K., Highton, J. and Whittaker, J.E. 1991. *Mesozoic Foraminifera from the Middle East at the Natural History Museum, London*. British Museum (Natural History), London, 30pp., 300pls.

Banner, F.T., Simmons, M.D. and Whittaker, J.E. 1991. The Mesozoic Chrysalinidae (Foraminifera, Textulariacea) of the Middle East: the Redmond (Aramco) taxa and their relatives. *Bulletin of the British Museum (Natural History), Geology Series*, **42**(2), 101–152.

Banner, F.T. and Whittaker, J.E. 1991. Redmond's new lituolid foraminifera from the Mesozoic of Saudi Arabia. *Micropaleontology*, **37**, 41–59.

Barbu, V. 2005. Lower cretaceous small benthic foraminifera from the Bucegi Mountains (South Carpathians) - paleoecologic implications. *Proceedings of the Romanian Academy, Series B, Chemistry Life Sciences and Geosciences*, **7**(1), 29–36.

Basson, P.W. and Edgell, H.S. 1971. Calcareous algae from the Jurassic and Cretaceous of Lebanon. *Micropaleontology*, **17**(4), 411–433.

Baum, G.R. and Vail, P.R. 1998. A new foundation for stratigraphy. *Geotimes*, **43**(11), 31–35.

Benzaggagh, M., Cecca, F., Schnyder, J., Seyed-Emami, K. and Majidifard, M.R. 2012. Calpionelles et microfaunes pélagiques du Jurassique supérieur–Crétacé inférieur dans les Formations Shal et Kolur (Montagnes du Talesh, chaîne de l'Elbourz, Nord-Ouest Iran). Répartition stratigraphique, espèces nouvelles, révision systématique et comparaisons régionales. *Annales de Paléontologie*, **98**(4), 253–301.

Beydoun, Z.R. 1964. The stratigraphy and structure of the eastern Aden Protectorate. *Overseas Geological Mining Resources Supplement*, **5**, HMSO, London, 107pp.

Beydoun, Z. R. 1988. *The Middle East: Regional geology and petroleum resources*. Beaconsfield, Bucks, U. K., Scientific Press Ltd., 291pp.

Beydoun, Z. R. 1991. Arabian plate hydrocarbon geology and potential - a plate tectonic approach. *American Association of Petroleum Geologists, Studies in Geology*, **33**, 77pp.

Bolli, H.M., Saunders, J.B. and Perch-Nielsen, K. (eds).1989. *Plankton Stratigraphy: Volume 1, Planktonic foraminifera, calcareous nannofossils and calpionellids*. Cambridge, Cambridge University Press, 599 pp.

Boudagher-Fadel, M.K., Banner, F.T., Whittaker, J.E. and Simmons, M.D. 1997. *The Early Evolutionary History of Planktonic Foraminifera*. British Micropalaeontological Society Publications Series, London, Chapman and Hall, 269pp.

BouDagher-Fadel, M.K. 2008. *Evolution and Geological Significance of Larger Benthic Foraminifera*. Elsevier, Amsterdam, 544pp.

Bramkamp, R. and Barger, T. 1938. Unpublished Aramco report, *In*: Powers *et al.* (eds.), *Sedimentary Geology of Saudi Arabia*, 1966, D74.

Brönnimann, P. and Zaninetti, L. 1966. Troisième note sur les foraminifères du Crétacé inférieur de la région genevoise: remarques stratigraphiques et description de *'Pseudotextulariella salevensis',* n. sp.; *'Haplophragmoides joukowskyi'* n. sp.; *'Citaella? favrei'* n. sp. *Archives des Sciences*, **19**(1), 23pp.

Brönnimann, P. 1976. Revision of the lectotype of *Favreina salevensis* (Paréjas) (Crustacea, Decapoda) and description of favreine form-species from the Jurassic and Cretaceous of Scotland, Portugal, Yugoslavia and Pakistan. *Paläontologische Zeitschrift*, **50**(1-2), 40–56.

Bruni, R., Bucur, I.I. and Preat, A. 2007. Uppermost Jurassic–Lower Cretaceous carbonate deposits from Fara San Martino (Maiella, Italy): biostratigraphic remarks. *Studia Universitatis Babes– Bolyai, Geologia*, **52**(2), 45–54.

Bucur, I.I. 1988. Les foraminifères du Crétacé inférieur (Berriasian-Hauterivian) de la zone de Reşiţa-Moldova Nouă (Carpathes Méridionales, Roumanie). Remarques biostratigraphiques. *Revue de Paléobiologie, Genéve*, Special Volume **2,** Benthos ‘86, 379–389.

Bucur, I.I. 1993. Representatives of the genus *Protopeneroplis* Weynschenk from the Lower Cretaceous deposits in the Reşiţa-Moldova Nouă Zone (Southern Carpathians, Romania). *Revue de Micropaléontologie*, **36**, 213–223.

Bucur, I.I. 1997, Representatives of the genus *Protopeneroplis* (Foraminifera) in the Jurassic and Lower Cretaceous Deposits in Romania. Comparisons with other Regions of the Tethyan Area. *Acta Palaeontologica Romaniae*, **1**, 65–71.

Bucur, I.I. 2000. Lower Cretaceous dasyclad algae from the Padurea Craiului Massif (northern Apuseni Mountains, Romania). *Acta Palaeontologica Romaniae*, **2**, 53–72.

Bucur, I.I. 2011. Early Barremian dasycladalean algae from Serre de Bleyton (Drôme, SE France). *Annalen des Naturhistorischen Museums in Wien. Serie A für Mineralogie und Petrographie, Geologie und Paläontologie, Anthropologie und Prähistorie*, 619–653.

Bucur, I.I. and Onac, P.B. 2000. New data concerning the age of the Mesozoic limestones from Scărişoara (Bihor Mountains). *Studia Universitatis Babeş-Bolyai, Geologia*, **45**(2), 13–20.

Bucur, I.I. and Săsăran, E. 2005a. Relationship between algae and environment: an Early Cretaceous case study, Trascău Mountains, Romania*. Facies*, **51**(1-4), 275–287.

Bucur, I.I. and Săsăran, E. 2005b. Micropaleontological assemblages from the Upper Jurassic- Lower Cretaceous deposits of Trascău Mountains and their biostratigraphic significance. *Acta Palaeontologica Romaniae*, **5**, 27–38.

Bucur, I.I. and Săsăran, E. (eds). 2011. *Calcareous Algae from Romanian Carpathians*. Field Trip Guidebook of the 10th International Symposium on Fossil Algae, Cluj University Press, Cluj-Napoca, Romania, 137pp.

Bucur, I.I., Conrad, M.A., and Radoičić, R. 1995. Foraminifers and calcareous algae from Valanginian limestones in the Jerma River Canyon, Eastern Serbia. *Revue de Paléobiologie, Genéve*, **14**(2), 349–377.

Bucur, I.I., Grădinaru, E., Lazăr, I. and Grădinaru, M. 2014. Early Cretaceous micropaleontological assemblages from a condensed section of the Codlea area (Southern Carpathians, Romania). *Acta Palaeontologica Romaniae*, **9**, 67–84.

Bucur, I.I., Granier, B. and Krajewski, M. 2014a. Calcareous algae, microbial structures and microproblematica from Upper Jurassic-lowermost Cretaceous limestones of southern Crimea. *Acta Palaeontologica Romaniae*, **10**(1-2), 61–86.

Bucur, I.I., Hoffmann, M. and Kolodziej, B. 2005. Upper Jurassic-Lowermost Cretaceous benthic algae from Tethys and the European platform: a case study from Poland. *Revista Española Micropaleontologia*, **37**, 105–129.

Bucur, I.I., Majidifard, M.R. and Senowbari-Daryan, B. 2013. Early Cretaceous Calcareous Benthic Microfossils from the Eastern Alborz and Western Kopet Dagh (Northern Iran) and their stratigraphic significance. *Acta Palaeontologica Romaniae*, **9**(1), 23–37.

Bucur, I.I., Piteiu, M.-A., and Săsăran, E. 2004. The Mesozoic carbonate deposits from the borehole 6042 Deleni (Transylvanian Depression). *Studia UBB* Geologia, **49**(2), 27–48.

Bucur, I.I., Săsăran, L., Săsăran, E., and Schuller, V. 2004. Micropaleontological Study of the Limestone Olistoliths within the Upper. *Acta Palaeontologica Romaniae,* **4**(1), 55–67.

Bucur, I.I., Săsăran, E., Balica, C., Beles, D., Bruchental, C., Chendes, C., Chendes, O., Hosu, A., Lazar, D., Lapadat, A., Vlad Marian, A., Mircescu, C., Turi, V. and Ungureanu, R. 2010. *Mesozoic carbonate deposits from some areas of the Romanian Carpathians- case studies*. Cluj University Press, Cluj-Napoca, Romania, 203pp.

Bucur, I., Senowbari-Daryan, B. and Abate, B. 1996. Remarks on some Foraminifera from the Upper Jurassic (Tithonian) reef limestone of Madonie Mountins (Sicily). *Bollettino della Società Paleontologica Italiana*, **35**(1), 65–80.

Burchfiel, H. L. and Hoover, J. W. 1935. Unpublished Aramco report, *In*: Powers *et al.* (eds.), *Sedimentary Geology of Saudi Arabia*, 1966, D74.

Carras, N., Conrad, M.A. and Radoičić, R. 2006. *Salpingoporella*, a common genus of Mesozoic Dasycladales (calcareous green algae). *Revue de Paléobiologie, Genéve*, **25**(2), 457–517.

Carter, D. J., and Hart, M. B. 1977. Micropalaeontological investigations for the site of the Thames Barrier, London. *Quarterly Journal of Engineering Geology and Hydrogeology*, **10** (3), 321-337.

Catuneanu, O., Abreu, V., Bhattacharya, J.P. Blum, M.D., Dalrymple, R.W., Eriksson, P. G., Fielding, C.R., Fisher, W.L., Galloway, W.E., Gibling, M.R., Giles, K.A., Holbrook, J.M., Jordan, R., Kendall, C.G.St.C., Macurda, B., Martinsen, O.J., Miall, A.D., Neal, J.E., Nummendal, D., Pomar, L., Posamentier, H.W. *et al*. 2009. Towards the standardization of sequence stratigraphy. *Earth-Science Reviews*, **92**(1), 1–33.

Catuneanu, O., Bhattacharya, J. P., Blum, M. D., Dalrymple, R. W., Eriksson, P. G., Fielding, C. R., *et al*. 2010. Thematic Set: Sequence stratigraphy: common ground after three decades of development. *First Break*, **28**(1), 41–54.

Charollais, J., Brönnimann, P. and Zaninetti, L. 1966. Troisième note sur les foraminifères du Crétacé inférieur de la région genevoise. Remarques stratigraphiques et description de *Pseudotextulariella salevensis* n. sp.; *Haplophragmoides joukowskyi* n. sp.; *Citaella? favrei* n. sp. *Archives des Sciences, Genéve,***19**(1), 23–48.

Chen, D. and Tucker, M.E. 2003. The Frasnian–Famennian mass extinction: insights from high-resolution sequence stratigraphy and cyclostratigraphy in South China. *Palaeogeography, Palaeoclimatology, Palaeoecology*, **193**(1), 87–111.

Chiocchini, M.P. and Mancinelli, A. 1978. Ricerche geologiche sul Mesozoica del Gran Sasso d'Italia (Abruzzo) lll. Corelazioni microbiostratigrafiche tra

facies di margine della piattaforma carbonatica e facies pelagiche del Giurasico e Cretacico inferire. *Studi Geologici Camerti*, **IV**, 19–36.

Chiocchini, M., Farinacci, A., Mancinelli, A., Molinari, V. and Potetti, M. 1994. Biostratigrafia a foraminiferi, dasicladali e calpionelle delle succesioni carbonatiche mesozoiche dell'Appenino centrale (Italia). *Studi Geologici Camerti, Vol. Spec*. "Biostratigrafia dell'Italia centrale", 9–128.

Choquette, P. W., and Pray, L. C. 1970. Geologic nomenclature and classification of porosity in sedimentary carbonates. *American Association of Petroleum Geologists, Bulletin*, **54** (2), 207-250.

Christian, L. 1997. Cretaceous subsurface geology of the Middle East Region. *GeoArabia*, **2**(3), 239–256.

Clark, G.N. and Boudagher-Fadel, M.K. 2001. The larger benthic foraminifera and stratigraphy of the Upper Jurassic/Lower Cretaceous of Central Lebanon. *Revue de Micropaléontologie*, **44**(3), 215–232.

Colombié, C. and Strasser, A. 2005. Facies, cycles, and controls on the evolution of a keep-up carbonate platform (Kimmeridgian, Swiss Jura). *Sedimentology*, **52**(6), 1207–1227.

Conrad, M.A., Praturlon, A. and Radoičić, R. 1974. *The genus Actinoporella* Guembel in Alth 1882, Dasycladales, green algae. A revision. *Geologica Romana*, **13**, 1–15.

Conrad, M.A. and Peybernès, B.1976. Hauterivian-Albian Dasycladaceae from the Urgonian limestones in the French and Spanish Eastern Pyrenées. *Geologica Romana*, **15**, 175–197.

Crescenti, U. 1969. Biostratigrafi a delle facies mesozoiche dell' Appennino centrale. Corelazioni. *Geologiga Rom*ana, **8**, 15–40.

Cushman, J.A. 1927. An Outline of the Re-Classification of the Foraminifera. *Contributions from the Cushman Laboratory for Foraminiferal Research*, **3**, 1–105.

Cushman, J.A. 1947. *Foraminifera, their Classification and Economic use* [3rd Edition]. Harvard University Press, Cambridge, MA, 535pp.

Cushman, J. A., and Alexander, C. I. 1930. Some Vaginulinas and other foraminifera from the Lower Cretaceous of Texas. *Contributions from the Cushman Laboratory for Foraminiferal Research*, **6** (8), 1-8.

Cushman, J.A. and Glazewski, K. 1949. Upper Jurassic Foraminifera from the Nizniow Limestone of Podole, Poland. *Contributions to the Cushman Laboratory for Foraminiferal Research*, **25**(1), 1–24.

Dercourt, J., *et al*. 2000. *Peri-Tethys Atlas*. Paleogeographical Maps. Gauthier-Villars, Paris.

Desai, D. and Banner, F.T. 1987. The evolution of Early Cretaceous Dorothiinae (Foraminiferida). *Journal of Micropalaeontology*, **6**,13–27.

Dessauvagie, T. F. J. 1963. On the occurrence of *Neotrocholina* in Turkey. *Bulletin of the Mineral Research and Exploration Institute of Turkey,* **60**, 71–75.

Dragastan, O. 1999. Jurassic-Cretaceous calcareous algae of the Transylvanides, Inner Dacised and Moesian Platform (Romania). *Revista Española de Micropaleontología*, **31**(2), 185–218.

Dragastan, O. 2011. Early Cretaceous foraminifera, algal Nodules and calpionellids from the Lapoş Valley, Bicaz Gorges (Eastern Carpathians, Romania). *Analele Stiintifice ale Universitatii "Al. I. Cuza" din Iasi Seria Geologie,* **57** (1), 91–113.

Dragastan, O.N., Antoniade, C. and Stoica, M. 2014. Biostratigraphy and Zonation of the Lower Cretaceous Carbonate Succession from Cernavoda-Lock Section, South Dobrogea, Eastern Part of the Moesian Platform (Romania). *Carpathian Journal of Earth and Environmental Sciences*, **9**(1), 231–260.

Dunham, R. J., 1962, Classification of Carbonate rocks according to their depositional texture. *In*: Ham, W.E. (Ed.), *Classification of Carbonate Rocks*, *A Symposium*, American Association of Petroleum Geologists,Tulsa, OK, 108–121.

Dunnington, H.V., Wetzel, R. and Morton, D.M. 1959. Mesozoic and Palaeozoic. *Asie, Fasc. 110a, Lexique stratigraphique international, 3 Iraq. Centre National de Recherches Scientifique, Paris*, 1–333.

Dupeuble, P., Boillot, G. and Mougenot, D.1987. Upper Jurassic–Lowest Cretaceous Limestones dredged From the Western Galicia Margin. *In*: Boillot, G., Winterer, E.L., Meyer, A.W., *et al*., *Proceedings of the Ocean Drilling Program*, *Initial Reports, College Station, TX,***103**, 99–105.

Egger, J.G. 1902. Foraminiferen und Ostakoden aus den Kreidemergeln der oberbayerischen Alpen. *Abhandlungen der Königlichen bayerischen Akademie der Wissenschaften zu München, Mathematische-Naturwissenschaftlische Klasse*, **21**, 3–230.

El-Azabi, M.H. and A. El-Araby 1996. Depositional facies and palaeoenvironments of the Albian Cenomanian sediments in Gabal El-Minshera, north central Sinai, *Egypt. Geological Society of Egypt*, *Special Publication*, **2**, 151–198.

El-Azabi, M. H. and El-Araby, A. 2007. Depositional framework and sequence stratigraphic aspects of the Coniacian–Santonian mixed siliciclastic/carbonate Matulla sediments in Nezzazat and Ekma blocks, Gulf of Suez, Egypt. *Journal of African Earth Sciences*, **47**(4), 179–202.

Edgell, H.S. 1992. Basement tectonics of Saudi Arabia as related to oil field structures. *In*: Rickard, M.H. *et al*. (eds), *Basement tectonics*, Kluwer Academic Publishers, Dordrecht, The Netherlands, **9**, 169–193.

Elliott, G.F. 1957. New calcareous algae from the Arabian Peninsula. *Micropaleontology*, **3**(3), 227–230.

Elliott, G.F. 1959. Fossil calcareous algal floras of the Middle East with a note on a Cretaceous problematicum, *Hensonella cylindrica* gen. et sp. nov. *Quarterly Journal of the Geological Society, London*, **115**(1-4), 217–232.

Elliott, G.F. 1968. Permian to Palaeocene calcareous algae (Dasycladaceae) of the Middle East. *Bulletin of the British Museum, Natural History (Geology), Supplement* **4**, 101pp.

Embry III, A. F., and Klovan, J. E. 1971. A Late Devonian reef tract on northeastern Banks Island, NWT. *Bulletin of Canadian Petroleum Geology*,**19** (4), 730-781.

Emery, D. and Myers, K.J. 1996. *Sequence Stratigraphy*. Oxford, Blackwell Science, 297pp.

Flügel, E. 1982. *Microfacies Analysis of Limestones*. Springer-Verlag, Heidelberg and Berlin, 633pp

Flügel, E. 2004. *Microfacies of Carbonate Rocks. Analysis, Interpretation and Application*. Springer-Verlag, Heidelberg and Berlin, 976pp.

Folk, R. L. 1959. Practical petrographic classification of limestones. *AAPG Bulletin*, **43** (1), 1-38.

Galloway, W.E. 1989. Genetic stratigraphic sequences in basin analysis. 1. Architecture and genesis of flooding-surface bounded depositional units. *American Association of Petroleum Geologists, Bulletin*, **73**, 125–142.

Glaessner, M.F. 1945. *Principles of Micropalaeontology*. Melbourne University Press and Oxford University Press, Oxford, xvi + 296pp.

Gorbatchik, T. 1986. *Jurassic and Early Cretaceous Planktonic Foraminifera of the Southern SSSR*. Akademia Nauk SSSR, 'Nauka', Moscow [in Russian], 239pp.

Gorbatchik, T.N. and Mohamad, G.K. 1997. New species of Lituolida (Foraminifera) from the Tithonian and Berriasian of the Crimea. *Paleontological Journal*, **4**, 3–9.

Görög, Á. and Wernli, R. 2003. Palaeobiogeography of the middle Jurassic protoglobigerinids. *Eclogae Geologica Helvetiae*, **96**, 237–248.

Görög, Á. and Wernli, R. 2013. Protoglobigerinids of the Early Kimmeridgian of the Jura Mountains (France). *Journal of Foraminiferal Research*, **43**(3), 280–290.

Grabowski, C.G., Jr., and Norton, I.O. 1995. Tectonic controls on the stratigraphic architecture and hydrocarbon systems of the Arabian Plate, *In:*

Al-Husseini, M.I., (Ed.), *Geo-94, Middle East Petroleum Geosciences Conference*: Gulf Petrolink, Manama, Bahrain, **1**, 413–430.

Gradstein, F.M. 1978. Jurassic Grand Banks foraminifera. *Journal of Foraminiferal Research,* **8**(2), 97–109.

Granier, B. and Brun, R. 1991. *Cylindroporella cruciformis* et *Holosporella arabica*, deux Dasycladace'es nouvelles du Groupe Thamama, (?Portlandien-) Berriasien-Aptien d'Abu Dhabi, Emirats Arabes Unis. *Cretaceous Research*, **12**(4), 403–410.

Granier, B. and Busnardo, R. 2013. New stratigraphic data on the Aptian of the Persian Gulf. *Cretaceous Research*, **39,** 170–182.

Gray, D.R., Gregory, R.T. and Miller, J.M. 2005. Comment on "Structural evolution, metamorphism and restoration of the Arabian continental margin, Saih Hatat region, Oman Mountains" by Searle, M.P., *et al., Journal of Structural Geology*, **27** (2), 371–374.

Greig, D.A. 1958. Oil Horizons in the Middle East. *In*: Weeks, L.G. (Ed.) *Habitat of Oil: a Symposium conducted by the American Association of Petroleum Geologists*, Tulsa, U.S.A. 1182–1193.

Grigelis, A. A., and Gorbatchik, T.N. 1980. The Systematics of Jurassic and Early Cretaceous Globigerinacea. Translated from "K sistematike yurskikh I rannemelovykh Globigerinacea". *Paleontolgical Journal,*1980, **1**, 20–30.

Haq, B.U., Hardenbol, J. and Vail, P.R. 1988. Mesozoic and Cenozoic chronostratigraphy and cycles of sea-level change. *In*: Wilgus, C.K., Hastings, B.S., Kendall, C.G.StC., Posamentier, H.W., Ross, C.A. and Van Wagoner, J.C. (eds), *Sea-Level Changes: An Integrated Approach*, Society of Economic Paleontologists and Mineralogists, Tulsa, OK, Special Publication, **42**, 71–108.

Haq, B.U. and Boersma, A. 1998. *Introduction to marine micropaleontology*. Elsevier, New York, Amsterdam, Oxford, 376 pp.

Haq B. U. and Al-Qahtani, M. 2005. Phanerozoic cycles of sea-level change on the Arabian Plate. *GeoArabia*, **10**(2), 127–160.

Haq, B. U. 2014. Cretaceous eustasy revisited. *Global and Planetary Change*, **113**, 44-58.

Hariri, Mustafa M. 2003. Sedimentary Strata, Part 2 of Regional Geology (GEOL–318). *Power point lecture from King Fahd University for Petroleum and Minerals, Earth Sciences Department. Saudi Arabia*.

Hart, M.B. 1991. The Late Cenomanian calcisphere global bioevent. *Proceedings of the Ussher Society*, **7**(4), 413–417.

Hart, M.B., Hudson, W., Smart, C.W. and Tyszka, J. 2012. A reassessment of ‘Globigerina bathoniana’ Pazdrowa, 1969 and the palaeoceanographic

significance of Jurassic planktic foraminifera from southern Poland. *Journal of Micropalaeontology*, **31**(2), 97–109.

Haas, J. 1999. Genesis of Late Cretaceous toe-of-slope breccias in the Bakony Mts, Hungary. *Sedimentary Geology*, **128**(1), 51–66.

Haas, J., Görög, Á., Kovács, S., Ozsvárt, P., Matyók, I. and Pelikán, P. 2006. Displaced Jurassic foreslope and basin deposits of Dinaridic origin in Northeast Hungary. *Acta Geologica Hungarica*, **49**(2), 125–163.

Haynes, J.R. 1981. *Foraminifera*. Palgrave Macmillan UK, Oxford, 467pp.

Haynes, J.R., 1990. The classification of the foraminifera-a review of historical and philosophical perspectives. *Palaeontology*, **33**(3), 503–528.

Henson, F.R.S. 1948. Larger imperforate foraminifera of south-western Asia. Families Lituolidae, Orbitolinidae and Meandropsinidae. *British Museum (Natural History)*, *London*, 126pp.

Henson, R. S. 1951. Observations on the geology and petroleum occurrences in the Middle East. *In*: *Proceedings of the 3rd World Petroleum Congress*, The Hague, Vol. 1,118–140.

Hinnov, L.A. 2000. New perspectives on orbitally forced stratigraphy. *Annual Review of Earth and Planetary Sciences*, **28**, 419–475.

Hosseini, S.A. and Conrad, M.A. 2008. Calcareous algae, foraminifera and sequence stratigraphy of the Fahliyan Formation at Kuh-e-Surmeh (Zagros Basin, SW of Iran). *Geologia Croatica*, **61**(2-3), 215–237.

Hottinger, L. 1967. Foraminifères imperforés du Mésozoïque marocain. *Mémoires Service Géologique du Maroc (Rabat)*, **209**, 1–129.

Hudson, R.G.S. 1953. LVII.–The systematic position of the Mesozoic stromatoporoid *Cladocoropsis* Felix, 1907. *Annals and Magazine of Natural History: Series 12*, **6**(68), 615–619.

Hudson, R.G.S. 1954. Jurassic stromatoporoids from the Lebanon. *Journal of Paleontology*, **28**(5), 657–661.

Hughes, G. 2000. Bioecostratigraphy of the Shu'aiba Formation, Shaybah field, Saudi Arabia. *GeoArabia*, **5**(4), 545–578.

Hughes, G. 2008. Biofacies and palaeoenvironments of the Jurassic Shaqra Group of Saudi Arabia. *Volumina Jurassica*, **6**(1), 33–45.

Hughes, G. 2009. Using Jurassic Micropaleontology to Determine Saudi Arabian Carbonate Paleoenvironments*. In*: Demchuk, T.D. and Gary, A.C. (eds), *Geologic Problem solving with Microfossils.* SEPM, Special Publication, **93**, 127–152.

Hughes, G. 2013. Late Permian to Late Jurassic “microproblematica” of Saudi Arabia: Possible palaeobiological assignments and roles in the palaeoenviromental reconstructions*. GeoArabia*, **1**, 57–92.

Hughes, G. and Naji, N. 2008. Sedimentological and micropalaeontological evidence to elucidate post-evaporitic carbonate palaeoenvironments of the Saudi Arabian. *Volumina Jurassica***, 6**(1), 61–73.

Hughes, G., Al-khaled, M. and Varol, O. 2008a. Oxfordian biofacies and palaeoenvironments. *Volumina Jurassica*, **6**(1), 47–60.

Hughes, G., Varol, O. and Al-khalid, M. 2008b. Late Oxfordian Micropalaeontology , nannopalaeontology and palaeoenvironments of Saudi Arabia. *GeoArabia*, **13**(2), 15–46.

Hughes, G. W., Al-Khaled, M and Varol, O. 2009. Oxfordian biofacies and palaeoenvironments of Saudi Arabia. *Volumina Jurassica*, **6**(4), 47–60.

Husinec, A. and Sokač, B. 2006. Early Cretaceous benthic associations (foraminifera and calcareous algae) of a shallow tropical-water platform environment (Mljet Island, southern Croatia). *Cretaceous Research*, **27**(3), 418–441.

Ivanova, D. and Kołodziej, B., 2004. New foraminiferal data on the age of Stramberk-type limestones, Polish Carpathians. *Comptes rendus de l’ Académie bulgare des Sciences*, **57**, 69–74.

Ivanova , D. Kolodziej, B., Koleva- Rekalova, E. and Roniewicz, E. 2008. Oxfordian evolution on the western Moesian Carbonate Platform: a case study from SW Bulgaria. *Annales Societatis Poloniae*, **78**, 65–90.

Ivanova, D. and Kołodziej, B. 2010. Late Jurassic-Early Cretaceous Foraminifera from Štramberk-type Limestones, Polish Outer Carpathians. *Studia Universitatis Babes-Bolyai, Geologia*, **55**(2), 3–31.

Ivanova, D. and Kolodziej, B. 2010. Late Jurassic–Early Cretaceous foraminifera from Štramberk-type limestones, Polish outer Carpathians.*Studia UBB Geologia*, **55**(2), 3-31.

Kaminski, M. A., Gradstein, F. M., and Geroch, S. 1992. Uppermost Jurassic to Lower Cretaceous benthic foraminiferal biostratigraphy at ODP Site 765 on the Argo Abyssal Plain. *In*: Gradstein, F.M., Ludden, J.N., *et al*. (eds), *Proceedings of the Ocean Drilling Program: Scientific Results, College Station, TX*, **123**, 239–269.

Kaminski, M. A. 2000. The New and Reinstated Genera of Agglutinated Foraminifera published between 1986 and 1996. *In*: Hart, M.B., Kaminski, M.A. and Smart, C.W. (eds), *Proceedings of the Fifth International Workshop on Agglutinated Foraminifera,* Grzybowski Foundation, Special Publication, **7**, 185–219.

Kaminski, M. A. 2004. The Year 2000 Classification of the Agglutinated Foraminifera. *In:* Bubik, M. and Kaminski, M.A. (eds), *Proceedings of the*

Sixth International Workshop on Agglutinated Foraminifera, Grzybowski Foundation, Special Publication, **8** 237–255.

Kaminski, M.A., Setoyama, E. and Cetean, C.G. 2008. Revised Stratigraphic Ranges and the Phanerozoic Diversity of Agglutinated Foraminiferal Genera. Romania. *In*: *Proceedings of the Seventh International Workshop on Agglutinated Foraminifera*, Grzybowski Foundation, Special Publication, **13**, 79–106.

Kano, A., Kakizaki, Y., Takashima, C., Wang, W. and Matsumoto, R. 2007. Facies and depositional environment of the uppermost Jurassic stromatoporoid biostromes in the Zagros Mountains of Iran. *GFF (The Geological Society of Sweden)*, **129**(2), 107–112.

Kassler, P. 1973. The structural and geomorphic evolution of the Persian Gulf. *In*: Purser, B.H. (Ed.), *The Persian Gulf. Holocene carbonate sedimentation and diagenesis in a shallow epicontinental sea,* Springer, New York, Heidelberg and Berlin, 11–32.

Katz, M.E., Browning, J.V., Miller, K.G., Monteverde, D.H., Mountain, G.S., and Williams, R.H. 2013. Paleobathymetry and sequence stratigraphic interpretations from benthic foraminifera: Insights on New Jersey shelf architecture, IODP Expedition 313. *Geosphere*, **9**(6), 1488–1513.

Kauffman, E.G. and Hart, M.B.1996. Cretaceous bio-events. *In*: Walliser, O (Ed.), *Global events and event stratigraphy in the Phanerozoic*, Springer, Berlin and Heidelberg, 285–312.

Kaźmierczak, J. 1976. Cyanophycean nature of stromatoporoids. *Nature,* **264**, 49–51.

Kendall, G.StC., Bowen, B., Alsharhan, A., Cheong, D.-K. and Stoudt, D. 1991. Eustatic controls on carbonate facies in reservoirs, and seals associated with Mesozoic hydrocarbon fields of the Arabian Gulf and the Gulf of Mexico. *Marine Geology*, **102**, 215–238.

Kendall, G.StC., Alsharhan, A. and Marlow, L. 2010. Regional stratigraphy of the Southern Tethyan margin, lithofacies, sequence stratigraphy, source, seal and reservoir rocks. *Search and Discovery Article #10273, Adapted from oral presentation at AAPG Annual Convention, New Orleans, Louisiana, April 11-14, 2010*.

Keupp, H. 1978. Calcisphaeren des Untertithon der sudlichen Frankenalbund die systematische Stellung von *Pithonella* Lorenz 1901. *Neues Jahrbuch für Geologie und Palaontologie, Monatshefte,* **2***,* 87–98.

Keupp H., 1979. Lower Cretaceous Calcisphaerulidae and their relationship to calcareous dinoflagellate cysts. *Bulletin des Centres de Recherches Exploration-Production, Elf-Aquitaine*,**3**(2), 651–663.

Kietzmann, D. A.and Palma, R. M. 2010. New crustacean microcoprolites from the Lower Cretaceous (middle Berriasian–lower Valanginian) of the Neuquén Basin, southern Mendoza, Argentina. *Journal of South American Earth Sciences*, **30**(1), 58–64.

King, C., Bailey, H. W., Burton, C. and King, A. D. 1989. Cretaceous of the North Sea. *In*: Jenkins, D. G. and Murray J. W., *Stratigraphical Atlas of Fossil Foraminifera* [2nd edition], British Micropalaeontological Society Series, Ellis Horwood Ltd, Chichester, 372–417.

Kirby, R. H., Carr, B. S., Al-humoud, J., Safar, A. I., Al-Matar, D., and Naser, W. 1998. Characterization of a Vertically Compartmentalized Reservoir in a Supergiant Field, Burgan Formation, Greater Burgan Field, Kuwait; Part 1: Stratigraphy and Water Encroachment. In *SPE Annual Technical Conference and Exhibition,* New Orleans, Louisiana, 509-516.

Kobayashi, F. and Vuks, V.J. 2006. Tithonian–Berriasian foraminiferal faunas from the Torinosu-type calcareous blocks of the southern Kanto Mountains, Japan: their implications for post-accretionary tectonics of Jurassic to Cretaceous terranes. *Geobios*, **39**(6), 833–843.

Kolodzieg, B. 1997. Boring Foraminifera from Exotics of the Stramberk-Type Limestones (Tithonian- Lower Berriasian, Polish Carpathians). *Annales Societatis Geologrum Poloniae*, **67**, 249–256.

Konert, G., Afifi, A.M., Al-Hajri, S.A., and Droste, H.J. 2001, Palaeozoic stratigraphy and hydrocarbon habitat of the Arabian Plate. *GeoArabia*, **6**, 407–442.

Koutsoukos, E.A. and Hart, M.B. 1990. Cretaceous foraminiferal morphogroup distribution patterns, palaeocommunities and trophic structures: a case study from the Sergipe Basin, Brazil. *Transactions of the Royal Society of Edinburgh: Earth Sciences*, **81**(3), 221–246.

Kowal, J., Olszewska, B., and Cieszkowski, M. 2011. Uppermost Jurassic–Lower Cretaceous exotic limestones with algae from the Silesian Nappe, Polish Outer Carpathians (Żegocina, Olszyny and Lanckorona area). *In*: *10th International Symposium on Fossil Algae Cluj-Napoca, Romania, 12–18 September,* 2011, 43 [abstract].

Kowal-Kasprzyk, J. 2014. North-Tethyan Tithonian chitinoidellids from exotic limestone pebbles in the Silesian Nappe (Polish Outer Carpathians). *Geologica Carpathica*, **65**(1), 25–34.

Krajewski, M., 2008. Lithology of the Upper Jurassic-Lower Cretaceous (Tithonian-Lower Berriasian) Ay-Petri reef complex (southern Ukraine, the Crimea Mountains). *Neues Jahrbuch für Geologie und Paläontologie*, **5**, 298–312.

Krajewski, M., 2010. Facies, microfacies and development of the Upper Jurassic-Lower Creataceous of the Crimean carbonate platform from the

Yalta and Ay-Petri massifs (Crimea Mountain, Southern Ukraine). Dissertation Monographs 217, Wydawnictwa AGH, Kraków, 253 pp.

Krajewski, M. and Olszewska, B. 2007. Foraminifera from the Late Jurassic and Early Cretaceous carbonate platform facies of the southern part of the Crimea Mountains; Southern Ukraine. *Annales Societatis Geologorum Poloniae*, **77**, 291–311.

Krische, O., Bujtor, L. and Gawlick, H.J. 2013. Calpionellid and ammonite biostratigraphy of uppermost Jurassic to Lower Cretaceous sedimentary rocks from the Leube quarry (Northern Calcareous Alps, Salzburg, Austria). *Austrian Journal of Earth Science* **106**(1), 26–45.

Kuss, J. 1994. Cretaceous (Albian–Turonian) Calcareous algae from Egypt and Jordan–systematics, stratigraphy and paleogeography*, Abhandlungen Geologischen Bundesanstalt*, **50**, 295–317.

Kuss, J. and Conrad, M.A. 1991. Calcareous algae from Cretaceous carbonates of Egypt, Sinai, and southern Jordan. *Journal of Paleontology*, **65**(5), 869–882.

Kuznetsova, K.I., Grigelis, A.A., Adjamian, J., Jarmakani, E. and Hallaq, L. 1996. *Zonal Stratigraphy and Foraminifera of the Tethyan Jurassic (Eastern Mediterranean)*. OPA (Overseas Publishers Association) Amsterdam B.V., Published in the Netherlands under license by Gordon and Breach Science, 256pp.

Lakova, I., Stoykova, K. and Ivanova, D. 1999. Calpionellid, nannofossil and calcareous dinocyst bioevents and integrated biochronology of the Tithonian to Valanginian in the Western Balkanides, Bulgaria. *Geologica Carpathica*, **50**(2), 151–168.

Smith, L.B., and Read, J.F. 1999. Application of high-resolution sequence stratigraphy to tidally influenced Upper Mississippian carbonates, Illinois basin. *In* Harris, P. M. *et al*. (eds.), *Advances in carbonate sequence stratigraphy: Application to reservoirs, outcrops, and models*, Society for Sedimentary Geology (SEPM), Special Publication **63**, 107-126pp.

Larson, R.L. 1991. Latest pulse of earth: evidence for a mid-Cretaceous superplume. *Geology,* **19,** 547–550.

Lehmann, R. 1975. Crustacean Coproliths from Topmost Jurassic or Basal Cretaceous Deposits of the Northwestern Pacific. *In*: Larson, R.L., Moberly, R., *et al.* (eds), *Preliminary Reports, Deep Sea Drilling Project, Leg 32, U.S. Government Printing Office, Washington*, 827–833.

Le Nindre, Y.M., Manivit J., Manivit, H. and Vaslet, D. 1990. Stratigraphie sequentielle du Jurassique et du Crétacé en Arabia Saoudite. *Société Géologique de France, Bulletin,* **6**(6), 1025–1034.

Leupold, W. and Bigler, H., 1936. Coscinoconus eine neue Foraminiferenform aus Tithon-Unterkreide-Gesteinen der Helvetischen Zone der Alpen. *Eclogae Geologicae Helvetiae*, **28**(2), 606-624.

Lloyd, A.J. 1962. Polymorphid, miliolid and rotaliform foraminifera from the type Kimmeridgian. *Micropaleontology*, **8**, 369–383.

Loeblich, A.R. and Tappan, H. 1950. Foraminifera of the Type Kiowa Shale, Lower Cretaceous. *Palaeontological Contributions*, *Protozoa*, University of Kansas, **3**, 1–15.

Loeblich, A. R. and Tappan, H. 1964. Protista 2. Chiefly 'Thecamoebians' and Foraminiferida. *In*: Moore, R.C. (Ed.), *Treatise on Invertebrate Paleontology*, The Geological Society of America and the University of Kansas. Lawrence Kansas, Part C. **1**: 1–510, text-figs 1–399; 2: 511–900, text-figs 400-653.

Loeblich, A.R., and Tappan, H. 1982. A revision of mid-Cretaceous Textularian foraminifers from Texas. *Journal of Micropalaeontology*, **1**(1), 55–69.

Loeblich, A.R. and Tappan, H. 1984. Suprageneric classification of the Foraminiferida (Protozoa). *Micropaleontology*, **30**, 1–70.

Loeblich, A.R. and Tappan, H. 1985. Some new and redefined genera and families of agglutinated foraminifera. *Journal of Foraminiferal Research*, **15**(2), 91–104.

Loeblich, A. R. and Tappan, H. 1987. *Foraminiferal Genera and their Classification*. Van Nostrand Reinhold, New York, 970pp. + 847pls.

Loeblich, A.R. and Tappan, H. 1992. Present Status of Foraminiferal Classification. *In*: Takayanagi, Y. and Saito, T (eds), *Studies in Benthic Foraminifera*. Tokai University Press, 93–102.

Longoria, J. F. 1974. *Stratigraphic, morphologic and taxonomic studies of Aptian planktonic foraminifera*. *Revista Española de Micropaleontología*, No. Extraord., 1–107.

Lucia, F.J., 1995, Rock-fabric/petrophysical classification of carbonate pore space for reservoir characterization. *American Association of Petroleum Geologists, Bulletin*, **79**(9), 1275–1300.

Macrides, C.G. and Neves, F.A. 2008. Lithology estimation from a multicomponent 3D-4C OBC seismic survey over a clastic reservoir in the Arabian Gulf. **13**(1), 15–34.

Mansour, A. T. 1975. *Pfenderina* (Foraminifera) from the Jurassic sediments of Ethiopia. *Mitteilungen der Abteilung für Geologie, Paläontologie und Bergbau am Landesmuseum Joanneum, Graz*, **35**, 113–131.

Masse, J. P. and Arnaud-Vanneau, A. 1999. Early Cretaceous calcareous algae of the mid-Pacific Mountains. *Revue de Micropaléontologie*, **42**(1), 57–69.

Masters, B. A. 1977. Mesozoic Planktonic Foraminifera. *Oceanic Micropaleontology*, **1**, 301-731.

Masters, B.A. and Scott, R.W. 1978. Microstructure, affinities and systematicsof Cretaceous calcispheres. *Micropaleontology,* **24**, 210–221.

Maync, W. 1959. Deux nouvelles espèces crétacées du genre *Pseudocyclammina* (Foraminifères). *Revue de Micropaléontologie*. **1**(4), 179–189.

Maync, W. 1965. Some comments on C. D. Redmond's new lituolid foraminifera from Saudi Arabia. *Revue de Micropaléontologie*, **8**, 37–40.

Miall, A.D. 1997. *The Geology of Stratigraphic Sequences*. Springer-Verlag, Berlin, 433pp.

Mitchum Jr, R.M. 1977. Seismic stratigraphy and Global Changes of Sea Level: Part 11. Glossary of Terms used in Seismic Stratigraphy. *In*: Payton, C.E. (Ed.), *Seismic Stratigraphy: Applications to Hydrocarbon Exploration*, American Association of Petroleum Geologists, Memoir **26**, 205–212.

Mitchum, R. M., and Van Wagoner, J. C. 1991. High-frequency sequences and their stacking patterns: sequence-stratigraphic evidence of high-frequency eustatic cycles. *Sedimentary Geology*, **70**(2), 131-160.

Michetiuc, M., Catincuţ, C., and Bucur, I.I. 2012. An Upper Jurassic-Lower Cretaceous carbonate platform from the Vâlcan Mountains (Southern Carpathians, Romania): paleoenvironmental interpretation. *Geologica Carpathica*, **63**(1), 3348.

Mohler, W. 1938. Mikropaläontologische Untersuchungen in der nordschweizerischen Juraformation. *Mémoires Suisses de Paléontologie*, **60**, 1–53.

Morozowa, V. G., and Moskalenko, T. A. 1961. Planktonic Foraminifera of the Boundary Deposits of the Bajocian and Bathonian Stages of Central Dagestan (Northeast Caucasus). *Voprosy Mikropaleontologii*, **5**, 3-30.

Murillo-Muñetón, G. and Dorobek, S. L. 2003. Controls on the Evolution of Carbonate Mud Mounds in the Lower Cretaceous Cupido Formation, Northeastern Mexico. *Journal of Sedimentary Research*, **73** (6), 869-886.

Murris, R. J. 1980. Middle East--Stratigraphic Evolution and Oil Habitat: Abstract. *American Association of Petroleum Geologists, Bulletin*, **64**(7), 597-618.

Murris, R. J. 1984. Middle East: stratigraphic evolution and oil habitat.

Neagu, T. 1968. Study of the Miliolidaceae in the lower Cretaceous (Barremian) of Southern Dobrogea. *Travaux du Muséum National d'Histoire Naturelle 'Grigore Antipa', Bucharest, Romamia,* **8**, 563–572.

Neagu T. 1984. Nouvelle données sur la morphologie du test, sur la systématique et la nomenclature des Miliolides agaisthegues du Mésozoïque. *Revista Española de Micropaleontología*, **16**, 75–90.

Neagu T. 1986. Barremian–Lower Aptian miliolid fauna in Southern Dobrogea (Romania). *Revista Espanola de Micropaleontología,* **18**(3), 313–348.

Neagu, T. 1994. Early Cretaceous *Trocholina* Group and some related genera from Romania, Part l. *Revista Espanõla de Micropaleontología*, **26**, 117–143.

Neagu, T. 1995. Early Cretaceous *Trocholina* Group and some related genera from Romania, Part ll. *Revista Espanõla de Micropaleontología*, **27**, 5–40.

Neagu, T. 2000. Lower Cretaceous calcareous agglutinated Foraminifera from Southern Dobrogea, Romania. Part II. Early Cretaceous Cuneolinidae. *In*: Hart, M.B., Kaminski, M.A. and Smart, C.W. (Eds), *Proceedings of the Fifth International Workshop on Agglutinated Foraminifera*. Grzybowski Foundation, Special Publication, **7**, 363–386.

Neagu, T. 2004. Smaller agglutinated foraminifera from an olistolith of Adneth Limestones, Tipea Valley, Persani Mountains, Romania. *In*: Bubík, M. and Kaminski, M.A. (eds), *Proceedings of the Sixth International Workshop on Agglutinated Foraminifera*. Grzybowski Foundation, Special Publication, **8**, 381–392.

Neagu, T. and Neagu, M. 1995a. Smaller agglutinated foraminifera from the Achanticum Limestone (Upper Jurassic), Eastern Carpathians – Romania. *In*: Kaminski, M.A., Geroch, S. and Gasinski, M.A. (eds), *Proceedings of the*

Fourth International Workshop on Agglutinated Foraminifera. Grzybowski Foundation Special Publication, **3**, 211–225.

Neagu, T. and Neagu, M. 1995b. Smaller Agglutinated Foraminifera from the Acanthicum *Limestone (Upper Jurassic), Eastern Carpathians, Romania*. *In*: Kaminski, M.A., Geroch, S. and Gasinski, M. (Eds), *Proceedings of the 4th International Workshop on Agglutinated Foraminifera* Grzybowski Foundation Special Publication, **3**, 211–225.

Neagu, T. and Platon, E. 1994. Genera *Haplophragmoides* Cushman, 1910; *Recurvoides* Earland, 1934; *Thalmannammina* Pokorny, 1951; *Plectorecurvoides* Noth, 1952 and *Pokornyammina* n. gen. from Upper Cretaceous Flysch facies, Eastern Carpathians, Romania. *Revista Espanõla de Micropaleontología*, **26**(1), 5–30.

Neumann, A. C. 1965. Processes of Recent Carbonate Sedimentation in Harrington Sound, Bermuda. *Bulletin of Marine Science*, **15**(4), 987-1035.

Nowak W. 1980. Suborder Tintinnina Claparede and Lachman 1858. *In*: Malinowska L. (Ed.): Geology of Poland, Vol. III: Atlas of guide and characteristic fossils. Part 2b: Mesozoic, Jurassic. Wydawnictwa Geoleologiczne, Warszawa, 329–338.

Nunn, E.V., and Price, G.D. 2010. Late Jurassic (Kimmeridgian–Tithonian) stable isotopes ($\delta^{18}O$, $\delta^{13}C$) and Mg/Ca ratios: new palaeoclimate data from

Helmsdale, northeast Scotland. *Palaeogeography, Palaeoclimatology, Palaeoecology*, **292**(1), 325–335.

Nunn, E.V., Price, G.D., Gröcke, D.R., Baraboshkin, E.Y., Leng, M.J. and Hart, M.B. 2010. The Valanginian positive carbon isotope event in Arctic Russia: Evidence from terrestrial and marine isotope records and implications for global carbon cycling. *Cretaceous Research*, **31**(6), 577–592.

Okla, S.M. 1991. Dasycladacean algae from the Jurassic and Cretaceous of central Saudi Arabia. *Micropaleontology*, **37**(2),183–190.

Olszewska, B. 2010. Microfossils of the Upper Jurassic-Lower Cretaceous formations of the Lublin Upland (SE Poland) based on thin section studies. *Polish Geological Institute,* **26**.

Olszewska, B., Szydlo A., Jugowiec-Nazarkiewcz, M. and Nescieruk, P. 2008. Integrated biostratigraphy of carbonate deposits of the Cieszyn Beds in the Polish Western Carpathians. *Geologia*, **24**, 33–59.

Omaña, L. and González Arreola, C. 2008. Late Jurassic (Kimmeridgian) larger benthic Foraminifera from Santiago Coatepec, SE Puebla, Mexico*. Geobios*, **41**(6), 799–817.

Payton, C.E. (Ed.).1977. *Seismic Stratigraphy: Applications to Hydrocarbon Exploration.* American Association of Petroleum Geologists, Memoir **26**, 516pp.

Petrova, S. 2010. Calpionellid data on Berriasian age of the Sarbenitsa Wedge, Cherni Osam Formation (Western Balkan Mountains, Bulgaria). *Comptes rendus de l'Académie bulgare des Sciences*, **63**(5), 733–740.

Petrova, S., Rabrenović, D., Lakova, I., Koleva-Rekalova, E., Ivanova, D., Metodiev, L. and Malešević, N. 2012. Biostratigraphy and microfacies of the pelagic carbonates across the Jurassic/Cretaceous boundary in eastern Serbia (Stara Planina-Poreč Zone). *Geologica Balcanica*, **41**(1–3) 53–76.

Pfender, J. 1938. Les Foraminifères du Valanginien provencal. *Société Géologique de France, Bulletin*, **8**, 5th series, no. 3–4, 231–242.

Platonov, E., Lakova, I., Petrova, S. and Arkadiev, V. 2014.Tithonian and Lower Berriasian calpionellid against ammonite biostratigraphy of the Dvuyakornaya Formation in eastern Crimea. *Geologica Balcanica*, **43**(1–3), 63–76.

Pollastro, R.M. 2003.Total Petroleum Systems of the Paleozoic and Jurassic, Greater Ghawar Uplift and Adjoining Provinces of Central Saudi Arabia andNorthern Arabian-Persian Gulf. *United States, Geological Survey,* **2202 – H**, 107pp.

Pop, G. and Bucur, I.I. 2001. Upper Jurassic and Lower Cretaceous sedimentary formations from the Vâlcan Mountains (South Carpathians). *Studia Universitatis Babes-Bolyai, Geologia*, **XLVI** (2), 77–94.

Powers, R.W., Ramirez, L.F., Redmond C.D. and Elberg E.L.Jr. 1966. Geology of the Arabian Peninsula: Sedimentary Geology of Saudi Arabia. *United States, Geological Survey, Professional Papers*, **560-D**, 147pp.

Powers, R. W. 1968. Lexique Stratigraphique International : Saudi Arabia. *Centre National de la Recherche Scientifique*, Paris, **3**, Asie, fasc. 10 b 1, 177pp .

Premoli Silva, I. and Verga, D. 2004. Practical Manual of Cretaceous planktonic foraminifera. In: Verga, D. and Rettori, R. (eds), *International School on Planktonic Foraminifera*, Universities of Perugia and Milan, Perugia, Italy, 3rd Course, Tipografia Ponte Felcino, 283pp.

Price, G.D., Wilkinson, D., Hart, M.B., Page, K.N., and Grimes, S.T. 2009. Isotopic analysis of coexisting Late Jurassic fish otoliths and molluscs: Implications for upper-ocean water temperature estimates. *Geology*, **37**(3), 215–218.

Radoičić, R. 2005. New Dasycladales and microbiota from the lowermost Valanginian of the Mirdita Zone. *Annales Géologiques de la Péninsule Balkanique*, **66**, 27–53.

Read, J.F. 1982. Carbonate platforms of passive (extensional) continental margins: types, characteristics and evolution. *Tectonophysics*, **81**(3), 195–212.

Read, J.F. 1985. Carbonate platform facies models. *American Association of Petroleum Geologists, Bulletin,* **66**, 860–878.

Redmond, C.D. 1964a. The foraminiferal family Pfenderinidae in the Jurassic of Saudi Arabia. *Micropaleontology*, **10**(2), 251–263.

Redmond, C.D. 1964b. Lituolid foraminifera from the Jurassic and Cretaceous of Saudi Arabia. *Micropaleontology*, **10**, 405–414.

Redmond, C.D. 1965. Three new genera of Foraminifera from the Jurassic of Saudi Arabia. *Micropaleontology*, **11**(2), 133–140.

Reháková, D. and Michalík, J. 1997. Evolution and distribution of calpionellids – the most characteristic constituents of Lower Cretaceous Tethyan microplankton. *Cretaceous Research*, **18**(3), 493–504.

Reháková, D. 2000. Calcareous dinoflagellate and calpinellid bioevents versus sea-level fluctuations recorded in the West-Carpathian (Late Jurassic/Early Cretaceous) pelagic environments. *Geologica Carpathica*, **51**(4), 229–243.

Remane, J. 1989. Calpionellids. In: Bolli, H.M., Saunders, J.B., and Perch-Nielsen, K. (eds), *Plankton Stratigraphy: Volume 1, Planktic foraminifera, calcareous nannofossils and calpionellids,* Cambridge, Cambridge University Press, 555–572.

Remane, J. 1998. Calpionellids. In: Haq, B. U. and Boersma, A. (eds), *Introduction to Marine Micropaleontology, Elsevier Biomedical, New York, Amsterdam, Oxford*, 161–170.

Rigaud, S., Blau, J., Martini, R. and Rettori, R. 2013. Taxonomy and phylogeny of the Trocholinidae (Involutinina). *Journal of Foraminiferal Research*, **43**(4), 317–339.

Roux, A. and Deloffre, R: 1990. Revision des Gymnocodiaceae (Algues Rouges, Permien-Crétacé), Taxonomie, Biostratigraphie, Paleogeographie. I. Partie: Géneralites sur la famille. *Revue de Micropaléontologie*, **33**(2), 123–137.

Schlager, W. 2002. *Sedimentology and sequence stratigraphy of carbonate rocks*. Vrije Universiteit, Amsterdam. Earth and Life Sciences, 146 pp.

Schlagintweit, F. and Ebli, O. 1999. New Results on Microfacies, Biostratigraphy and Sedimentology of Late Jurassic – Early Cretaceous platform carbonate of the Northern Calcareous Alps: Part1 Tressenstein Limestone, Plassen Formation. *Abhandlungen der Geologischen Bundesanstalt, Wien,* **56**(2), 379–418.

Schlagintweit, F. 2005. *Neogyroporella? gawlicki* n. sp., a new Dasycladale from the Upper Jurassic–Lower Cretaceous Lärchberg Formation of the Northern Calcareous Alps, Austria. *Geologia Croatica*, **58**(2), 103–117.

Schlagintweit, F. and Gawlick, H. 2006. *Subbdelloidina luterbacheri* Riegraf, 1987 (Encrusting Foraminifera) from Late Jurassic to Early Cretaceous Reefal Limestones of Albania and the Northern Calcareous Alps (Austria). *Jahrb Geol Bundesanst*, **146**, 53-63.

Schlagintweit, F., Dieni, I. and Radoičić, R. 2009. Two look-alike dasycladalean algae: *Clypeina isabellae* Masse, Bucur, Virgone and Delmasso, 1999 from the Berriasian of Sardinia (Italy) and *Clypeina loferensis* sp. n. from the Upper Jurassic of the Northern Calcareous Alps (Austria). *Geoloski anali Balkanskoga poluostrva*, (70), 43–59.

Schlagintweit, F., Bover-Arnal, T and Salas, R 2010. New insights into *Lithocodium aggregatum* Elliott 1956 and *Bacinella irregularis* Radoičić 1959 (Late Jurassic – Lower Cretaceous): two ulvo-phycean green algae (?Order Ulotrichales) with a heteromorphic life cycle (epilithic/euendolithic). *Facies*, **56**, 509–547.

Schlagintweit, F. 2012. New insights into Troglotella incrustans Wernli and Fookes, 1992, a fascinating Upper Jurassic–Upper Cretaceous foraminifer. *Studia Universitatis Babes-Bolyai, Geologia*, **57** (2), 17–26.

Scholle P.A. and Ulmer-Scholle, D.S. 2003. A Colour Guide to the Petrography of Carbonate Rocks: Grains, Textures, Porosity**,** Diagenesis. *American Association of Petroleum Geologists, Memoir,* **77,** 474pp.

Schulze, F., Kuss, J. and Marzouk, A. 2005. Platform configuration, microfacies and cyclicities of the upper Albian to Turonian of west-central Jordan. *Facies,* **50** (3-4), 505–527.

Scotese, C. R., Gahagan, L. M. and Larson, R. L. 1988. Plate tectonic reconstructions of the Cretaceous and Cenozoic ocean basins. *Tectonophysics*, **155**(1), 27–48.

Scotese, C. R. 2007. www.scotese.com/cretaceous.htm [accessed throughout research]

Senowbari-Daryan, B., Bucur, I. I., Schlagintweit, F., Săsăran, E., and Matyszkiewicz, J. 2007. *Crescentina*, a new generic name for "*Tubiphytes*" *morronensis* Crescenti, 1969. In *9th International Symposium of Fossil Algae, Zagreb, Croatia,* 19–20.

Senowbari-Daryan, B., Bucur, I.I., Schlagintweit, F., Săsăran, E., and Matyszkiewicz, J. 2008. *Crescentiella*, a new name for "*Tubiphytes*" *morronensis* Crescenti, 1969: an enigmatic Jurassic–Cretaceous microfossil. *Geologia Croatica*, **61**(2-3), 185–214.

SEPM STRATA. Website produced by the Society for Sedimentary Geology, Tulsa, OK, as a database for Sequence Stratigraphy [www.sepmstrata.org], accessed during 2015 and 2016.

Septfontaine, M. 1977. Niveaux à Foraminifères (Pfenderininae et Valvulininae) dans le Dogger des Préalpes médianes du Chablais occidental (Haute-Savoie, France). *Eclogae Geologicae Helvetiae*, **70**, 599-625.

Septfontaine, M. 1988. Towards an Evolutionary Classification of Jurassic lituolids (Foraminifera) in Carbonate Platform Environment. *Revue de Paléobiologie Special Volume*, **2**, 229-256.

Sharland, P.R., Archer, R., Casey, D.M., Davies, R.B., Hall, S.H., Heward, A.P., Horbury, A.D. and Simmons, M.D. 2001. Arabian Plate sequence stratigraphy. *GeoArabia Special Publication,* **2**, Gulf PetroLink, Bahrain, 371pp, with 3 charts.

Shebl, H.T. and Alsharhan, A.S.1994. Sedimentary facies and hydrocarbon potential of Berriasian- Hauterivian carbonates of Saudi Arabia. *In*: Simmons, M.D. (Ed.), *Micropalaeontology and Hydrocarbon Exploration in the Middle East*, British Micropalaeontological Society, Special Publication, Chapman and Hall, London, 159–175.

Shebl, H. T. and Al Sharhan, A.S. 2000. Microfacies analysis of Berriasian-Hauterivian Carbonates, Central Saudi Arabia. SPEM Special Publication, **69**, 115-127.

Simmons, M.D. and Hart, M.B. 1987. The biostratigraphy and microfacies of the Early to mid-Cretaceous carbonates of Wadi Mi'aidin, Central Oman

Mountains. *In*: Hart, M.B. (Ed.), *Micropalaeontology of Carbonate Environments*, Ellis Horwood Ltd, Chichester, 176–207.

Simmons, M.D., Emery, D. and Pickard, N.A.H. 1991. *Hensonella dinarica*, an originally calcitic Early Cretaceous dasycladacean alga. *Palaeontology*, **34**(4), 955–961.

Simmons, M.D. and Williams, C.L. 1992. Sequence stratigraphy and eustatic sea-level change: the role of micropalaeontology. *Journal of Micropalaeontology*, **11**(2), 112.

Simmons, M.D., Boudagher-Fadel, M.K., Banner, F.T. and Whittaker, J E. 1997. The Jurassic Favusellacea, the earliest Globigerinina. *In*: Boudagher-Fadel, M.K., Banner, F.T., Whittaker, J.E. and Simmons, M.D. (eds), *The Early Evolutionary History of Planktonic Foraminifera*, Chapman and Hall, London, 17–51.

Skelton, P. W., Spicer, R.A., Kelley, S.P. and Gilmour, I. 2003. *The Cretaceous World*. Cambridge University Press, Cambridge, United Kingdom, 360pp.

Sloss, L. L., 1963. Sequences in the Cratonic interior of North America: *Geological Society of America, Bulletin,* **74**, 93-114.

Spence, G.H. and Tucker, M.E. 1999. Modeling carbonate microfacies in the context of high-frequency dynamic relative sea-level and environmental changes. *Journal of Sedimentary Research*, **69**(4), 947–961.

Spence, G.H. and Tucker, M.E. 2000. Modelling carbonate microfacies within the context of high frequency dynamic relative sea-level and environmental changes –Reply. *Journal of Sedimentary Research*, **70**, 1335–1336.

Spence, G.H. and Tucker, M.E. 2007. A proposed integrated multi-signature model for peritidal cycles in carbonates. *Journal of Sedimentary Research*, **77**(10), 797–808.

Spence, G.H., Arnaud-Vanneau, A., Arnaud, H. and Tucker, M.E. 2004. Unravelling the microfacies signatures of para-sequences using computer optimized similarity matrices. *Sedimentology*, **51**, 1243–1271.

Stearn, C.W. 1972. The relationship of the stromatoporoids to the sclerosponges. *Lethaia*, **5**(4), 369–388.

Stearn, C.W., Webby, B.D., Nestor, H. and Stock, C.W. 1999. Revised classification and terminology of Palaeozoic stromatoporoids. *Acta Palaeontologica Polonica*, **44**(1), 369–388.

Steinke, M. 1937. Unpublished Aramco report, *In*: Powers *et al.* (eds.), *Sedimentary geology of Saudi Arabia*, 1966.

Steinke, M. 1940. Unpublished Aramco report, *In*: Powers *et al.* (eds.), *Sedimentary geology of Saudi Arabia*, 1966.

Steinke, M. and Bramkamp, R.A. 1952. Mesozoic rocks of eastern Saudi Arabia. *American Association of Petroleum Geologists*, Bulletin, **36**, 909.

Streng, M., Hildebrand-Habel, T. and Willems, H. 2004. A proposed classification of archeopyle types in calcareous dinoflagellate cysts. *Journal of Paleontology*, **78**(3), 456–483.

Strohmenger, C.J., Weber, L.J., Ghani A., Al-Mehsin, K., Al-Jeelani, O., Al-Mansoori, A., Al-Dayyani, T., Vaughan, L., Khan, S.A. and Mitchell, J.C. 2006. High-resolution sequence stratigraphy and reservoir characterization of Upper Thamama (Lower Cretaceous) reservoirs of a giant Abu Dhabi oil field, United Arab Emirates. In: Harris, P.M. and Weber, L.J. (eds), *Giant hydrocarbon reservoirs of the world: from rocks to reservoir characterization and modelling*, American Association of Petroleum Geologists, Memoir, **88**, 139–171.

Strohmenger, C. J., Mitchell, J. C., Feldman, H. R., Lehmann, P. J., Broomhall, R. W., Patterson, P. E., Al-Sahlan, G., Mitchell, j. C., Feldman, H. R., Demko, T. M., Wellner, R. W., Lehmann, P. J., McCrimmon, G. G., Broomhall, R. W., and Al-Ajmi, N. 2006. Sequence Stratigraphy and Reservoir Architecture of the Burgan and Mauddud formations (Lower Cretaceous), Kuwait, *in* P. M. Harris and L. J. Weber, (eds.), *Giant hydrocarbon reservoirs of the world: From rocks to reservoir characterization and modelling*: AAPG Memoir **88**/SEPM Special Publication, 213-245.

Sugden, W., and Standring, A. J., 1975. Qatar Peninsula. *Lexique Strat. Internat., Centre Nat. Rech. Scientifique,* Paris, III, Asie, Fasc. 10b3, 120 p.

Tasli, K. 2001. Benthic foraminifera of the Upper Jurassic platform carbonate sequence in the Aydincik (Içel) Area, Central Taurides, S. Turkey. *Geologia Croatica*, **54**(1), 1–13.

Tappan, H., and Loeblich, A. R. 1988. Foraminiferal evolution, diversification, and extinction. *Journal of Paleontology*, **62**(05), 695-714.

Tucker, M.E. and Wright, V.P. (with a chapter by Dickson, J.A.D.). 1990. *Carbonate Sedimentology*. Blackwell Science, Oxford, 496pp.

Turi, V., Săsăran, E. and Bucur, I.I. 2011. New data on the Upper Jurassic–Lower Cretaceous limestones from Bihor Mountains: case study of Gârda Seacă-Hodobana region, Romania. *Studia UBB Geologia*, **56**(1), 11–27.

Vail, P.R., Mitchum Jr, R.M. and Thompson lll, S. 1977. Seismic Stratigraphy and Global Changes of Sea Level: Part 3. Relative Changes of Sea level from Coastal Onlap. In: Payton, C.E. (Ed.), *Seismic Stratigraphy: Applications to Hydrocarbon Exploration,* American Association of Petroleum Geologists, Memoir **26**, 63–81.

van Buchem, F. S., Pittet, B., Hillgarten, H., Grotsch, J., Al-Mansouri, A., Billing, I. M., ... and Van Steenwinkel, M. 2002. High-Resolution Sequence Stratigraphic Architecture of the Barremian-Aptian Carbonate Systems in Northern Oman and the United Arab Emirates Kharaib and Shu'aiba Formations. *Geoarabia-Manama-*, ***7*****,** 461-500.

Vaslet, D., Al-Muallem, M.S. Maddah, S.S. Brosse, J. M. Fourniguet, J. Breton, J.P. and Le Nindre, Y.M. 1991. Explanatory notes to the geologic map of the Ar Riyad Quadrangle, Kingdom of Saudi Arabia. Geoscience map GM-121, scale 1:250,000, sheet 24I. *Deputy Ministry for Mineral Resources, Ministry of Petroleum and Mineral Resources*, Kingdom of Saudi Arabia, 54pp.

Védrine, S. 2008. Co-occurrence of the foraminifer *Mohlerina basiliensis* with *Bacinella-Lithocodium* oncoids: palaeoenvironmental and palaeoecological implications (Late Oxfordian, Swiss Jura). *Journal of Micropalaeontology*, **27**(1), 35–44.

Védrine, S., Strasser A. and Hug, W. 2007. Oncoid growth and distribution controlled by sea-level fluctuations and climate (Late Oxfordian, Swiss Jura Mountains). *Facies,* **53**, 535–552.

Velić, I. 1977. Jurassic and lower cretaceous assemblage-zones in Mt. Velika Kapela, Central Croatia*. Acta Geologica,* **9**(2), 15-37.

Walker, R.G. and James, N.P. 1992. *Facies Models. Response to Sea Level Change.* Geological Association of Canada, Toronto, 454pp.

Wanner J. 1940. Gesteinsbildende Foraminiferen aus Malm undUnterkreide des östlichen Ostindischen Archipels. *Paläontologische Zeitschrift*, **22**, 75–99.

Webster, R.E. 2004. Takutu Basin, Guyana and Brazil: Paleogeography and Climate. http://www.searchanddiscovery.com/documents/2004/webster02/images/poster03.pdf.

Wendler, J. and Willems, H. 2002. Distribution pattern of calcareous dinoflagellate cysts across the Cretaceous-Tertiary boundary (Fish Clay, Stevns Klint, Denmark): Implications for our understanding of species-selective extinction. *In*: Koeberl, C. and MacLeod, K.G. (eds), *Catastrophic events and mass extinctions: impacts and beyond*, Geological Society of America, Special Paper, 356, Boulder, Colorado, 265–276.

Wendler, I., Zonneveld, K.A. and Willems, H. 2002. Calcareous cyst-producing dinoflagellates: ecology and aspects of cyst preservation in a highly productive oceanic region. *In*: Clift, P.D., Kroon, D., Gaedicke, C. and Craig, J. (eds), *The tectonic and climate evolution of the Arabian Sea Region*, *Geological Society, London, Special Publications*, **195**, 317–340.

Wernli, R. and Fookes, E. 1992. *Troglotella incrustans* n. gen., n. sp., un étrange et nouveau foraminifère calcicavicole du complexe récifal Kimméridgien de Saint-Germain-de-Joux (Ain, France). *Bolletino della Societa Paleontologica Italiana*, **31**, 95–103.

Wiesner, H. 1931. Die Foraminiferen der Deutschen Sudpolar Expedition 1901–1903. Deutschen Subpolar Expedition. *Berlin (Zoology)*, **20**, 53–165.

Wilgus, C.K., Hastings, B.S., Kendall, C.G.StC., Posamentier, H.W. and Ross, C.A. 1988. *Sea Level Changes: An integrated approach*. SEPM, Tulsa, OK, Special Publication, 42, 407pp.

Wilson, J.L. 1970. Depositional facies across carbonate shelf margins. *Transactions of the Gulf Coast Association of Geological Societies,* **20**, 229–233.

Wilson, J.L. 1974. Characteristics of carbonate - platform margins. *American Association of Petroleum Geologists, Bulletin,* **58**, 810 –824.

Wilson, J.L. 1975. *Carbonate Facies in Geologic History*. Springer, New York, N.Y., 471pp.

Wood, A. 1947. The supposed Cambrian Foraminifera from the Malverns. *Quarterly Journal of the Geological Society, London*, **102**, 447–460.

Wood, A. 1949. The structure of the wall of the test in the Foraminifera; its Value in classification. *Quarterly Journal of the Geological Society, London*, **104**, 229–255.

Yabe, H. and Sugiyama, T. 1927. *Cladocoropsis mirabilis* Felix from the Torinosu Limestone of Japan. *Japanese Journal of Geology and Geography*, **5**, 107–110.

Yabe, H. and Sugiyama, T. 1935. Jurassic stromatoporoids from Japan. *Science Reports of the Tohoku Imperial University, 2nd Series, Geology*, **14**(2), 135–164.

Yilmaz, İ.Ö. 2000. Taxonomic and paleogeographic approaches to the dasyclad algae in the Upper Jurassic (Kimmeridgian)-Upper Cretaceous (Cenomanian) peritidal carbonates of the Fele (Yassıbel) Area (Western Taurides, Turkey). *Turkish Journal of Earth Sciences*, **8**(2-3), 81–102.

Yose, L.A., Ruf, A.S., Strohmenger, C.J., Schuelke, J.S., Gombos, A., Al-Hosani, I., Al-Maskary, S., Bloch, G., Al-Mehairi, Y. and Johnson, I.G. 2006, Three dimensional characterization of a heterogeneous carbonate reservoir, Lower Cretaceous, Abu Dhabi (United Arab Emirates). *In*: Harris, P.M. and Weber, L.J. (eds), *Giant hydrocarbon reservoirs of the world: From rocks to reservoir characterization and modeling*, American Association of Petroleum Geologists, Memoir, 88 [co-published as an SEPM Special Publication],173– 212.

Zaninetti, L., Salvini-Bonnard, G. and Decrouez, D. 1987. *Montsalevia*, n. gen. (Montsaleviidae, n. fam., Foraminifère), dans le Crétacé inférieur (Berriasien moyen-Valanginien) du Mont Salève et du Jura Meridional (Haute-Savoie, France); note préliminaire. *Revue de Paléobiologie, Genéve*, **6**(1), 165–168.

Zell, P., Stinnesbeck, W., Beckmann, S., Adatte, T. and Hering, F. 2015. The Berriasian–Valanginian (Early Cretaceous) boundary transition at Santa Catarina Ticuá, Oaxaca State, southern Mexico: Ammonites, bivalves, calpionellids and their paleobiogeographic significance. *Journal of South American Earth Sciences*, **62**, 33–57.

Ziegler, M.A. 2001. Late Permian to Holocene paleofacies evolution of the Arabian Plate and its hydrocarbon occurrences. *GeoArabia*, **6**(3), 445–504.

List of Plates

Plate 1

A. *Troglotella incrustans* Wernli and Fookes (1992) in *Lithocodium aggregatum* Elliott, 1956, Well-B, 8425.9’, , field of view 2.5 mm.

B. *Troglotella incrustans* Wernli and Fookes (T) (1992) in *Lithocodium aggregatum* Elliott, 1956, Well-G, 6761.3’, field of view 6.3 mm.

Plate 2

A. *Troglotella incrustans* (T) Wernli and Fookes (1992) in *Lithocodium aggregatum* (LCe) Elliott, 1956, Well-G, 6768.5’, field of view 6.3 mm.

B. *Troglotella incrustans* (T) Wernli and Fookes (1992) in encrusting *Lithocodium aggregatum* (LCe) Elliott (1956) on bivalve shell, microbial micritization of encrusting *Lithocodium aggregatum* Elliott and *Troglotella incrustans* Wernli and Fookes borings have been intensive on weak parts of the shell, Well-I, 5524.2’.

Plate 3

A. *Troglotella incrustans* (T) Wernli and Fookes (1992) in *Lithocodium aggregatum* (LCe) Elliott, 1956, Well-H, 7325.5’, field of view 6.3 mm.

B. *Conoglobigerina* sp. cf. *C. gulekhensis* (Cq) (Gorbatchik and Poroshina 1979), Well-D, 8630.7’, field of view 2.5 mm. Three specimens in tempestitic, laminated peloidal bindstone.

Plate 4

A. *Conoglobigerina* sp. cf. *C. gulekhensis* (Gorbatchik and Poroshina, 1979), Well-D, 8587.2', field of view 2.5 mm. Associated with monaxon spicules in tempestitic, laminated peloidal bindstone.

B. *Conoglobigerina* sp. cf. *C. gulekhensis* (Gorbatchik and Poroshina, 1979), a close-up image, width (0.14 mm), length (0.144 mm), Well-D, 8587.2', field of view 1.25 mm. Associated with monaxon spicules in tempestitic, laminated peloidal bindstone.

Plate 5

A. *Conoglobigerina* sp. cf. *C. gulekhensis* (Gorbatchik and Poroshina, 1979), a close-up image, maximum width is 0.25 mm, Well-D, 8639.7', field of view 2.5 mm. Associated with monaxon spicules in tempestitic, laminated peloidal bindstone.

B. *Conoglobigerina* sp. cf. *C. gulekhensis* (Gorbatchik and Poroshina, 1979), close-up from image A.

Plate 6

A. *Coscinoconus alpina* Leupold, 1935, Well-H, 6427.5', field of view 2.5 mm. The blue colour is voids.

B. *Coscinoconus alpina* Leupold, 1935, Well-H, 6421.5', field of view 2.5 mm. The blue colour is voids.

Plate 7

A. *Coscinoconus alpina* Leupold (1935), Well-F, 8390.5', field of view 6.3 mm.

B. *Coscinoconus alpina* Leupold (1935), Well-H, 6417.6', field of view 2.5 mm.

Plate 8

A. *Coscinoconus delphinensis* (Arnaud-Vanneau *et al*., 1988), Well-H, 6422.5, field of view 2.5 mm.

B. *Coscinoconus delphinensis* (Arnaud-Vanneau *et al.*, 1988), Well-H, 6422.5, field of view 6.3 mm.

Plate 9

A. *Coscinoconus delphinensis* (Arnaud-Vanneau *et al*., 1988), Well-H, 6422.5', field of view 2.5 mm.

B. *Coscinoconus delphinensis* (Arnaud-Vanneau *et al*., 1988), Well-H, 6422.5', field of view 6.3 mm.

Plate 10

A. *Coscinoconus elongata* (Leupold, 1935), Well-G, 6765.4', field of view 2.5 mm.

B. *Coscinoconus elongata* (Leupold, 1935), Well-F, 8390.5', field of view 6.3 mm.

Plate 11

A. *Coscinoconus cherchiae* Arnaud-Vanneau *et al.* (1988), Well-D, from the base of the Yamama Formation, 8204.2', field of view 2.5 mm.

B. *Coscinoconus cherchiae* Arnaud-Vanneau *et al. (*1988), Well-B, 8357', field of view 2.5 mm.

Plate 12

A. *Coscinoconus sagittaria* Arnaud-Vanneau *et al.* (1988), Well-H, 6427.5', field of view 2.5 mm.

B. *Coscinoconus sagittaria* Arnaud-Vanneau *et al.* (1988), Well-A, 4064.5' field of view 2.5 mm.

Plate 13

A. *Coscinoconus sagittaria* Arnaud-Vanneau *et al.* (1988), Well-D, from the top of the Yamama Formation, 7960.2', field of view 2.5 mm.

B. *Coscinoconus sagittaria* Arnaud-Vanneau *et al.* (1988), Well-I, 5448.7', field of view 2.5 mm.

Plate 14

A. *Coscinoconus sagittaria* Arnaud-Vanneau *et al.* (1988), Well-D, common *C. sagittaria* wackestone from the base of the Yamama Formation, 7975.2', field of view 2.5 mm.

B. *Neotrocholina valdensis* Reichel (1955), Well-I, from the base of the Yamama Formation, 5474.7', field of view 2.5 mm.

Plate 15

A. *Protopeneroplis ultragranulata* (Gorbatchik, 1971), Well-G, 6767.5', field of view 2.5 mm.

B. *Protopeneroplis ultragranulata* (Gorbatchik, 1971), Well-G, 6810.5', field of view 2.5 mm.

C. *Protopeneroplis ultragranulata* (Gorbatchik, 1971), Well-H, 6423.5', field of view 2.5 mm.

D. *Protopeneroplis ultragranulata* (Gorbatchik, 1971), Well-H, 6414.8', field of view 2.5 mm.

E. *Protopeneroplis ultragranulata* (Gorbatchik, 1971), Well-I, 5524.2', field of view 2.5 mm.

F. *Protopeneroplis ultragranulata* (Gorbatchik, 1971), Well-A, from the base of the Yamama Formation, 4061.6', field of view 2.5 mm.

Plate 16

A. *Protopeneroplis ultragranulata* (Gorbatchik, 1971), Well-D, 8639.7', field of view 2.5 mm.

B. *Protopeneroplis ultragranulata* (Gorbatchik, 1971), Well-H, 6423.5', field of view 2.5 mm.

C. *Protopeneroplis ultragranulata* (Gorbatchik, 1971), Well-H, 6414.8', field of view 2.5 mm.

D. *Protopeneroplis ultragranulata* (Gorbatchik, 1971), Well-H, 6424.5', field of view 2.5 mm.

E. *Protopeneroplis ultragranulata* (Gorbatchik, 1971), Well-H, 6247.5', field of view 2.5 mm.

F. *Protopeneroplis ultragranulata* (Gorbatchik, 1971), Well-H, 6414.8', field of view 2.5 mm.

Plate 17

A. *Protopeneroplis ultragranulata* (Gorbatchik, 1971), Well-I, 5448.7', field of view 2.5 mm.

B. *Protopeneroplis ultragranulata* (Gorbatchik, 1971), Well-I, 5471.7', field of view 2.5 mm.

C. *Protopeneroplis ultragranulata* (Gorbatchik, 1971), Well-D, from the Yamama Formation, 7957.2', field of view 1.25 mm.

D. *Protopeneroplis banatica* Bucur (1993), Well-A, from the Yamama Formation, 4061.6', field of view 2.5 mm.

E. *Protopeneroplis banatica* Bucur (1993), Well-B, from the Yamama Formation, 8375.9', field of view 2.5 mm.

F. *Lenticulina* sp., Well-D, from the Yamama Formation, 7960.2', field of view 1.25 mm.

Plate 18

A. *Lenticulina* sp., Well-D, 8639.7', field of view 1.25 mm.

B. *Lenticulina* sp., Well-D, 8639.7', field of view 2.5 mm.

C. *Lenticulina* sp., Well-D, 8639.7', field of view 0.61 mm.

D. *Lenticulina* sp., Well-D, 8620.2', field of view 2.5 mm.

E. *Cf. Lenticulina* sp., Well-I, 5448.7', field of view 2.5 mm.

F. *Cf. Lenticulina* sp., Well-I, 5518.2', field of view 2.5 mm.

Plate 19

A. *Cf. Pyrulinoides* sp., Well-B, 8365.1', field of view 1.25 mm.

B. *Nodosaria* sp., Well-D, 8639.7', field of view 2.5 mm.

Plate 20

A. *Nodosaria* sp., Well-I, 5451.7', field of view 2.5 mm.

B. *Ophthalmidium* sp., Well-F, 8441.5', field of view 2.5 mm.

Plate 21

A. *Ophthalmidium* sp., Well-G, 6762.6', field of view 2.5 mm.

B. *Ophthalmidium* sp., Well-H, 6416.5', field of view 2.5 mm.

C. *Ophthalmidium* sp., Well-H, 6423.5', field of view 2.5 mm.

D. *Ophthalmidium* sp., Well-B, 8444.4', field of view 6.3 mm.

E. *Ophthalmidium* sp., Well-I, 5448.7', field of view 2.5 mm.

F. *Ophthalmidium* sp., Well-I, 5448.7', field of view 2.5 mm.

Plate 22

A. *Ophthalmidium* sp., Well-I5448.7', field of view 2.5 mm.

B. *Meandrospira favrei* (Charollais *et al*., 1966), Well-B, from the Yamama Formation, 8361.8', field of view 2.5 mm.

C. *Meandrospira favrei* (Charollais *et al*., 1966), Well-D, from the Yamama Formation, 7957.2', field of view 1.25 mm.

D. *Meandrospira favrei* (Charollais *et al*., 1966), Well-D, from the Yamama Formation, 7957.2', field of view 2.5 mm.

E. *Meandrospira favrei* (Charollais *et al*., 1966), three specimens in wackestone, Well-D, from the Yamama Formation, 7957.2', field of view 2.5 mm.

F. *Meandrospira favrei* (Charollais *et al*., 1966), Well-D, from the Yamama Formation, 7957.2', field of view 2.5 mm.

Plate 23

A. *Meandrospira favrei* (Charollais *et al*., 1966), Well-D, from the Yamama Formation, 7957.2', field of view 1.25 mm.

B. *Meandrospira favrei* (Charollais *et al*., 1966), Well-D, from the Yamama Formation, 7957.2', field of view 2.5 mm.

C. *Nubecularia* sp., surrounded by microlayers (dark, concentric micrites) of *Crescentiella morronensis* forma *morronensis* (Crescenti, 1969), Well-H, 6414.8', field of view 2.5 mm.

D. *Nubecularia* sp., Well-H, 6414.8', field of view 2.5 mm.

E. *Nubecularia* sp., surrounded by microlayers (dark, concentric micrites) of *Crescentiella morronensis* forma *morronensis* (Crescenti, 1969), Well-I, 5534.7', field of view 2.5 mm.

F. *Nubecularia* sp., surrounded by microlayers (dark, concentric micrites) of *Crescentiella morronensis* forma *morronensis* (Crescenti, 1969), Well-I, 5448.7', field of view 2.5 mm.

Plate 24

A. *Nubecularia* sp., Well-H, 6421.5’, field of view 2.5 mm.

B. *Nubecularia* sp., surrounded by microlayers (dark, concentric micrites) of *Crescentiella morronensis* forma *morronensis* (Crescenti, 1969), Well-H, 6421.5’, field of view 2.5 mm.

C. *Nubecularia* sp., surrounded by microlayers (dark, concentric micrites) of *Crescentiella morronensis* forma *morronensis* (Crescenti, 1969), Well-I, 5448.7’, field of view 2.5 mm.

D. *Nubecularia* sp., surrounded by microlayers (dark, concentric micrites) of *Crescentiella morronensis* forma *morronensis* (Crescenti, 1969), Well-I, 5448.7’, field of view 2.5 mm.

E. *Nubecularia* sp., surrounded by microlayers (dark, concentric micrites) of *Crescentiella morronensis* forma *morronensis* (Crescenti, 1969), Well-I, 5448.7’, field of view 2.5 mm.

F. *Nubecularia* sp., surrounded by microlayers (dark, concentric micrites) of *Crescentiella morronensis* forma *morronensis* (Crescenti, 1969), Well-I, 5448.7’, field of view 2.5 mm.

Plate 25

A. *Nodobacularia* sp., surrounded by microlayers (dark, concentric micrites) of *Crescentiella morronensis* forma *morronensis* (Crescenti, 1969), Well-B, 8388.8’, field of view 6.3 mm.

B. *Nodobacularia* sp., surrounded by microlayers (dark, concentric micrites) of *Crescentiella morronensis* forma *morronensis* (Crescenti, 1969), Well-B, 8445.5', field of view 6.3 mm.

C. *Nodobacularia* sp., surrounded by microlayers (dark, concentric micrites) of *Crescentiella morronensis* forma *morronensis* (Crescenti, 1969), Well-B, 8353.3'.

D. *Derventina filipescui* Neagu (1968), Well-A, from the Yamama Formation, 4058.7', field of view 2.5 mm.

E. *Derventina filipescui* Neagu (1968), Well-I, from the Yamama Formation5451.7', field of view 2.5 mm.

F. *Derventina filipescui* Neagu (1968), Well-A, from the Yamama Formation, 4058.7', field of view 2.5 mm.

Plate 26

A. *Derventina filipescui* Neagu (1968), Well-D, from the Yamama Formation, 7960.2', field of view 1.25 mm.

B. *Istriloculina emiliae* Neagu (1984), Well-H, 7305.2', field of view 2.5 mm.

C. *Istriloculina emiliae* Neagu (1984), Well-H, 7305.2', field of view 2.5 mm.

D. *Istriloculina eliptica* (Iovcheva, 1962), Well-G, 6762.6', field of view 2.5 mm.

E. *Istriloculina eliptica* (Iovcheva, 1962), Well-B, 5408.1', field of view 2.5 mm.

F. *Quinqueloculina egmontensis* Lloyd (1962), Well-H, 7339', field of view 2.5 mm.

Plate 27

A. *Quinqueloculina egmontensis* Lloyd (1962), Well-H, 7325.5', field of view 2.5 mm.

B. *Quinqueloculina egmontensis* Lloyd (1962), Well-H, 7325.5', field of view 2.5 mm.

C. *Quinqueloculina egmontensis* Lloyd (1962), Well-H, 7328.6', field of view 2.5 mm.

D. *Quinqueloculina egmontensis* Lloyd (1962), Well-I, 5531.7', field of view 2.5 mm.

E. *Quinqueloculina egmontensis* Lloyd (1962), Well-I, 5531.7', field of view 2.5 mm.

F. *Quinqueloculina egmontensis* Lloyd (1962), Well-H, 6416.5', field of view 2.5 mm.

Plate 28

A. *Quinqueloculina* sp., Well-H, 6427.5', field of view 2.5 mm.

B. *Quinqueloculina* sp., Well-H, 6423.5', field of view 2.5 mm.

C. *Quinqueloculina* sp., Well-H, 6423.5', field of view 2.5 mm.

D. *Quinqueloculina* sp., Well-B, 8411.5', field of view 2.5 mm.

E. *Quinqueloculina* sp., Well-I, 5524.2', field of view 2.5 mm.

F. *Quinqueloculina* sp., Well-I, 5543.2', field of view 2.5 mm.

Plate 29

A. *Mohlerina basiliensis* (Möhler, 1938), Well-G, 6779.5', field of view 2.5 mm.

B. *Mohlerina basiliensis* (Möhler, 1938), Well-G, 6809.5', field of view 2.5 mm.

C. *Mohlerina basiliensis* (Möhler, 1938), Well-B, 8431.3', field of view 2.5 mm.

D. *Reophax* sp., Well-I, 5524.2', field of view 2.5 mm.

E. *Reophax* sp., Well-G, 6762.6', field of view 2.5 mm.

F. *Haplophragmoides joukowskyi* Charollais *et al.* (1966), Well-I, from the Yamama Formation, 5448.7', field of view 2.5 mm.

Plate 30

A. *Haplophragmoides joukowskyi* Charollais *et al.* (1966), Well-D, from the Yamama Formation, 7957.2', field of view 2.5 mm.

B. *Haplophragmoides joukowskyi* Charollais *et al.* (1966), Well-D, from the Yamama Formation, 7957.2', field of view 2.5 mm.

C. *Haplophragmoides joukowskyi* Charollais *et al.* (1966), Well-D, from the Yamama Formation, 7957.2', field of view 1.25 mm.

D. *Haplophragmoides joukowskyi* Charollais *et al.* (1966), Well-D, 7957.2', field of view 2.5 mm.

E. *Haplophragmoides joukowskyi* Charollais *et al.* (1966), Well-D, 8638.2', field of view 2.5 mm.

F. *Haplophragmoides joukowskyi* Charollais *et al.* (1966), Well-D, 8639.7', field of view 2.5 mm.

Plate 31

A. *Nautiloculina bronnimanni* Arnaud-Vanneau and Peybernes (1978), Well-H, 6421.5', field of view 2.5 mm.

B. *Nautiloculina bronnimanni* Arnaud-Vanneau and Peybernes, (1978), Well-H, 6427.5', field of view 2.5 mm.

C. *Nautiloculina bronnimanni* Arnaud-Vanneau and Peybernes, (1978), Well-H, 6427.5', field of view 2.5 mm.

D. *Nautiloculina bronnimanni* Arnaud-Vanneau and Peybernes, (1978), Well-I, 5518.2', field of view 2.5 mm.

E. *Nautiloculina oolithica* Möhler (1938), Well-H, 7331.8', field of view 2.5 mm.

F. *Nautiloculina oolithica* Möhler (1938), Well-H, 6417.5', field of view 2.5 mm.

Plate 32

A. *Nautiloculina oolithica* Möhler (1938), Well-B, 8361.8', field of view 2.5 mm.

B. *Nautiloculina oolithica* Möhler (1938),, Well-H, 7331.8', field of view 2.5 mm.

C. *Freixialina planispiralis* Ramalho (1969), Well-I, 5448.7', field of view 2.5 mm.

D. *Freixialina planispiralis* Ramalho (1969), Well-G, 6775.6', field of view 2.5 mm.

E. *Ammobaculites* sp. aff. *A. celatus* Arnaud-Vanneau (1980), Well-I, 5474.1', field of view 1.25 mm.

F. *Ammobaculites* sp. aff. *A. celatus* Arnaud-Vanneau (1980), Well-I, 5524.2', field of view 2.5 mm.

Plate 33

A. *Ammobaculites subcretaceus* Cushman and Alexander (1930), Well-F, 8412.5', field of view 6.3 mm.

B. *Ammobaculites subcretaceus* Cushman and Alexander (1930), Well-G, 6760.6', field of view 2.5 mm.

C. *Ammobaculites subcretaceus* Cushman and Alexander (1930), Well-G, 6762.6', field of view 2.5 mm.

D. *Ammobaculites subcretaceus* Cushman and Alexander (1930), Well-G, 6762.6', field of view 2.5 mm.

E. *Charentia cuvillieri* Neumann (1965), Well-H, 6408.1', field of view 1.25 mm.

F. *Charentia evoluta* (Gorbatchik, 1968), Well-I, 5480.2', field of view 6.3 mm.

Plate 34

A. *Charentia evoluta* (Gorbatchik, 1968), Well-I, 5471.7', field of view 6.3 mm.

B. *Montsalevia salevensis* Charollais *et al.* (1966), Well-A, plug # 4, field of view 6.3 mm.

C. *Montsalevia salevensis* Charollais *et al.* (1966), Well-I, 5465.7', field of view 2.5 mm.

D. *Anchispirocyclina lusitanica* (Egger, 1902), Well-I, 5385.7', field of view 6.3 mm.

E. *Anchispirocyclina lusitanica* (Egger, 1902), Well-I, 5385.7', field of view 6.3 mm.

F. *Anchispirocyclina lusitanica* (Egger, 1902), Well-I, 5385.7', field of view 6.3 mm.

Plate 35

A. *Anchispirocyclina lusitanica* (Egger, 1902), Well-I, 5385.7', field of view 6.3 mm.

B. *Anchispirocyclina lusitanica* (Egger, 1902), Well-B, 8357', field of view 6.3 mm.

C. *Anchispirocyclina lusitanica* (Egger, 1902), Well-B, 8357', field of view 2.5 mm.

D. *Anchispirocyclina lusitanica* (Egger, 1902), Well-I, 5385.7', field of view 16 mm.

E. *Anchispirocyclina lusitanica* (Egger, 1902), Well-I, 5385.7', field of view 6.3 mm.

F. *Everticyclammina kelleri* (Henson, 1948), Well-D, 8639.7', field of view 2.5 mm.

Plate 36

A. *Everticyclammina kelleri* (Henson, 1948), Well-D, 8641.2', field of view 2.5 mm.

B. *Everticyclammina kelleri* (Henson, 1948), Well-D8641.2', field of view 2.5 mm.

C. *Everticyclammina kelleri* (Henson, 1948), Well-D8641.2', field of view 2.5 mm.

D. *Everticyclammina kelleri* (Henson, 1948), Well-D8644.2', field of view 2.5 mm.

E. *Everticyclammina kelleri* (Henson, 1948), Well-B, 8370.5', field of view 2.5 mm.

F. *Everticyclammina kelleri* (Henson, 1948) (right), and *Pseudocyclammina cylindrica* Redmond (1964) (left), Well-B, 8370.5', field of view 6.3 mm.

Plate 37

A. *Everticyclammina virguliana* Koechlin (1942), Well-H, 7328.6', field of view 2.5mm.

B. *Everticyclammina virguliana* Koechlin (1942), Well-H, 7328.6’, field of view 2.5 mm.

C. *Everticyclammina virguliana* Koechlin (1942), Well-G, 6811.3’, field of view 2.5 mm.

D. *Everticyclammina virguliana* Koechlin (1942), Well-D, 8644.2’, field of view 2.5 mm.

E. *Bramkampella arabica* Redmond (1964), Well-I, 5479.2’, field of view 6.3 mm.

F. *Bramkampella arabica* Redmond (1964), Well-B, 8370.5’, field of view 2.5 mm.

Plate 38

A. *Bramkampella arabica* Redmond (1964), Well-A, 4110.5,, field of view 6.3 mm.

B. *Bramkampella arabica* Redmond (1964), Well-D, 7957.2’, field of view 2.5 mm.

C. *Bramkampella arabica* Redmond (1964), Well-B, from the Yamama Formation, 8370.5’, field of view 6.3 mm.

D. *Pseudocyclammina cylindrica* Redmond (1964), Well-A, 4061.6’, field of view 2.5 mm.

E. *Pseudocyclammina cylindrica* Redmond (1964), Well-I, 5479.2’, field of view 6.3 mm.

F. *Pseudocyclammina cylindrica* Redmond (1964), Well-B, 8370.5', field of view 2.5 mm.

Plate 39

A. *Pseudocyclammina cylindrica* Redmond (1964), axial section,Well-I, 5480.7', field of view 6.3 mm.

B. Two *Pseudocyclammina lituus* Yokoyama (1890), upper, lateral section, and *Pseudocyclammina cylindrica* Redmond (1964), lower, Well-A, 4061.6', field of view 6.3 mm.

C. *Pseudocyclammina lituus* Yokoyama (1890), transverse section, Well-H, plug # 6427.5, field of view 2.5 mm.

D. *Pseudocyclammina lituus* Yokoyama (1890), transverse section, Well-D, 7969.2'.

E. *Pseudocyclammina lituus* Yokoyama (1890), tangential section, Well-D, 7960.2'.

F. *Pseudocyclammina lituus* Yokoyama (1890), tangential section, Well-D, 7960.2'.

Plate 40

A. *Pseudocyclammina lituus* Yokoyama (1890), tangential section, the wall is agglutinated by sponge spicules (monaxon type) in deep water setting, Well-A, 4061.6', field of view 6.3 mm.

B. *Pseudocyclammina lituus* Yokoyama (1890), tangential section, Well-B, 8370.5', field of view 6.3 mm.

C. *Pseudocyclammina lituus* Yokoyama (1890), tangential section, Well-H, 6408.1', field of view 6.3 mm.

D. *Pseudocyclammina lituus* Yokoyama (1890), (left) transverse section, and *Bramkampella arabica* Redmond, 1964 (right) transverse section, Well-B, 8370.5', field of view 6.3 mm.

E. *Plectinella virgulinoides* Marie (1956), tangential section, Well-H, 7328.6', field of view 2.5 mm.

F. *Plectinella virgulinoides* Marie (1956), tangential section, Well-H, 7327.1', field of view 2.5 mm.

Plate 41

A. *Plectinella virgulinoides* Marie (1956), tangential section, Well-B, 8420.6', field of view 2.5 mm.

B. *Plectinella virgulinoides* Marie (1956), tangential section, Well-B, 8420.6', field of view 2.5 mm.

C. *Plectinella virgulinoides* Marie (1956), tangential section, Well-B, 5408.1', field of view 6.3 mm.

D. *Plectinella virgulinoides* Marie (1956), tangential section, Well-H, 7331.8', field of view 2.5 mm.

E. *Plectinella virgulinoides* Marie (1956), tangential section, Well-H, 7330.8', field of view 2.5 mm.

F. *Eomarssonella* sp., tangential section, Well-H, 6421.5', field of view 6.3 mm.

Plate 42

A. *Eomarssonella* sp. Well-H, plug # 6424.5', field of view 2.5 mm.

B. *Eomarssonella* sp., Well-G, 5380.2', field of view 2.5 mm.

C. *Eomarssonella* sp., Well-B, 8395.4', field of view 2.5 mm.

D. *Eomarssonella* sp., Well-I, 5533.2', field of view 6.3 mm.

E. *Bitaxia* sp., Well-B, 5408.1', field of view 6.3 mm.

F. *Uvigerinammina uvigeriniformis* (Seibold and Seibold, 1960), Well-G, 5382.2', field of view 2.5 mm.

Plate 43

A. *Uvigerinammina uvigeriniformis* (Seibold and Seibold, 1960), Well-H, 6423.5', field of view 2.5 mm.

B. *Uvigerinammina uvigeriniformis* (Seibold and Seibold, 1960), Well-B, 8427', field of view 2.5 mm.

C. *Verneuilinoides neocomiensis* Mjatliuk (1939), Well-G, 5385.7', field of view 6.3 mm.

D. *Verneuilinoides neocomiensis* Mjatliuk (1939), Well-H, 7332.5', field of view 2.5 mm.

E. *Verneuilinoides neocomiensis* Mjatliuk (1939), Well-H, 6421.5', field of view 6.3 mm.

F. *Verneuilinoides neocomiensis* Mjatliuk (1939), Well-H, 6422.5', field of view 2.5 mm.

Plate 44

A. *Verneuilinoides neocomiensis* Mjatliuk (1939), Well-H, plug # 7331.8', field of view 2.5 mm.

B. *Verneuilinoides polonicus* (Cushman and Glazewski, 1949), Well-G, 6761.3', field of view 2.5 mm.

C. *Verneuilinoides polonicus* (Cushman and Glazewski, 1949), Well-G, 6772.5', field of view 2.5 mm.

D. *Verneuilinoides polonicus* (Cushman and Glazewski, 1949), Well-G, 6779.5', field of view 2.5 mm.

E. *Verneuilinoides polonicus* (Cushman and Glazewski, 1949), Well-G, 6779.5', field of view 2.5 mm.

F. *Verneuilinoides polonicus* (Cushman and Glazewski, 1949), Well-H, 7339', field of view 2.5 mm.

Plate 45

A. *Verneuilinoides polonicus* (Cushman and Glazewski, 1949), intruded by wispy seam micro-stylolite filled by clay minerals, Well-B, 8361.8', field of view 2.5 mm.

B. *Verneuilinoides polonicus* (Cushman and Glazewski, 1949), Well-B, 8410.5', field of view 2.5 mm.

C. *Verneuilinoides polonicus* (Cushman and Glazewski, 1949), Well-I, 5524.2', field of view 2.5 mm.

D. *Siphovalvulina variabilis* Septfontaine, 1988, Well-H, 7316.2', field of view 2.5 mm.

E. *Siphovalvulina variabilis* Septfontaine, 1988, Well-D, 8639.7', field of view 2.5 mm.

F. *Siphovalvulina variabilis* Septfontaine, 1988, Well-D, 8639.7', field of view 2.5 mm.

Plate 46

A. *Gaudryina ectypa* Arnaud-Vanneau (1980), Well-D, 8638.2', field of view 2.5 mm.

B. *Gaudryinella* sp., Well-H, 7328.6', field of view 6.3 mm.

C. *Gaudryinella* sp., Well-H, 7328.6', field of view 2.5 mm.

D. *Gaudryinella* sp., Well-G, 6779.5', field of view 2.5 mm.

E. *Gaudryinella* sp., Well-H, 6410.2', field of view 2.5 mm.

F. *Gaudryinella* sp., Well-B, 8427', field of view 2.5 mm.

Plate 47

A. *Verneuilina minuta* Wiesner (1931), Well-H, 7331.3', field of view 2.5 mm.

B. *Verneuilina minuta* Wiesner (1931), Well-H, 7328.6', field of view 2.5 mm.

C. *Protomarssonella kummi* (Zedler, 1961), Well-H, 7328.6', field of view 2.5 mm.

D. *Protomarssonella kummi* (Zedler, 1961), Well-H, 7339, field of view 2.5 mm.

E. *Protomarssonella kummi* (Zedler, 1961), Well-I, 5543.2', field of view 2.5 mm.

F. *Praedorothia* sp. cf. *P. praehauteriviana* (Dieni and Massari, 1966), Well-G, 6768.5', field of view 2.5 mm.

Plate 48

A. *Praedorothia* sp. cf. *P. praehauteriviana* (Dieni and Massari, 1966), Well-A, 4061.6', field of view 2.5 mm.

B. *Kurnubia palastiniensis* Henson (1948), transverse section, Well-F, 3255.5', field of view 6.3 mm. Note that porosity type is intra-skeletal, in which it enhances the reservoirs quality by increasing primary porosity value.

C. *Kurnubia palastiniensis* Henson (1948), transverse section, Well-F, 3255.5', field of view 2.5 mm.

D. *Kurnubia palastiniensis* Henson (1948), oblique section, Well-F, 3255.5', field of view 2.5 mm.

E. *Kurnubia palastiniensis* Henson (1948), transverse section, Well-F, 3255.5', field of view 2.5 mm.

F. *Kurnubia palastiniensis* Henson (1948), oblique section, Well-F, 3255.5', field of view 2.5 mm.

Plate 49

A. *Kurnubia palastiniensis* Henson (1948), transverse section, Well-F, 3255.5', field of view 6.3 mm. Note that porosity type is intra-skeletal, in which it enhances the reservoirs quality by increasing primary porosity value and as a consequence permability increses.

B. *Kurnubia palastiniensis* Henson (1948), transverse section, Well-F, 3255.5', field of view 6.3 mm.

C. *Kurnubia palastiniensis* Henson (1948), transverse section, Well-F, 3255.5', field of view 2.5 mm.

D. *Kurnubia palastiniensis* Henson (1948), oblique section, Well-F, 3243.5', field of view 1.25 mm.

E. *Kurnubia palastiniensis* Henson (1948), transverse section, Well-F, 3255.5', field of view 1.25 mm.

F. *Pfenderina neocomiensis* (Pfender, 1938), Well-G, 6768.5', field of view 2.5 mm.

Plate 50

A. *Pfenderina neocomiensis* (Pfender, 1938), Well-H, 7332.5', field of view 2.5 mm.

B. *Pfenderina neocomiensis* (Pfender, 1938), Well-H, 7331.8', field of view 2.5 mm.

C. *Pfenderina neocomiensis* (Pfender, 1938), Well-H, 7328.6', field of view 2.5 mm.

D. *Pfenderina neocomiensis* (Pfender, 1938), Well-H, 7331.8’, field of view 2.5 mm.

E. *Pfenderina neocomiensis* (Pfender, 1938), Well-H, 7331.8’, field of view 2.5 mm.

F. *Pfenderina neocomiensis* (Pfender, 1938), Well-H, 7330.8’, field of view 2.5 mm.

Plate 51

A. *Pfenderina neocomiensis* (Pfender, 1938), Well-H, 7332.5’, field of view 2.5 mm.

B. *Pfenderina neocomiensis* (Pfender, 1938), Well-G, 6809.5’, field of view 2.5 mm.

C. *Pfenderina neocomiensis* (Pfender, 1938), Well-B, 8420.6’, field of view 2.5 mm.

D. *Pfenderina neocomiensis* (Pfender, 1938), Well-I, 5524.2’, field of view 2.5 mm.

E. *Haghimashella arcuata* (Haeusler, 1890), Well-H, 7323.7’, field of view 2.5 mm.

F. *Haghimashella arcuata* (Haeusler, 1890), Well-H, 6424.5’, field of view 2.5 mm.

Plate 52

A. *Haghimashella arcuata* (Haeusler, 1890), Well-H, 7316.9’, field of view 2.5 mm.

B. *Haghimashella arcuata* (Haeusler, 1890), Well-B8404.1', field of view 2.5 mm.

C. *Textulariopsis jurassica* (Gümbel, 1862), Well-D, 8642.7', field of view 2.5 mm.

D. *Textulariopsis jurassica* (Gümbel, 1862), Well-D, 8642.7', field of view 2.5 mm.

E. *Textulariopsis jurassica* (Gümbel, 1862), Well-D, 8642.7', field of view 2.5 mm.

F. *Textulariopsis jurassica* (Gümbel, 1862), Well-H, 6421.5', field of view 2.5 mm.

Plate 53

A. *Textulariopsis jurassica* (Gümbel, 1862), Well-D, 7957.2', field of view 1.25 mm.

B. *Textulariopsis jurassica* (Gümbel, 1862), Well-D, 7957.2', field of view 1.25 mm.

C. *Textulariopsis jurassica* (Gümbel, 1862), Well-H, 6423.5', field of view 2.5 mm.

D. Monaxon sponge spicules (red arrow), Well-B, 8365.1', field of view 2.5 mm.

E. Monaxon (red arrow) and triaxon sponge spicules (yellow arrow), Well-B, 8370.5', field of view 2.5 mm.

F. Monaxon sponge spicules (red arrow), Well-H, 6426.5’, field of view 6.3 mm.

Plate 54

A. Large monaxon sponge spicules (red arrow), Well-D, 8644.2’, field of view 2.5 mm.

B. Large monaxon sponge spicules (red arrow), Well-D, 8644.2’, field of view 2.5 mm.

C. Monaxon sponge spicules (red arrow), Well-D, 8644.2’, field of view 6.3 mm.

D. Monaxon sponge spicules (red arrow), Well-D, 8644.2’, field of view 6.3 mm.

E. Triaxon sponge spicules (yellow arrow), Well-D, 8644.2’, field of view 2.5 mm.

F. Triaxon sponge spicules (yellow arrow), Well-D, 8644.2’, field of view 2.5 mm.

Plate 55

A. Meandering wall structure type of calcareous sponge, possibly cf. *Raphidonema* sp., Well-D, 7957.2’, field of view 5 mm.

B. *Cladocoropsis mirabilis* Felix (1927), Well-I, 5482.2’.

C. *Cladocoropsis mirabilis* Felix (1927), Well-I, 5482.2’.

D. *Cladocoropsis mirabilis* Felix (1927), Well-I, 5482.2’.

E. *Cladocoropsis mirabilis* Felix (1927), Well-I, 5531.7’.

F. Stromatoporoid, Well-I, 5531.7’.

Plate 56

A. Possibly calcisponge clotted roots wackestone, Well-I, 5474.7’, field of view 16 mm.

B. Dinocyst, Well-A, 4058.7’, field of view 2.5 mm.

C. *Comittosphaera sublapidosa* (Volger, 1941), showing uneven inner and outer walls, Well-A, 4061.6’, field of view 2.5 mm.

D. Dinocyst, Well-G, 6775.6’, field of view 2.5 mm.

E. *Colomisphaera cieszynica* Nowak (1968), Well-G, plug # 100, field of view 2.5 mm.

F. Dinocyst, Well-B, 8427’, field of view 2.5 mm.

Plate 57

A. Possible Calcisphere, (D) Length 0.25 mm, d (internal length) 0.13 mm, Well-B, 8432.5’.

B. *Stomiosphaera wanneri* Borza (1969), stratigraphical range is from upper Berriasian to Hauterivian, Well-G, 6811.3’, field of view 2.5 mm.

Plate 58

A. *Stomiosphaera wanneri* Borza (1969), image taken with polarized light (XPL), not the cross extinction, Well-G, 6811.3’, field of view 2.5 mm.

B. *Stomiosphaera wanneri* Borza (1969), stratigraphical range is from Berriasian to Valanginian, Well-G, 6811.3’, field of view 2.5 mm.

C. *Crustocadosina semiradiata* (Wanner, 1940), Well-G, 6809.5', field of view 2.5 mm.

D. *Crustocadosina semiradiata* (Wanner, 1940), Well-G, 6811.3', field of view 2.5 mm.

E. *Macroporella praturloni* Dragastan (1999), Well-G, 6809.5', field of view 2.5 mm.

F. *Macroporella praturloni* Dragastan (1999), Well-G, 6809.5', field of view 2.5 mm.

Plate 59

A. *Actinoporella podolica* (Alth, 1878), Well-B, 8365.1', field of view 6.3 mm.

B. *Actinoporella podolica* (Alth, 1878) and a gastropod mold in lagoonal skeletal wackestone, Yamama Formation, Well-B, 8365.1', field of view 6.3 mm.

C. *Actinoporella podolica* (Alth, 1878), Well-B, 8365.1', field of view 6.3 mm.

D. *Actinoporella podolica* (Alth, 1878), Well-B, 8365.1', field of view 6.3 mm.

E. *Actinoporella podolica* (Alth, 1878), Well-B, 8365.1', field of view 2.5 mm.

F. *Holosporella arabica* Granier and Brunn (1991), Well-B, 8365.1', field of view 6.3 mm.

Plate 60

A. *Salpingoporella annulata* Carozzi (1953), Well-A, 4064.5', field of view 6.3 mm.

B. *Salpingoporella annulata* Carozzi (1953), Well-A, 4064.5', field of view 2.5 mm.

C. *Salpingoporella annulata* Carozzi (1953), Well-D, 8638.2', field of view 6.3 mm.

D. *Salpingoporella annulata* Carozzi (1953), Well-D, 8644.2', field of view 2.5 mm.

E. *Salpingoporella annulata* Carozzi (1953), Well-H, 7323.7', field of view 2.5 mm.

F. *Salpingoporella annulata* Carozzi (1953), Well-H, 6408.1', field of view 2.5 mm.

Plate 61

A. *Salpingoporella annulata* Carozzi (1953), Well-H, 7330.5', field of view 2.5 mm.

B. *Salpingoporella annulata* Carozzi (1953), Well-B, 8365.1', field of view 2.5 mm.

C. *Salpingoporella annulata* Carozzi (1953), Well-I, 5474.7', field of view 6.3 mm.

D. *Salpingoporella annulata* Carozzi (1953), Well-B, 8361.8', field of view 2.5 mm.

E. *Salpingoporella annulata* Carozzi (1953), with micrite envelope and micritization activity left by calcite cement, Well-H, 6414.8', field of view 2.5 mm.

F. *Salpingoporella annulata* Carozzi (1953), with micrite envelope and micritization activity left by calcite cement, Well-H, 6414.8', field of view 2.5 mm.

Plate 62

A. *Salpingoporella circassa* Farinacci and Radoičić (1991), Well-B, 8431.3', field of view 1.25 mm.

B. *Salpingoporella circassa* Farinacci and Radoičić (1991), Well-A, 4061.6', field of view 2.5 mm.

C. *Salpingoporella annulata* Carozzi (1953), Well-A, 4064.5', field of view 2.5 mm.

D. *Salpingoporella* ex gr*. pygmaea* (Gümbel, 1891), Well-G, 6760.6', field of view 2.5 mm.

E. *Salpingoporella* ex gr*. pygmaea* (Gümbel, 1891), Well-G, 6760.6', field of view 2.5 mm.

F. *Salpingoporella* ex gr*. pygmaea* (Gümbel, 1891), Well-G, 6767.5', field of view 2.5 mm.

Plate 63

A. *Salpingoporella* ex gr*. pygmaea* (Gümbel, 1891), Well-H, 6217.5', field of view 2.5 mm.

B. *Salpingoporella* ex gr*. pygmaea* (Gümbel, 1891), Well-H, 6217.5', field of view 2.5 mm.

Plate 64

A. *Salpingoporella* ex gr*. pygmaea* (Gümbel, 1891), Well-G, 6779.5', field of view 2.5 mm.

B. *Salpingoporella* ex gr*. pygmaea* (Gümbel, 1891), Well-G, 6779.5', field of view 6.3 mm.

C. *Clypina isabellae* Masse *et al.* (1999), Well-H, 6410.2', field of view 6.3 mm.

D. *Clypina isabellae* Masse *et al.* (1999), Well-H, 6422.5', field of view 6.3 mm.

E. *Clypina isabellae* Masse *et al.* (1999), Well-A, 4064.5', field of view 6.3 mm.

F. *Iranella inopinata* Gollestaneh (1965), Well-A, 4061.6', field of view 2.5 mm.

Plate 65

A. *Permocalculus ampullaceus* (P) Elliott (1959), Gastropod (G) and *Salpingoporella annulata* (S) Carozzi, Well-A, 4063.4', field of view 2.5 mm.

B. *Salpingoporella dinarica* Radoičić (1959), Well-G, 6768.5', field of view 6.3 mm.

C. *Salpingoporella dinarica* Radoičić (1959), Well-H, 6423.5', field of view 6.3 mm.

D. *Permocalculus ampullaceus* Elliott (1959), Well-H, 6410.2', field of view 2.5 mm.

E. *Permocalculus ampullaceus* Elliott (1959), Well-B, 8357', field of view 6.3 mm.

F. *Permocalculus ampullaceus* Elliott (1959), Well-B, 8375.9', field of view 6.3 mm.

Plate 66

A. *Salpingoporella dinarica* Radoičić (1959), Well-I, 5524.2', field of view 2.5 mm.

B. *Thaumatoporella parvovesiculifera* (Raineri, 1922), Well-G, 6760.6', field of view 2.5 mm.

C. *Thaumatoporella parvovesiculifera* (Raineri, 1922), Well-G, 6767.5', field of view 2.5 mm.

D. *Thaumatoporella parvovesiculifera* (Raineri, 1922), Well-H, 6416.5', field of view 2.5 mm.

E. *Arabicodium aegagrapiloides* Elliott (1957), Well-H, 6407.2', field of view 6.3 mm.

F. *Marinella lugeoni* Pfender (1939), Well-H, 6407.2', field of view 6.3 mm.

Plate 67

A. *Aeolisaccus dunningtoni* Elliott (1958), Well-B, 8429.3', field of view 2.5 mm.

B. *Aeolisaccus dunningtoni* Elliott (1958), Well-H, 7328.6', field of view 1.25 mm.

C. *Aeolisaccus dunningtoni* Elliott (1958), Well-H, 7316.2', field of view 2.5 mm.

D. *Aeolisaccus dunningtoni* Elliott (1958), Well-G, 6775.6', field of view 2.5 mm.

E. *Aeolisaccus dunningtoni* Elliott (1958), Well-D, 8644.2', field of view 2.5 mm.

F. *Aeolisaccus dunningtoni* Elliott (1958), Well-B, 8410.5', field of view 1.25 mm.

Plate 68

A. *Hensonella* sp., Well-G, 6760.6', field of view 6.3 mm.

B. *Hensonella* sp., Well-G, 6809.5', field of view 2.5 mm.

C. *Hensonella* sp., Well-G, 6811.3', field of view 2.5 mm.

D. *Lithocodium aggregatum* Elliott (1956), encrusting type surrounding and micritizing a multi-layered bivalve, Well-G, 6761.3', field of view 6.3 mm.

E. *Lithocodium aggregatum* Elliott (1956), encrusting type surrounding and micritizing a multi-layered bivalve, Well-G, 6761.3', field of view 6.3 mm.

F. *Lithocodium aggregatum* Elliott (1956), encrusting type surrounding and micritizing a multi-layered bivalve, Well-G, 6761.3', field of view 6.3 mm.

Plate 69

A. *Lithocodium aggregatum* Elliott (1956), encrusting type surrounding and micritizing a multi-layered bivalve, Well-G, 6761.3', field of view 6.3 mm.

B. *Lithocodium aggregatum* Elliott (1956), encrusting type surrounding and micritizing a multi-layered bivalve, Well-G, 6761.3', field of view 6.3 mm.

C. *Lithocodium aggregatum* Elliott (1956), large, encrusting oncoidal type, mesh-like structure, Well-I, 5531.7', field of view 6.3 mm.

D. *Lithocodium aggregatum* Elliott (1956), large, encrusting type surrounding and micritizing a coral, miesh-like structure, Well-H, 6420.6', field of view 6.3 mm.

E. *Lithocodium aggregatum* Elliott (1956), large, encrusting oncoidal type, mesh-like structure, Well-F, 8402.5', field of view 6.3 mm.

F. *Lithocodium aggregatum* Elliott (1956), encrusting type surrounding and micritizing a hard lithoclast, mesh-like structure, Well-G, 6761.3', field of view 6.3 mm.

Plate 70

A. *Lithocodium aggregatum* Elliott (1956), Boundstone, Well-G, 6768.5', image maximum width is16 mm.

B. *Lithocodium aggregatum* Elliott (1956), with mesh-like structure, Well-I, 6411.1', field of view 6.3 mm.

C. *Lithocodium aggregatum* Elliott (1956), a small lump of *lithocodium* oncoid, less than 1mm, Well-I, 6416.5', field of view 6.3 mm.

D. *Lithocodium aggregatum* Elliott (1956), large oncoidal type, over 2mm, Well-I, 6427.5', field of view 6.3 mm.

E. *Lithocodium aggregatum* Elliott (1956), large oncoidal type, over 2mm, common with mesh-like structures Well-I, 6427.5', field of view 6.3 mm.

F. *Lithocodium aggregatum* Elliott (1956), large oncoidal type, over 2mm, , Well-F, 8423.5', field of view 6.3 mm.

Plate 71

A. *Lithocodium aggregatum* Elliott (1956), Boundstone, Well-F, 8423.5', field of view 6.3 mm.

B. *Lithocodium aggregatum* Elliott (1956), Well-I, 6411.1', field of view 6.3 mm.

C. *Lithocodium aggregatum* Elliott (1956) in wackestone matrix, Well-F, 8469.5', field of view 6.3 mm.

D. *Lithocodium aggregatum* Elliott (1956), encrusting a bivalve and a mold of ex-aragonitic, could be coral (see coralline form like lower corner), Well-D, 8015.2', field of view 6.3 mm.

E. *Lithocodium aggregatum* Elliott (1956), encrusting oncoidal type, over 2mm, common with mish-like structures Well-H, 6406.4', field of view 6.3 mm.

F. *Lithocodium aggregatum* Elliott (1956), large nodule type, over 2mm, , Well-G, 6760.6', field of view 6.3 mm.

Plate 72

A. *Pseudolithocodium carpathicum* Míšík (1979), Well-G, 6811.3', field of view 6.3 mm.

B. *Crescentiella morronensis* forma *morronensis* (Crescenti, 1969), emend. Senowbari-Daryan *et al*. (2007), Well-H, 6417.5', field of view 2.5 mm.

C. *Crescentiella morronensis* forma *morronensis* (Crescenti, 1969), emend. Senowbari-Daryan *et al*. (2007), Well-H, 6417.5', field of view 2.5 mm.

D. *Crescentiella morronensis* forma *morronensis* (Crescenti,1969), emend. Senowbari-Daryan *et al*. (2007), Well-H, 6417.5', field of view 2.5 mm.

E. *Crescentiella morronensis* forma *morronensis* (Crescenti, 1969), emend. Senowbari-Daryan *et al*. (2007), Well-H, 6417.5', field of view 2.5 mm.

F. *Crescentiella morronensis* forma *morronensis* (Crescenti, 1969), emend. Senowbari-Daryan *et al*. (2007), Well-H, 6417.5', field of view 2.5 mm.

Plate 73

A. *Crescentiella morronensis* forma *morronensis* (Crescenti, 1969), emend. Senowbari-Daryan *et al*., 2007, Well-H, 6417.5' , field of view 2.5 mm.

B. *Crescentiella morronensis* forma *morronensis* (Crescenti, 1969), emend. Senowbari-Daryan *et al*. (2007), Well-B, 8357', field of view 6.3 mm.

C. *Crescentiella morronensis* forma *morronensis* (Crescenti, 1969), emend. Senowbari-Daryan *et al*. (2007), Well-B, 8361.8', field of view 6.3 mm.

D. *Crescentiella morronensis* forma *morronensis* (Crescenti, 1969), emend. Senowbari-Daryan *et al*. (2007), Well-B, 8444.4', field of view 6.3 mm.

E. *Crescentiella morronensis* forma *morronensis* (Crescenti, 1969), emend. Senowbari-Daryan *et al*. (2007), Well-B, 8444.4', field of view 6.3 mm.

F. *Calpionellopsis simplex* (Colom, 1938.), Width (W) 0.08 mm, length (L) 0.14 mm, Well-D, 8638.2', field of view 2.5 mm.

Plate 74

A. *Crassicollaria brevis* Remane (1962), Width (W) 0.1 mm, length (L) 0.12 mm, Well-D, 8609.7', field of view 1.25 mm.

B. *Calpionella alpina* Lorenz (1902), Well-D, 8627.7', field of view 2.5 mm.

C. *Calpionella alpina* Lorenz (1902), Well-F, 8202.5', field of view 2.5 mm.

D. Serpulid sp., Well-I, 5531.7, field of view 6.3 mm.

E. Serpulid sp., Well-D, 8608.2', field of view 6.3 mm.

F. *Terebella* sp. cf.*T. lapilloides* Münster (1833), Well-B, 8361.8', field of view 2.5 mm.

Plate 75

A. Scleractinian coral, Well-B, 8361.8', field of view 6.3 mm.

B. Gastropoda sp1. (pelagic?), Well-D, 8609.7', field of view 6.3 mm.

C. Cerithiidae sp., Well-H, 6414.8', field of view 6.3 mm.

D. Gastropoda sp., Well-D, 7957.2', field of view 1.25 mm.

E. Gastropoda sp., Well-F, 8455.5', field of view 6.3 mm.

F. Gastropoda sp., Well-I, 5477.7', field of view 6.3 mm.

Plate 76

A. Bivalve fragment, crushed bivalve mosaic spar cement Well-A, 4058.7', field of view 6.3 mm.

B. Bivalve fragment, Well-G, 6775.6’, field of view 6.3 mm.

C. Bivalve fragment, Well-D, 8641.2’, field of view 2.5 mm.

D. Costate bivalve sp., Well-B, 8357’, field of view 6.3 mm.

E. *Inoceramus* sp. (fragment), thick prismatic calcite piece, Well-D, 7960.2’, field of view 6.3 mm.

F. Costate bivalve sp., Well-D, 7960.2’, field of view 6.3 mm.

Plate 77

A. Oyster, Well-G, 6761.3’, field of view 6.3 mm.

B. Oyster, affected by *Lithocodium* borings and microbial activity, Well-G, 6761.3’, field of view 6.3 mm.

C. Oyster, affected by *Lithocodium* borings and microbial activity, Well-G, 6761.3’, field of view 6.3 mm.

D. Possible asteroid species within pellet packstone of protected internal shoal, Well-F, 8425.5’, field of view 6.3 mm.

E. Echinoid plate, Well-D, 7957.2’, field of view 2.5 mm.

F. Echinoid plate with syntaxial overgrowth cement, Well-H, 6422.5’, field of view 2.5 mm.

Plate 78

A. Echinoid plate with syntaxial overgrowth cement, Well-I, 5533.2’, field of view 6.3 mm.

B. Echinoid plates with syntaxial overgrowth cement, Well-I, 5543.2', field of view 6.3 mm.

C. Echinoid plate with syntaxial overgrowth cement, Well-I , 5533.2', field of view 2.5 mm.

D. Echinoid plates with syntaxial overgrowth cement, Well-I, 5542.2', field of view 6.3 mm.

E. Crinoid plate with syntaxial overgrowth cement, Well-H, 6414.8', field of view 2.5 mm.

F. Crinoid plate with syntaxial overgrowth cement, Well-D, 8521.2', field of view 6.3 mm.

Plate 79

A. Spine of regular echinoid with syntaxial overgrowth cement, Well-D, 8521.2', field of view 2.5 mm.

B. Spine of regular echinoid, Well-I, 5536.2', field of view 2.5 mm.

C. Spine of regular echinoid, Well-I, 5543.2', field of view 1.25 mm.

D. Oblique section through a spine of a regular echinoid in pelagic mudstone, Well-I, 5542.2', field of view 6.3mm.

E. *Saccocoma* sp., Well-A, 4061.6', field of view 2.5 mm.

F. *Saccocoma* sp., in cross-polarized light XPL, Well-A, 4061.6', field of view 2.5 mm.

Plate 80

A. Section through an ostracod valve, Well-A, 4058.7', field of view 2.5 mm.

B. Section through the carapace if an ostracod valve, Well-D, 8638.2', field of view 2.5 mm.

C. Section through an ostracod valve, Well-D, 8644.2', field of view 0.61 mm.

D. Section through the carapace if an ostracod valve, Well-I, 5448.7', field of view 2.5 mm.

E. Section through the carapace if an ostracod valve, Well-I, 5448.7', field of view 2.5 mm.

F. *Favreina* sp. cf. *F. dinarica* Brönnimann (1976), Well-B, 8421.6', field of view 2.5 mm.

Plate 81

A. *Favreina* sp. cf. *F. dinarica* Brönnimann (1976), Well-G, 6779.5', field of view 6.3 mm.

Plate 82

A. HMF 1: Porous, Intraclastic, Foraminferal and Peloidal Packstone, Well-H, 6427.5', This microfacies is highly porous (~20%) and has potential reservoir quality with fenestral (FE), interparticle (BP) and intraparticle (IP) porosities.

B. HMF 1: Porous, Intraclastic, Foraminferal and Peloidal Packstone, Well-H, 6427.5‘.

Plate 83

A. HMF 2: Finely Laminated Mudstone, Well-H, 6426.5‘. Microfacies porosity is from 0 % to <0.5 % of a moldic (MO) porosity type. Almost all of the porosity is formed by the empty spaces left by dissolved grains.

B. HMF 2: Finely Laminated Mudstone, Well-H, 6415.7‘. This microfacies is characterised by being barren of microfossils to one of very low biodiversity. It only contains occasional, thin-walled ostracods.

Plate 84

A. HMF 3: Peloidal, Foraminiferal and Intraclastic Packstone , Well-H, 6409.2‘. This microfacies contains diagnostic microfossils indicating a lagoonal to protected open marine environment. This includes *Quinqueloculina* spp., miliolids, *Istriloculina* spp., *Gaudryinopsis* sp., and *Verneuilinoides polonicus*. Blue colour is void and representing (5–20%) interparticle (BP) and intraparticle (IP) porosities.

B. HMF 3: Peloidal, Foraminiferal and Intraclastic Packstone , Well-H, 6425.5’ (x2). Blue colour is void and representing (5–20%) interparticle (BP) and intraparticle (IP) porosities.

Plate 85

A. HMF 3: Peloidal, Foraminiferal and Intraclastic Packstone , Well-H, 6391.1‘. This microfacies is characterized by fine grained packstone

and grainstone made of peloids, coated grains, lithoclastics and benthic foraminifera.

B. HMF 3: Peloidal, Foraminiferal and Intraclastic Packstone , Well-H, 6416.5'. The vadose zone micro-stalactite dripstone cement or pendant type of cement.

Plate 86

A. HMF 3: Peloidal, Foraminiferal and Intraclastic Packstone , Well-H, 6414.8. bivalve enveloped by microbial micrite.

B. HMF 3: Peloidal, Foraminiferal and Intraclastic Packstone , Well-H, 6401.3'. This microfacies is common with moldic and cavern porosities. This includes *Quinqueloculina* spp., miliolids, Istriloculina spp., *Gaudryinopsis* sp., and *Verneuilinoides polonicus*.

Plate 87

A. HMF 4a (low energy, *Lithocodium aggregatum* large oncoids): *Lithocodium*, Intraclastic and Peloidal Wackestone-Packstone-Grainstone-Rudstone, Well-H, 6420.6'. Large oncoid of *Lithocodium aggregatum* sorrounding a coral.

B. HMF 4a (low energy, *Lithocodium aggregatum* large oncoids): *Lithocodium*, Intraclastic and Peloidal Wackestone-Packstone-Grainstone-Rudstone, Well-H, 6420.6'. This microfacies has potential reservoir quality with intermediate to highly porous moldic (Mo), interparticle (IP) and intraparticle (BP) porosities, with a range of porosity from 5% to 20%.

Plate 88

A. HMF 4a (low energy, *Lithocodium aggregatum* large oncoids): *Lithocodium*, Intraclastic and Peloidal Wackestone-Packstone-Grainstone-Rudstone, Well-H, 6418.5‘.

B. HMF 4a (low energy, *Lithocodium aggregatum* large oncoids): *Lithocodium*, Intraclastic and Peloidal Wackestone-Packstone-Grainstone-Rudstone, Well-H, 6418.5‘.

Plate 89

A. HMF 4a (low energy, *Lithocodium aggregatum* large oncoids): *Lithocodium*, Intraclastic and Peloidal Wackestone-Packstone-Grainstone-Rudstone, Well-H, 6423.5.

B. HMF 4a (low energy, *Lithocodium aggregatum* large oncoids): *Lithocodium*, Intraclastic and Peloidal Wackestone-Packstone-Grainstone-Rudstone, Well-H, 6418.5'.

Plate 90

A. HMF 4a (low energy, *Lithocodium aggregatum* large oncoids): *Lithocodium*, Intraclastic and Peloidal Wackestone-Packstone-Grainstone-Rudstone, Well-H, 6420.6’. Microbialite pellets from *Lithocodium* microbialite activity on skeletal grains.

B. HMF 4a (low energy, *Lithocodium aggregatum* large oncoids): *Lithocodium*, Intraclastic and Peloidal Wackestone-Packstone-Grainstone-Rudstone, Well-H, 6422.5’.

Plate 91

A. HMF 4b (high energy, *Lithocodium aggregatum* smaller oncoids): *Lithocodium*, Intraclastic and Peloidal Wackestone-Packstone-Grainstone-Rudstone, Well-H, 6404.3‘. This microfacies has potential reservoir quality with intermediate to highly porous moldic (Mo), interparticle (IP) and intraparticle (BP) porosities, with a range of porosity from 5% to 20%.

B. HMF 4b (high energy, *Lithocodium aggregatum* smaller oncoids): *Lithocodium*, Intraclastic and Peloidal Wackestone-Packstone-Grainstone-Rudstone, Well-H, 6404.3‘.

Plate 92

A. HMF 5: *Terebella*, *Crescentiella*, *Ophthalmidium* and Allochthonous Bio-lithoclastic Packstone/Grainstone , Well-H, 6417.6‘. Fine grained packstone and grainstone formed of allochthonous peloids, ooids, coated grains, lithoclastics and allochthonous benthic foraminifera. These are an admixture of reworked sediments transported by gravity flows from both the platform interior and platform margin.

B. HMF 5: *Terebella*, *Crescentiella*, *Ophthalmidium* and Allochthonous Bio-lithoclastic Packstone/Grainstone , Well-H, 6417.6‘. This has has potential reservoir quality with highly porous (~20%) with both interparticle (BP) and intraparticle (IP) porosities.

Plate 93

A. HMF 5: *Terebella*, *Crescentiella*, *Ophthalmidium* and Allochthonous Bio-lithoclastic Packstone/Grainstone, Well-B, 8388.8'. *Crescentiella morronensis* forma *morronensis* cortex surrounding *Nodobacularia* sp.

B. HMF 6: Laminated Peloidal Packstone/Grainstone/Bindstone, Well-H, 6408.1'. Fine, very well-sorted peloidal grainstone has a potential reservoir quality with an interparticle (IP) porosity of ~5%.

Plate 94

A. HMF 6: Laminated Peloidal Packstone/Bindstone, Well-H, 6406.4'. Encrusting *Lithocodium* piece.

B. HMF 6: Laminated Peloidal Packstone/Bindstone, Well-H, 6405.3'. This microfacies is characterized by alternations of micrite and fine peloidal laminations. It is composed of fine grained packstone and grainstone.

Plate 95

A. F 1: Spiculite, Calcisiltite Wackestone, Well-D, 8609.7'. This microfacies has very poor reservoir quality as it contains no porosity. It is characterised by deeper slope microfossils that includes common echinoderms, triaxon spicules, monaxon spicules, planktonic foraminifera (*Conoglobigerina* sp. cf. *C. gulekhensis*) and calpionellids.

B. DMF 1: Spiculite, Calcisiltite Wackestone, Well-D, 8644.2. This microfacies is characterised by deeper slope microfossils that includes

common echinoderms, triaxon spicules, monaxon spicules, planktonic foraminifera (*Conoglobigerina* sp. cf. *C. gulekhensis*) and calpionellids.

Plate 96

A. DMF 2: Extraclastic, *Nodosaria, Lenticulina* and *Saccocoma* Packstone, Well-D, 8642.7'. It is composed of angular, well-sorted lithoclasts and echinoderm fragments. The main matrix is transported lithoclasts in the form of microbreccia. Oil stains are common and implicating fair porosity. This microfacies has fair reservoir quality as it contains reasonable levels of porosity that is evident from the oil staining (brown colour staining).

B. DMF 2: Extraclastic, *Nodosaria, Lenticulina* and *Saccocoma* Packstone, Well-D, 8642.7'. Higher close-up on the microfacies.

Plate 97

A. DMF 3: Slope-Laminated Peloidal Bindstone/ Wackestone/ Packstone, Well-D, 8635.2'. This microfacies is densely packed and has poor reservoir quality as it contains no visible porosity. Chemical compaction and stylolite are very common.

B. DMF 3: Slope-Laminated Peloidal Bindstone/ Wackestone/ Packstone, Well-D, 8635.2'. It is common planktonic foraminifera (*Conoglobigerina* sp. cf*. C. gulekhensis*).

Plate 98

A. DMF 3: Slope-Laminated Peloidal Bindstone/ Wackestone/ Packstone, Well-D, 8635.2'. A close-up view of the planktonic foraminifera (*Conoglobigerina* sp. cf*. C. gulekhensis*).

B. DMF 3: Slope-Laminated Peloidal Bindstone/ Wackestone/ Packstone, Well-D, 8635.2'. A close-up view of the planktonic foraminifera (*Conoglobigerina* sp. cf*. C. gulekhensis*).

Plate 99

A. DMF 4: *Lenticulina*, Oyster, Peloidal Packstone, Well-D, 8630.7'. The texture is abundant with very well sorted fine peloids and it is the main matrix. This microfacies is characterised by *Lenticulina* spp. and transported Platform Margin microfossils such as gastropods, oyster type of bivalves, echinoderms and agglutinated foraminifera.. The microfacies has poor porosity with (<3%). It is commonly represented by a moldic (MO) porosity.

B. DMF 5: *Lenticulina*, Saddle Dolomite Wackestone, Well-D, 8620.2'. This microfacies texture has mainly that of wackestone. The crystalline saddle dolomite is secondary that has possibly been developed by hydrothermal fluids. The main matrix in this lithofacies is very dolomitic, dense micrite. Solution seams and microstylolites are very common. This microfacies is characterised by slope microfossils that include *Lenticulina* spp., *Nodosaria* spp., *Everticyclammina virguliana* and *Pseudocyclammina lituus*.

Plate 100

A. DMF 6: *Protopeneroplis*, Peloidal WackestoneWell-D, 8611.2’. This microfacies texture is mainly that of peloidal wackestone. The well sorted fine peloids were created within the back-shoal side of the protected open marine floor and they are probably localised as a result of the very low energy conditions. This microfacies is characterised by sheltered open marine microfossils that is include common gastropods, bivalves, echinoderm fragments, *Protopeneroplis ultragranulata*, *P. lituus* and thin-shelled ostracods.

B. DMF 6: *Protopeneroplis*, Peloidal WackestoneWell-D, 8611.2’. The microfacies has low reservoir quality as it contains no porosity.

Plate 101

A. DMF 7: Foraminifera, Peloidal Mud-lean Packstone, Well-D, 8584.2’. Texture is almost completely that of a mud-lean packstone. It is mainly formed of very fine and very well-sorted peloids. Bioclastic contents have been coated by micrite envelopes as a result of microbial activity. The reservoir quality is poor as a result of the calcite cemented fabric

B. DMF 7: Foraminifera, Peloidal Mud-lean Packstone, Well-D, 8584.2’. This microfacies is characterised by inner-shoal foraminifera with high diversity. It contains abundant, and variable, miliolids and other benthic, agglutinated foraminifera.

Plate 102

A. DMF 8: *Nodosaria*, Peloidal Microstylolitic/Dolomitic Grainstone /Bindstone, Well-D, 8563.2'. This microfacies is characterized by alternations of dolomitic, microstylolitic laminae with very well-sorted, fine peloidal laminations. Texture is mainly that of a peloidal grainstone, where peloids and dolomite crystals are the main constituents. This microfacies has common signs of chemical dissolution and compaction. The microfacies has poor to fair porosities (~ 3%). The porosities have been destroyed by the chemical compaction and the stylolites. These laminae are densely packed and this results in poor reservoir quality; there is no visible porosity.

B. DMF 8: *Nodosaria*, Peloidal Microstylolitic/Dolomitic Grainstone /Bindstone, Well-D, 8563.2'. The most important recorded microfossil is *Nodosaria* spp.

Plate 103

A. DMF 9: Peloidal, Reworked-Skeletal Wakestone, Well-D, 8558.7'. This microfacies texture is mainly that of wakestone. Transported and reworked peloids and skeletal fragments are the main constituents. Planktic foraminifera (*Conoglobigerina* sp. cf. *C. gulekhensis*), are relatively common. The microfacies is characterised by (IP) inter-particle porosity ranging from 3 % - 15%.

B. DMF 10: *Conoglobigerina* sp., Extraclastic, Peloidal Wakestone, Well-D, 8542.2'. This microfacies is that of wackestone and it is abundant

with well sorted fine peloids. The lithofacies is characterised by very poor moldic (Mo) porosity.

Plate 104

A. DMF 11: *Lenticulina*, Peloidal Wackestone to Packstone , Well-D, 8540.7’. This microfacies texture is mainly that of wackestone. The main matrix in this lithofacies is micrite that is abundantly recorded with moldic porosity. It is characterised by the presence of very well-sorted peloids that were created within the lagoon floor.

B. DMF 11: *Lenticulina*, Peloidal Wackestone to Packstone , Well-D, 8540.7’. This microfacies is characterised by slope microfossils that include common *Lenticulina* spp ; very common fragments and debris of molluscs and echinoderms; rare polymorphinids; and commonly transported *Nautiloculina* spp. from the lagoonal environment.

Plate 105

A. DMF 12: Superficial Ooid Grainstone , Well-D, 8406.2’. The main matrix is micritized concentric ooids with an abundant syntaxial cement growth surrounding echinoderm plates. Well-sorted concentric ooids have been created within the shallow shoal and attributed to the very high energy conditions and the agitation of waves and currents within the platform sand bank. This microfacies has very good reservoir quality in which it contains interparticle (IP) porosity ranging from 15% to 25 %. Meniscus cements, suggesting emergence, are formed in this environment by a relatively sharp fall in sea level.

B. DMF 13: Leached Superficial Ooid Grainstone, Well-D, 8410.7’. The main matrix is leached concentric ooids that is characterised by an abundant syntaxial cement growth surrounding echinoderm plates. This microfacies has very good reservoir quality in which it contains moldic (MO) and interparticle (IP) porosity above 25 %. This is may indicate a subaerial exposure surface and possibly a sequence boundary.

Plate 106

A. DMF 14: Peloidal, Coated Bioclastics Packstone and Grainstone, Well-D, 8392.7’. This microfacies texture is mainly that of packstone and grainstone. Micritised peloids, ooids and coated skeletal fragments are the main constituents in association with common rounded lithoclasts and microbial micritization. This microfacies has very good reservoir quality in which it contains moldic (MO) and interparticle (IP) porosity ranging from 10 to 25 %.

B. DMF 14: Peloidal, Coated Bioclastics Packstone and Grainstone, Well-D, 8392.7’. This microfacies is characterised by Platform Margin microfossils that include oyster bivalves and *Protopeneroplis* spp. and *P. Lituus.*

Plate 107

A. DMF 14: Peloidal, Coated Bioclastics Packstone and Grainstone, Well-D, 8392.7’. This microfacies is characterised by Platform Margin microfossils that include oyster bivalves and *Protopeneroplis* spp. and *P. Lituus.*

B. DMF 15: Lithocodium Boundstone, Well-D, 8385.2'. This microfacies texture is mainly that of boundstone to packstone. It is mainly composed of *Lithocodium aggregatum* large oncoids indicating categories 3 and 4 of Vědrine *et al*. (2007) and Michetiuc *et al*. (2012), in which they are characterized by encrusting microbial meshwork shapes. This microfacies has very good reservoir quality in which it contains moldic (MO) and intraparticle (IP) porosity above 15 %.

Plate 108

A. DMF 16: Non-Laminated Peloidal, Miliolids Grainstone, Well-D, 8320.7'. This microfacies texture is mainly that of grainstone. The main matrix is clean fine, very well-sorted peloids that is abundant by syntaxial cement growth surrounding echinoderm plates. The very well sorted peloids have been created within the lagoonal floor. This microfacies has very good reservoir quality in which it contains interparticle (IP) porosity of up to 20 %. This microfacies is characterised by lagoonal microfossils that include abundant *Quinqueloculina* spp, rare *Textulariopsis jurassica* and echinoderm fragments with syntaxial cement overgrowth.

B. DMF 17: Peloidal Intraclastic Skeletal Grainstone , Well-D, 8295.7'. This microfacies texture is mainly that of grainstone. The main matrix is of non-laminated, fairly sorted, intraclastic, peloidal, *Quinquloculina* grainstone. This microfacies is associated with reworked lithoclasts and coated skeletal fragments. These are very well-sorted peloids and minor to poorly sorted, sub-rounded lithoclasts. This microfacies has

very good reservoir quality in which it contains moldic (MO) and interparticle (IP) porosity above 30%.

Plate 109

A. DMF 17: Peloidal Intraclastic Skeletal Grainstone , Well-D, 8295.7. Note the high porosity and the grain sorting.

B. DMF 18: Poorly sorted, Intraclastic Grainstone to Rudstone, Well-D, 8249.7‘. This microfacies texture is mainly that of sparry calcite cemented rudstone and grainstone. The main matrix is leached out, poorly sorted, intraclastic peloids and coated reef skeletal fragments (such as *Macroporella praturloni*, encrusting type of *Lithocodium aggregatum* and oyster bivalves) by micritic envelopes. This microfacies has poor reservoir quality in which it contains a moldic (MO) porosity ~ 3 %.

Plate 110

A. DMF 18: Poorly sorted, Intraclastic Grainstone to Rudstone, Well-D, 8249.7. This microfacies is characterised by platform margin microfossils *Macroporella praturloni*, encrusting type of *Lithocodium aggregatum* and the oyster bivalves.

B. DMF 18: Poorly sorted, Intraclastic Grainstone to Rudstone, Well-D, 8249.7. This microfacies is characterised by platform margin microfossils such as *Mohlerina basiliensis.*

Plate 1

A. *Troglotella incrustans* Wernli and Fookes (1992) in *Lithocodium aggregatum* Elliott, 1956, Well-B, 8425.9', field of view 2.5 mm.

B. *Troglotella incrustans* Wernli and Fookes (T) (1992) in *Lithocodium aggregatum* Elliott, 1956, Well-G, 6761.3', field of view 6.3 mm.

Plate 1

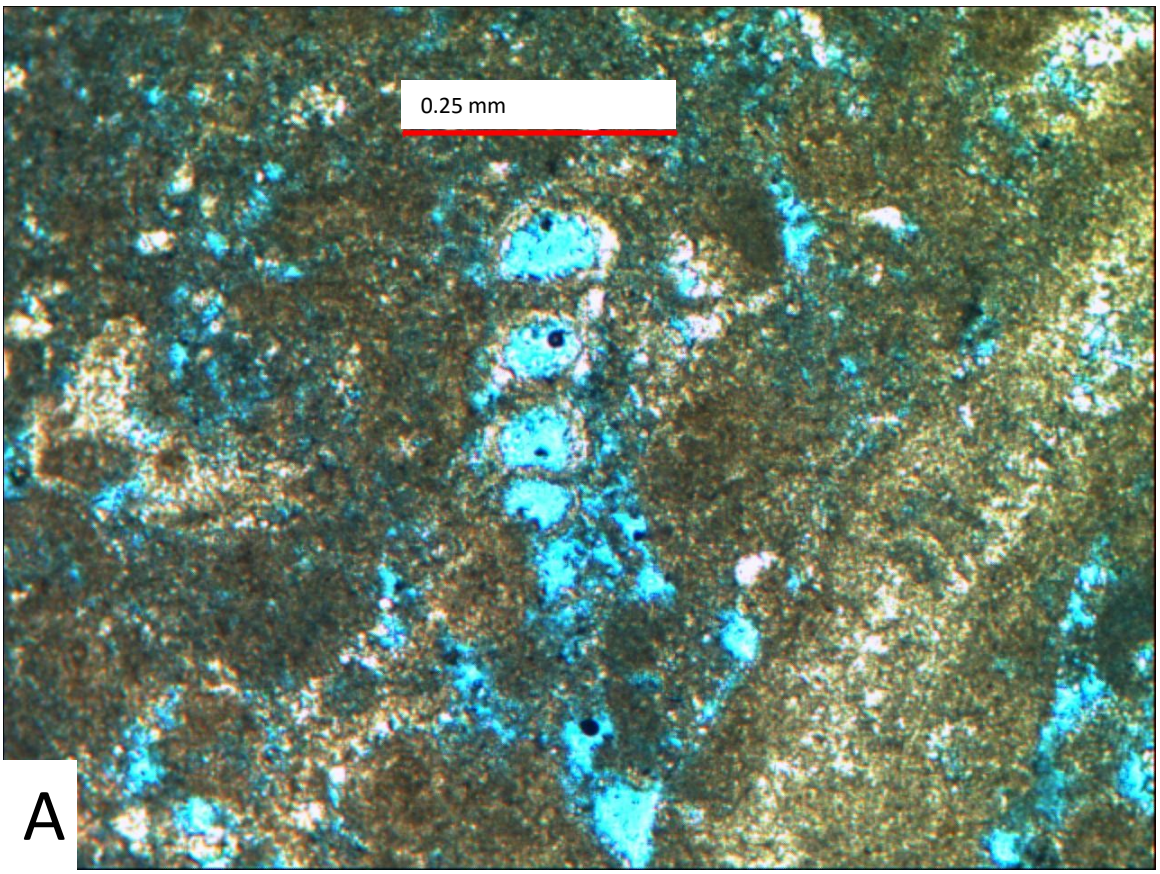

A

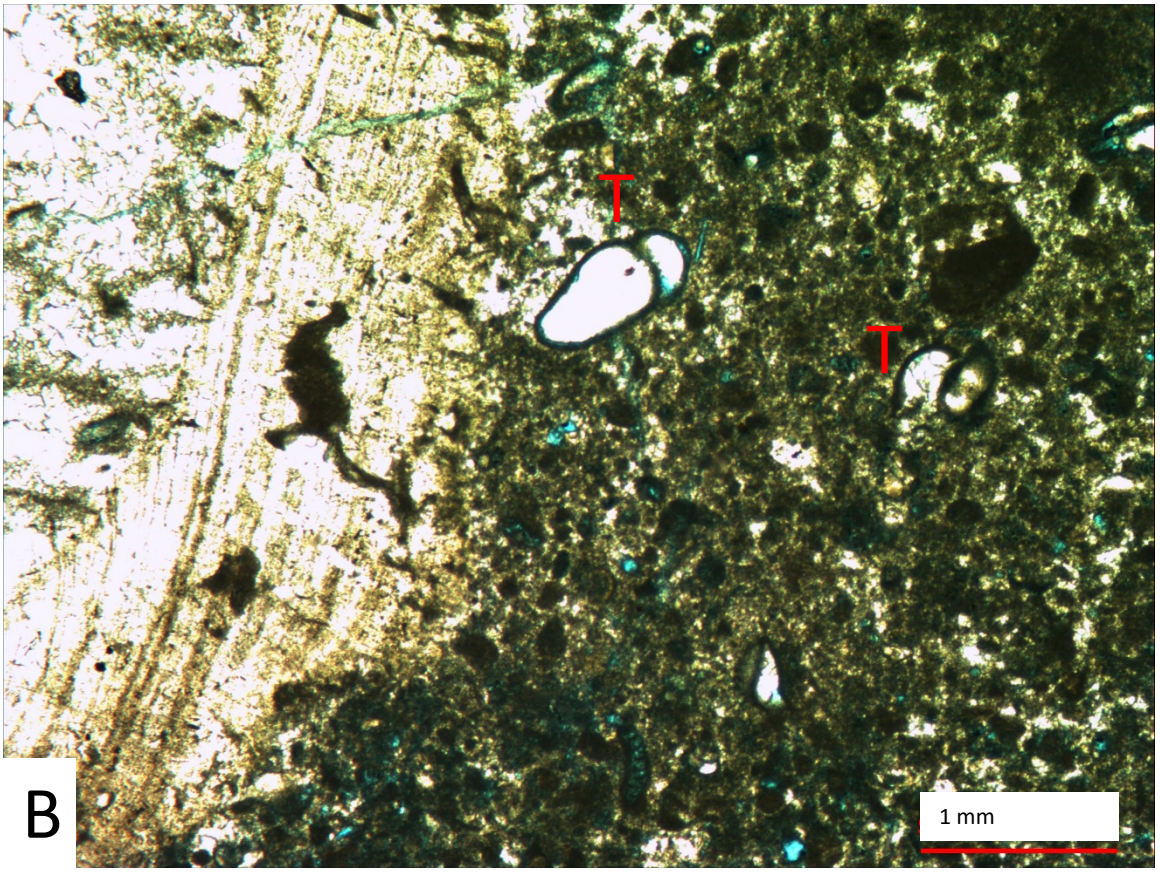

B

Plate 2

A. *Troglotella incrustans* (T) Wernli and Fookes (1992) in *Lithocodium aggregatum* (LCe) Elliott, 1956, Well-G, 6768.5', field of view 6.3 mm.

B. *Troglotella incrustans* (T) Wernli and Fookes (1992) in encrusting *Lithocodium aggregatum* (LCe) Elliott (1956) on bivalve shell, microbial micritization of encrusting *Lithocodium aggregatum* Elliott and *Troglotella incrustans* Wernli and Fookes borings have been intensive on weak parts of the shell, Well-I, 5524.2'.

Plate 2

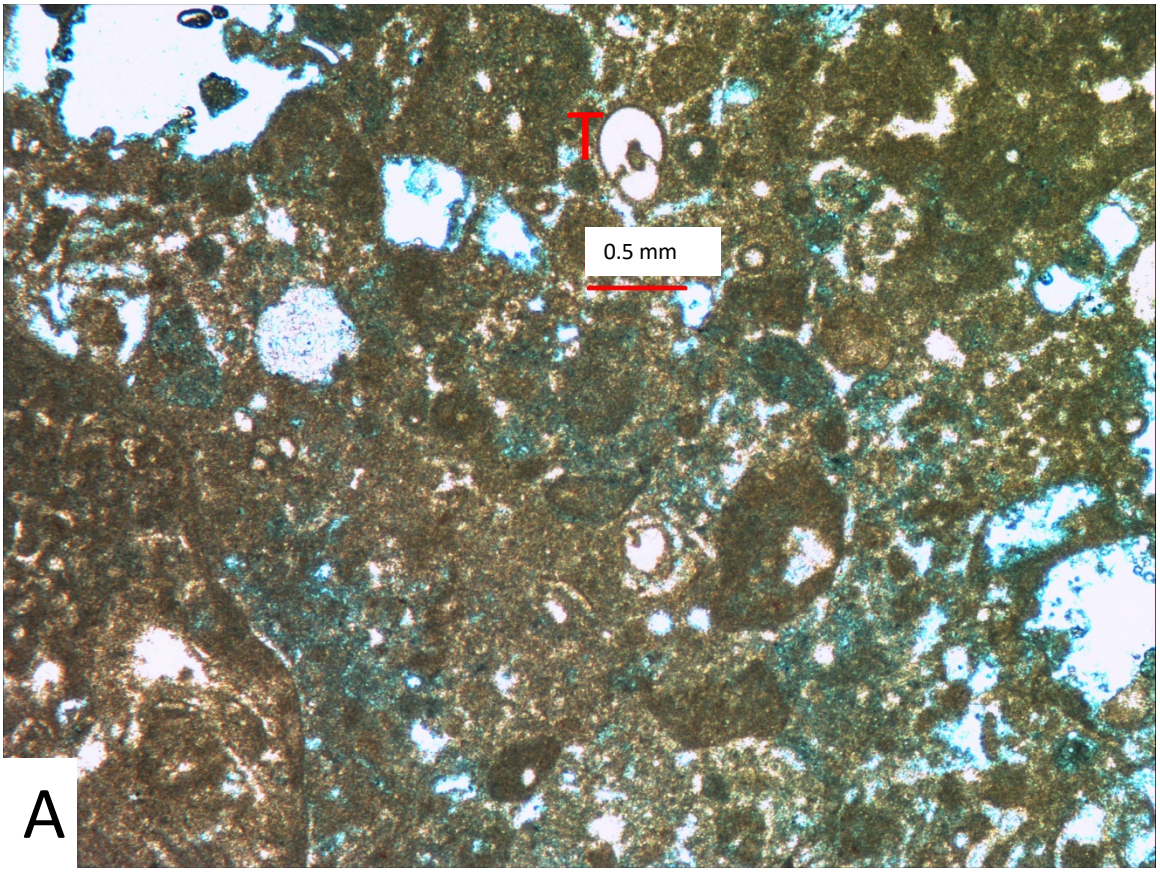

A

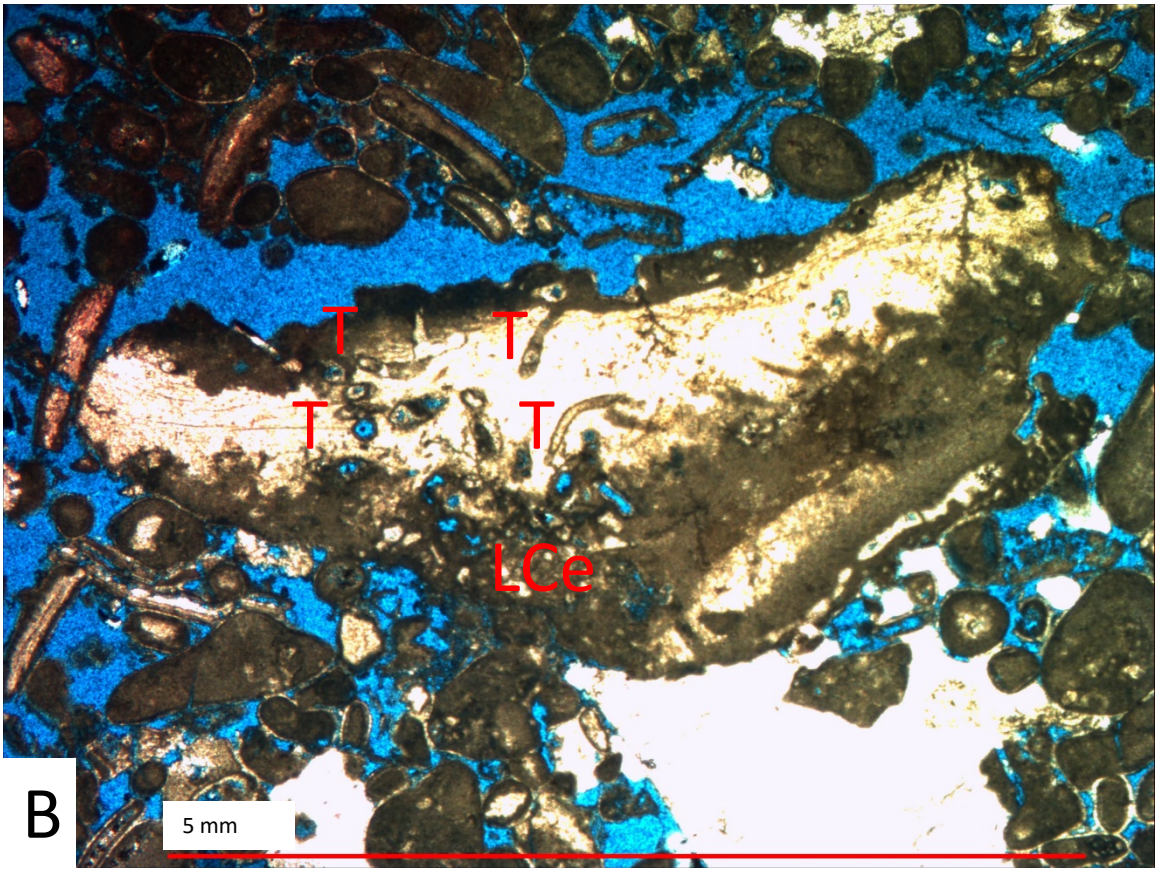

B

Plate 3

A. *Troglotella incrustans* (T) Wernli and Fookes (1992) in *Lithocodium aggregatum* (LCe) Elliott, 1956, Well-H, 7325.5', field of view 6.3 mm.

B. *Conoglobigerina* sp. cf. *C. gulekhensis* (Cq) (Gorbatchik and Poroshina 1979), Well-D, 8630.7', field of view 2.5 mm. Three specimens in laminated peloidal bindstone.

Plate 3

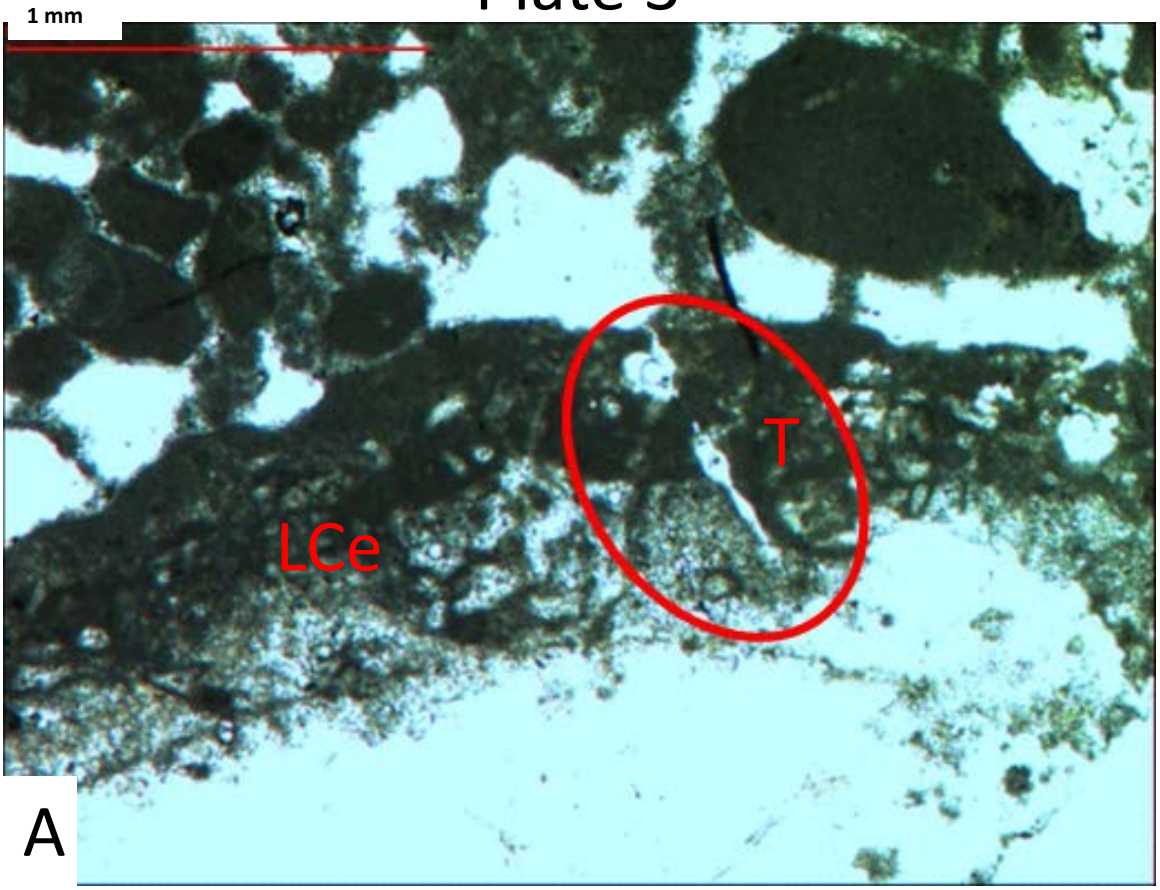

A

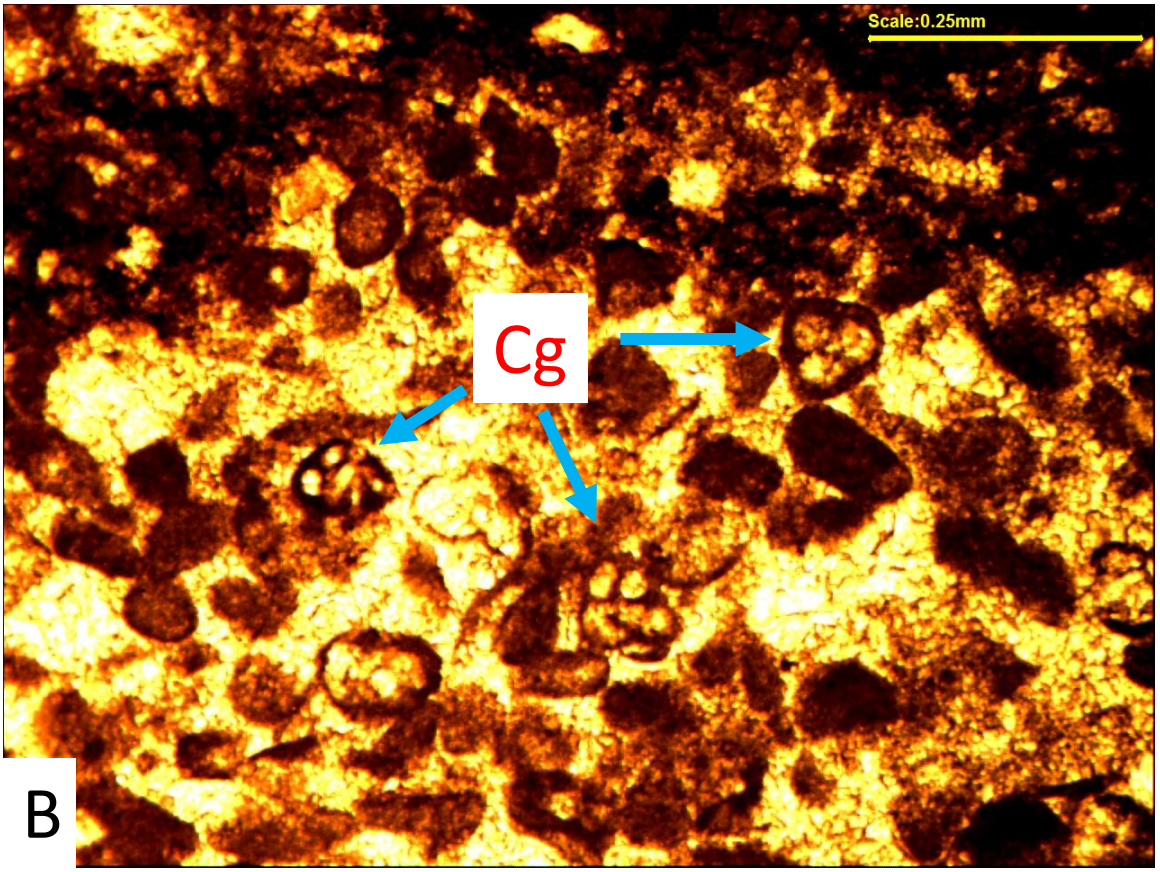

B

Plate 4

A. *Conoglobigerina* sp. cf. *C. gulekhensis* (Gorbatchik and Poroshina, 1979), Well-D, 8587.2', field of view 2.5 mm. Associated with monaxon spicules in tempestitic, laminated peloidal bindstone.

B. *Conoglobigerina* sp. cf. *C. gulekhensis* (Gorbatchik and Poroshina, 1979), a close-up image, width (0.14 mm), length (0.144 mm), Well-D, 8587.2', field of view 1.25 mm. Associated with monaxon spicules in tempestitic, laminated peloidal bindstone.

Plate 4

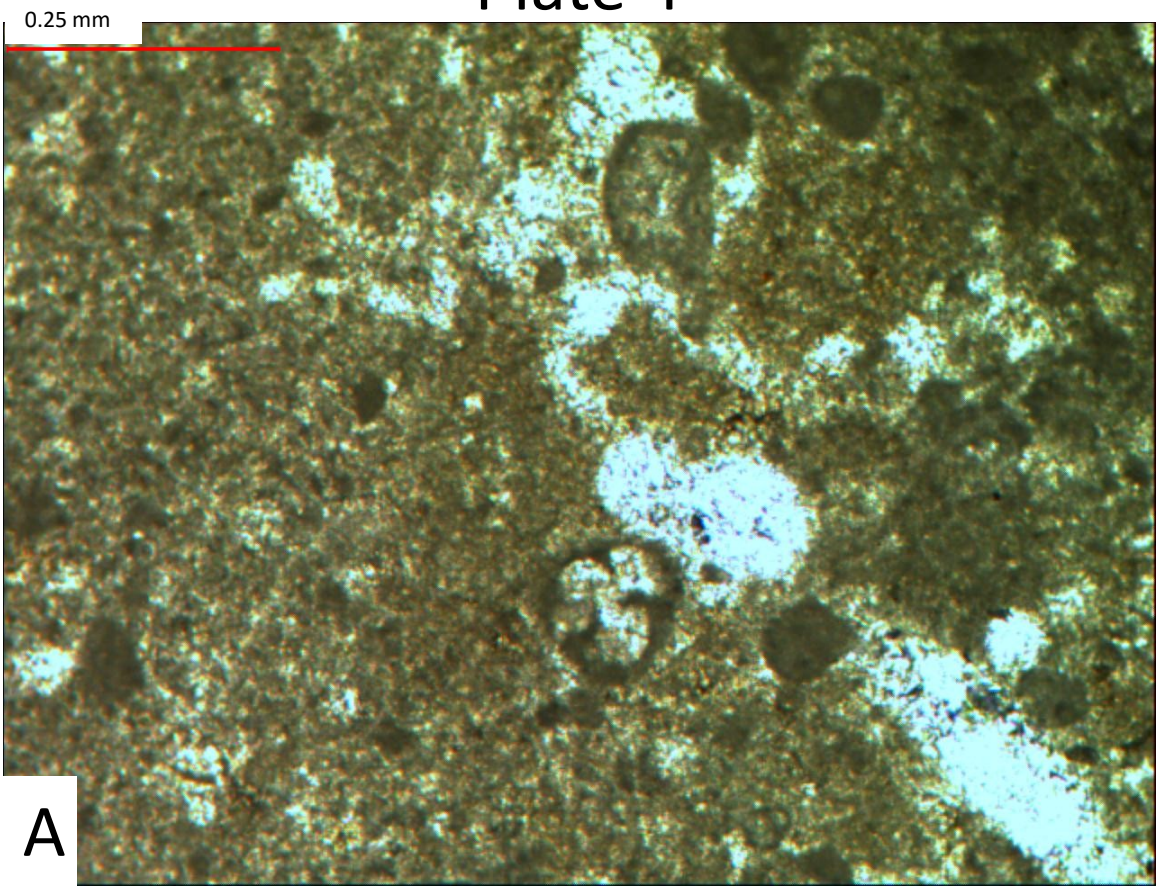

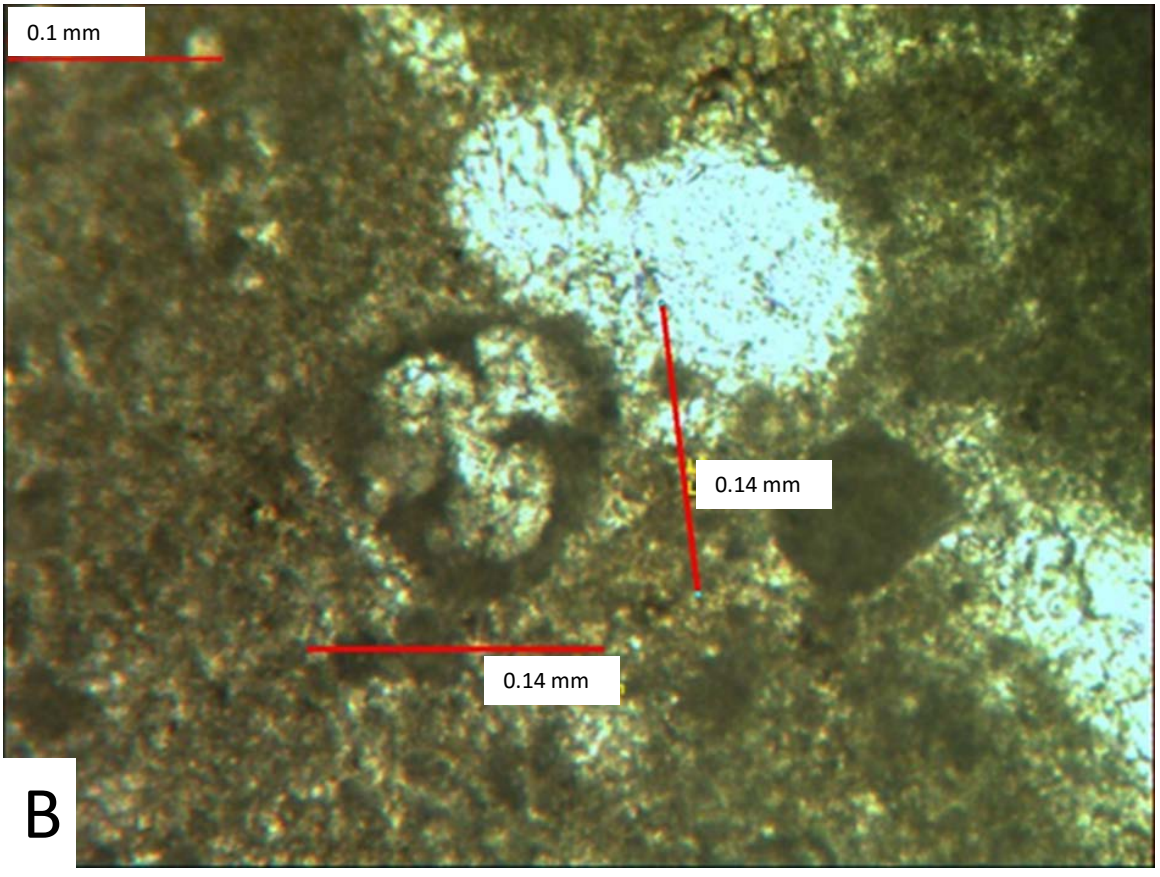

Plate 5

A. *Conoglobigerina* sp. cf. *C. gulekhensis* (Gorbatchik and Poroshina, 1979), a close-up image, maximum width is 0.25 mm, Well-D, 8639.7', field of view 2.5 mm. Associated with monaxon spicules in tempestitic, laminated peloidal bindstone.

B. *Conoglobigerina* sp. cf. *C. gulekhensis* (Gorbatchik and Poroshina, 1979), close-up from image A.

Plate 5

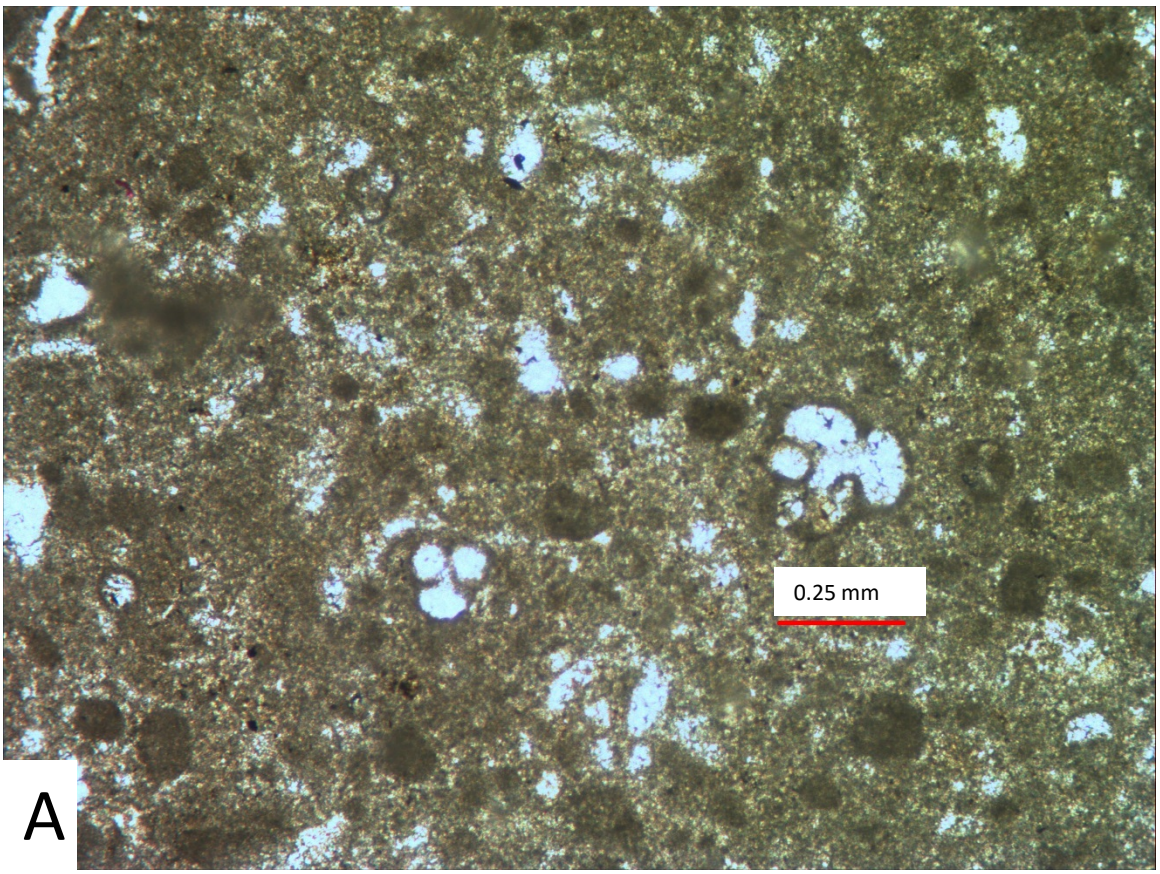

A

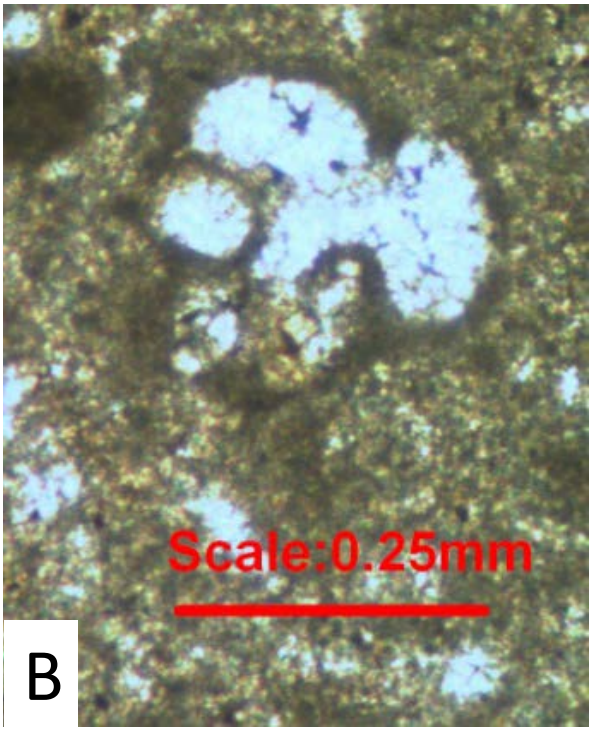

B

Plate 6

A. *Coscinoconus alpina* Leupold, 1935, Well-H, 6427.5', field of view 2.5 mm. The blue colour is voids.

B. *Coscinoconus alpina* Leupold, 1935, Well-H, 6421.5', field of view 2.5 mm. The blue colour is voids.

Plate 6

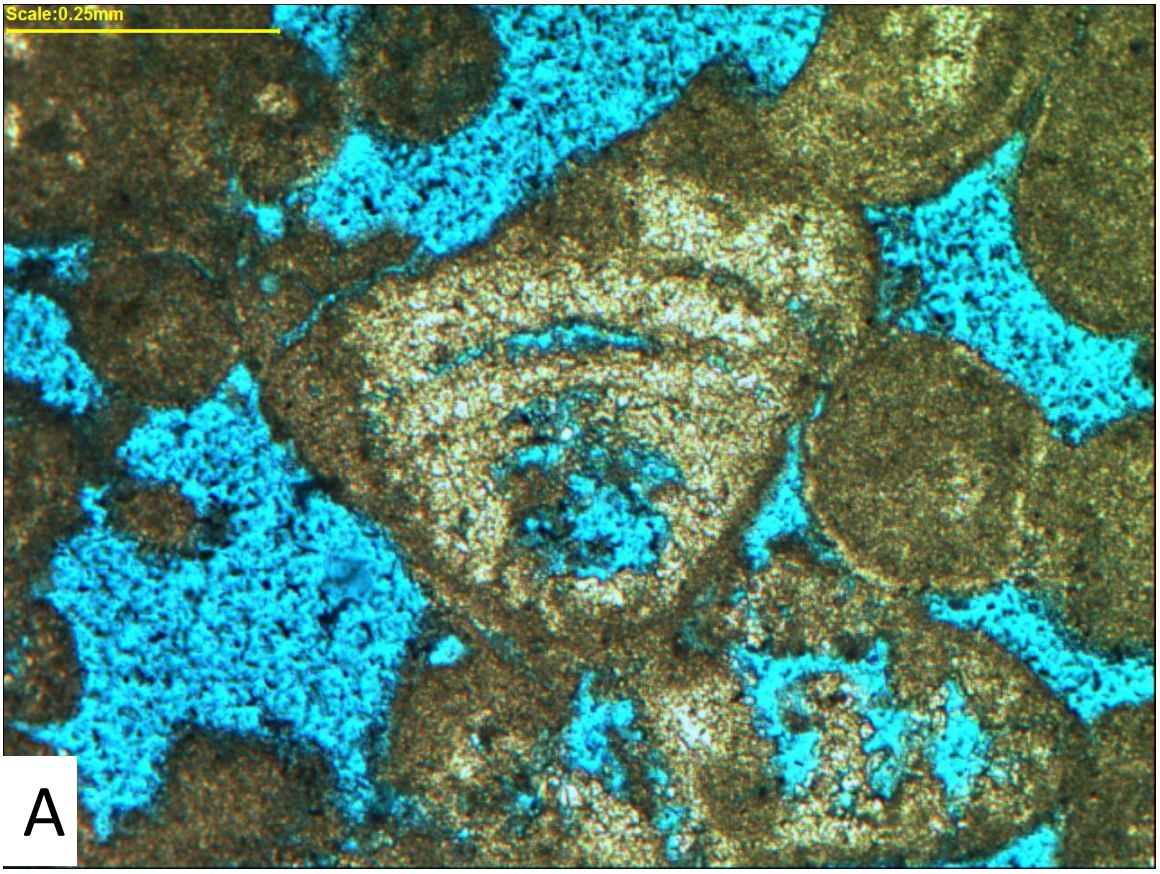

A

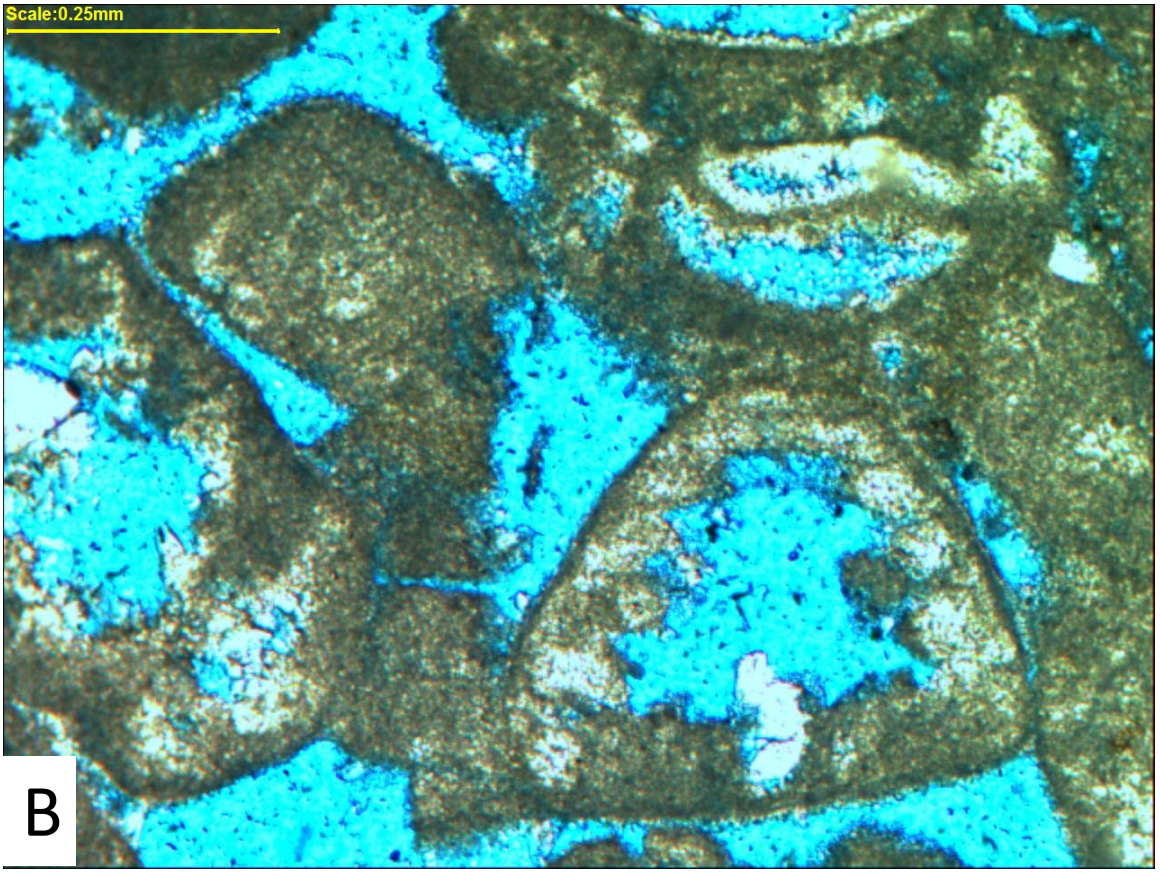

B

Plate 7

A. *Coscinoconus alpina* Leupold (1935), Well-F, 8390.5', field of view 6.3 mm.

B. *Coscinoconus alpina* Leupold (1935), Well-H, 6417.6', field of view 2.5 mm.

Plate 7

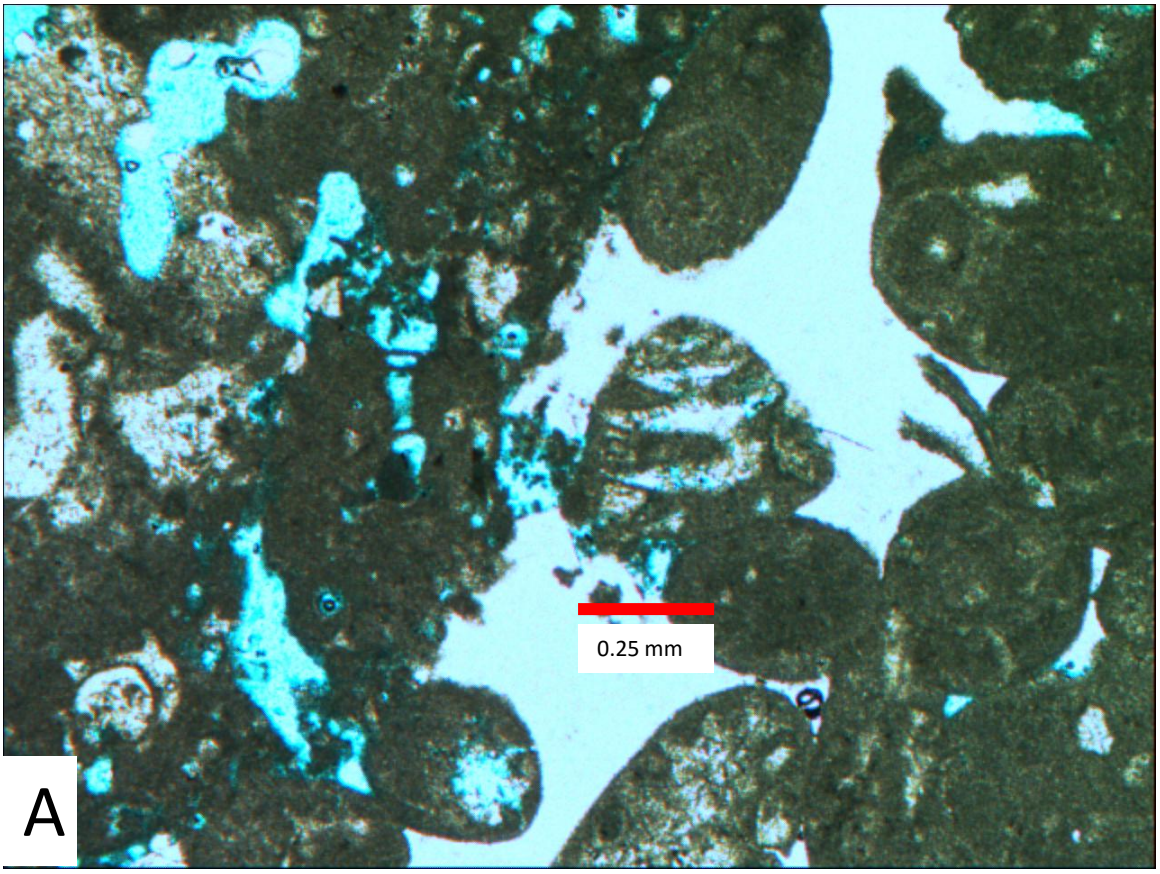

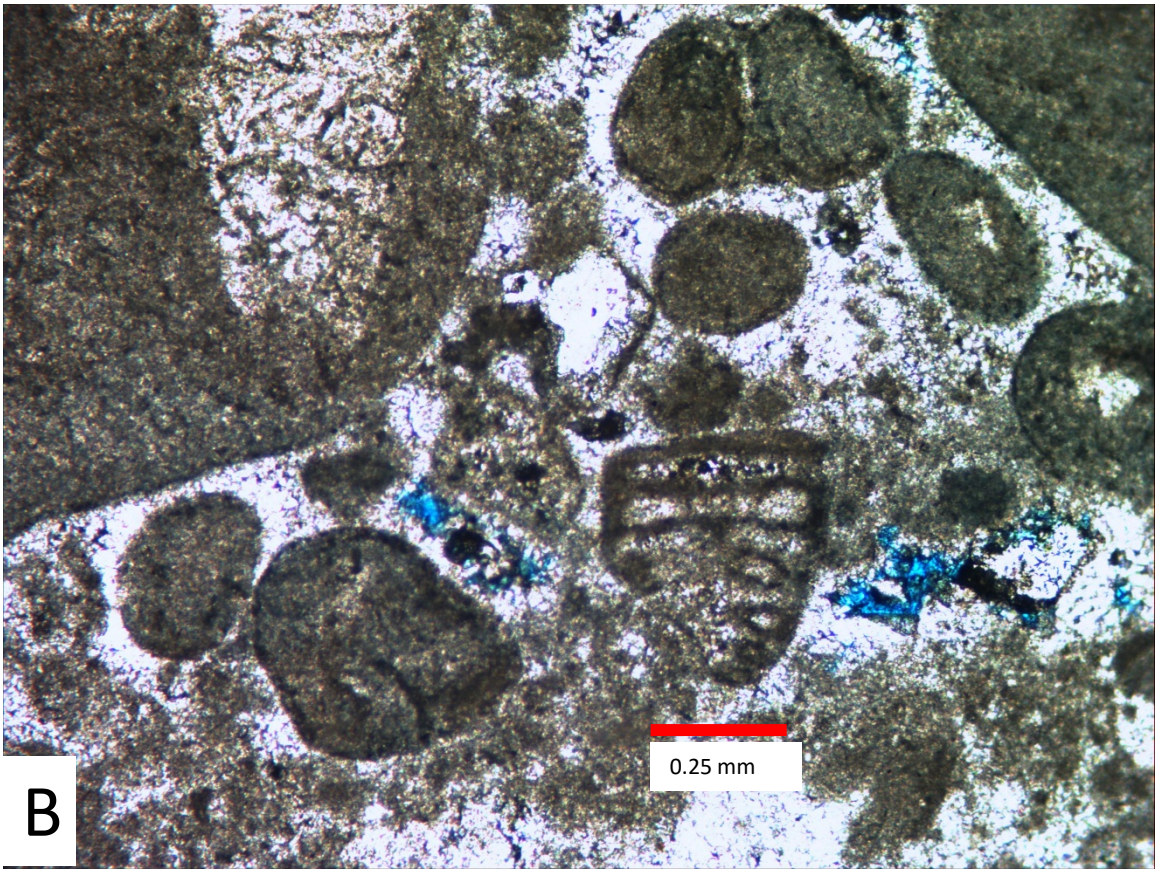

Plate 8

A. *Coscinoconus delphinensis* (Arnaud-Vanneau *et al*., 1988), Well-H, 6422.5, field of view 2.5 mm.

B. *Coscinoconus delphinensis* (Arnaud-Vanneau *et al.*, 1988), Well-H, 6422.5, field of view 6.3 mm.

Plate 8

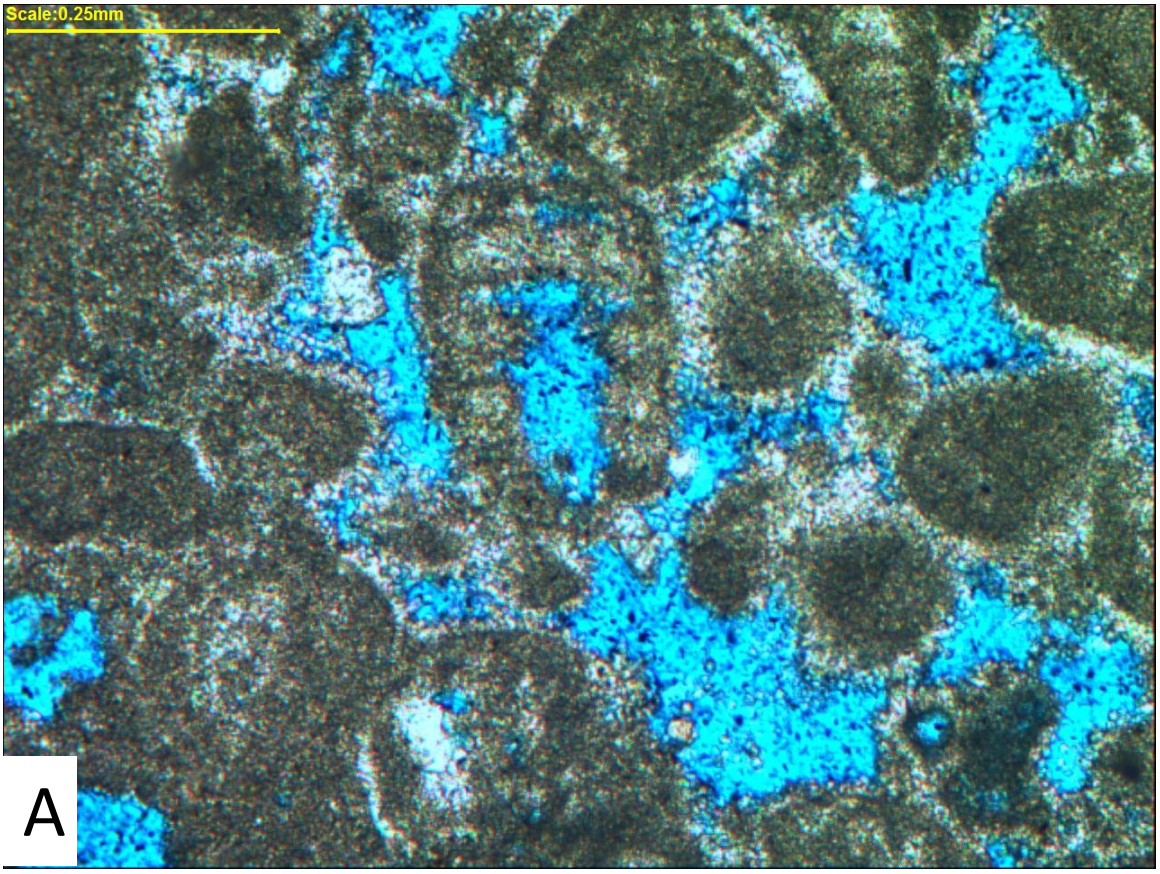

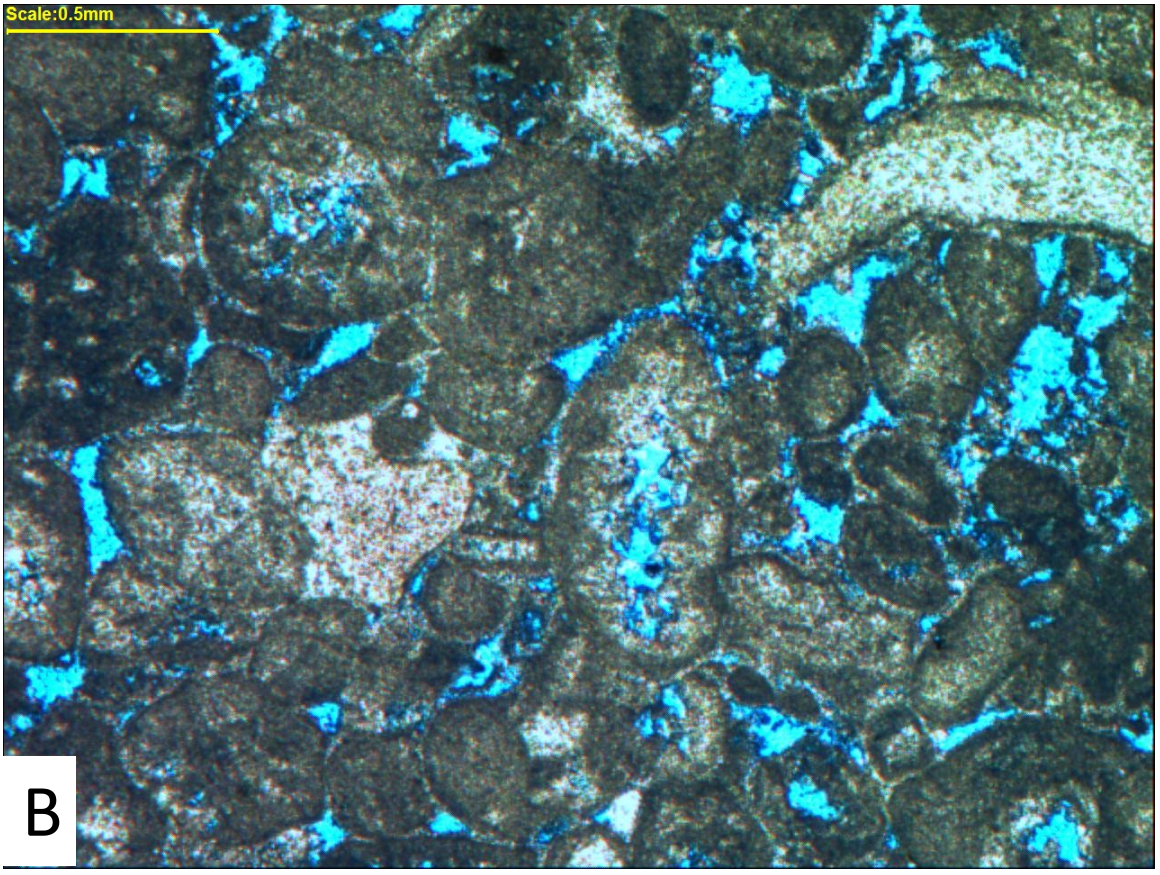

Plate 9

A. *Coscinoconus delphinensis* (Arnaud-Vanneau *et al*., 1988), Well-H, 6422.5', field of view 2.5 mm.

B. *Coscinoconus delphinensis* (Arnaud-Vanneau *et al*., 1988), Well-H, 6422.5', field of view 6.3 mm.

Plate 9

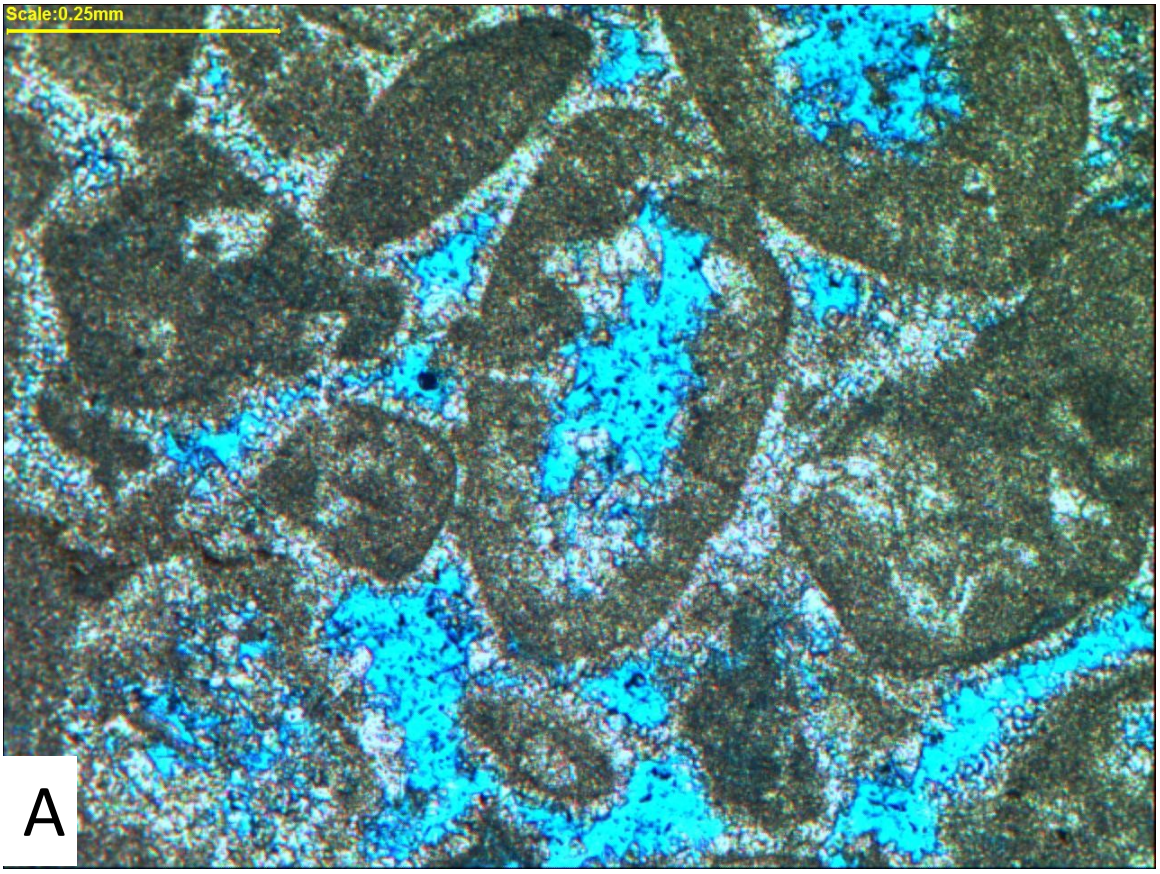

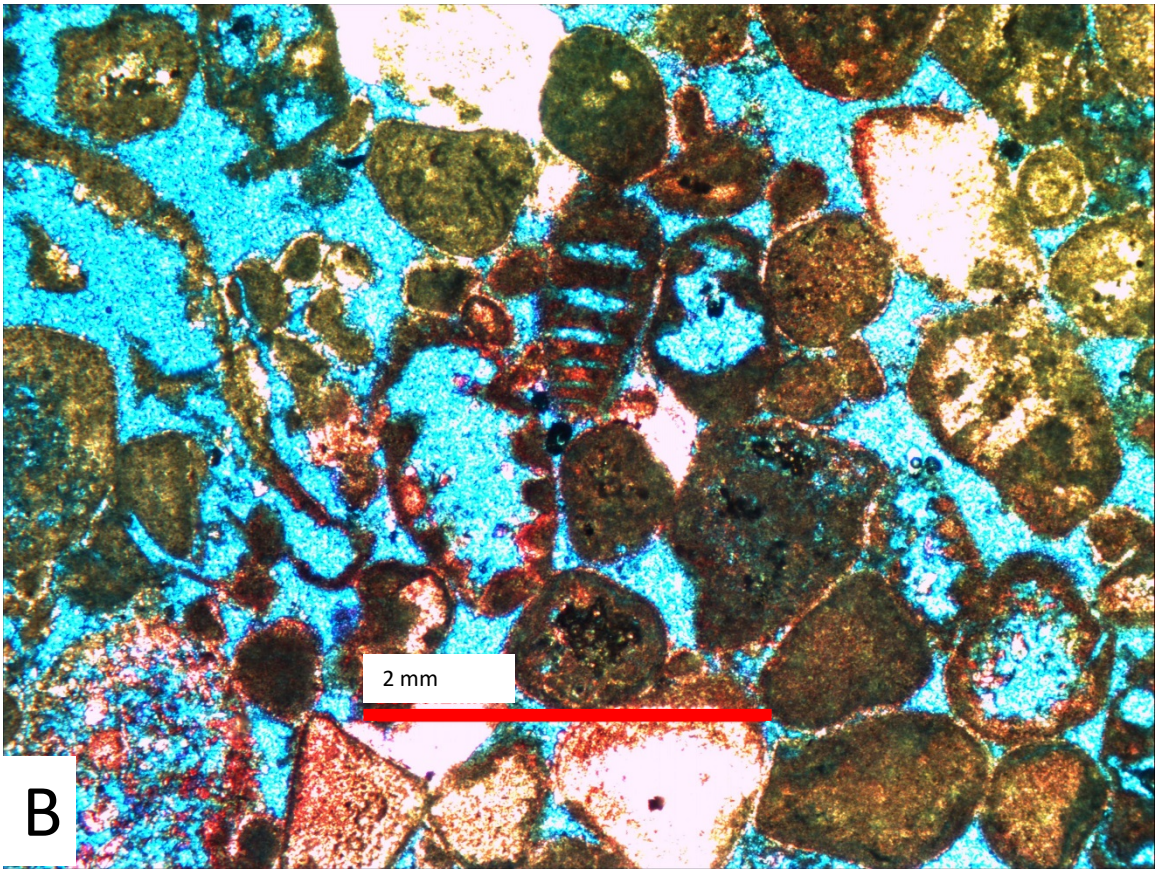

Plate 10

A. *Coscinoconus elongata* (Leupold, 1935), Well-G, 6765.4', field of view 2.5 mm.

B. *Coscinoconus elongata* (Leupold, 1935), Well-F, 8390.5', field of view 6.3 mm.

Plate 10

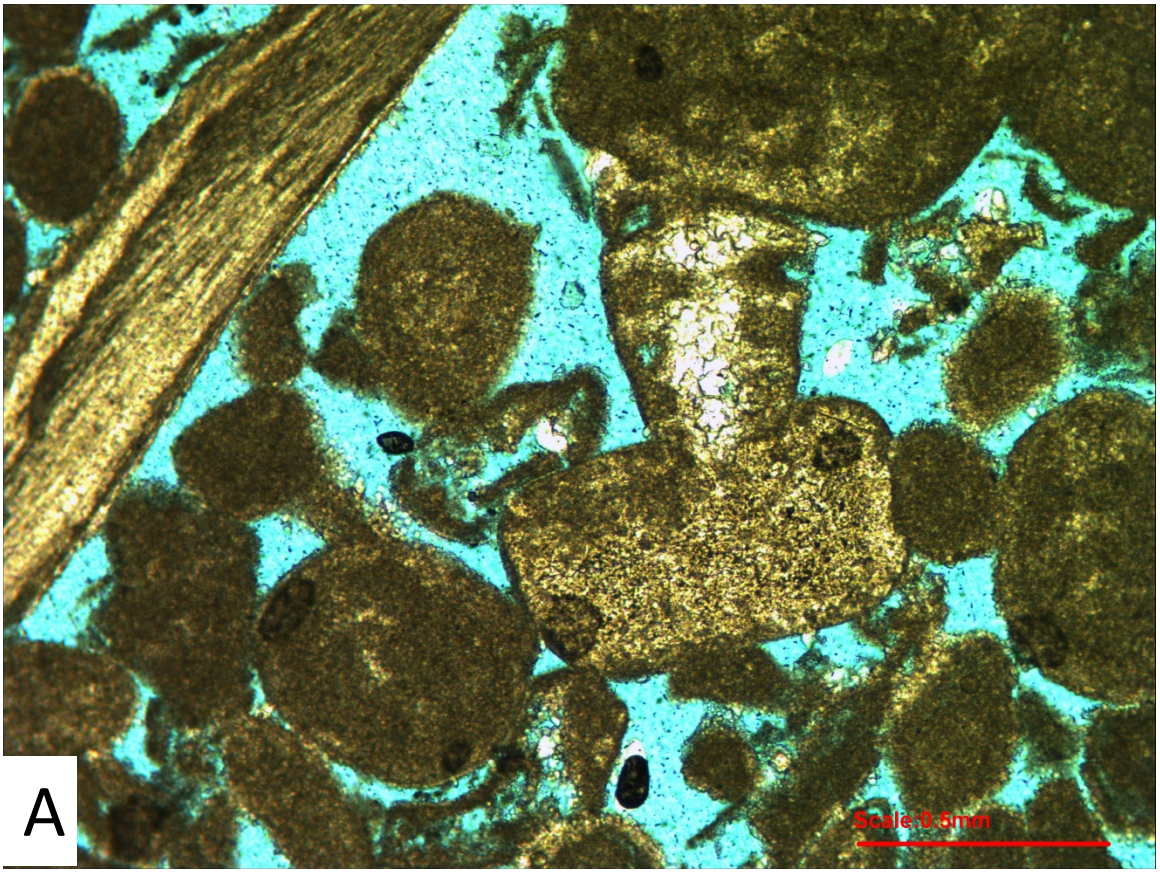

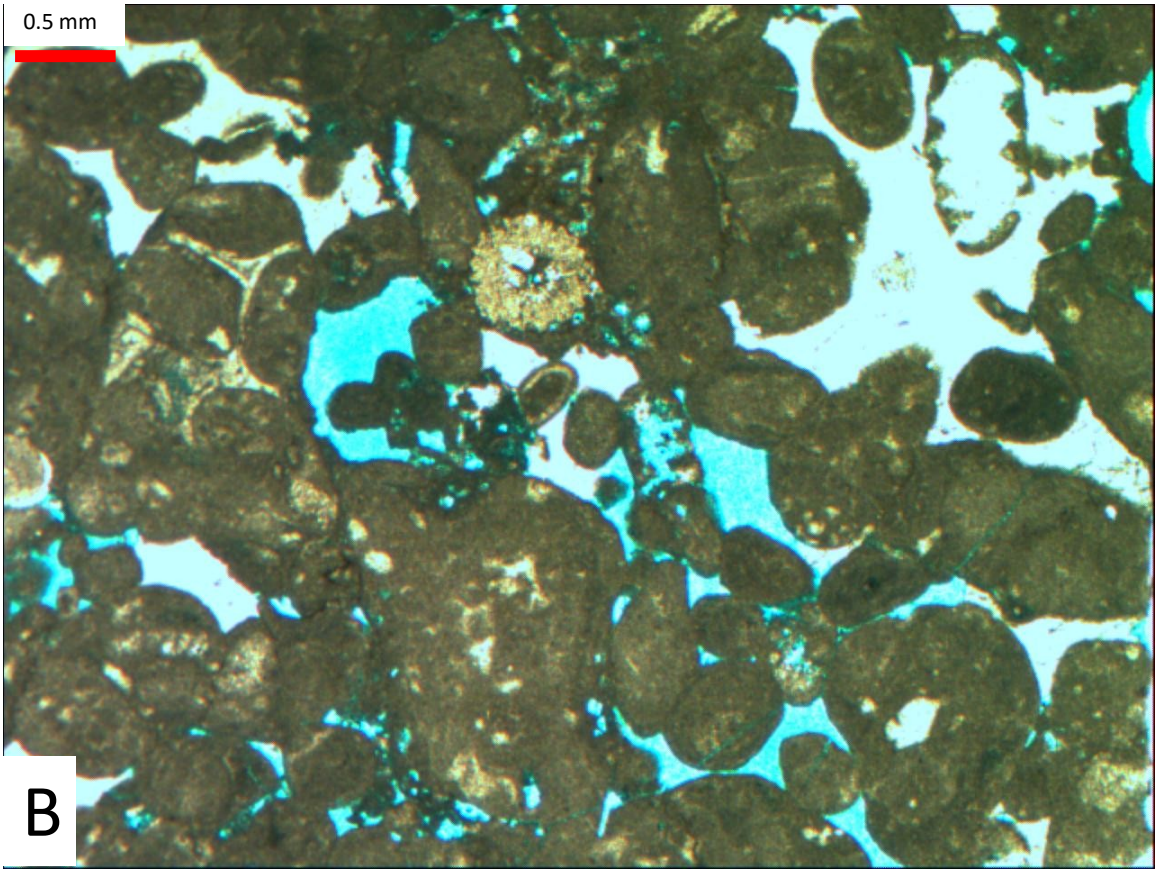

Plate 11

A. *Coscinoconus cherchiae* Arnaud-Vanneau *et al.* (1988), Well-D, from the base of the Yamama Formation, 8204.2', field of view 2.5 mm.

B. *Coscinoconus cherchiae* Arnaud-Vanneau *et al. (*1988), Well-B, 8357', field of view 2.5 mm.

Plate 11

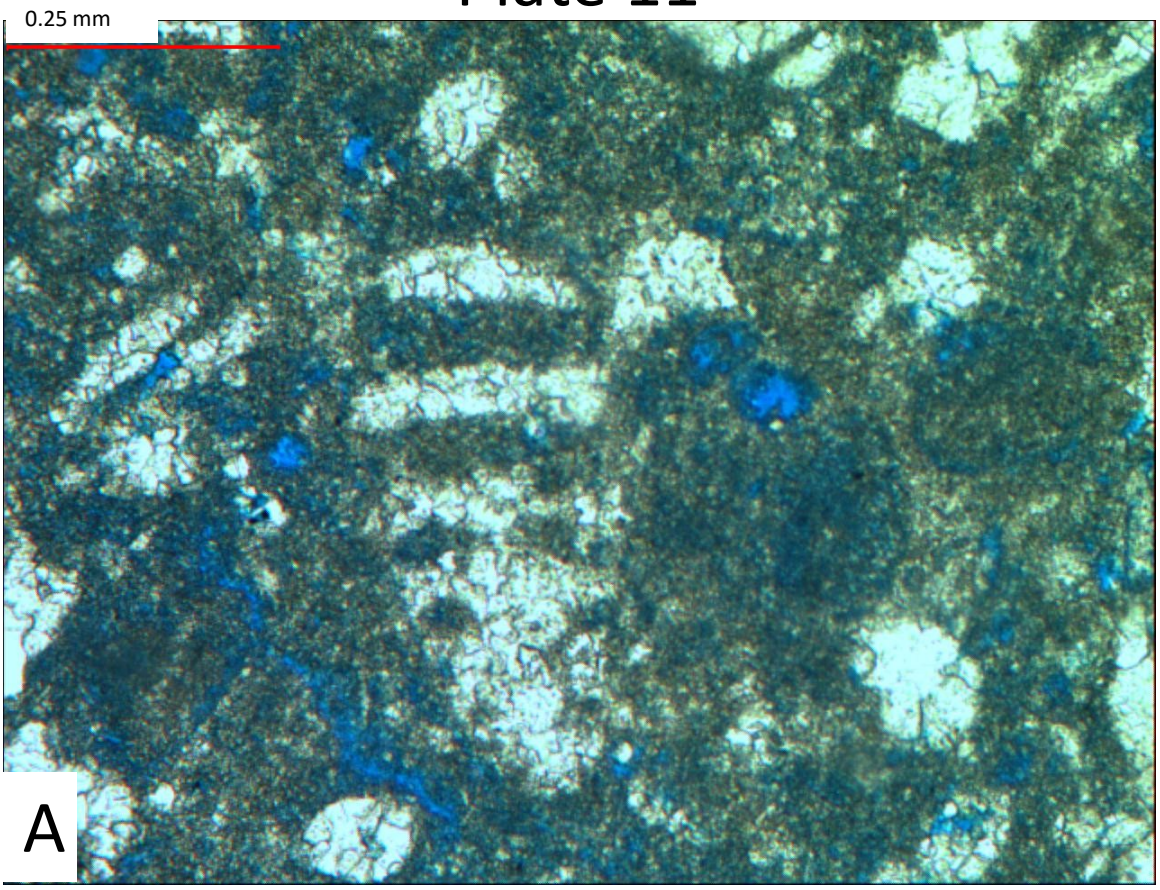

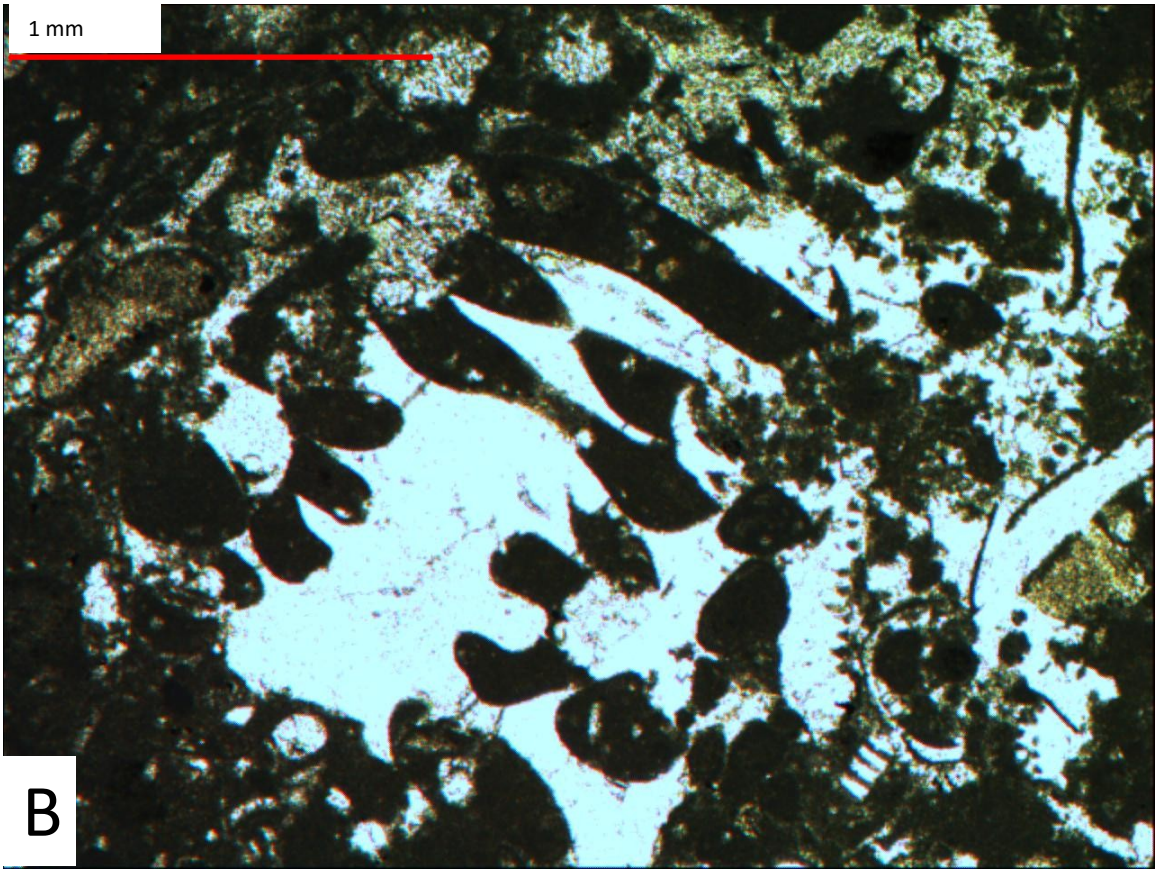

Plate 12

A. *Coscinoconus sagittaria* Arnaud-Vanneau *et al.* (1988), Well-H, 6427.5', field of view 2.5 mm.

B. *Coscinoconus sagittaria* Arnaud-Vanneau *et al.* (1988), Well-A, 4064.5' field of view 2.5 mm.

Plate 12

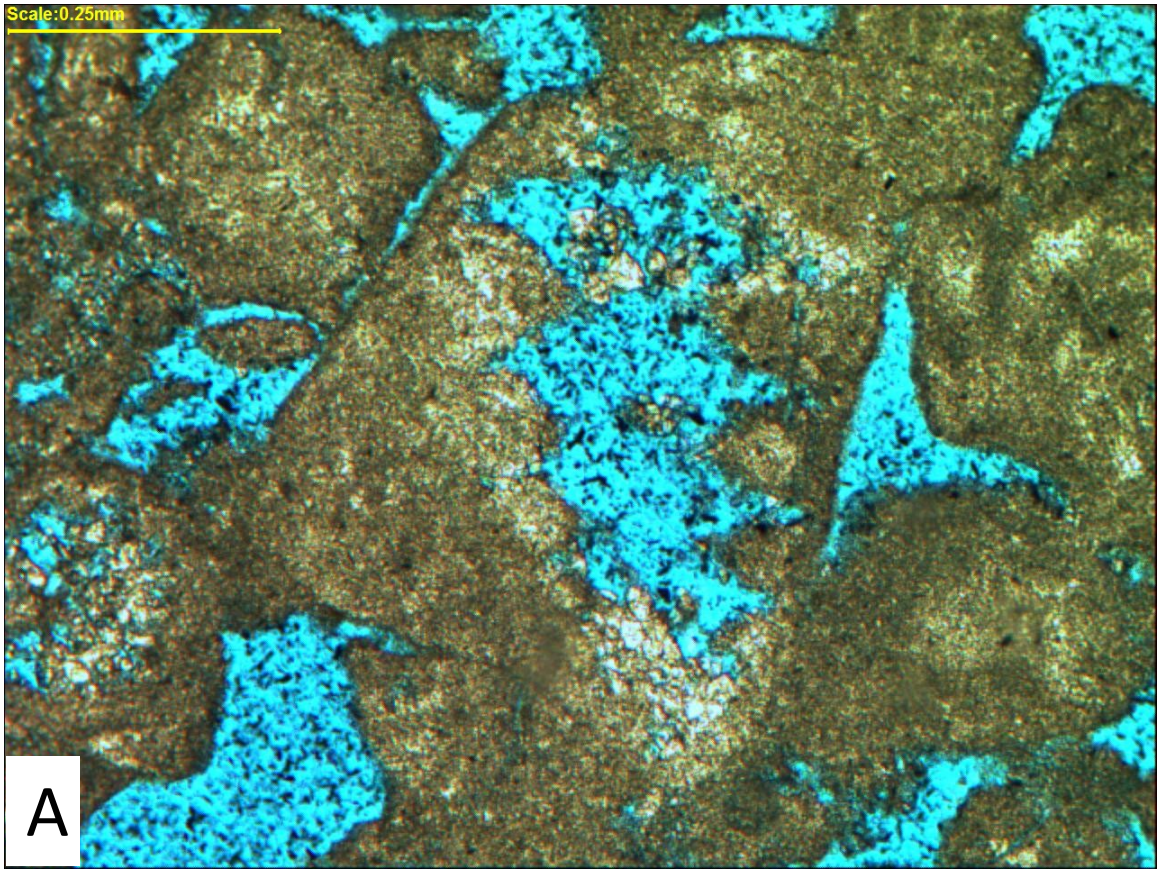

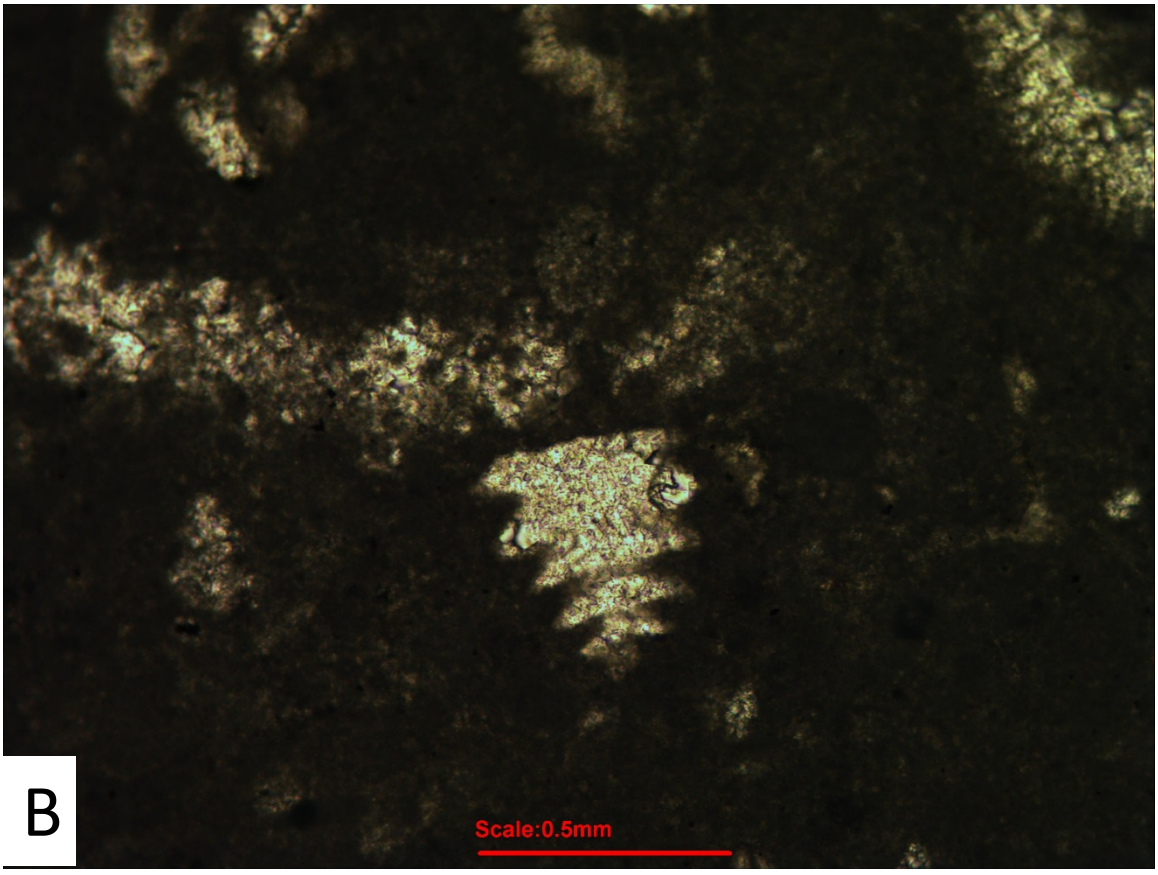

Plate 13

A. *Coscinoconus sagittaria* Arnaud-Vanneau *et al.* (1988), Well-D, from the top of the Yamama Formation, 7960.2', field of view 2.5 mm.

B. *Coscinoconus sagittaria* Arnaud-Vanneau *et al.* (1988), Well-I, 5448.7', field of view 2.5 mm.

Plate 13

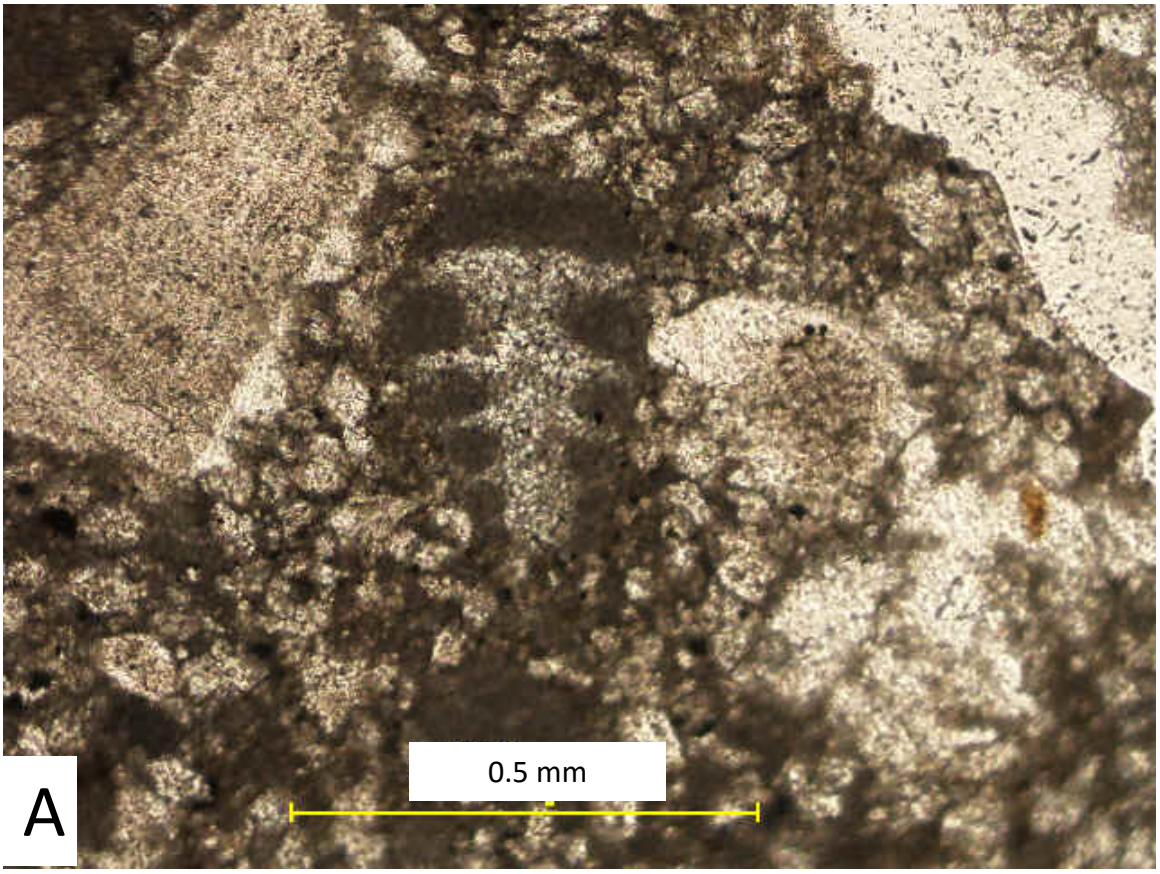

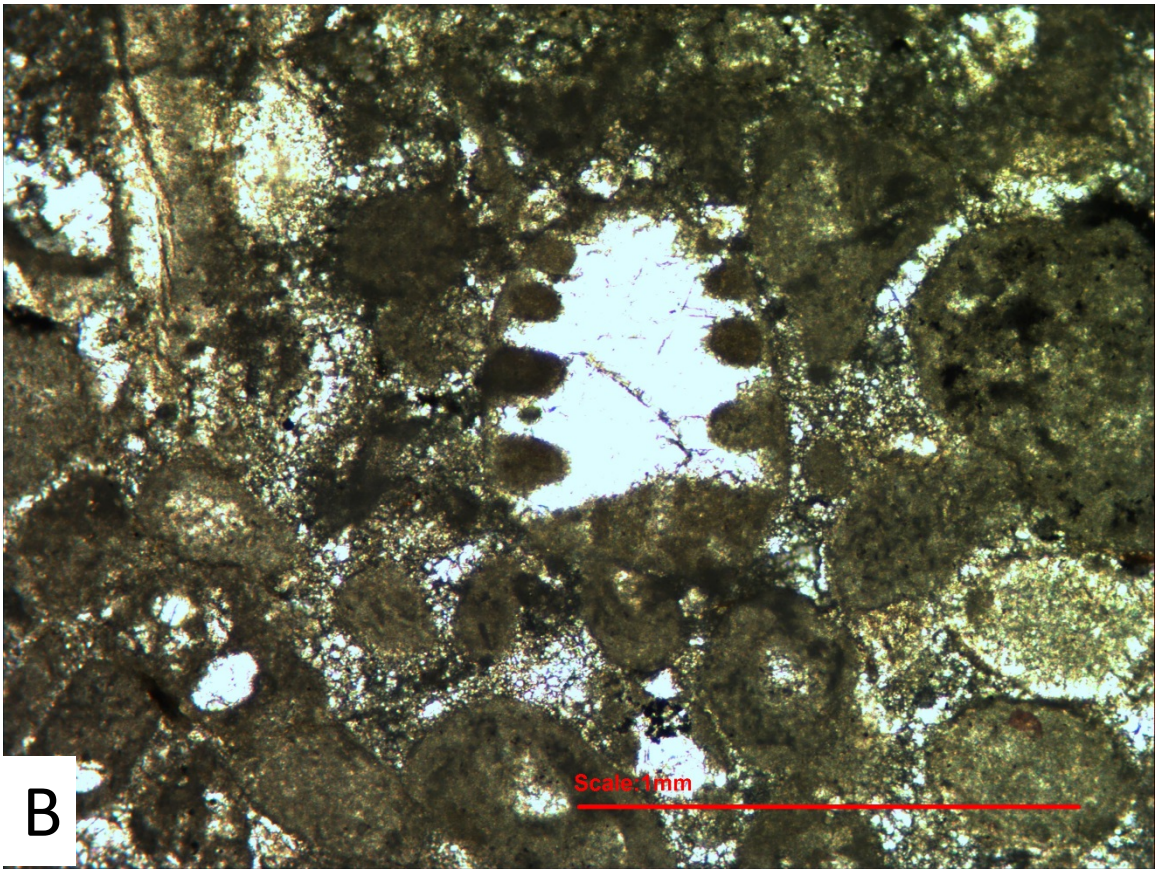

Plate 14

A. *Coscinoconus sagittaria* Arnaud-Vanneau *et al.* (1988), Well-D, common *C. sagittaria* wackestone from the base of the Yamama Formation, 7975.2', field of view 2.5 mm.

B. *Neotrocholina valdensis* Reichel (1955), Well-I, from the base of the Yamama Formation, 5474.7', field of view 2.5 mm.

Plate 14

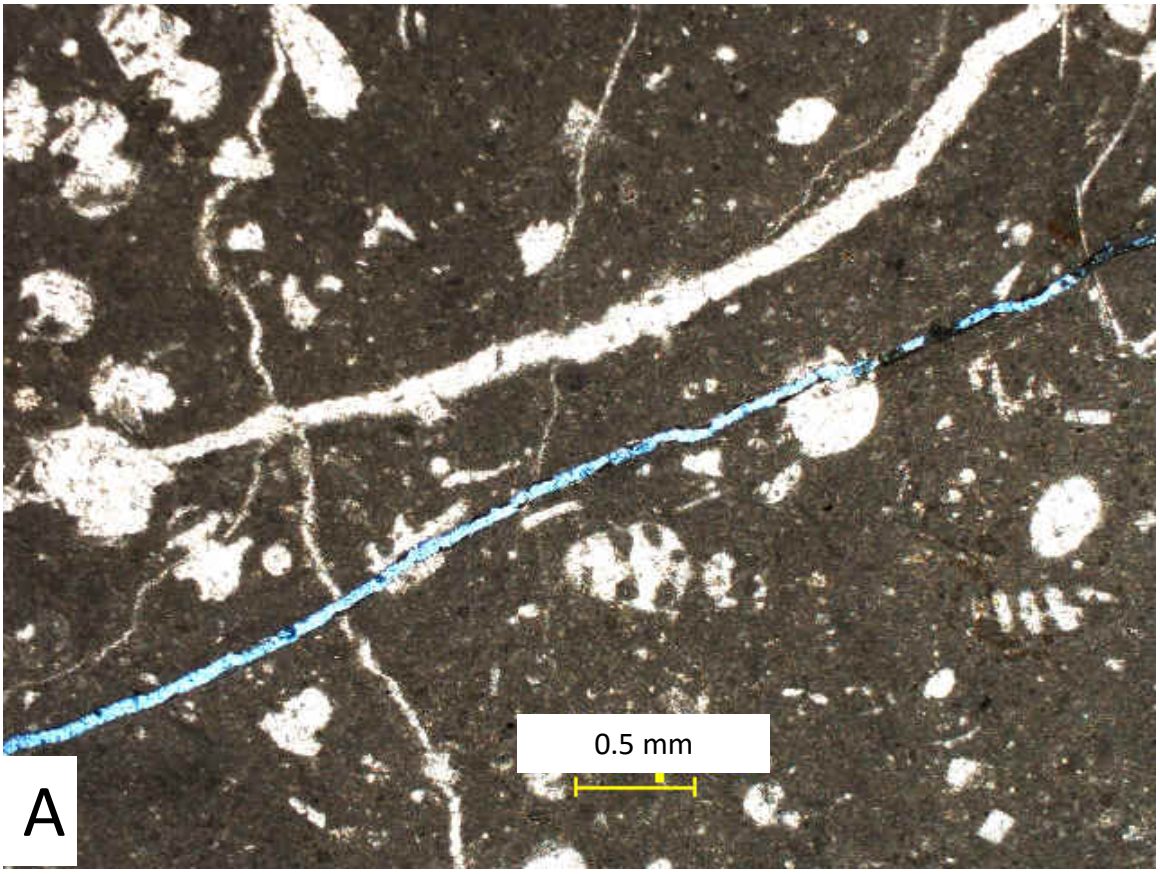

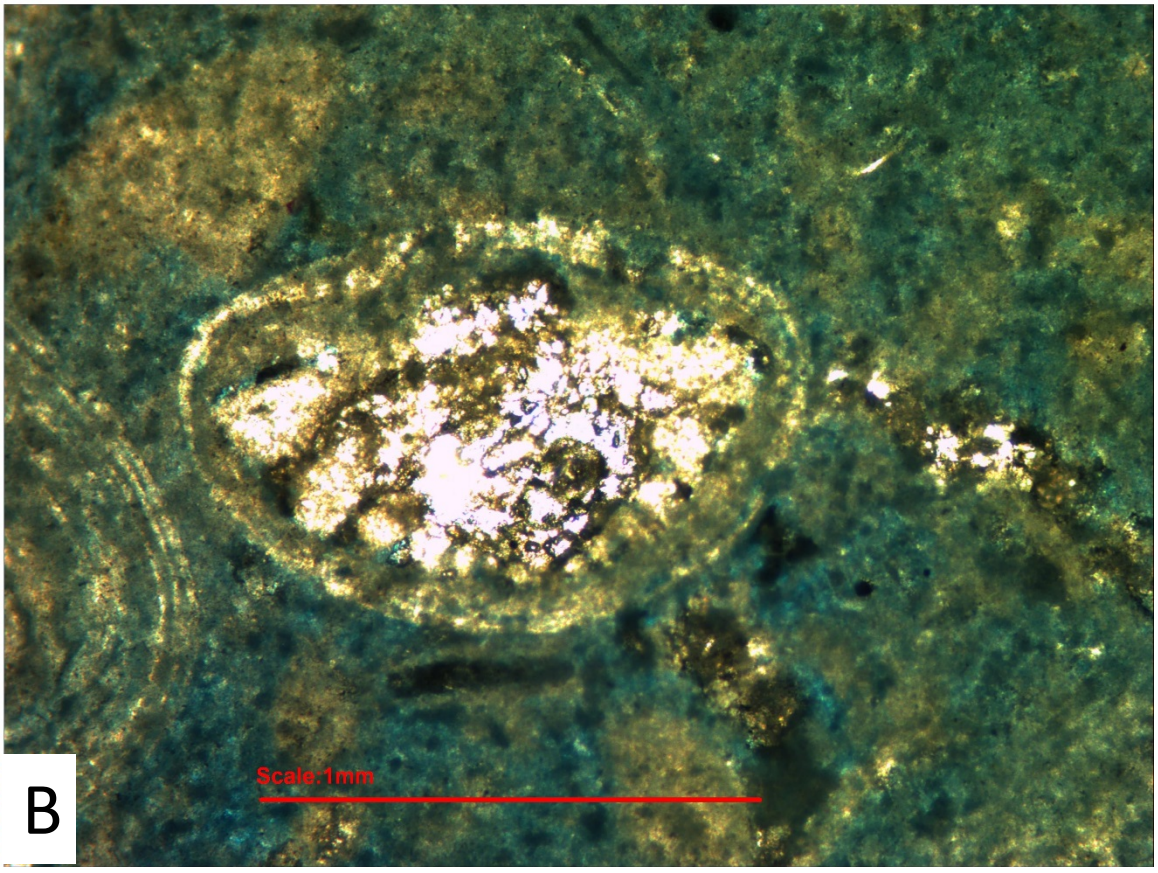

Plate 15

A. *Protopeneroplis ultragranulata* (Gorbatchik, 1971), Well-G, 6767.5', field of view 2.5 mm.

B. *Protopeneroplis ultragranulata* (Gorbatchik, 1971), Well-G, 6810.5', field of view 2.5 mm.

C. *Protopeneroplis ultragranulata* (Gorbatchik, 1971), Well-H, 6423.5', field of view 2.5 mm.

D. *Protopeneroplis ultragranulata* (Gorbatchik, 1971), Well-H, 6414.8', field of view 2.5 mm.

E. *Protopeneroplis ultragranulata* (Gorbatchik, 1971), Well-I, 5524.2', field of view 2.5 mm.

F. *Protopeneroplis ultragranulata* (Gorbatchik, 1971), Well-A, from the base of the Yamama Formation, 4061.6', field of view 2.5 mm.

Plate 15

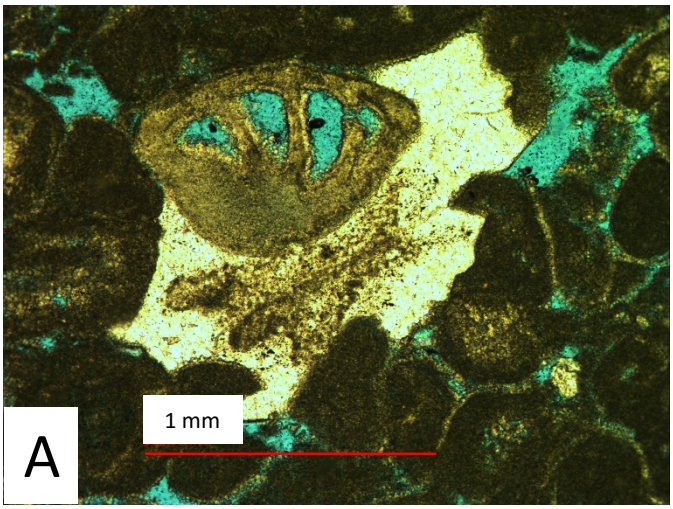

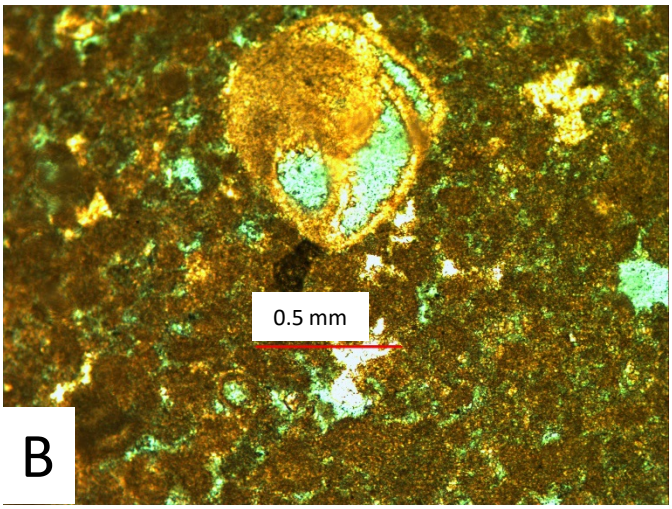

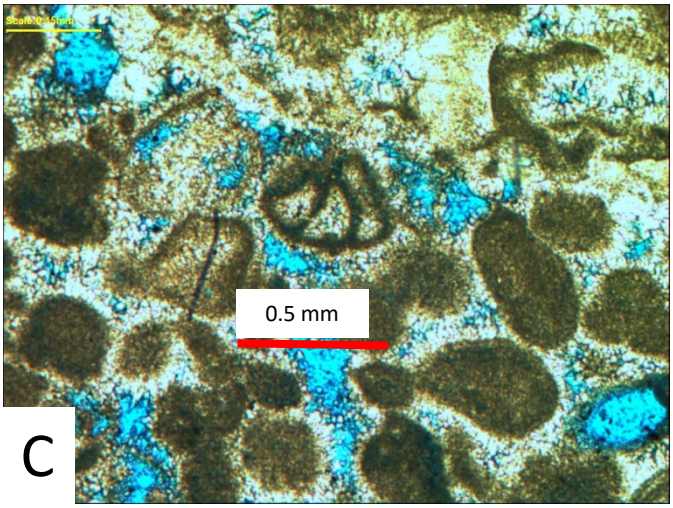

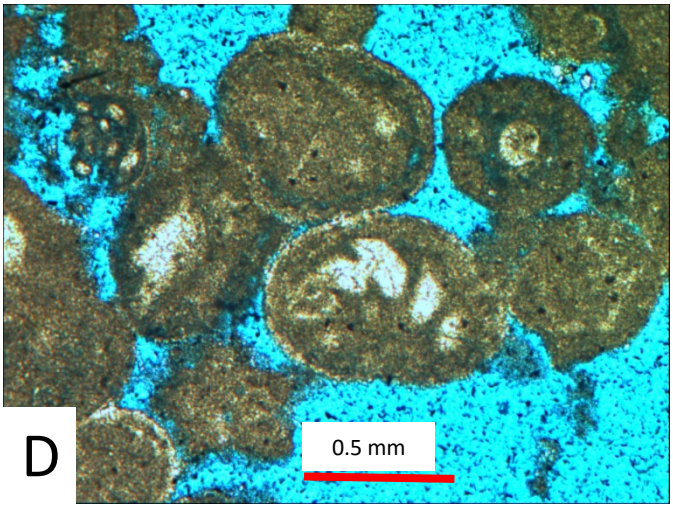

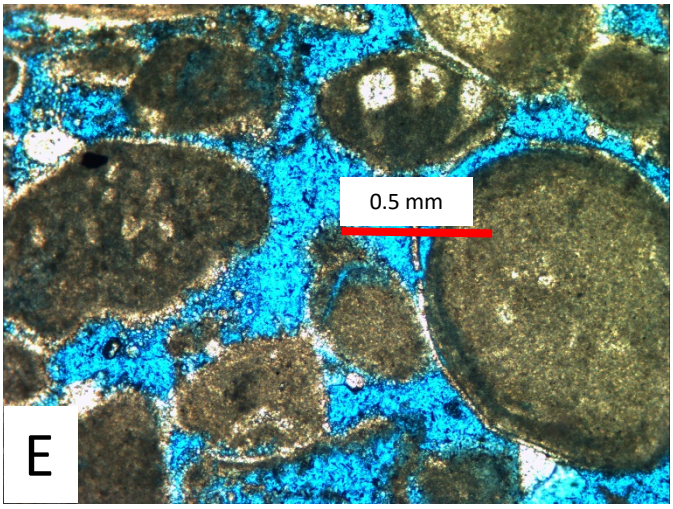

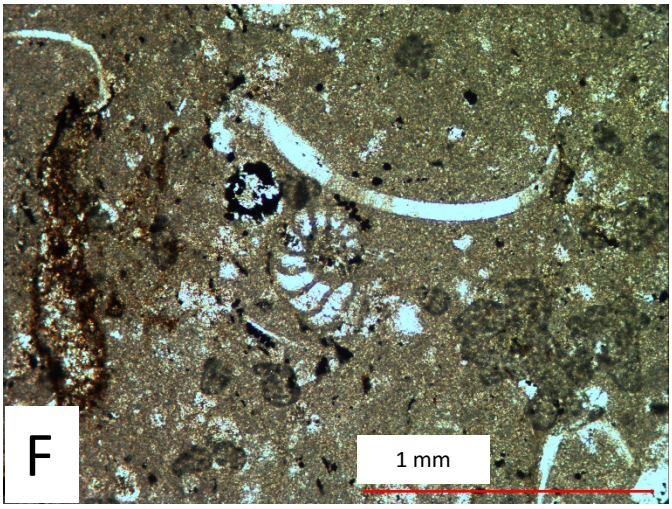

Plate 16

A. *Protopeneroplis ultragranulata* (Gorbatchik, 1971), Well-D, 8639.7', field of view 2.5 mm.

B. *Protopeneroplis ultragranulata* (Gorbatchik, 1971), Well-H, 6423.5', field of view 2.5 mm.

C. *Protopeneroplis ultragranulata* (Gorbatchik, 1971), Well-H, 6414.8', field of view 2.5 mm.

D. *Protopeneroplis ultragranulata* (Gorbatchik, 1971), Well-H, 6424.5', field of view 2.5 mm.

E. *Protopeneroplis ultragranulata* (Gorbatchik, 1971), Well-H, 6247.5', field of view 2.5 mm.

F. *Protopeneroplis ultragranulata* (Gorbatchik, 1971), Well-H, 6414.8', field of view 2.5 mm.

Plate 16

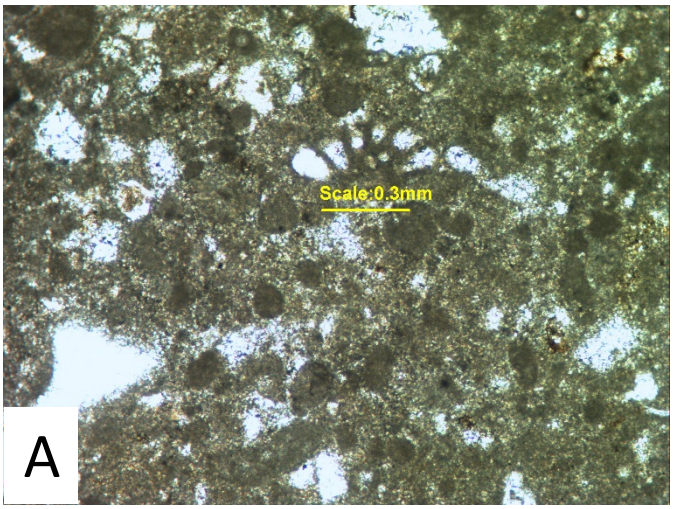

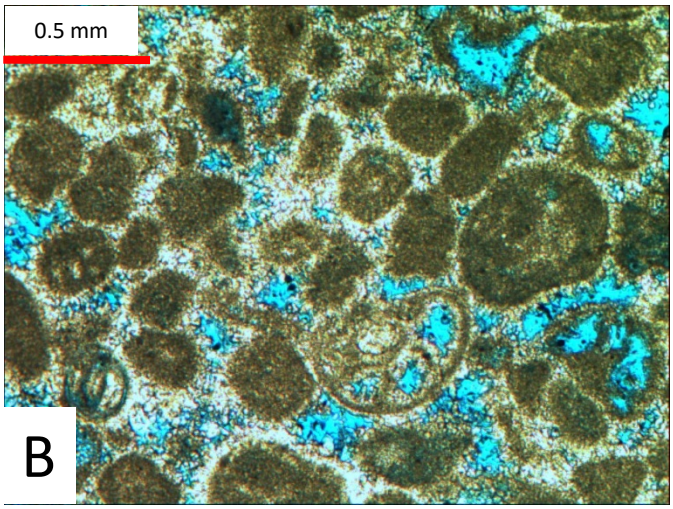

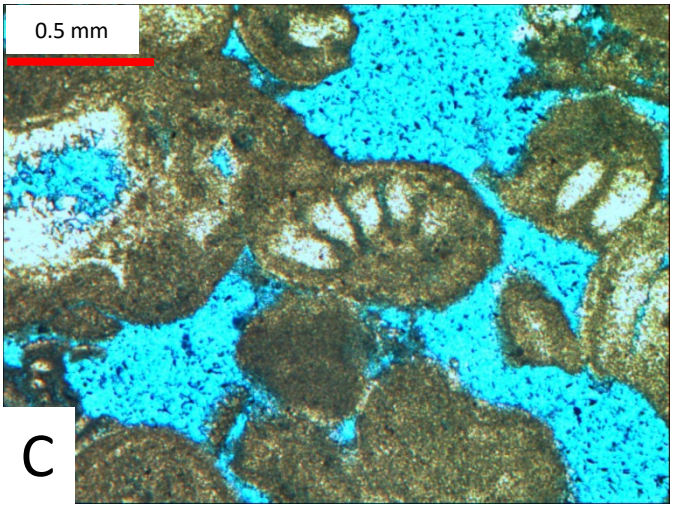

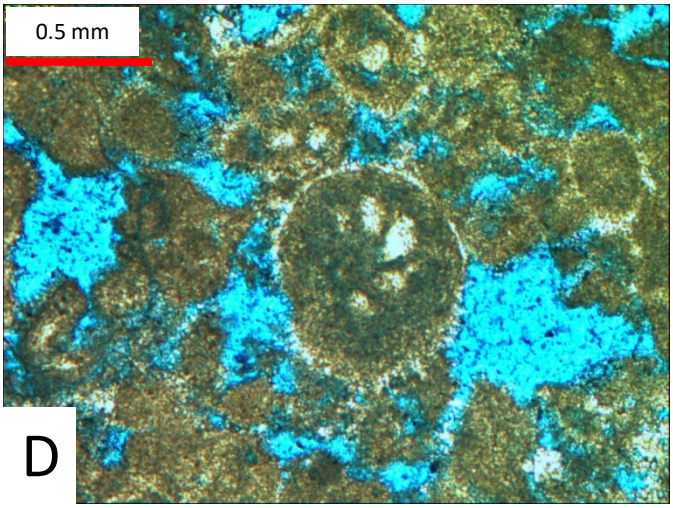

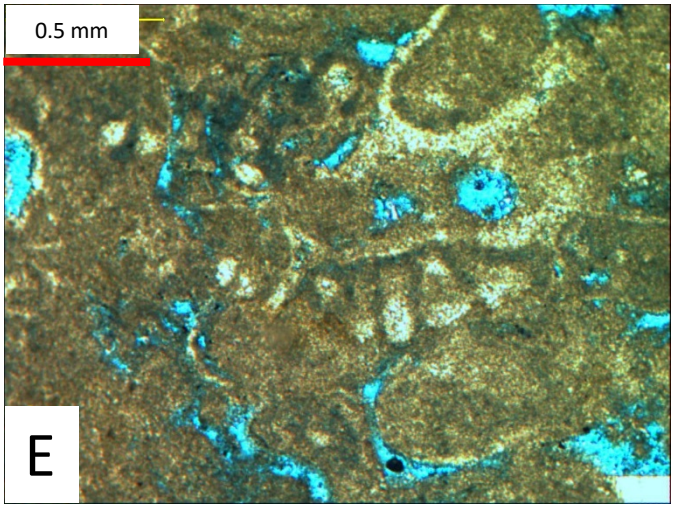

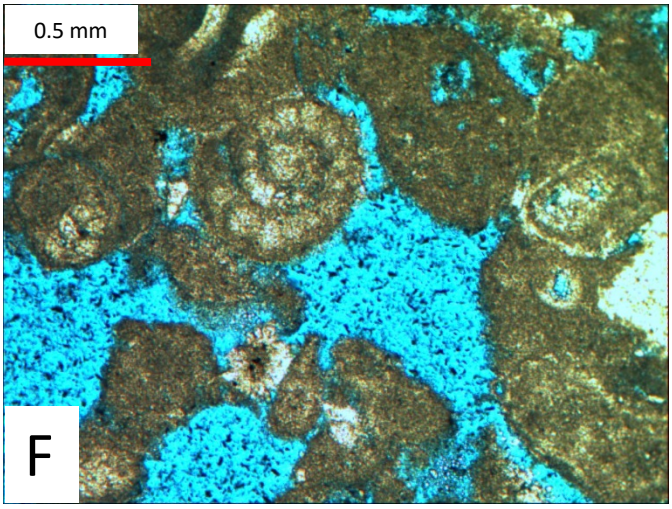

Plate 17

A. *Protopeneroplis ultragranulata* (Gorbatchik, 1971), Well-I, 5448.7', field of view 2.5 mm.

B. *Protopeneroplis ultragranulata* (Gorbatchik, 1971), Well-I, 5471.7', field of view 2.5 mm.

C. *Protopeneroplis ultragranulata* (Gorbatchik, 1971), Well-D, from the Yamama Formation, 7957.2', field of view 1.25 mm.

D. *Protopeneroplis banatica* Bucur (1993), Well-A, from the Yamama Formation, 4061.6', field of view 2.5 mm.

E. *Protopeneroplis banatica* Bucur (1993), Well-B, from the Yamama Formation, 8375.9', field of view 2.5 mm.

F. *Lenticulina* sp., Well-D, from the Yamama Formation, 7960.2', field of view 1.25 mm.

Plate 17

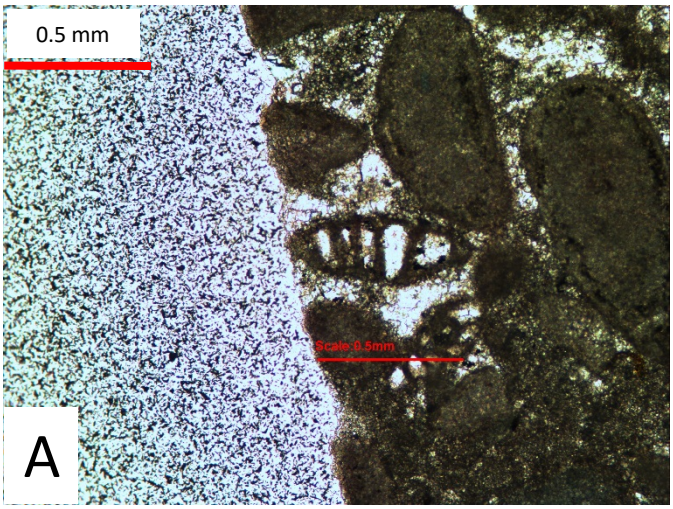

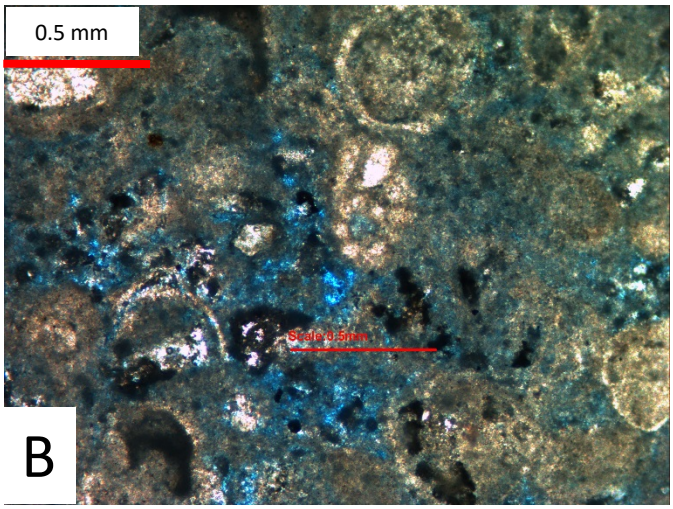

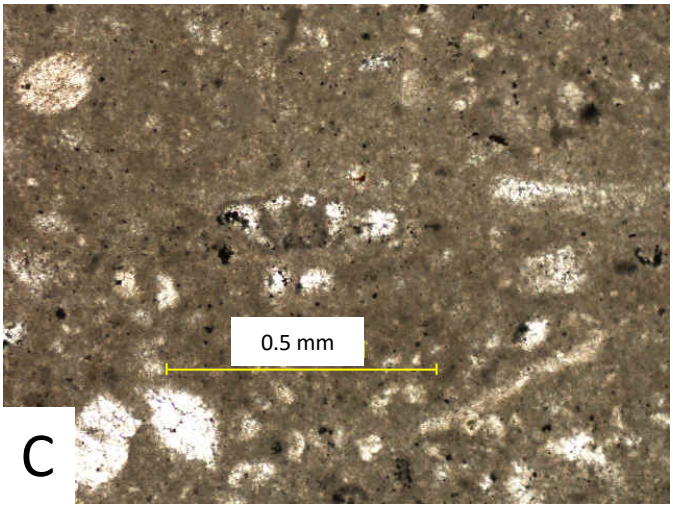

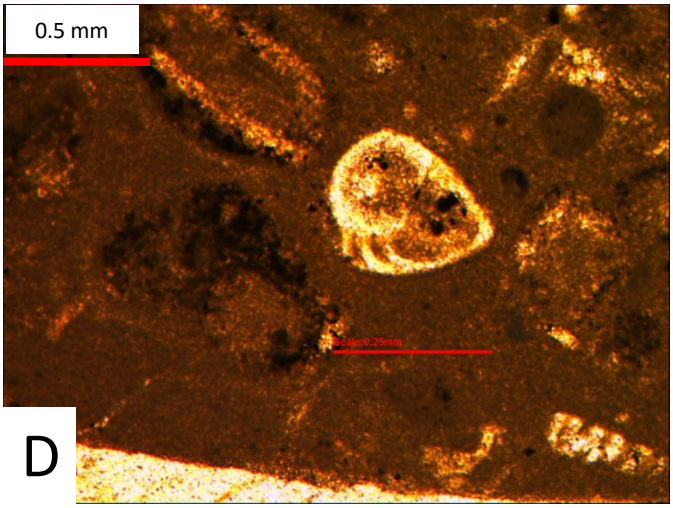

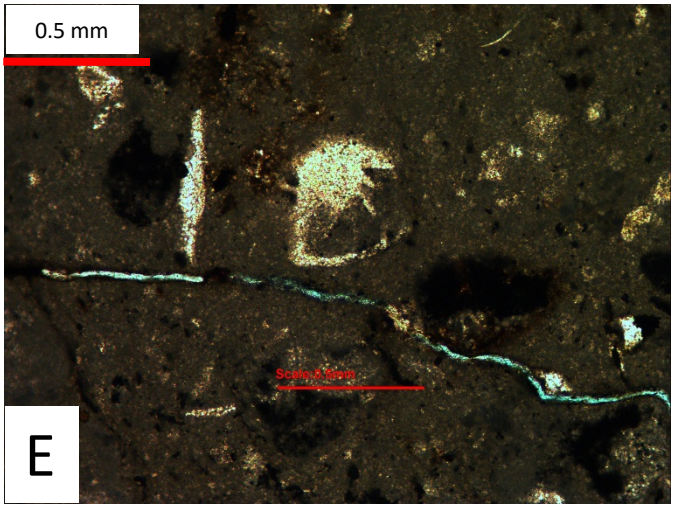

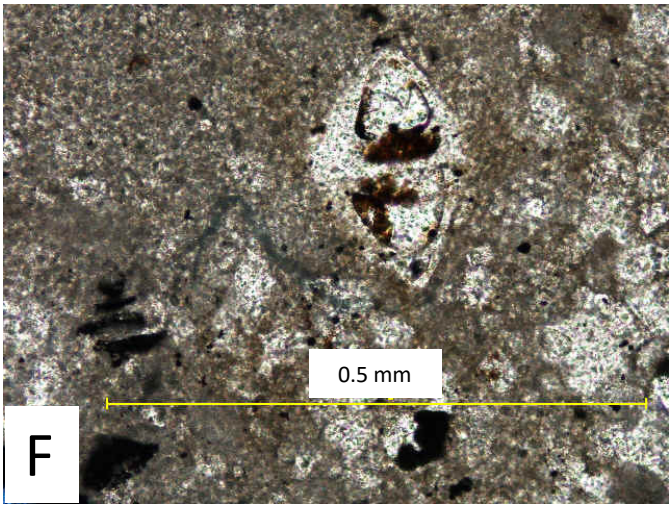

Plate 18

A. *Lenticulina* sp., Well-D, 8639.7’, field of view 1.25 mm.

B. *Lenticulina* sp., Well-D, 8639.7’, field of view 2.5 mm.

C. *Lenticulina* sp., Well-D, 8639.7’, field of view 0.61 mm.

D. *Lenticulina* sp., Well-D, 8620.2’, field of view 2.5 mm.

E. *Cf. Lenticulina* sp., Well-I, 5448.7’, field of view 2.5 mm.

F. *Cf. Lenticulina* sp., Well-I, 5518.2’, field of view 2.5 mm.

Plate 18

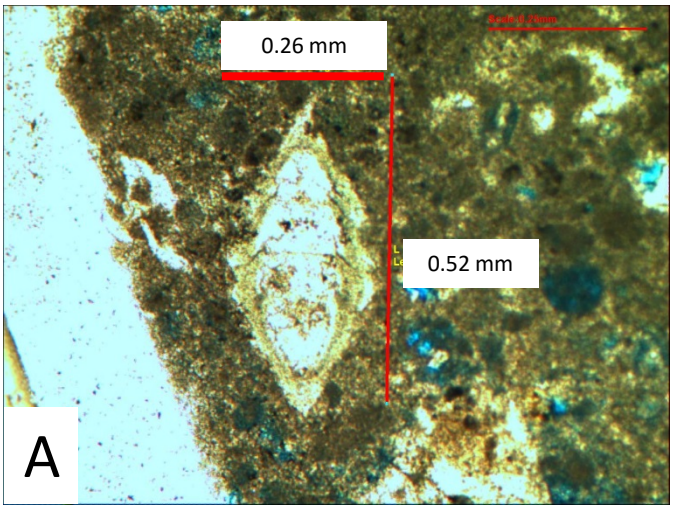
0.26 mm
0.52 mm
A

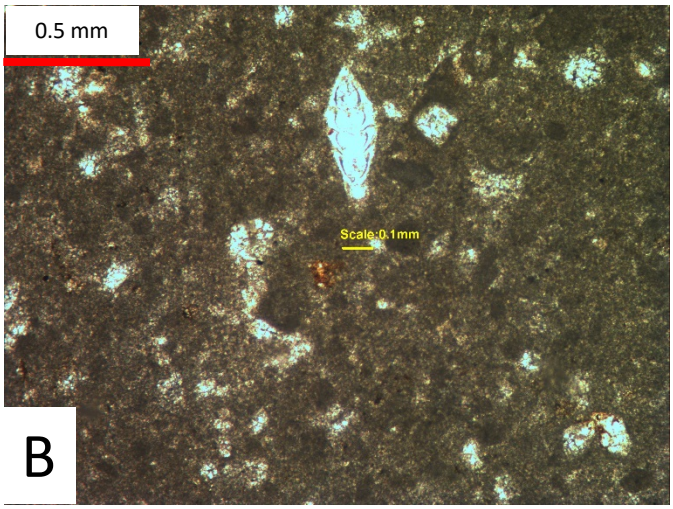
0.5 mm
Scale:0.1mm
B

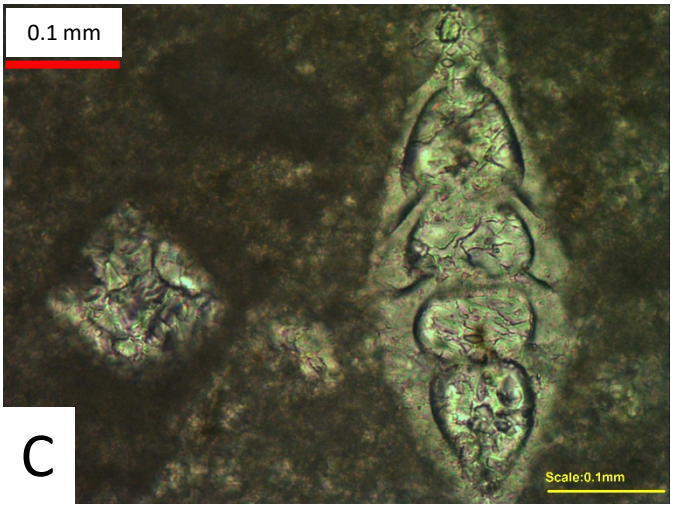
0.1 mm
Scale:0.1mm
C

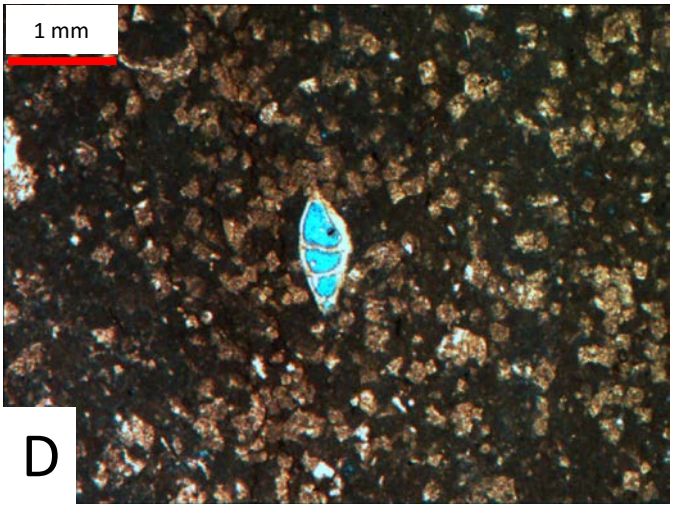
1 mm
D

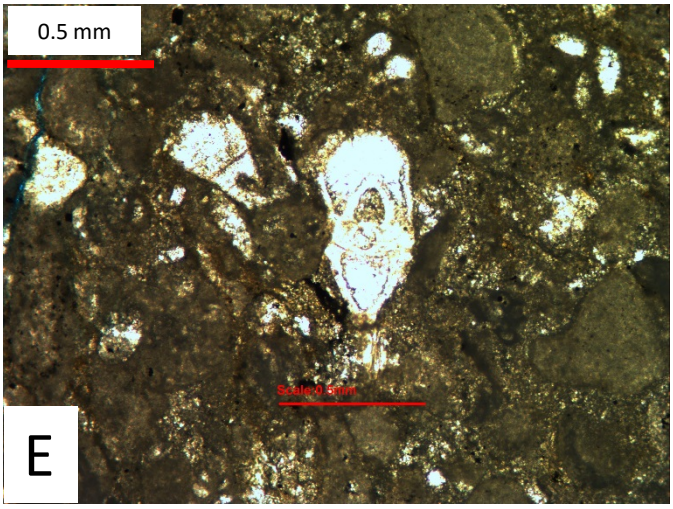
0.5 mm
E

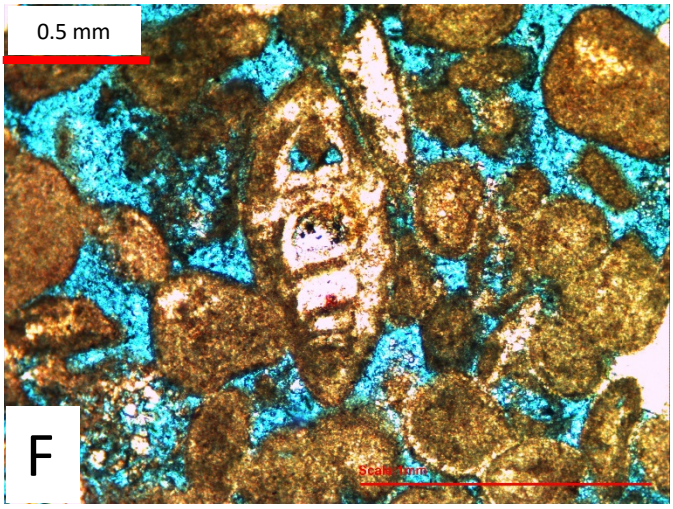
0.5 mm
F

Plate 19

A. *Cf. Pyrulinoides* sp., Well-B, 8365.1', field of view 1.25 mm.

B. *Nodosaria* sp., Well-D, 8639.7', field of view 2.5 mm.

Plate 19

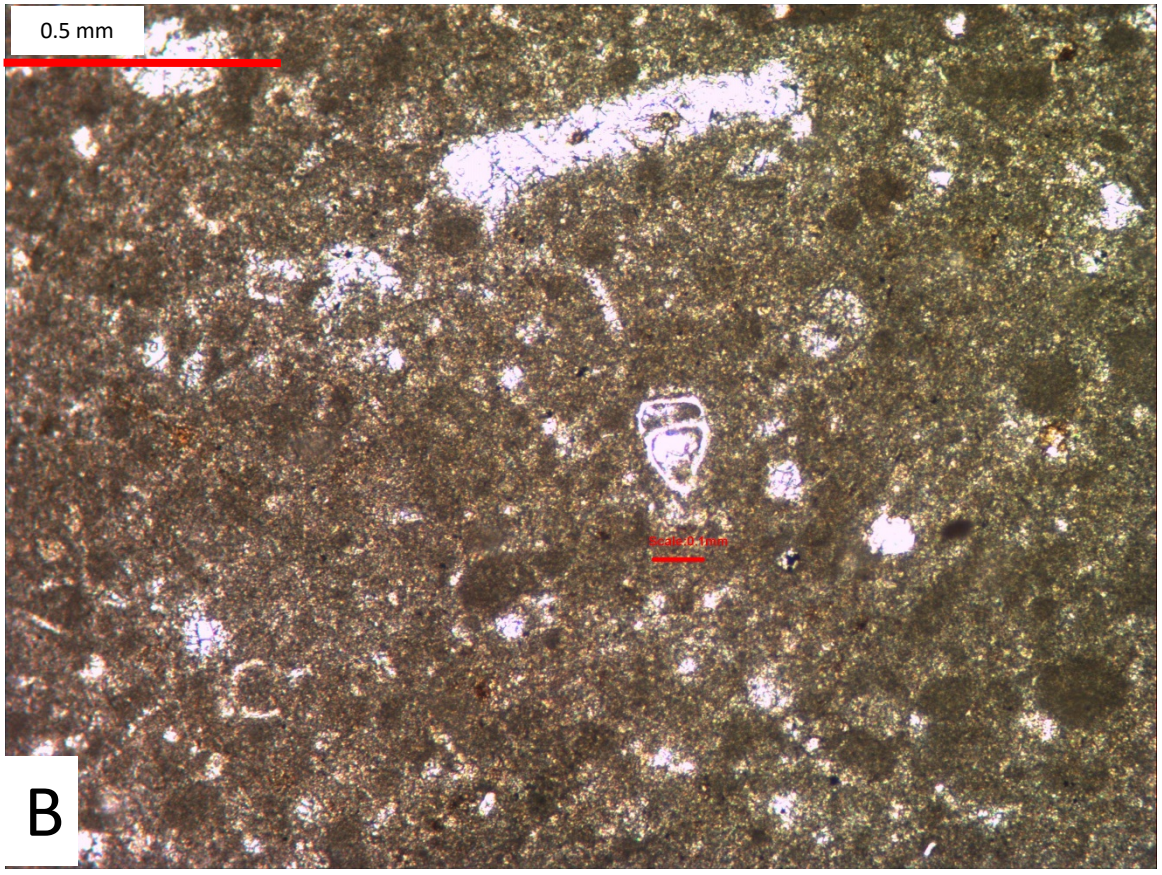

Plate 20

A. *Nodosaria* sp., Well-I, 5451.7’, field of view 2.5 mm.

B. *Ophthalmidium* sp., Well-F, 8441.5’, field of view 2.5 mm.

Plate 20

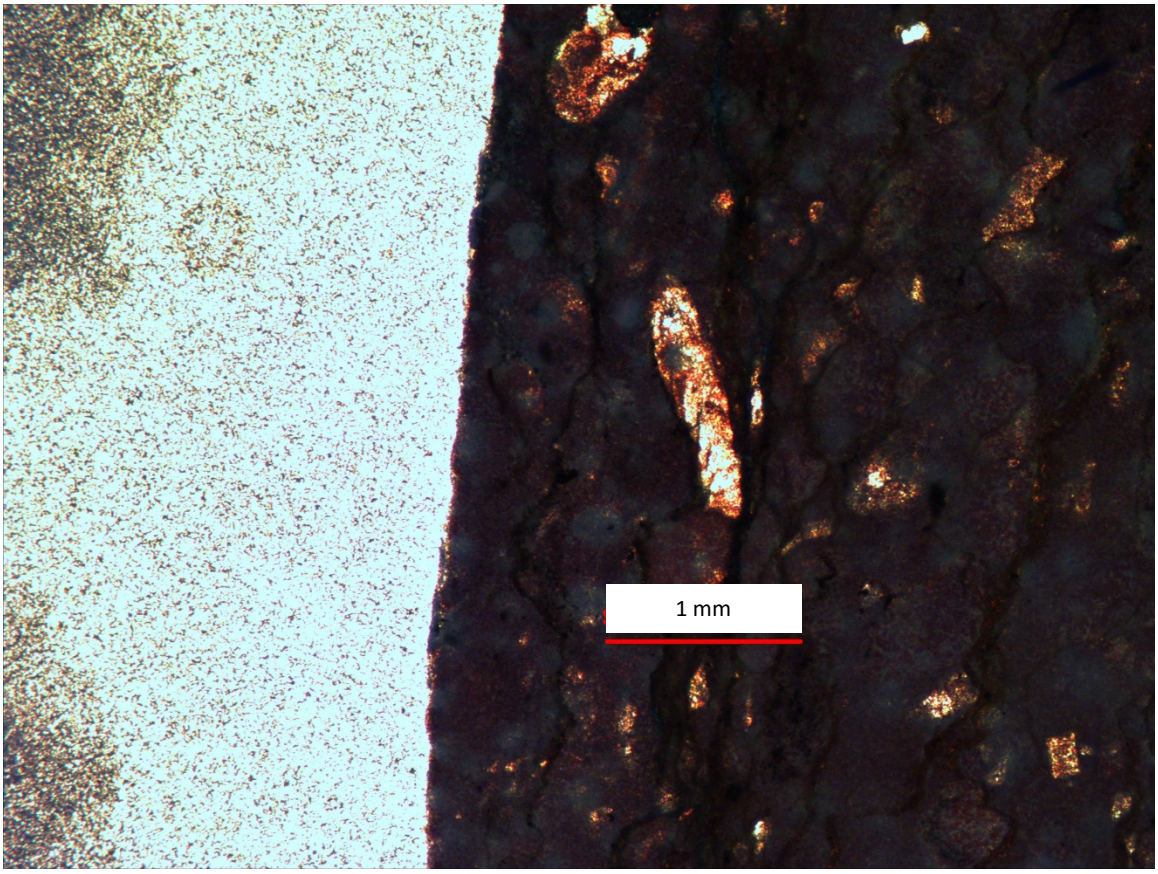

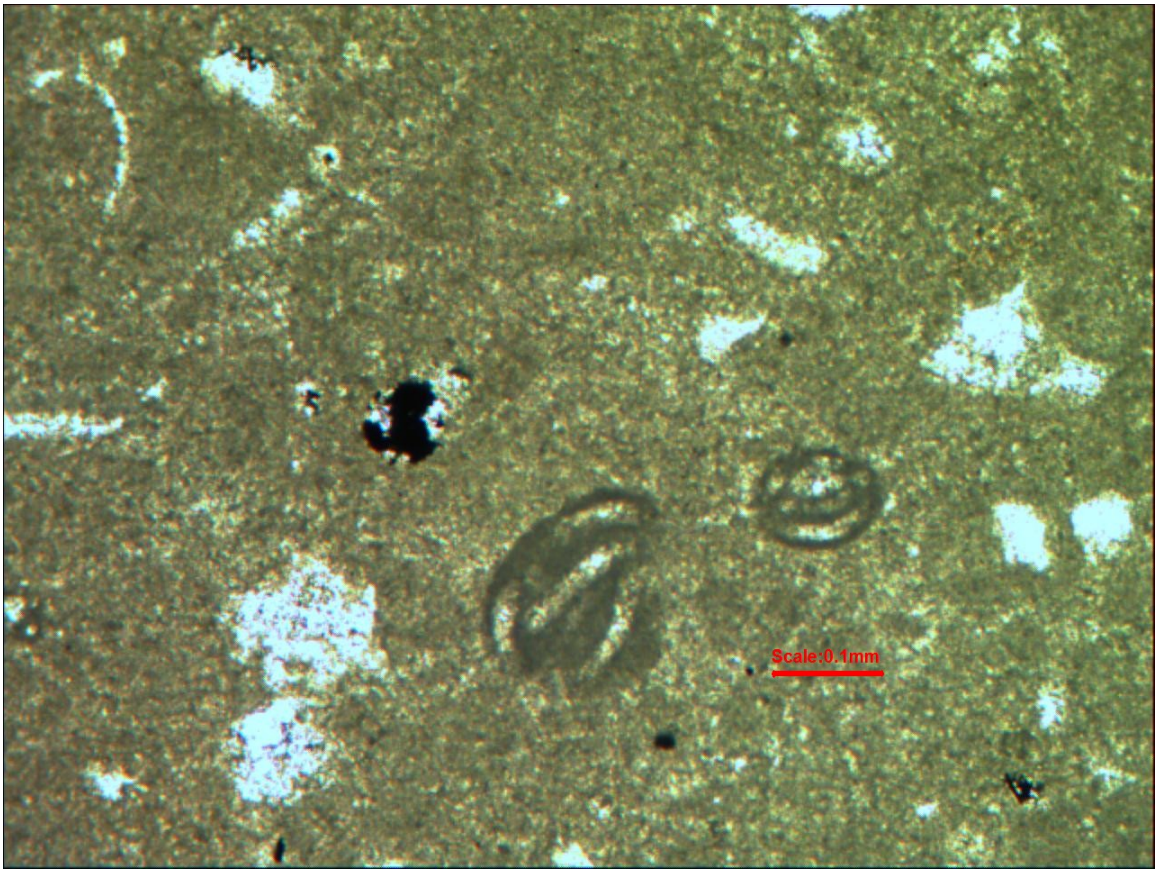

Plate 21

A. *Ophthalmidium* sp., Well-G, 6762.6’, field of view 2.5 mm.

B. *Ophthalmidium* sp., Well-H, 6416.5’, field of view 2.5 mm.

C. *Ophthalmidium* sp., Well-H, 6423.5’, field of view 2.5 mm.

D. *Ophthalmidium* sp., Well-B, 8444.4’, field of view 6.3 mm.

E. *Ophthalmidium* sp., Well-I, 5448.7’, field of view 2.5 mm.

F. *Ophthalmidium* sp., Well-I, 5448.7’, field of view 2.5 mm.

Plate 21

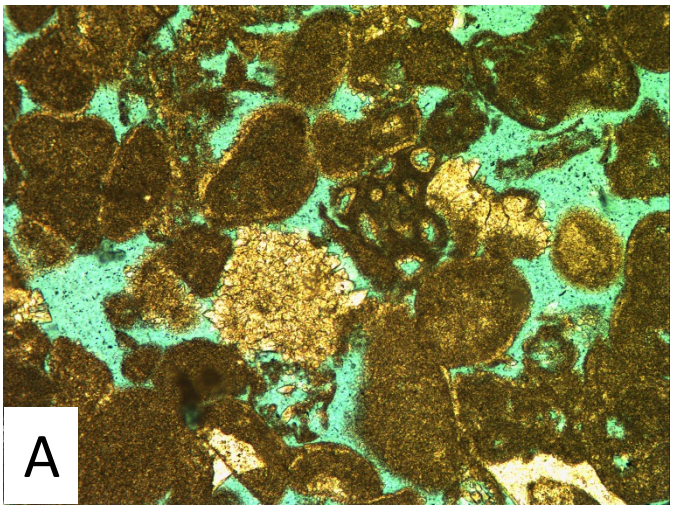

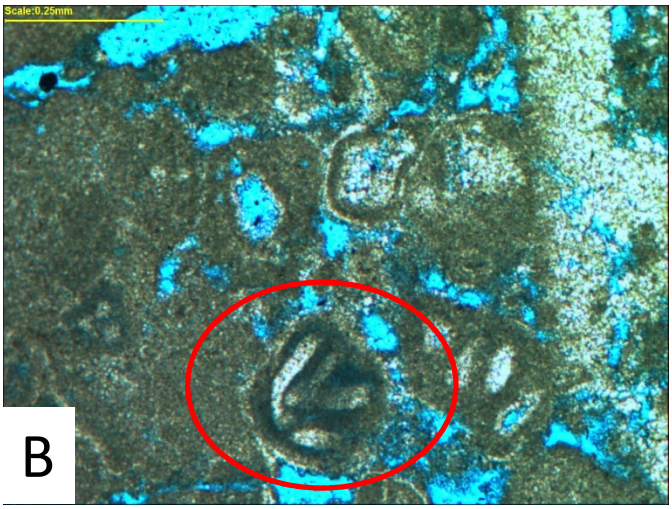

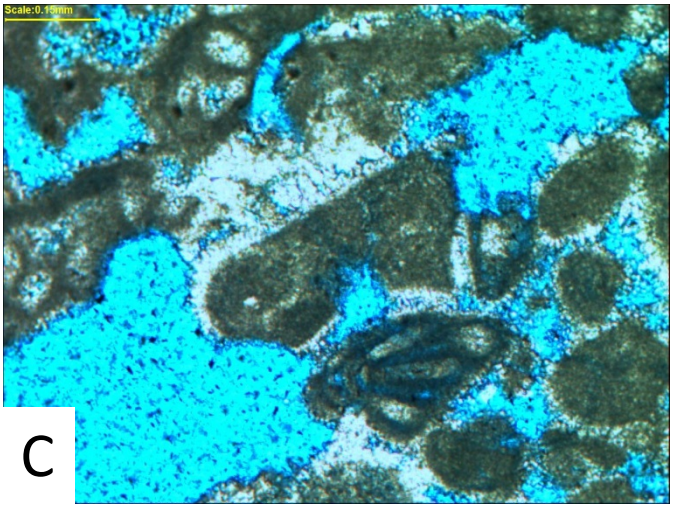

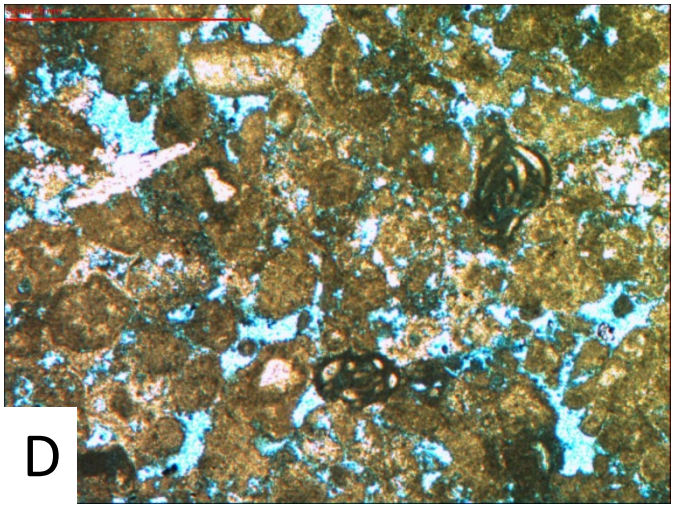

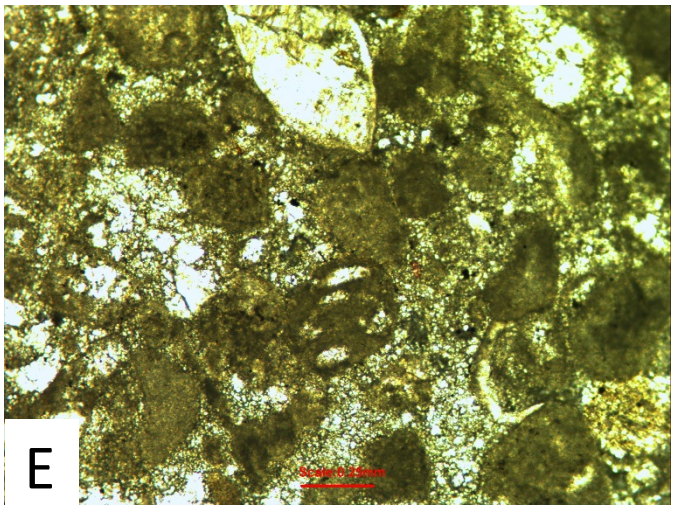

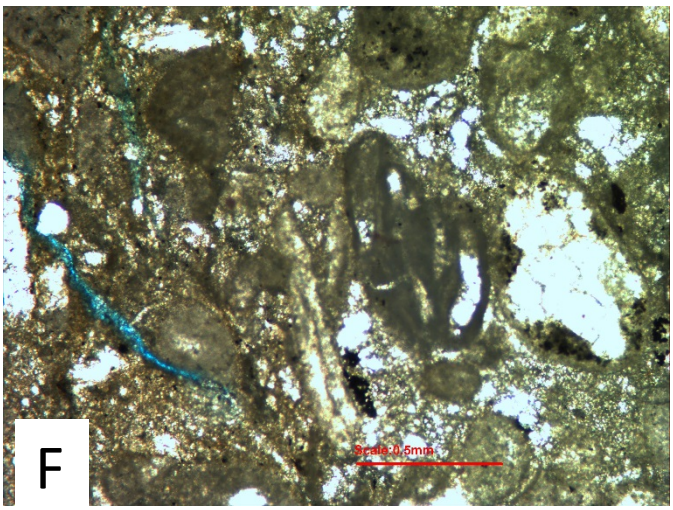

Plate 22

A. *Ophthalmidium* sp., Well-I5448.7', field of view 2.5 mm.

B. *Meandrospira favrei* (Charollais *et al*., 1966), Well-B, from the Yamama Formation, 8361.8', field of view 2.5 mm.

C. *Meandrospira favrei* (Charollais *et al*., 1966), Well-D, from the Yamama Formation, 7957.2', field of view 1.25 mm.

D. *Meandrospira favrei* (Charollais *et al*., 1966), Well-D, from the Yamama Formation, 7957.2', field of view 2.5 mm.

E. *Meandrospira favrei* (Charollais *et al*., 1966), three specimens in wackestone, Well-D, from the Yamama Formation, 7957.2', field of view 2.5 mm.

F. *Meandrospira favrei* (Charollais *et al*., 1966), Well-D, from the Yamama Formation, 7957.2', field of view 2.5 mm.

Plate 22

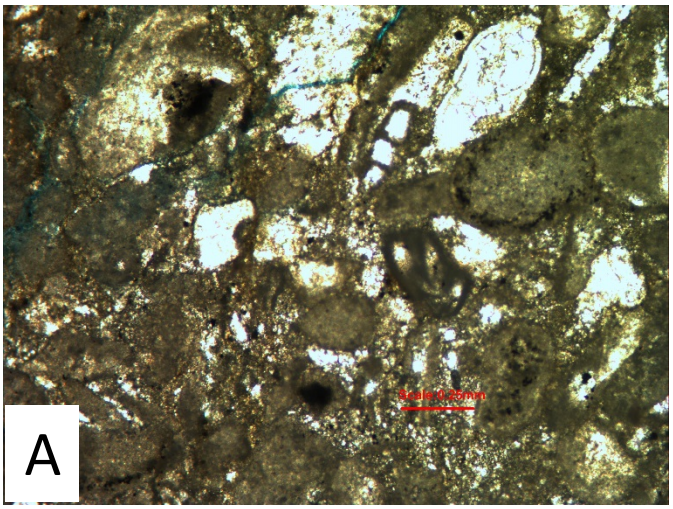

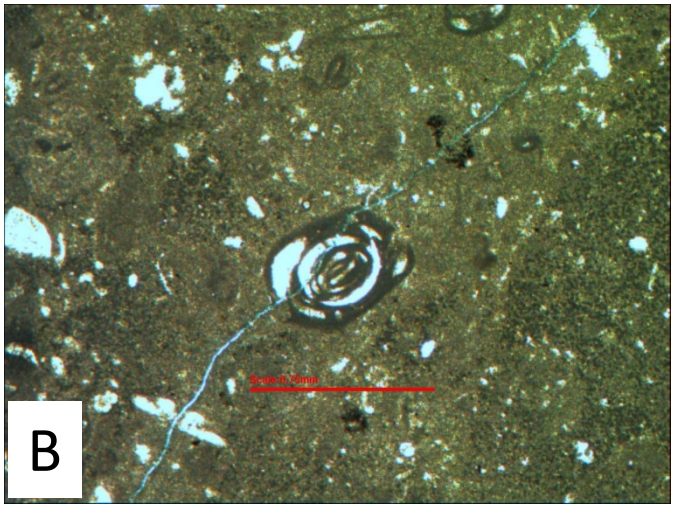

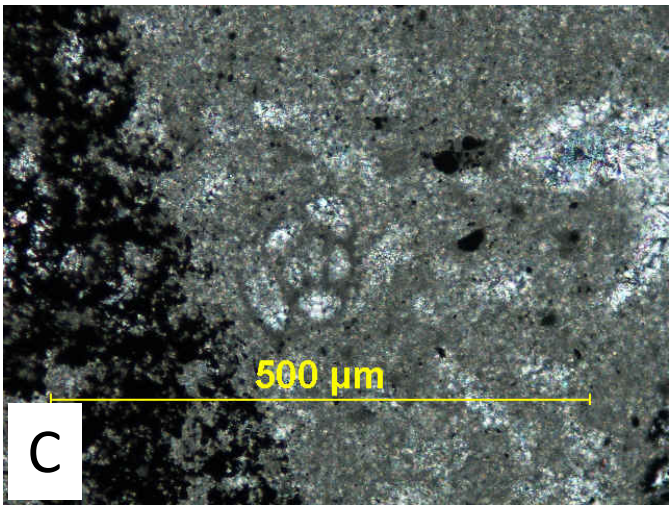

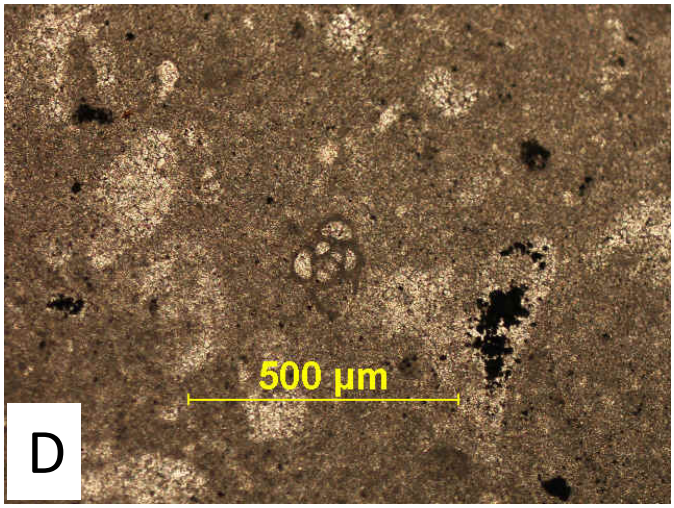

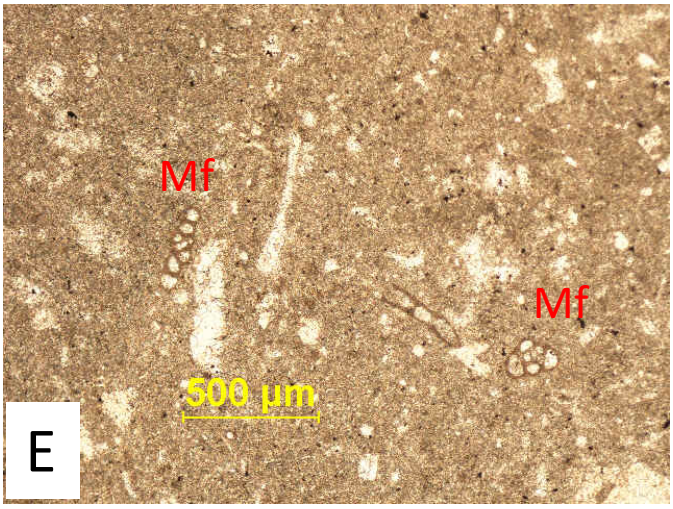

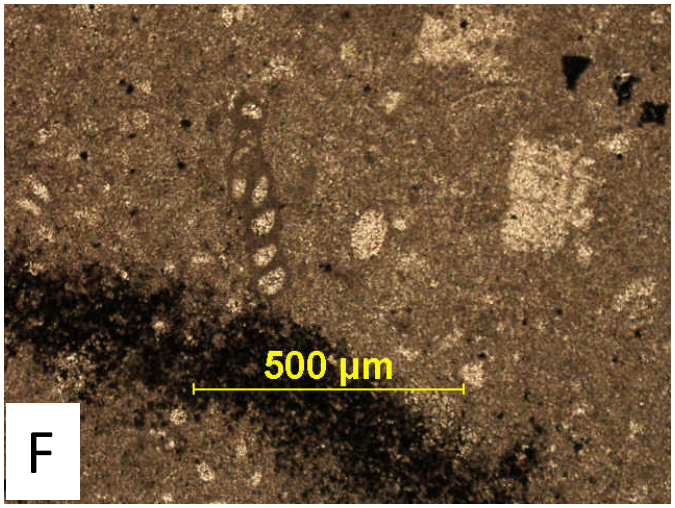

Plate 23

A. *Meandrospira favrei* (Charollais *et al*., 1966), Well-D, from the Yamama Formation, 7957.2', field of view 1.25 mm.

B. *Meandrospira favrei* (Charollais *et al*., 1966), Well-D, from the Yamama Formation, 7957.2', field of view 2.5 mm.

C. *Nubecularia* sp., surrounded by microlayers (dark, concentric micrites) of *Crescentiella morronensis* forma *morronensis* (Crescenti, 1969), Well-H, 6414.8', field of view 2.5 mm.

D. *Nubecularia* sp., Well-H, 6414.8', field of view 2.5 mm.

E. *Nubecularia* sp., surrounded by microlayers (dark, concentric micrites) of *Crescentiella morronensis* forma *morronensis* (Crescenti, 1969), Well-I, 5534.7', field of view 2.5 mm.

F. *Nubecularia* sp., surrounded by microlayers (dark, concentric micrites) of *Crescentiella morronensis* forma *morronensis* (Crescenti, 1969), Well-I, 5448.7', field of view 2.5 mm.

Plate 23

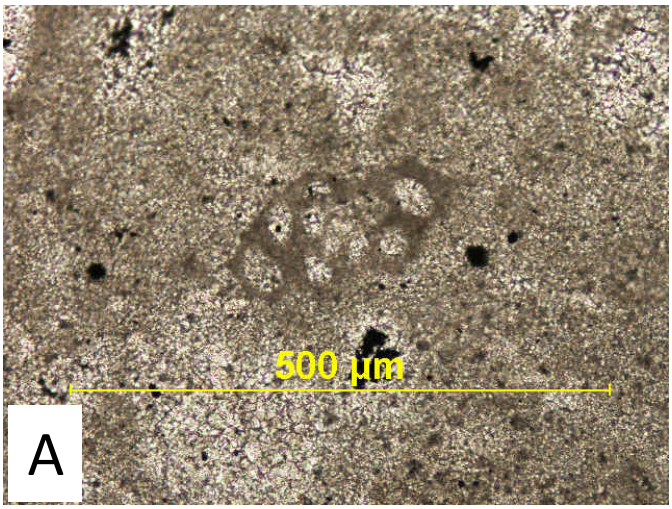

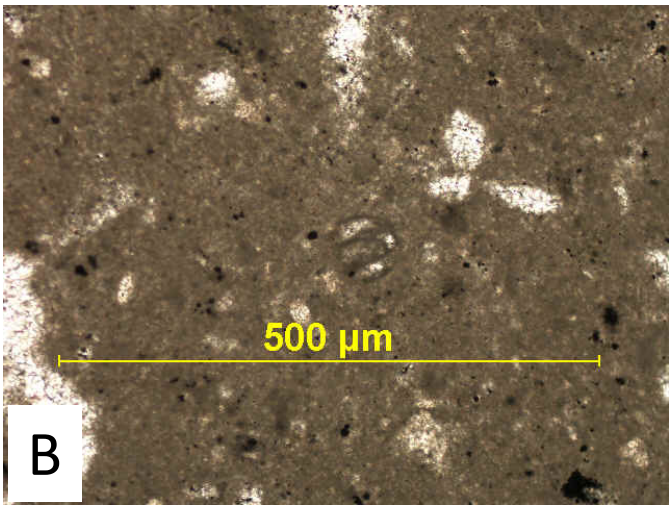

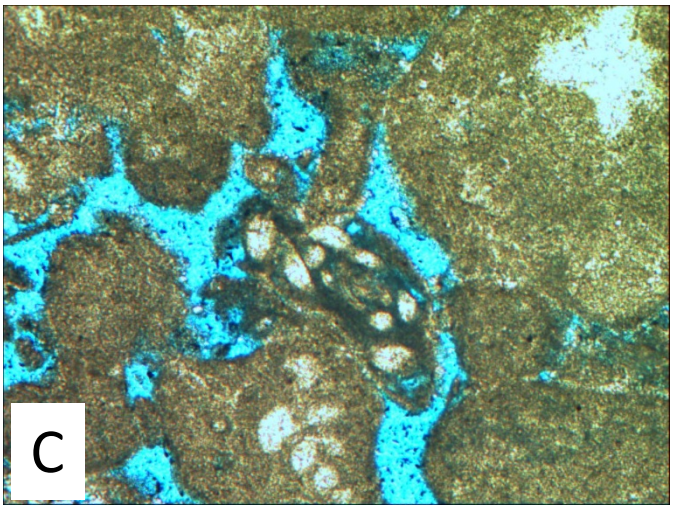

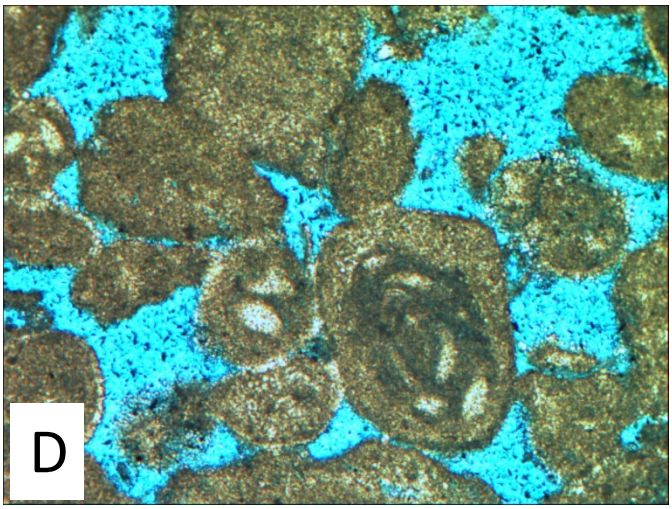

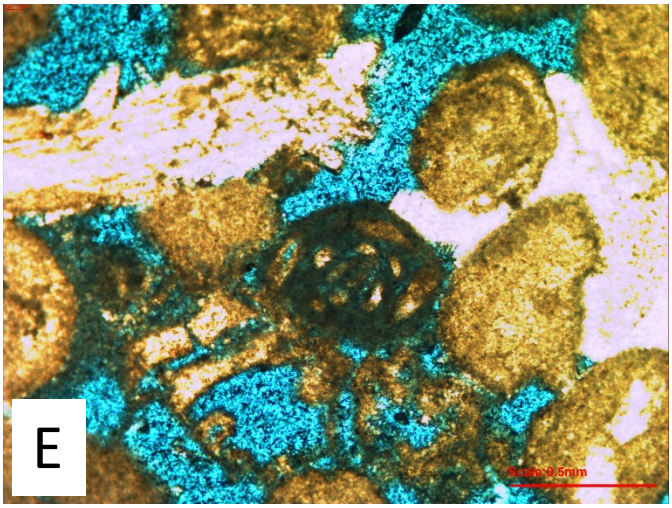

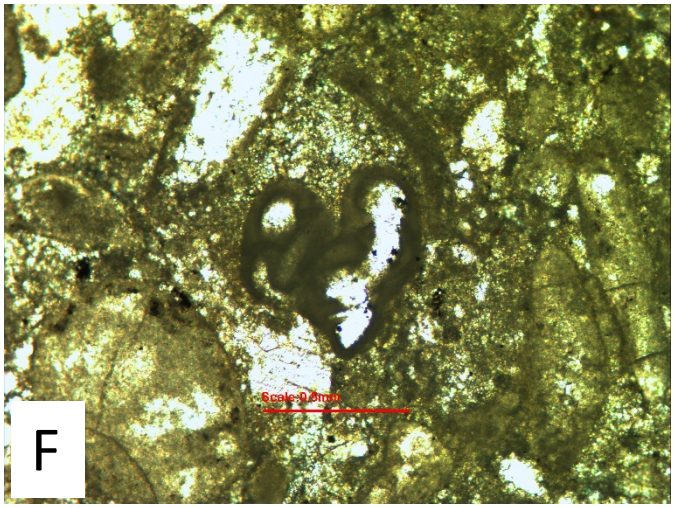

Plate 24

A. *Nubecularia* sp., Well-H, 6421.5', field of view 2.5 mm.

B. *Nubecularia* sp., surrounded by microlayers (dark, concentric micrites) of *Crescentiella morronensis* forma *morronensis* (Crescenti, 1969), Well-H, 6421.5', field of view 2.5 mm.

C. *Nubecularia* sp., surrounded by microlayers (dark, concentric micrites) of *Crescentiella morronensis* forma *morronensis* (Crescenti, 1969), Well-I, 5448.7', field of view 2.5 mm.

D. *Nubecularia* sp., surrounded by microlayers (dark, concentric micrites) of *Crescentiella morronensis* forma *morronensis* (Crescenti, 1969), Well-I, 5448.7', field of view 2.5 mm.

E. *Nubecularia* sp., surrounded by microlayers (dark, concentric micrites) of *Crescentiella morronensis* forma *morronensis* (Crescenti, 1969), Well-I, 5448.7', field of view 2.5 mm.

F. *Nubecularia* sp., surrounded by microlayers (dark, concentric micrites) of *Crescentiella morronensis* forma *morronensis* (Crescenti, 1969), Well-I, 5448.7', field of view 2.5 mm.

Plate 24

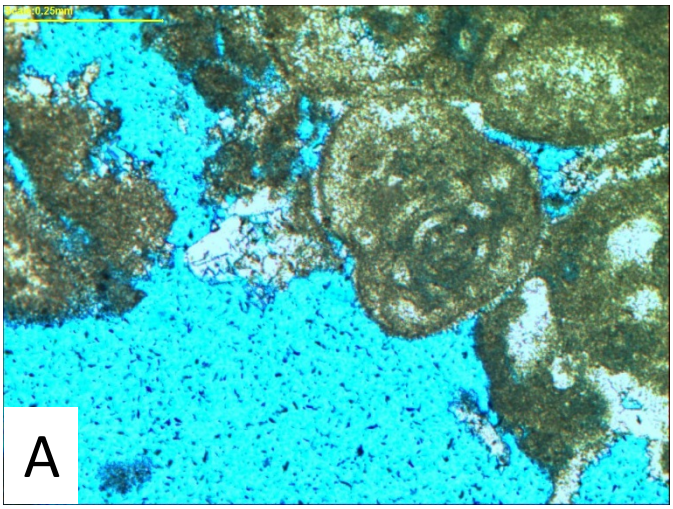

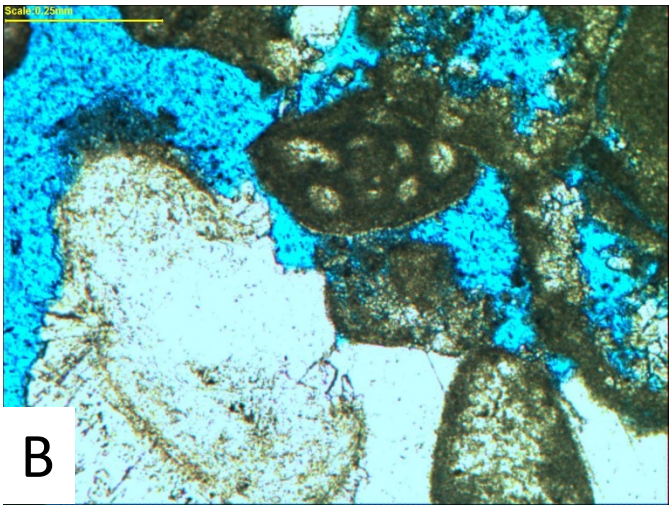

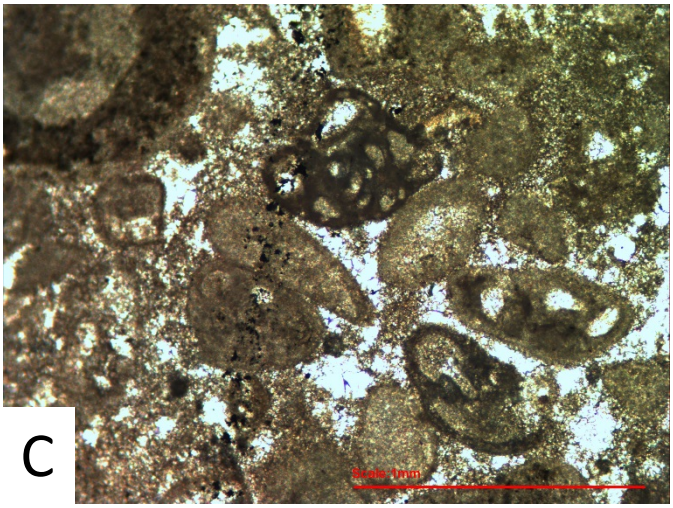

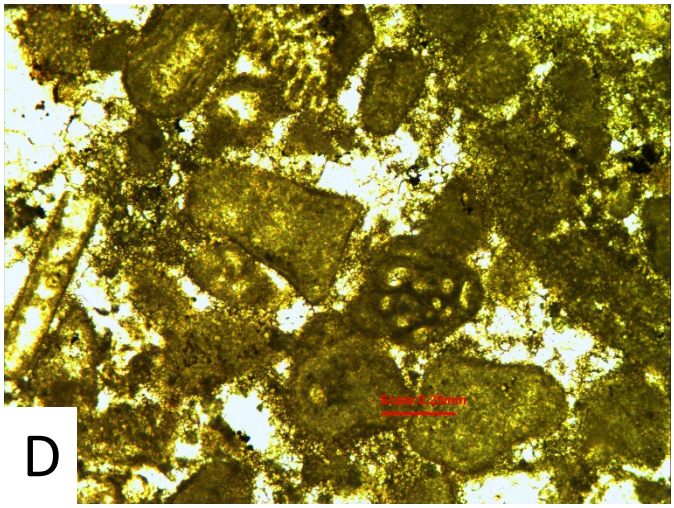

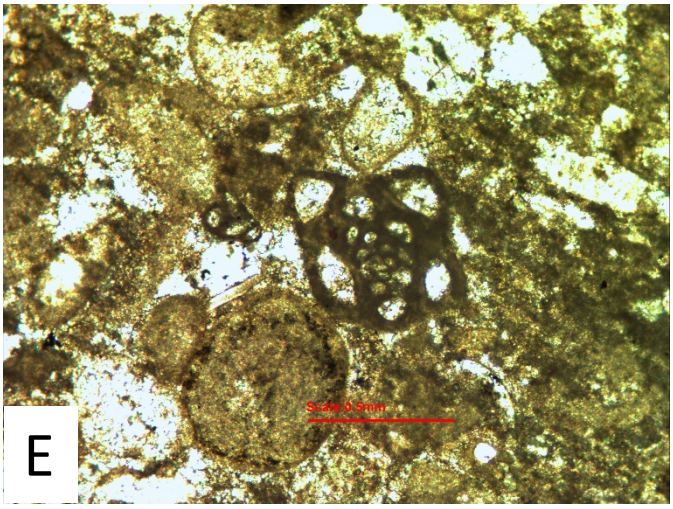

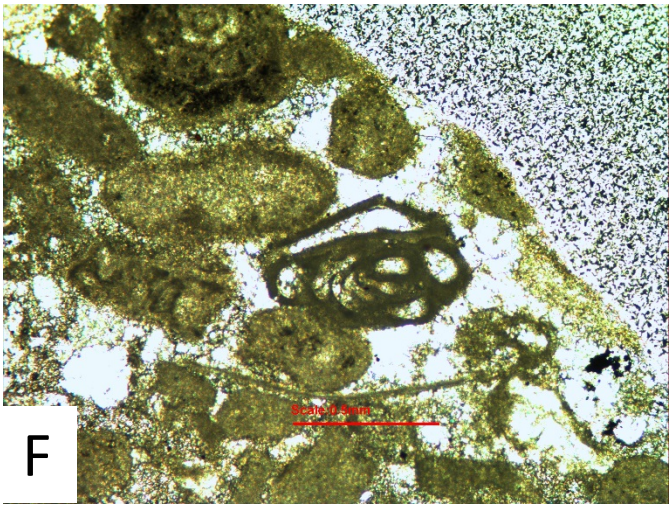

Plate 25

A. *Nodobacularia* sp., surrounded by microlayers (dark, concentric micrites) of *Crescentiella morronensis* forma *morronensis* (Crescenti, 1969), Well-B, 8388.8', field of view 6.3 mm.

B. *Nodobacularia* sp., surrounded by microlayers (dark, concentric micrites) of *Crescentiella morronensis* forma *morronensis* (Crescenti, 1969), Well-B, 8445.5', field of view 6.3 mm.

C. *Nodobacularia* sp., surrounded by microlayers (dark, concentric micrites) of *Crescentiella morronensis* forma *morronensis* (Crescenti, 1969), Well-B, 8353.3'.

D. *Derventina filipescui* Neagu (1968), Well-A, from the Yamama Formation, 4058.7', field of view 2.5 mm.

E. *Derventina filipescui* Neagu (1968), Well-I, from the Yamama Formation5451.7', field of view 2.5 mm.

F. *Derventina filipescui* Neagu (1968), Well-A, from the Yamama Formation, 4058.7', field of view 2.5 mm.

Plate 25

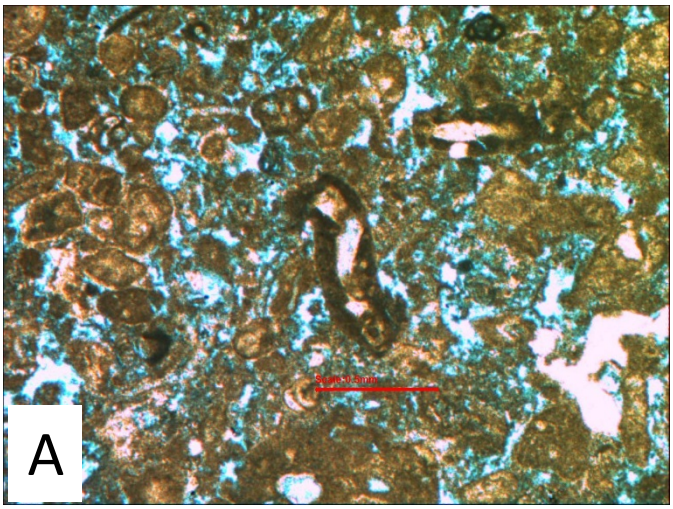

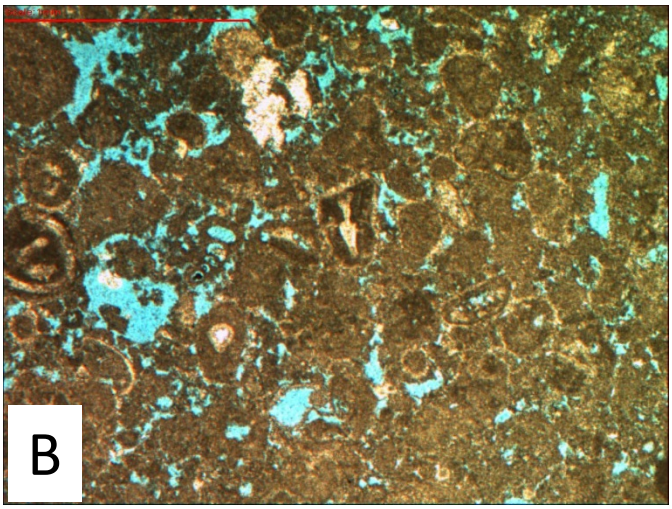

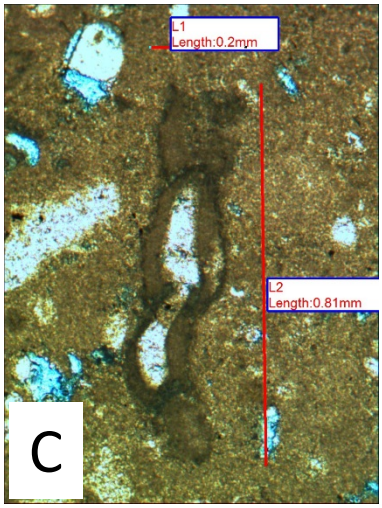

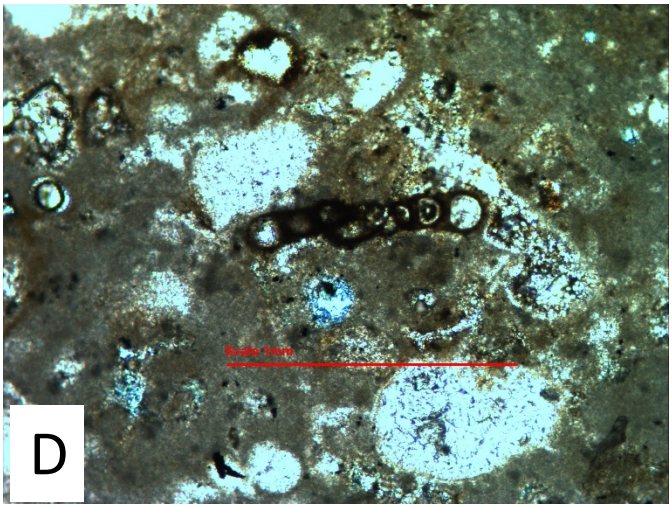

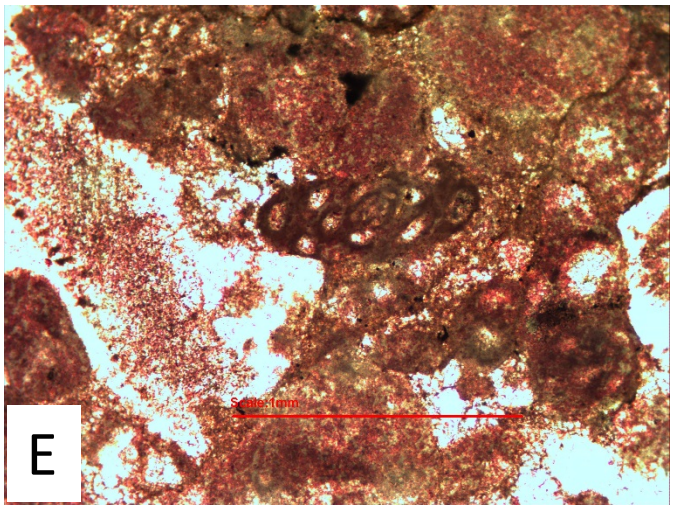

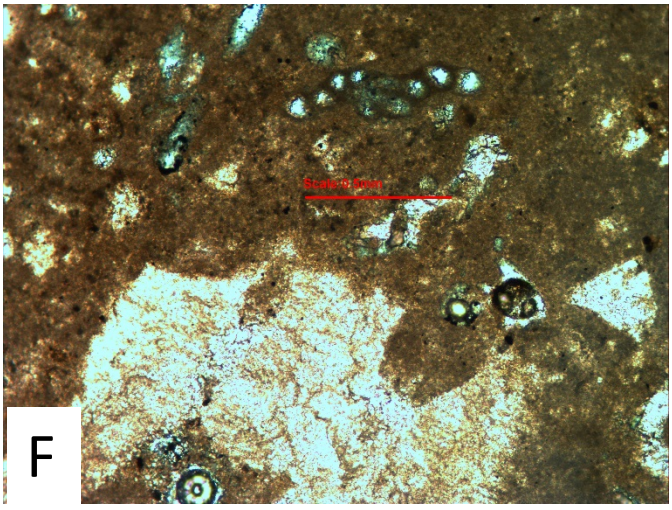

Plate 26

A. *Derventina filipescui* Neagu (1968), Well-D, from the Yamama Formation, 7960.2', field of view 1.25 mm.

B. *Istriloculina emiliae* Neagu (1984), Well-H, 7305.2', field of view 2.5 mm.

C. *Istriloculina emiliae* Neagu (1984), Well-H, 7305.2', field of view 2.5 mm.

D. *Istriloculina eliptica* (Iovcheva, 1962), Well-G, 6762.6', field of view 2.5 mm.

E. *Istriloculina eliptica* (Iovcheva, 1962), Well-B, 5408.1', field of view 2.5 mm.

F. *Quinqueloculina egmontensis* Lloyd (1962), Well-H, 7339', field of view 2.5 mm.

Plate 26

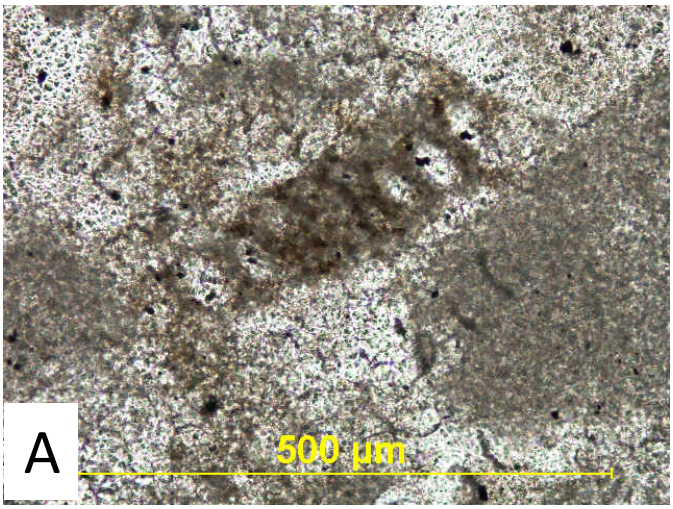

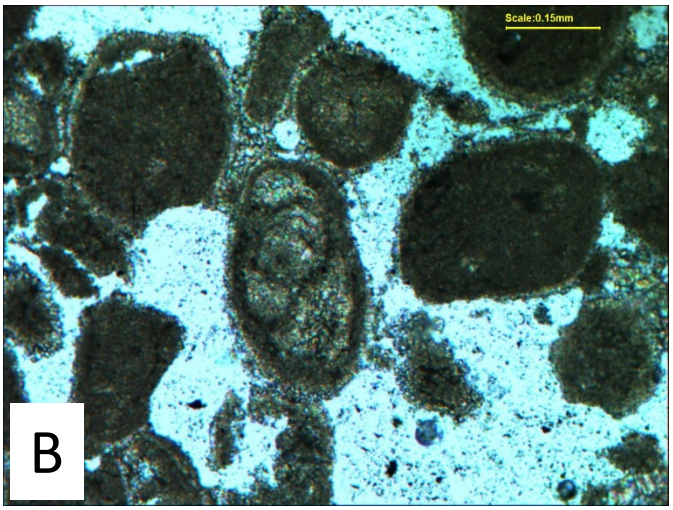

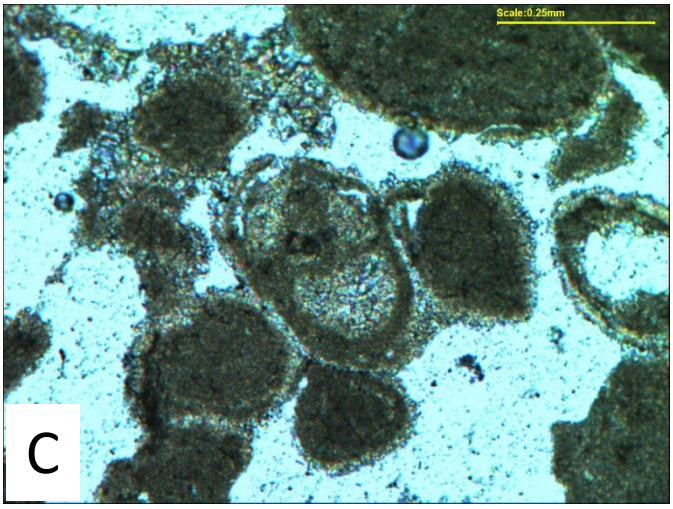

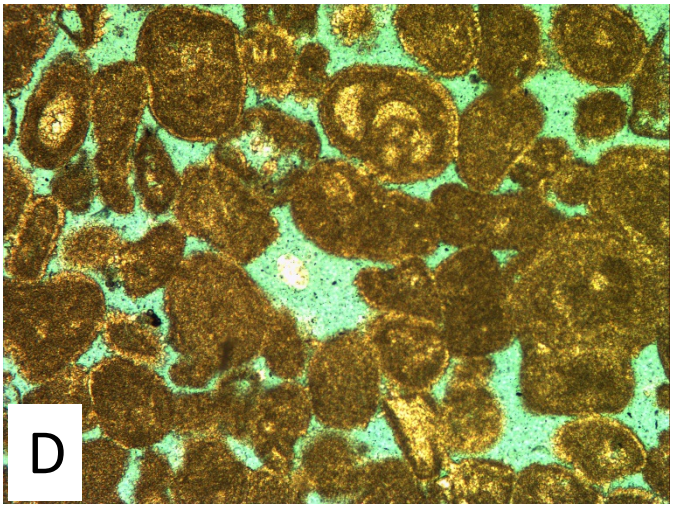

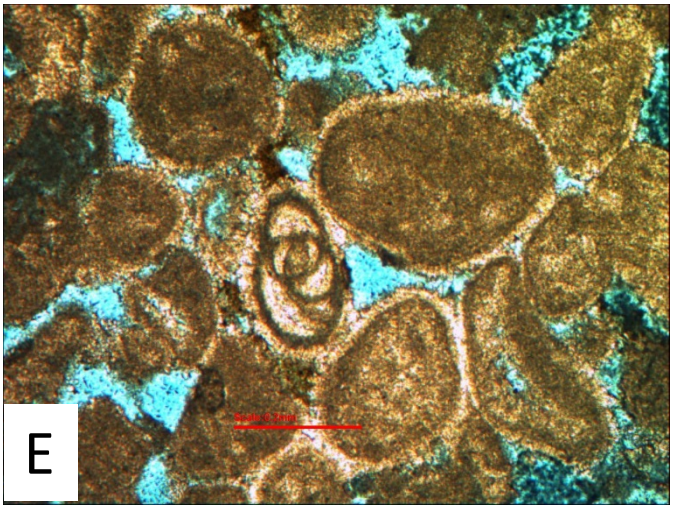

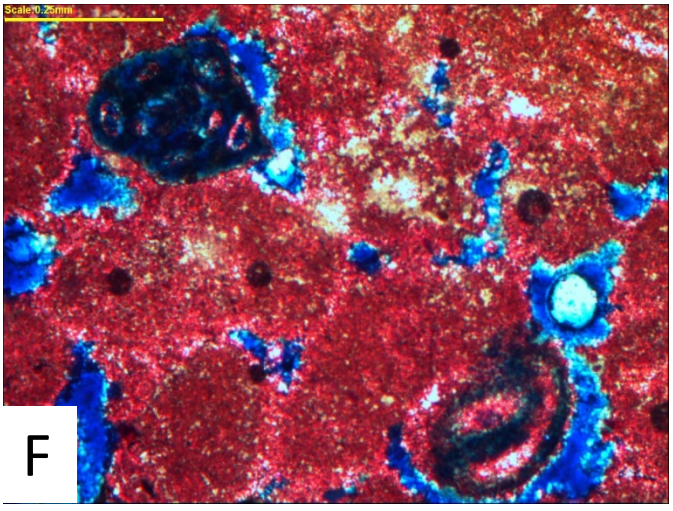

Plate 27

A. *Quinqueloculina egmontensis* Lloyd (1962), Well-H, 7325.5', field of view 2.5 mm.

B. *Quinqueloculina egmontensis* Lloyd (1962), Well-H, 7325.5', field of view 2.5 mm.

C. *Quinqueloculina egmontensis* Lloyd (1962), Well-H, 7328.6', field of view 2.5 mm.

D. *Quinqueloculina egmontensis* Lloyd (1962), Well-I, 5531.7', field of view 2.5 mm.

E. *Quinqueloculina egmontensis* Lloyd (1962), Well-I, 5531.7', field of view 2.5 mm.

F. *Quinqueloculina egmontensis* Lloyd (1962), Well-H, 6416.5', field of view 2.5 mm.

Plate 27

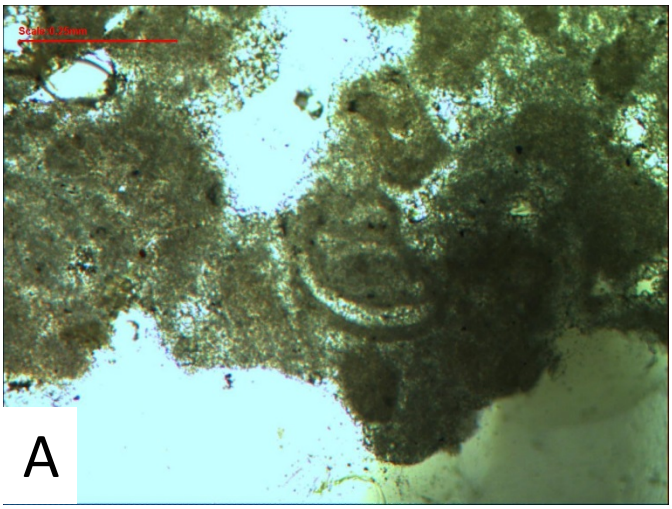

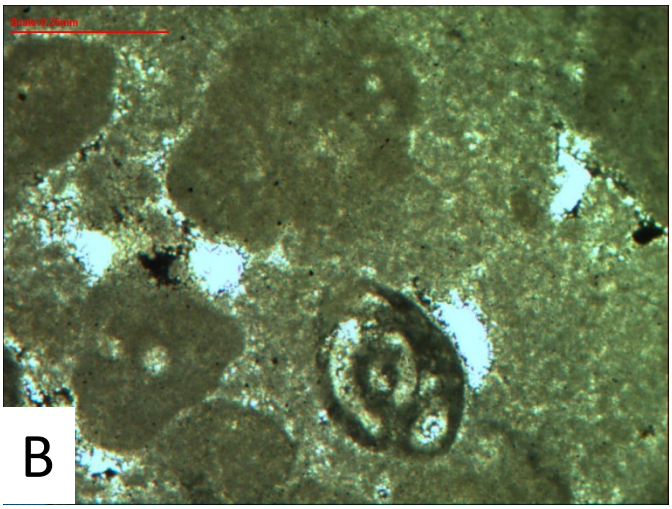

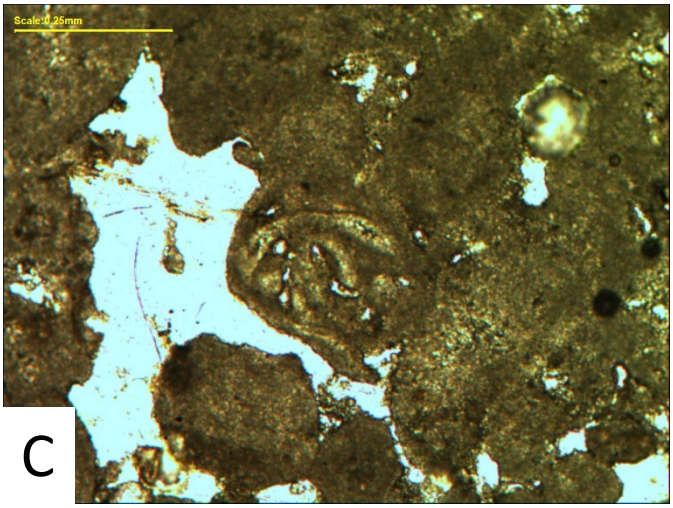

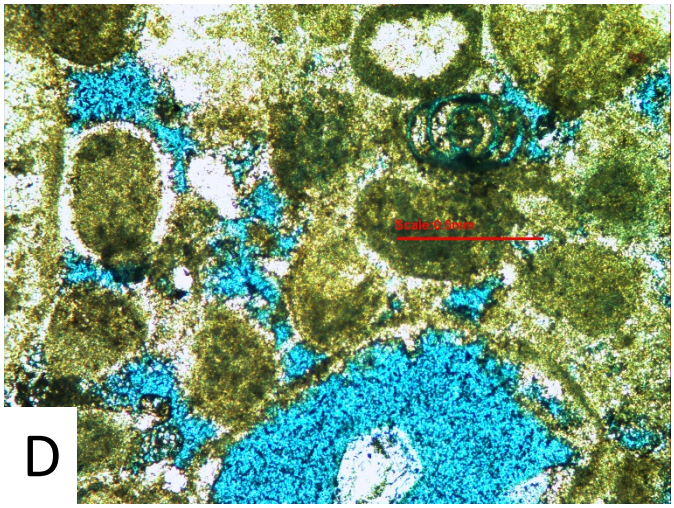

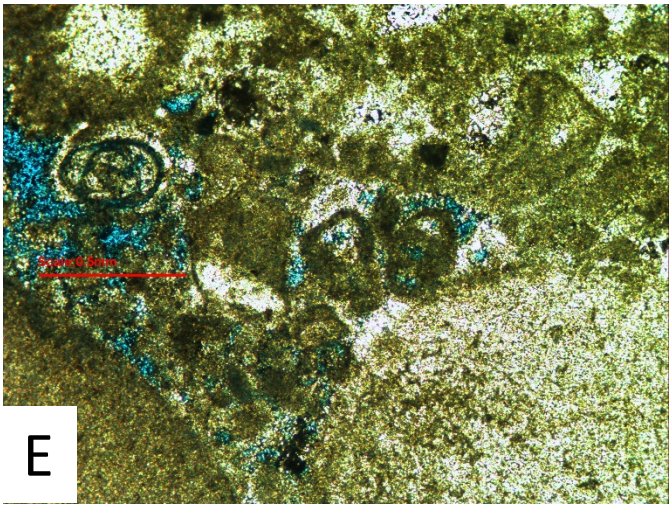

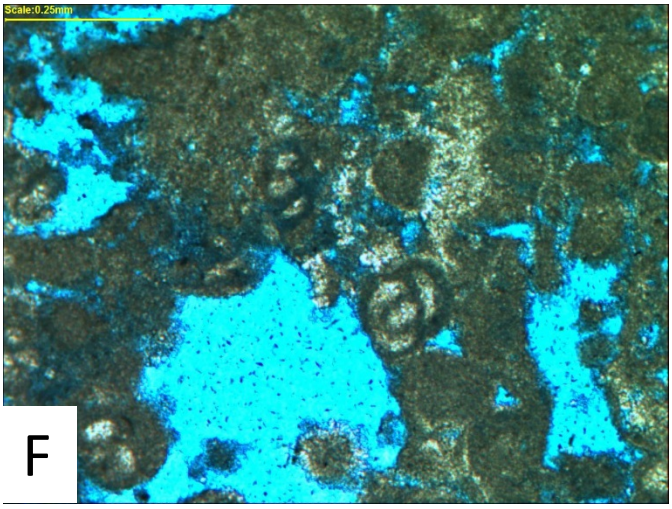

Plate 28

A. *Quinqueloculina* sp., Well-H, 6427.5', field of view 2.5 mm.

B. *Quinqueloculina* sp., Well-H, 6423.5', field of view 2.5 mm.

C. *Quinqueloculina* sp., Well-H, 6423.5', field of view 2.5 mm.

D. *Quinqueloculina* sp., Well-B, 8411.5', field of view 2.5 mm.

E. *Quinqueloculina* sp., Well-I, 5524.2', field of view 2.5 mm.

F. *Quinqueloculina* sp., Well-I, 5543.2', field of view 2.5 mm.

Plate 28

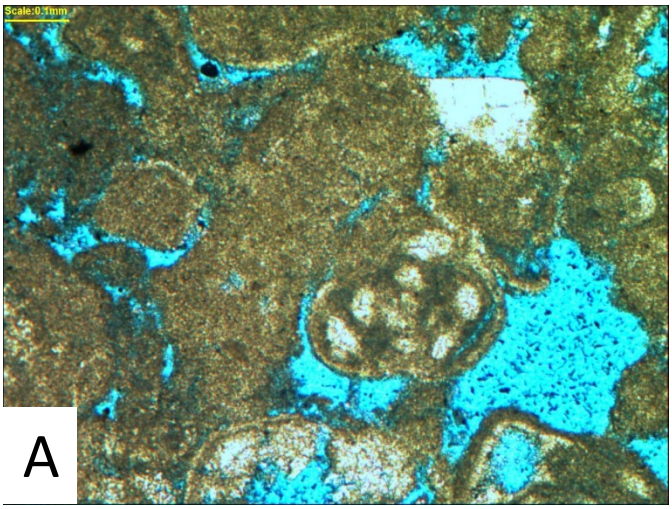

A

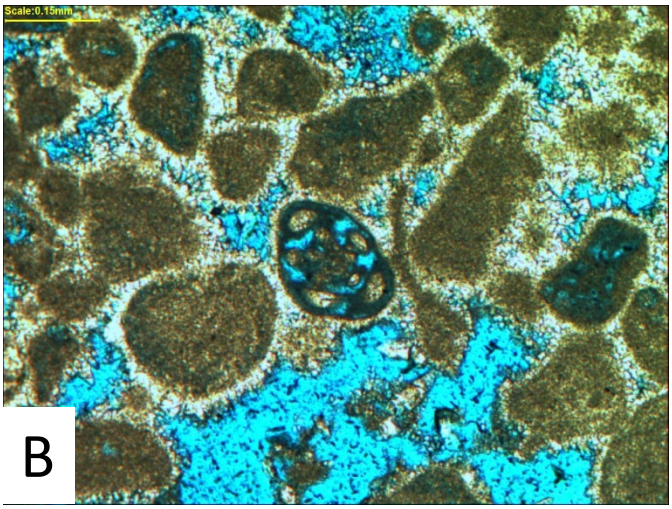

B

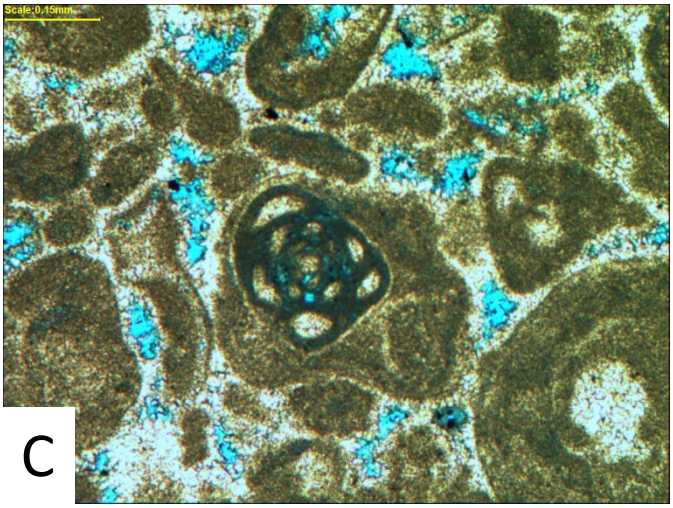

C

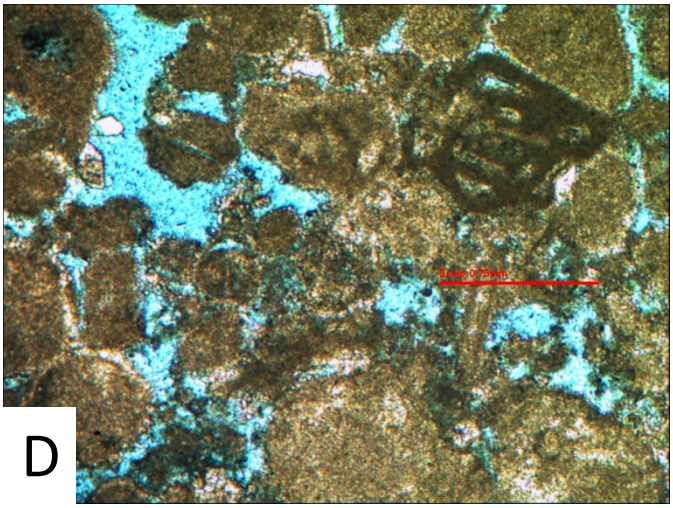

D

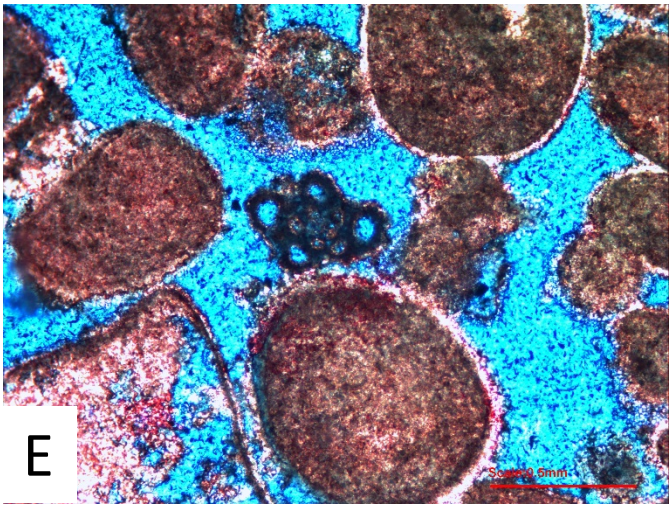

E

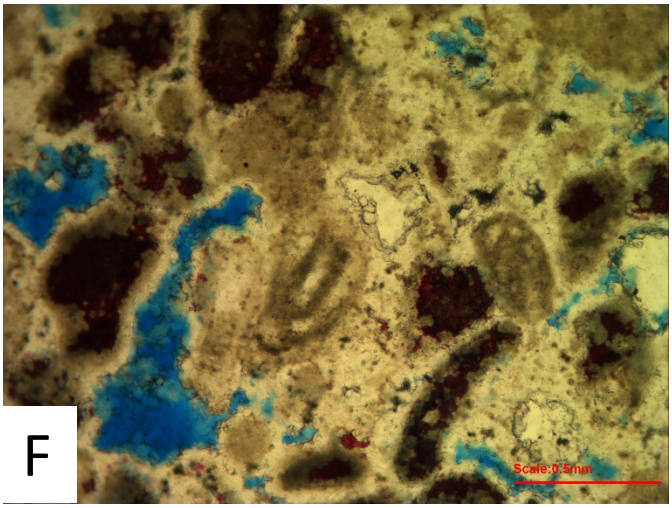

F

Plate 29

A. *Mohlerina basiliensis* (Möhler, 1938), Well-G, 6779.5', field of view 2.5 mm.

B. *Mohlerina basiliensis* (Möhler, 1938), Well-G, 6809.5', field of view 2.5 mm.

C. *Mohlerina basiliensis* (Möhler, 1938), Well-B, 8431.3', field of view 2.5 mm.

D. *Reophax* sp., Well-I, 5524.2', field of view 2.5 mm.

E. *Reophax* sp., Well-G, 6762.6', field of view 2.5 mm.

F. *Haplophragmoides joukowskyi* Charollais *et al.* (1966), Well-I, from the Yamama Formation, 5448.7', field of view 2.5 mm.

Plate 29

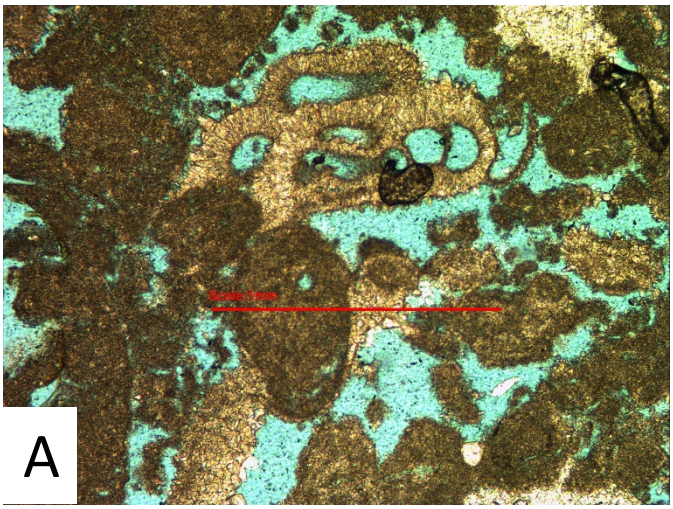

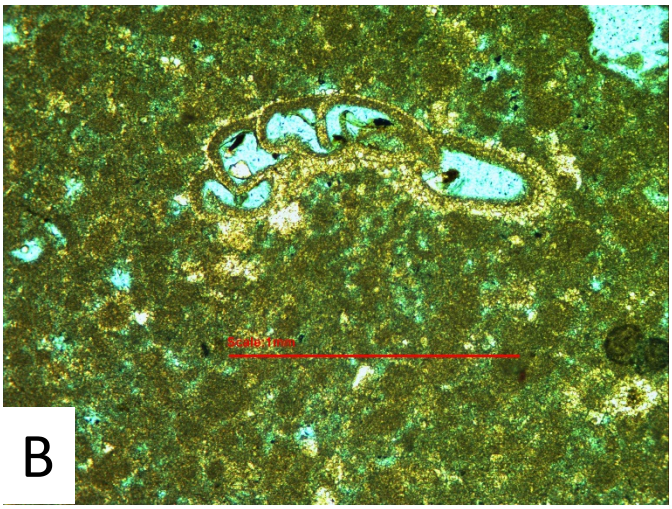

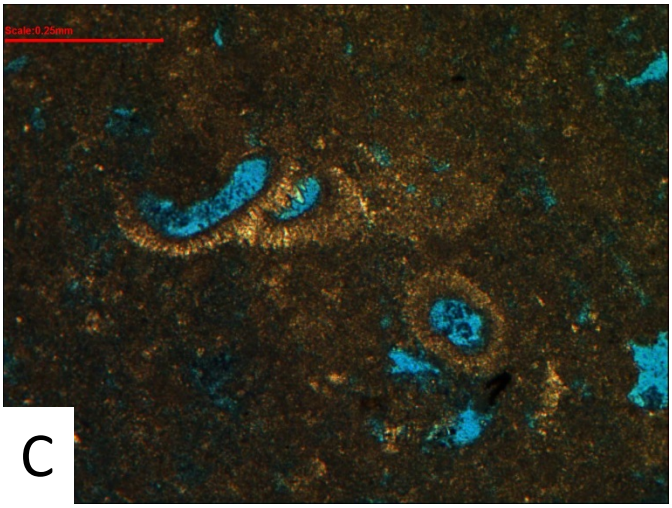

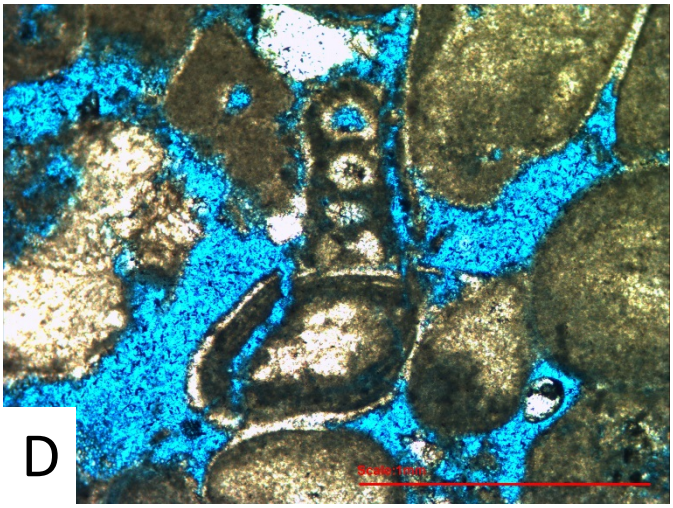

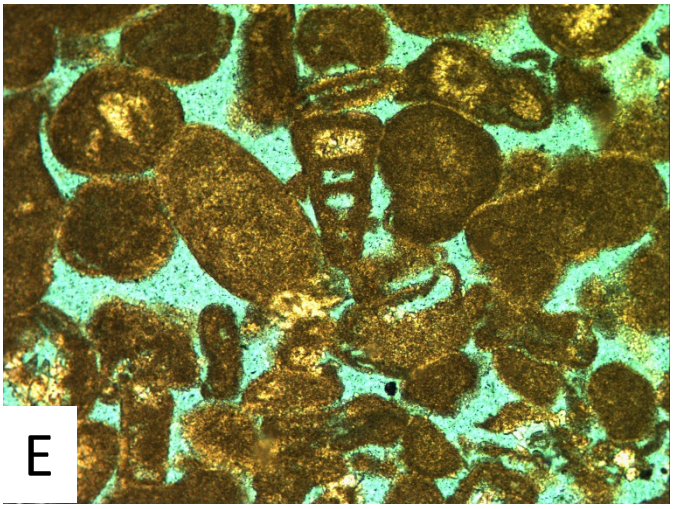

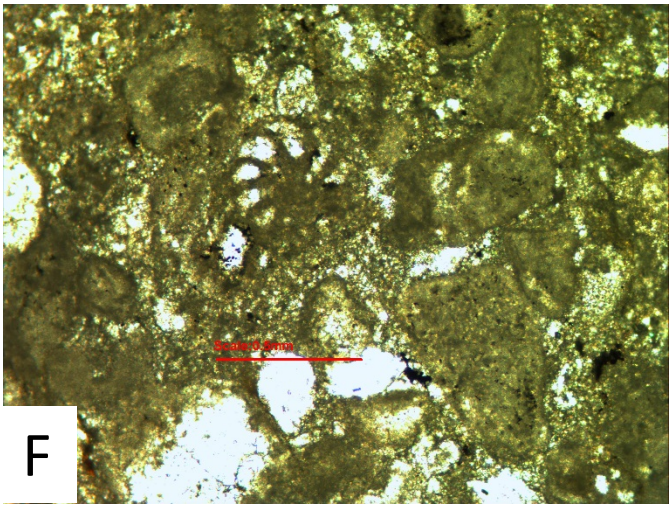

Plate 30

A. *Haplophragmoides joukowskyi* Charollais *et al.* (1966), Well-D, from the Yamama Formation, 7957.2', field of view 2.5 mm.

B. *Haplophragmoides joukowskyi* Charollais *et al.* (1966), Well-D, from the Yamama Formation, 7957.2', field of view 2.5 mm.

C. *Haplophragmoides joukowskyi* Charollais *et al.* (1966), Well-D, from the Yamama Formation, 7957.2', field of view 1.25 mm.

D. *Haplophragmoides joukowskyi* Charollais *et al.* (1966), Well-D, 7957.2', field of view 2.5 mm.

E. *Haplophragmoides joukowskyi* Charollais *et al.* (1966), Well-D, 8638.2', field of view 2.5 mm.

F. *Haplophragmoides joukowskyi* Charollais *et al.* (1966), Well-D, 8639.7', field of view 2.5 mm.

Plate 30

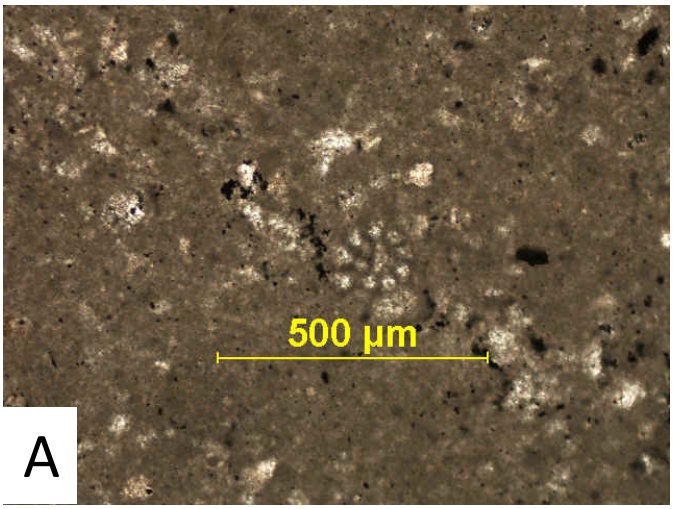

A

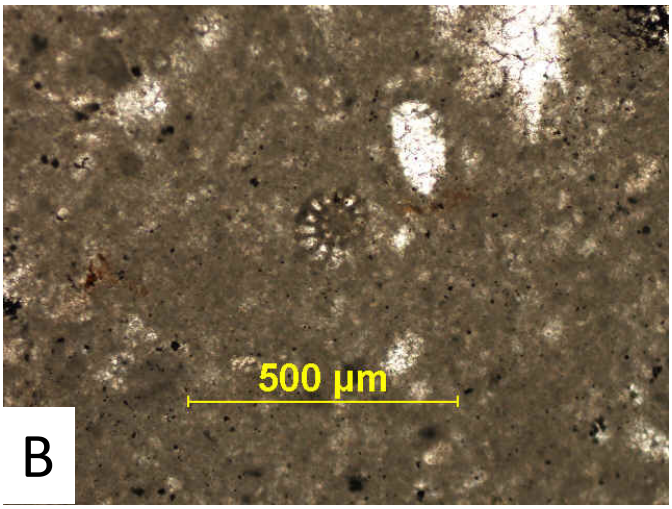

B

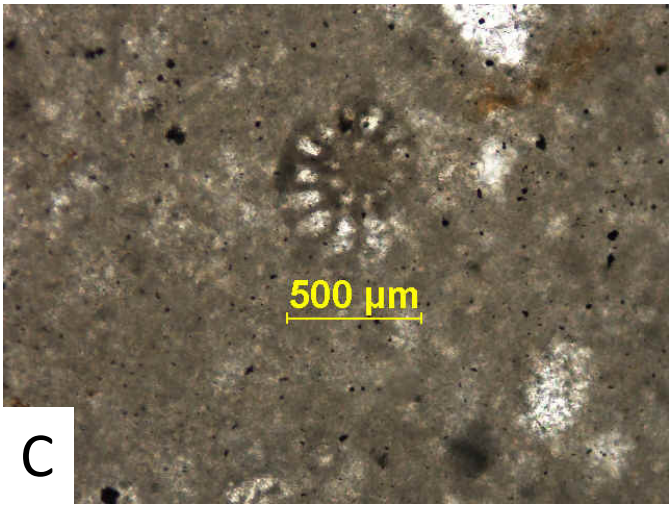

C

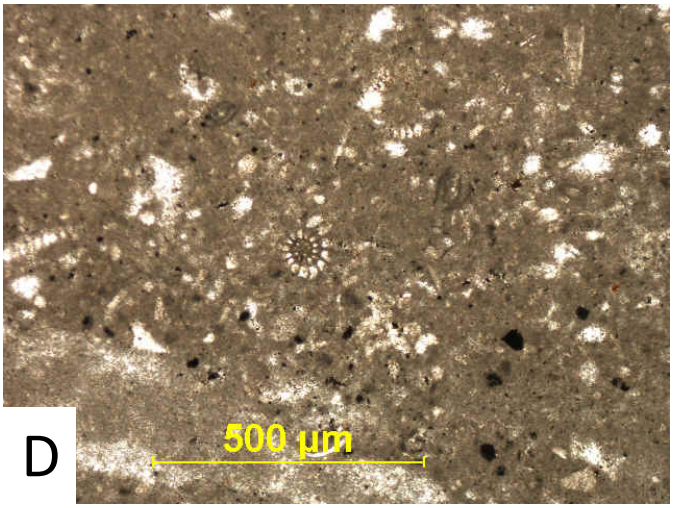

D

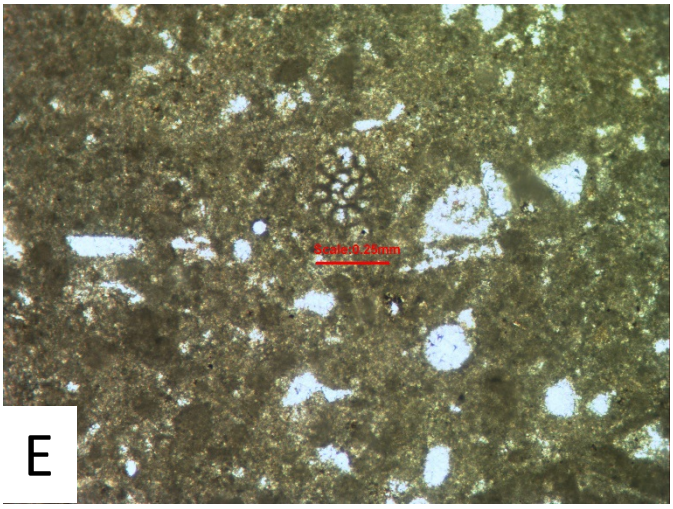

E

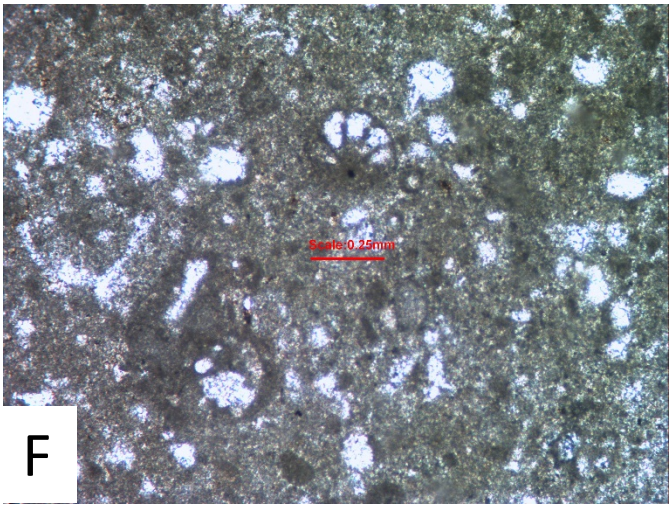

F

Plate 31

A. *Nautiloculina bronnimanni* Arnaud-Vanneau and Peybernes (1978), Well-H, 6421.5', field of view 2.5 mm.

B. *Nautiloculina bronnimanni* Arnaud-Vanneau and Peybernes, (1978), Well-H, 6427.5', field of view 2.5 mm.

C. *Nautiloculina bronnimanni* Arnaud-Vanneau and Peybernes, (1978), Well-H, 6427.5', field of view 2.5 mm.

D. *Nautiloculina bronnimanni* Arnaud-Vanneau and Peybernes, (1978), Well-I, 5518.2', field of view 2.5 mm.

E. *Nautiloculina oolithica* Möhler (1938), Well-H, 7331.8', field of view 2.5 mm.

F. *Nautiloculina oolithica* Möhler (1938), Well-H, 6417.5', field of view 2.5 mm.

Plate 31

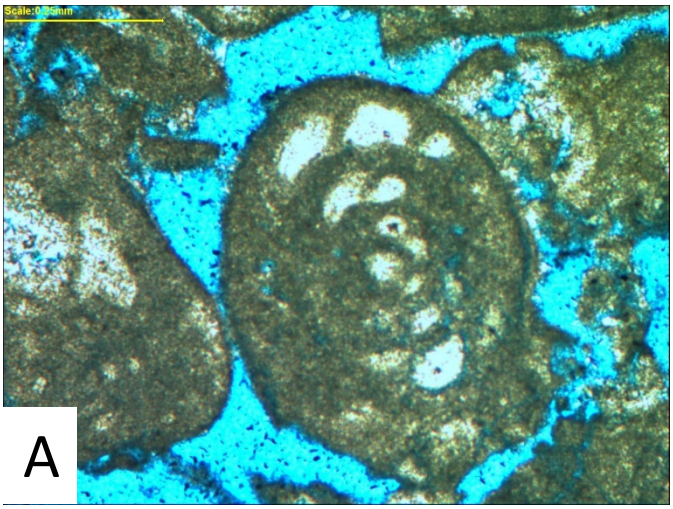

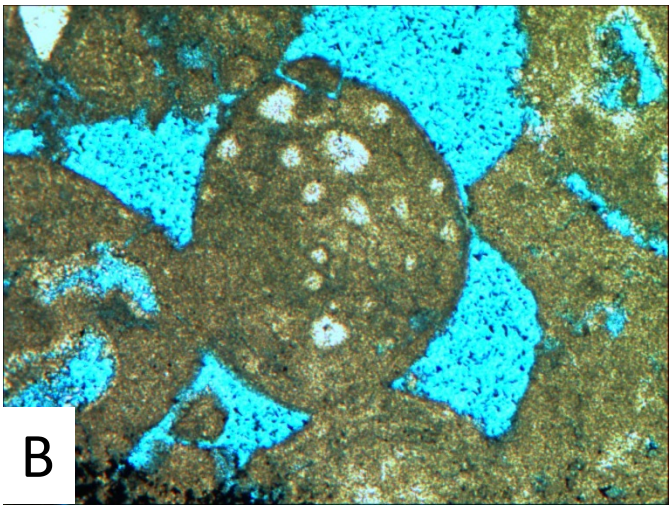

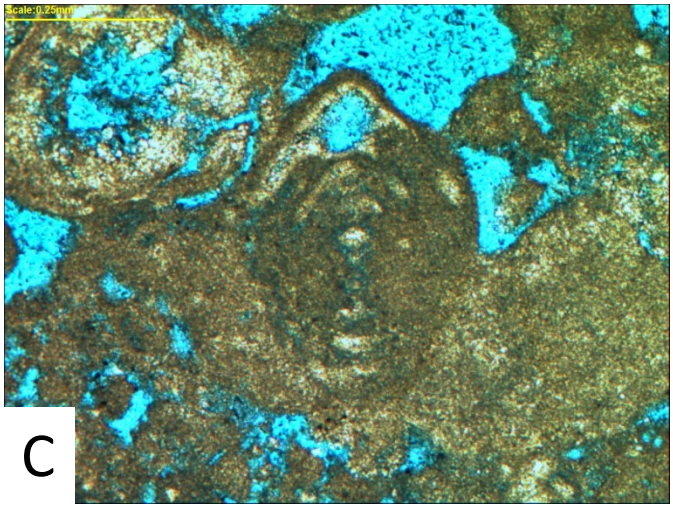

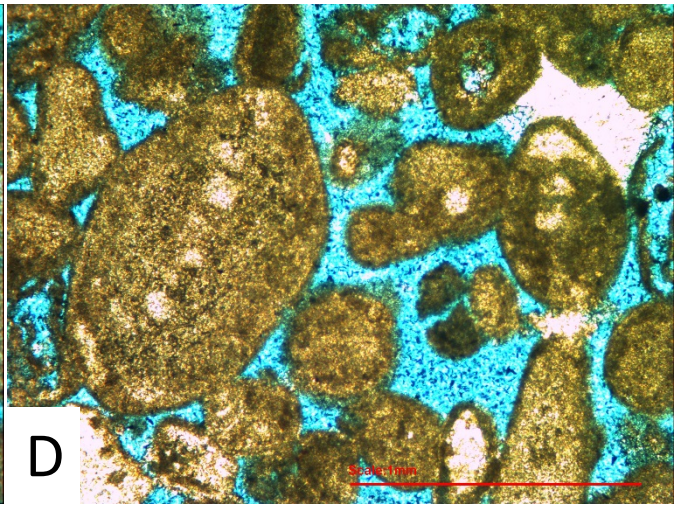

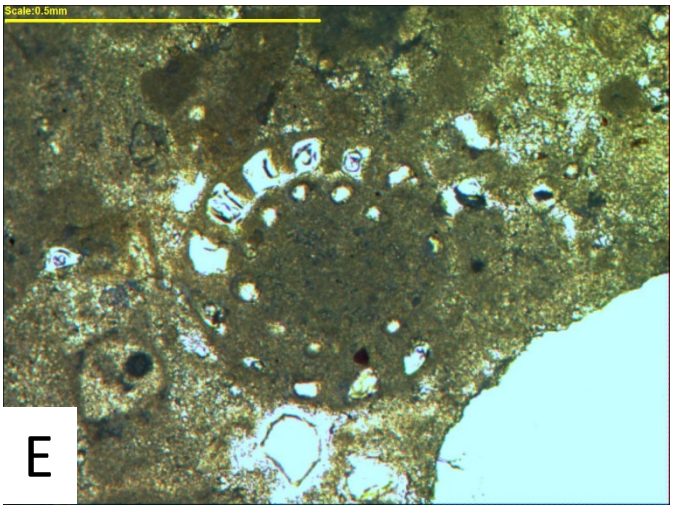

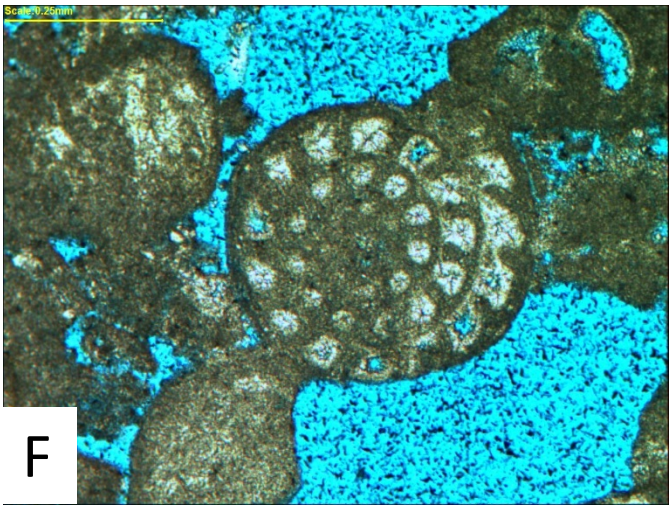

Plate 32

A. *Nautiloculina oolithica* Möhler (1938), Well-B, 8361.8', field of view 2.5 mm.

B. *Nautiloculina oolithica* Möhler (1938),, Well-H, 7331.8', field of view 2.5 mm.

C. *Freixialina planispiralis* Ramalho (1969), Well-I, 5448.7', field of view 2.5 mm.

D. *Freixialina planispiralis* Ramalho (1969), Well-G, 6775.6', field of view 2.5 mm.

E. *Ammobaculites* sp. aff. *A. celatus* Arnaud-Vanneau (1980), Well-I, 5474.1', field of view 1.25 mm.

F. *Ammobaculites* sp. aff. *A*. *celatus* Arnaud-Vanneau (1980), Well-I, 5524.2', field of view 2.5 mm.

Plate 32

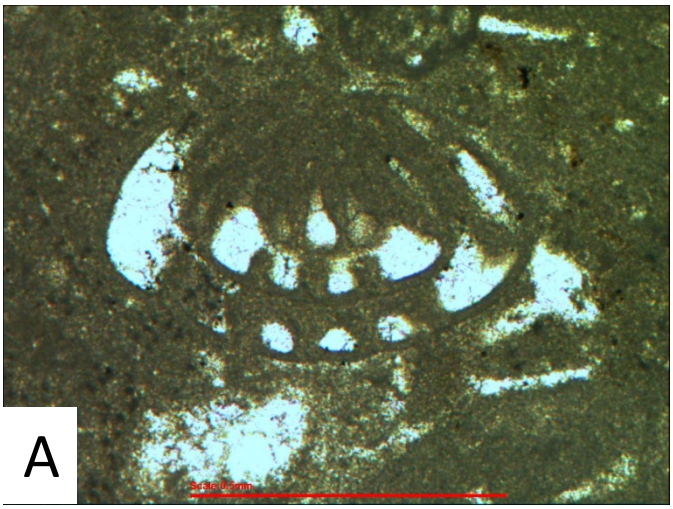

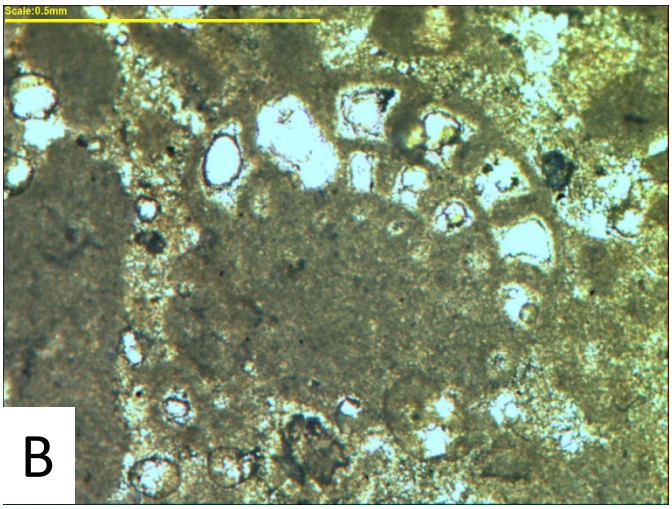

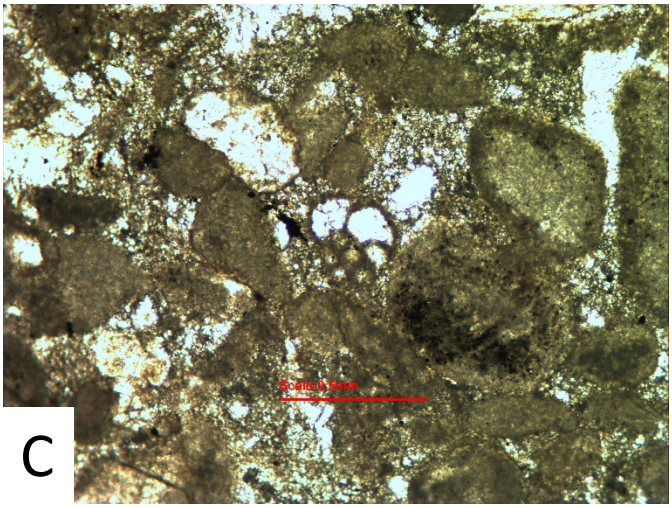

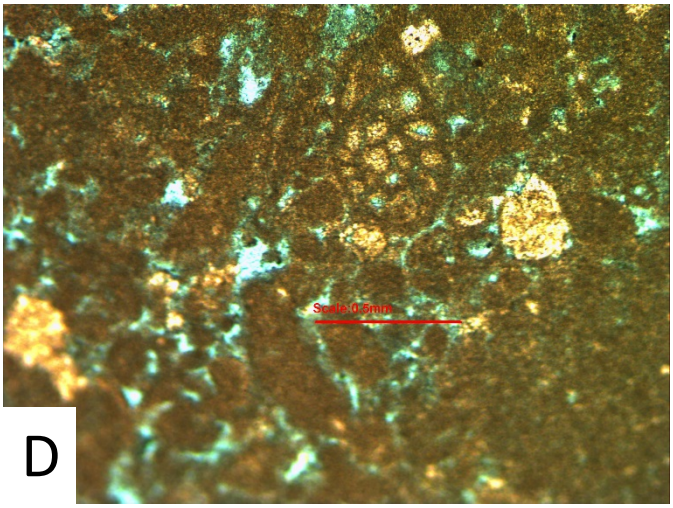

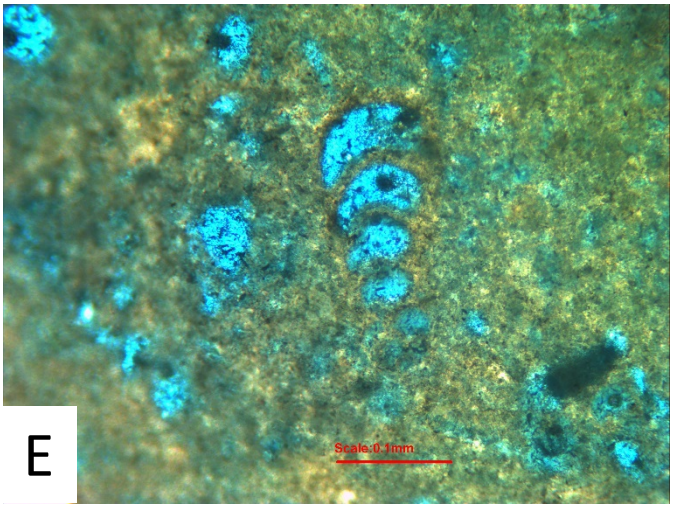

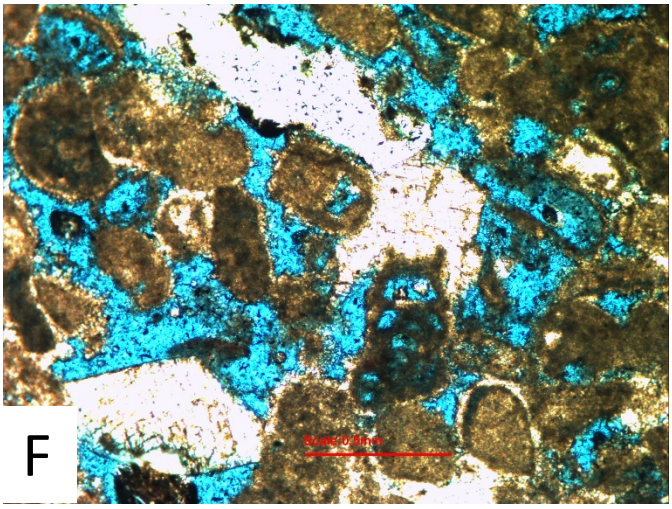

Plate 33

A. *Ammobaculites subcretaceus* Cushman and Alexander (1930), Well-F, 8412.5', field of view 6.3 mm.

B. *Ammobaculites subcretaceus* Cushman and Alexander (1930), Well-G, 6760.6', field of view 2.5 mm.

C. *Ammobaculites subcretaceus* Cushman and Alexander (1930), Well-G, 6762.6', field of view 2.5 mm.

D. *Ammobaculites subcretaceus* Cushman and Alexander (1930), Well-G, 6762.6', field of view 2.5 mm.

E. *Charentia cuvillieri* Neumann (1965), Well-H, 6408.1', field of view 1.25 mm.

F. *Charentia evoluta* (Gorbatchik, 1968), Well-I, 5480.2', field of view 6.3 mm.

Plate 33

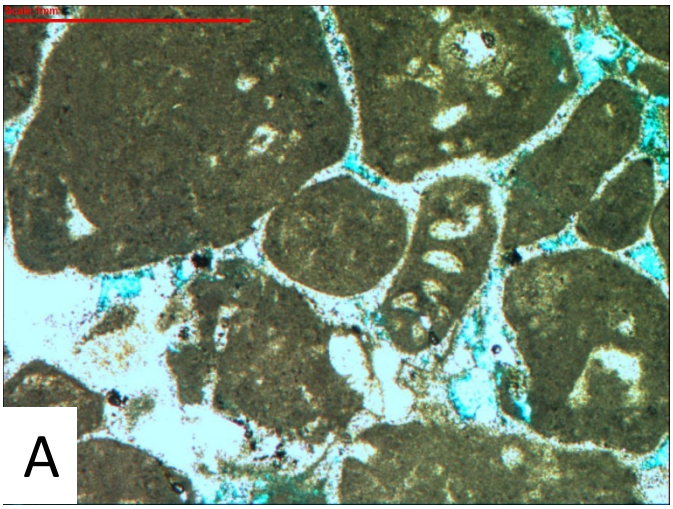

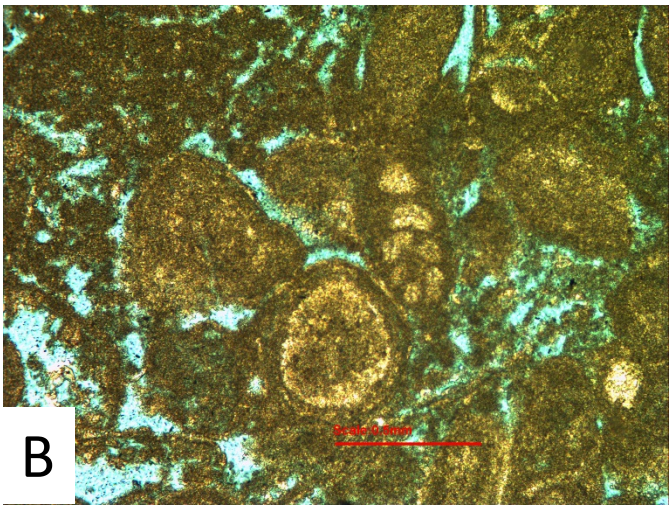

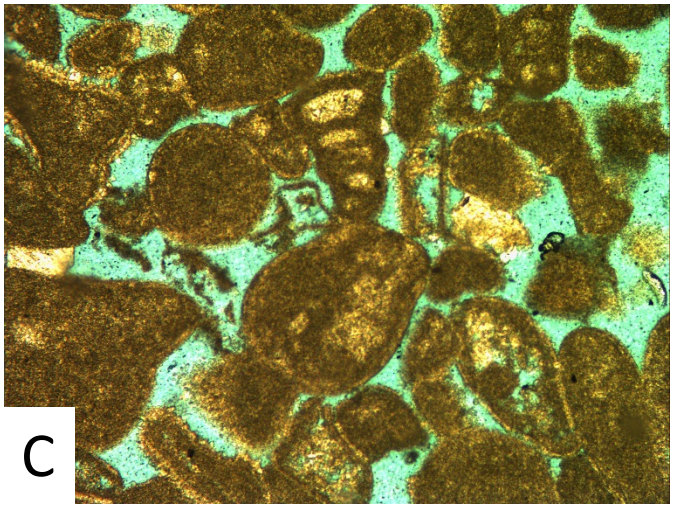

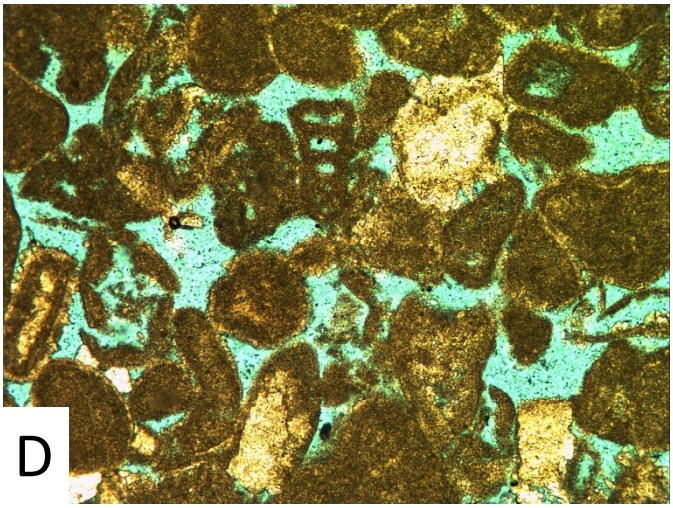

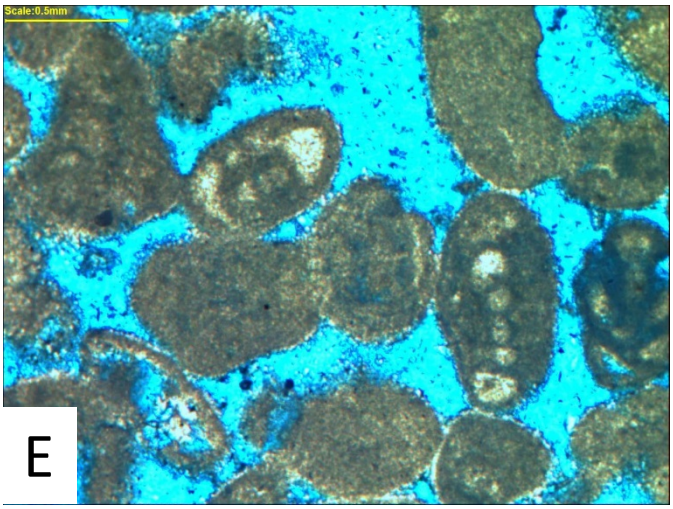

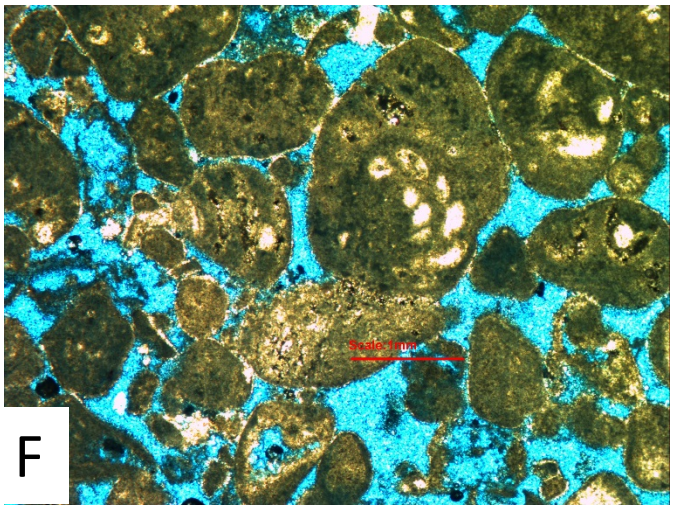

Plate 34

A. *Charentia evoluta* (Gorbatchik, 1968), Well-I, 5471.7', field of view 6.3 mm.

B. *Montsalevia salevensis* Charollais *et al.* (1966), Well-A, plug # 4, field of view 6.3 mm.

C. *Montsalevia salevensis* Charollais *et al.* (1966), Well-I, 5465.7', field of view 2.5 mm.

D. *Anchispirocyclina lusitanica* (Egger, 1902), Well-I, 5385.7', field of view 6.3 mm.

E. *Anchispirocyclina lusitanica* (Egger, 1902), Well-I, 5385.7', field of view 6.3 mm.

F. *Anchispirocyclina lusitanica* (Egger, 1902), Well-I, 5385.7', field of view 6.3 mm.

Plate 34

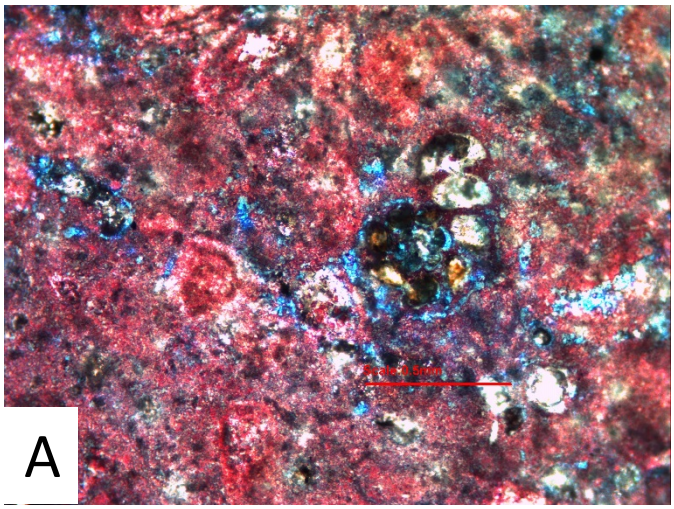

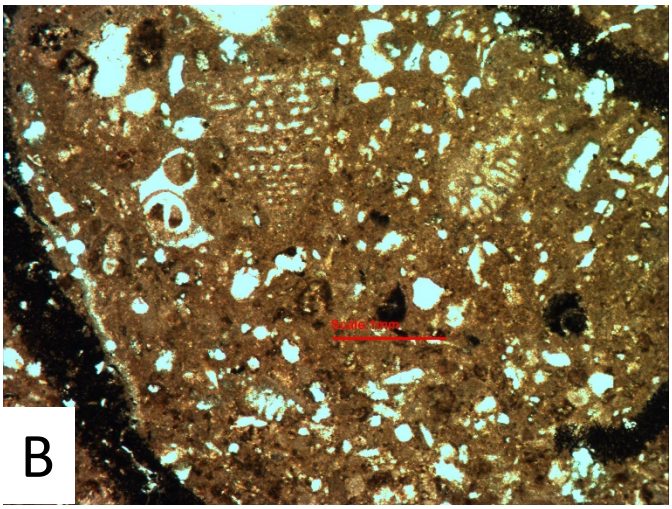

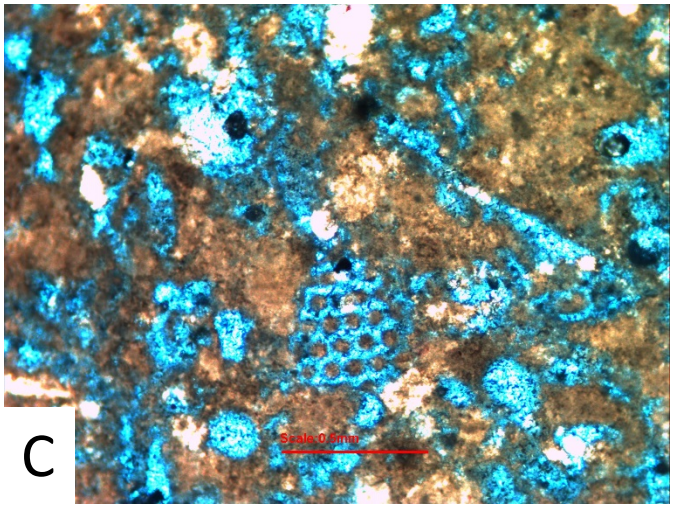

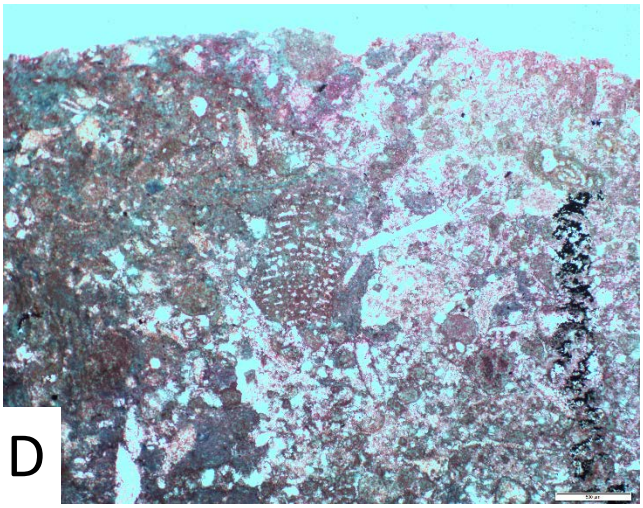

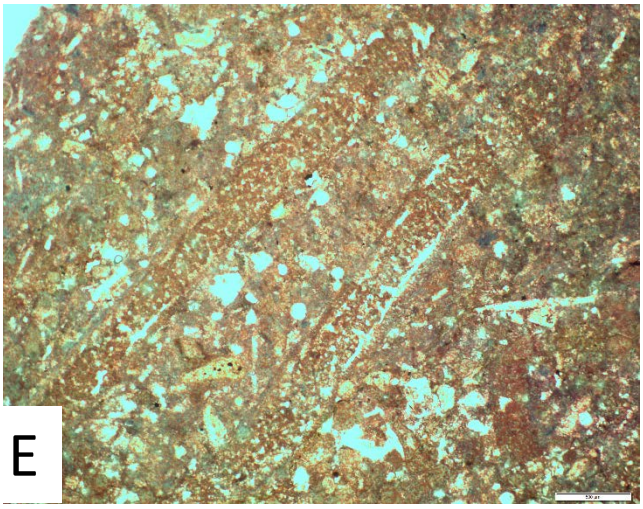

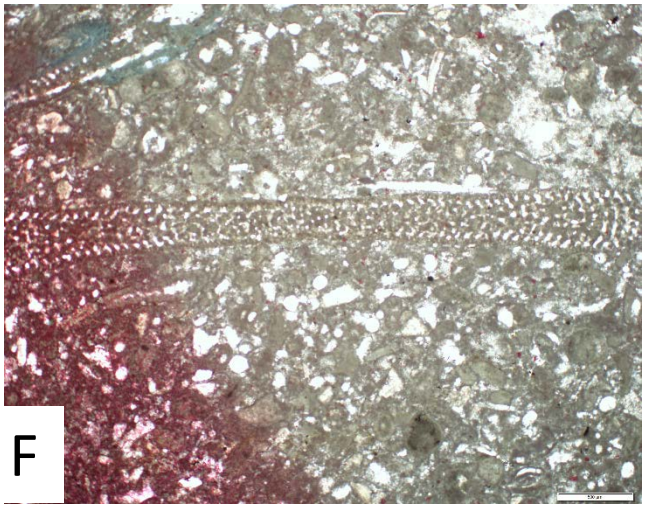

Plate 35

A. *Anchispirocyclina lusitanica* (Egger, 1902), Well-I, 5385.7', field of view 6.3 mm.

B. *Anchispirocyclina lusitanica* (Egger, 1902), Well-B, 8357', field of view 6.3 mm.

C. *Anchispirocyclina lusitanica* (Egger, 1902), Well-B, 8357', field of view 2.5 mm.

D. *Anchispirocyclina lusitanica* (Egger, 1902), Well-I, 5385.7', field of view 16 mm.

E. *Anchispirocyclina lusitanica* (Egger, 1902), Well-I, 5385.7', field of view 6.3 mm.

F. *Everticyclammina kelleri* (Henson, 1948), Well-D, 8639.7', field of view 2.5 mm.

Plate 35

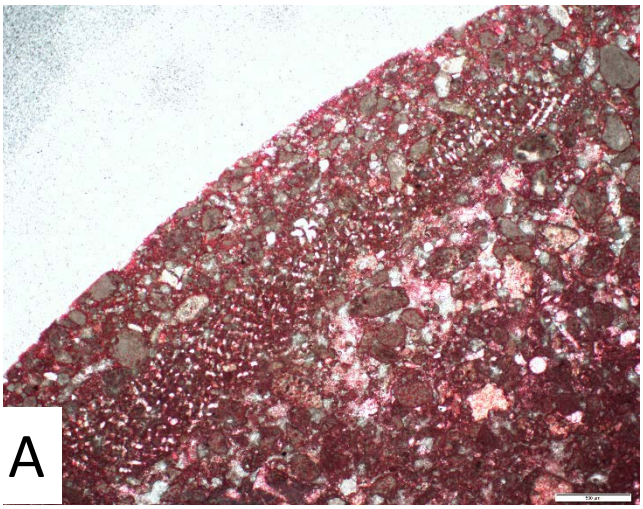

A

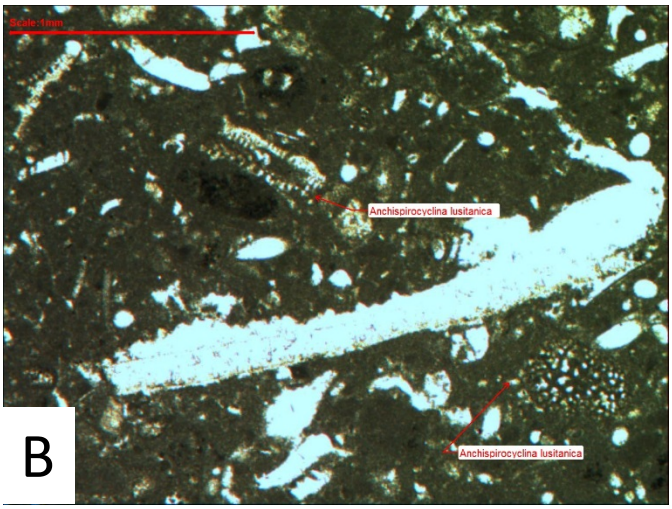

B

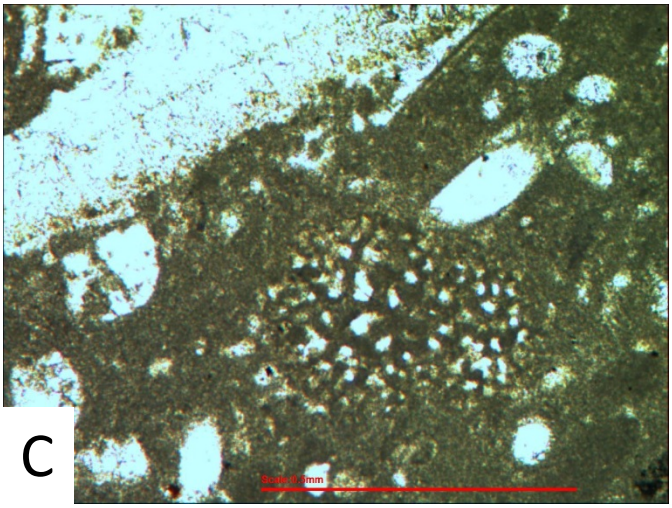

C

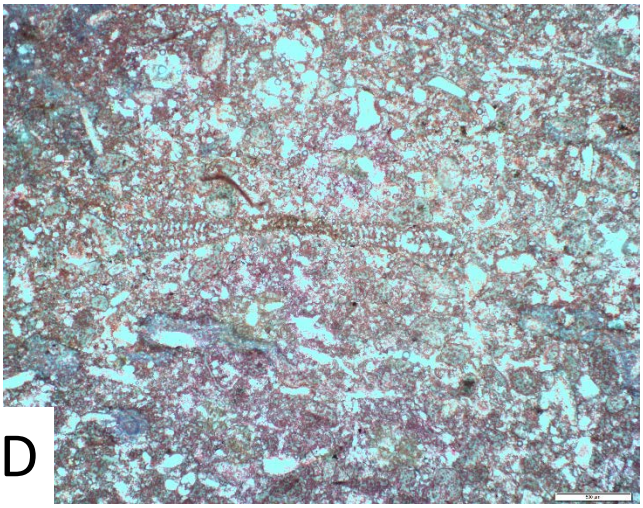

D

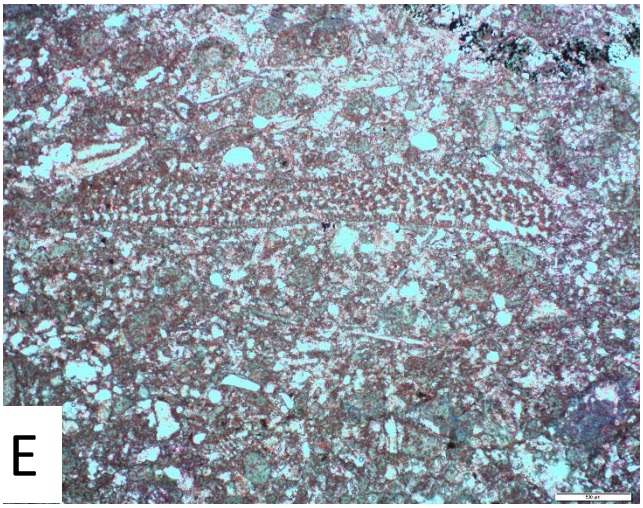

E

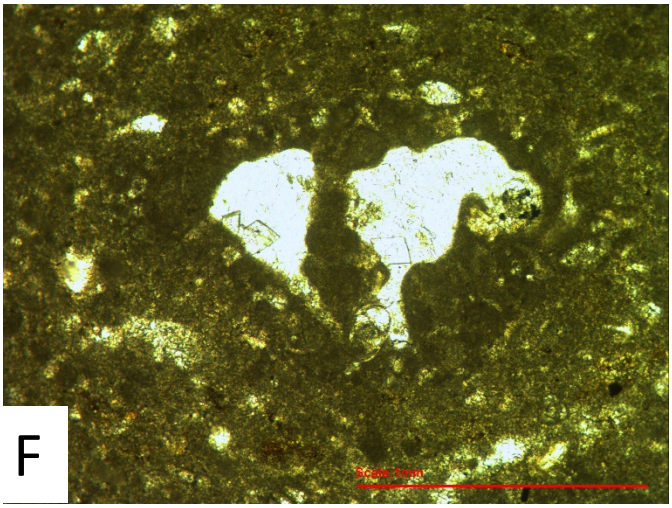

F

Plate 36

A. *Everticyclammina kelleri* (Henson, 1948), Well-D, 8641.2', field of view 2.5 mm.

B. *Everticyclammina kelleri* (Henson, 1948), Well-D8641.2', field of view 2.5 mm.

C. *Everticyclammina kelleri* (Henson, 1948), Well-D8641.2', field of view 2.5 mm.

D. *Everticyclammina kelleri* (Henson, 1948), Well-D8644.2', field of view 2.5 mm.

E. *Everticyclammina kelleri* (Henson, 1948), Well-B, 8370.5', field of view 2.5 mm.

F. *Everticyclammina kelleri* (Henson, 1948) (right), and *Pseudocyclammina cylindrica* Redmond (1964) (left), Well-B, 8370.5', field of view 6.3 mm.

Plate 36

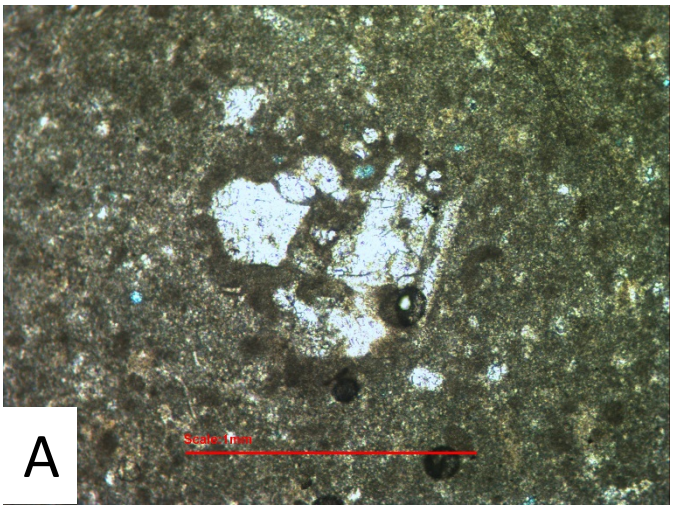

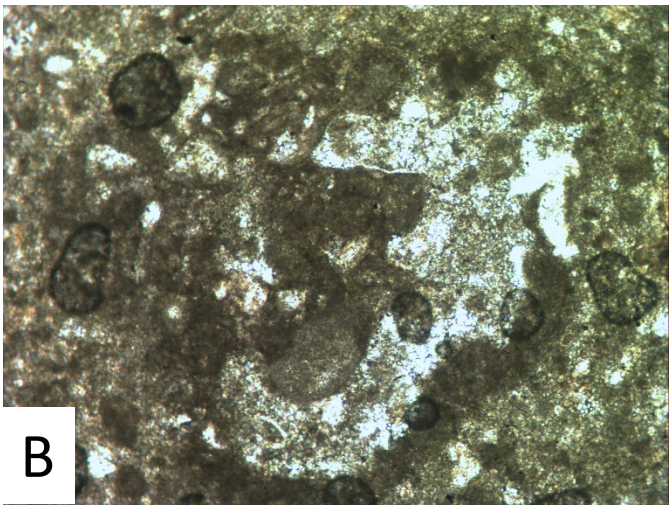

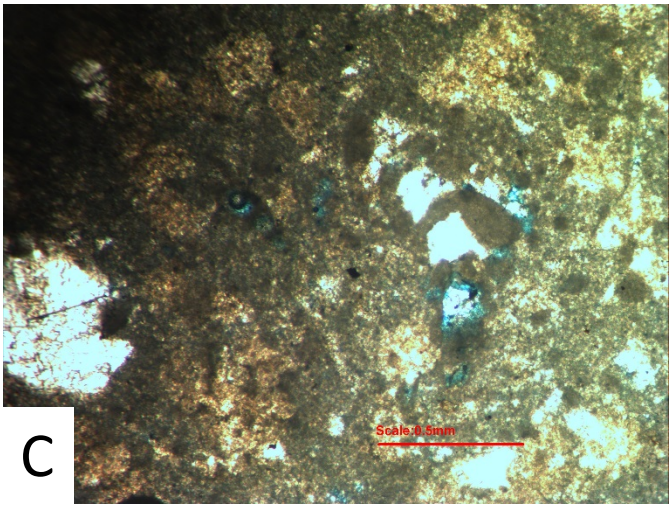

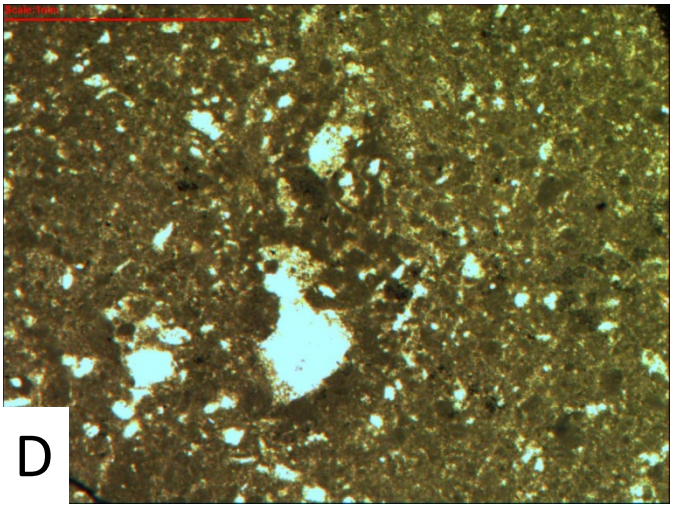

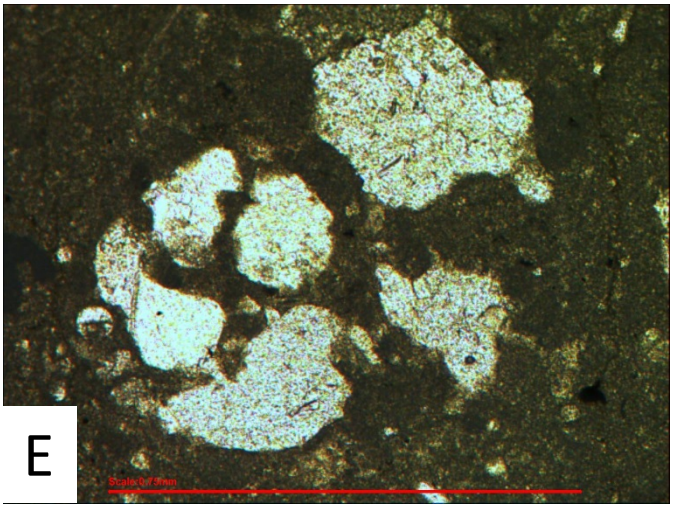

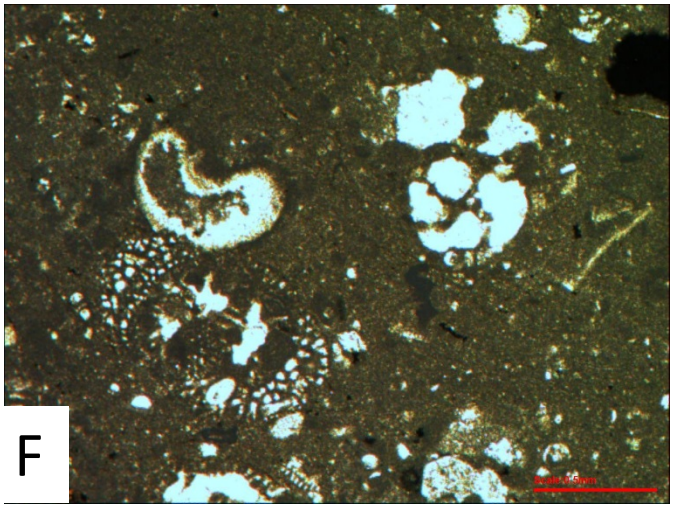

Plate 37

A. *Everticyclammina virguliana* Koechlin (1942), Well-H, 7328.6', field of view 2.5mm.

B. *Everticyclammina virguliana* Koechlin (1942), Well-H, 7328.6', field of view 2.5 mm.

C. *Everticyclammina virguliana* Koechlin (1942), Well-G, 6811.3', field of view 2.5 mm.

D. *Everticyclammina virguliana* Koechlin (1942), Well-D, 8644.2', field of view 2.5 mm.

E. *Bramkampella arabica* Redmond (1964), Well-I, 5479.2', field of view 6.3 mm.

F. *Bramkampella arabica* Redmond (1964), Well-B, 8370.5', field of view 2.5 mm.

Plate 37

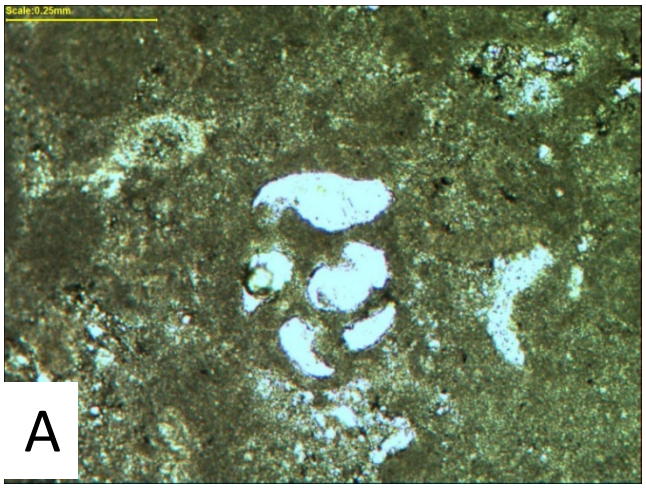

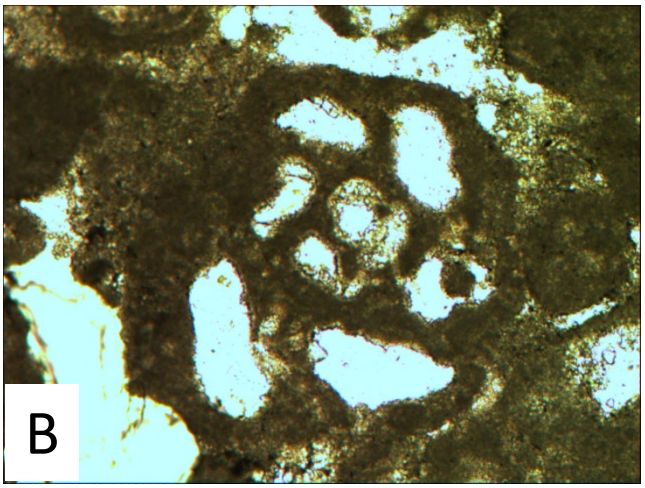

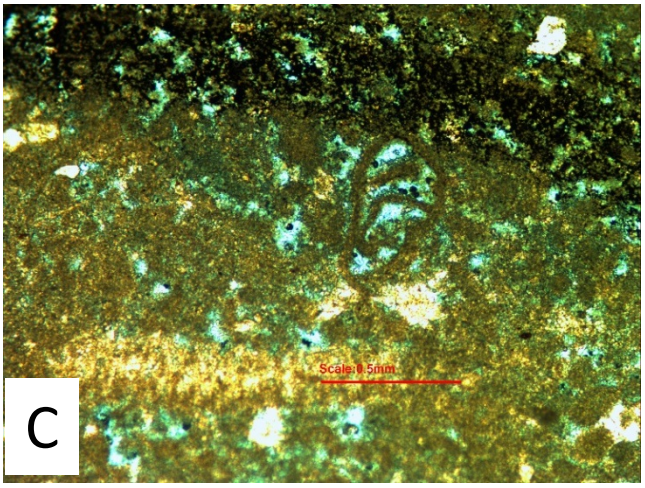

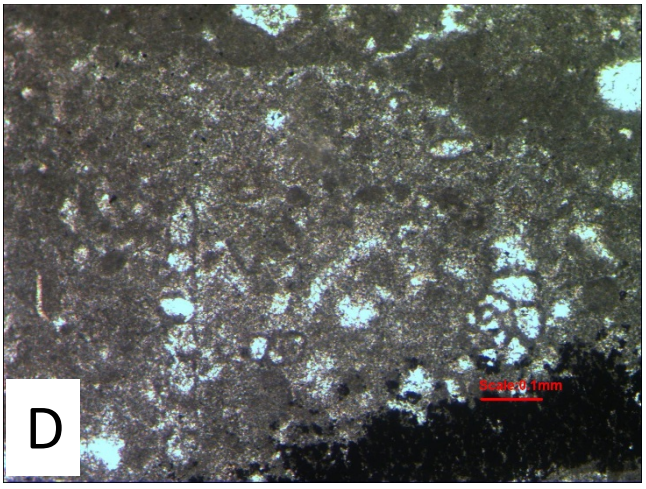

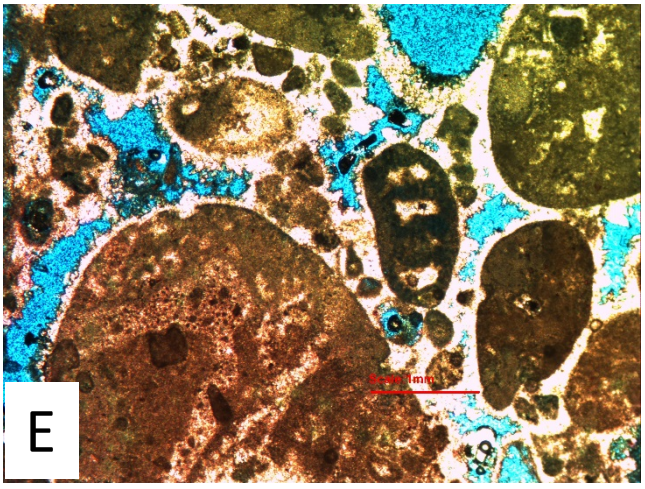

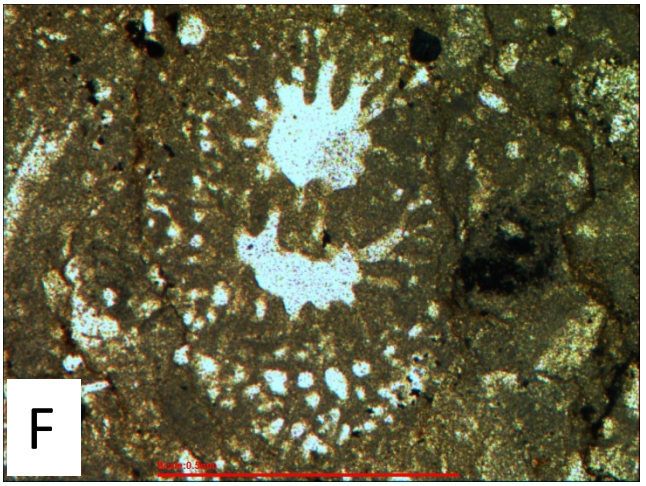

Plate 38

A. *Bramkampella arabica* Redmond (1964), Well-A, 4110.5,, field of view 6.3 mm.

B. *Bramkampella arabica* Redmond (1964), Well-D, 7957.2', field of view 2.5 mm.

C. *Bramkampella arabica* Redmond (1964), Well-B, from the Yamama Formation, 8370.5', field of view 6.3 mm.

D. *Pseudocyclammina cylindrica* Redmond (1964), Well-A, 4061.6', field of view 2.5 mm.

E. *Pseudocyclammina cylindrica* Redmond (1964), Well-I, 5479.2', field of view 6.3 mm.

F. *Pseudocyclammina cylindrica* Redmond (1964), Well-B, 8370.5', field of view 2.5 mm.

Plate 38

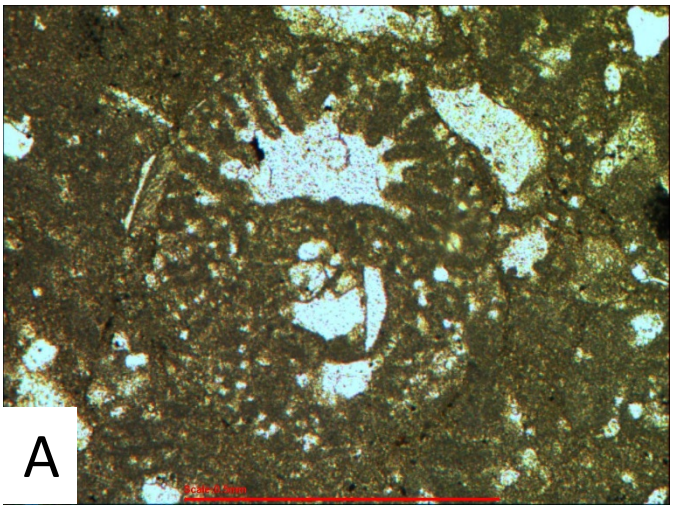
A

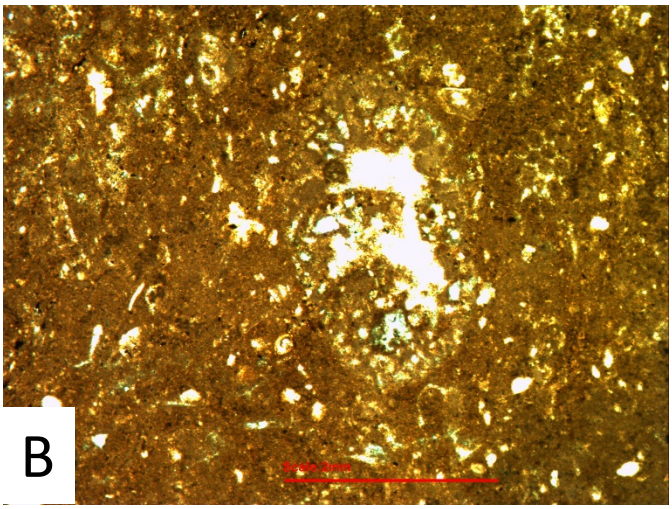
B

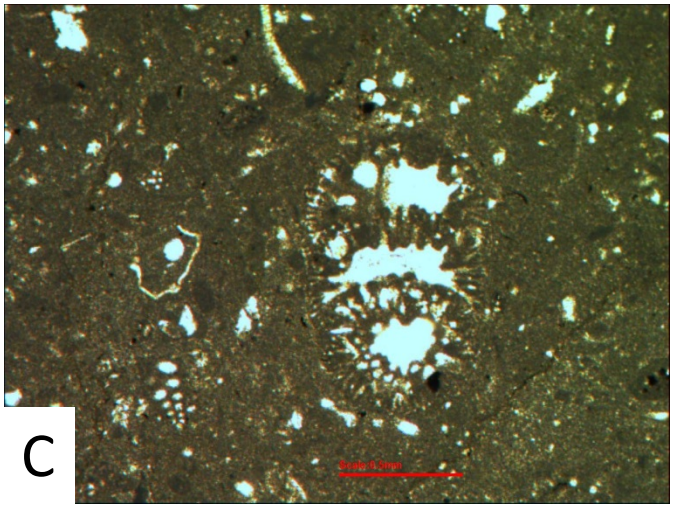
C

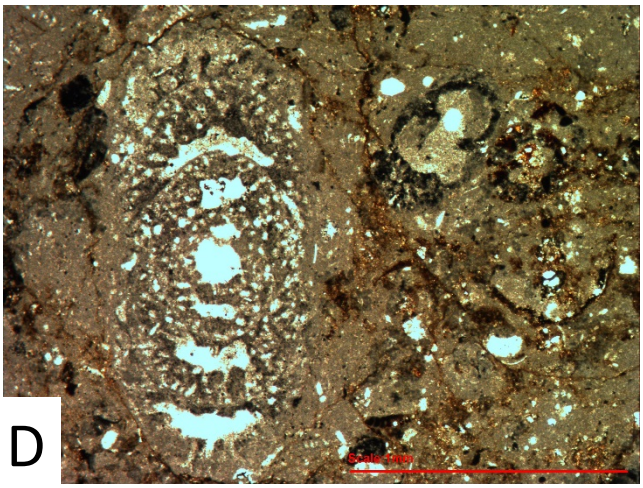
D

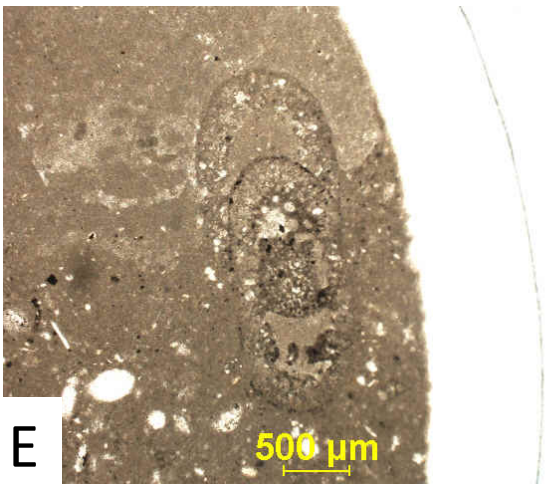

E

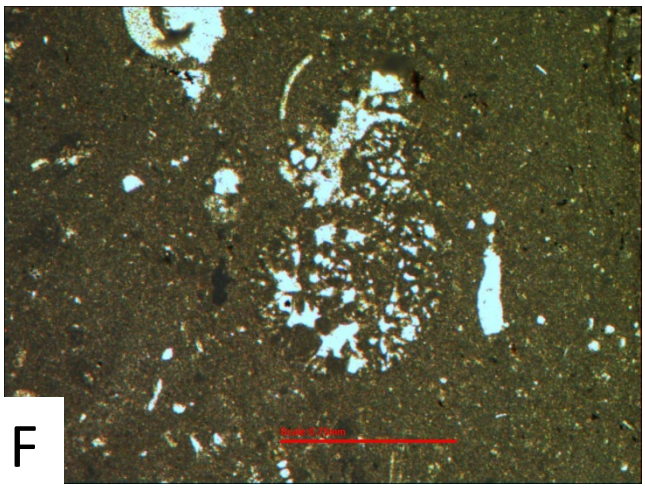
F

Plate 39

A. *Pseudocyclammina cylindrica* Redmond (1964), axial section,Well-I, 5480.7', field of view 6.3 mm.

B. Two *Pseudocyclammina lituus* Yokoyama (1890), upper, lateral section, and *Pseudocyclammina cylindrica* Redmond (1964), lower, Well-A, 4061.6', field of view 6.3 mm.

C. *Pseudocyclammina lituus* Yokoyama (1890), transverse section, Well-H, plug # 6427.5, field of view 2.5 mm.

D. *Pseudocyclammina lituus* Yokoyama (1890), transverse section, Well-D, 7969.2'.

E. *Pseudocyclammina lituus* Yokoyama (1890), tangential section, Well-D, 7960.2'.

F. *Pseudocyclammina lituus* Yokoyama (1890), tangential section, Well-D, 7960.2'.

Plate 39

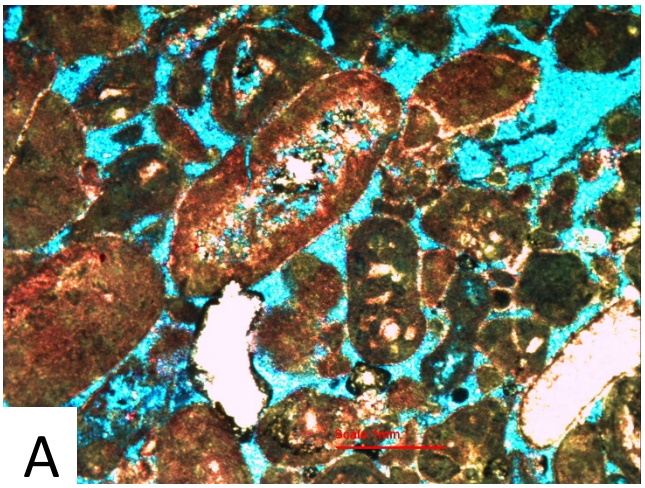
A

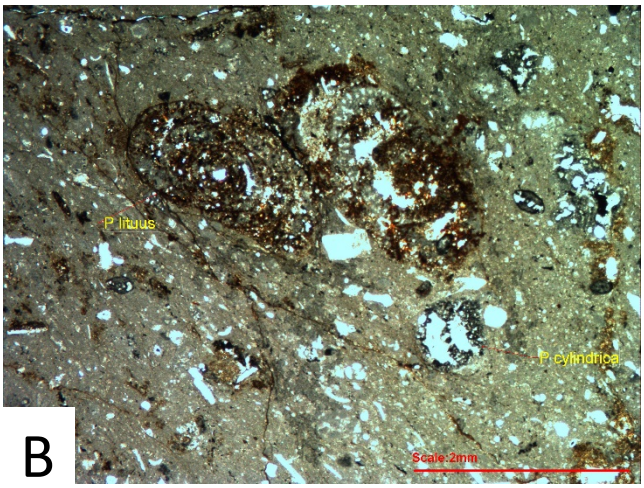
P. lituus
P. cylindrica
Scale:2mm
B

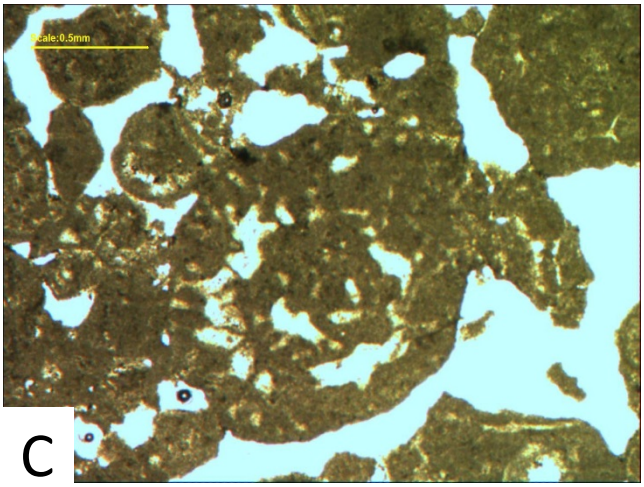
Scale:0.5mm
C

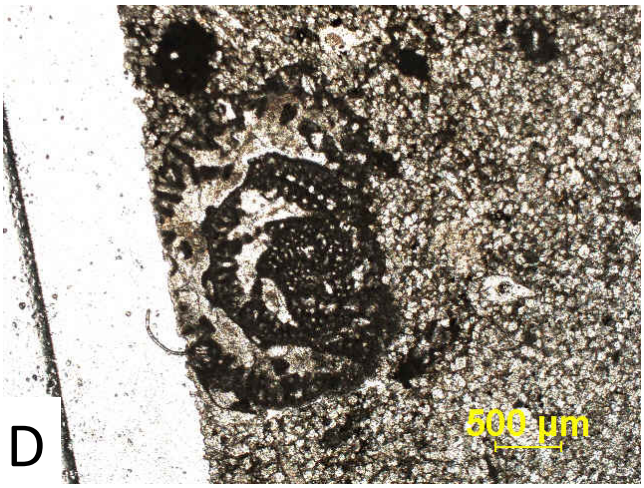
500 µm
D

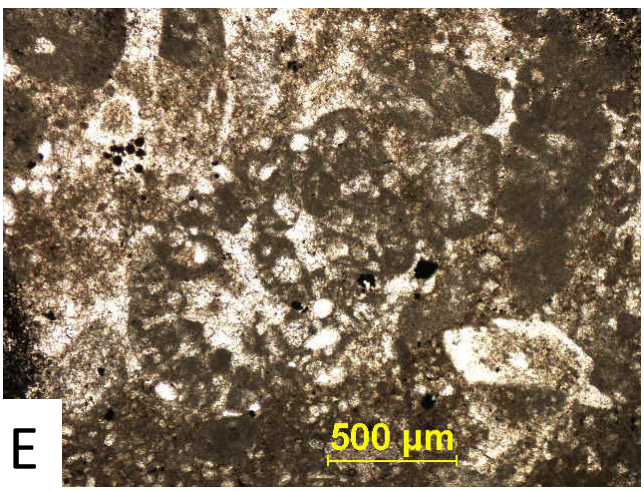
500 µm
E

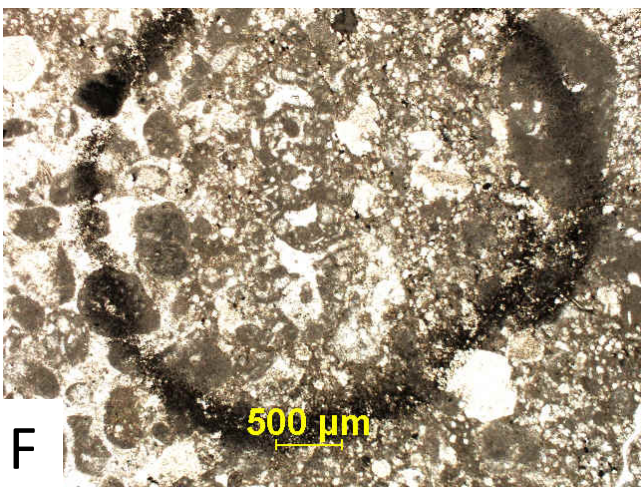
500 µm
F

Plate 40

A. *Pseudocyclammina lituus* Yokoyama (1890), tangential section, the wall is agglutinated by sponge spicules (monaxon type) in deep water setting, Well-A, 4061.6', field of view 6.3 mm.

B. *Pseudocyclammina lituus* Yokoyama (1890), tangential section, Well-B, 8370.5', field of view 6.3 mm.

C. *Pseudocyclammina lituus* Yokoyama (1890), tangential section, Well-H, 6408.1', field of view 6.3 mm.

D. *Pseudocyclammina lituus* Yokoyama (1890), (left) transverse section, and *Bramkampella arabica* Redmond, 1964 (right) transverse section, Well-B, 8370.5', field of view 6.3 mm.

E. *Plectinella virgulinoides* Marie (1956), tangential section, Well-H, 7328.6', field of view 2.5 mm.

F. *Plectinella virgulinoides* Marie (1956), tangential section, Well-H, 7327.1', field of view 2.5 mm.

Plate 40

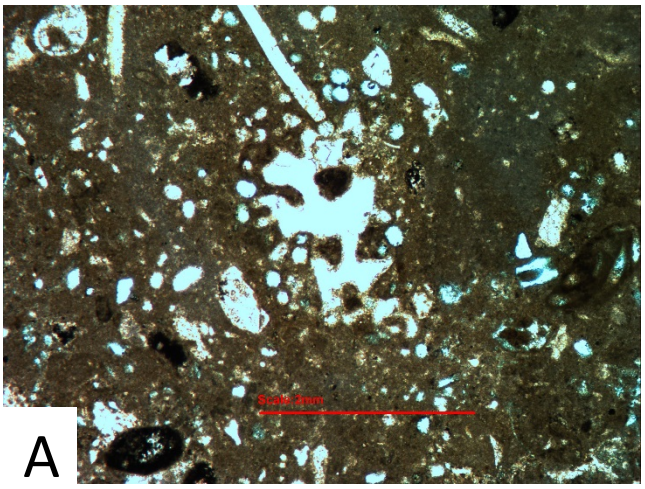

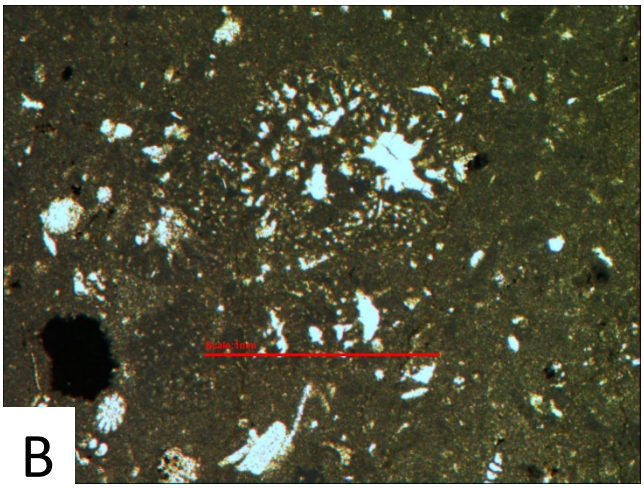

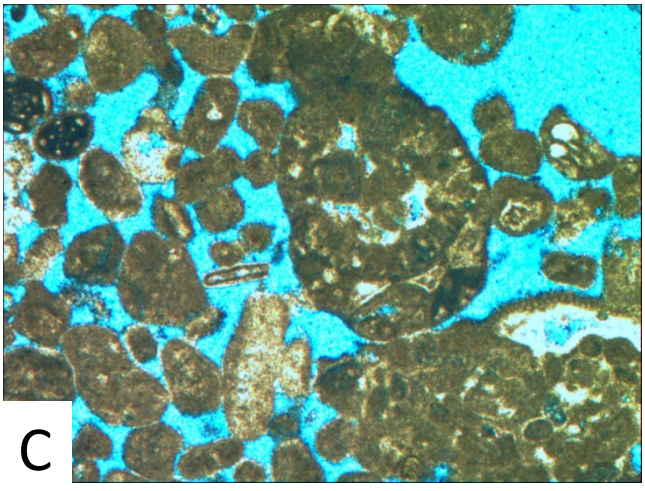

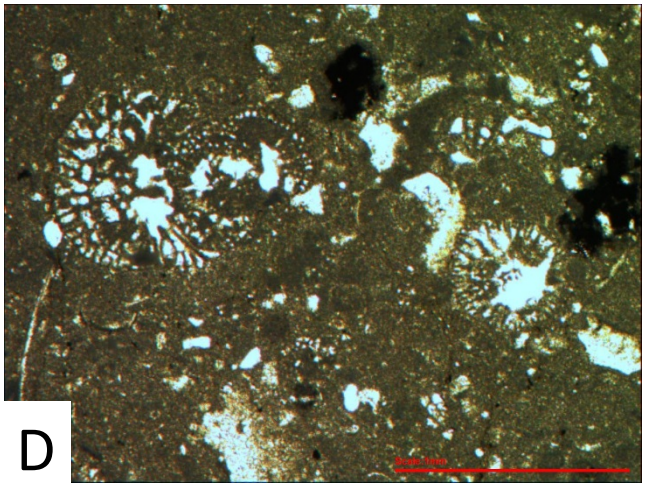

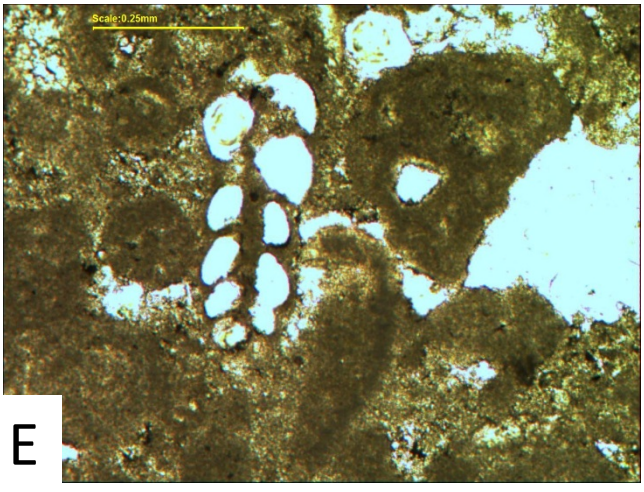

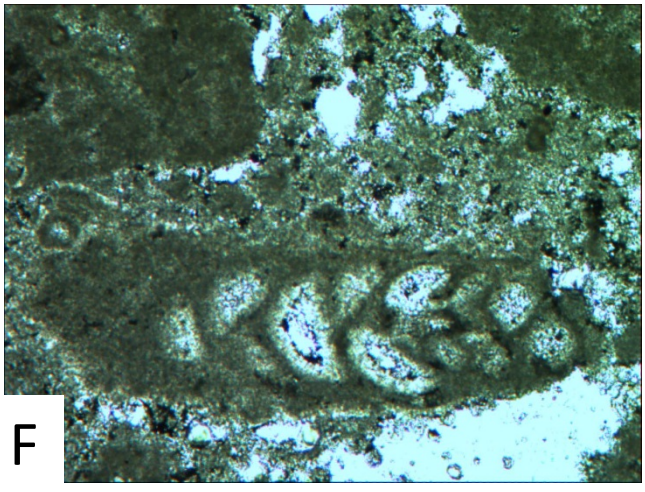

Plate 41

A. *Plectinella virgulinoides* Marie (1956), tangential section, Well-B, 8420.6', field of view 2.5 mm.

B. *Plectinella virgulinoides* Marie (1956), tangential section, Well-B, 8420.6', field of view 2.5 mm.

C. *Plectinella virgulinoides* Marie (1956), tangential section, Well-B, 5408.1', field of view 6.3 mm.

D. *Plectinella virgulinoides* Marie (1956), tangential section, Well-H, 7331.8', field of view 2.5 mm.

E. *Plectinella virgulinoides* Marie (1956), tangential section, Well-H, 7330.8', field of view 2.5 mm.

F. *Eomarssonella* sp., tangential section, Well-H, 6421.5', field of view 6.3 mm.

Plate 41

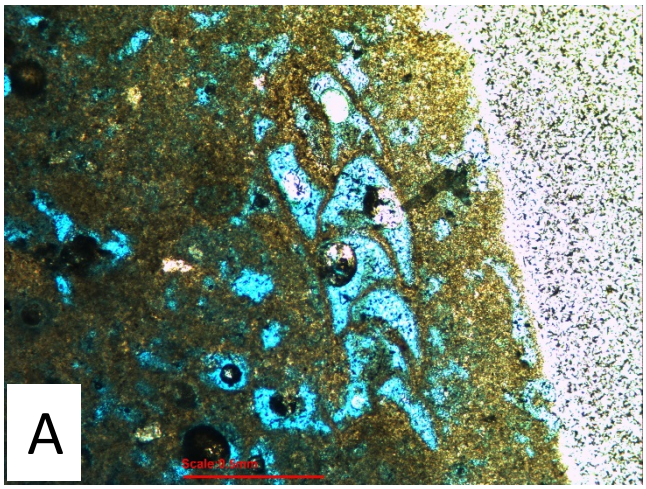

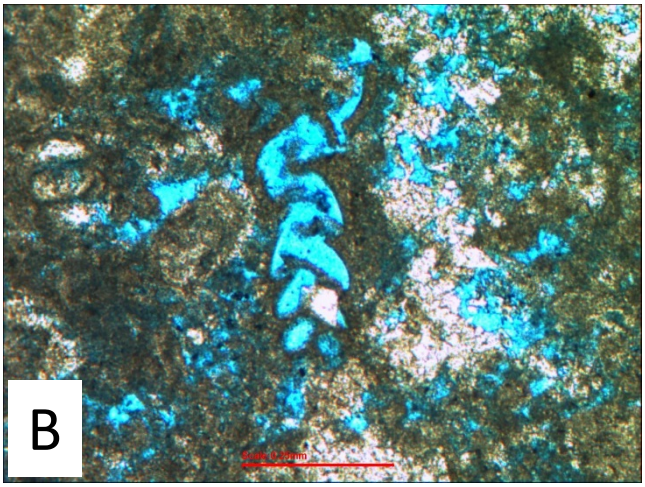

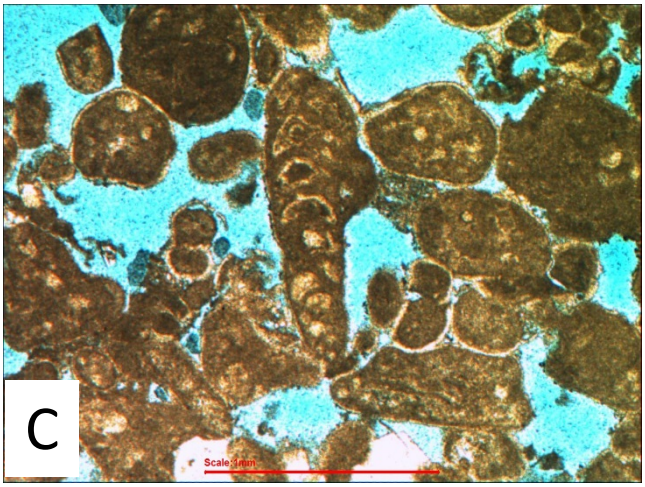

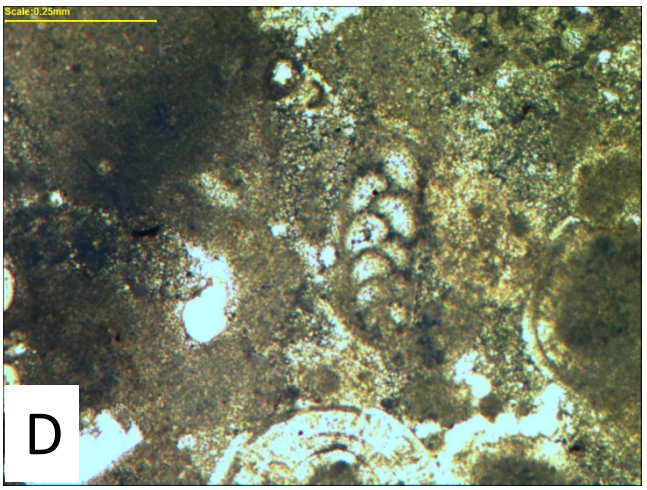

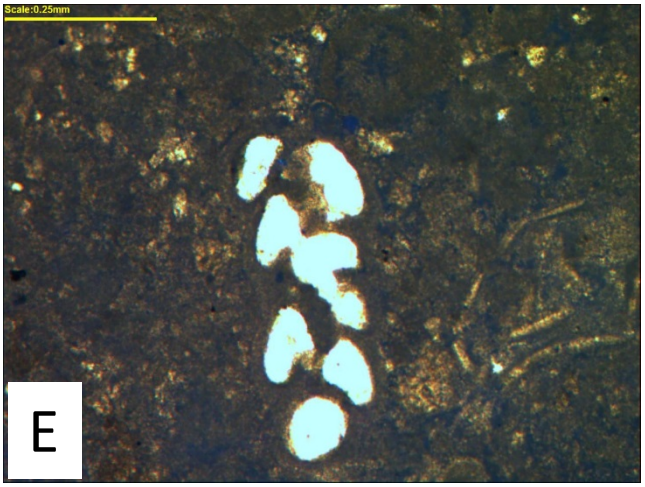

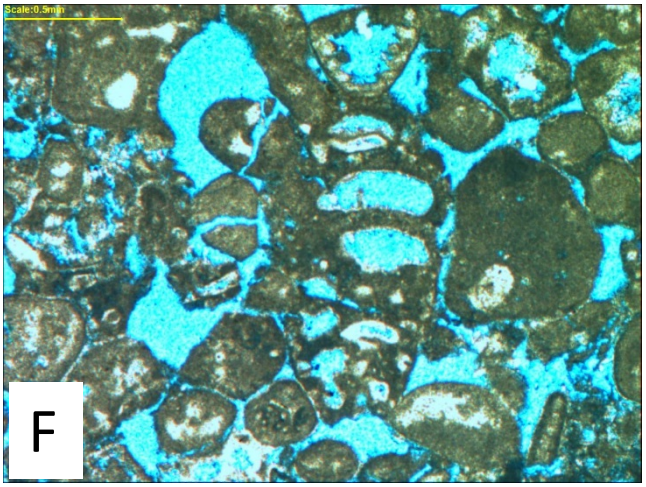

Plate 42

A. *Eomarssonella* sp. Well-H, plug # 6424.5', field of view 2.5 mm.

B. *Eomarssonella* sp., Well-G, 5380.2', field of view 2.5 mm.

C. *Eomarssonella* sp., Well-B, 8395.4', field of view 2.5 mm.

D. *Eomarssonella* sp., Well-I, 5533.2', field of view 6.3 mm.

E. *Bitaxia* sp., Well-B, 5408.1', field of view 6.3 mm.

F. *Uvigerinammina uvigeriniformis* (Seibold and Seibold, 1960), Well-G, 5382.2', field of view 2.5 mm.

Plate 42

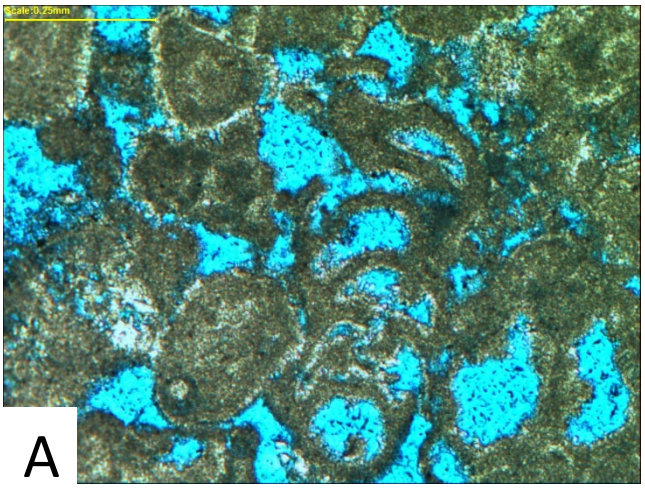

A

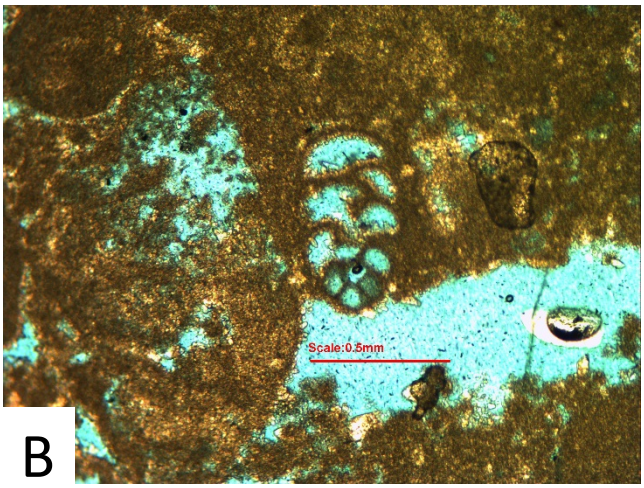

B

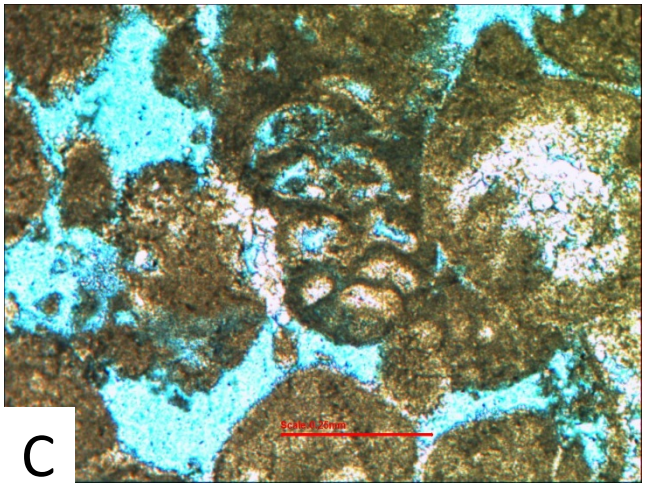

C

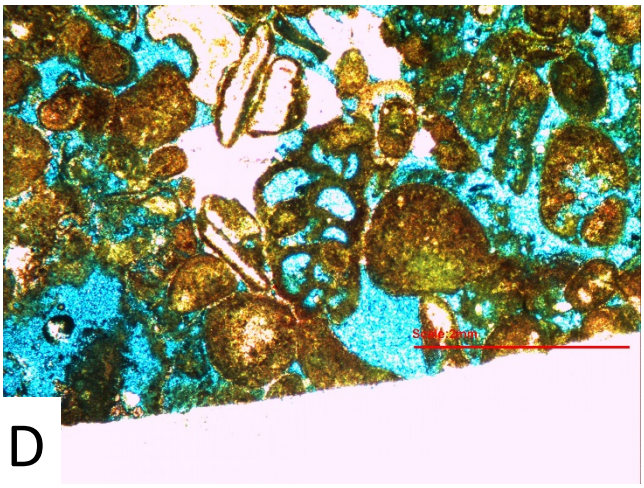

D

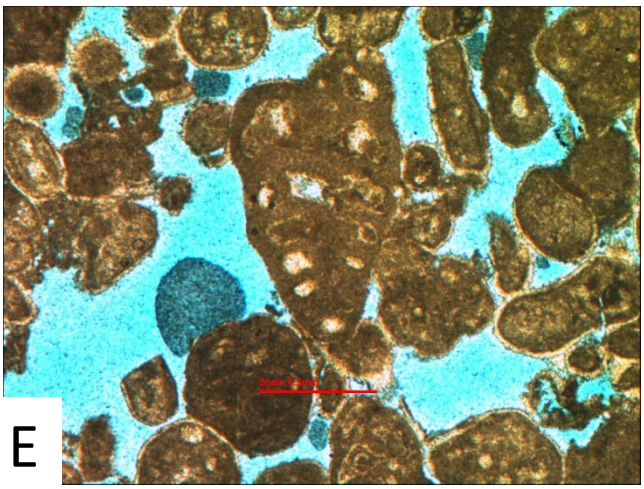

E

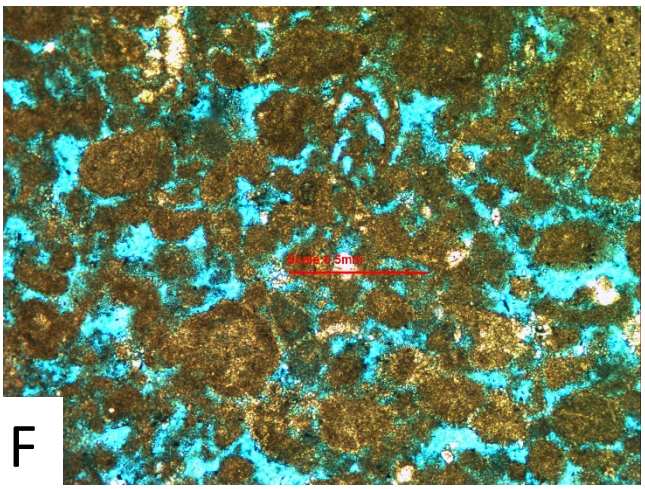

F

Plate 43

A. *Uvigerinammina uvigeriniformis* (Seibold and Seibold, 1960), Well-H, 6423.5', field of view 2.5 mm.

B. *Uvigerinammina uvigeriniformis* (Seibold and Seibold, 1960), Well-B, 8427', field of view 2.5 mm.

C. *Verneuilinoides neocomiensis* Mjatliuk (1939), Well-G, 5385.7', field of view 6.3 mm.

D. *Verneuilinoides neocomiensis* Mjatliuk (1939), Well-H, 7332.5', field of view 2.5 mm.

E. *Verneuilinoides neocomiensis* Mjatliuk (1939), Well-H, 6421.5', field of view 6.3 mm.

F. *Verneuilinoides neocomiensis* Mjatliuk (1939), Well-H, 6422.5', field of view 2.5 mm.

Plate 43

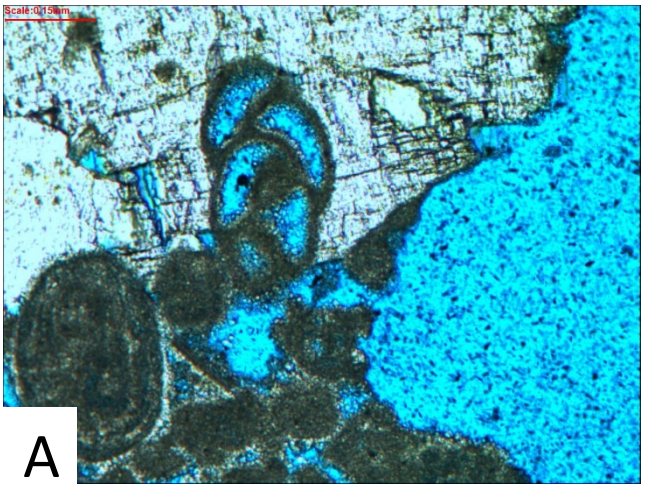

A

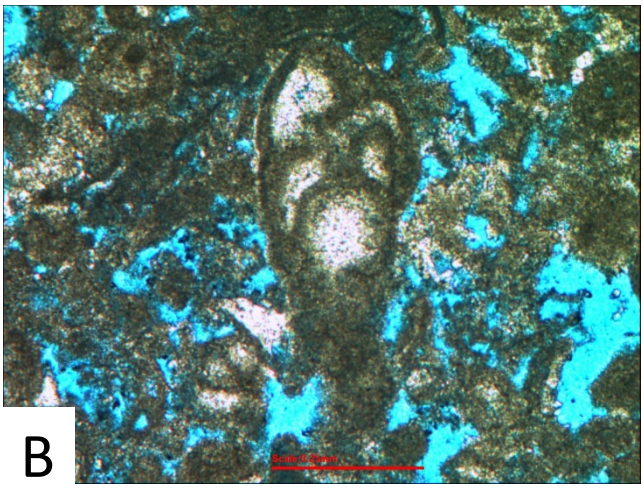

B

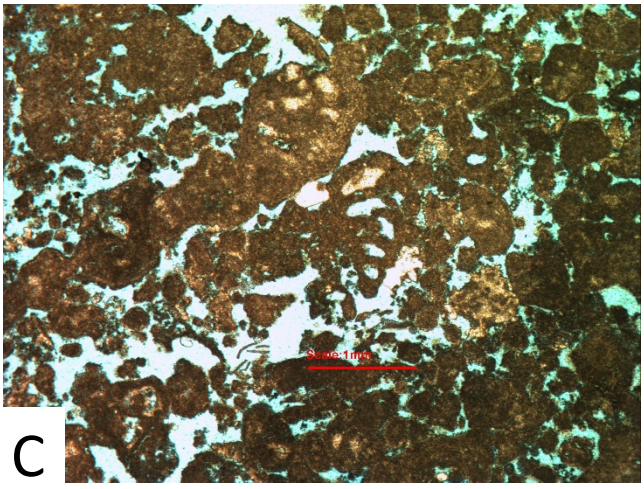

C

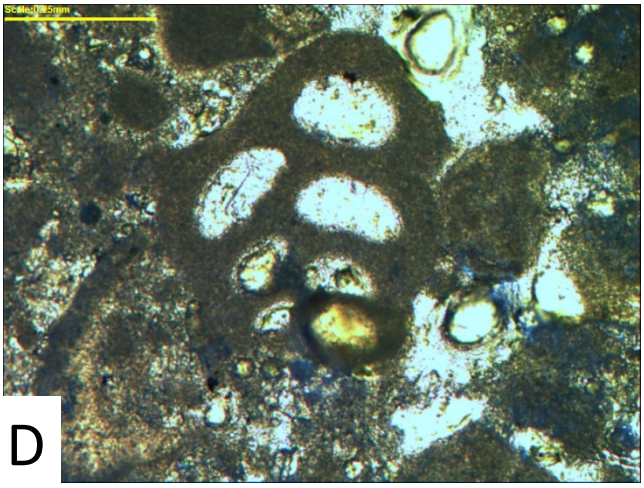

D

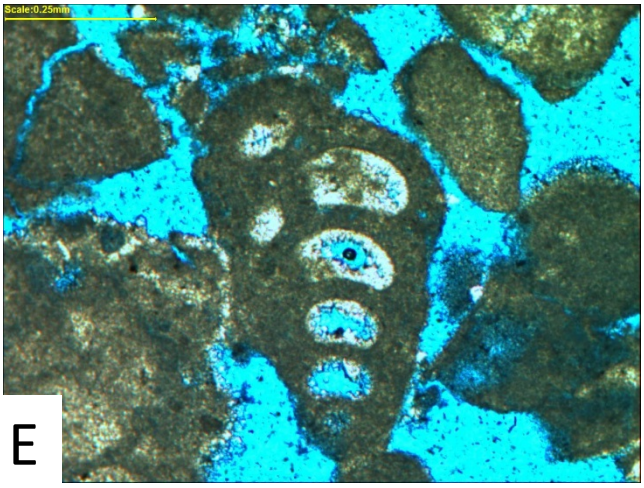

E

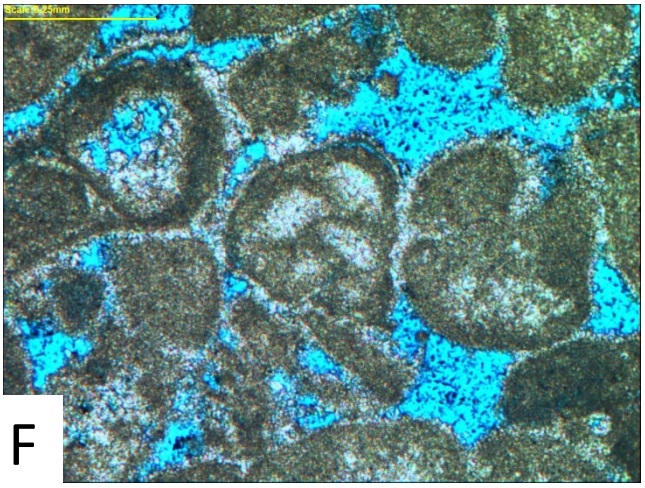

F

Plate 44

A. *Verneuilinoides neocomiensis* Mjatliuk (1939), Well-H, plug # 7331.8', field of view 2.5 mm.

B. *Verneuilinoides polonicus* (Cushman and Glazewski, 1949), Well-G, 6761.3', field of view 2.5 mm.

C. *Verneuilinoides polonicus* (Cushman and Glazewski, 1949), Well-G, 6772.5', field of view 2.5 mm.

D. *Verneuilinoides polonicus* (Cushman and Glazewski, 1949), Well-G, 6779.5', field of view 2.5 mm.

E. *Verneuilinoides polonicus* (Cushman and Glazewski, 1949), Well-G, 6779.5', field of view 2.5 mm.

F. *Verneuilinoides polonicus* (Cushman and Glazewski, 1949), Well-H, 7339', field of view 2.5 mm.

Plate 44

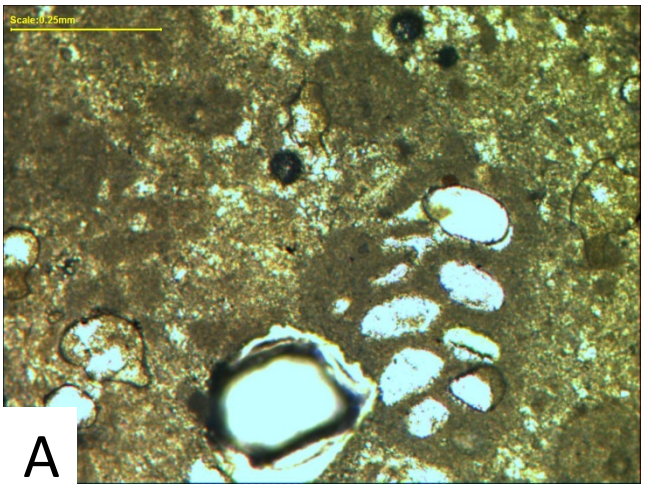

A

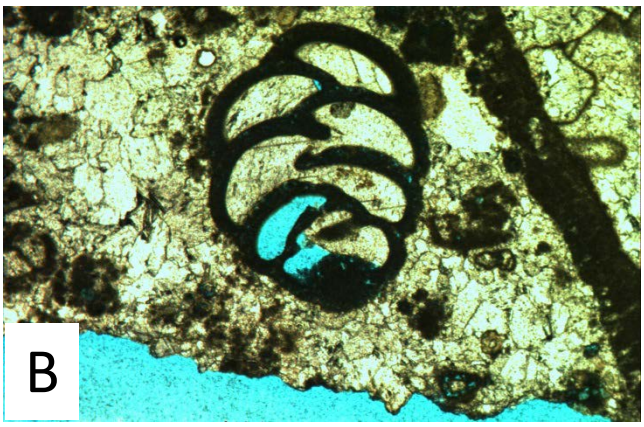

B

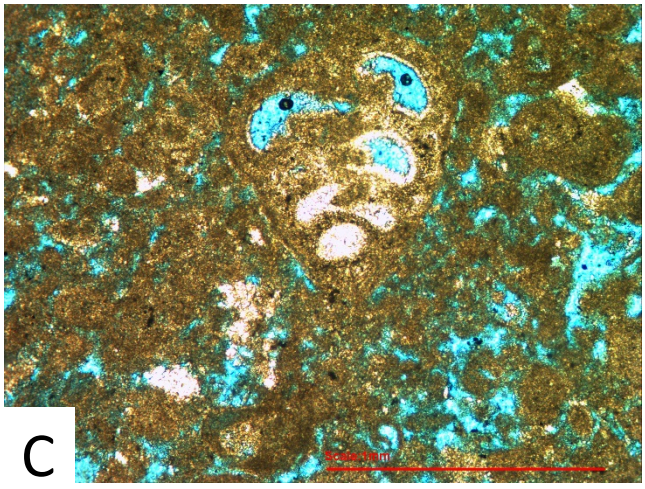

C

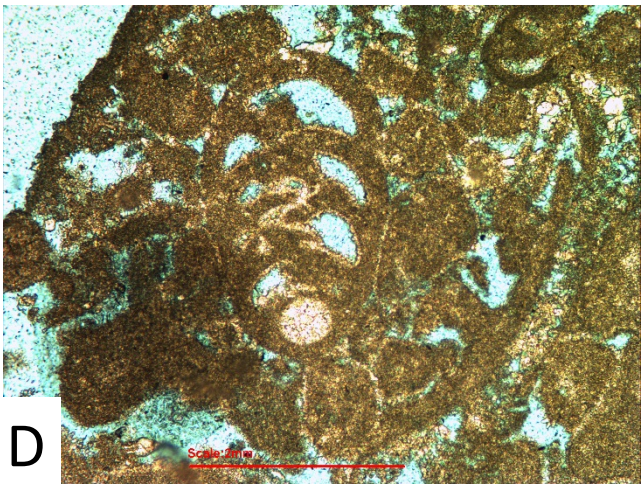

D

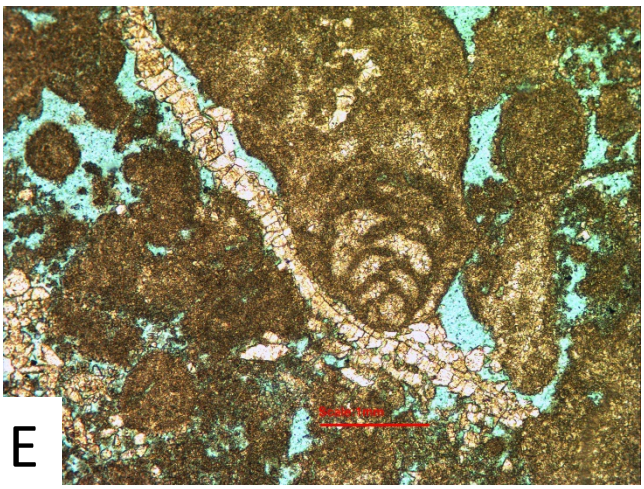

E

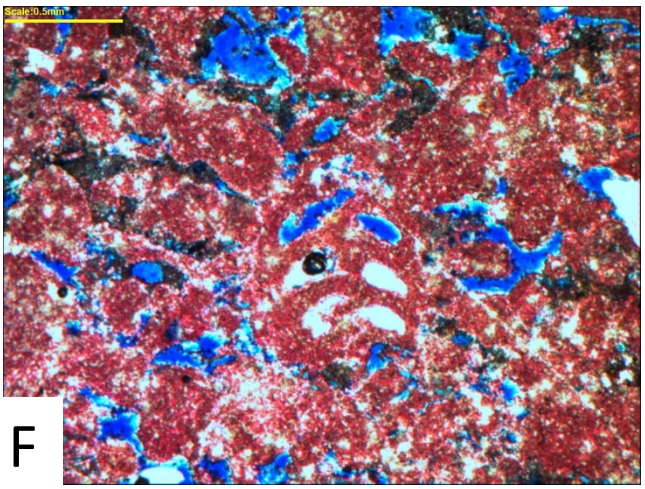

F

Plate 45

A. *Verneuilinoides polonicus* (Cushman and Glazewski, 1949), intruded by wispy seam micro-stylolite filled by clay minerals, Well-B, 8361.8', field of view 2.5 mm.

B. *Verneuilinoides polonicus* (Cushman and Glazewski, 1949), Well-B, 8410.5', field of view 2.5 mm.

C. *Verneuilinoides polonicus* (Cushman and Glazewski, 1949), Well-I, 5524.2', field of view 2.5 mm.

D. *Siphovalvulina variabilis* Septfontaine, 1988, Well-H, 7316.2', field of view 2.5 mm.

E. *Siphovalvulina variabilis* Septfontaine, 1988, Well-D, 8639.7', field of view 2.5 mm.

F. *Siphovalvulina variabilis* Septfontaine, 1988, Well-D, 8639.7', field of view 2.5 mm.

Plate 45

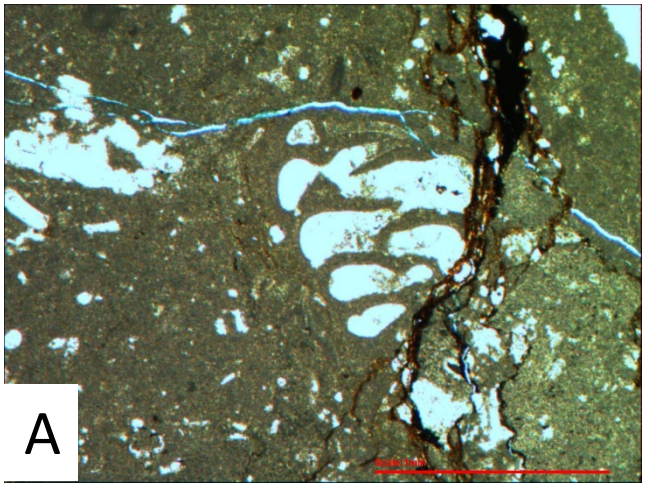

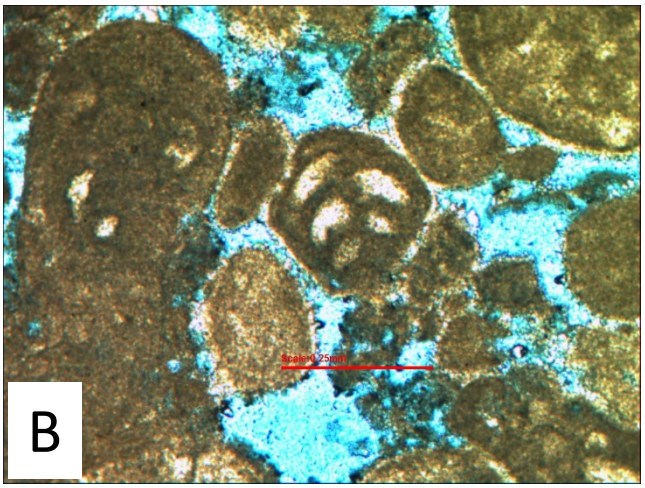

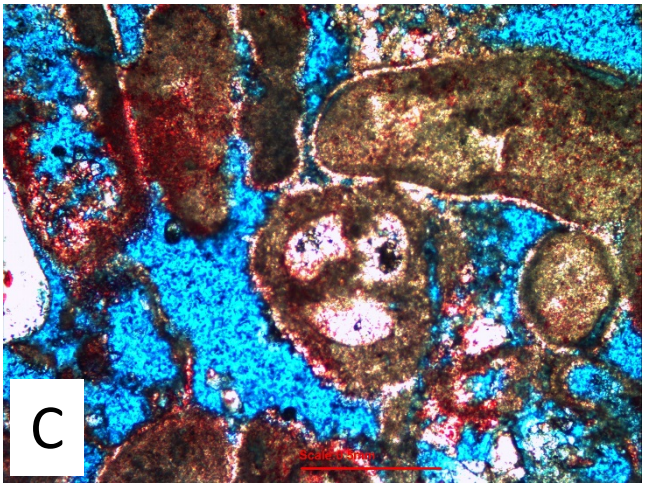

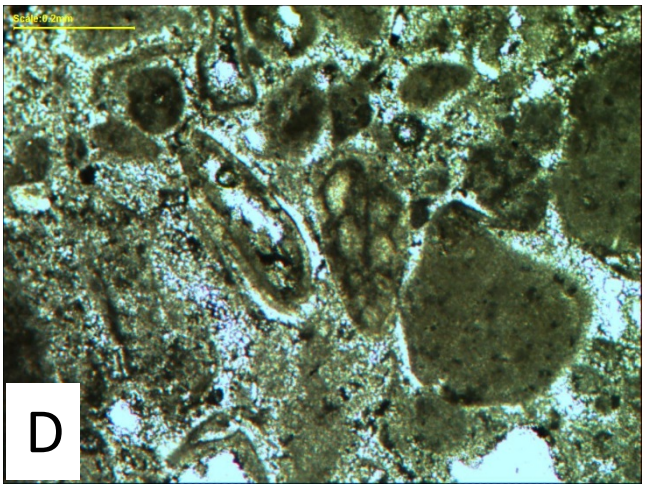

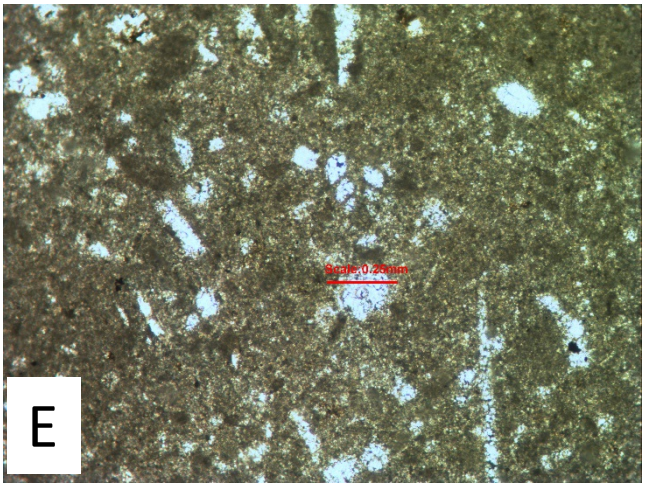

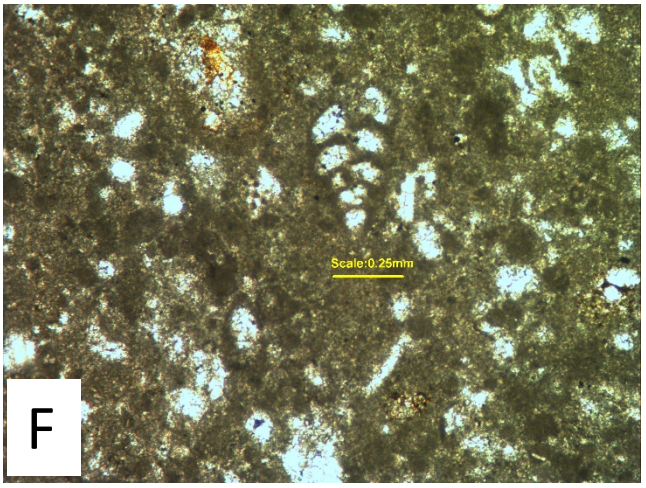

Plate 46

A. *Gaudryina ectypa* Arnaud-Vanneau (1980), Well-D, 8638.2’, field of view 2.5 mm.

B. *Gaudryinella* sp., Well-H, 7328.6’, field of view 6.3 mm.

C. *Gaudryinella* sp., Well-H, 7328.6’, field of view 2.5 mm.

D. *Gaudryinella* sp., Well-G, 6779.5’, field of view 2.5 mm.

E. *Gaudryinella* sp., Well-H, 6410.2’, field of view 2.5 mm.

F. *Gaudryinella* sp., Well-B, 8427’, field of view 2.5 mm.

Plate 46

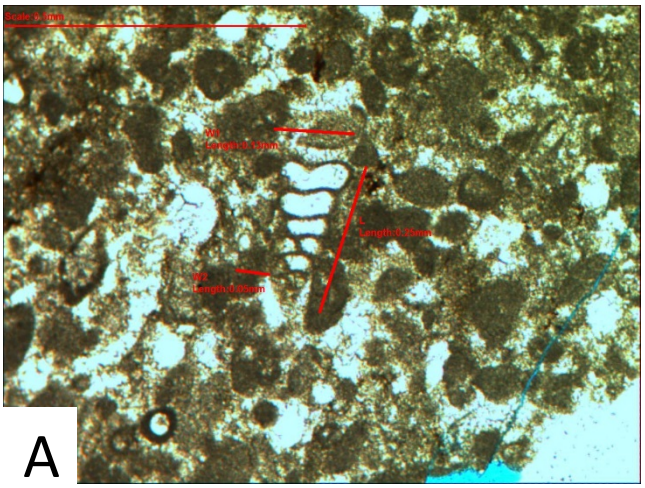

A

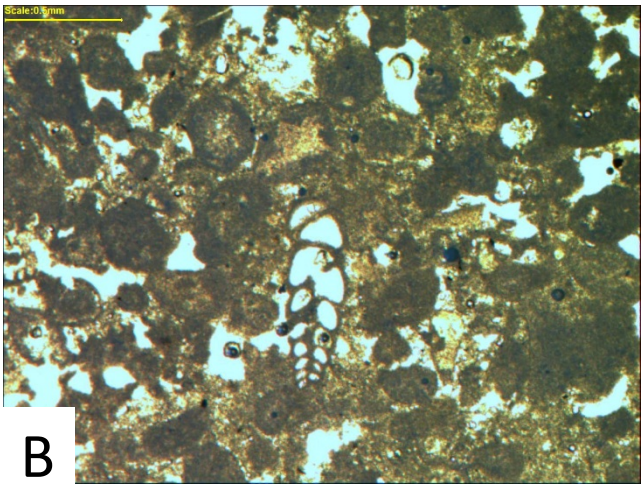

B

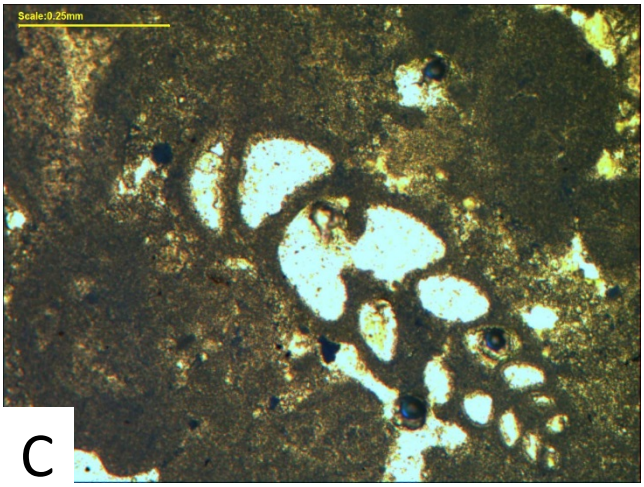

C

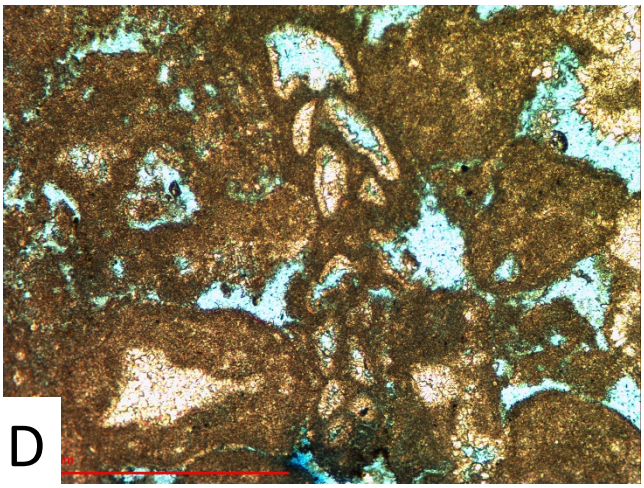

D

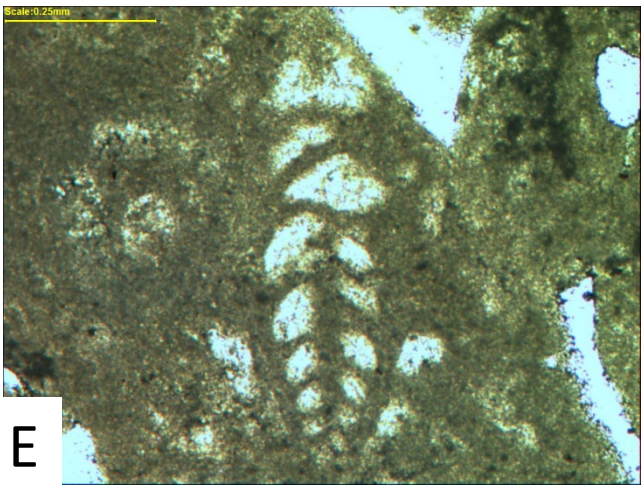

E

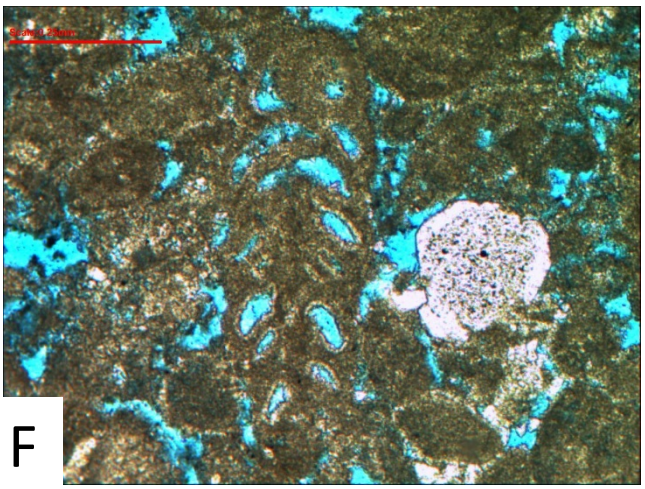

F

Plate 47

A. *Verneuilina minuta* Wiesner (1931), Well-H, 7331.3', field of view 2.5 mm.

B. *Verneuilina minuta* Wiesner (1931), Well-H, 7328.6', field of view 2.5 mm.

C. *Protomarssonella kummi* (Zedler, 1961), Well-H, 7328.6', field of view 2.5 mm.

D. *Protomarssonella kummi* (Zedler, 1961), Well-H, 7339, field of view 2.5 mm.

E. *Protomarssonella kummi* (Zedler, 1961), Well-I, 5543.2', field of view 2.5 mm.

F. *Praedorothia* sp. cf. *P. praehauteriviana* (Dieni and Massari, 1966), Well-G, 6768.5', field of view 2.5 mm.

Plate 47

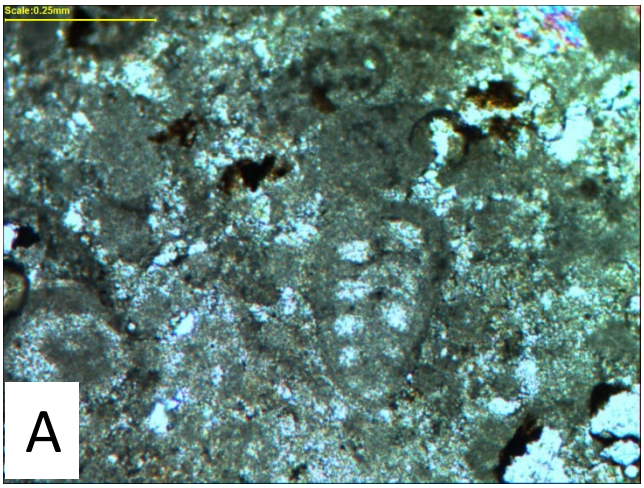
Scale:0.25mm
A

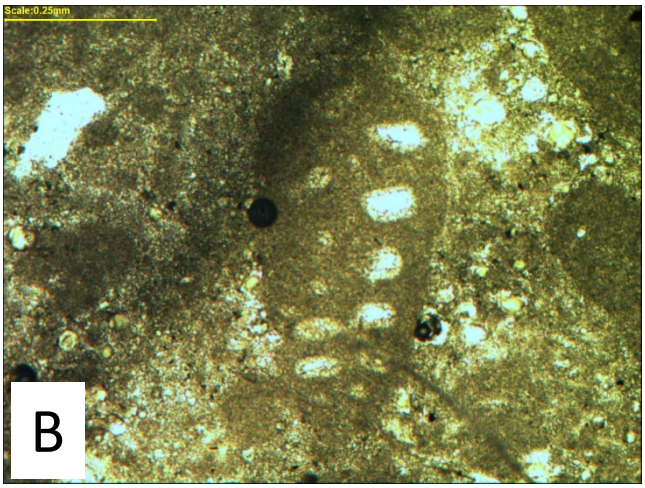
Scale:0.25mm
B

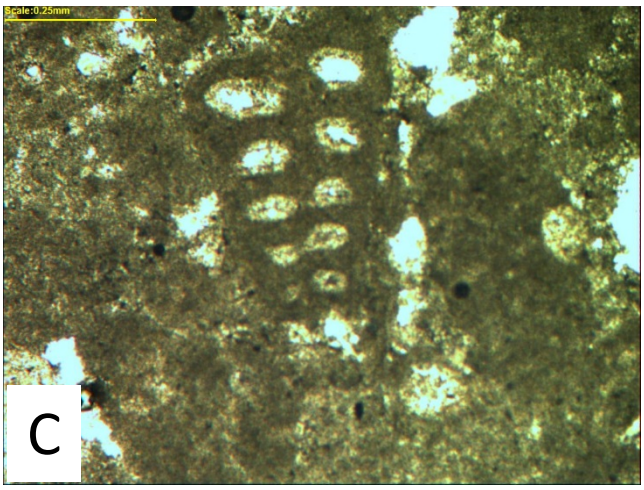
Scale:0.25mm
C

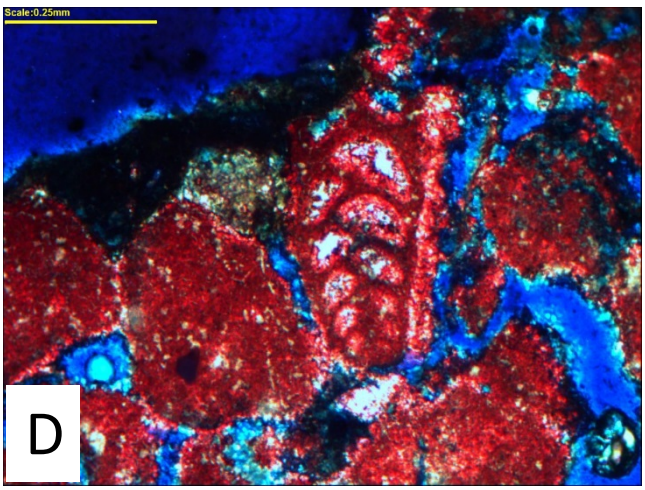
Scale:0.25mm
D

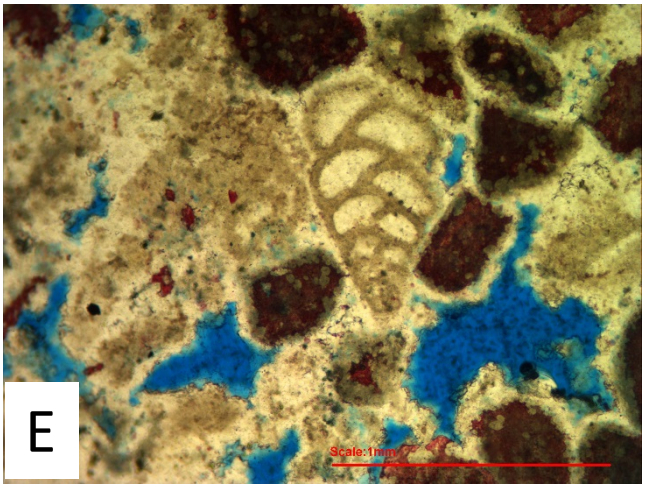
Scale:1mm
E

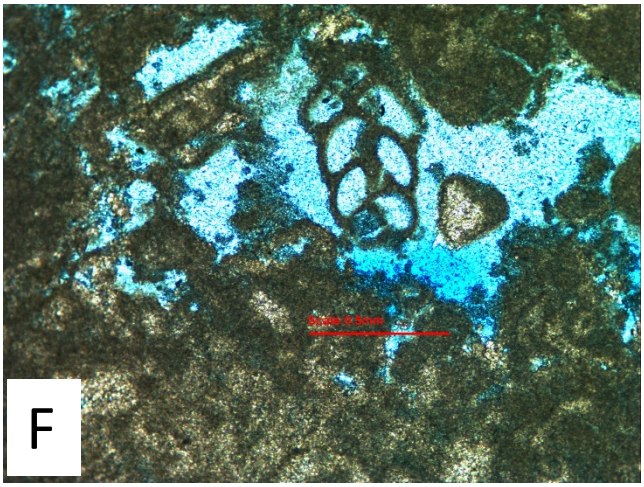
F

Plate 48

A. *Praedorothia* sp. cf. *P. praehauteriviana* (Dieni and Massari, 1966), Well-A, 4061.6', field of view 2.5 mm.

B. *Kurnubia palastiniensis* Henson (1948), transverse section, Well-F, 3255.5', field of view 6.3 mm. Note that porosity type is intra-skeletal, in which it enhances the reservoirs quality by increasing primary porosity value.

C. *Kurnubia palastiniensis* Henson (1948), transverse section, Well-F, 3255.5', field of view 2.5 mm.

D. *Kurnubia palastiniensis* Henson (1948), oblique section, Well-F, 3255.5', field of view 2.5 mm.

E. *Kurnubia palastiniensis* Henson (1948), transverse section, Well-F, 3255.5', field of view 2.5 mm.

F. *Kurnubia palastiniensis* Henson (1948), oblique section, Well-F, 3255.5', field of view 2.5 mm.

Plate 48

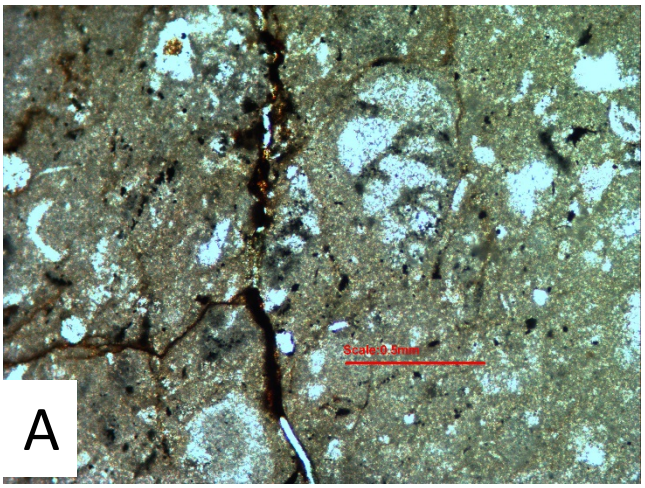

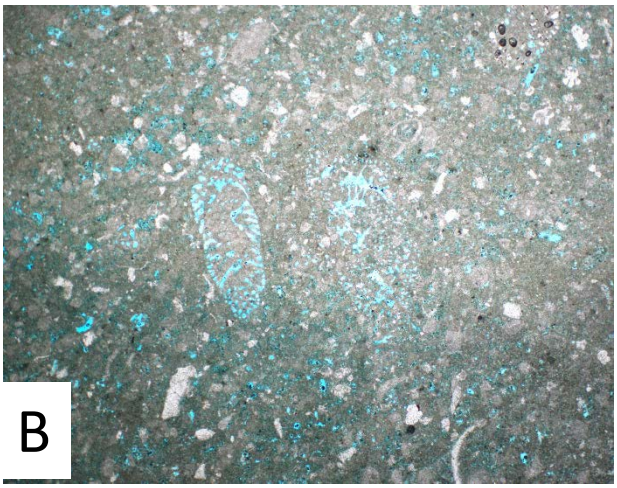

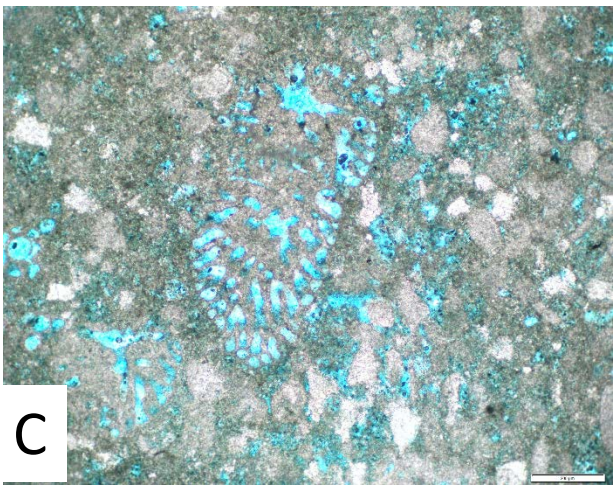

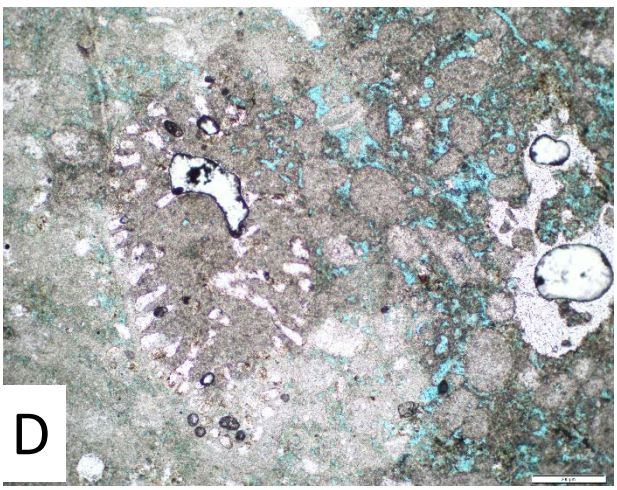

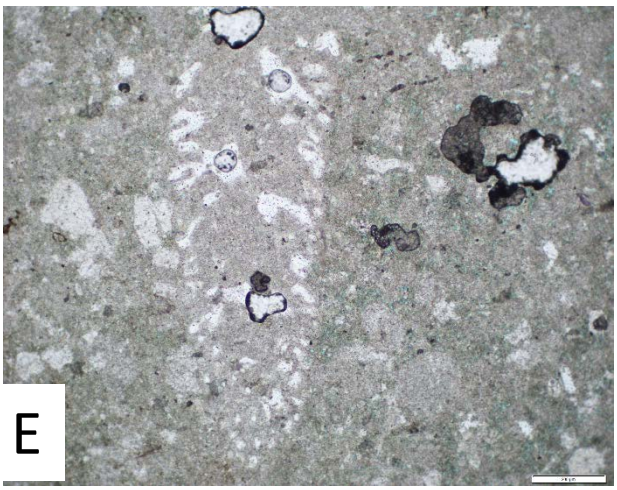

Plate 49

A. *Kurnubia palastiniensis* Henson (1948), transverse section, Well-F, 3255.5', field of view 6.3 mm. Note that porosity type is intra-skeletal, in which it enhances the reservoirs quality by increasing primary porosity value and as a consequence permability increses.

B. *Kurnubia palastiniensis* Henson (1948), transverse section, Well-F, 3255.5', field of view 6.3 mm.

C. *Kurnubia palastiniensis* Henson (1948), transverse section, Well-F, 3255.5', field of view 2.5 mm.

D. *Kurnubia palastiniensis* Henson (1948), oblique section, Well-F, 3243.5', field of view 1.25 mm.

E. *Kurnubia palastiniensis* Henson (1948), transverse section, Well-F, 3255.5', field of view 1.25 mm.

F. *Pfenderina neocomiensis* (Pfender, 1938), Well-G, 6768.5', field of view 2.5 mm.

Plate 49

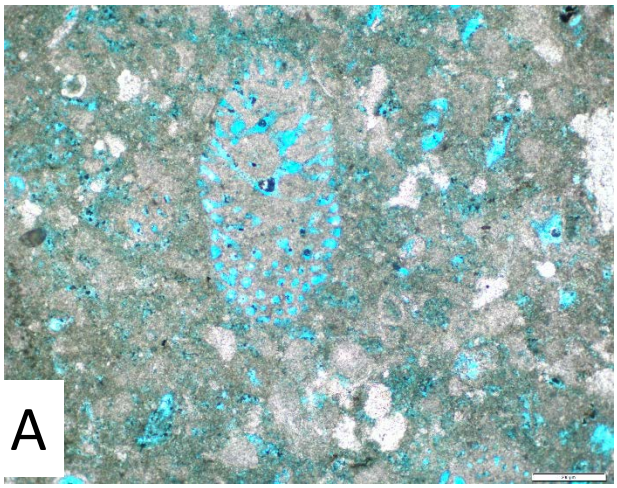
A

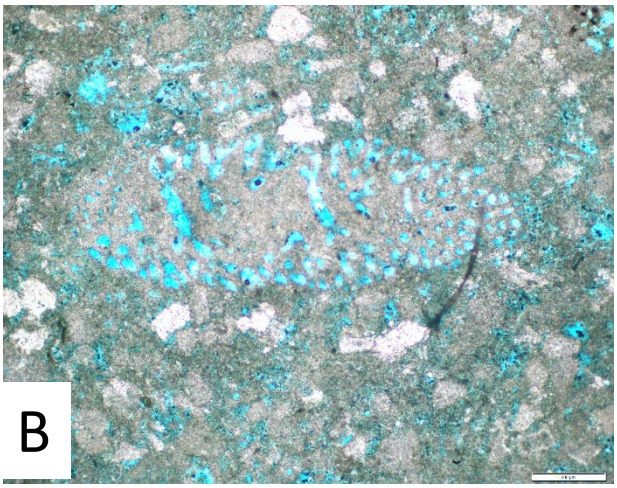
B

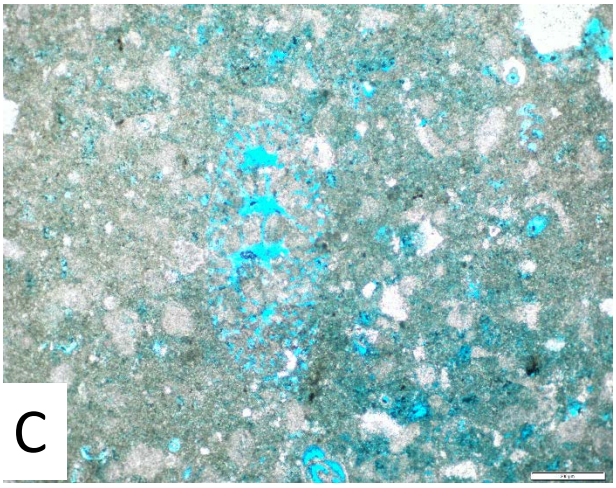
C

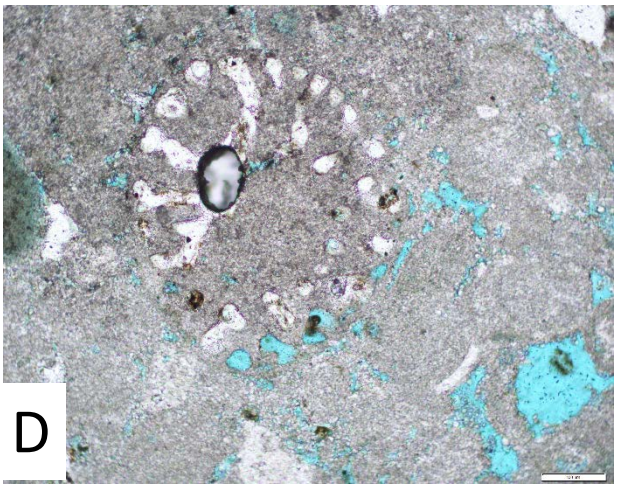
D

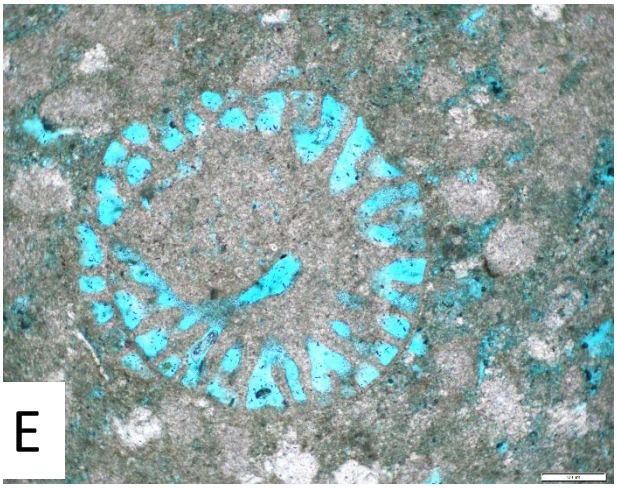
E

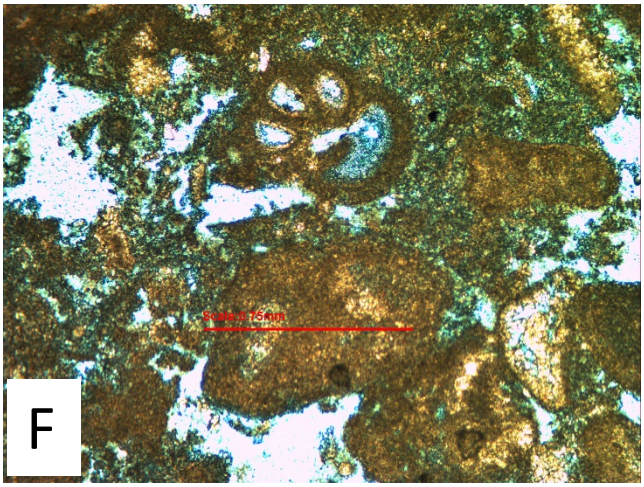
F

Plate 50

A. *Pfenderina neocomiensis* (Pfender, 1938), Well-H, 7332.5', field of view 2.5 mm.

B. *Pfenderina neocomiensis* (Pfender, 1938), Well-H, 7331.8', field of view 2.5 mm.

C. *Pfenderina neocomiensis* (Pfender, 1938), Well-H, 7328.6', field of view 2.5 mm.

D. *Pfenderina neocomiensis* (Pfender, 1938), Well-H, 7331.8', field of view 2.5 mm.

E. *Pfenderina neocomiensis* (Pfender, 1938), Well-H, 7331.8', field of view 2.5 mm.

F. *Pfenderina neocomiensis* (Pfender, 1938), Well-H, 7330.8', field of view 2.5 mm.

Plate 50

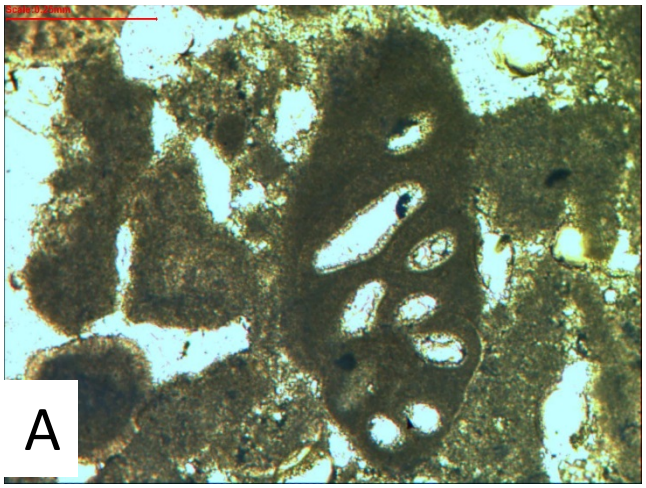

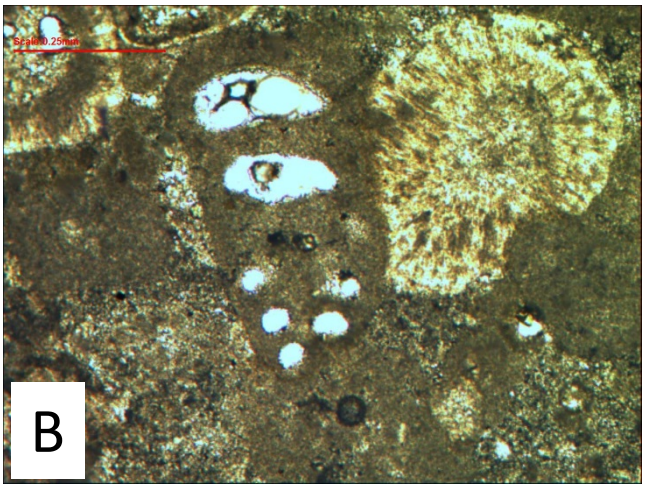

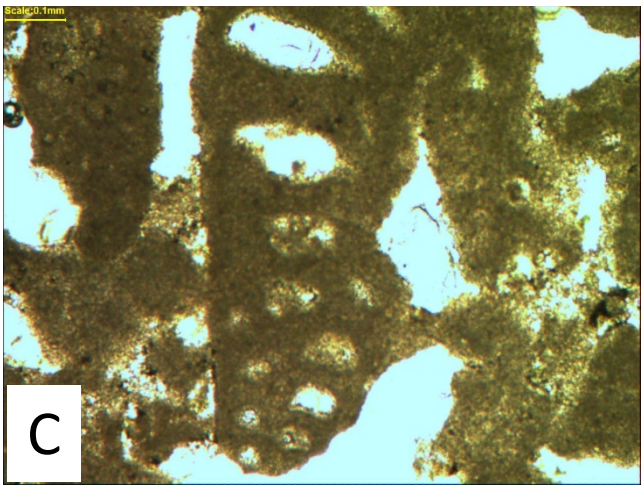

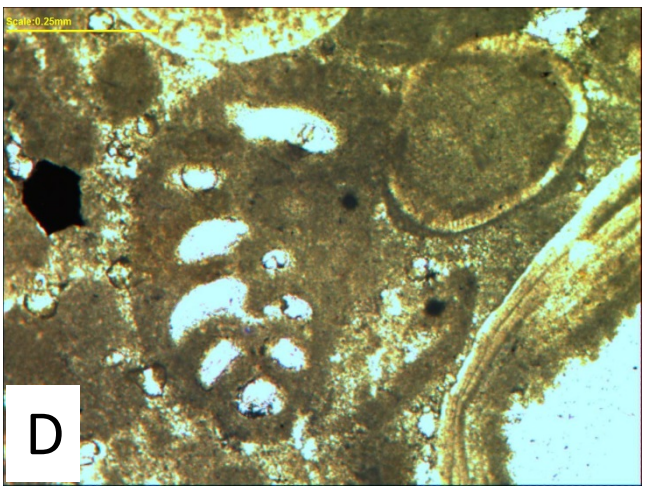

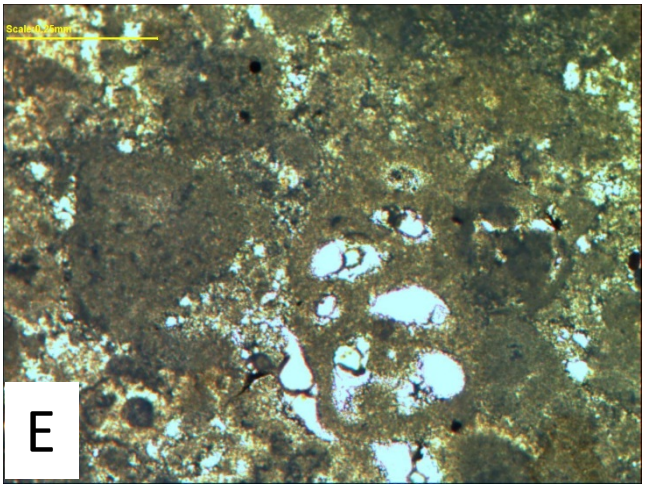

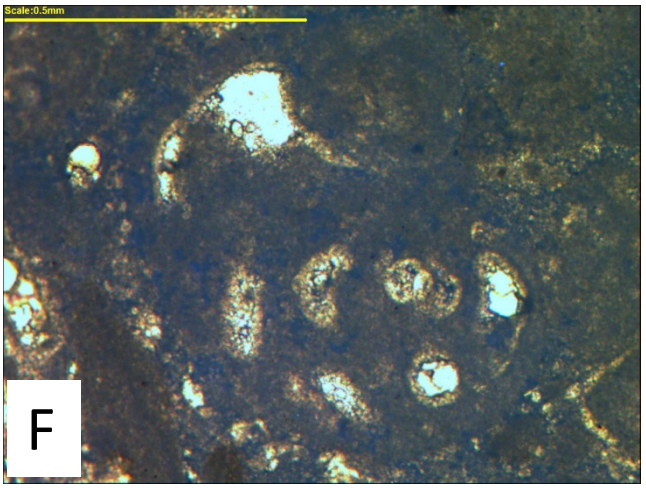

Plate 51

A. *Pfenderina neocomiensis* (Pfender, 1938), Well-H, 7332.5', field of view 2.5 mm.

B. *Pfenderina neocomiensis* (Pfender, 1938), Well-G, 6809.5', field of view 2.5 mm.

C. *Pfenderina neocomiensis* (Pfender, 1938), Well-B, 8420.6', field of view 2.5 mm.

D. *Pfenderina neocomiensis* (Pfender, 1938), Well-I, 5524.2', field of view 2.5 mm.

E. *Haghimashella arcuata* (Haeusler, 1890), Well-H, 7323.7', field of view 2.5 mm.

F. *Haghimashella arcuata* (Haeusler, 1890), Well-H, 6424.5', field of view 2.5 mm.

Plate 51

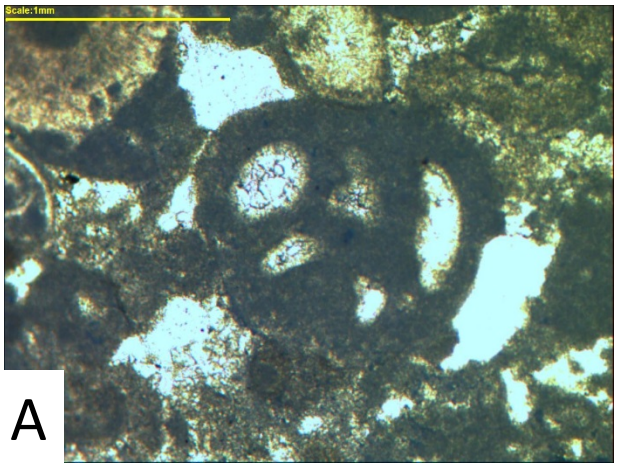

A

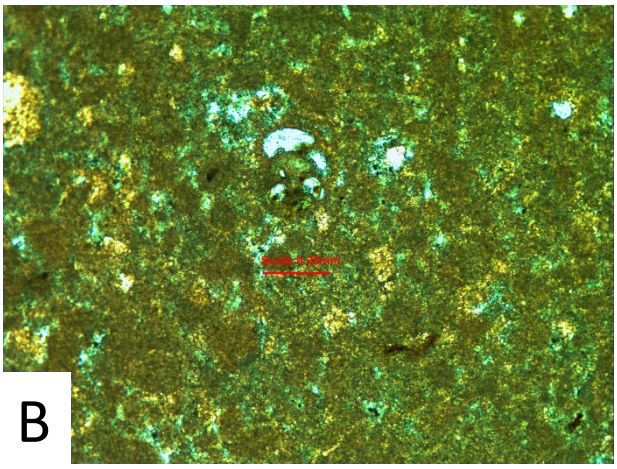

B

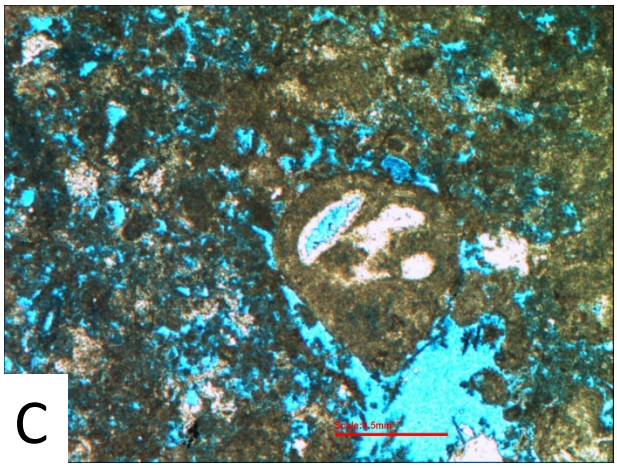

C

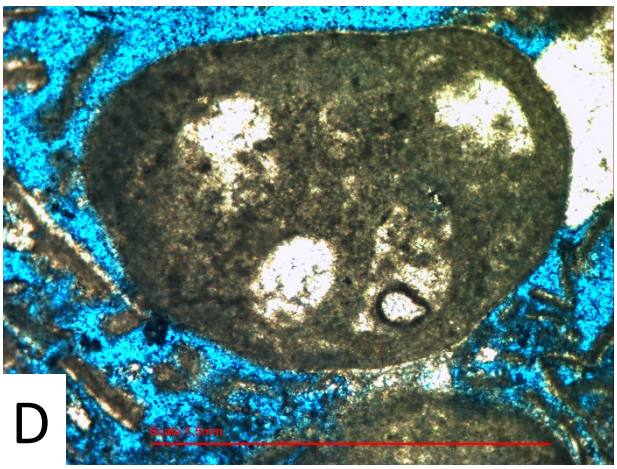

D

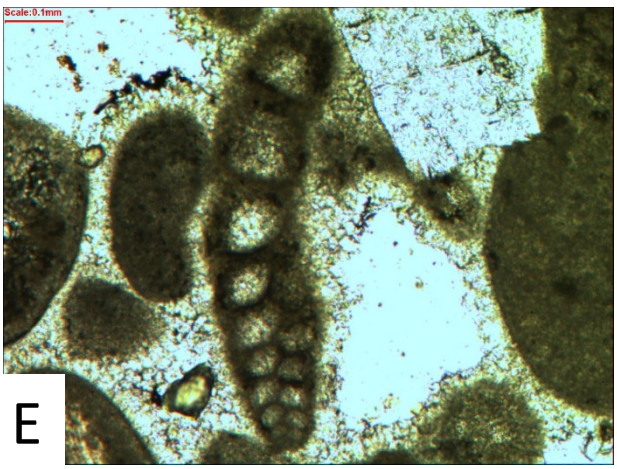

E

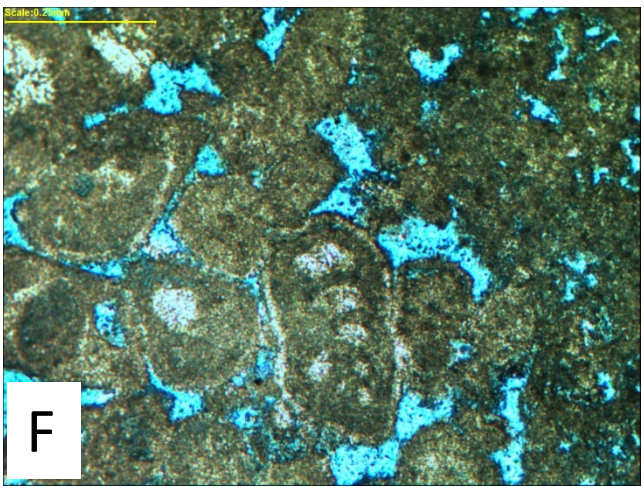

F

Plate 52

A. *Haghimashella arcuata* (Haeusler, 1890), Well-H, 7316.9', field of view 2.5 mm.

B. *Haghimashella arcuata* (Haeusler, 1890), Well-B8404.1', field of view 2.5 mm.

C. *Textulariopsis jurassica* (Gümbel, 1862), Well-D, 8642.7', field of view 2.5 mm.

D. *Textulariopsis jurassica* (Gümbel, 1862), Well-D, 8642.7', field of view 2.5 mm.

E. *Textulariopsis jurassica* (Gümbel, 1862), Well-D, 8642.7', field of view 2.5 mm.

F. *Textulariopsis jurassica* (Gümbel, 1862), Well-H, 6421.5', field of view 2.5 mm.

Plate 52

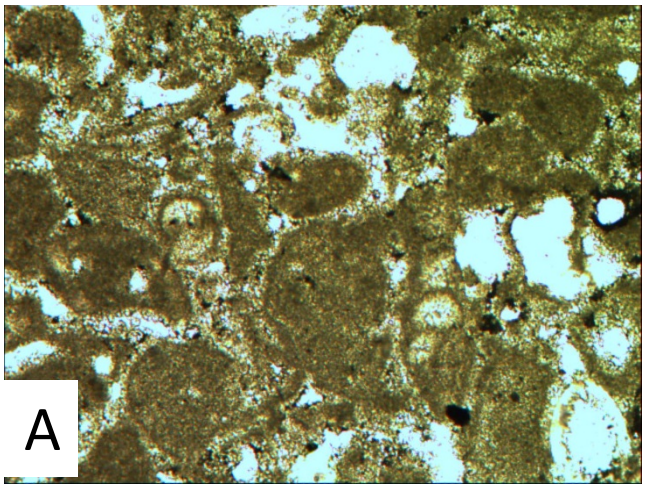

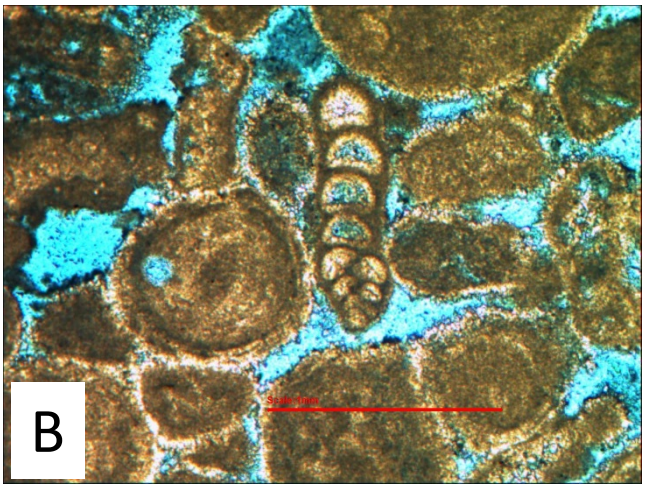

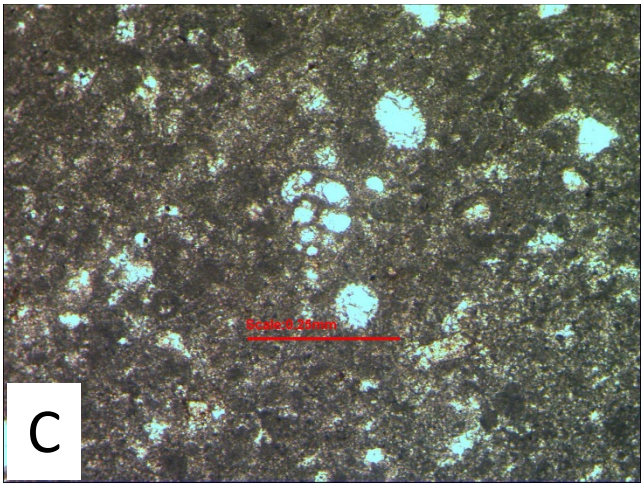

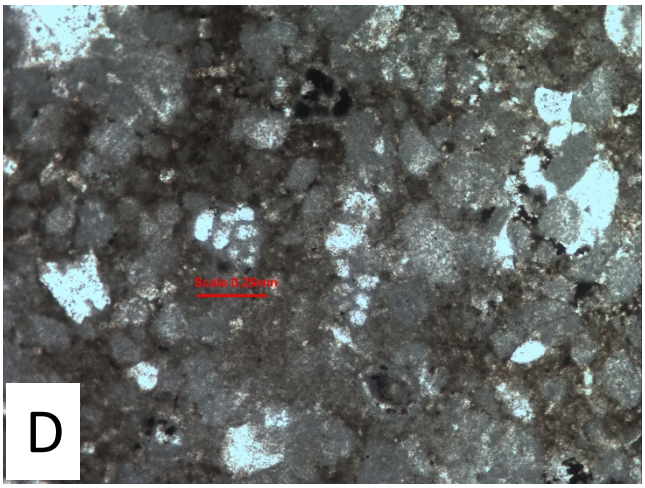

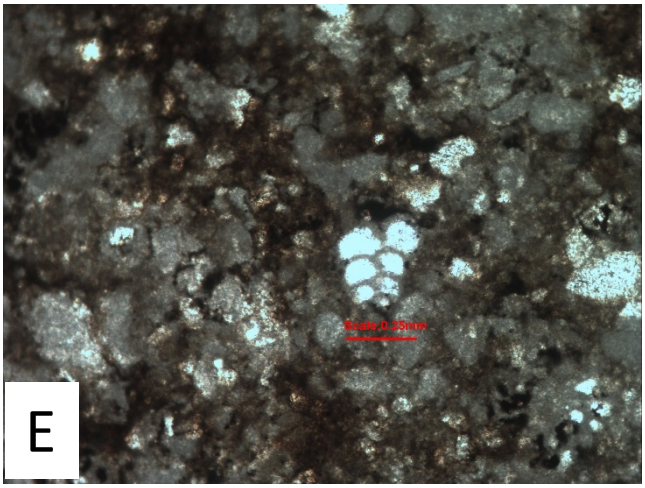

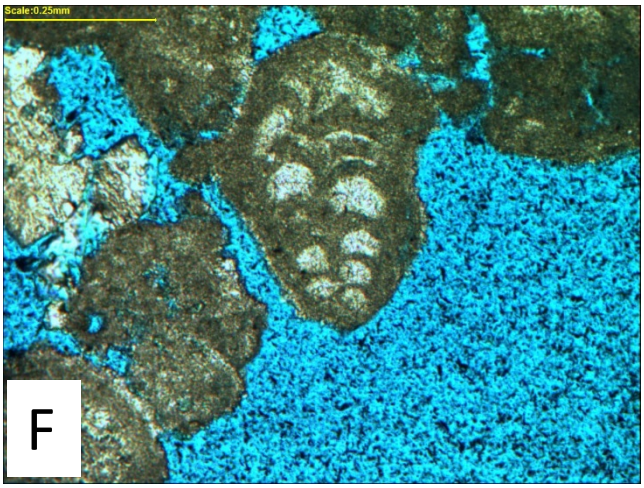

Plate 53

A. *Textulariopsis jurassica* (Gümbel, 1862), Well-D, 7957.2', field of view 1.25 mm.

B. *Textulariopsis jurassica* (Gümbel, 1862), Well-D, 7957.2', field of view 1.25 mm.

C. *Textulariopsis jurassica* (Gümbel, 1862), Well-H, 6423.5', field of view 2.5 mm.

D. Monaxon sponge spicules (red arrow), Well-B, 8365.1', field of view 2.5 mm.

E. Monaxon (red arrow) and triaxon sponge spicules (yellow arrow), Well-B, 8370.5', field of view 2.5 mm.

F. Monaxon sponge spicules (red arrow), Well-H, 6426.5', field of view 6.3 mm.

Plate 53

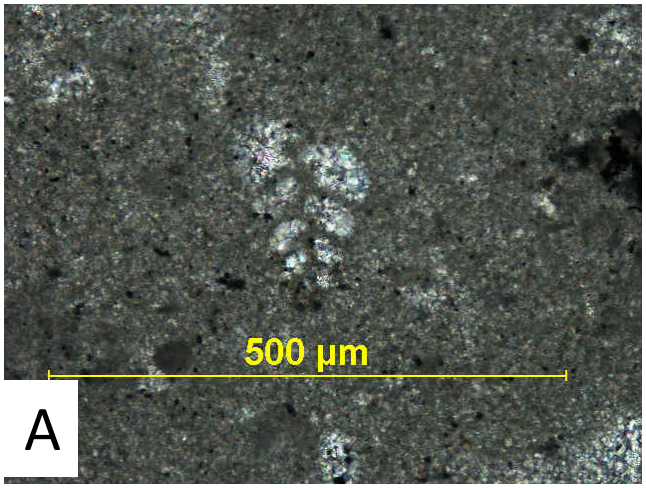

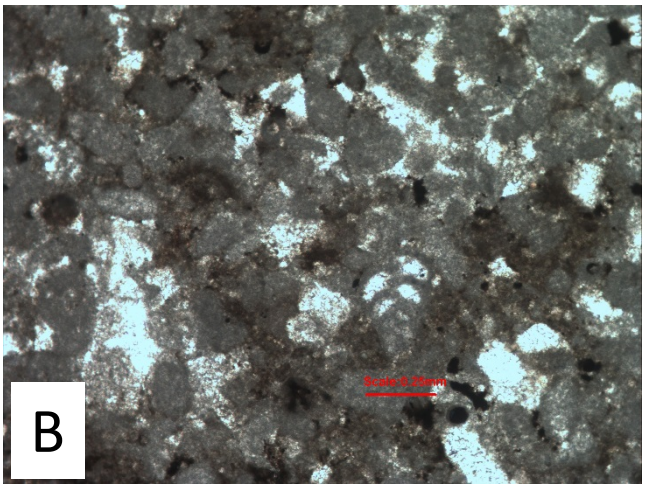

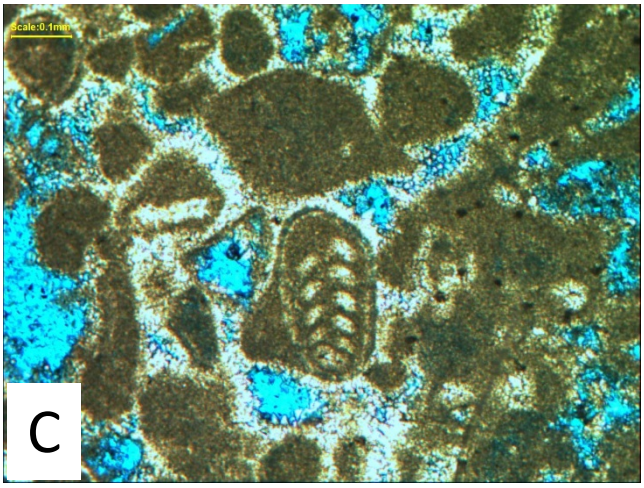

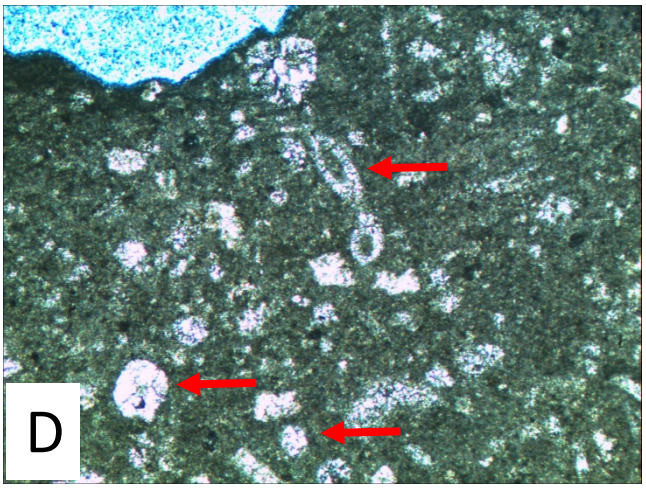

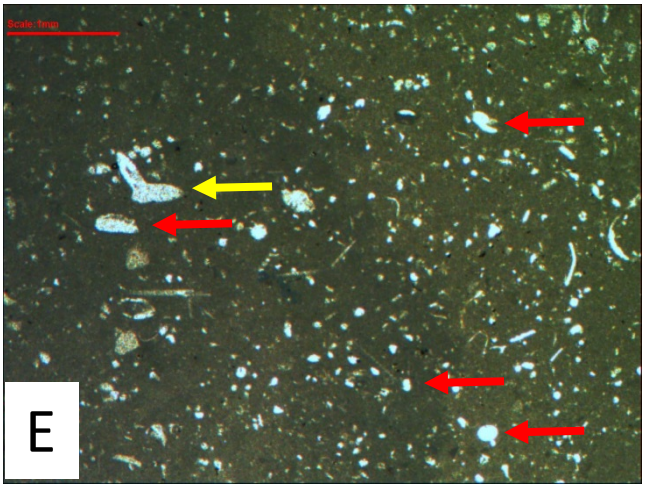

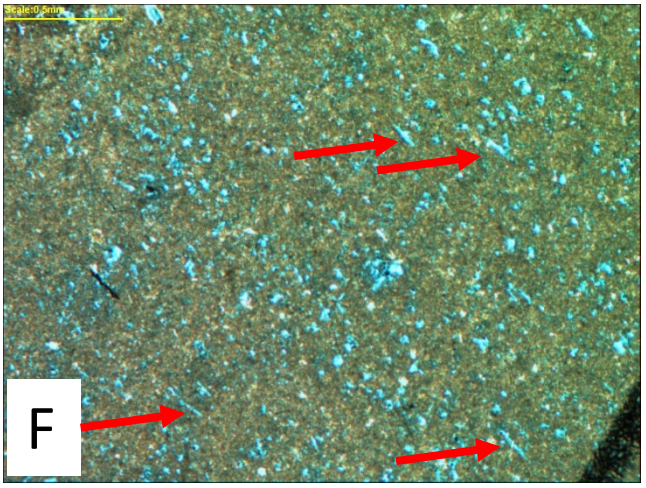

Plate 54

A. Large monaxon sponge spicules (red arrow), Well-D, 8644.2’, field of view 2.5 mm.

B. Large monaxon sponge spicules (red arrow), Well-D, 8644.2’, field of view 2.5 mm.

C. Monaxon sponge spicules (red arrow), Well-D, 8644.2’, field of view 6.3 mm.

D. Monaxon sponge spicules (red arrow), Well-D, 8644.2’, field of view 6.3 mm.

E. Triaxon sponge spicules (yellow arrow), Well-D, 8644.2’, field of view 2.5 mm.

F. Triaxon sponge spicules (yellow arrow), Well-D, 8644.2’, field of view 2.5 mm.

Plate 54